NASA Contractor Report 159242

ASSESSMENT OF THE USE OF SPACE TECHNOLOGY IN THE MONITORING OF OIL SPILLS AND OCEAN POLLUTION - TECHNICAL VOLUME

U. R. Alvarado (Editor)

(NASA-CR-159242) ASSESSMENT OF THE USE OF SPACE TECHNOLOGY IN THE MONITORING OF OIL SPILLS AND OCEAN POLLUTION: TECHNICAL VOLUME. EXECUTIVE SUMMARY (General Electric Co.) 464 p HC A20/MF A01 CSCL 13B G3/43

N80-26745

Unclas 23632

GENERAL ELECTRIC COMPANY
Philadelphia, Pennsylvania 19101

NASA Contract NAS1-15657
April 1980

National Aeronautics and Space Administration
Langley Research Center
Hampton, Virginia 23665

SD DOCUMENT NO. 80SDS4203
CONTRACT NO. NAS-1-15657

FINAL REPORT

ASSESSMENT OF THE USE OF SPACE TECHNOLOGY IN THE MONITORING OF OIL SPILLS AND OCEAN POLLUTION

TECHNICAL VOLUME

PREPARED FOR

NATIONAL AERONAUTICS AND SPACE ADMINISTRATION

LANGLEY RESEARCH CENTER
HAMPTON, VIRGINIA 23665

TECHNICAL OFFICER: WILLIAM F. CROSWELL

GENERAL ELECTRIC
SPACE DIVISION
Valley Forge Space Center
P. O. Box 8555 • Philadelphia, Penna. 19101

The key contributors to this report include:

U. Alvarado
G. Chafaris
J. Chestek
J. Contrad
G. Frippel
R. Gulatsi
A. Heath
H. Hodara (Tetra Tech.)
H. Kritikos (U. of Pennsylvania)
K. Tomiyasu

The authors gratefully acknowledge the support of the representatives within the U.S. Government and Industry, the Canadian Centre for Remote Sensing, and many technical consultants within the General Electric Company throughout the conduct of the study.

TABLE OF CONTENTS

SECTION 1
INTRODUCTION

In 1978 the United States Congress directed the National Aeronautics and Space Administration to investigate the utility of satellite systems and space technology in the detection and monitoring of oceanic oil spills and waste pollution. NASA's program in response to this directive has included the management of the study that is the subject of this report. The study was performed by the General Electric Company, Space Division.

1.1 STUDY OBJECTIVES

The study addressed the following basic goals that are pertinent to an assessment of the potential of space systems and technology in this important application:

- Determination of the measurement requirements and the end-products required by other agencies who are assigned operational responsibilities.
- Assessment of the present state-of-the-art, adequacy of the current technology, and the Advances in technology needed to meet the requirements.
- Definition of the characteristics of a future satellite system that would meet the requirements.

In addition, the study examined the potential impact of other space-related technologies such as communications and data handling.

1.2 SCOPE

A broad spectrum of topics were treated in the study, ranging from user needs to overall system implementation.

Serving as the framework of the study were the requirements of the various governmental users of ocean pollution data. Thus, a very important part of the study was the continuing dialog between NASA, the GE Study Team, and key representatives of the various government user organizations. An assessment of present and projected capabilities to meet these user requirements necessitated a broad system approach that sought to find realistic system concepts for utilizing the current and projected technology. Thus, in addition to the scientific aspects of remote sensing technology; the impact of various choices in instruments, sensor characteristics, sensor platforms, orbits and supporting equipment was also addressed.

A progression as shown in Figure 1.2-1 was followed in the study. The user's needs form the basis for mission requirements to satisfy the necessary knowledge objectives. These, in turn, are translated into measurement requirements necessary for pollution detection and monitoring as well as the input parameters to "fate" models to predict the trajectory of pollutants. Based on a technology assessment, sensors, platforms and other elements of the monitoring system are postulated to meet the measurement requirements. The selection of viable system implementation approaches is performed through analyses of mission operations and preliminary cost trades.

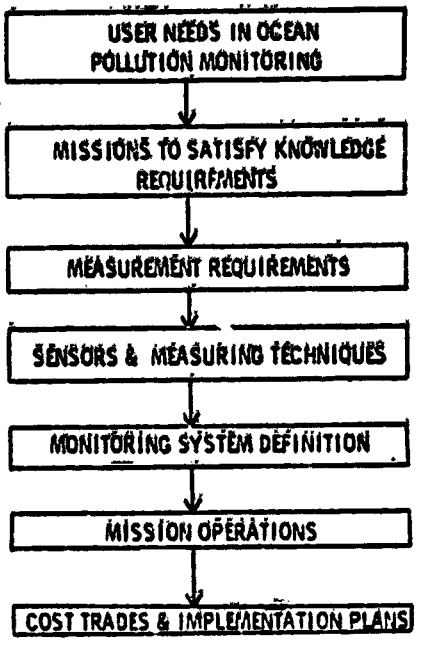

Figure 1.2-1 Elements of the Study

1.3 STUDY CONTRIBUTORS

The study benefitted greatly from the interest and cooperation of a large community of users and researchers who provided useful comment and technical inputs during the course of the study. Since many of these personnel were members of the Ad-Hoc Committee on Space Monitoring of Oil Spills, NASA-Langley arranged to hold study review meetings concurrently with Committee meetings, an arrangement which proved to be very successful in terms of benefits to the overall endeavor. Many individual interviews were held with experts in various aspects of oceanic pollution and related remote sensing. Member of the study team participated in the 1979 Oil Spill Conference and other related symposia. The following is a partial list of organizations that were represented in the study:

- NASA Langley Research Center
- NASA Goddard Space Flight Center
- National Oceanic and Atmospheric Administration, Department of Commerce
- U.S. Coast Guard, Department of Transportation
- U.S. Geological Survey, Department of Interior
- U.S. Bureau of Land Management, Department of Interior
- U.S. Environmental Protection Agency
- University of Rhode Island
- University of California, Santa Barbara
- Massachusetts Institute of Technology
- Jet Propulsion Laboratory
- ERIM
- JBF Scientific
- Intera Environmental Consultants
- Canadian Centre for Remote Sensing

The General Electric study team contracted the consultant services of Tetra Tech, Inc., Pasadena California, to assist in the expert assessment of remote sensing techniques relative to waste disposal pollutants. Fegley Associates, Inc., whose members are from the University of Pennsylvania, provided consultation and scientific liaison services relative to oil trajectory (fate) and impact modeling.

To all the individuals from the participating organizations, acknowledgement is made of their excellent contributions to the program, and we offer our sincere thanks for their enthusiastic cooperation.

SECTION 2
SUMMARY OF RESULTS

- TECHNOLOGY
- SYSTEM ELEMENTS
- SYSTEM CONCEPTS
- RECOMMENDATIONS

SECTION 2
SUMMARY OF RESULTS

The results of the study are summarized, considering three basic aspects:

- State of Technology Applicable to the Ocean Pollution Monitoring Mission
- Elements of a Possible Monitoring System
- Concept of the Systems to Fulfill the User Requirements

2.1 TECHNOLOGY

An initial technology base exists for space monitoring of oil spills and waste pollutants. This initial baseline has led to several measuring techniques and sensor concpets which make use of present knowledge of the characteristics of electromagnetic reflectance and emission of oil films and waste pollutant dispersions on water. Additional technology enhancement is needed leading to a better understanding of the environmental effects on the measurements, particularly those related to ocean dynamics. Much of this knowledge can only be attained through carefully controlled field testing, employing aircraft, spacecraft and surface truth instruments.

More technologically advanced than pollution monitoring itself are those techniques related to some of the inputs to the pollutant trajectory models. Examples of these measurements are wind speed & direction, and ocean surface temperature. However, in some measurements such as significant wave-height and ocean current speed/direction, a fairly mature measurement technology has limited ability due to the inability to provide extensive and frequent spatial-temporal coverage using only one or two satellites. Table 2.1-1 highlights remain aspects of this technological status.

MEASUREMENT TYPE	(A) KEY USER REQUIREMENTS	(B) STATE OF KNOWLEDGE OF DETECTION	(C) SENSING TECHNOLOGY ASSESSMENT	(D) NEEDED TECHNOLOGY ADVANCES	(E) KEY SYSTEM CHARACTERISTICS/CAPABILITIES	(F) OVERALL ASSESSMENT
1. OIL SPILL AREAL DISTRIBUTION	• 10-15 m RESOLUTION, • TWO MEASUREMENTS/DAY TO 200 n. mi.	• EFFECT OF OIL ON MICROWAVE BACKSCATTER IS UNDERSTOOD; • NEED KNOWLEDGE OF OCEAN DYNAMICS (1) TO RESOLVE AMBIGUITIES, (2) IDENTIFY OPTICAL SIGNATURES	BASIC RADAR & OPTICAL SENSORS/TECHNIQUES AVAILABLE; NEED TO TAILOR TO POLLUTION MISSION	• WIDE-SWATH, HIGH RESOLUTION, POINTABLE RADAR (SAR) AND OPTICAL IMAGER • INFO EXTRACTION TO RESOLVE AMBIGUITIES	• 10-15 m RESOLUTION IS NOT COST EFFECTIVE 60-100 m ADEQUATE TO DETECT MOST SPILLS	• SPACE SENSING REQUIRES RESEARCH IN INFORMATION EXTRACTION. • HIGH TEMPORAL FREQUENCY REQUIRES COMPLEMENTARY USE OF SPACECRAFT & AIRCRAFT
2. OIL SPILL THICKNESS REQUIRED FOR QUANTIFICATION	• 0.1 μm-2mm THICKNESS RANGE • 10-15 m RESOLUTION	PHYSICS OF THICKNESS MEASUREMENTS IN MICROWAVE ARE KNOWN	PASSIVE MICROWAVE RADIOMETER TECHNIQUES AVAILABLE FOR CROSS RESOLUTIONS & THICKNESS ABOVE 1mm.	• LARGE MICROWAVE ANTENNAS • OPTICAL TECHNIQUE DEVELOPMENT FOR THIN DK FILMS (E.G. LASER FLUORESCENCE	• LARGE SPACE PLATFORMS FOR ANTENNAS & LASER OPTICS	• OIL THICKNESS MEASUREMENT NOT FEASIBLE FROM SPACE IN FORESEEABLE FUTURE • CAN MEASURE FROM AIRCRAFT
3. OIL SPILL CLASSIFICATION	• OIL TYPE - CRUDE - REFINED - CHARACTERISTICS	OIL FLUORESCENCE PHENOMENON IS WELL UNDERSTOOD	LASER FLUOROSENSOR TECHNOLOGY IS IN EXPERIMENTAL STAGE	• ADVANCED LASER FLUOROSENSORS FOR SPACE	• LARGE SPACE PLATFORMS • ATMOSPHERIC ATTENUATION AND DISTANCE WOULD NECESSITATE LARGE OPTICS FROM SPACE	• OIL CLASSIFICATION NOT FEASIBLE FROM SPACE IN FORESEEABLE FUTURE • CAN MEASURE FROM AIRCRAFT
4. WASTE POLLUTANT SPATIAL DISTRIBUTION	>30 METER RESOLUTION	OPTICAL RADIANCE CONTRAST RELATIONSHIPS ARE DEVELOPED, NEED EXPANSION FOR SPACE OBSERVATIONS	OPTICAL SENSOR TECHNOLOGY AVAILABLE FOR CROSS RESOLUTION (e.g. 1 Km).	NEED WIDE SWATH, HIGH RESOLUTION SENSOR DEVELOPMENT	• HANDLING OF HIGH DATA RATES	• CAN MEASURE FROM SPACE; NEED ADDITIONAL DEVELOPMENT
5. WASTE POLLUTANT CONCENTRATION (DILUTION)	>30 METER RESOLUTION; DETECTION OF SMALL TRACES OF HAZARDOUS SUBSTANCES	STATISTICAL DATA HANDLING TECHNIQUES HAVE BEEN SUCCESSFUL IN MEASURING CONCENTRATIONS	OPTICAL SENSOR ARE AVAILABLE FOR GROSS RESOLUTION	NEED EXPERIMENTAL DATA UNDER VARIOUS ATMOSPHERIC & SURFACE CONDITIONS, FROM SPACE SENSORS	• HIGH SENSOR DETECTIVITY • MULTI-CHANNEL INSTRUMENT	• PROMISING TECHNIQUES; REQUIRE ADDITIONAL SPACE-BASED DATA

Table 2.1-1 Space Technology Capability Summary

MEASUREMENT TYPE	(a) KEY USER REQUIREMENTS	(b) STATE OF KNOWLEDGE OF DETECTION	(c) SENSOR TECHNOLOGY ASSESSMENT	(d) NEEDED TECHNOLOGY ADVANCES	(e) KEY SYSTEM CHARACTERISTICS/CAPABILITIES	(f) OVERALL ASSESSMENT
6. WASTE POLLUTANT CLASSIFICATION	• DIFFERENTIATE: – ACIDS – SLUDGE – BIO-DIGESTED WASTE	DIFFERENCE IN REFLECTANCE SPECTRAL CHARACTERISTICS IS KNOWN	ADVANCED OPTICAL SENSOR (POLA) WOULD BE SUITABLE FOR CROSS CLASSIFICATION	• MULTISPECTRAL LINEAR ARRAYS • WIDE-SWATH	HIGH DATA RATES	CROSS CLASSIFICATION POSSIBLE WITH MULTISPECTRAL LINEAR ARRAY
7. WIND SPEED AND DIRECTION	• 10 KM RESOLUTION CELLS • SPEED MEASUREMENTS EVERY 3 HOURS	RELATIONSHIPS BETWEEN SPEED/DIRECTION & NORMALIZED RADAR CROSS-SECTION IS KNOWN	SCATTEROMETER HAS DEMONSTRATED CAPABILITY	• ELIMINATION OF WIND-DIRECTION AMBIGUITY • FILLING OF CENTRAL GAP AREA IN SWATH	SATELLITE MUST ACCOMMODATE MULTIPLE ANTENNAS	CAN MEASURE WITH SCATTEROMETER
8. OCEAN CURRENT SPEED AND DIRECTION	• 10 KM GRID • MEASUREMENTS EVERY 6 HOURS	• SEA TOPOGRAPHY VS. CURRENTS IS UNDERSTOOD • IR MAPPING OF BOUNDARIES IS A MATURE SCIENCE	• MICROWAVE & LASER ALTIMETRY SUFFICIENTLY ACCURATE, BUT, • CANNOT PROVIDE 10 KM, ONCE/6 HR. COVERAGE	• MULTI-BEAM ALTIMETRY AT VERY HIGH INCIDENCE ANGLES	• ALTIMETER CAN ONLY MEASURE AT POINTS ALONG ORBIT TRACK. 10 KM GRID IS DIFFICULT TO ATTAIN	• NOT FEASIBLE WOULD REQUIRE A FLEET OF SATELLITES TO PROVIDE COVERAGE • CAN MEASURE FROM AIRCRAFT
9. WAVE HEIGHT (H 1/3)	• 10 KM GRID • MEASUREMENTS EVERY 3 HRS.	• CORRELATION BETWEEN ALTIMETER PULSE RISE-TIME AND WAVE HEIGHT IS KNOWN	• ALTIMETER SENSOR TECHNOLOGY IS MATURE	• TECHNIQUES FOR COMBINING ALTIMETRY DATA WITH SEA-STATE MODEL OUTPUTS • EXPLORE NEW TECHNIQUES USING SAR/SCATTEROMETER	• ALTIMETER CAN ONLY MEASURE AT POINTS ALONG ORBIT TRACK. 10 KM GRID IS DIFFICULT TO ATTAIN	• NOT FEASIBLE WOULD REQUIRE A FLEET OF SATELLITES TO PROVIDE COVERAGE • CAN MEASURE FROM AIRCRAFT
10. WAVE DIRECTION AND LENGTH	• MEASUREMENTS EVERY 3 HRS. • WAVE LENGTH RANGE: 0.3 METERS TO 1 KM	• SAR IMAGE DATA INTERPRETATION TECHNIQUES ARE AVAILABLE	• BASIC RADAR TECHNOLOGY IS AT HAND; NEED TO TAILOR TO POLLUTION MISSION • SPATIAL RESOLUTION IS THE LOWER LIMIT OF MEASUREMENT CAPABILITY	• NEED DIFFERENT TECHNIQUES FOR LONG-RANGE OF WAVE-LENGTHS	• MANY SATELLITES NEEDED FOR ONCE/3 HRS COVERAGE • HIGH DATA RATES, HIGH-POWER, FOR FINE RESOLUTION	• SAR CAN ONLY MEASURE WAVES ABOVE SAR RESOLUTION, i.e. LIMIT

Table 2.1-1 Space Technology Capability Summary (Cont'd)

A more specific summary of measurement technology must consider each individual user requirement parameter. The Executive Summary, Section IV contains a discussion of each of the main measurement parameters and its state of technology.

2.2 SYSTEM ELEMENTS

The analysis of the various ocean pollution monitoring scenarios and missions permitted a correlation of the applicability of selected sensors and platforms to the various aspects of the missions. This correlation is summarized on Table 2.2-1. The primary spaceborne sensors are as follows:

- Synthetic Aperture Radar
- Pointable Optical Linear Array
- Scatterometer
- Passive Microwave Radiometer
- Microwave Altimeter

The primary airborne sensors are as follows:

- Side Looking Airborne Radar (USCG-ARI)
- UV/IR Line Scanner (USCG-ARI)
- Low Light Level TV (USCG-ARI)

Additional sensors recommedned for a future airborne system such as Advanced ARI (AARI) are as follows:

- Airborne Sythetic Aperture Radar
- Airborne Passive Microwave Radiometer
- Airborne RF Altimeter
- Laser Stimulated Fluorosensor

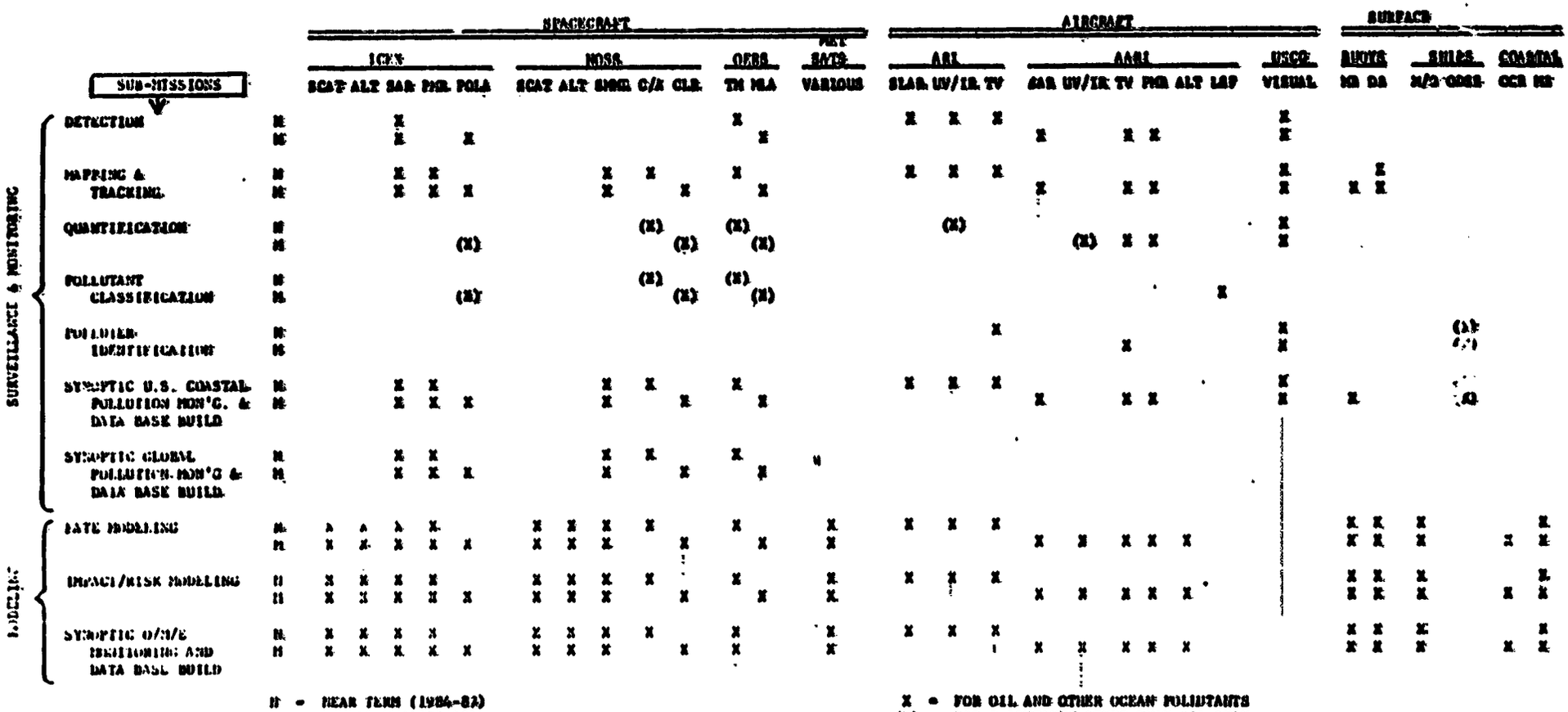

N = NEAR TERM (1984-87)
M = MID-TERM (1988-91)

X = FOR OIL AND OTHER OCEAN POLLUTANTS
(X) = FOR POLLUTANTS OTHER THAN OIL ONLY

AARI - ADVANCED AIRBORNE REMOTE INSTRUMENTATION
ALT - ALTIMETER
ARI - AIRBORNE REMOTE INSTRUMENTATION
C/A - COASTAL ZONE COLOR SCANNER/ADV VERY HIGH RESOLUTION RADIOMETER (CZCS/AVHRR)
CCR - COASTAL CURRENT RADAR
CLR - COMBINER
DB - DRIFTING BUOYS
LSF - LASER STIMULATED FLUOROSENSOR
MB - MOORED BUOYS
METSATS - METEOROLOGICAL SATELLITES
MLA - MULTISPECTRAL LINEAR ARRAY
M/O - METEOROLOGICAL & OCEANOGRAPHIC SENSING SYSTEMS
MS - METEOROLOGICAL STATIONS
NOSS - NATIONAL OCEANIC SATELLITE SYSTEM
OOSS - OCEAN DUMPING SURVEILLANCE SYSTEM
OERS - OPERATIONAL EARTH RESOURCES SYSTEM
PMR - PASSIVE MICROWAVE RADIOMETER
POLA - POINTABLE OPTICAL LINEAR ARRAY
SAR - SYNTHETIC APERTURE RADAR
SCAT - SCATTEROMETER
SLAR - SIDE-LOOKING AIRBORNE RADAR
SMMR - SCANNING MULTICHANNEL MICROWAVE RADIOMETER
TM - THEMATIC MAPPER
USCG - U.S. COAST GUARD
UV/IR - ULTRAVIOLET/INFRARED LINE SCANNER

Table 2.2-1 Platforms and Sensors (Employment Concept)

Support spaceborne sensors useful to correlate or complement data from primary sensors or to provide secondary data relative to pollution are as follows:

- Thematic Mapper
- Multi-spectral Linear Array (narrow swath)
- Coastal Zone Color Scanner (narrow swath)
- Advanced Very High Resolution Radiometer

The most important future space platforms applicable to the mission are the National Oceanic Satellite System and future spacecraft equipped with SAR, niminally that for the Ice Processes and Climate Mission. Spacecraft such as Landsat and Operational Earth resources Satellite and Metecrological Satellites are envisioned as providing valuable mission support.

2.3 SYSTEM CONCEPTS

The future system for ocean pollution monitoring is envisioned as having the following general characteristics:

- It is an EVOLUTIONARY system, with gradually increased capability relative to full attainment of the mission goals.
- The system elements will be SHARED to a great extent; for instance there will not be any dedicated space platform, since multi-mission systems such as NOSS can be utilized effectively.
- The system will use the COMPLEMENTARY capabilities of ai-borne, spaceborne, and surface elements. This complementary approach will be particulary useful in providing the necessary spatial/tempotal coverage over the 200 mile coastal zone. A comprehensive analysis of the operational asepcts of this coverage, using various orbits is included in Section 5.2.

A comparative analysis examined six alternative system concepts and ranked them using criteria such as cost, coverage capabilities, and timeliness of the information. The option exhibiting the highest rating utilizes NOSS and the spacecraft for ICEX as the primary space platforms. The latter would contain wide-swath pointable SAR and Pointable Optical Linear Array with 100 meters resolution. The pointability feature was found to be very useful in providing the desired coastal coverage. An important element of the system is the centralized Data Processing System which permits data from many sources to be processes and disseminated to the users.

2.4 RECOMMENDATIONS

Oceanic pollution due to petroleum and the disposal of wastes is a serious global environmental problem, the control of which represents a major technological and institutional challenge. Aspects of the problem where space technology can contribute include communications, ship navigation, remote sensing of pollutants, and data management. As the results of the study summarized above indicate, the capability to monitor large ocean areas synoptically through space-borne instruments is feasible. Furthermore, the satisfaction of user needs realative to the location, extent, and dispersion of pollutants necessitates the cooperative coverage by spacecraft, aircraft and surface platforms.

In order to enable the realization of the potential of space endeavors in the cost-effective satisfaction of the user needs, the following research and development efforts are recommended:

INFORMATION EXTRACTION TECHNIQUES

Research is recommended leading to the development of techniques for high-certainty, unambiguous detection and delineation of oil spills and waste pollution in the ocean. A major part of this effort will involve the building of a comprehensive baseline of experimental data concerning space and aircraft observations of natural and controlled pollution events under a wide variety of environmental conditions. Both the effects of the environmental variables upon the observation, as well as the nature of the environmental phenomenon itself should be investigated. Due to the likelihood that the ultimate observational techniques will be multi-spectral in nature, it is recommended that the field testing be conducted using a variety of simultaneous observations in the optical and microwave spectral bands. Accurate surface-truth data will be essential to the development of the proper information extraction relationships for pollution monitoring.

DEVELOPMENT OF INSTRUMENTS FOR BROAD SPATIAL/TEMPORAL COVERAGE

Parametric design studies are recommended on the types of space instruments for oil and waste pollution monitoring that are suitable for frequent coverage of the 200 n.mi. coastal zone. The two prime instruments identified in this study are the wide-swath pointable SAR and the Pointable Optical Lindear Array. Some of the parameters to be examined in the use of SAR are swath-width, power, microwave frequency, and resolution. Typical trades will include the determination of optimum method of illumination (i.e. fixed vs. scanned beam), number of beams, and antenna configuration. Results of these parametric analyses are needed for the potential incorporation of the ocean pollution mission in the future development of multi-application instruments such as in the SAR for geological research and Ice Processes and Climate Experiments.

OIL QUANTIFICATION METHODS

New or improved techniques should be developed for sensing oil slick thickness, a measurement that is necessary in the quantification of oil spills. Multi-frequency passive microwave radiometry techniques for high resolution (e.g. 0.1 to 0.2 Km.) mapping of thickness distribution from space should be explored.

NEW TECHNIQUES FOR FATE-MODEL INPUT DATA

A substitute for nadir-altimetry should be found, for measuring significant wave height and ocean current speed and direction. A potential area of research here is the development of automated data processing techniques using signal returns from sensors such as synthetic aperture and laser radars.

DATA HANDLING AND COMMUNICATION SYSTEM APPROACHES

The requirements of the oil spills and ocean pollution mission are typical of many emerging applications where data must be collected from many diverse sources, processed in real-time or near real-time, and formatted to meet the

user's needs. Consideration of the pollution mission needs is recommended for inclusion in future R&D efforts relative to end-to-end data processing and communication techniques and systems.

A great deal of the data currently being gathered through satellites such as Tiros, Nimbus, Landsat, and DMSP would be useful to the users of ocean pollution data. Similarly, some of the data from planned systems such as NOSS will be directly applicable to this mission. Thus, the specific data processing and dissemination needs of the users should be examined relative to these programs, to implement means of making the data available to the users within the required time-interval.

SECTION 3
USER REQUIREMENTS

- THE OCEAN POLLUTION PROBLEM
- DEFINITION OF USERS
- KNOWLEDGE OBJECTIVES AND MEASUREMENT REQUIREMENTS
- OIL SPILL TARGET CHARACTERIZATION OF SPATIAL RESOLUTION REQUIREMENTS

SECTION 3

USER REQUIREMENTS

Information concerning oceanic pollution is of great interest to a large segment of the population, primarily due to the hazard to human health due to potential contamination of ocean-derived food resources. In addition, private concerns such as commercial fisheries need this data to ensure the quality of their product. Similarly, the ocean resort managers, the vacationing public and private beach owners are interested in information regarding the cleanliness and aesthetic quality of the coastal environment. To satisfy these needs in the protection of health and property, the various governmental agencies need ocean pollution-related data in order to discharge the following general responsibilities:

- To prevent or reduce pollution at the sources.
- To eliminate, diminish or evaluate the detrimental effects of pollution events.
- To permit proper planning for the construction of new facilities or installations while avoiding potential damage natural or man-made resources.
- To insure payment by the polluter for environmental damage, clean-up costs and legal fines.

This section of the report deals with the user needs by: (1) defining the pollution problem and its severity;(2) identifying the key government organizations whose responsibilities require the use of pollution monitoring data; (3) stating the user requirements in terms of the knowledge to be gained and the measurements to attain that knowledge; (4) defining the scope of the observational missions which provide an operational structure for the accomplishment of these measurements.

3.1 THE OCEAN POLLUTION PROBLEM

Although the oceans cover a great portion (≈ 71%) of the world's surface, the coastal waters bounded by the continental shelf, where 99% of the world fish catch originates, is only 7% of that surface. Ecologically sensitive regions within the coastal zone, including estuaries and areas of upwelling are spread widely throughout this coastal zone. Furthermore, most of man's activities is the ocean are conducted within this zone, including the aesthetic enjoyment of the coastal environment. Unfortunately, this most sensitive and vulnerable area relative to pollution, is also the area where most of the man-induced pollution occurs. It is reasonable to assume that long before the deep oceans would be polluted, the coastal zone would be thoroughly polluted. Such occurrence is not inevitable, and there are signs of sufficient international concern about the problem, as evidenced by many international treaties to justify optimism about the improbability of long-term catastrophic coastal pollution. However, the quantities and types of pollutants dumped in the ocean justify concern about the long-term damage that will be made to local, environmentally fragile areas that constitute significant elements of our ocean resources.

Well publicized pollution events such as those by the Argo Merchant[9] (1976) and Amoco Cadiz [58](1978), while having serious temporary consequences, do not constitute the major problem. The larger problem in terms of detrimental effects on the environment are caused by the sustained, rather than the occasional rate of flow of contaminants into the coastal waters. This relentless contamination due to oil and disposed wastes often does not permit time for marine biological species in certain regions to recover from the disruptive effects of pollution.

Oil Pollution affects marine ecosystems in many ways, generally through: (1) toxicity, acting directly on the marine organism; (2) physical coating of the organism; (3) loss of habitat; and (4) change in food supply. Other ocean pollutants are lethal to marine species in small pollutant concentrations, while others have a debilitating effect characterized by retardation of growth, alteration of chemoreception in food finding and mating, aberrant behavior, physiological stresses affecting vigor, and reproductive failure (ref. no. 99). Table 3.1-1 summarizes the major types of ocean pollution and their environmental impact.

Table 3.1-1 Categories of Ocean Areas and Types of Pollution, Effects on Uses and their Duration

Ocean Area	Types of Pollution	Effects on Uses and Pollution Trends	Duration of Effects
Coastal waters (10% of total area; 99% of total fish production, including that from upwelling areas).	Sewage; industrial wastes; litter; petroleum hydrocarbons.	Living resources destroyed or rendered unusable; industrial uses of sea water adversely influenced; amenities reduced; recreational values diminished.	Mainly during period of discharge. Can be short-term, in the case of a sporadic event; or long-term in a sustained period of discharge.
	Synthetic organic chemicals; metals; radioactivity.	Living resources decreased or rendered unusable.	Long-term; metals and synthetic organic chemical deposited in sediments may be released for a long time through normal leaching and/or dredging disturbance.
Open ocean (90% of total area; 1% of total fish production, excluding that from upwelling areas).	Synthetic organic chemicals; metals; petroleum hydrocarbons; radioactivity.	Increasing concentrations in water and organisms may indicate dangerous trends.	Long-term; duration depends on the residence time of pollutant.

Following are some of the pertinent statistics concerning the quantity of pollutants introduced into the ocean environment.

The sources of oil pollution, on a worldwide basis, are shown in Table 3.1-2. Out of the total of 45.2 million barrels annually (1.9 billion gallons), about 29.6 million barrels are due to uncontrollable, non-point or fixed sources. The remainder, approximately 15.6 million barrels are due to transportation activities. Only 14% of the transportation segment are due to accidents such as groundings, strandings, and collisions. The remaining 86% are due to operational activities such as oil tanker tank washing (50.6%), loading and docking activities (12%), and bilge and bunker tank pumping (23.4%). It is clear from these quantities that an operational system for monitoring oil spills needs to consider many types of sources: natural, accidental and intentional.

Table 3.1-2. Annual Input of Petroleum Hydrocarbons In The Ocean

Source of Oil	Million Barrels Per Year	Percent Of Annual Input
Transportation Tankers, dry docking, terminal operations, bilges, accidents	15.6	34.6
Coastal refineries, municipal and industrial waste	6.6	14.6
River and urban runoff	14.2	31.4
Atmospheric fallout	4.4	9.7
Natural seeps	4.4	9.7
Totals	45.2	100.0

(Source: From National Academy of Sciences)

Waste disposal accounts for a large portion of the total ocean pollution input. The estimated rate of introduction of the major waste categories in U.S. coastal waters are as follows:

Sewage Sludge:	4540 million kg/yr
Industrial Wastes:	1544 million kg/yr (Mid-Atlantic & Gulf of Mexico)
Incineration of Organochlorides:	27 million kg/yr
Ocean Outfalls:	7.6 million cubic meters/day (2740 billion kg/yr)
Dredged Material:	31.5 million cubic meters/yr

One of the major waste pollutants is metals, the origins of which are the natural processes and mining practices. By far the largest portion of metals transported into the world's ocean (e.g. through river effluents) is iron (3.4×10^8 metric tons per year). Other abundant metal pollutants include manganese, copper, zinc, nickel, lead, molybdenum, silver, mercury, tin and antimony. Highest toxicity in these metals relative to marine organisms is found in mercury, silver, copper, and zinc; which together constitute approximately 2% of the total metal input to the oceans.

Chemical industrial waste has constituted a significant source of pollution, however, recent legislative restrictions on the dump sites and/or concentrations are tending to reduce the harmful effects of these pollutants. "Toxic pollutants" as defined by the Clean Water Act include the following substances:

Aldrin/Dieldrin; Arsenic; Benzidine; Carbon tetrachloride; Cadmium

Dichlorobenzidine

Chlorinated ethanes

Chloroform

Chromium; Demeton; Dichloroethylenes

Dinitrotoluene

Fluoranthene

Diphenylhydrazine; Endrin; Hexachlorocyclopentadiene; Ethylbenzene; Lindane; Mercury; Nickel

Nitrobenzene; Naphthalene

Silver; Vinyl Chloride

Acenaphthene; Antimony; Chlorinated benzenes; Chloroalkyl ethers; DDT

Dichloropropane and dichloropropene; Halomethanes; Malathion; Tetrachloroethylene

Trichloroethylene

Polynuclear aromatic hydrocarbons; Endosulfan; Mirex; Pentachlorophenol

Phenol; Acrylonitrite

Asbestos; Benzene

Beryllium; Chlorinated Naphthalene; 2-Chlorophenol; Chlorophenols; Chlorophenoxy herbicides; Cyanide; 2,4-Dichlorophenol

Acrolein; Chlordane; Nitrosamines; Copper; dichlorobenzenes; Guthion; Haloethers

Heptachlor

Hexachlorobutadiene; Hexachlorocyclohexane; Isophorone

Lead; Methoxychlor; Nitrophenols; parathion; Phthalate Esters; PCB's

Selenium; P-Dioxin

Thallium, Toluene

Toxaphene; Zinc

2,4-dimethylphenol.

Summarizing the severity of the ocean pollution problem: the number of pollutant substances that are harmful to the environment, and the large quantity of pollutant material entering into our coastal waters suggests that this global problem ranks not much lower than atmospheric pollution in severity. Predictions of how the problem will develop during the next two decades is difficult, considering all the variable that are involved. Our general assessment is that causes of the problem would not subside significantly during that period, and that its detrimental effects will be significant unless the proper operational practices and surveillance are instituted. For instance, although there will be a decrease in ocean transportation of fossil hydrocarbon fuels, increased transportation of other chemicals, such as synthetic fuels with characteristics similar to crude and processed oil will tend to compensate. Similarly, in the waste disposal pollution area, the improved regulatory countermeasures may be balanced by increased demands for waste disposal capacity due to increased population and accelerated industrial development in the emerging nations.

3.2 DEFINITION OF USERS

The need for ocean pollution related data derives primarily from federal legislation for the protection the coastal environment. Table 3.2-1 identifies some of the main statutes that relate to this subject, and the U.S. agencies involved in carrying out the provisions of those laws. The following sections present a brief description of the responsibilities of the main users of ocean pollution-related data.

3.2.1 U.S. DEPARTMENT OF TRANSPORATION - U.S. COAST GUARD (USCG)

In accordance with the Federal Water Pollution Control Act (33USC1251), the USCG has primary responsibility for enforcement of U.S. laws concerning ocean pollution due to oil and other hazardous substances. Jurisdiction for this responsibility encompassed the contiguous waters and the prohibited zones, and has been extended to the 200 miles controlled coastal zone as defined by the Fishery Conservation and Management Act of 1976.

The monitoring task by the USCG encompasses the following:

1. Detection and identification harmful discharges of oil and hazardous substances. A discharge of oil that causes a sheen or discoloration of the water surface or adjoining shoreline or causes a sludge or emulsion to be deposited beneath the water surface or upon adjoining shorelines violates the Federal Water Pollution Control Act of 1972. The "hazardous substances" include the toxic pollutants that were listed in Section 3.1 above.

2. Assessment of the spatial extent of the pollution events, including their areal and volumetric extent.

3. Determination and prediction of the movement (trajectory) of the pollutants.

4. Evaluation of effectiveness of efforts to remove (or neutralize the effects of) discharges of oil and hazardous substances.

5. Gather legal evidence to permit the prosecution of violators of ocean pollution laws.

The Airborne Oil Surveillance System (AOSS) became fully operational in 1977. This system carries remote sensing instrumentation (described in Section 4.2.5)

TABLE 3.2-1

MAJOR LEGISLATION APPLICABLE TO OIL SPILLS & OCEAN POLLUTION

STATUTE	SUBJECT OF THE STATUTE	AGENCIES INVOLVED	TERRITORIAL APPLICABILITY
FEDERAL WATER POLLUTION CONTROL ACT (33 USC 1251)	OIL OR HAZARDOUS SUBSTANCE DISCHARGES IN U.S. WATERS. NATIONAL STANDARDS.	EPA, DOT, CORPS OF ENG., CUSTOMS, DOI	U.S. WATERS, SHORELINES, CONTIGUOUS ZONE
NATIONAL OIL & HAZARDOUS SUBSTANCES POLLUTION CONTINGENCY PLAN (TITLE 40, CFR)	COORDINATED & INTEGRATED RESPONSE BY FED. DEPTS. AND AGENCIES TO MINIMIZE DAMAGE FROM OIL AND HAZARDOUS SUBSTANCE DISCHARGES	COUNCIL ON ENV. QUAL, DOC, DOD, HEW, HUD, DOI, DOJ, USCG, STATE DEPT., ABC, EPA	NAVIGABLE WATERS, ADJOINING SHORELINES, WATERS OF CONTIGUOUS ZONE
REFUSE ACT (33 USC 407)	DISCHARGE FROM SHIP, OR SHORE FACILITY ANY KIND OF REFUSE MATTER	USCG, CUSTOMS, CORPS OF ENG., DOI, STATE DEPT.	U.S. NAVIGABLE WATERS, TRIBUTARIES, BANKS
OIL POLLUTION ACT OF 1961 (33 USC-1001-1015) REF. TO "INTERNATIONAL CONVENTION FOR THE PREVENTION OF POLLUTION OF THE SEA BY OIL"	ESCAPE OR DISCHARGE OF OIL FROM U.S. SEAGOING VESSELS (E.G., RATE OF DISCHARGE: 60 LITERS/MILE; 100 PPM, TOTAL DISCHARGE 1/15000 OF TOTAL CARGO.	USCG, CUSTOMS, CORPS OF ENG., DOJ, STATE DEPT.	PROHIBITED ZONES (50 MILES TO SEA 100 MILES OFF NE COAST)
CLEAN WATER ACT & 1977 AMENDMENTS	ELIMINATION OF POLLUTANT DISCHARGE IN NAVIGABLE WATERS, BY 1985. WATER QUALITY GOALS, FEDERAL FINANCIAL ASSISTANCE, WATER QUALITY SURVEILLANCE SYSTEM.	EPA (ADMINISTRATION) NASA USCG USGS NOAA	NAVIGABLE WATERS, CONTIGUOUS ZONE, OPEN OCEAN
COASTAL ZONE MANAGEMENT ACT (16 USC 1451)	CONSERVATION, PROTECTION, DEVELOPMENT, AND ENHANCEMENT OF COASTAL RESOURCES. MANAGEMENT PROGRAMS INVOLVE U.S. AGENCIES AND THE AFFECTED STATES.	EES, NOAA, DOI AND INDIVIDUAL STATES.	COASTAL WATERS (TERRITORIAL WATERS, GREAT LAKES, SHORELANDS)
NATIONAL OCEAN POLLUTION RESEARCH AND DEVELOPMENT & MONITORING PLANNING ACT	PREPARATION OF A 5-YEAR PLAN FOR FEDERAL OCEAN POLLUTION R&D AND MONITORING.	NOAA (LEAD), EPA, DOI, NASA, USCG.	MARINE ENVIRONMENT: U.S. TERRITORIAL WATERS, 200 MILE ZONE, HIGH SEAS, SEABED, SUBSOIL
MARINE PROTECTION, RESEARCH, AND SANCTUARIES ACT (MPRSA)	OCEAN DUMPING OF WASTES: DREDGE MAT'L,	EPA, USCE, USCG (REGULATORY AUTHORITY); NOAA (RESEARCH & DESIG. OF SANCTUARIES, MONITORING PROG.	OCEAN WATERS, COASTAL WATERS, & GREAT LAKES

on an HC-130B aircraft flying oil spill detection patrols along the East Coast and Gulf of Mexico. The AOSS capabilities will be expanded with the advent of the Airborne Remote Instrumentation (ARI) system which will be operational in 1981 (ref. Section 4.2.5.2). The ARI system will be flown on six medium-range Falcon jet-aircraft.

3.2.2 ENVIRONMENTAL PROTECTION AGENCY (EPA)

EPA is the primary agency administering the Clean Water Act, as ammended in 1977. Its region of concern in ocean pollution matters is the nation's navigable water, waters of the contiguous zone and the oceans. Under the provisions of the Clean Water Act, EPA will ensure the reduction and elimination of pollution discharges in navigable waters; conduct investigations concerning pollution of navigable waters; establish and maintain water quality surveillance system for inland waters utilizing resources of NASA, NOAA, USGS, and USCG; and take action to insure international measures for prevention of harmful discharges by other countries.

EPA supports efforts in response to the National Contingency Plan, which takes action in the event of major pollution incidents. That support includes the on-site coordination of activities in response of pollution events or inland waters (except the Great Lakes) in the same way that USGS coordinates activities for coastal waters and the Great Lakes. EPA also provides assistance in major oil spills through the "Aerial Remote Sensing Program", which provides aerial photographic coverage with a turn-around time of approximately one day.

3.2.3 DEPARTMENT OF INTERIOR/BUREAU OF LAND MANAGEMENT (BLM)

BLM is responsible for preparing environmental impact statements which are used as one of the major criteria in granting or withholding leases of off-shore areas for economic development. A vital part of an impact statement is the

prediction of the probable damage to the coastal environment in the event of a major pollution event (e.g. oil spill due to an off-shore oil well blow-out). In order to determine the probable oil spill trajectory and damage to sensitive coastal areas, a baseline of environmental statistics must be assembled. This data includes parameters such as wind speed and direction, ocean currents, significant wave height, and other data necessary for pollutant trajectory modeling. Remotely sensed data will be a useful complement to detailed, in-situ measurements, and provide synoptic, repeated coverage of the required areas.

3.2.4 DEPARTMENT OF INTERIOR - GEOLOGICAL SURVEY (USGS)

In conjunction with the BLM, USGS is responsible for conducting risk analyses relative to sensitive shore resources. The Water Resources Division of USGS has developed a model for the determination of the risk of oil spills and their impact on shore areas. USGS is a participant is one of the primary agencies in the National Contingency Plan.

USGS has performed analyses of Landsat multi-spectral image data under the EROS program. Image data from oil slicks was enhanced using computer aided image enhancement techniques.

3.2.5 U.S. DEPARTMENT OF COMMERCE - NATIONAL OCEANIC AND ATMOSPHERIC ADMINISTRATION (NOAA)

NOAA provides leadership, research and advisory support in the use and conservation of ocean resources. Its responsibilities encompass the ocean and its biological resources through functions such as defining, monitoring, exploring, mapping, forecasting, managing and conserving. An important part of the research activity concerns the determination of the effect of pollution or biological resources and ultimately the fishing industry. In addition, NOAA shares the responsibility with the USCG for administering the provisions of the Fishery Conservation and Management Act, which deals with the 200-mile coastal zone.

Research that is highly relevant to the ocean pollution mission is being carried out in several NOAA facilities. For instance, the Atlantic Oceanographic and Meteorological Laboratories is conducting a program of space observations of major ocean current boundaries and circulation patterns, using imaging data from satellites such as Tiros and GOES (ref. No. 83). Another example is the work being conducted in the Environmental Research Laboratories, concerning oil spills and the properties of oil that are relevant in remote sensing applications. In addition, the NWS-Systems Development Office is developing models for oil-spill trajectory.

NOAA was a leadership role in the "National Ocean Pollution Research and Development and Monitoring Planning Act of 1978". The preparation of this national plan for action is the responsibility of the Committee on Ocean Pollution, under NOAA direction. The special task force includes the following subcommittees: Research and Development, Monitoring, Data and Information, and National Needs.

3.2.6 NATIONAL AERONAUTICS AND SPACE ADMINISTRATION

Relative to ocean pollution activities, NASA has an important supportive role: research and development of sensors, platforms and measurement techniques.

The Coastal Zone Color Scanner's capabilities for oil spill and waste pollutant monitoring are being analyzed. The Landsat Multispectral Scanner, although not intended specifically for ocean applications, has produced images of oil spills and waste pollution dumps.

NASA Langley Research Center (LRC) has performed and is continuing research in remote sensing techniques for the identification and quantification of waste pollutants such as sewage sludge, acid dumps and other industrial wastes disposed in the ocean. LRC is the center of considerable research development

concerning microwave sensors such as the radiometer scatterometer, which is used in the measurement of wind speed and direction.

3.2.7 DEPARTMENTS OF DEFENSE; HEALTH, EDUCATION AND WELFARE; AND STATE

The DoD Naval Research Laboratory develops measurement techniques for oil spill detection and quantification. For instance, multifrequency microwave techniques have been developed for measuring the thickness distribution of oil slicks. DoD also provides assistance through manpower and equipment in major pollution incidents.

The State Department provides leadership in developing joint international contingency plans with neighboring countries such as Canada and Mexico.

HEW provides expert consultation and assistance in the assessment of the effects of actual or potential pollution incidents upon public health.

3.3 KNOWLEDGE OBJECTIVES AND MEASUREMENT REQUIREMENTS

A survey of user needs was performed, based on interviews with key representatives of the user community, as well as a review of current user literature. Results of the initial survey were presented during the first and second study research reviews, and user inputs from those reviews were factored into the final results. Table 3.3-1 summarizes the results of that survey, in terms of knowledge items which are useful to the various agencies in carrying out their responsibilities. The items on this table listed vertically represent what the users need to know about the pollutant, polluter, or the environment; the major users of the information are listed across the top of the matrix. Although there is a large degree of commonality in the requirements among the various user agencies, the manner in which the information is used and the degree of utility varies with the user. For instance, although item No. 2 in Table 3.3-1,

TABLE 3.3-1

KNOWLEDGE REQUIREMENTS BY USERS

KNOWLEDGE REQUIREMENTS	DOT USCG	DOC NOAA	DOC MAR AD	EPA	DOI USGS	DOI BLM	DOD NAVY	STATE DEPT.	HEM
1. DETECTION & LOCATION OF POLLUTANT	X	X		X			X	X	
2. QUANTITY & SPATIAL DISTRIBUTION	X	X	X	X	X	X	X	X	X
3. RATE OF DISCHARGE	X		X	X			X		
4. POLLUTANT CLASSIFICATION, COARSE	X		X		X	X	X	X	
5. POLLUTANT CLASSIFICATION, DETAILED	X	X		X					
6. SOURCE LOCATION	X		X	X			X	X	X
7. SOURCE IDENTIFICATION	X		X	X			X	X	
8. MOTION AND DISPERSION	X	X		X	X	X	X	X	
9. PREDICTED MOTION, SPREADING & SHORE IMPACT	X	X		X	X	X		X	
10. OPTIMUM POLLUTION ABATEMENT MEASURES	X	X		X	X				X
11. PREDICTION OF PROBABILITY OF DAMAGE TO ECOLOGY OR PROPERTY		X		X	X	X		X	X
12. ASSESSMENT OF DAMAGE	X	X	X	X	X	X		X	X
13. ECOSYSTEM INFORMATION		X		X					X

"Quantity and Spatial Distribution" is of some relevance to all the agencies listed, the main user is the USCG since it constitutes the primary enforcement agency. Due to the complementary nature of inter-agency responsibilities regarding ocean pollution, many of the agencies need certain information to enable support to agencies like USCG, EPA and DOI which have operational responsibility in current or projected ocean pollution incidents. This complementarity accounts for the large commonality of knowledge requirements among users.

Following is a brief definition of each of the knowledge requirements and a general statement about the measurements that are needed to support these objectives.

1. Detection and Location of Pollutant.

The pollutant must be detected as being distinct from other phenomena or conditions of the sea. A certain amount of identification is implied in this knowledge, since as the pollutant needs to be resolved from other types of matter on the sea surface such as, fish-oil and emissions or plant life on the water surface. With respect to the location, it is necessary that upon finding an oil slick or a waste dump the coordinates of the slick or waste must be known. The measurements necessary to attain this knowledge are essentially the image of the pollutant on the water or a point or a series of points within that pollutant.

2. Quantity and Spatial Distribution

In order to determine the quantity in gallons or barrels of pollutant that have been spilled it will be necessary to determine not only the areal distribution but also the vertical or depth distribution of such pollutant. It must be recognized that measurement of the thickness of the oil slick for instance will not determine the total volumetric extent of the pollution since there may be

layers of sub-surface pollutants that will have different geometric and velocity characteristics than the surface pollution.

3. Rate of Discharge.

This knowledge item refers to the rate at which the pollutant is being introduced into the ocean environment. The measurement can only be performed by inference since there is no physical observable that can be indicative of the rate at which, for instance, a ship in distress is discharging oil. The measurement of rate of discharge can be inferred from consecutive measurements of the quantity and spatial distribution of the pollutant. In this manner, one can plot the volumetric extent versus time and determine by the slope of this curve what the actual rate of discharge is at any particular time.

4. Pollutant Classification, Coarse.

A Coarse Classification can be defined as one that would differentiate between gross categories of pollutants. For instance, it will definitely define whether the pollutant is oil or sewage sludge, or acid waste, etc.

5. Pollutant Classification, Detailed.

Detailed Classification entails the differentiation between the various types of oil and, in the case of waste, the differentiation among the many types of toxic pollutants which are prohibited in accordance of the Clean Water Act. It can be seen that the detailed classification of pollutants is a very difficult task using remote sensing. For this reason early in the study a guideline was given to us by NASA whereby the detailed pollutant classification was not to be a primary goal for space monitoring.

6. Source Location.

A very important knowledge requirement for producing legal evidence is the location of the source of the pollutant, whether it would be a ship or a point source on the shore. Again, what is needed here is the coordinates of the

oil slick or waste dump and in many cases the relationship between that coordinate and the various ships in the vicinity of the particular pollution event.

7. Motion and Dispersion.

The exact meaning of this knowledge is where the pollutant is going and how is it spreading with respect to time. The measurement necessary to determine motion and dispersion is a sequence of areal images with respect to time so that the vector and the distribution of the pollutant can be determined.

8. Predicted Motion, Spreading and Shore Impact.

In contrast with item No. 7 which defines motion and dispersion in real time, the Predicted Motion, Spreading and Shore Impact deals with forecasting based on the characteristics of the pollution and the extent environmental conditions such as wind - stress, and current. The measurements needed for this particular knowledge are inputs to the models that define the oil pollutant trajectory on the surface and within the sub-surface. From these predictions the points and areas upon which the pollutant will impact the shore can be predicted.

9. Optimum Pollution Abatement Measures.

In order to determine the optimum ways in which the pollutant can be either diverted, stoppped or neutralized, it is necessary that several factors be considered: In these factors, in essence is a combination of the above items 1 through 8, which defines where the pollution is, how it is moving, and what its predicted impact would be. In addition, the environmental conditions at the time are important in this determination, since the deployment of equipment & people will be highly influenced by the type of weather conditions existing at the time.

10. Prediction of Probability of Damage to Ecology or Property.

Considering this item, there are two types of predictions that are important. One of these deals with prediction of damage due to an event that has already

occurred, the other deals with the prediction of a probable event on the basis of the statistics of traffic or pollution events for that particular area. In order to make this prediction the motion and dispersion of pollutants as well as it predicted motion spreading and shore impact are important. Statistics must be built concerning the environmental conditions at various times of the year for a particular area when dealing with predictions of future events.

11. Assessment of Damage.

This item of knowledge pertains to the examination of the extent of the pollution in a particularly sensitive area of the shore and determination from the knowledge of the sensitivities, the degree of damage that has been sustained by that particular area. When dealing with an area such as an estuary for instance, the degree of damage is difficult to assess based solely on the image of for instance the oil slick and its impact upon the shore. Other factors are very important here, for instance, the degree of mixing of the pollutant in the water and the amount of pollutant that adheres to the ocean floor.

12. Ecological Information.

The type of information required here deals with the environmental conditions that are pertinent to the sustenance of marine organisms, including fish, and plants. The measurement of chlorophyll content, for instance, is very important in this knowledge objective. Also important is the degree of turbulence and mixing in the ocean.

Measurement Requirements

The measurements necessary to satisfy the knowledge objectives were derived from a dialog with the users. This was an iterative process, wherein the initial specification, based on discussions, analyses and documentation, was reviewed by representatives of the user community and the results of that review were incorporated in the final specification. The requirements of the various agencies are generally represented by those of the USCG, USDI and NOAA, since the requirements of these agencies cover the range, including pollution law enforcement, planning for coastal mineral resource utilization, and protecting the coastal marine environment.

REQUIREMENTS SPECIFICATION

Table 3.3-2 shows the compilation of the requirements of the various users and represents the most stringent specifications for each measurement parameter. The parameters, numbered 1 through 23 belong to three general categories:

a. Oil pollution characteristics, such as areal distribution, classification, etc.

b. Waste pollutant characteristics, such as spatial distribution, concentration, etc.

c. Ocean and atmospheric conditions which determine the motion and dispersion of pollutants; t se relate to winds, ocean currents, waves, air-water interface temperatures, etc.

The "Mission Type" column (Table 3.3-2) refers to the following generic categories of ocean pollution missions:

(a) Surveillance and Monitoring - includes search and detection of pollution, and tracking of the pollutant after detection.

(b) Modeling - includes the measuring of parameters for oil trajectory modeling and building of environmental data bases.

The measurement requirements corresponding to the first four parameters (Table 3.3-2) lists two sets of specifications, one for each of the types of missions in (a) and (b) above. The detailed mission analysis is summarized in section 5.1.

Table 3.3-2. Measurement Requirements - A Compilation of the Most Stringent Specifications by the Users

PARAMETER	MISSION TYPE	RANGE OR SCOPE	PRECISION (±)	ACCURACY (±)	SPATIAL RESOLUTION OR GRID SIZE	FREQUENCY (EVERY X HRS)	DATA DELAY (HRS)
1. OIL SPILL AREAL DISTRIBUTION	SURV. & MONITOR	>10m	5%	5%	10m	12	3
	MODELING	>15m	10%	10%	15m	12	3
2. OIL SPILL COORDINATES	SURV. & MONITOR	US COASTAL AREA	0.5Km	1Km	N/A	12	6
	MODELING	US COASTAL AREA	-	250m	N/A	12	6
3. OIL SPILL THICKNESS	SURV. & MONITOR	0.1μm - 2mm	-	5%	10	12	6
	MODELING	0.1μm - 2mm	-	-	15	12	3
4. OIL CLASSIFICATION	SURV. & MONITOR	MAJOR TYPES	N/A	N/A	-	12	6
	MODELING	GROSS CLASSIFICATION	N/A	N/A	-	12	6
5. POLLUTANT DUMP SPATIAL DISTRIBUTION	SURV. & MONITOR	>30m	-	-	30m	24	1 to 3
6. POLLUTANT DUMP COORDINATES	SURV. & MONITOR	US COASTAL ZONE	200m	200m	N/A	12(FOR ACIDS)	3
7. WASTE POLLUTANT CLASSIFICATION	SURV. & MONITOR	ACID/INDUSTRIAL OR SEWAGE	GENERIC CLASS	GENERIC CLASS	>30m	12(FOR ACIDS)	3
8. WASTE POLLUTANT CONCENTRATION	SURV. & MONITOR	PPM TO MG/L	POLLUTANT DEPENDENT	POLLUTANT DEPENDENT	>30m	12	3
9. POLLUTION SOURCE(E.G. VESSEL) IDENTIFICATION	SURV. & MONITOR	TANKERS, BARGES, RIVER EFFLUENT, NATURAL SOURCE	SUFFICIENT FOR LEGAL EVIDENCE		N/A	12	3
10. WIND SPEED	MODEL	0-50m/sec.	0.5m/sec	2m/sec	10Km	3	3
11. WIND DIRECTION	MODEL	0-360°	5°	10°	10Km	6	3
12. OCEAN CURRENT SPEED	MODEL	0-300cm/sec	5cm	5cm	10Km	6	3
13. OCEAN CURRENT DIRECTION	MODEL	0-360°	10°	10°	10Km	6	3
14. ICE COVER AREAL EXTENT	MODEL	0-100%	-	2%	10m	24	6
15. ICE THICKNESS	MODEL	0-50m	0.2m	0.3m	10m	24	6
16. SIG. WAVE HEIGHT	MODEL	0.3-25m	0.3m	0.3m	10Km	3	3
17. WAVE LENGTH	MODEL	0.3-1000m	10%	10%	10Km	3	3
18. WAVE DIRECTION	MODEL	0-360°	10%	10%	10Km	3	3
19. AIR TEMPERATURE	MODEL	-30°to40°C	1°C	1.5°C	10Km	12	3
20. WATER TEMP. (SURFACE)	MODEL	-2°to30°C	0.25°C	1°C	10Km	24	6
21. WEATHER FRONTS	MODEL	-	-	-	10Km	12	6
22. PRECIPITATION	MODEL	-	-	-	10Km	12	6
23. SUSPENDED SEDIMENT	MODEL				10Km	12	6

Several definitions that may be useful in the interpretation of the measurement requirements in Table 3.3-2 are:

a. "Accuracy" refers to the range of deviations from an absolute reference.

b. "Precision" refers to relative accuracy.

c. "Spatial resolution" is the diameter of the object that can be resolved in the image data.

d. "Frequency" refers to how often the measurement must be performed over the 200 mile coastal zone.

e. "Data Delay" is the permissible delay between data acquisition and availability of the data to the user.

At this point, it may be well to clarify an important aspect of the requirements: the spatial region (volume) within which knowledge concerning the extent and movement of pollutants is needed. From the point of view of areal extent, the region of interest (as stated previously) is the 200-mile "controlled" zone as established by the Fishery Conservation Management Action of 1976. Theoretically the depth of interest is from the surface to the sea floor, principally in the region of the continental shelf. This is due to the fact that sub-surface transport of pollutants, including oil, is significant. (This is illustrated in Appendix C, which shows calculated trajectories and areal extent of surface and sub-surface oil.) From the point of view of remote sensing of pollutants and the "model" parameters, the concern is only with surface phenomena, since that is virtually all that can be monitored. From these surface measurements, however, some of the sub-surface effects are inferred.

An initial review of the measurement requirements highlighted two areas of high potential impact on a space-based monitoring system: spatial resolution and sampling frequency. Specifically, the resolution requirements for determining the areal distribution (extent) of oil spills and waste pollutants require relatively fine resolution, ranging from 10 to 30 meters. Regarding temporal coverage, the frequency of coverage ranges from two to eight times per day. These coverage-related requirements

were found to be sufficiently stringent to require special examination in the light of practical implementation approaches.

Through dialog with the users, it was determined that the coverage requirements were flexible, that is, the effectiveness of the space measurements related to spatial coverage do not decrease abruptly as we depart from the ideal or most stringent requirement (e.g. 10 meter resolution). This requirements flexibility, concurred to by the representatives of the user community, enabled three important analyses in the study:

(a) Establishment of effective (or reasonable) spatial resolution requirements, based on the percentage of significant pollution incidents able to be acquired. (Reference Section 3.4).

(b) Determination of the area coverage that is possible by utilizing the orbits associated with existing or planned spacecraft such as NOSS (instead of idealized orbits for hypothetical dedicated spacecraft). (Reference Section 5.2).

(c) Determination of the optimum role of aircraft sensors and spacecraft sensors is in meeting the coverage requirements. (Reference Section 5.1).

The results of these analyses, from a requirements point-of-view, can be summarized as follows: (1) Spatial resolution goals of 60-100 meters from space were found to be reasonable, considering the high percentage of significant oil spills that will be detected in that range. (2) Coastal coverage of once a day in a large portion of the U.S. coast and twice and three times a day in selected portions of the coast are possible assuming the use of existing or planned spacecraft. This constitutes a great improvement over present capabilities and would be of significant value to the users. (3) A "complementary" approach utilizing the best coverage capabilities of aircraft and spacecraft instrument would be optimum. This approach combines the synoptic coverage of all-weather space-borne sensors with the detailed, higher resolution coverage of airborne sensors over high density traffic shipping lanes and any gaps in spacecraft coverage.

3.4 OIL SPILL TARGET CHARACTERIZATION FOR SPATIAL RESOLUTION REQUIREMENTS

Federal law imposes extremely challenging - but at times qualitatively-defined - objectives on those agencies charged with marine pollution monitoring and enforcing the law. (Reference 10) The general result is that some of the user requirements of Table 3.3-2 are based not on the Federal law directly but on an interpretation of the wording of one or more laws, taking many other factors into account...The shape and size characteristics of illegal oil spills are the case in point of this section. An example of the problem is that the Coast Guard, in procuring remote sensing systems to monitor for illegal marine pollution, must state specifications based on indefinite guidelines prohibiting pollution which causes "any visible sheen" on the water surface.

The following sections are based on research into the types of marine hydrocarbon pollution that are targets for remote sensing systems: investigating the rate of occurrence; cumulative pollutant volume; and causes, mechanisms, and fates characteristic of the different types. The objective of these analyses is to quantify from these basic facts the spatial characteristics of the different types of oil spill targets and weight them according to their priorities as system targets.

3.4.1 Operational Discharges

This type of discharge applies to the type of spill made deliberately (and therefore not reported) by a ship while underway. This would involve the dumping overboard of an oil-water mixture either from tank washing or from bilge pumping. Tank washing includes washing of "empty" oil cargo tanks on tankers traveling in ballast or "empty" bunker fuel tanks on any large ship. It may put on the order of hundreds of gallons of oil per minute into the water. Bilge pumping will contribute a substantially lower rate of oil pollution -- ranging from on the order of a gallon per minute for engine oil leakage into the bilges on small boats up to tens of gallons per minute for large ships - particularly with leakage from large pumping systems.

Figure 3.4-1 is a good example of a tank washing discharge photographed by an aircraft system developed for oil spill surveillance by the Swedish Coast Guard (Ref. 10). A few points are made for future use on this type of spill.

- It is long and narrow -- and hence can be called a linear feature for pattern recognition purposes.
- Its length grows primarily according to the ship velocity (with some secondary perturbation due to surface and near surface currents and surface winds aligned with the ship motion).
- Its width has stabilized (on the order of 1 to 3 times the ship's width) shortly after discharge, and appears to grow more slowly thereafter.

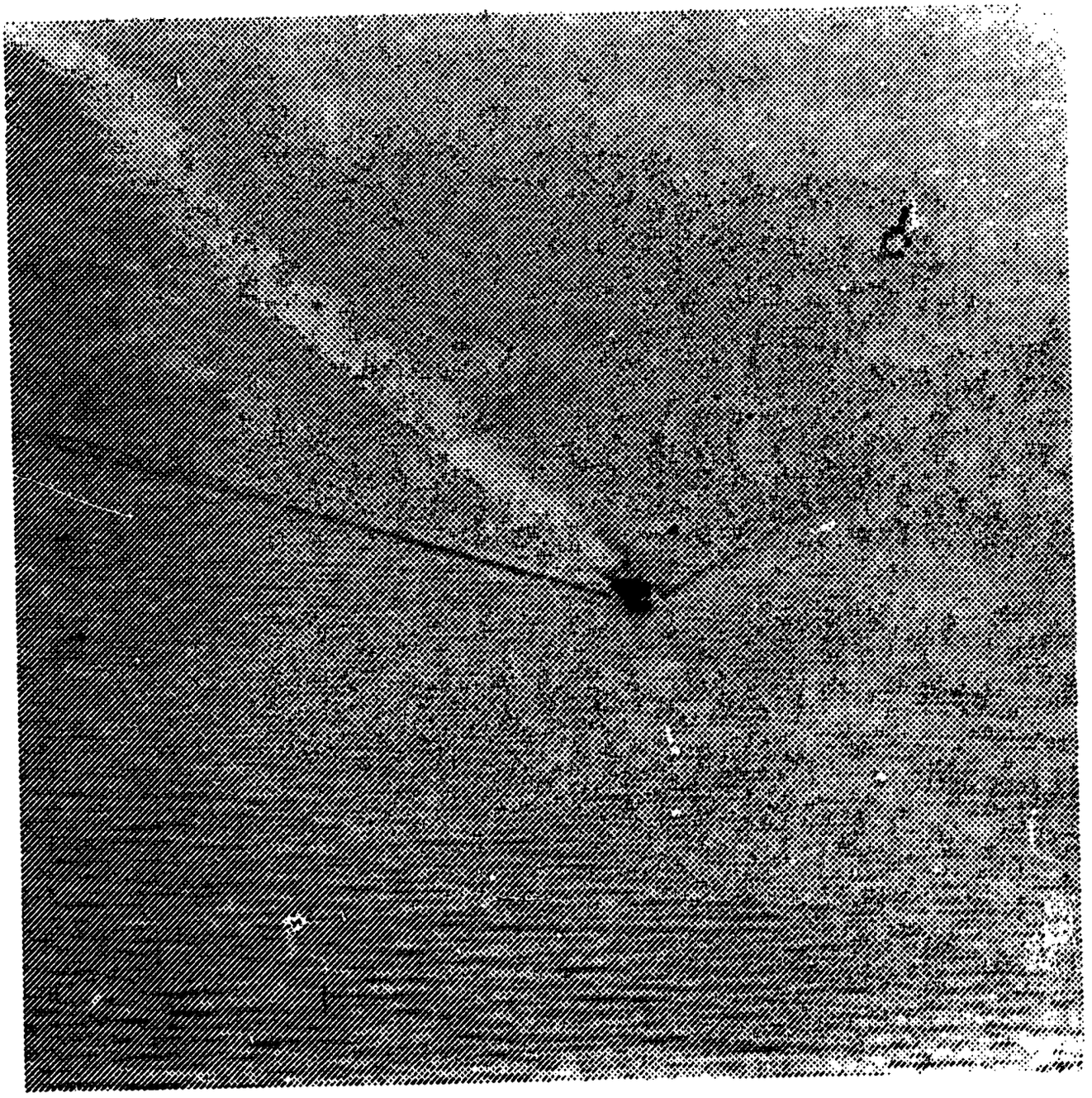

FIGURE 3.4-1: A vessel illegally cleaning its tanks in the Baltic Sea (photo taken with the hand-held camera) (Extracted from Ref. 1)

- The continuity (unbrokenness) of the slick depends on several factors, including discharge rate, ship speed, sea state, and type of oil.

- As discussed later, the major part (thin portion) of a spill area spreads as a power of time since spill (exponent of 0.6 from NRL tests). (Ref. 2)

The following table shows some typical parameters on different ships whose discharges are of interest (Ref. 5):

Type of Ship	Width (m)	Speed (kts)
VLCC (Very Large Crude Carrier)	> 50	15-25
Tugboat	10	10-15
Pleasure Craft	< 10	10-15

The analyses which follow are intended to bracket oil spill detection system targets for operational discharges, from the largest (VLCC tank washing) to the smallest (pleasure craft bilge pumping).

3.4.1.1. VLCC Tank Washing. Oil supertankers carry tens of millions of gallons of oil and references (18, 25) indicate that the oil portion of tank washing "slops" can amount to 0.4% of this volume (40,000 gallons or more). The following assumes this is pumped overboard at a rate of 100 gallons per minute. Figure 3.5-2 illustrates the assumed spill growth geometry wherein initial area growth is linear (proportional to time) until thickness of 0.01 mm (10 micrometers) is reached. After time t_1 the area grows proportional to the 0.6 power of time (the "spreading index" from Ref. 7 pp. 63-64). Thus, if we assume a VLCC speed of 25 knots, the target length grows at:

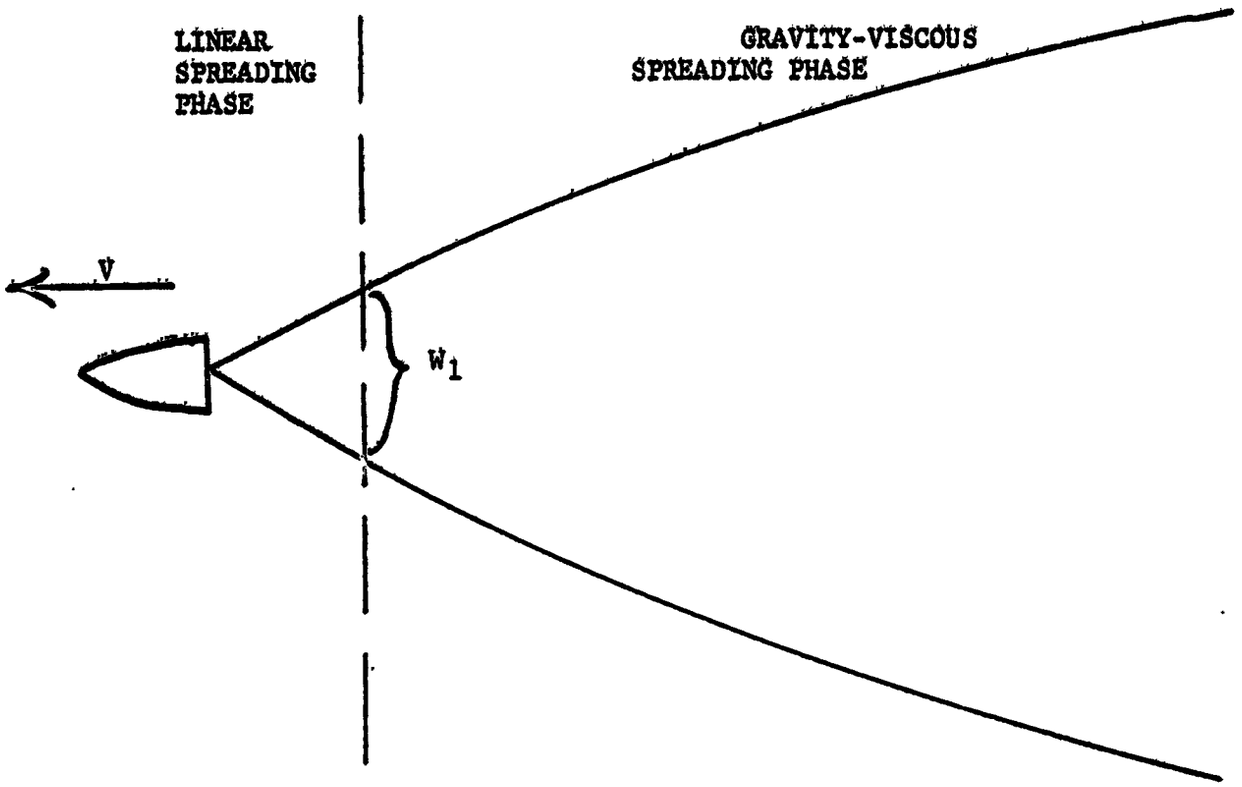

TIME	0	t_1	$t > t_1$
WIDTH	0	W_1	$W = W_1\left(\frac{t}{t_1}\right)^{0.6}$
LENGTH	0	$L_1 = Vt_1$	$L = Vt$
AREA	0	$A_1 = \frac{L_1 \times W_1}{2}$	$A = \frac{L_1 \times W_1}{2} + \int_{t_1}^{t} W_1\left(\frac{t}{t_1}\right)^{0.6} (Vdt)$

Figure 3.4-2. Tank Washing Spill Growth Geometry

$$\frac{25 \text{ nmi}}{\text{hour}} = \frac{46300 \text{ m}}{\text{hour}} = 772 \text{ m/min}$$

Since the spill area is related to the average thickness by:

$$\text{Area (in m}^2\text{)} = \frac{\text{Volume (in gal)} \times 3.78}{\text{Thickness (in mm)}},$$

at t_1, the time taken to spread linearly to a thickness of 0.01 mm,

$$A_1 = \frac{L_1 \times W_1}{2} = \frac{772\, W_1}{2} = \frac{100 \times 3.78}{0.01}$$

$$\therefore \quad W_1 = 98 \text{ m}$$

That yields a width about twice the tanker width at which gravity-viscous spreading at a rate proportional to the 0.6 power of time takes over. Since the spill length is bounded by continued discharging, the width will grow after t_1 as time to the 0.6 power:

W (meters)	Time (min)
98	t_1
149	$2t_1$
498	$15t_1$
1143	$60t_1$

Assuming t_1 is 1 minute, this target would be 772 m long by 0-98 m wide after only 1 minute, and over 10 km long by as much as 500 m wide (varies according to distance behind ship) after 15 minutes. The areal extent at 15 minutes can be calculated as:

$$A = \frac{L_1 \times W_1}{2} + \int_{t_1}^{t} \left(W_1 \left(\frac{t}{t_1}\right)^{0.6}\right) V dt.$$

$$= \frac{L_1 W_1}{2} + \frac{V W_1}{t_1} \left[\frac{t^{1.6}}{1.6}\right]_{t_1}^{t}$$

$$= \frac{L_1 W_1}{2} + \frac{V W_1}{1.6\, t_1} (t^{1.6} - t_1^{1.6})$$

$$= 37,800 + \frac{75,600}{1.6} (15^{1.6} - 1^{1.6}) = 3,589,268 \text{ m}^2$$

For 1500 gallons spilled, that indicates an average thickness of a couple micrometers (.0016 mm) which should be examined for validity. The work of Hollinger (Ref. 7) and Troy and Hollinger (Ref. 5) at NRL has led to the following points related to spill thickness, area, and spread rate:

(1) Most of an oil spill (90% or more) is concentrated in "thick" patches (on the order of one mm) in less than 10% of the spill area; the remainder is very much thinner (on the order of 1 micrometer).

(2) Based on numerous tests, the spill spreads with time at a rate proportional to wind speed (see Figure 3.4-3 from Ref. 7, p. 123). The steepness of each spill's growth curve is the spreading index used above and ranges from about 0.6 for calm days to 2.0 or more on very windy days. An index of 1.0 fits the 10-15 knot wind range and equates to area growth directly proportional to elapsed time: at 2 minutes, area twice as big as at 1 minute, etc.

Relative to the first point, the average thickness of a 90% thick/10% thin spill is 10 micrometers (0.01 mm) which is in line with the NRL test results.

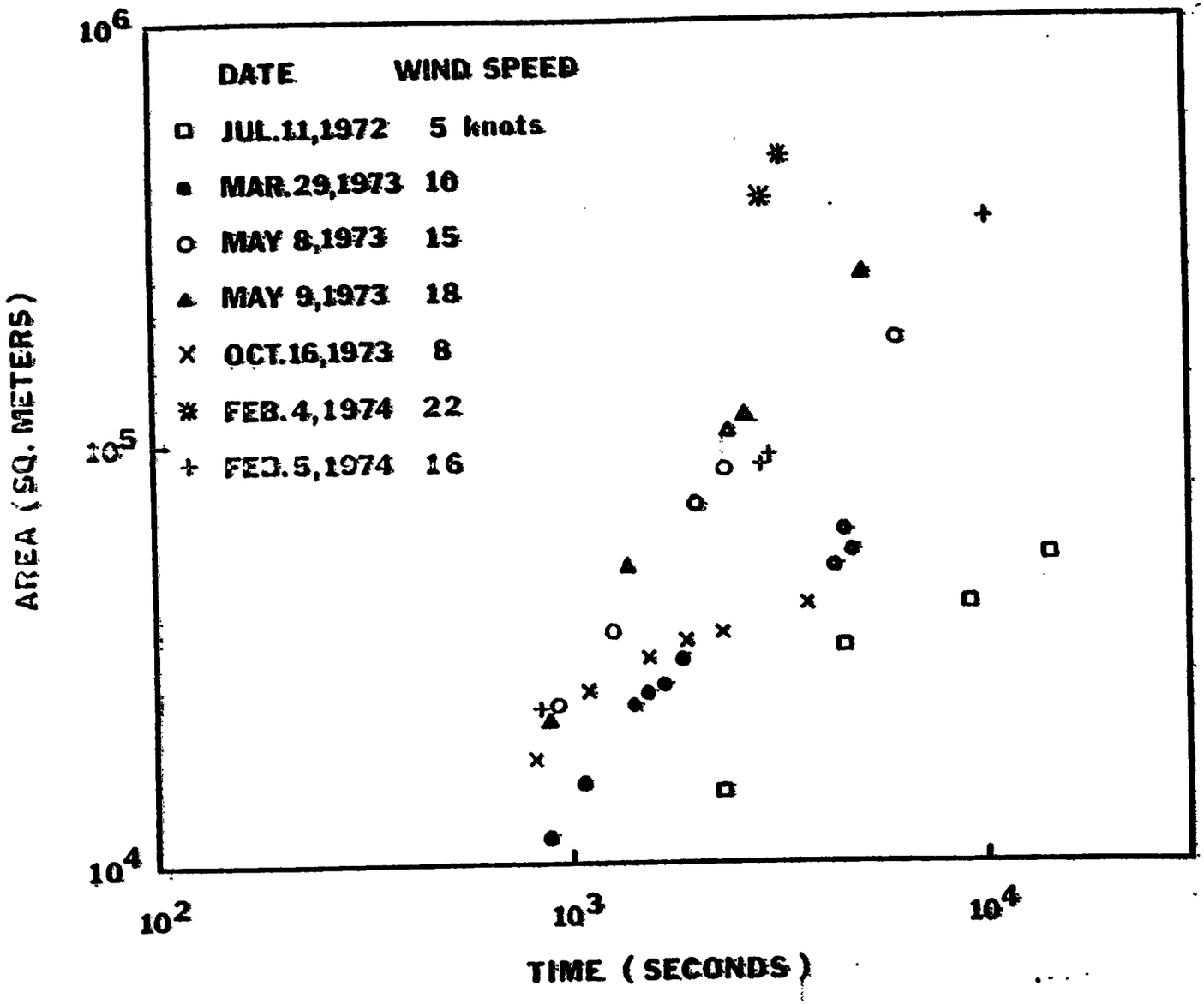

Figure 3.4-3. Spreading of Point Spills (Oil)
(Extracted from Reference 7)

Note: Volume of each spill was in the 500-630 gallon range.

We use this as the average spill thickness when gravity-viscous spreading begins, since a discharge of an oil-water mixture while underway (our target) is much less likely to produce "thick" regions ($\sim$ 1 mm) than the point spills of the NRL tests (full strength oil poured in the water while standing still). Also, we assume the thickness of operational discharges shortly after time t_1 is better represented by the "thin" regions ($\sim$ 1 micrometer) of the NRL tests.

Therefore, the above estimate of $\sim$ two micrometers average thickness after 15 minutes is credible for the assumed spill rate. The relationship of thickness and width to time from start of spill is shown in Figure 3.4-4 for three values of t_1. Several points can be noted from that figure:

- A slower ship or increased spill rate will result in greater target width.
- Shorter or longer linear spread times affect the timing of spill growth more than the spill geometry; slower initial spreading (longer t_1) results in slower spreading throughout the spill lifetime.
- Shorter t_1 results in more rapid spill thinning; for t_1 = 30 seconds, thickness is down to 1 micrometer only about 10 minutes behind the ship. This equates to shorter lifetimes for an unbroken sheen or slick.

For rougher seas, significant crosswinds, or a stiff headwind, the "neat, continuous" long and narrow spill would be broken up in proportion to its distance (and/or time) behind the ship.

Benchmarks such as Figure 3.4-1 indicate that t_1 of one minute is a useful estimate. Within the range of the parametric variations shown in Figure 3.4-4,

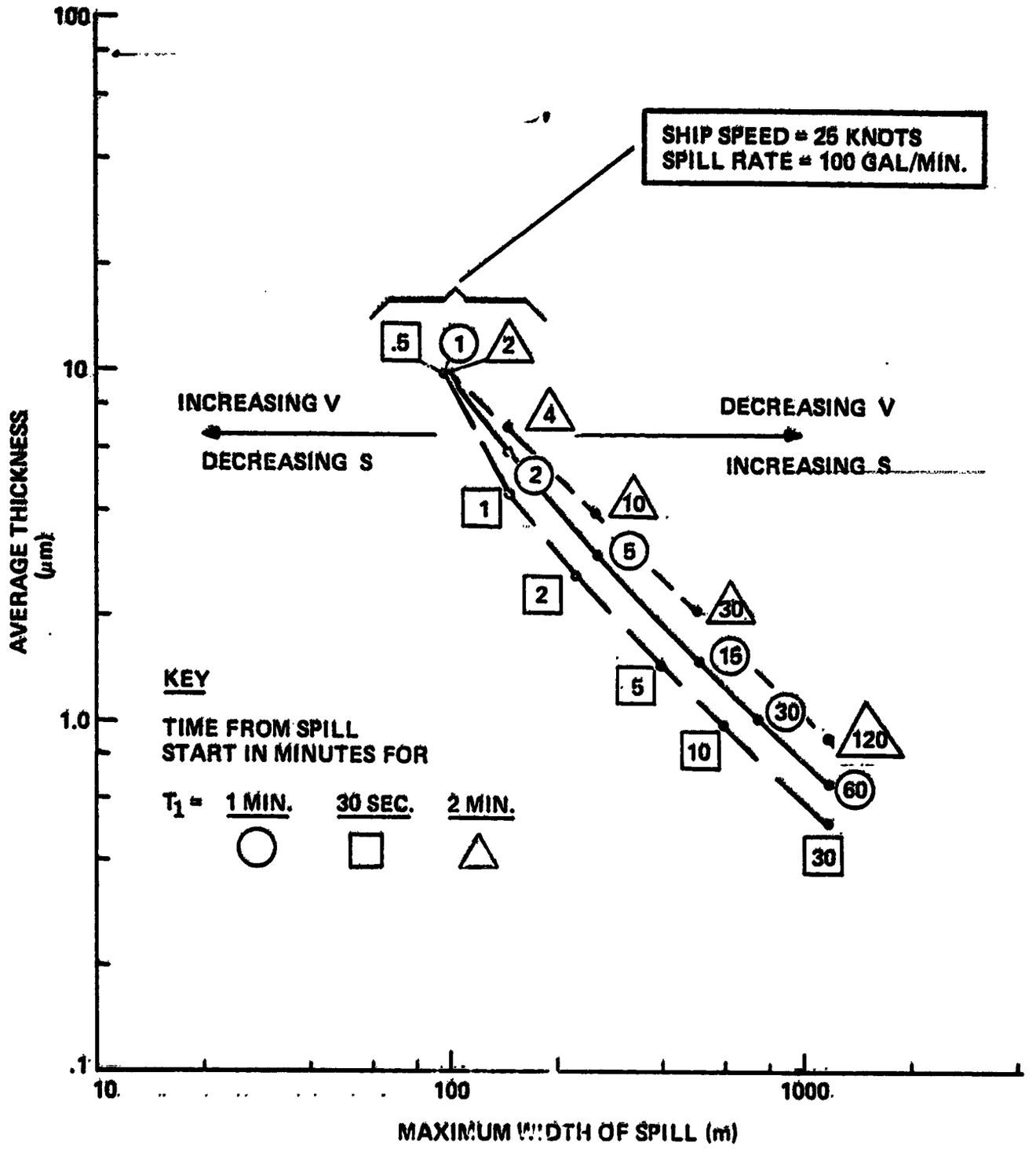

Figure 3.4-4. VLCC Tank Washing Spill Characteristics

it is therefore concluded that (1) the smallest dimension of a VLCC tank washing spill target will not be less than 100 meters (attained within about a minute); (2) this dimension will grow as discussed above to 500 or more meters within about 15 minutes; and (3) the overall target will be a long narrow linear feature.

3.4.1.2. Bilge Pumping. As discussed above, bilge pumping is another routine operational procedure which adds oil to the ocean from ships of all kinds and sizes. As reference 31 states: "Oil leakage is constant inside any ship's machinery and bunkering spaces. Lubricating and hydraulic oils drip from worn gaskets and areas of heavy lubrication. Fuel oil can leak from valves and connections of the lines that bring it from the bunkers to the machinery. All of this accumulates in the bilges with whatever water has leaked into the ship and the lot has to be pumped out from time to time." It is not hard to envision tens or even hundreds of gallons of leakage getting into the bilges -- depending on ship size, state of repair, length of cruise, number of pumps, and other factors. Pumping this overboard rapidly (to avoid detection) could at times put 10 gallons of oil per minute into the water for tens of minutes. Using a 10 gallon per minute spill rate and the same assumptions as in Part 1, the oil slick would grow as described here and illustrated in Figure 3.4-2 above:

LENGTH: V (Ship Speed) = 25 Knots = 772 m/min

WIDTH: Assuming a linear spread up to t_1 as above,

$$\text{Area} = V \times t_1 \times \frac{W_1}{2} = \frac{10 \times 3.78 \times t_1}{0.01}$$

$$\therefore \quad W_1 = 10 \text{ m}$$

The projected width at t_1 is inversely proportional to the average thickness assumed. If it were a micrometer (10 times thinner), the width would be 100 m, but that would probably result in too thin a slick to last as an unbroken viewable target. Therefore, 10 meters will be used as W_1.

As in Part 1, beginning at t_1, the 0.6 power of time spreading rate dominates and the length is bounded compared to the width. Therefore, the width and thickness over time will be:

Time (min)	W (m)	Approximate Thickness (mm)
1	10	0.01
2	15	0.006
5	26	0.003
15	50	0.002
30	75	0.001
60	114	0.0007

By the time the width gets into the 100 meter range, the thickness is dropping below 1 micrometer. Figure 3.4-5 shows the width-thickness-time relationships for the case just described as well as for slower ship speed, greater spill rate, and different t_1. The resulting curves support the following conclusions on bilge pumping spill targets:

- For speeds characteristic of large ships (25 knots), spill rates of 50 gal/min are needed to attain spill widths in the 100 meter range.
- For speeds characteristic of pleasure boats (15 knots), spill rates (~50 gal/min) yielding widths in the 100 meter range are probably too large to be typical.
- In summary, these targets will range from 10 to 100 meters wide for small ships and newer (less leakage) and/or faster large

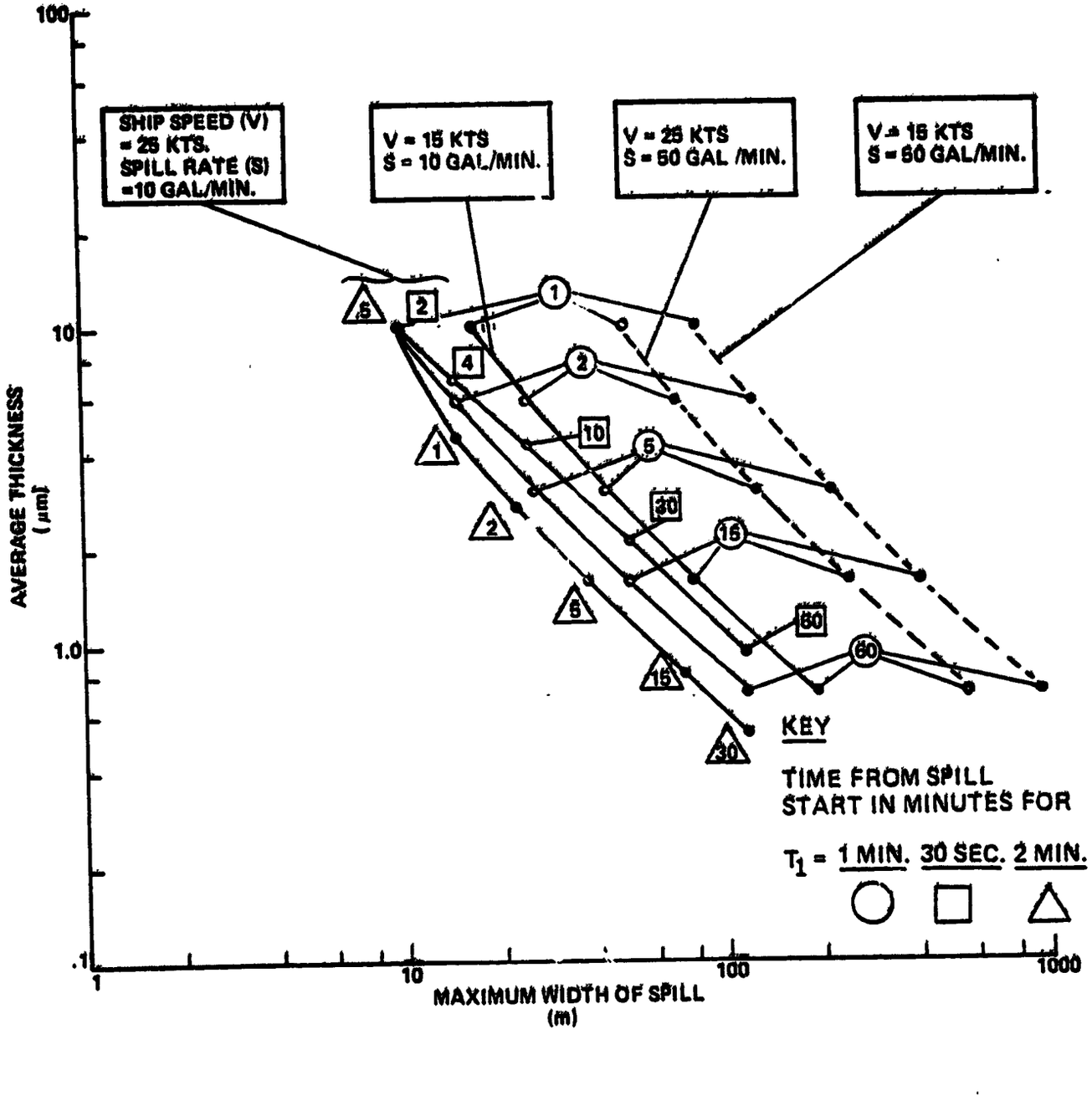

Figure 3.4-5. Bilge Pumping Spill Characteristics

ships, up to 50 to hundreds of meters wide for large ships, especially if they are older and/or have many pumps (more leakage).

3.4.2 Accidental Discharges

In contrast to operational discharges, spills are "easier" targets primarily because:

(1) They are much more likely to be reported, which greatly simplifies the target detection and location process.

(2) Usually the spill rates are higher and/or the ship speeds low or zero (collisions, groundings, leakage while docked, etc.).

Our analyses will treat these spills as point spills of two shapes:

- circular, growing radially
- elongated, where the length grows as width to the 1.2 power (to account for currents and winds).

Accidental spills while underway from inadvertent leakage are relatively too small in volume to be considered here, but are analogous to bilge pumping spills of very low rates (~1 gallon/minute).

The size of an accidental spill target is related to the amount spilled and average thickness by:

$$\text{Area}\,(m^2) = \frac{\text{Volume (gal)} \times 3.78}{\text{Thickness (mm)}}$$

The smallest dimension for the two geometries considered is:

CIRCULAR: diameter $= \sqrt{\frac{4A}{\pi}}$

ELONGATED: average width $= A^{\frac{1}{2.2}}$

(from $A = LW$; $L = W^{1.2}$)

The relationships among these key parameters are illustrated in Figure 3.4-6.

Typical spill statistics must be considered in using these parametric curves. The NRL work (references 5 and 7) shows point spills in the 500-gallon range reaching average thicknesses around 0.1 mm within 15-30 minutes (see Figure 3.4-3) and thinning out to the 0.01 mm range within 1-2 hours. Their conclusions support 0.01 mm as a typical average thickness for point spill with thick (millimeter range) and thin (micrometer range) areas. Area and volume statistics from other sources (e.g., reference 10) also fit this 0.01 mm average thickness range.

Therefore, the following inferences can be drawn from Figure 3.4-6 as to accidental spill targets:

- Spills of 200 gallons (circular geometry) or 500 gallons (elongated geometry) will attain a minimum dimension of 100 m within about 15-30 minutes.

- Given an hour or two to spread, most spills will have a minimum dimension of 100 m or more. Exceptions may be:
  - small spills (< 70 gal)
  - thick spills (> .01 mm average thickness)
  - unusually elongated geometry
  - combination of the above.

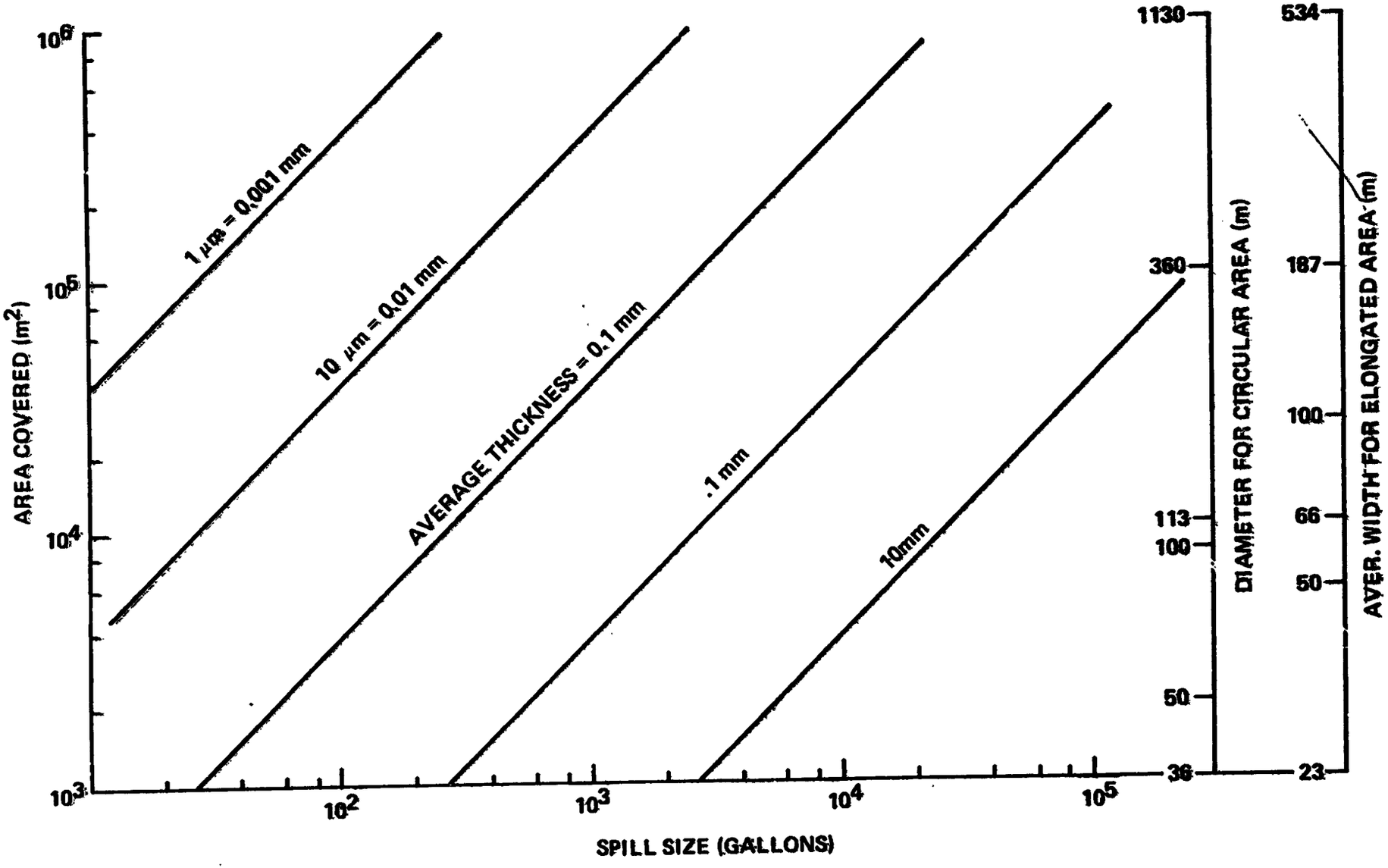

Figure 3.4-6. Spill Volume, Thickness, and Geometry Relationships

3.4.3 Summary of Target Spatial Characteristics

The results of these analyses are illustrated in Figures 3.4-7 and 3.4-8 for the highest probability types of spills. Note that most significant accidental discharges of oil reach a width of 100 meters or more in less than two hours from the spill incident. Moreover, operational tank washing and a large percentage of bilge pumping situations also provide spill targets of width 100 meters or more. The implication of these results is that a relaxation of the 10 to 15 meter resolution requirements for oil spill mapping may be appropriate; this possibility is explored in more detail in the System Options portion of this report.

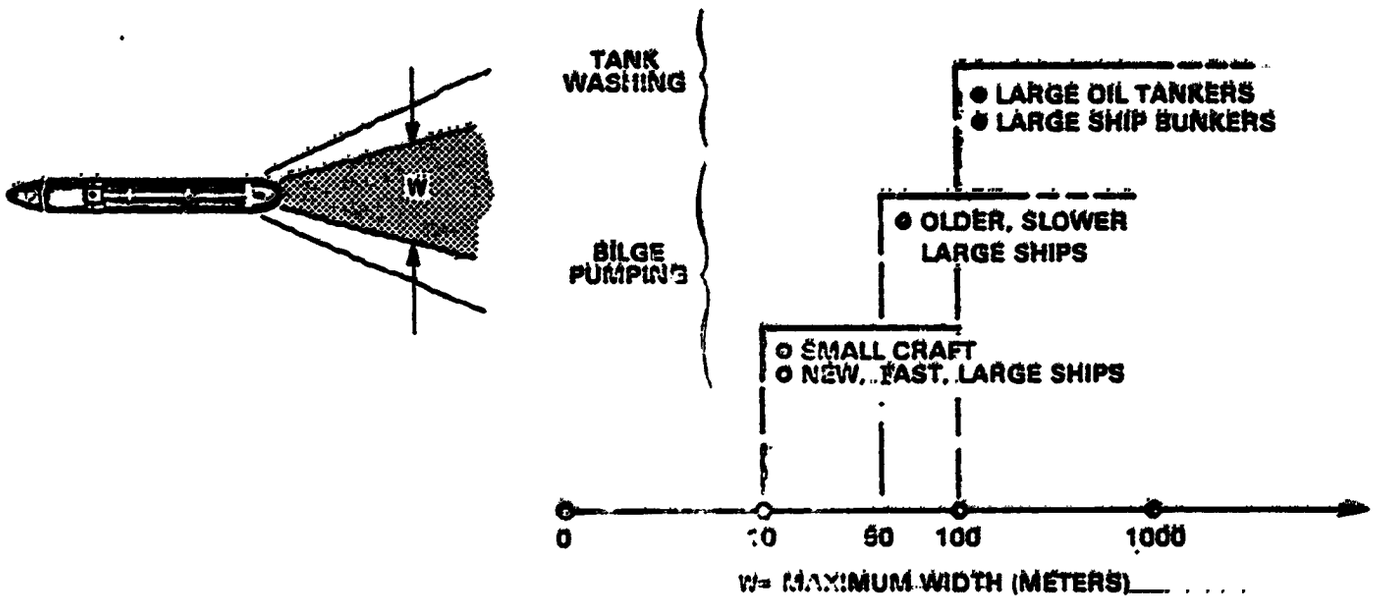

Figure 3.4-7. Spatial Characteristics of Accidental Oil Spills

Figure 8 similarly illustrates the minimum dimension attained within an hour or two of various size accidental spills.

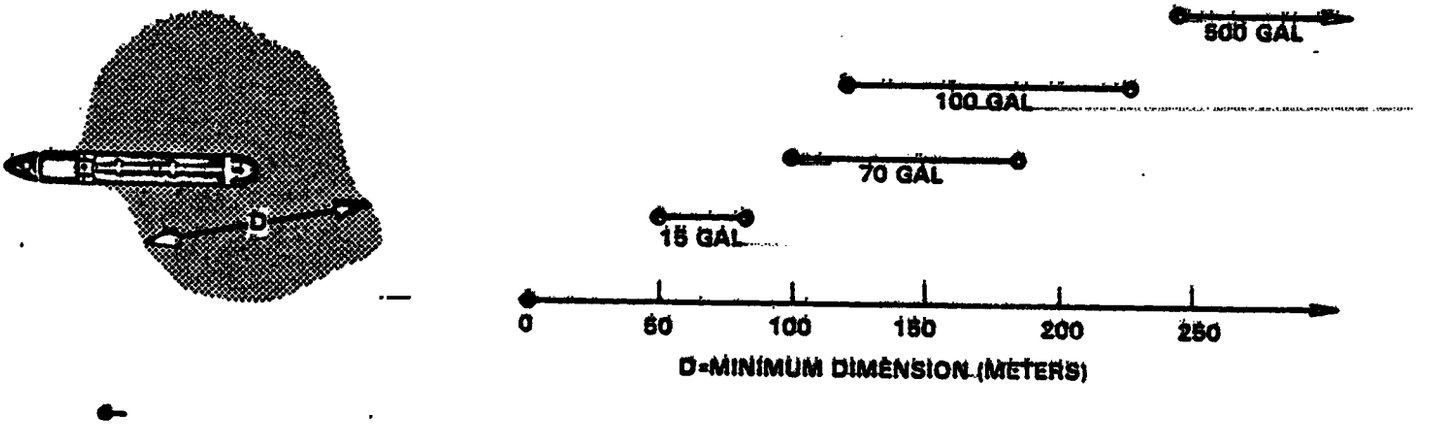

- TYPICALLY CIRCULAR OR ELONGATED FEATURES
- DIMENSIONS AFTER AN HOUR

Figure 3.4-8. Spatial Characteristics of Intentional Oil Spills (Operational Discharges)

SECTION 4
ASSESSMENT OF CANDIDATE SYSTEM ELEMENTS

- SENSORS AND SENSOR TECHNIQUES
- PLATFORMS
- SUPPORT SYSTEMS
- DATA SYSTEM FOR OCEAN POLLUTION MISSIONS

SECTION 4

ASSESSMENT OF CANDIDATE SYSTEM ELEMENTS

The assessment of the applicability of space technology to the Ocean Pollution Mission was performed relative to current and future system elements such as sensors, platforms and support systems. This focus on system elements rather than the underlying theory of detection was chosen to permit a realistic evaluation of present and projected capabilities, performed within the context of evolving earth observation system capabilities.

This section deals with that assessment, primarily with respect to sensors and sensing techniques, then with respect to the platforms and support systems that will permit the operation of these sensors.

4.1 SENSORS AND SENSING TECHNIQUES

This section deals with the analysis that leads from measurement requirements to the determination of which sensors and sensor characteristics are best suited to the performance of the measurements. As a prelude to the detailed assessment of sensors, a brief summary is presented of the state of the art in measurement technology relative to each of the measurements required by the users. This generalized discussion, found in Section 4.1.1 serves as a framework for the sensor analysis, which considers specific sensors and assesses their suitability and characteristics in the light of parallel considerations of missions and operational constraints.

4.1.1 MEASUREMENT TECHNOLOGY ASSESSMENT

The state of technology relative to the measurement requirements was assessed on the basis of discussions with remote sensing experts during the study research reviews, personal interviews with key technologists, and literature

research. The technology aspects of the requirements items specified in Section 3.4.1 are discussed in the paragraphs that follow.

Oil Spill Areal Extent

Optical techniques are being developed for detecting and mapping the extent of oil spills; these employ radiance contrast in the visible spectrum and emission in the thermal channels. Tests have shown that the reflectance of petroleum oils is different than that of water, the diffuse reflectivity for an oil slick being lower and specular reflectivity higher than the surrounding water. In the thermal infrared region corresponding with the atmospheric window (8 to 14 micrometer) the emittance of these oils is higher than water.

Synoptic mapping of oil slicks using optical techniques has shown its potential in two mission areas: (1) monitoring the progress of large spills, and (2) corroboration or filling in of gaps relative to all-weather microwave data. Recent imagery of the Bay of Campeche (IXTOC) oil spill, using Landsat, TIROS and Coastal Zone Color Scanner (CZCS) imagery has demonstrated that the potential utility of this monitoring technique is in providing a synoptic map of the entire oil spill area. For an example of CZCS imagery, see Figure 4.1-1. In mission applications requiring repeatable, frequent, wide-area coverage, the main disadvantage of optical techniques is the limitation due to cloud cover. In addition, the satellite data of oil spills obtained to date seems to be highly sensitive to sun-angle. Since adequate reflectivity contrast seems to be limited to the sun glint area of the image frame, the coverage swath-width from a satellite is correspondingly constrained. Figure 4.1-2 illustrates this dependence on sun angle relationship; the figure shows three TIROS images in the visible spectrum, during three consecutive days at various sun angles. The only image showing the IXTOC oil spill clearly is the one where the sun glint

Figure 4.1-1. CZCS Imagery of IXTOC Oil Spill in Gulf of Mexico

WAL 1 156:20:57:40 3320 1 N HRPT VIS IN 5 JUNE 79

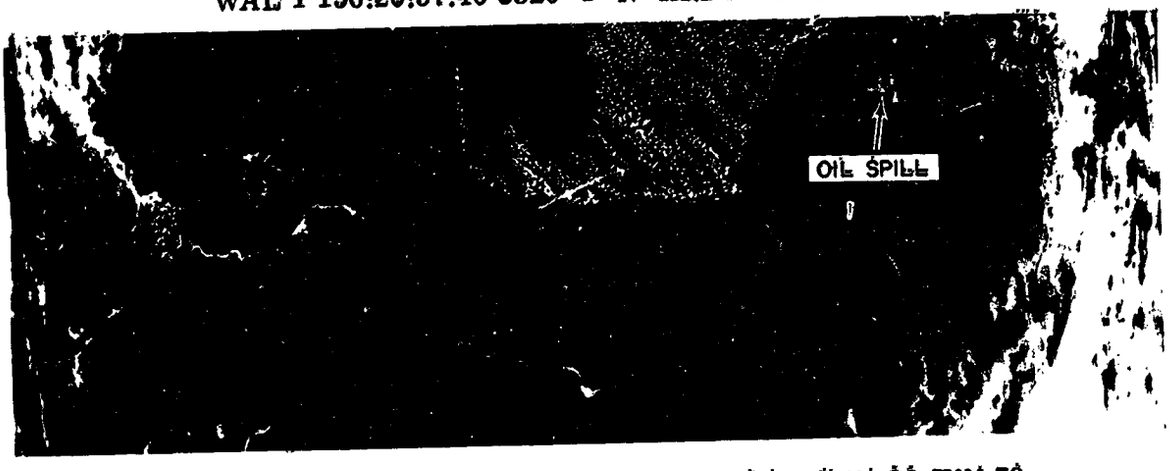

WAL 1 157:20:46:00 3334 1 N HRPT VIS IN 06 JUN 79

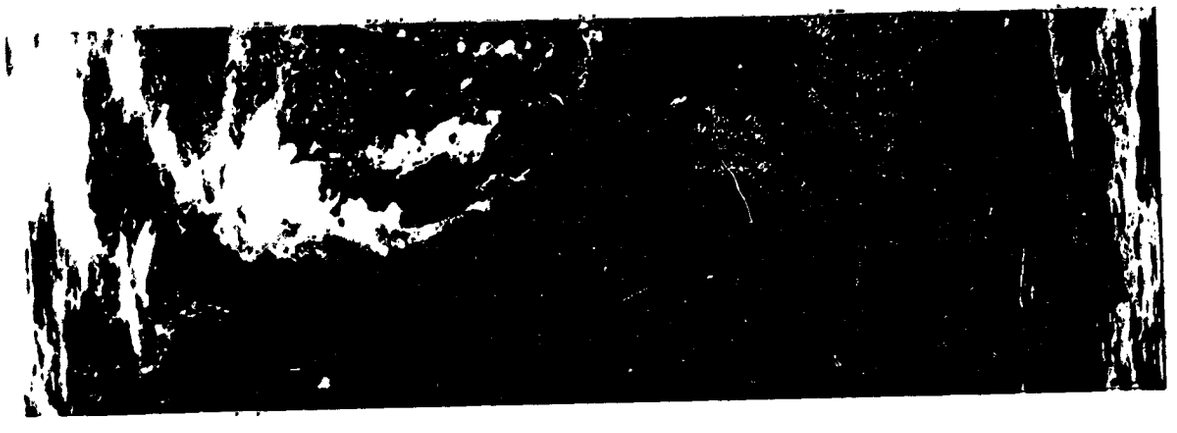

WAL 1 158:20:35:42 3348 1 N HRPT VIS IN 07 JUN 79

Figure 4.1-2. Sequence of TIROS Imagery Showing Effect of Sun Angle on Oil Spill Image
(Central Figure Shows Oil Spill When Sun Glint Is Directly Overhead)

is centered near the area of the spill.

In the microwave portion of the spectrum, the primary phenomenon that is exploited in the delineation of oil spills is the suppression of wind-driven capillary waves due to the presence of the oil film on the water. Images of oil slicks have been obtained using airborne, real aperture radars by the U.S. Coast Guard (AOSS Oil Surveillance Detection Radar) and the Swedish Coast Guard. Experimental tests, using controlled oil spills, have been conducted by the NASA and ERIM. Figure 4.1-3 is an example of the airborne imagery obtained through the use of an X-band experimental synthetic aperture radar.

Quantitative data has been obtained by the Canadian Centre for Remote Sensing[142], on the available signal contrast using microwave techniques to monitor an oil spill. Specifically, the tests showed that the suppression of the ocean backscatter cross section ranges from 7 dB to 12 dB for incidence angles (referenced at nadir) of 30° to 55°, and becomes negligible at incidence angles below 10°. Figure 4.1-4, obtained from the aforementioned CCRS/NASA tests, illustrates the effect of incidence angle on the backscatter suppression.

Still unresolved is the problem that other ocean dynamic features such as wind spills cause a similar suppression of the capillaries and thus create ambiguities in discriminating true oil spills from other ocean surface phenomena. Examples of these ambiguities have been observed in Seasat-SAR imagery over the Santa Barbara channel, where natural oil seepage forms oil slicks of resolvable dimensions. Figure 4.1-5, a mosaic of SAR imagery obtained by Seasat over the coastal region near Santa Barbara, shows a great abundance of ocean features. These ambiguities can also be observed in SAR imagery from aircraft, particularly when a high ratio of the area of the surrounding water to the oil slick is present. It is our assessment that research testing relative to this phenomenon could

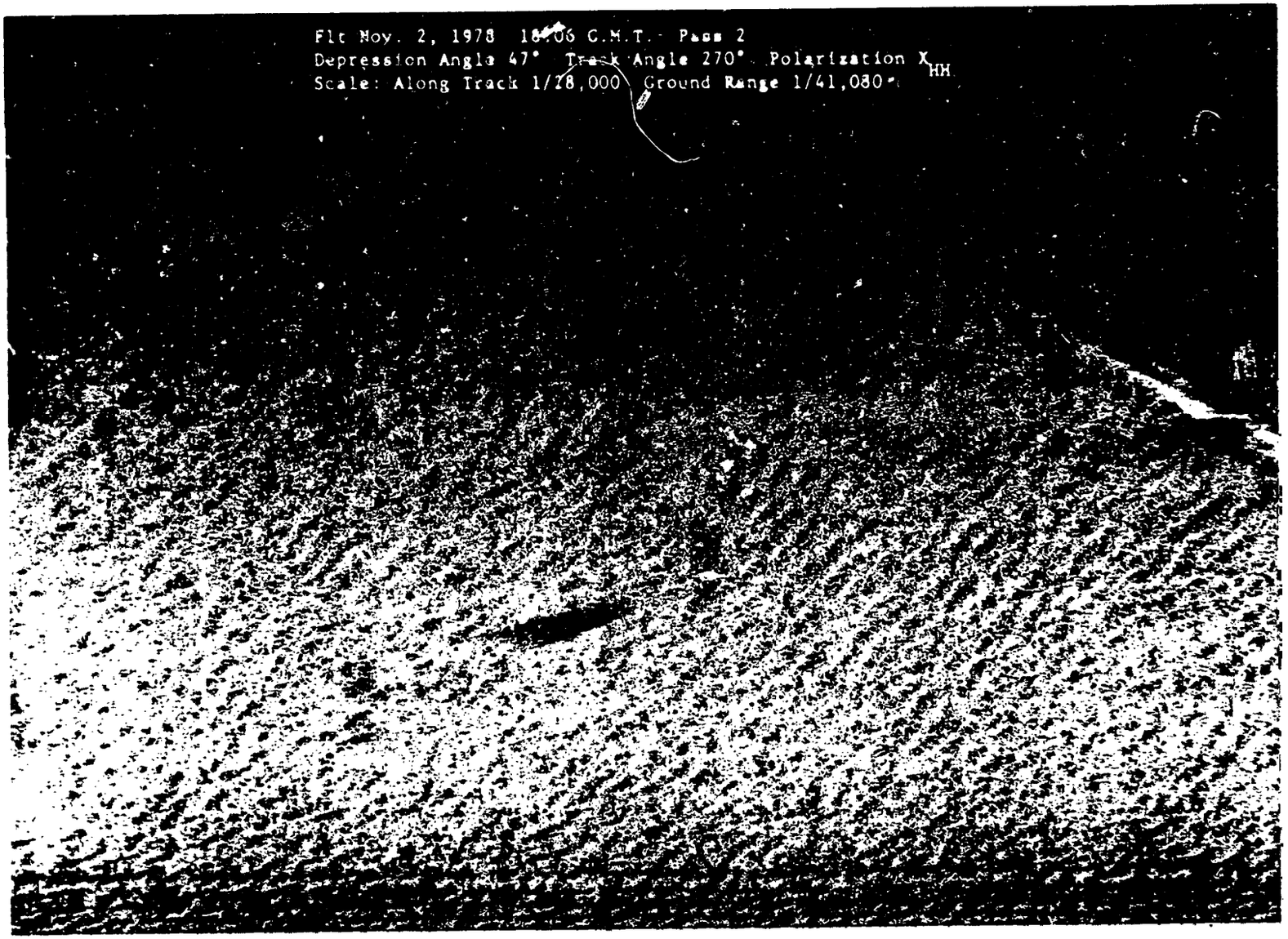

Figure 4.1-3. Example of Image of Oil Spill Using ERIM Airborne SAR

13.3 GHz SCATTEROMETER
WALLOPS ISLAND, NOVEMBER 2, 1978
FLIGHT LINE N°3
[illegible] POLARIZATION

(Source: CCRS Report "Observation of Two Oil Spills With A Microwave Scatterometer and a SAR")

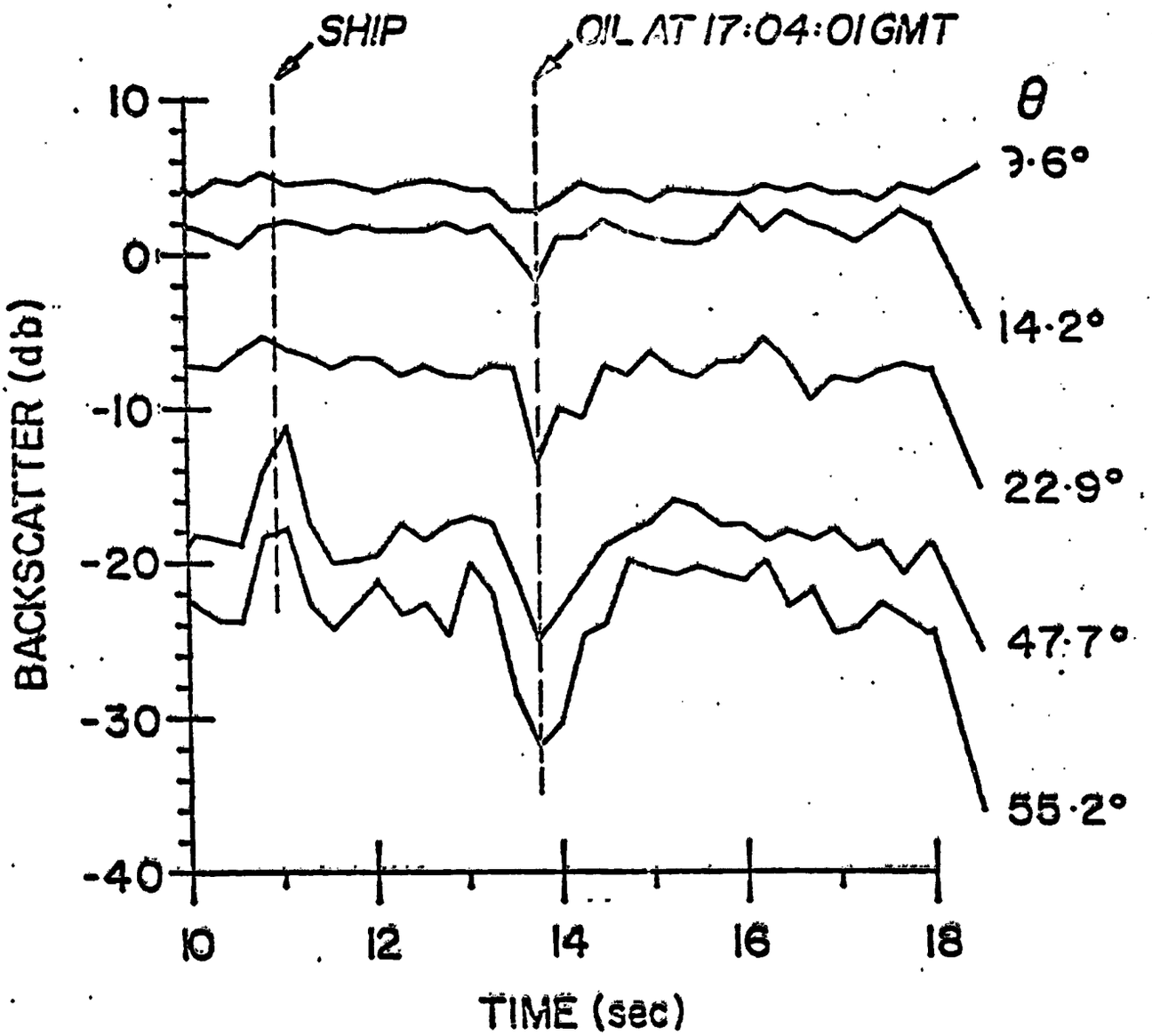

Figure 4.1-4. Backscatter Suppression Due To Oil Spill, Measured Various Incidence Angles.

Figure 4.1-5. SEASAT-SAR Imaging in Coastal Repair Near Santa Barbara.

determine whether: (a) differences in the signal level, dynamic characteristics, or geometric pattern between oil spills and oil slicks can permit adequate discrimination; or (b) the characteristics and random occurrence of these surface phenomena are such that an adequate frequency of false alarms is not feasible.

Important elements of that research are: (1) gaining better understanding of the ocean dynamic features; and (2) performance of tests using controlled spills or taking advantage of known spills under various wind and sea state conditions. Testing is required both from aircraft and space platforms, to determine the effect of altitude/synopticity on the detectivity of oil slicks.

Oil Film Thickness

Two techniques for measuring oil thickness, passive microwave radiometer and laser fluorescence, are complementary since the former is useful in thick oil films (above approximately 0.1 mm) and the latter is useful in thin films.

Using passive microwave radiometry, the region of the oil slick exhibits a higher brightness temperature than the surrounding water; this increase is dependent on oil thickness. NRL has developed a multi-frequency technique to eliminate ambiguities in the brightness versus thickness function. (References 6 and 7)

The brightness temperature due to an oil slick varies with oil film thickness. Since the dielectric constant of oil lies between that of air and water, the oil film behaves as a matching layer between the intermediate air column and the sea. This accounts for the alternating, oscillatory relationship observed in brightness temperature as oil thickness is increased. Emission amplitude is a maximum when the film thickness equals odd multiples of a quarter wavelength of the emitted signal. The oil thickness at which the first maximum occurs and the separation between maxima vary with frequency, as depicted in Figure 4.1-6,

thus making possible the unambiguous determination of oil thickness. NRL has determined that three frequencies are sufficient to measure the thickness range from approximately 0.1 to 3.0 millimeters.

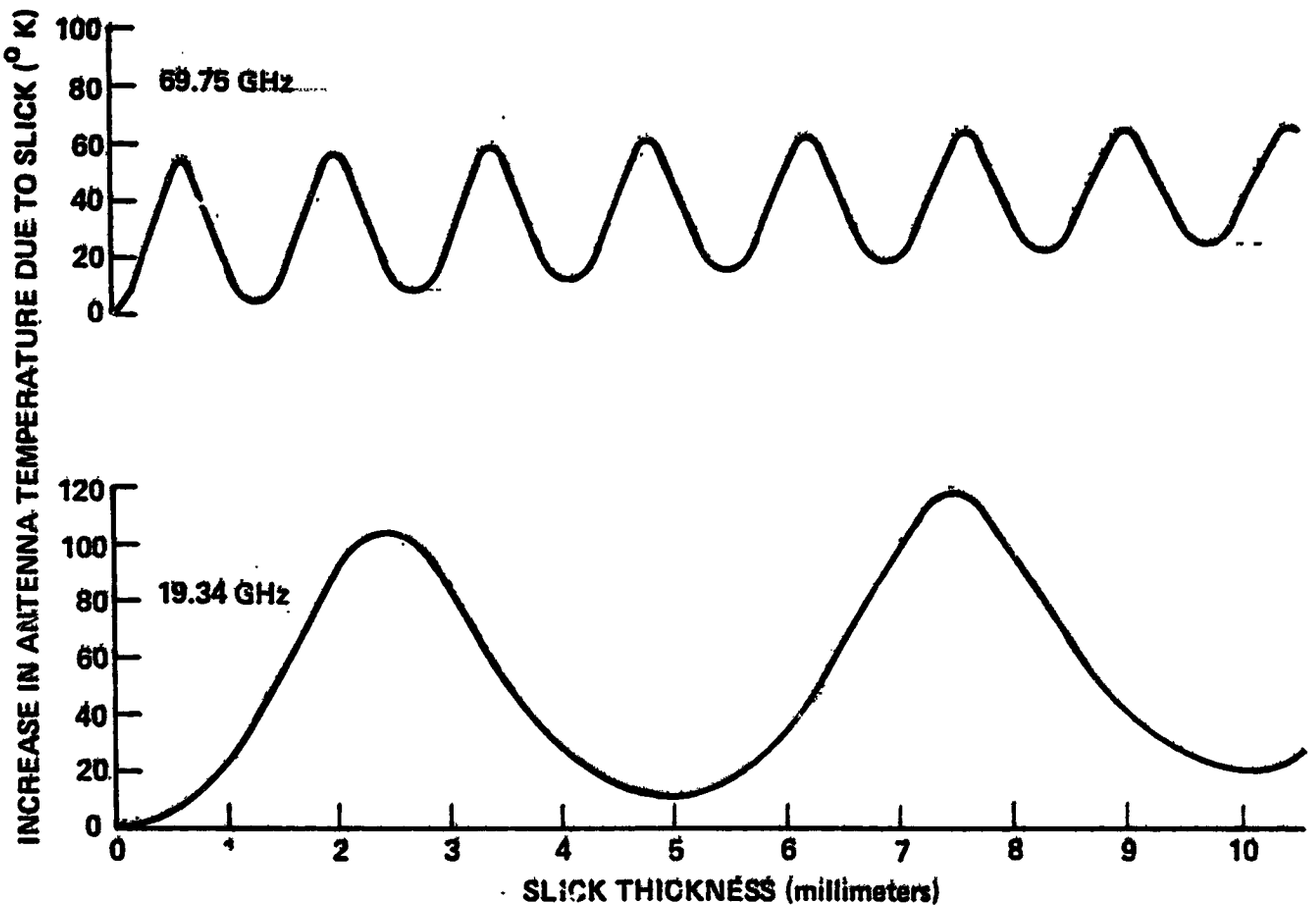

Figure 4.1-6. Oscillatory Relationship Between Microwave Brightness Temperature and Oil Thickness - (Data from J. Hollinger, Ref. 7)

The state of the art in passive microwave radiometers - at least for the next decade - will not permit the types of resolution required for this measurement, due to the multi-hundred meter antennas required to attain 15 or over 30 meter resolution. The technique is suitable, however, for measurement from aircraft. Future projections for multi-mission space platforms may permit the incorporation of large radiometer antennas for this and other applications.

A laser fluorosensor can measure oil thickness by detecting the difference in amplitude of the emitted fluorescence signal corresponding with the difference in oil film thicknesses. Figure 4.1-7 shows the relationship between fluorescence and thickness for a typical crude oil. Due to the attenuation effects of the atmosphere in the UV fluorescence region and the relatively long range from an orbiting satellite, the optics required for this application are very large.

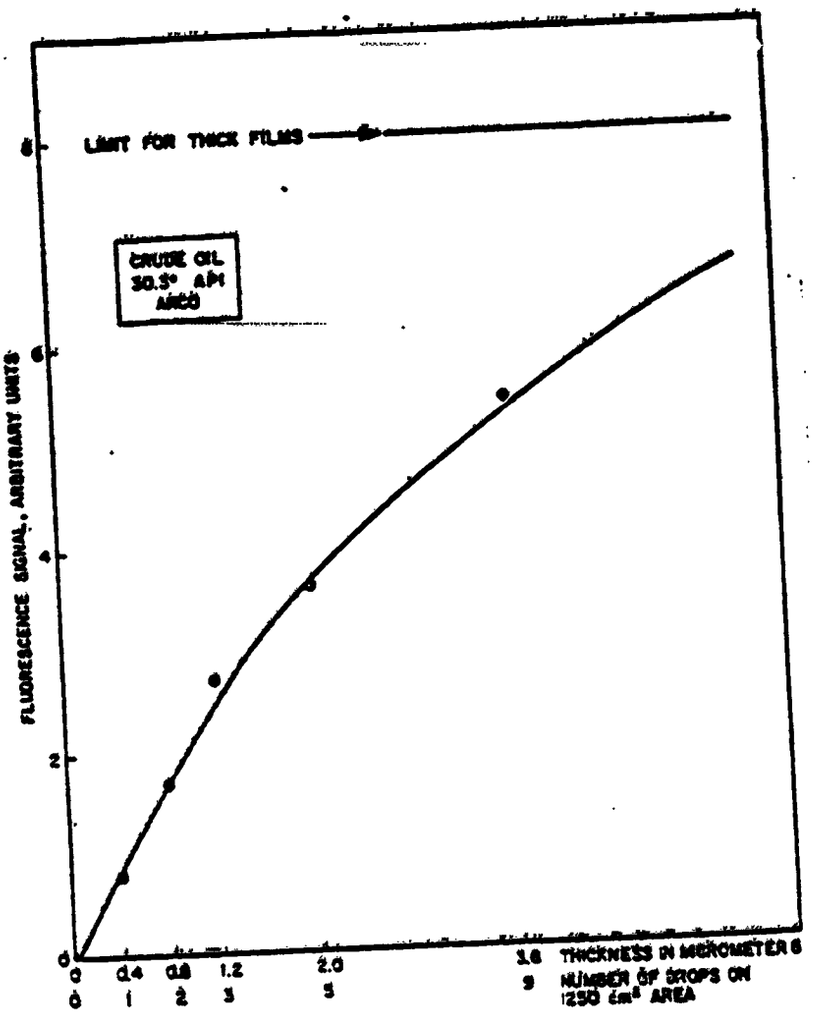

Figure 4.1-7 Relationship Between Fluorescence and Oil Film Thickness

As in the case of oil thickness measurements with microwave radiometers, the application may be feasible only when large space platforms are in operation. Both techniques are considered vital to successful quantification of oil spills from aircraft based sensors and require continued development.

Oil Spill Classification

Laser fluorescence has been successfully tested in the laboratory and from low altitudes to discriminate oil from water, and to classify among various oil types.[39] Specifically, tests have been conducted to measure fluorescence characteristics at different wavelengths. For instance, by measuring the ratio of fluorescent emissions at two different frequencies, gross classification of oils has been accomplished.

The same limitations in optics size discussed for the oil thickness measurement applies here. Therefore, this technique is suitable for aircraft-based sensing, until large space platforms become operational.

Waste Pollutant Detection and Mapping

Reflectance contrast between waste pollutants and the surrounding water in the visible spectrum has been employed as a means of detecting waste plumes. For instance, acid plumes were detected and mapped from space as early as 1973, using Landsat-1 (Ref. #17). Detection of sewage sludge plumes and other industrial wastes was not possible due to the short persistence of those plumes on the surface of the water.

The contrast between pollutant and the water varies with pollutant material, concentration, observation sun angle and atmospheric effects. Ambiguities arise

during the interpretation of spectral radiance data, since differentiation between waste pollution and the effect of clouds or sediment is sometimes difficult. Techniques to eliminate these ambiguities have been developed at the University of Delaware. They employ various spectral bands to produce distinctive two-dimensional (two-color) plots, as illustrated in Figure 4.1-8. The resulting eigenvector analysis provides statistical descriptions of characteristic regions in multi-dimensional color space, which serve as signatures for the various types of pollution.

Infrared sensing technology, highly advanced for the measurement of sea surface temperatures, may be useful in the detection of sewage plumes from sources such as ocean outfalls. These sources, which are common in many coast municipalities, produce a persistent surface temperature rise due to convection, in those regions where sewage diffusion takes place. Experimental data is needed to determine whether the spatial resolution and temperature sensitivity of current instruments is suitable for this application.

Waste Pollutant Concentration

The state of the art for this measurement is characterized by multispectral sensing in the visible spectrum, coupled with Multiple Regression Analysis (MRA) for data interpretation. In MRA, the spectral band having the highest correlation with concentration is determined. Statistical analysis (i.e., step-wise regression analysis) is applied, using other significant channels, to determine the relationship that will produce the highest accuracy of concentration measurement. NASA-Langley has employed this technique successfully, relative to airborne data.[78] Development testing from space platforms is required to adapt the technique for space monitoring applications.

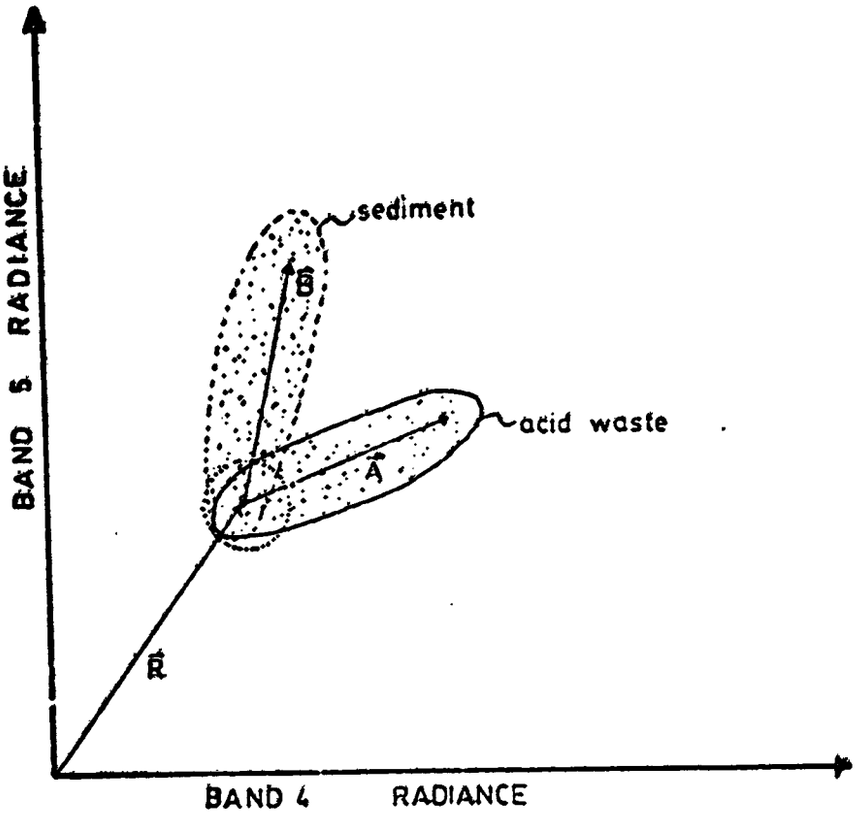

Figure 4.1-8. A two-band plot of Landsat data in which the regions corresponding to acid-waste, sediments and clear water. (Source: V. Klemas, reference 17)

Waste Pollutant Classification

The spectral radiance of polluted water varies with the type of pollutant. Atmospheric effects can mask the identifying signatures of the various pollutants such as acid waste, sewage sludge and bio-digested wastes. Information extraction techniques have been developed by NASA Langley to minimize the effects of variables such as atmospherics and sun angle. In-scene background elimination is accomplished by finding the ratios of waste plume radiances to unpolluted water radiance at various wavelengths in the visible spectrum. The characteristic relationship between these ratios and wavelenth is indicative of the type of pollutant. Figure 4.1-9 exemplifies this relationship. As in the case of pollutant concentration measurements, the multispectral data acquisition and information extraction techniques require further development using space data to adapt them to space observation. (Technique details appear in Ref. 70, 71, 72)

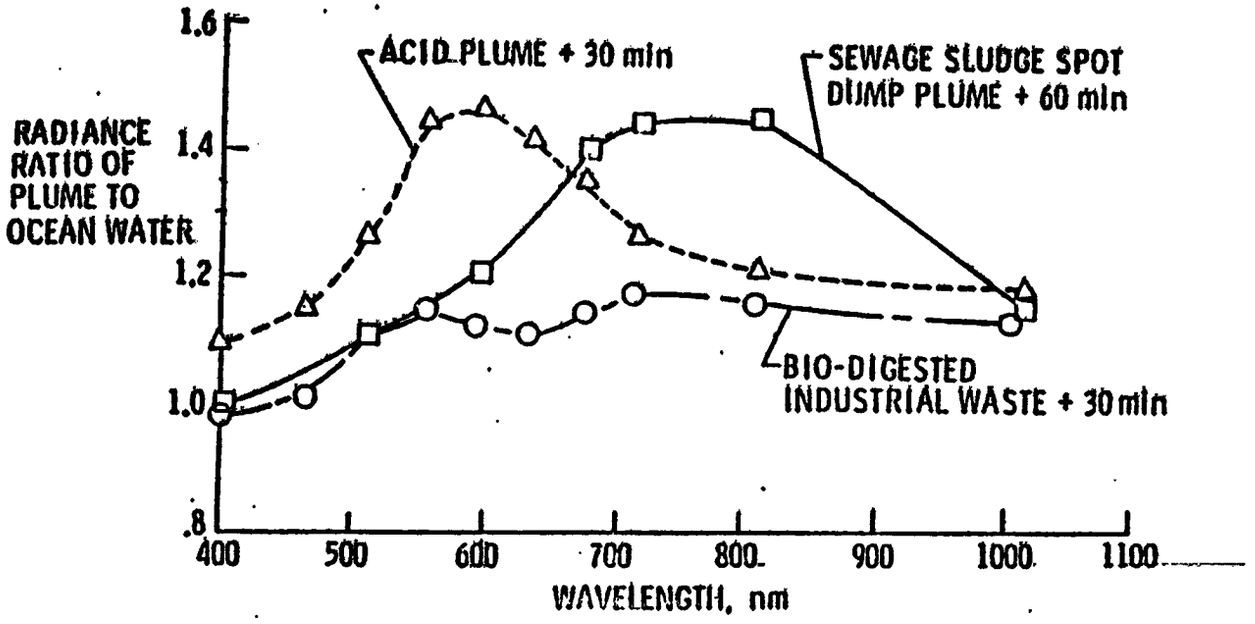

Figure 4.1-9. Spectral characteristics of plumes from sewage sludge, acid waste, and biosludge. (Data from R. Johnson, Reference 70)

Wind Speed and Direction

Wind speed and direction measurements have been successfully demonstrated from low earth orbit satellites such as Seasat. The scatterometer emits pulses at a uniform rate, and the electromagnetic waves are scattered and reflected from the illuminated portion of the ocean surface. A small portion of the scattered signal is detected by the scatterometer receiver, and permits the computation of the Normalized Radar Cross-Section (NRCS). The technique employed to determine wind direction is based on the fact that the NCRS is greatest when observing the scene in the up-wind direction, and lowest in the cross-wind direction. Two measurements per resolution element at different headings is usually sufficient to determine wind direction.

Scatterometers flown to date have had wind direction ambiguities (aliases) which sometimes can be resolved through the use of historical wind data. Development

of a scatterometer that eliminates these ambiguities will be important for this application. The use of more than four antenna beams at different headings has been proposed as a solution to this problem, and will be verified in future space systems.

All scatterometers built to date produce measurements within a swath containing a gap region centered about nadir. Methods of filling that gap need to be developed for this application.

Ocean Current Speed and Direction

Mapping the ocean current boundaries has been accomplished successfully from space, particularly with respect to large currents such as the Gulf Stream, where a significant thermal and color differential is produced by the stream.[84] However, the requirement for this application is quantitative: to map the speed and direction of the currents in this coastal zone with a resolution of 10 km. To date, the only technique that is applicable to this need is the inference of current through mapping of the sea surface contour. This method is based on the physical rise in the sea surface when crossing an ocean current. (In the Gulf Stream this averages about one meter.[83]) The state of the art of microwave or laser space altimeters is sufficiently advanced to permit the measurement of sea surface topography with the required precision. The determination of the precise ephemerides necessary to provide the altimeter reference is also within the state of the art.

The requirement for a 10 km grid every six hours persents a problem since state of the art altimeters make measurements only at nadir, at discrete points along the orbit track. A satellite at low earth orbit, for instance, could provide daily readings every 2800 km across the equator. Therefore, increasing the

number of satellites is not a practical solution. New techniques for ocean current measurements from satellites need to be developed; these need not be limited to altimetry, and should emphasize those methods that produce ocean current measurements across a wide swath.

Wave Height

Wave height has been successfully measured through the use of altimetry. Precise measurements of the rise time of the return radar pulse is interpreted in terms of significant wave height. The same limitations in grid size resolution discussed for current speed/direction measurement apply here.

A potential area of technological development for this application is the use of synthetic aperture radar data and/or scatterometer data in conjunction with new information extraction techniques. NASA Wallops has a promising concept for a multiple beam altimeter which produces altimetry data within a narrow swath (~50 km).[123] The expansion of these concepts to produce swaths in the order of 400 km should be explored.

Another possible solution is to combine sparse altimeter data with wave height models. Sophisticated models such as the Fleet Numerical Weather Model (FNWM) produce directional wave spectra with 300 km grid. Developments are underway that would permit predictions within smaller grids. The enhancement of these models with spacecraft data such as altimetry (for wave height calibration) and scatterometry (for wind speed input to the model) needs to be explored.

Wave Direction and Length

Radar images of the ocean surface reveal the wave patterns and from these we can measure wavelength and infer direction.

The requirement for measurements every three hours would necessitate multiple satellites even with a wide swath pointable SAR.

A similar solution to that discussed above is possible here. It consists of combining SAR data with ocean wave model predictions to produce the required frequency of wave direction and length measurement.

Another limitation of SAR data for this application is the fact that the SAR image would only show waves that are equal to or longer than the SAR resolution. Thus, using a 30 meter resolution SAR, the wavelength region from 0.3 meter to 30 meters would not be measurable. New technological developments are needed in this area. For instance, a scanned (pencil beam) SAR could measure ocean wavelengths across discrete lines instead of mapping the entire area, thus permitting high resolution with modest data rates and radar power.(Ref.Sect. 4.1.2.1.2)

Water Temperature

Measurements of sea surface have been obtained using thermal infrared and microwave radiometry. For instance, the Scanning Radiometer on board the ITOS satellite operates in the 10.5-12.5 micrometer region and has a theoretical accuracy of $\pm 0.2^{\circ}K$. Subsequent sensor developments in conjunction with Seasat A (i.e., VIRR sensor) have produced necessary improvements in thermal stability. Concerning the microwave spectrum, Seasat used multifrequency passive microwave techniques through the Scanning Multi-Channel Microwave Radiometer to measure surface temperatures with an accuracy of approximately $\pm 2^{\circ}K$. The projected accuracy for the radiometer that will fly on the National Oceanic Satellite System (NOSS) is $\pm 1^{\circ}C$ or better.

Air Temperature

Multifrequency optical radiometers such as the Vertical Temperature Profile Radiometer (ITOS-H and I) can measure the temperature of atmospheric layers up to 30 kilometers, with an accuracy of 3^{o} to 4^{o}C. The actual temperature at the air-water interface cannot be obtained directly, but must be inferred from the temperature profile measurements. The utility of space measurements is in the determination of the relative temperature distribution over a wide ocean expanse, using temperature calibrations from surface platforms such as data buoys in the coastal zone.

Weather Fronts

These fronts are monitored routinely through operational meteorological satellites.

Precipitation

Remotely sensed measurements of precipitation intensity and areal extent are feasible using passive microwave radiometry. The ocean emission is attenuated due to precipitation. The detected signal, then, is a function of the emissions from the ocean surface and rain, and the signal loss due to the rain. The radiative relationship necessary for extracting ocean temperature and precipitation attenuation information from the signal are known.

NASA developed an experimental sensor for measuring rain reflectivity and attenuation, the Multi-frequency Active Microwave Imaging System (MAMIS) under the Advanced Applications Flight Experiments Program. The instrument, operating in the 3.0 and 13.9 GHz bands, has flown on NOAA-sponsored aircraft tests.

Areal Distribution of Suspended Sediment

Techniques for detection of sediment are as described under "Waste Pollution Detection & Mapping".

METHODS FOR ASSESSMENT OF SENSORS/TECHNIQUES

An assessment of the state of technology in each of the measurement requirement areas preceeded the consideration of specific candidate sensors. Suitability of these sensors to the ocean pollution monitoring mission was determined on the basis of four criteria or "FILTERS", which served to analyze each sensor relative to its capability to perform the required measurements. These "filters are as follows:

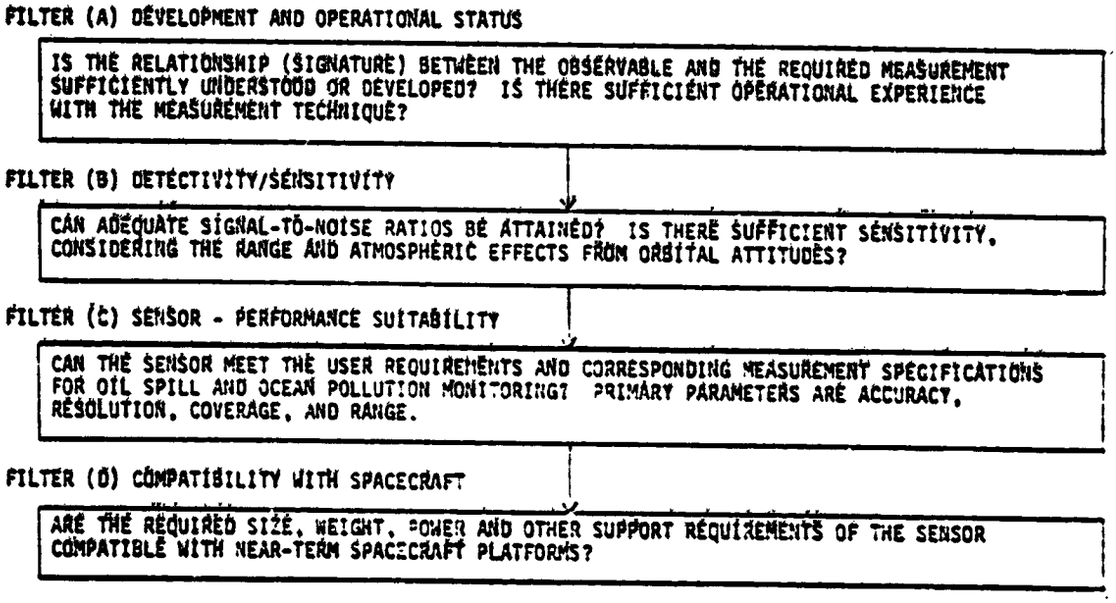

Particular emphasis in the analysis was placed on the selection of sensors having undergone actual field testing or operational documentation. We labeled this as sensor heritage, and categorized this heritage as follows:

I. SPACECRAFT SENSOR WITH PROVEN APPLICABILITY TO THE SPECIFIC MEASUREMENT

II. AIRCRAFT SENSOR WITH PROVEN APPLICABILITY TO THE SPECIFIC MEASUREMENT

III. SPACECRAFT SENSOR WITH RELATED CAPABILITY BUT NOT PROVEN APPLICABILITY TO THE SPECIFIC MEASUREMENT

IV. AIRCRAFT SENSOR - DEVELOPMENTAL RELATIVE TO THE SPECIFIC MEASUREMENT

V. SPACECRAFT SENSOR - ADVANCED CONCEPT

Parametric trades were performed in order to gain a better understanding of the system implications of a particular measurement approach. The methodology also made provisions for factoring in operational constraints such as the ability to attain the required temporal/spatial coverage using nominal orbits associated with current and planned spacecraft. This was accomplished by performing the suitability analysis in concurrently and interactively with the initial phases of the mission and operations analysis, as described in Section 5.1.

4.1.2 ASSESSMENT OF MICROWAVE SENSORS AND SENSING TECHNIQUES

The candidate sensors considered in this assessment were the Radar, Scatterometer, Passive Microwave Radiometer, and Altimeter. Within these categories of sensors there were many possible variations; for instance, radars can be imaging or non-imaging, real aperture or synthetic aperture, etc. Thus, in the "description of the sensor" and "Performance Parameters" segments, we quickly focus on the specific type or types of sensor that were potentially suitable for this mission. These sensors were then analyzed in accordance with the four "filters" discussed in the introduction to Section 4.1. The format, which follows for all major sensors considered, is as follows:

- o Parameters Measured
- o Description of the Sensor
- o Performance Parameters
- o Assessment of Sensor Suitability

4.1.2.1 Synthetic Aperture Radar

The synthetic aperture radar is an important candidate sensor for monitoring oil spills and ocean pollution. The capability of operating during day and night, and in clear and inclement weather offers a significant advantage to this sensor. Furthermore, spatial resolution of the sensor in the 30 to 100 meter range provides useful data in defining the boundaries of oil spills on the ocean.

4.1.2.1.1 Parameters Measured

The effect of oil on the ocean surface, as discussed in previous sections, is to reduce the amount of capillaries. When radar signals impinge on the ocean surface, the capillaries scatter the signals in all directions. Those signals returning to the radar are detected. Thus the presence of oil has the effect of reducing the radar return. It is this contrast in radar reflectivity that is utilized to detect oil spills. With the synthetic aperture radar the areal distribution can be determined to an accuracy established by the radar resolution.

From knowledge of the satellite ephemeides and the radar geometry, the earth surface coordinates of the oil spill can be computed.

In attempting to predict the oil spill trajectory, useful parameters obtained by the synthetic aperture radar are ocean wavelength and ocean wave direction. Further this radar is useful in establishing the extent of sea ice fields which will limit oil spill migration.

Tests performed by the NavalResearch Laboratory have investigated the effects of using horizontal polarization (HH) and vertical polarization (VV) of the antenna beam, upon the sensitivity of the instrument. Recent tests performed by the Canadian Centre for Remote Sensing have shown $^{\circ}$ contrasts of 10, 5, and 3 dB at incidence angles of 60°, 20°, and 15° respectively.

4.1.2.1.2 Description of the Synthetic Aperture Radar

A synthetic aperture radar (SAR) which comprises a pulsed transmitter, an antenna and a phase coherent receiver produces a two-dimensional image of a scene.[110-112] The SAR is borne by an aircraft or satellite, and the antenna is oriented typically at right angle to the velocity vector. See Figure 4.1-10. Range and azimuth ambiguity constraints impose restrictions on the overall geometry, antenna dimensions and coverage capability.

The only synthetic aperture radar successfully flown in a satellite is the SEASAT SAR.[118] The antenna is 2.2 m high in the elevation plane and 10.7 m long in the azimuth plane. The radar frequency is 1275 MHz and the beamwidth is about 6° in the elevation plane and 1° in the azimuth plane. The swath width is about 100 km. With this design approach, a wider swath is possible provided the antenna is made narrower and longer.

Figure 4.1-10

SAR BLOCK DIAGRAM

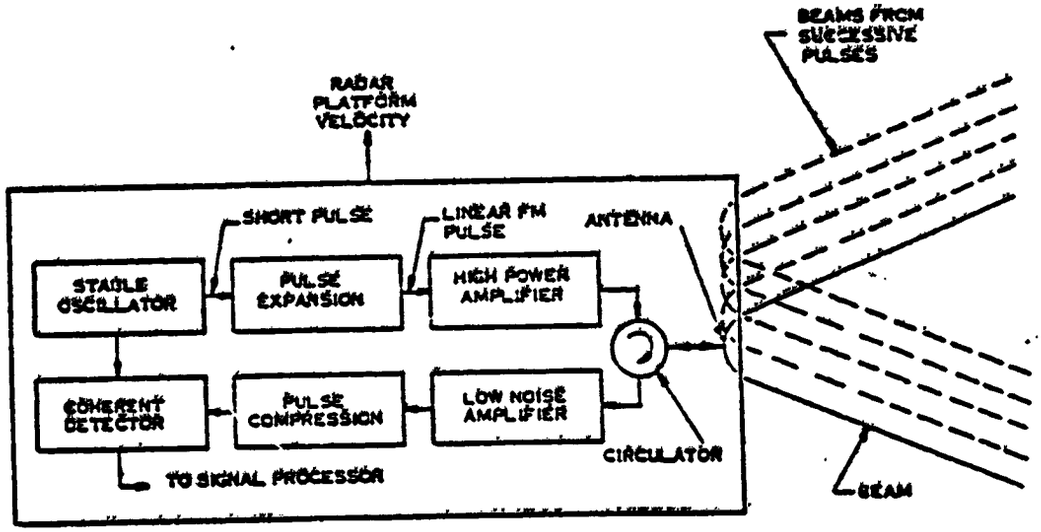

Another approach to obtain a wide swath proposed by Claassen in 1975 (Reference 119) utilizes an antenna beam that is scanned crosswise to the satellite ground track (see Figure 4.1-11). Scanned antenna beams to achieve wide swath coverage have also been reported by Cutrona (Reference 120).

The scanned beam configuration to be described is identical to that analyzed by Claassen (Reference 119). The discussion assumes a satellite platform for the SAR and a broadside antenna beam. The permissible number of scan beam positions is given by the ratio of the time period available for scanning across the swath to the integration time period required to form the synthetic aperture. A short integration time produces a short synthetic aperture and this results in a coarse azimuth resolution. The amount of scan angle in the elevation plane to image the swath is the product of the number of beam positions and elevation beam width of the antenna (Reference 128). A wide swath favors a small antenna area; however, the area must be sufficiently large to satisfy the ambiguity constraints at maximum slant range. Finally, the antenna area exerts a dominant influence on signal detection at maximum range. In the following paragraphs, performance trades are described in terms of swath width, resolution, antenna area, average power and data rate.

a) Swath Width - for the conventional SAR, the ground swath coverage W is given by

$$W = \frac{R}{\cos \theta_i} \cdot \frac{\lambda}{L_E}$$

where R is slant range, θ_i is incidence angle, λ is radar wavelength, and L_E is antenna dimension in the elevation plane. The other antenna dimension in the azimuth plane L_A is selected to satisfy the minimum antenna area A_m

FIGURE 4.1-11

SCANNED BEAM SAR

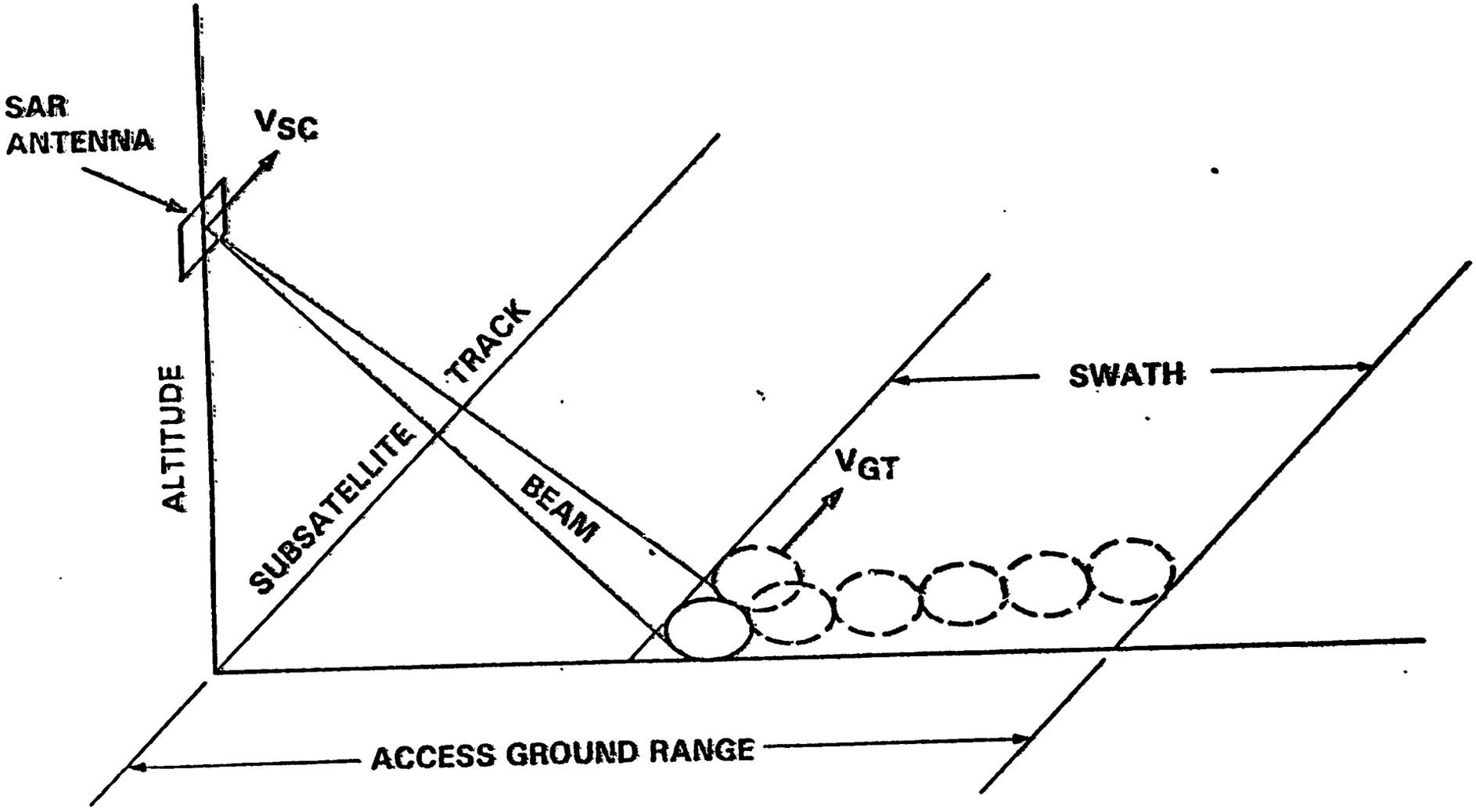

criterion dictated by the range and azimuth ambiguity constraints (Reference 144). An approximate equation for A_m is given by

$$A_m = L_A L_E = \frac{8 v_{sc} \lambda R \tan \Phi_i}{c} \qquad (1)$$

where v_{sc} is spacecraft velocity and c is light velocity. It is noted that A_m becomes smaller as the radar frequency is increased.

For the conventional focused SAR the ultimate one-look azimuth resolution is $L_A/2$, and with multiple looks the radar data processed azimuth resolution δ_{az} is given by

$$\delta_{az} = N_L L_A/2$$

where N_L is number of looks. In this configuration the synthetic aperture length L_{SA} is equal to the distance of satellite travel during which time, T_B, the scene area, is illuminated by the antenna beam. The distance $L_{SA} = T_B v_{sc}$ and the illumination time T_B is

$$T_B = \frac{\lambda R}{L_A v_{gt}} \qquad (2)$$

where v_{gt} is ground track velocity. With a modest antenna length L_A, the ultimate one-look high azimuth resolution of $L_A/2$ may exceed the requirement for some applications. For coarse resolution the synthetic aperture length required for imaging is less than L_{SA}. The time required to form the synthetic aperture is less than T_B so that time becomes available to scan the antenna beam to other directions in the elevation plane.

In a scanned beam SAR the time period T_W available to scan across the swath is given by the illumination time available from the beam geometry at the nearest range R_N so that

$$T_W = \frac{\lambda}{L_A} \frac{R_N}{v_{gt}}$$

where v_{gt} is ground track velocity. The antenna beam dwell time T_d required to form the synthetic aperture is

$$T_d = \frac{N_L \lambda/2}{\delta_{az} v_{sc}/R_F} .$$

For a conservative design, T_d is computed for operation at the farthest range R_F. The number of possible scanned beam positions N_B is given by the ratio T_W/T_d and

$$N_B = \frac{v_{sc}}{v_{gt}} \frac{R_N}{R_F} \frac{\delta_{az}/N_L}{L_A/2}$$

$$= \frac{\delta_{az}/N_L}{L_A/2}$$

The ratio v_{sc}/v_{gt} is slightly greater than unity, and R_N/R_F is slightly less than unity. In words, the potential number of beam positions is given by the ratio of the quantity δ_{az}/N_L to the ultimate focused azimuth resolution $L_A/2$. For a given value of δ_{az}/N_L the product of $N_B L_A$ is fixed so that a hardware design trade is indicated between L_A and N_B. The antenna length $L_A = 2\ \delta_{az}/(N_B N_L)$, and L_A assumes its longest value of $2\ \delta_{az}$ when $N_B = 1$ and $N_L = 1$.

The beam is scanned in the elevation plane. Assuming that the elevation beamwidth Θ_E is constant with scan angle, the available scan angle range $\Delta\Theta_{scan}$ is $N_B \Theta_E$, so that

$$\Delta\Theta_{scan} = \frac{\delta_{az}}{N_L} \frac{2}{L_A} \frac{\lambda}{L_E} .$$

Since the antenna area $A = L_A L_E$,

$$\Delta\Theta_{scan} = \frac{\delta_{az}}{N_L} \frac{2\lambda}{A} \qquad (3)$$

This equation implies that the scan angle $\Delta\Theta_{scan}$ is independent of the shape of the antenna aperture. The selection of particular values of the antenna dimensions is a hardware design trade involving the values of N_B and L_A. An example of a SAR with 18 beam positions has been reported. A wide scan angle favors a small area A; however, this is constrained by ambiguity considerations. Further, a small value of A will require greater transmitter power to achieve a given signal-to-noise ratio.

If the minimum antenna area criterion given by (1) is combined with (3)

$$\Delta\Theta_{scan} = \frac{\delta_{az}}{N_L} \frac{c}{4v_{sc} R_F \tan \Theta_{iF}} .$$

This is the largest value of $\Delta\Theta_{scan}$ attainable and it is constrained by ambiguity at the farthest range. A coarse azimuth resolution will permit wide swath coverage. It is noted that when constrained by ambiguity, $\Delta\Theta_{scan}$ is independent of wavelength. The $\Delta\Theta_{scan}$ is measured from the beam axis angle at the farthest range towards nadir. The minimum usable value of incidence angle can be dictated by the scene to be imaged or by range resolution. Because of the geometry, the projected surface range resolution δ_{gr} is governed by the radar slant range resolution δ_{sr} (commensurate with the radar bandwidth) by the equation $\delta_{gr} = \delta_{sr}$ cosecant Θ_i. An incidence angle near zero is not usable by any SAR (Reference 112).

b) Transmitter Power - The average transmitter power of a SAR depends on many parameters, and it is given by

$$P_{ave} \sqrt{N_L} A^2 \eta^2 \delta_{sr} \sigma^o = SNR\, 8\pi R_F^3 kT_s v_{sc} \lambda L_s$$

where N_L = number of looks

A = Antenna area

η = antenna efficiency

δ_{sr} = slant range resolution

σ^o = normalized radar cross section

SNR = S/N at beam center

R_F = slant range to far edge of swath

k = Boltzmann's constant.

T_s = system noise temperature

v_{sc} = spacecraft velocity

λ = radar wavelength

L_S = system loss factor, greater than unity.

A small value of P_{ave} favors small values of λ and R_F but large values of A, δ_{sr} and σ^o. The average power is independent of antenna shape but decreases rapidly by increasing area A. A large value of A is counter to wide swath coverage so that a performance trade is indicated. The average power is inversely related to δ_{sr}. In order to maintain a given value of ground image resolution δ_{gr} across the swath δ_{sr} must be varied in accordance to $\delta_{sr} = \delta_{gr} \sin \Phi_i$, where Φ_i is the incidence angle. There is a hardware design limit on δ_{sr} and an operational limit on Φ_i which is scene dependent.

If the SAR design is ambiguity limited at the far edge of the swath, the average power is given by

$$P_{ave} \sqrt{N_L}\, \eta^2\, \delta_{sr}\, \sigma^o = \frac{SNR\, \pi^3 c^2\, k\, T_s L_s}{8\, v_{sc}} \frac{R_F}{\lambda \tan^2 \Theta_{iF}} .$$

For a given geometry, it is noted that the average power decreases with radar frequency.

c) Data Rate - The return signal received by the radar is usually recorded first and processed later to produce images of scenes. Because the received signal pulse length is a fraction of the interpulse period, it is assumed that signal buffering is employed to stretch out in time the data stream until it almost fills the interpulse period. This technique will reduce the data rate to a minimum. The data rate is given by the product of three quantities, viz., (a) number of range bins per pulse; (b) number of bits per range bin; and (c) the pulse repetition frequency.

Compression of the signal in range is reasonably convenient to achieve within the radar electronics and this is assumed. After range compression the received signal is sampled in time at a rate so as to provide amplitude and phase data for each range resolution bin. The number of range bins is given by the ratio of range extent of the antenna beam footprint to the ground range resolution, δ_{gr}. The extent is given approximately by $R\Theta_E/\cos \Theta_i$, and the number of range bins N_{RB} is

$$N_{RB} = \frac{R \lambda}{\delta_{gr} L_E \cos \Theta_i} .$$

When the analog received signal is digitized, a sufficient number of bits (B_{IQ}/S) is required for each sample period of the received signal to provide

adequate accuracy or fidelity. Since the phase of the received signal is required in addition to its amplitude, both the in-phase and quadrature phase components are recorded.

A very critical parameter in a SAR is the pulse repetition frequency, PRF. To achieve high quality imagery, the PRF is typically about 30% higher than the minimum value required that meets the azimuth ambiguity constraint. The minimum value is given by $v_{sc}/(L_A/2)$ which in words states that the satellite platform travel distance cannot exceed one-half the physical antenna length between successive pulses. The typical PRF is about $2.6\ v_{sc}/L_A$.

Finally, the data rate DR is given by

$$DR = \frac{B_{IQ}}{S} \times N_{RB} \times PRF$$

$$= \frac{B_{IQ}}{S} \times \frac{R}{\cos \phi_i} \times \frac{2.6\lambda\, v_{sc}}{A\, \delta_{az}}$$

where $A = L_A L_E$. It is assumed that the ground range resolution δ_{gr} is equal to the azimuth resolution δ_{az}. The data rate depends on position within the swath, and the highest value occurs at the far edge of the swath. It is noted that the data rate is independent of antenna aperture shape, and also independent of λ and R if the design is ambiguity limited. The data rate is highest when ambiguity limited and it decreases as A is increased.

d). Signal Processing - The principles of processing SAR signals to produce two-dimensional images have been discussed in the literature (References 145, 146). Optical techniques have been widely used, and recently digital techniques have been reported. In the proposed scanned beam radar, the antenna beam at any instant of time illuminates a fraction of the swath width. The beam dwell

duration in this position is such as to generate the required synthetic aperture length. In this time period sufficient radar return signals are transmitted and received to produce an image of this illuminated area called a "patch." All of the patches across the swath are combined to form an image of the full swath width. After traversing the swath, the antenna beam returns and an image is formed of the adjacent in-track patch. All of these cross-track and in-track patches are combined to produce an image of the scene. The transmitted radar signal and received signal processing have to be sufficiently accurate to permit joining adjacent patches within a fraction of the resolution dimension. Resampling of the data may be required to achieve patch alignment. A digital buffer memory is required to store the image data of the patches and to read out the data to produce a single image of the scene.

e) Computations for 30 Meter Resolution - The available swath widths under ambiguity-limited operation were computed for one-look imaging and 30-meter resolution. The computations were performed for a spherical earth geometry with the SAR satellite at three different altitudes of 700, 900 and 1100 km. The ground ranges from the subsatellite point to the far edge of the swath were computed for several incidence angles. With an incidence angle of 45°, the ground range is 880 km from the 1100-km altitude (see Figure 4.1-13). The minimum antenna area required to meet both the range and azimuth ambiguity constraints is 9.07 m^2 (see Figure 4.1-12). An ambiguity-limited swath width of 358 km is attainable and this is shown in Figure 4.1-13. With a greater incidence angle, the ground range can be further increased. On the other hand, if the incidence angle and ground range are decreased, the required antenna size decreases and the ambiguity limited swath width increases. An arbitrary minimum incidence angle of 10° is selected at the near edge of the swath because of

Figure 4.1-12

AMBIGUITY LIMITED MINIMUM ANTENNA AREA

30-M AZIMUTH RESOLUTION
9375 MHZ

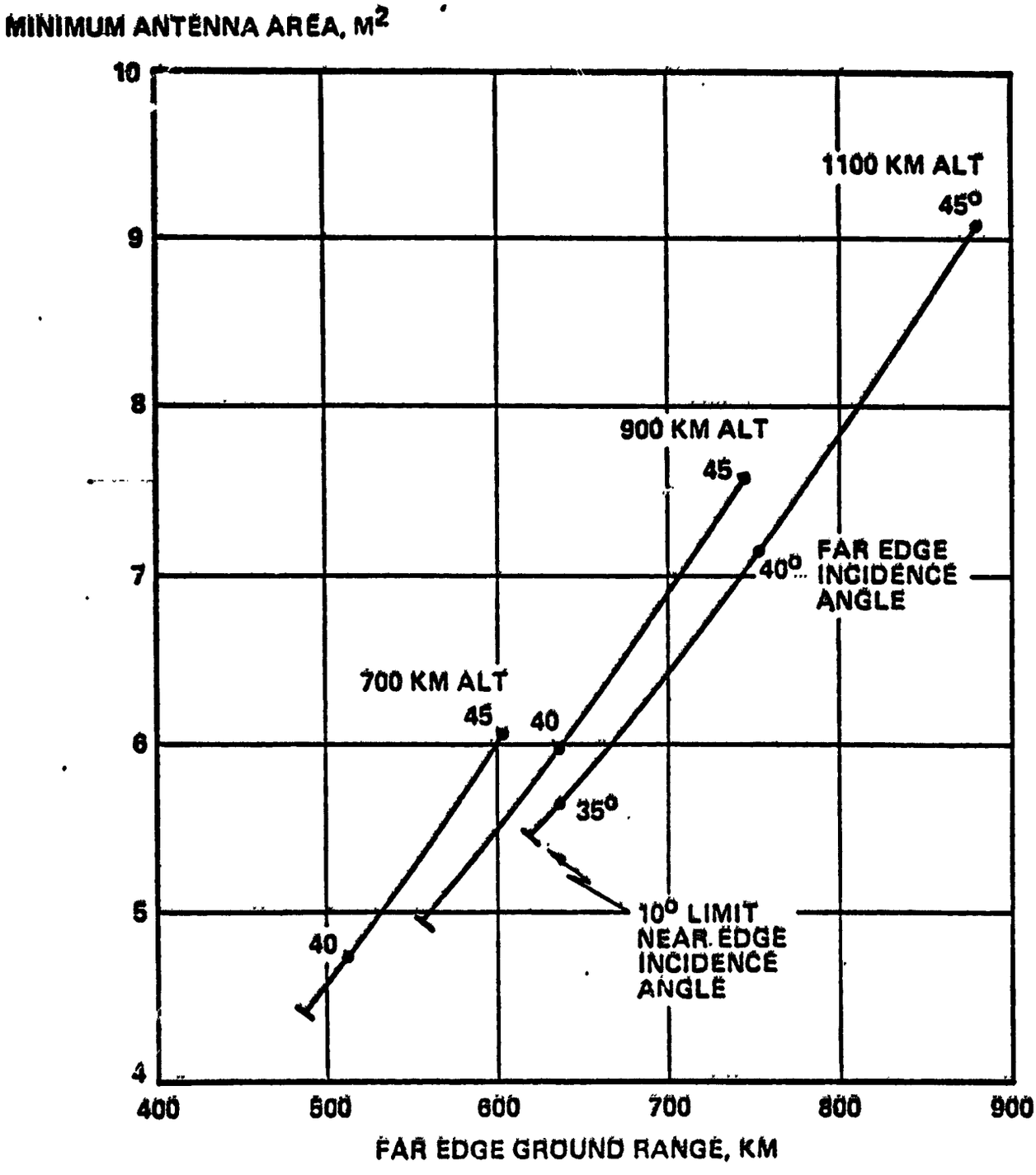

FIGURE 4.1-13

AMBIGUITY LIMITED SWATH WIDTH
(INDEPENDENT OF WAVELENGTH)

30-M AZIMUTH RESOLUTION
ONE-LOOK IMAGING

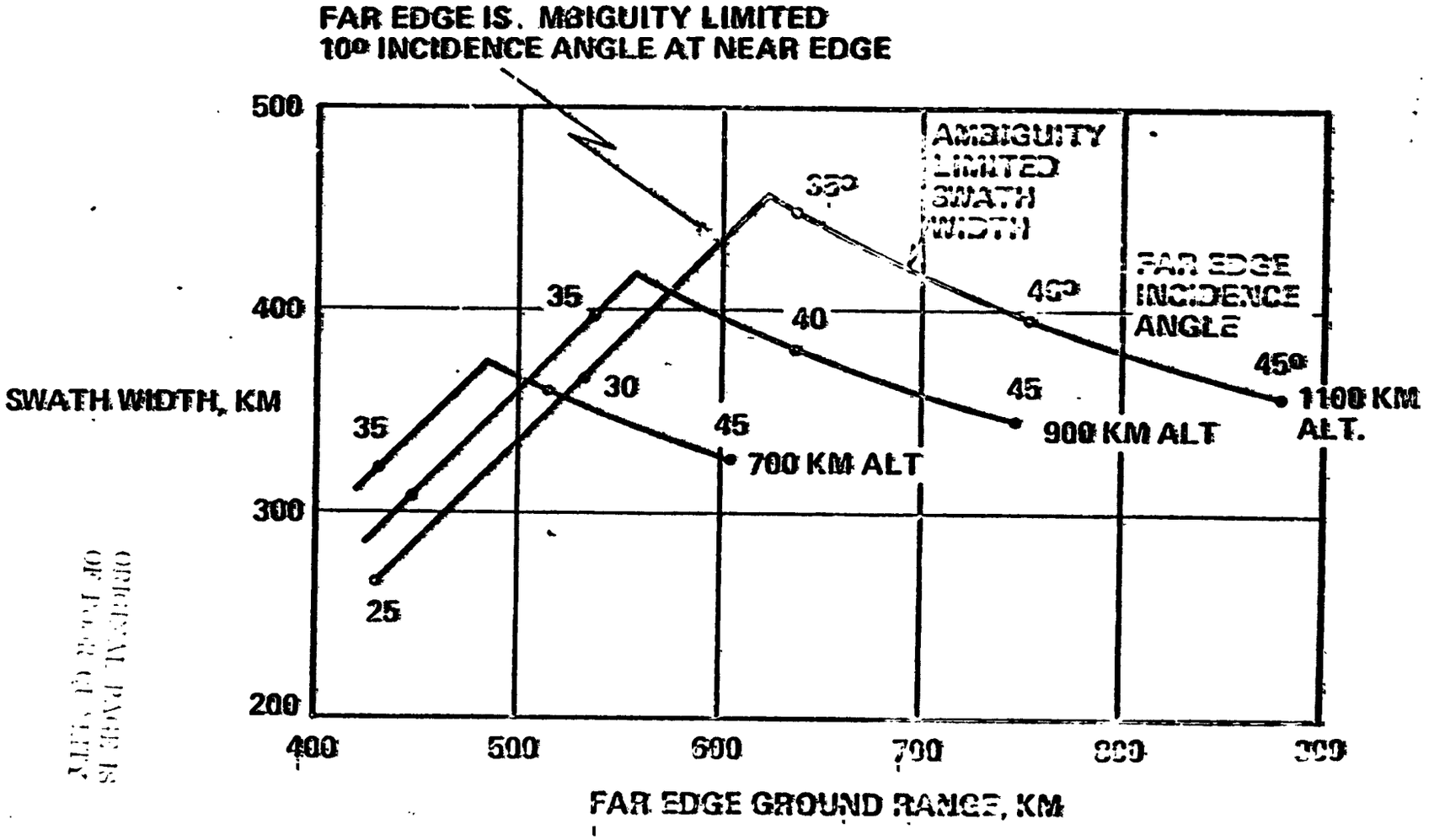

excessive degradation in ground range resolution for a given slant range resolution. With this minimum incidence angle constraint, the maximum swath width of 453.5 km is obtained from the 1100 km altitude when the far edge incidence angle is 34.25° and the ground range is 619 km. The antenna area for this geometry is 5.46 m^2. If a swath width narrower than 453.5 km and a ground range closer than 619 km are acceptable, then the antenna area can be made larger than 5.46 m^2. This will decrease both the average transmitter-power and the digital data rate. From Figure 4.1-13 it can be seen that the maximum swath width decreases with decreasing satellite altitude.

The average power and data rate were computed for several incidence angles and the three satellite altitudes. The following assumptions were made:

S/N = 3 dB at beam edge, 9 dB at beam center

f = 9375 MHz

N_L = 1 look

δ_{az} = 30 m

T_s = 817°K

L_S = 6 dB

σ^o = 0.005 $\cot^2 \Phi_{iF}$

δ_{sr} = $\delta_{az} \sin \Phi_i$

η = 55%

$v_{sc} = \sqrt{398601.2/(H + R_e)}$, km/sec

H = satellite altitude, km

R_e = earth radius, 6378 km.

The average power for ambiguity limited operation, one-look imaging and 30-m resolution are:

		700 km	900 km	1100 km
$\theta_i = 40^\circ$	swath	360 km	379 km	394 km
	P_{ave}	1423 W	1840 W	2263 W
$\theta_i = 45^\circ$	swath	326 km	344 km	358 km
	P_{ave}	1383 W	1784 W	2188 W

The maximum ambiguity limited data rate depends only on the far edge incidence angle, and it is 46.7 and 42.4 MBPS for 40° and 45° incidence angles respectively. It is assumed that 8 bits are required to record the amplitude and phase of the signal in each range resolution cell.

e) Computations for 100-m Resolution - Computations were performed for one-look imaging and 100-meter azimuth resolution. Images with 100-m resolution may have utility in mapping sea ice, ocean surface roughness, in addition to oil spills. With ambiguity limited operation at the far edge of the swath, the computed swath widths were so wide that the near edge incidence angles were less than 10°. By increasing the antenna area, the near edge incidence angle can be increased to 10°. The use of a larger antenna area will decrease the average power and data rate. The largest antenna areas were calculated which provided specified swath widths and satisfied the near edge incidence angle requirement of 10°. Three swath widths of 300, 500 and 700 km were selected for each of the three satellite altitudes of 700, 900 and 1100 km. The radar frequency is 9375 MHz. The largest antenna areas as a function of swath width are plotted in Figure 4.1-14. From the 100 km altitude, the 700 km swath has a far edge incidence angle of 44.5° and a 13.03 m^2 antenna is used. The far edge incidence

Figure 4.1-14

ANTENNA AREA FOR OPTIMUM DESIGN
(10° NEAR EDGE INCIDENCE ANGLE, MINIMUM POWER AND DATA RATE)

100-M RESOLUTION
ONE LOOK, .9375 MHZ

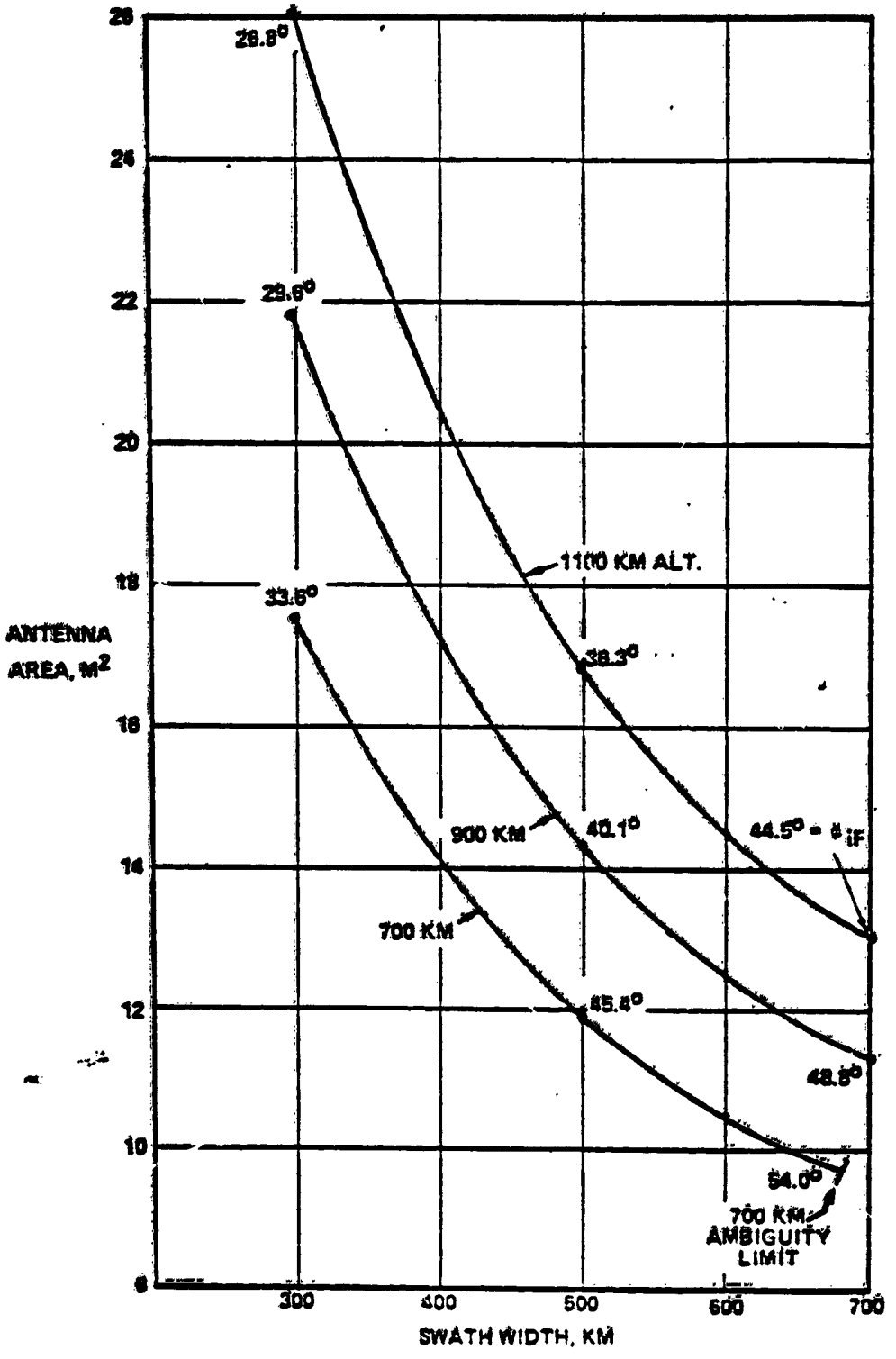

C-2

angles are also given in the figure for other swath widths and satellite altitudes.

If the satellite is in a 700-km altitude orbit, a 700 km swath cannot be imaged since the ambiguity constraint is violated at the far edge of the swath. The maximum swath width which can be imaged from this altitude is 691.5 km, and the far edge incidence angle is 34.05°. If the far edge incidence angle is constrained to 45° due to operational reasons, a 500 km swath can be imaged from the 700-km altitude. The required antenna area for this swath is 11.86 m^2.

With the antenna area optimized for each combination of swath and altitude, the average powers were computed, and a wide variation was found. As before, it is assumed that $\sigma^{\circ} = 0.005 \cot^2 \theta_{iF}$. The average powers were calculated for detection at the far edge of the swath. The computational results are shown in Figure 4.1-15. For a 300-km swath the average power of about 18.5 watts is almost independent of satellite altitude between 700 and 1100 km. With wider swaths, the average power decreases with increasing altitudes.

With the optimum antenna area for the particular swath and altitude, the digital data rates were computed. It is assumed that 8 bits are required to record the amplitude and phase of the signal in each range resolution cell. The results are plotted in Figure 4.1-16. For a 700-km swath, the data rate is in the vicinity of 10 MBPS.

f) Comments on Scanned Beam Synthetic Aperture Radar - The swath width coverage capability of a synthetic aperture radar is proportional to its azimuth resolution and inversely to its antenna area. The widest swath is obtained when the geometry is ambiguity limited. In instances where the maximum obtainable swath exceeds requirement, the antenna area can be increased, which will reduce transmitter power and digital data rate.

Figure 4.1-15

AVERAGE POWER WITH OPTIMUM ANTENNA AREA

(10° NEAR EDGE INCIDENCE ANGLE)

100-M RESOLUTION
ONE LOOK
9375 MHZ
$\sigma^0 = 0.005 \cot^2 \phi_{iF}$

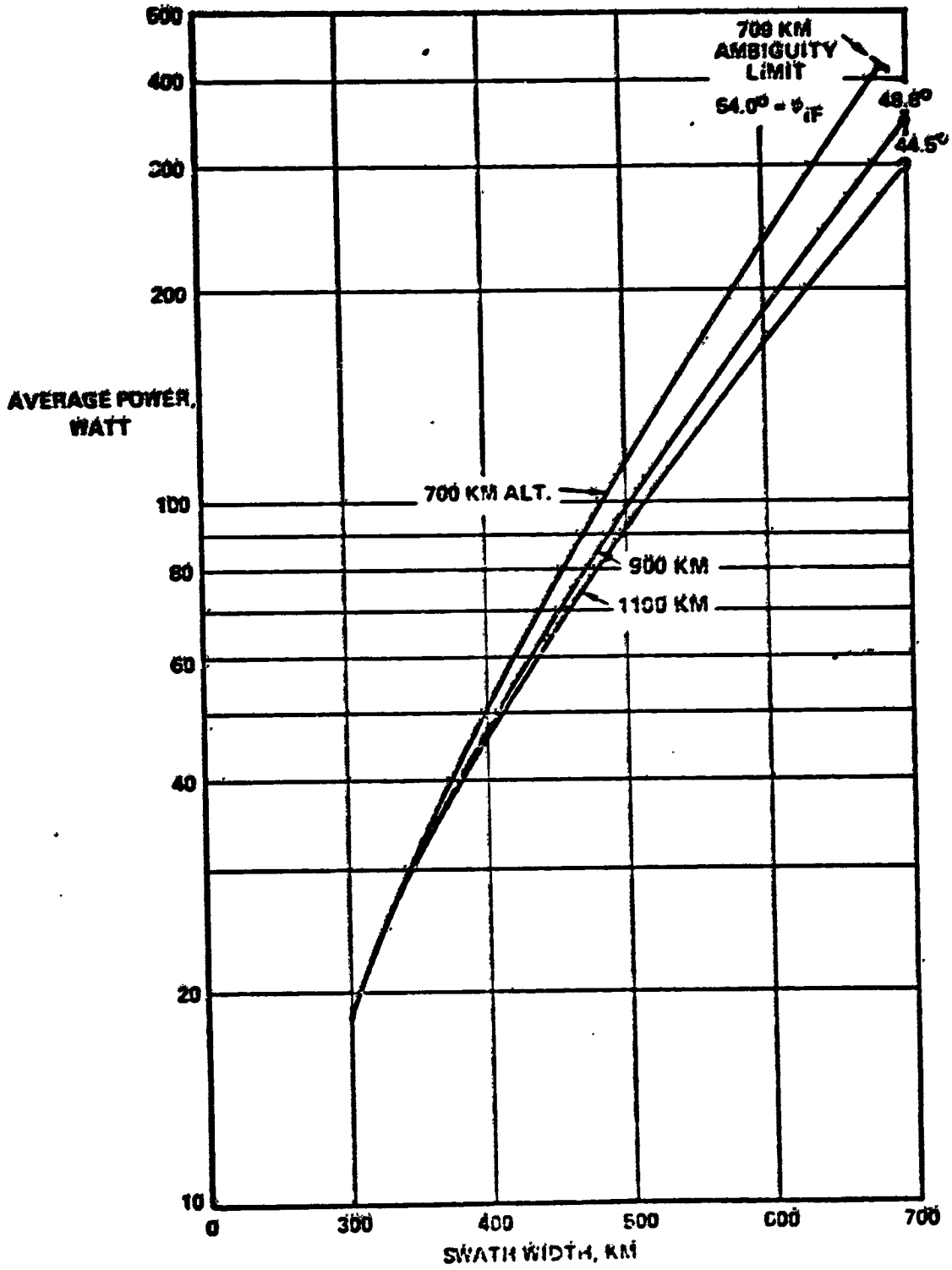

The antenna aperture shape controls the number of beam positions in the elevation plane to cover the swath and this is a hardware design trade factor. Performance trade computations suitable for configurational purposes are presented involving resolution, antenna area, swath width, average transmitter power and digital data rate.

The processing of radar data to produce an image of a wide swath is probably best achieved by employing digital techniques. Images of subswath scenes illuminated by the antenna beam in each scan position are combined to form an image of the full swath (see Figure 4.1-17). An alignment accuracy of a fraction of the resolution dimension is required to combine the subswath images.

Figure 4.1-15
AVERAGE POWER WITH OPTIMUM ANTENNA AREA
(10° NEAR EDGE INCIDENCE ANGLE)
100-M RESOLUTION
ONE LOOK
9375 MHZ
$\delta^o = 0.005 \cot^2 \theta_{iF}$

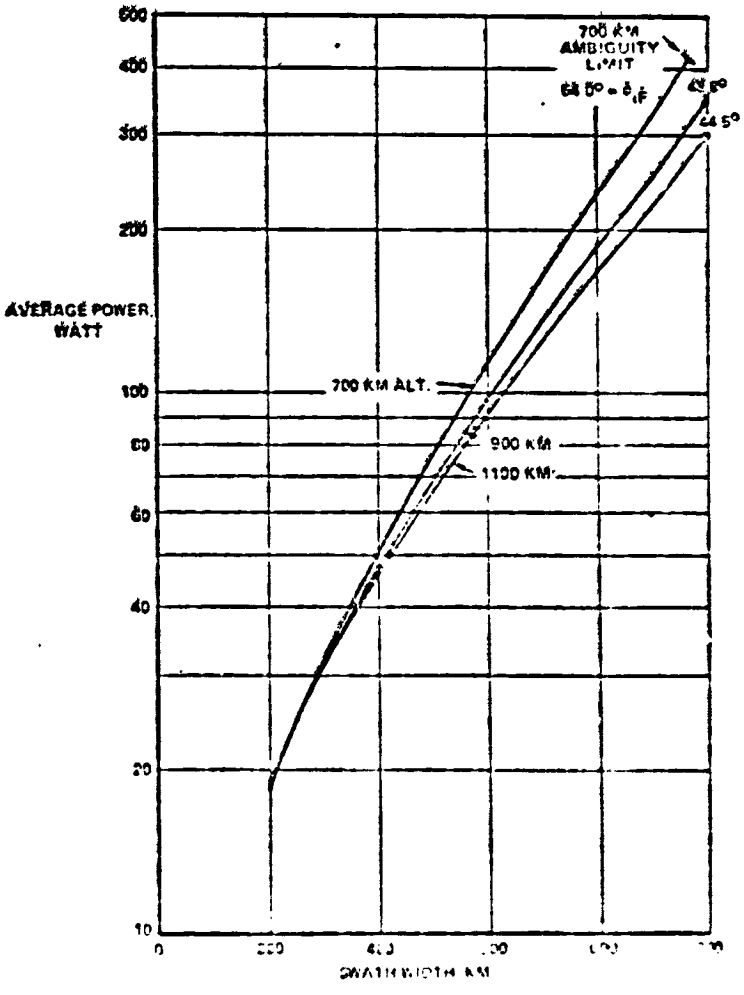

DATA RATE WITH OPTIMUM ANTENNA AREA
(10° NEAR EDGE INCIDENCE ANGLE)

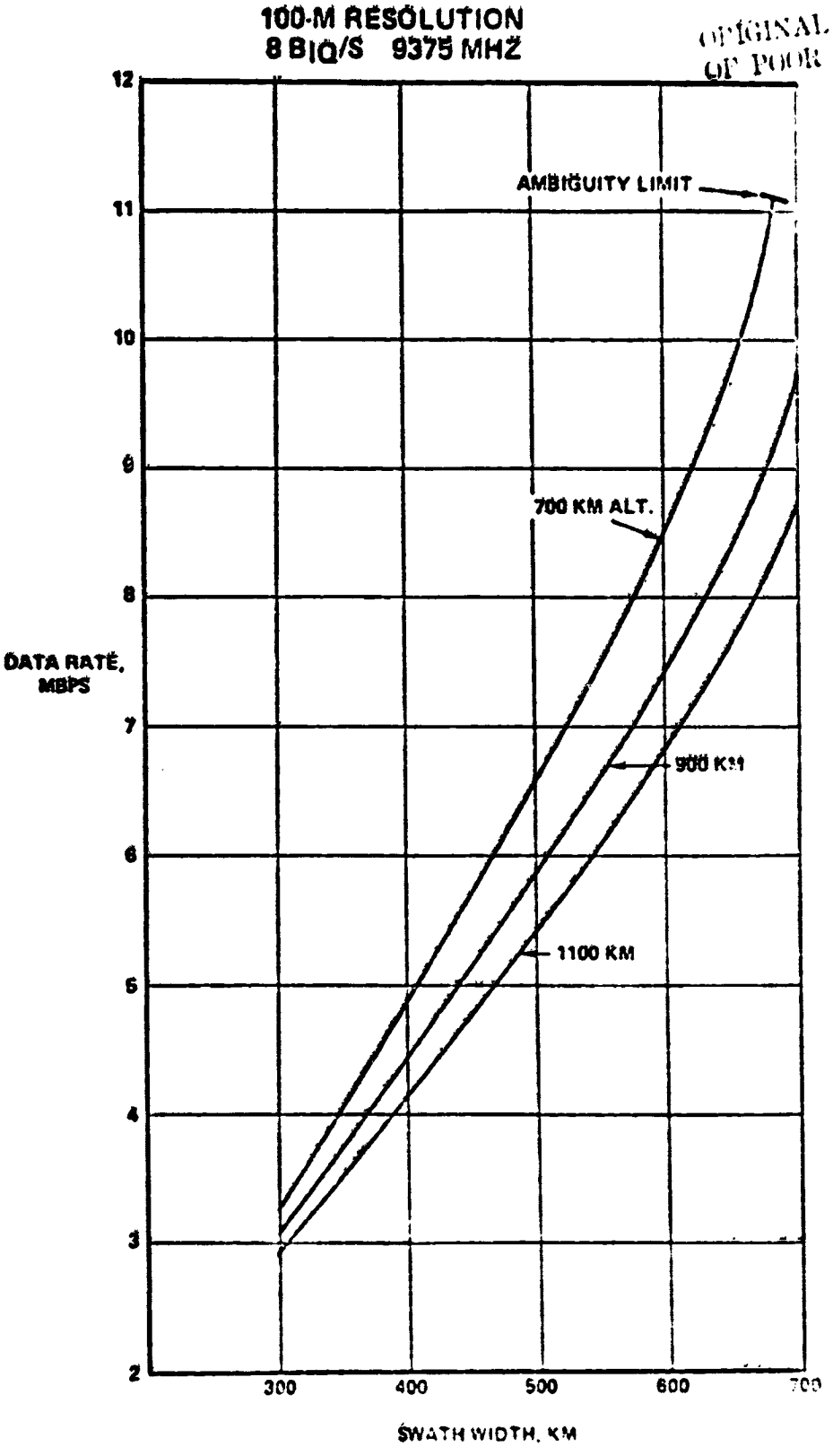

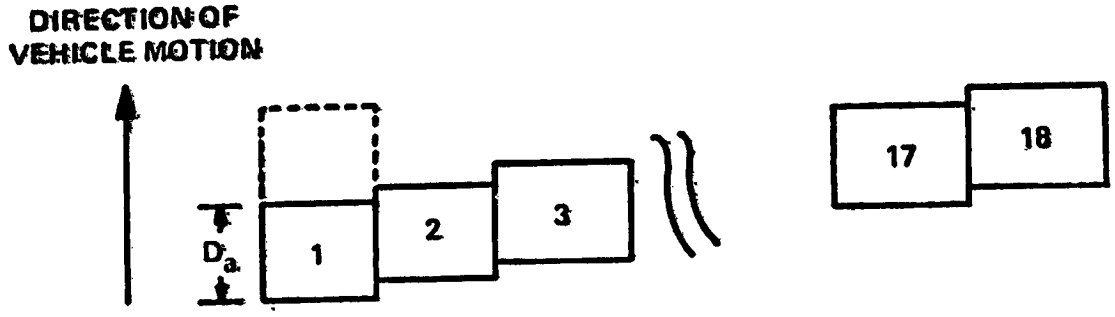

Figure 4.1-17. Relative Patch Locations

4.1.2.1.3 Performance Parameters

Calculations on performance were carried out for satellite altitudes covering a range that is representative of the ocean pollution mission: satellite altitudes of 567 and 803 km; swath widths of 110, 180, 280 and 392 km with maximum ground ranges of 500, 500, 600 and 600/cm respectively. A representative coverage access of the SAR swaths is shown in Figure 4.1-18. The azimuth and ground resolutions were 30 km, system noise figure was 4 dB, system loss of 6 dB, one-look imaging, and 3 dB SNR at path edge. For the two narrows swaths, the maximum incidence angle at the far edge of the swath was 45° and the normalized radar cross section σ^{o} was -25 dB. For the two wider swaths the corresponding values were 38.4° and -20 dB. The average radiated power and the antenna area presented in Table 4.1-1. For comparison purposes the relevant values for the SEASAT SAR and the SAR for the Ice Processes and Climate mission are also given in Table 4.1-1.

The SAR for MOPS* was reconfigured for four levels of capability, and the various parameter values for a one-look design are given in Table 4.1-2. In the fifth level of capability, a four-look design was configured. The resolutions used were 30, 60 and 100 meters. The swath widths were 360 and 390 km. In three designs the swath location could be pointed within a maximum ground range of 600 km. In one design the maximum ground range was 500/cm and the 360 km swath was fixed in its location relative to the satellite. The results are shown in Table 4.1-2. The following assumptions were made:

frequency	9375 MHz
altitude	900 km
NCRS, ^{o}	-23 dB
A/D Converter	8 bits IPQ per sample
noise figure	4 dB
system loss	6 dB
SNR	3 dB at patch edge

The average power levels varied from 50 W to 1872 W. The data rate ranged from 4.3 to 48.5 MBPS, and the antenna area from 4.6 to 18.5 m^2.

*MOPS is a study designation for a potential Monitor of Oceanic Pollution System".

Table 4.1-1

MOPS-SAR PARAMETERS & COMPARISON WITH IPAC & SEASAT-SAR

PARAMETER	MOPS VERY NARROW SWATH	MOPS NARROW SWATH	MOPS MEDIUM SWATH	MOPS WIDE SWATH	SEASAT SAR	IPAC SAR
FREQUENCY (MHz)	9375	9375	9375	9375	1275	12000
ALTITUDE (KM)	567	567	893	567	808	777
NOISE FIGURE (dB)	4	4	4	4	-	4.5
SYSTEM LOSS (dB)	6	6	6	6	-	6
NO. OF LOOKS	1	1	1	1	4	2
δ_{ground} RESOLUTION (M)	30	30	30	30	25	100
$\delta_{slant\ r}$ RESOLUTION (M)	15	15	15	15	8.6	50
$\delta_{azimuth}$ RESOLUTION (M)	30	30	30	30	25	100
σ^o NRCS (dB)	-25	-25	-20	-20	-	-20
SNR, PATCH EDGE (dB)	3	3	3	3	-	3
INCIDENCE ANGLE (deg. max.)	45	45	38.4	38.4	20.4	37
GROUND RANGE (KM) MAX	500	500	600	600	376	506
SWATH WIDTH (KM)	110	180	280	392	100	264
AVE. RF POWER (WATTS)	300	1000	1000	2000	55	128
PK RF POWER (WATTS)	-	-	3000	6000	-	-
DC POWER ESTIMATE (WATTS)	1500	3800	3800	6800	500	650
ANTENNA AREA (M^2)	15	8.2	7.7	5.5	11.8	7.2

Figure 4.1-18

REPRESENTATIVE COVERAGE ACCESS FOR SAR SENSOR SWATHS

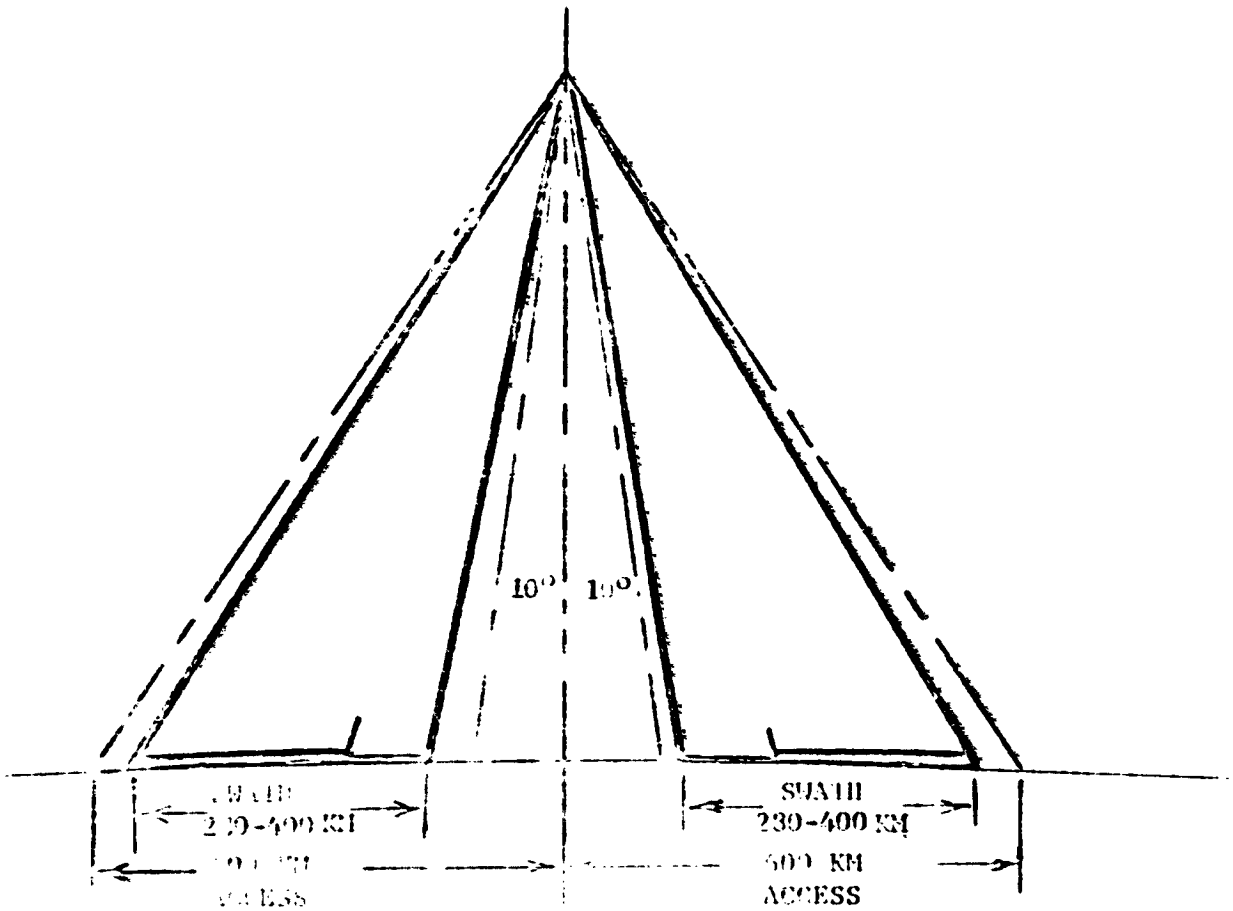

TABLE 4.1-2

ALTERNATE MOPS SAR CONFIGURATIONS

CAPABILITY	#1	#2	#3	#4	#5
LOOKS	1	1	1	1	1
RESOLUTION	30 M	60 M	60 M	100 M	100 M
SWATH	390/cm	360 km	360 km	360 km	364 km
MAX GROUND RANGE	600 km	600 km	500 km	600 km	500 km
AVERAGE POWER	187.2 W	226 W	160 W	50 W	263 W
DATA RATE	48.5 MBPS	11.9 MBPS	10.9 MBPS	4.3 MBPS	15.4 MBPS
ANTENNA AREA	5.5 m^2	11.2 m^2	11.0 m^2	18.5 m^2	4.6 m^2

A block diagram for a SAR is shown in Figure 4.1-17. The electrical values for many of the component boxes are given for a typical design. The output power of the TWT will be dictated by detection requirements as given in the preceding paragraphs.

4.1.2.1.4 Assessment of Sensor Suitability

The synthetic aperture radar has been used successfully to detect oil spills by various experiments. The detection is based on the reduction of radar backscatter of oil-film covered sea caused by the reduction in surface capillaries, and this radar backscatter reduction occurs in contrast with the surrounding sea with natural surface capillaries. On occasion a patch of sea with reduced radar backscatter has been observed in the absence of oil on the surface, and these patches of calm sea surface have been called "wind slicks" or localized areas of wind shear where wind conditions change so rapidly that capillaries do not sufficient time to develop.

Thus while the SAR will detect oil spills there is a possibility of ambiguous or false detection.

The SAR can easily detect ice cover since the radar cross sections of the ice and the contiguous sea are quite different. The SAR imagery offers the capability of providing the crest-to-crest distance between waves, or wave length. SAR imagery of this type have been shown by NRL and JPL. As a consequence of this wave imagery, the SAR can be used to provide wave direction. Without auxiliary information such as synoptic or historical data, there is a 180° ambiguity in the wave direction.

Another question addressed is the sensor sensitivity from orbit. Depending on orbit altitude and performance requirements the average RF power ranges between 50 and 1872 watts. Assuming a 33% efficiency for the transmitter tube, the prime power for only the high power amplifer ranges from 150 to 5616 watts.

For utility in the monitoring the coastal zone, it is postulated that the SAR should have a 600 km ground range capability from the subsatellite track, on a total access swath width of 1200 km. Configuration designs have been presented with the 1200 km swath width capability.

The near-term satellites have finite size, weight and power constraints, and different configurational designs have been present in the preceding paragraphs to meet a variety of combinational constraints.

4.1.2.1.5 Technology Implication

Investigations are suggested to examine the mechanism of wind slicks that are ambiguous with oil spills. The temporal characteristics of wind slicks and occurrence probabilities should be examined. The utility of time-delayed imagery requires experimentation. The range of radar frequency, incidence angle, heading angle relative to the local wind vector, polarization, resolution and oil type should be investigated.

In the scanned beam approach, many subswath radar images have to be combined to generate a composite full-swath image. The use of digital techniques appears to be feasible and exploratory studies are required. Further the feasibility of on-board signal processing to generate imagery on the spacecraft should be examined for this application. It appears that the data rate associated with formed images should be considerably lower than that of the raw radar data stream.

A most critical area of development in the SAR hardware is a long life, high efficiency, high power transmitter. Future SAR applications are all constrained by the available transmitter tubes.

4.1.2.1.6 SAR Assessment Summary

A summary assessment has been prepared for the synthetic aperture radar as a sensor for oil spill detection. This summary is given in Table 4.1-3.

Table 4.1-3. SAR Assessment Summary

PARAMETER	COMMENTS
o SPILL DETECTION	NEEDS DEVELOPMENT OF DATA ENHANCEMENT TO REDUCE AMBIGUITIES WITH "WIND SLICKS"
o ICE COVER	MEET REQUIREMENTS
o WAVE LENGTH	MEET REQUIREMENTS
o WAVE DIRECTION	MEET REQUIREMENTS EXCEPT 180° AMBIGUITY
o SPACECRAFT DRIVERS	DC POWER = 6.8×10^3 WATTS FOR 30 M RESOLUTION, 390 KM SCANNED SWATH
	RF TRANSMIT POWER = 2.0×10^3 WATTS/AVG., 6.0×10^3 WATTS/PK (SPACE QUALIFIED TUBE DEVELOPMENT REQUIRED)
	DATA RATE = 77.5×10^6 BPS
	ANTENNAS = 2 REQUIRED, 5.5 M^2 EACH

4.1.2.2 Microwave Scatterometer

Parameters Measured

Through the measurement of the Radar Backscatter Coefficient (σo) in two mutually orthogonal directions, ocean surface wind speed and direction can be inferred. A secondary measurement that can be inferred from σo is Ice Cover Extent.

The most stringent requirements, based on user requirement specifications are as follows:

	Wind Speed	Wind Direction	Ice Cover
Precision	0.5 m/s	5^{o}	10%
Accuracy	2 m/s	10^{o}	2%
Range	0-50 m/s	$0-360^{o}$	0-100%
Frequency (every N hrs.)	3	3	3
Delay (hrs.)	3	3	3
Spatial Resolution	10 km	10 km	5 km

Description of the Sensor - Theory of Operation - A microwave scatterometer is a remote sensor which has demonstrated utility by enabling the calculation of geophysical parameters from its measurements. In basic form, a scatterometer comprises a transmitter, an antenna and a receiver. The transmitter emits pulses at a uniform rate. The pulsed signals are radiated by the antenna, and reflected or scattered by the illuminated scene. A small portion of the scattered signal is detected by the sensitive receiver, and the ratio of received to transmitted signals is a measure of the radar cross section, RCS, of the scene. When the scene is the ocean surface, its roughness increases with wind speed and it is this observation that is utilized to infer oceanic wind speed from the radar cross section. The units of RCS are area (meter squared) and when divided by the physical area of the scatterer, a quantity called normalized RCS, or NRCS and symbolized by σ_o is obtained.

Aircraft experiments at 13.9 GHz conducted by NASA Langley have shown that the NRCS is wind speed and wind heading dependent. The sensitivity and magnitude of NRCS also depends on the incidence angle. See Figures 4.1-19 and 4.1-20. In general the magnitude of NRCS is larger when the radiated beam is vertically instead of horizontally polarized.

The typical size of resolution cells on the oceanic surface attainable by scatterometers on satellites is in the order of several kilometers. Thus, the satellite borne scatterometers are useful in determining oceanic wind fields and ice cover extent but not useful in mapping oil spills that are usually much smaller in size.

The scatterometer is capable of mapping a wide swath, in excess of 1000 km. To cover this swath. The antenna may be either a scanning pencil beam or a stationary fan beam. The scatterometer resolution cell size is determined by the antenna beam and electronic factors. With a pencil beam the cell size is determined the antenna beam width and the size decreases as the antenna dimension is increased. To fulfill a requirement for contiguous coverage, a narrower pencil beam antenna means that the antenna must scan azimuthally at a faster rate. With a fan beam type scatterometer the beam axis is oriented obliquely to the flight vector and the major dimension of the beam ellipse is aligned in the elevation plane. The resolution cell size in the azimuth direction is determined by the azimuth beamwidth of the antenna. In the elevation plane or range direction, the range position is determined by Doppler shift and the range cell resolution is determined by the Doppler spread. The use of narrow bond Doppler filters results in fine range resolution.

The technique employed to determine wind direction is based on the observation that the NRCS is greatest when observing the surface in the upwind direction and lowest when observing the surface in the cross wind direction (see Figure 4.1-19). Two measurements on each patch of seas differing in headings is usually sufficient

Figure 4.1-19

DOWNWIND σ^0_{vv} VERSUS WIND SPEED

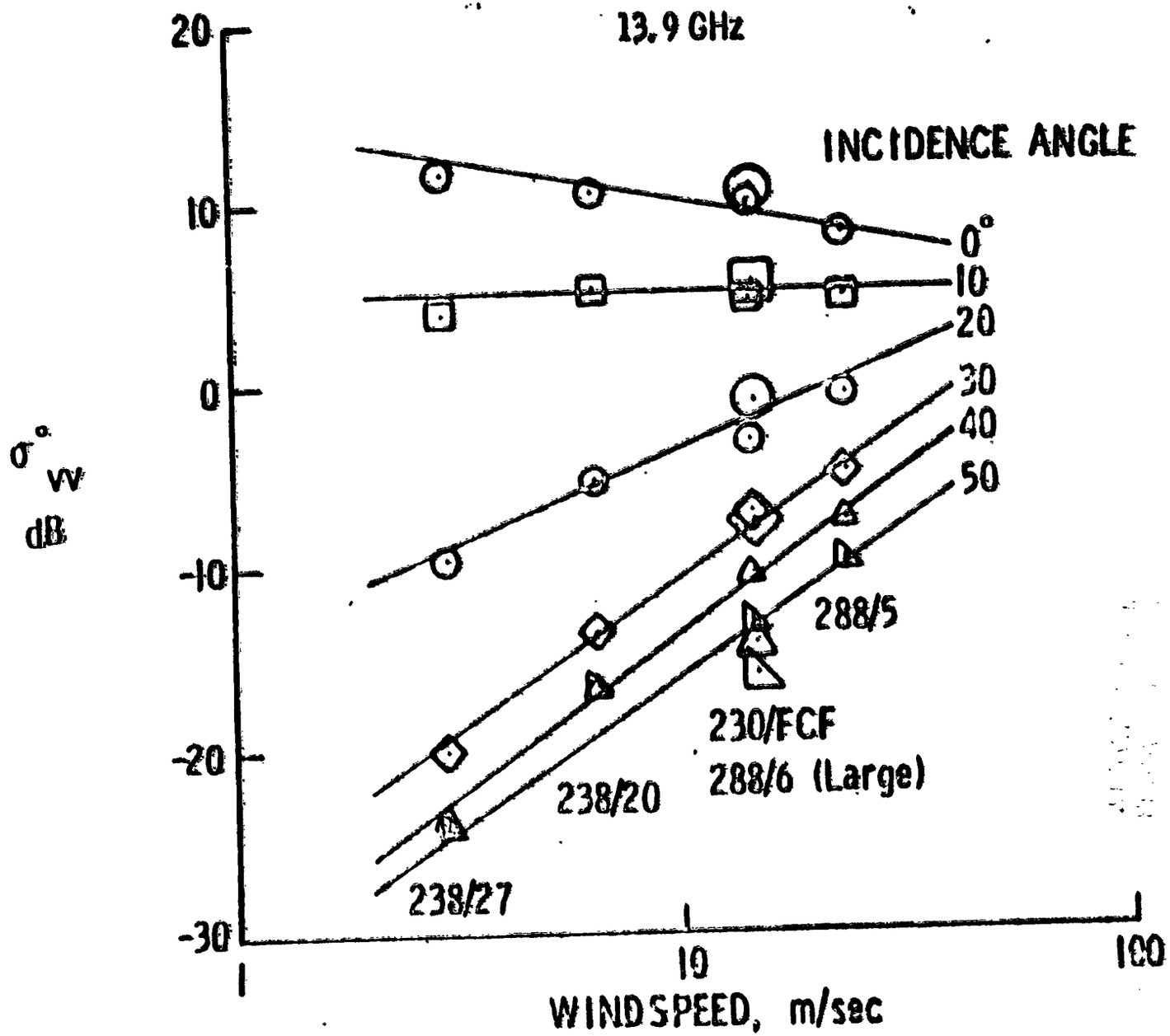

Figure 4.1-20

AAFE RADSCAT SCATTEROMETER WIND DIRECTION SENSITIVITY

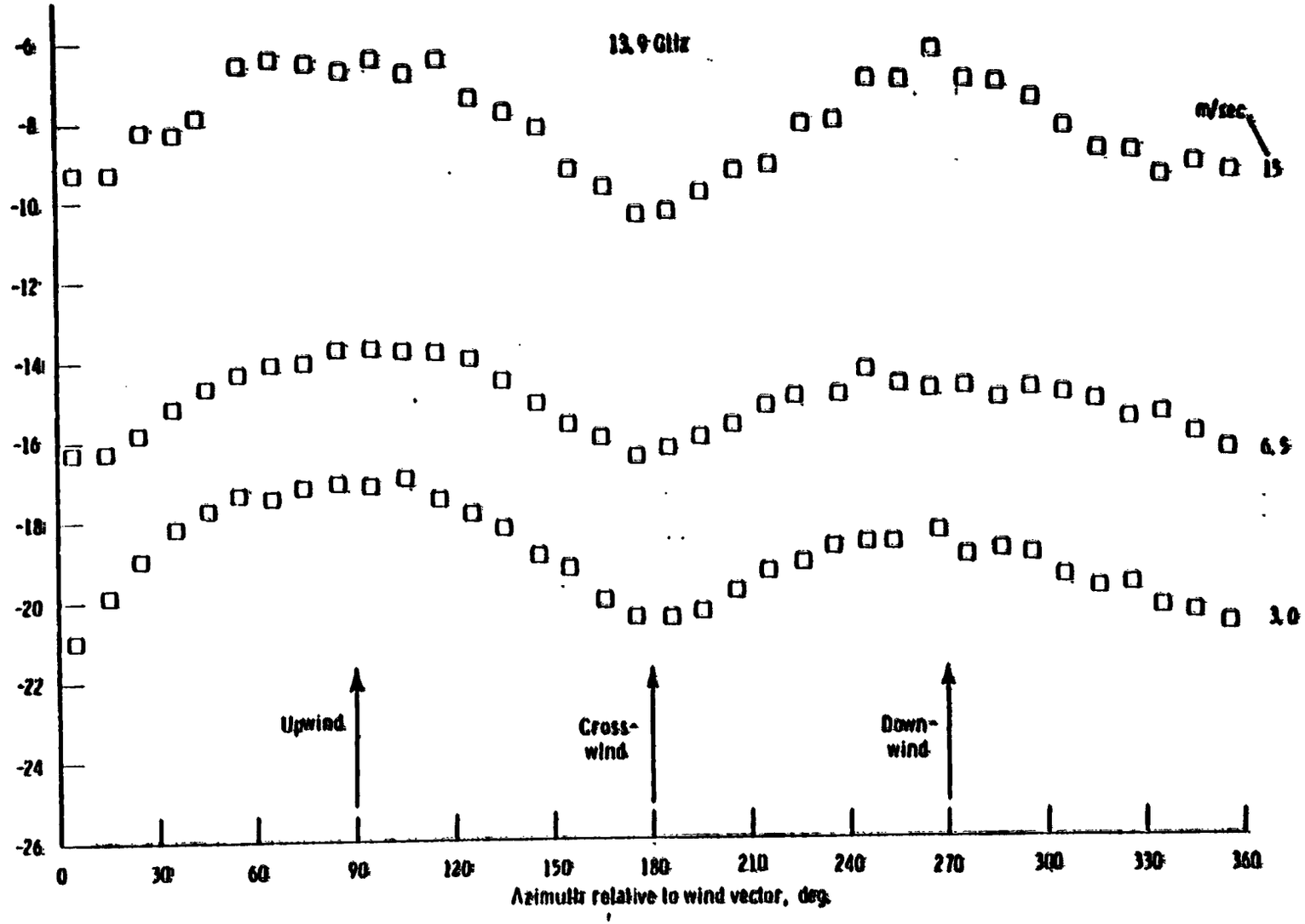

to determine wind direction except for a 180° direction ambiguity. Historical data sometimes can be employed to resolve the ambiguity. Additional beams differing in heading will uniquely determine the wind direction.

The fan beam scatterometer with four beams can map wide swaths but a central gap in coverage is produced. A method of mapping the central region has been proposed.[132]

The scatterometer can provide useful data almost all of the time except during heavy rainfall. During cloudy conditions and through moderate rain, the microwave signals suffer little in attenuation. When raining, the rain impacts the ocean surfaces, and significant efforts occur only during heavy rain.

Description of Sensor for Ocean Pollution Mission

The Microwave Scatterometer operates within the range of 13-14 GHz and is essentially a long pulse doppler radar operating in a beam-width-limited mode. It transmits 450 watt peak power pulses of 4.8 millisecond duration for a total of 14 pulses at each of the sequentially illuminated fan beam antenna footprints and draws approximately 135 watts from the spacecraft bus. The signal processor uses the doppler shift of the return pulses to separate the signal into equal length cells within the illuminated patterns.

Figure 4.1-21 shows the doppler frequency shift versus time, from the beginning of the transmit pulse, for the precursor to the Ocean Pollution Mission instrument, the Seasat-A-Scatterometer. It is shown, by this curve, that individually controlled range gates will improve performance by integrating the receiver outputs only at the time the return signal is present. It also shows that for some period

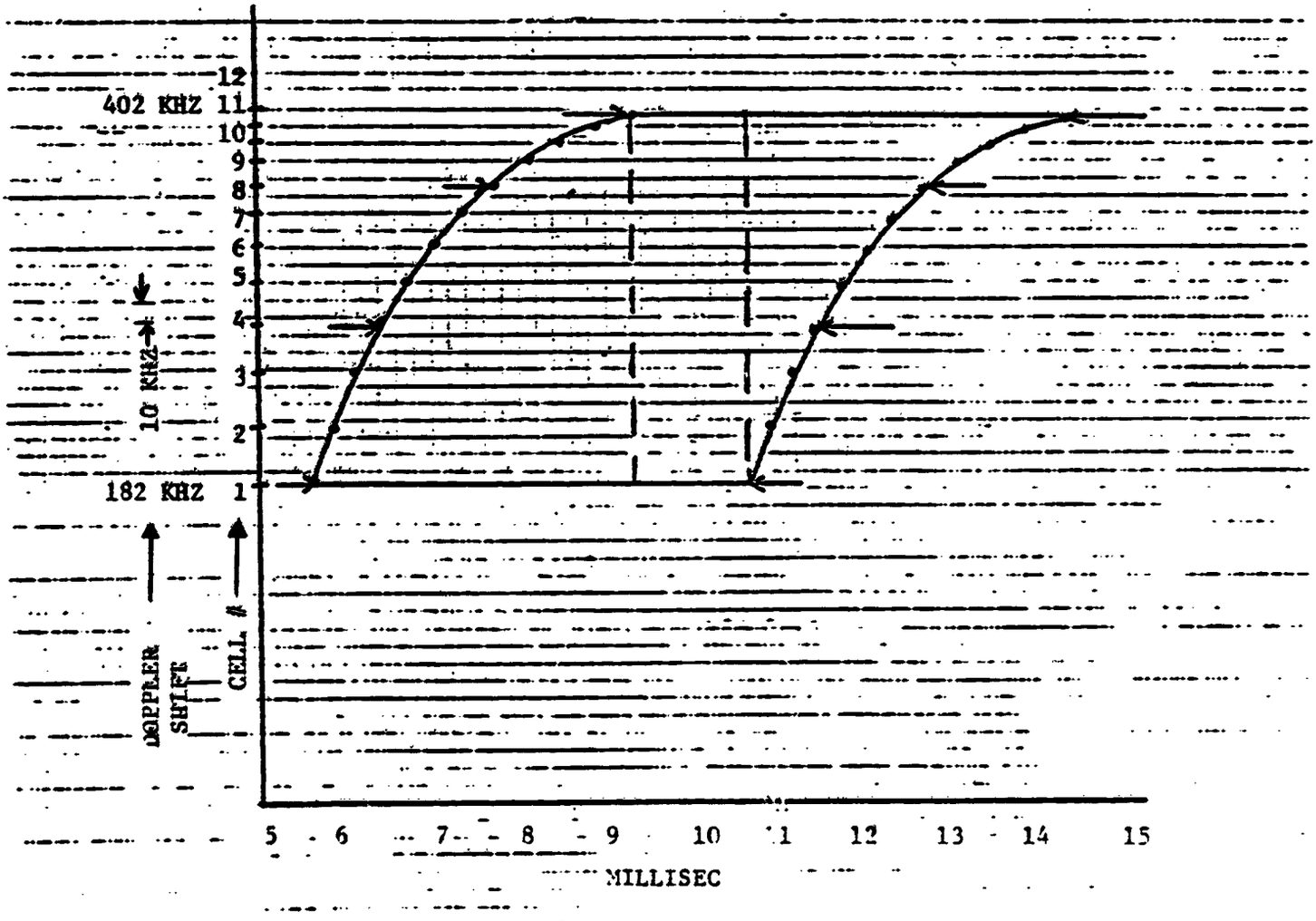

Figure 4.1-21. Seasat -A Scatterometer Doppler Return Vs. Time From Start of Transmit Pulse

of time, all doppler frequencies co-exist. These two factors indicate that Scatterometer performance is improved as orbit altitude and pointing angle control is tightened, as well as by incorporating some form of parallel signal processing.

Figure 4.1-22 is a functional block diagram of the microwave scatterometer. Two key features of this instrument are the calibration noise source for on-board, end-to-end, calibration of the receiver and signal processor and the frequency synthesizing technique of removing the sign of the doppler frequency shift to reduce the number of processing channels by a factor of two.

Performance Parameters

The overall performance of the scatterometer is determined by the K_p factor. This factor is equal to the normalized standard deviation or the standard deviation of the sigma-nought measurement divided by the mean of the measurement. The equation for evaluating K_p is:

$$K_p = \left[\frac{1}{B \tau_{sn}} \left(1 + \frac{2}{SNR} + \frac{\tau_g / \tau_s}{SNR^2} \right) \left(1 + \frac{\tau_g}{\tau_N} \right) \right]^{\frac{1}{2}}$$

where τ_{sn} = Noise integration Time
τ_s = Signal + Noise Integration Time
τ_g = Range gate time
B = Noise band width of Doppler filters
SNR = Signal/Noise ratio at detector.

The equation for the Scatterometer SNR is:

$$SNR = \frac{P_t \lambda^2 G_o^2 \left(\frac{G_n}{G_o}\right)^2 \phi L \sigma^o}{(4\pi R)^2 K T_s B L_s}$$

where:
P_t = Transmit power
λ = wavelength
G_o = PK antenna gain
G_n = Antenna gain at cell N
L = Length of resolution cell
ϕ = Antenna narrow 3-dB beamwidth
σ^o = Normalized scattering coefficient
R = Slant Range
K = Boltzmann's constant
T_s = System noise temperature
B = Doppler filter noise bandwidth
L_s = Total system losses from TWT output to receiver including atmospheric losses.

These two equations provide the basis for instrument level trade offs in optimizing mission performance.

Preliminary performance characteristics chosen for the instrument for this mission are shown on Table 4.1-4, along with those of Seasat A, for comparison purposes.

TABLE 4.1-4
PRELIMINARY SCATTEROMETER SENSOR CHARACTERISTICS

	Seasat	Ocean Pollution Mission
Assumed Altitude (km)	800	894
Resolution (km)	50	10
Wind Velocity Range (M/S)	4-24	4-24
Frequency (GHz)	14.6	13-14
Doppler Beams	12	65
Antenna Length (M)	3.04	3
Incidence Angles	25-55°	25-55°
Peak RF Power (W)	100	450
Duty Cycle (MS/MS)	6/30	6/27.5
Pulses Per Sample	61	14
Bus Power, (Watts DC)	135	500 (max)

Scatterometer Swath Coverage

The swath coverage of the Scatterometer is determined by the spacecraft altitude, antenna pointing azimuth, and the angle between the minimum and maximum acceptable earth incidence angles. The normal operating range for the Scatterometer is for earth incidence angles from 25° to 55° as shown in Figure 4.1-23. Some additional data can be obtained from 55° to 65° earth incidence angles but only at the higher windspeeds. Figure 4.1-23a shows the swath coverage and antenna footprints from a spacecraft altitude of 900 Km.

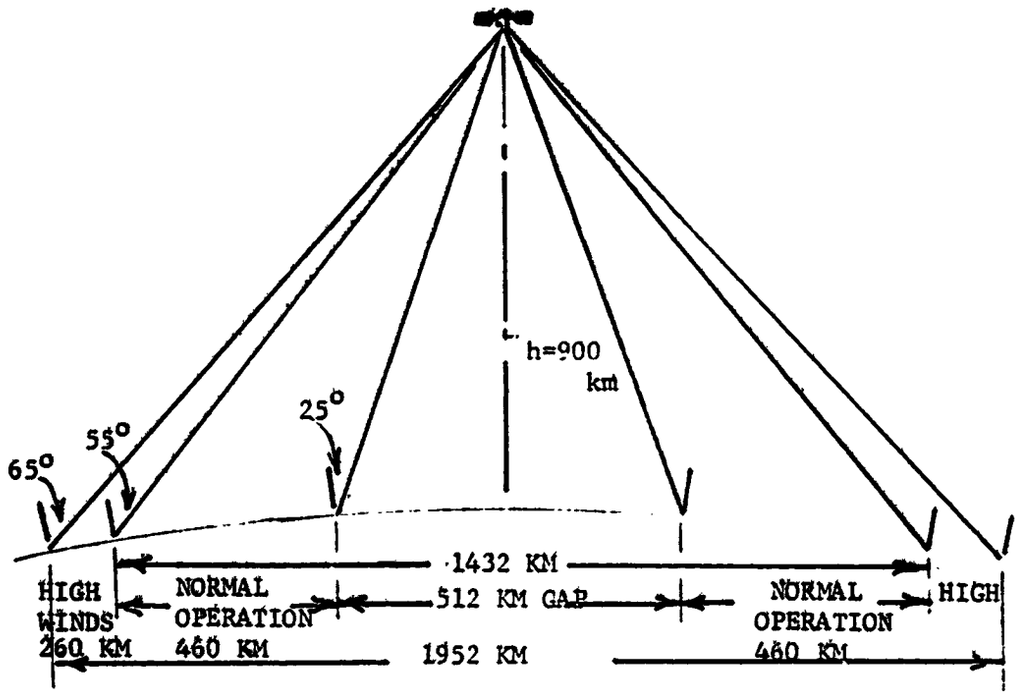

Figure 4.1-23 Scatterometer Incidence Angles

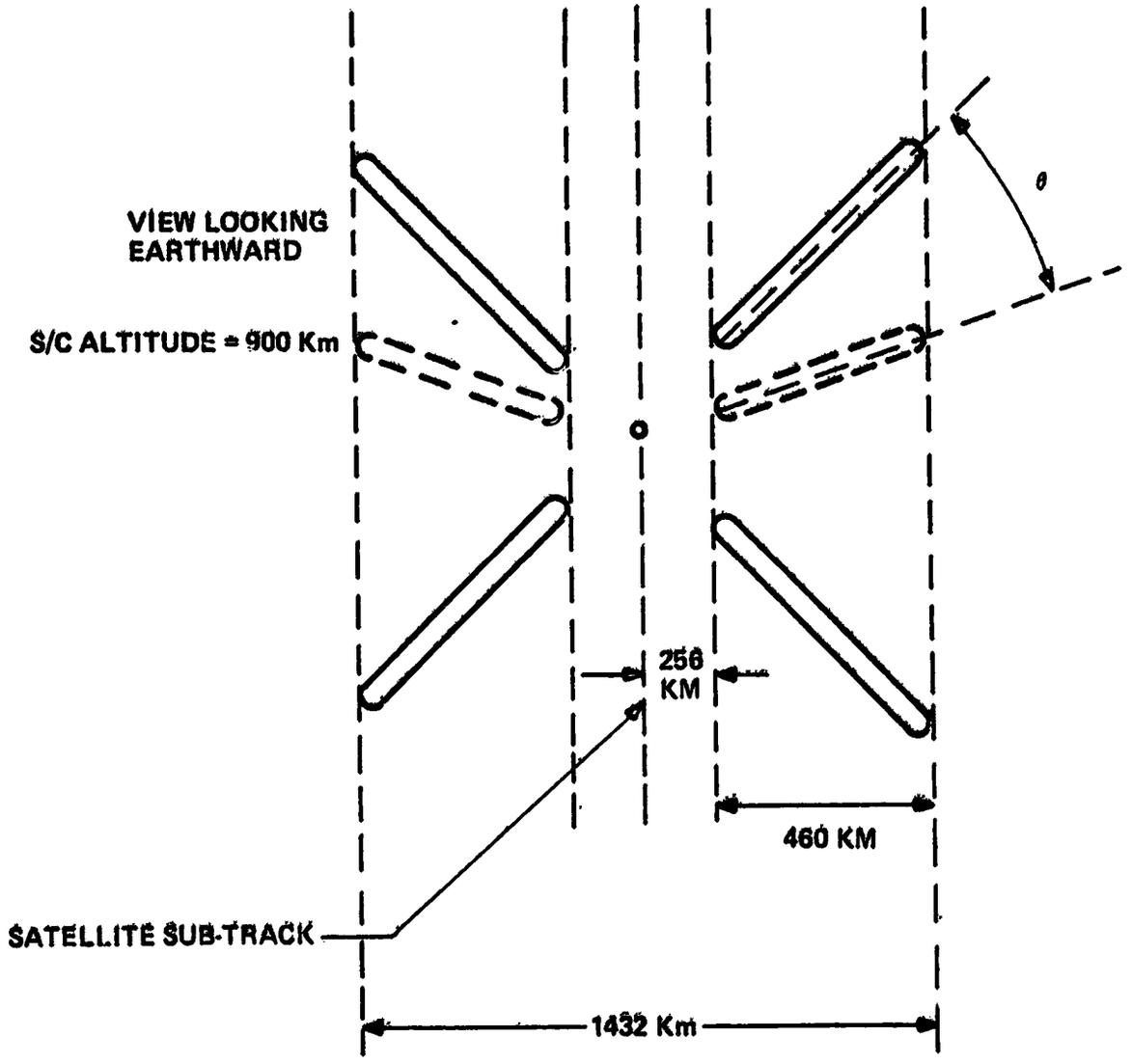

Figure 4.1-23a. Scatterometer Swath Width Coverage

Assessment of Sensor Suitability

Filter A: Is the relationship between observable and measurement well developed?

Yes; Algorithms have been developed for use on the Seasat-A-Scatterometer data which will provide wind speed directly and wind direction with up to four aliases. Recent studies show that wind direction aliases can be removed through the addition of two fan beam antennas, one for each side of the spacecraft.

Filter B: Is there sufficient sensitivity from orbit?

Yes; There will be sufficient sensitivity from orbit when the required modifications to re-existing (Seasat) design have been implemented, as described in "C" below.

Filter C: Can the sensor meet the user performance requirements?

Yes; With the following instrument modifications.

- o Improved antenna gain
- o Additional stick antenna on each side
- o Lower receiver noise temperature
- o Signal Processing and Timing modified.

Filter D: Are the required Wt. Vol. and power compatible with near-term satellite Systems?

Yes; Based on the Seasat and proposed NOSS designs.

Technology Implications

The hardware technology that needs to be developed for future scatterometers is that of digital signal processing. This type processing would provide the flexibility and resolution required for the Ocean Pollution mission.

4.1.2.3 Passive Microwave Radiometer

Parameters Measured

The primary function of the Microwave Radiometer is to measure the radiometric brightness Temperature (T_b) for the horizontal and vertical polarization components for each of five frequency ranges. These observations are made coincident in time and space at an earth incidence angles of $50^{\circ} \pm 1.5^{\circ}$.

Oil Thickness measurements is a very useful potential application of microwave radiometry, however, the spatial resolution limitations make it unsuitable for space measurement (see "Sensor Description").

Algorithms have been developed to convert this matrix of measurements for each cell into many geophysical parameters. The geophysical parameters measured by the Microwave Radiometer that can be used in the ocean pollution trajectory model are Ocean Surface Wind Speed, Ice Cover Extent, Ocean Surface Temperature and Precipitation.

The most stringent requirements for these parameters specified by the users are as follows:

	Wind Speed	Ice Cover	Surface Temp	Precipitation
Precision	0.5 m/sec	10 m/sec	0.5°C	*
Accuracy	2.0 m/sec	2 m/sec	1°C	*
Range	0 - 50	0 - 100	-2° to 30°C	*
Frequency (every N-hrs)	3	3	24	*
Delay (hrs)	3	3	6	6
Spatial Resolution	10	10	10	10

*Not Specified

Sensor Description - Theory of Operation

Radiometry is based on the observation that an object, or ocean surface, at absolute temperature T_o with surface emissivity E greater than zero emits noise like thermal radiation at all wavelengths. A radiometer is a very sensitive microwave receiver with a scanning narrow beam antenna. See Figure 4.1-24. The radiometer measures the apparent temperature T_a which is equal to the product ET_o. The ocean surface emissivity decreses as its surface becomes smoother. NRL has reported on the detection of oil spills with radiometer by an increase in T_a above that of the surrounding sea surface. Radiometry has proven useful in detecting precipitation since liquid water is electrically lossy at microwave frequencies and it has a finite value of emissivity. With an increase in precipitation rate. The apparent emissivity of the total rainfall intercepting the antenna beam will increase and it can be detected. The radiometer can also provide information on oceanic wind speed, sea ice extent and sea surface temperature.

The emissivity E of an arbitrary object has a value from zero to unity. A surface like that of the ocean has an emissivity which is a function of its roughness, its physical temperature, the complex dilectric constant, the beam incidence angle, the beam polaization, and the radiometer frequency. The temperature resolution in T or sensitivity of a Dicke radiometer is given by

$$T = \frac{2\,T_s}{\sqrt{B\,t_d}}$$

where T_s = system noise temperature

B = RF noise bandwidth

t_d = post detection integration time.

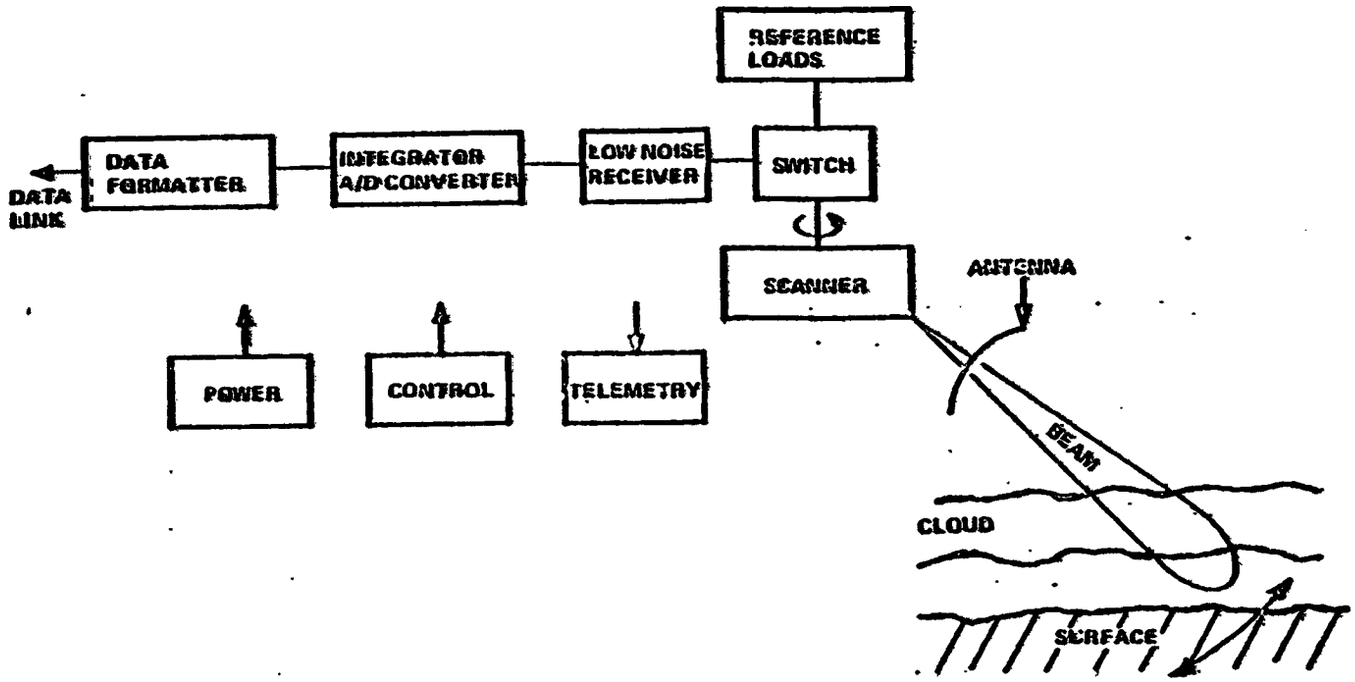

Figure 4.1-24 Passive μw Radiometer Block Diagram

In general, an object emits and also reflects thermal radiation. Thus if the atmosphere intervening between the radiometer and ocean surface is lossy for example due to rain, the rain will attentuate the signal emanating from the ocean surface and the rain itself will emit thermal radiation. The radiometer will yield an apparent temperature given by the radiative transfer equation:

$$T_A = t_a (E T_o + R_o T_a) + (1 - t_a) T_R$$

where t_a = atmospheric transmissivity, $0 \leq t_a \leq 1$

E = surface emissivity, $0 \leq E \leq 1$

R_o = power reflectivity of the ocean surface $0 \leq R_o \leq 1$

T_a = equivalent radiation temperature incident on the ocean surface

T_R = absolute temperature of the rain

T_o = absolute oceanic temperature

The apparent temperature T_A is dependent on the radiometer frequency, antenna beam polarization and beam incidence angle. The first term on the right is the radiation emanating from the ocean surface and the second term is that from the rain.

Microwave radiometers have been used to correlate oceanic wind speed to the apparent radiometric or brightness temperature. An example of this relationship is shown in Figure 4.1-25 for a radiometer operating at 1.55 cm wavelength. It is noted that foam effects occur at the higher wind speeds.

The choice of radiometer wavelengths has a profound effect on measurement utility. Because the radiometric temperature depends on a few factors, it becomes necessary to use a multi-frequency radiometer to help in the

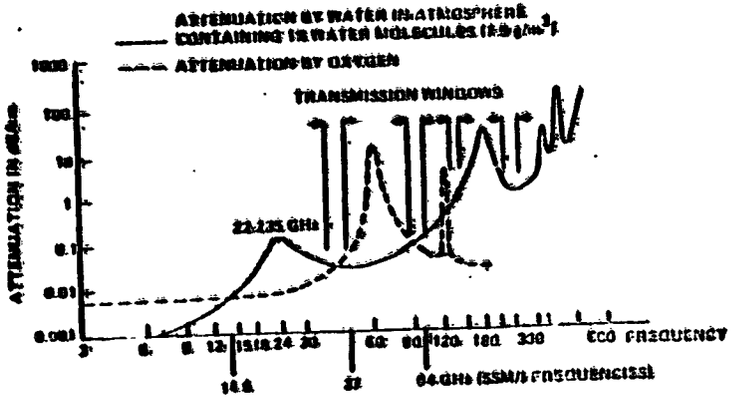

Atmospheric Attenuation of Microwaves Due to Water Vapor and Oxygen

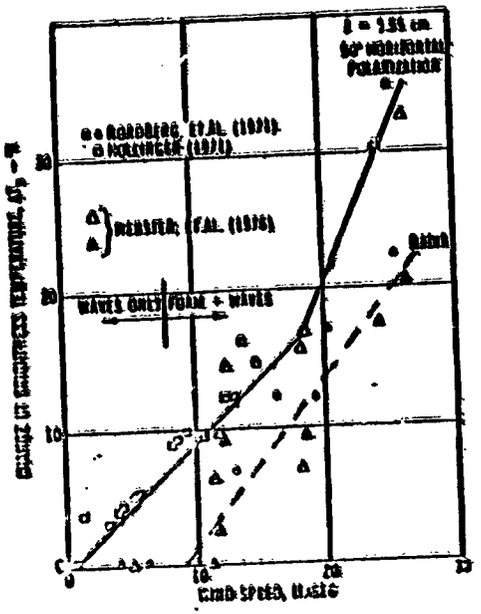

Change in Microwave Brightness Temperature vs. Wind Speed

Figure 4.1-25 Atmospheric Attenuation & Wind Effects Influencing Passive Microwave Radiometry

separation or identification of the various contributing geophysical parameters. The atmospheric attentuation and hence atmospheric emission of microwave signals due to water vapor and oxygen is also shown in Figure 4.1-25. The radiometer frequencies of signals that are most likely to observe the ocean surface are below 15 GHz and in the 37 GHz and 94 GHz "windows". Liquid water attenuates microwave signals at all frequencies and the amount of attenuation increases monotonically with frequency.

The NRL has successfully reported on the detection of oil spills using radiometer mounted in an aircraft. The aircraft was flown at a low altitude and this resulted in a short range and in a small beam spot size. The two radiometers operated at 19.3 and 31.0 GHz. A controlled oil spill was produced and the aircraft was flown over the spill. The increase in radiometric brightness temperature was measured over the spill and the results are shown in Figure 4.1-26. Also shown in the Figure are a photographic outline of the oil slick and an oil thickness contour. It is seen that the radiometers were responsive to only the thicker regions of the oil spill. The very thin oil film called "sheen" which was noted in the photograph did reveal that some "smoothing" of the surface occurred due to the oil. While the sheen was not observable by radiometry, it could be observed by a synthetic aperture radar.

A limitation of satellite borne microwave radiometry is its relatively large beam footprint and hence coarse spatial resolution due to the long slant range. Attempts to achieve fine resolution require the use of large antennas. A graph depicting the relationship between frequency, antenna size,

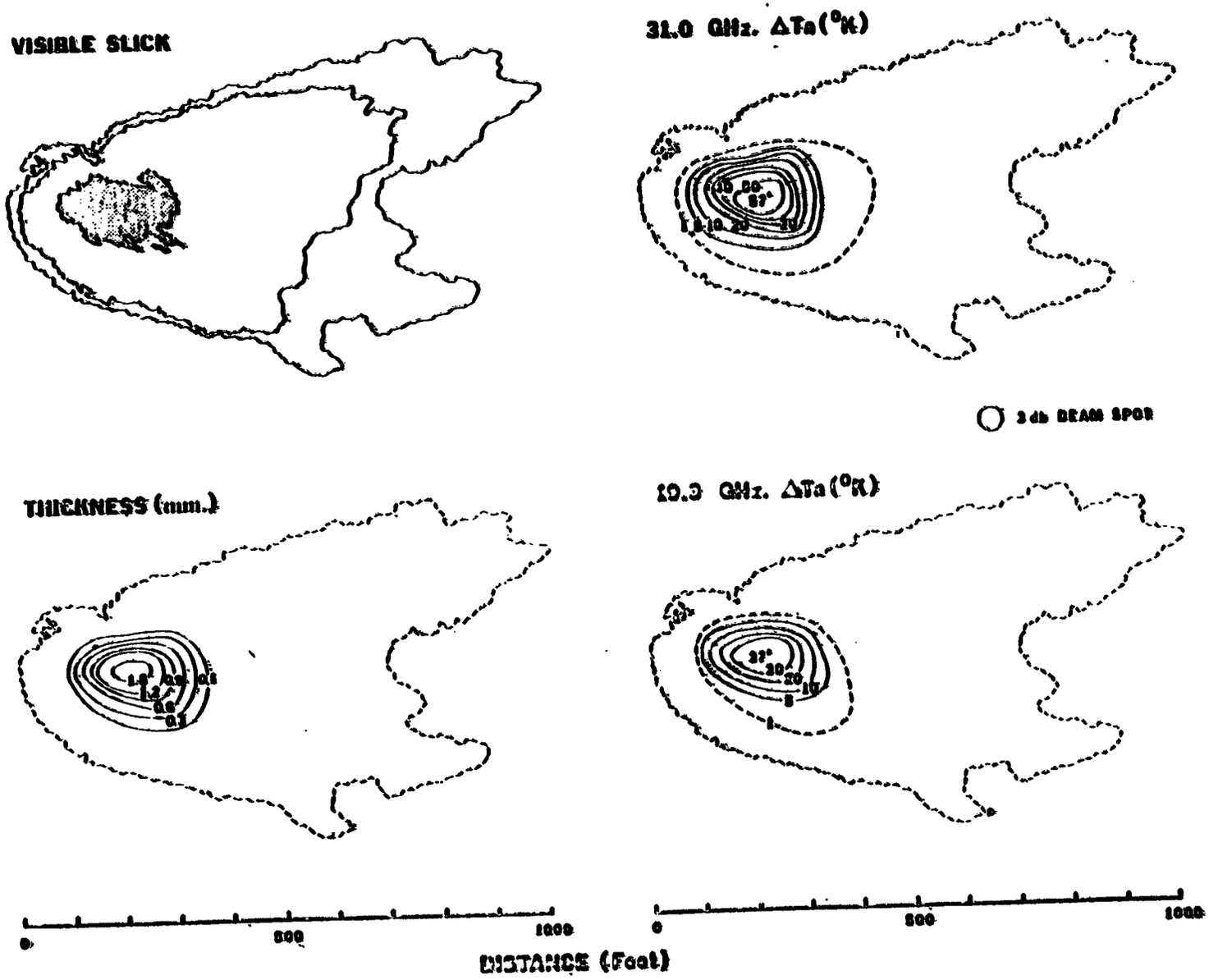

Data by J. P. Hollinger, NRL

Figure 4.1-26 Oil-Thickness Contours Based on △Brightness T

antenna beamwidth, slant range and circular footprint size is shown in Figure 4.1-27. In geometries where the circular footprint size approaches the antenna size D, the range to the scene becomes comparable to the far zone distance, $2D^2/\lambda$ where λ is the wavelength

For the geometries where the range to the scee is appreciably less than 2 , the antenna is focused in the near zone. Under this condition, there is a depth of focus associated with the geometry so that the focus may have to be adjusted across the field of view. With constant incidence angle scanning. The slant range is fixed and the focus does not require adjustment.

Briefly a microwave radiometer operated from a satellite, offers the capability of detecting the extent of ice cover and inferring ocean surface wind speed, ocean surface temperature and precipitation. A microwave radiometer borne in an aircraft can be used to detect oil spills and to quantify the oil if the thickness is greater than about 0.1 mm. An ambiguity in thickness occurs with increased sea state conditions.

Sensor Description for Ocean Pollution Mission

The Microwave Radiometer consists of a scanning 3.3 M aperture antenna followed by ten low noise, wideband receivers operating at 4.3 GHz, 10.65 GHz, 18.7 GHz, 21.3 GHz and 36.5 GHz. There are two separate receivers at each frequency to accommodate the horizontal and vertical components of the radiometric signal. The dual channel receivers/signal processors operate as total power radiometers with cold sky and hot load calibrations before and after each data scan. Figure 4.1-28 is a functional block diagram of the instrument.

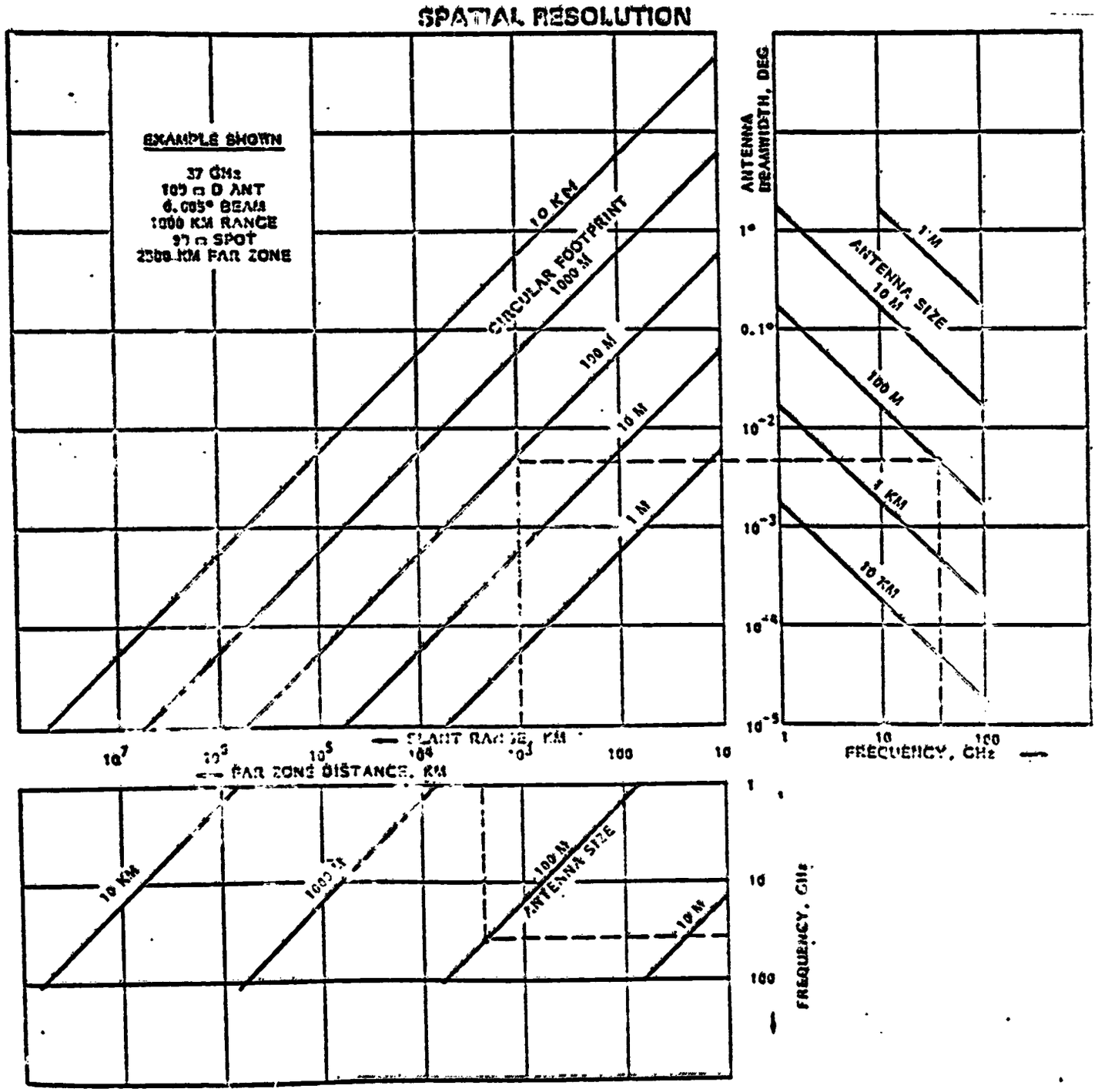

Figure 4.1-27 Passive Microwave Radiometer Performance Parameters

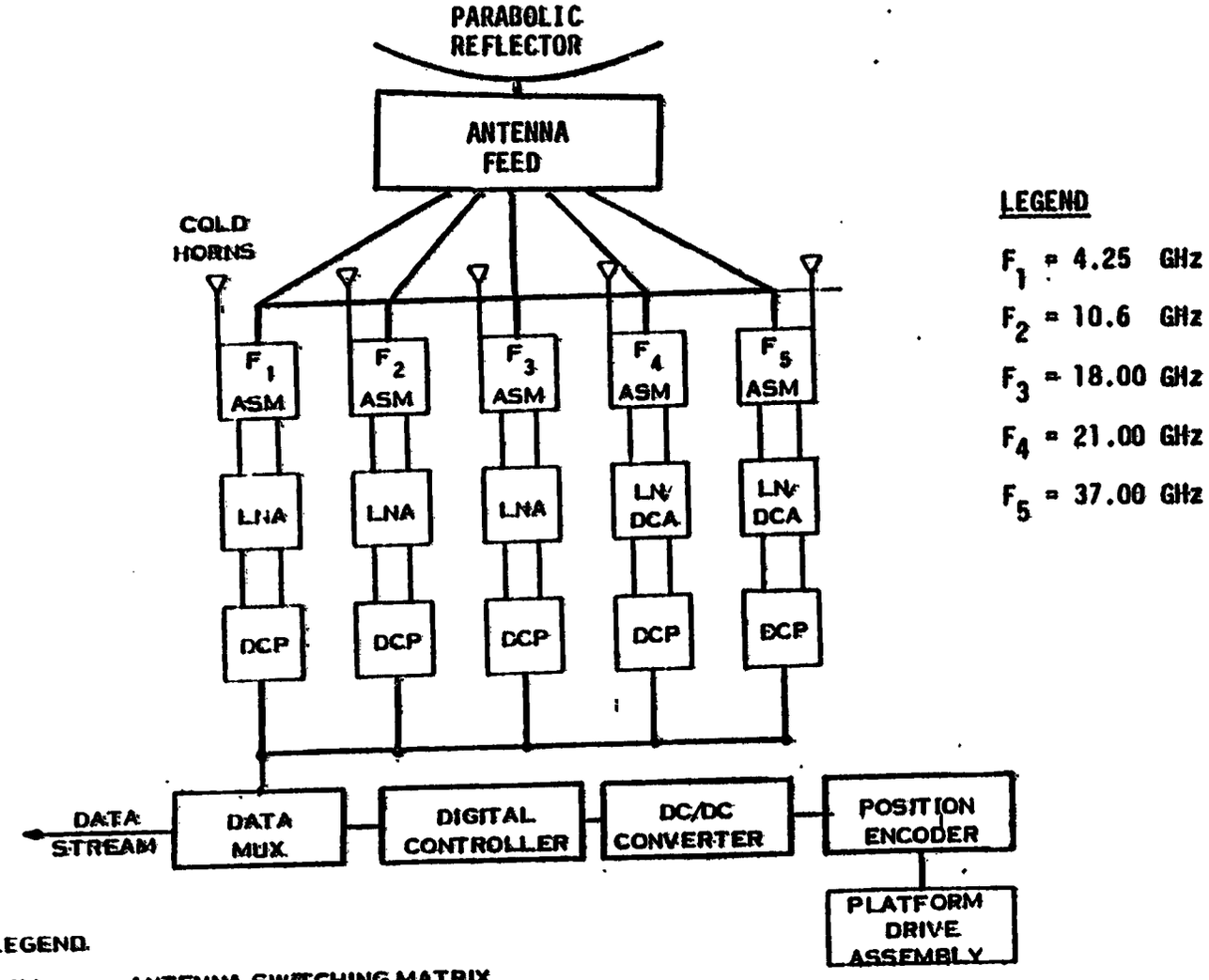

Figure 4.1-28 Microwave Radiometer Block Diagram

PERFORMANCE PARAMETERS

The overall performance of the Microwave Radiometer is determined by the end-to-end system ΔT is the minimum detectable change (or resolution), in radiometric rightness. The end-to-end system ΔT includes measurement accuracy of the sensor andthe accuracy with which the antenna pattern corrections can be made.

The equation for evaluating the instrument ΔT is:

$$\Delta T = T_s \left[\frac{1}{B\tau} + \left(\frac{\Delta G}{G} \right)^2 \right]^{\frac{1}{2}}$$

where: T_s = System Noise Temperature

B = Radiometer Bandwidth

τ = Integration Time

$\frac{\Delta G}{G}$ = Gain Stability Factor

The factors affecting the antenna pattern correction accuracy are:

- Spill over
- Side lobes
- Cross Polarization
- Knowledge of scene radiometric temperature observed by spillover and side lobes.

The factors of instrument T and Antenna Pattern correction provide the basis for end-to-end system level trade-offs for optimzing mission performance.

Table 4.1-5 shows representative parameters for a radiometer suitable for the ocean pollution mission. The instrument's spatial resolution for the 4.25 GHz channelused in ocean temperature is larger than the required 10 Km for that measurement. A much larger antenna dn some increasein power would be required to implement this 10 Km requirement for ocean temperature.

RADIOMETER SWATH COVERAGE

The swath coverage of the Microwave Radiometer is determined by the spacecraft altitude, the earth incidnce angle and the sector angle during the data taking portion of the scan. Table 4.1-6 shows the swath coverage for six spacecraft altitudes and two aximuth scans at a fixed earth incidence angle ($_i$). Figure 4.1-29 defines the terms used for the table.

TABLE 4.1-6 RADIOMETER SWATH COVERAGE

ALTITUDE	θ_i EARTH INCIDENCE	θ_N NADIR ANGLE	SWATH WIDTH 120°SECTOR	SWATH WIDTH 180°SECTOR
650 Km	50°	44.043°	1147 Km	1324 Km
700 Km	50°	43.653°	1221 Km	1410 Km
750 Km	50°	43.270°	1295 Km	1495 Km
800 Km	50°	42.896°	1366 Km	1578 Km
850 Km	50°	43.529°	1437 Km	1659 Km
900 Km	50°	43.169°	1505 Km	1738 Km

ASSESSMENT OF SENSOR SUITABILITY FILTER A:

Is the relationship between observable and measurement well developed?

Yes; Algorithms have been developed for use on the SeaSat-A SMMR data which will provide the four geophysical parameters desired.

Filter B: Is there sufficient sensitivity from orbit:

Yes; There is sufficient sensitivity from orbit when the conditions described under Filter C are met.

TABLE 4.1-5

MICROWAVE RADIOMETER PARAMETERS AND COMPARISON WITH SEASAT-SMMR AND NOSS-LMMR

PARAMETER DESCRIPTION	NOSS	SEASAT	OCEAN POLLUTION
ALTITUDE	700	800 KM	900 KM
SCAN ANGLE FROM SATELLITE SUB TRACK	±600	± 25°	± 60°
SWATH WIDTH	1221	643.6 KM	1676.0 KM
FREQUENCIES	6.63, 10.69, 18,21,31 GHz	6.63, 10.69, 18, 21, 37 GHz	4.25, 10.69, 18,21,37GHz (1.4 & 91 GHz OPTIONAL)**
POLARIZATION	V&H	V&H	V&H
SPATIAL RESOLUTION @ 37 GHz	7.2	21 KM	* 10 KM
ANTENNA APERTURE	3.6	0.79 M	3.3 M
NADIR ANGLE	43.7°	42°	45°
EARTH INCIDENCE ANGLE	50°	48.8°	53.8°
BUS POWER (AVG.)	300 WATTS	61 WATTS	250 WATTS

* REFLECTOR UNDER ILLUMINATED @ 37 GHz

** NOT REQUIRED FOR MOPS

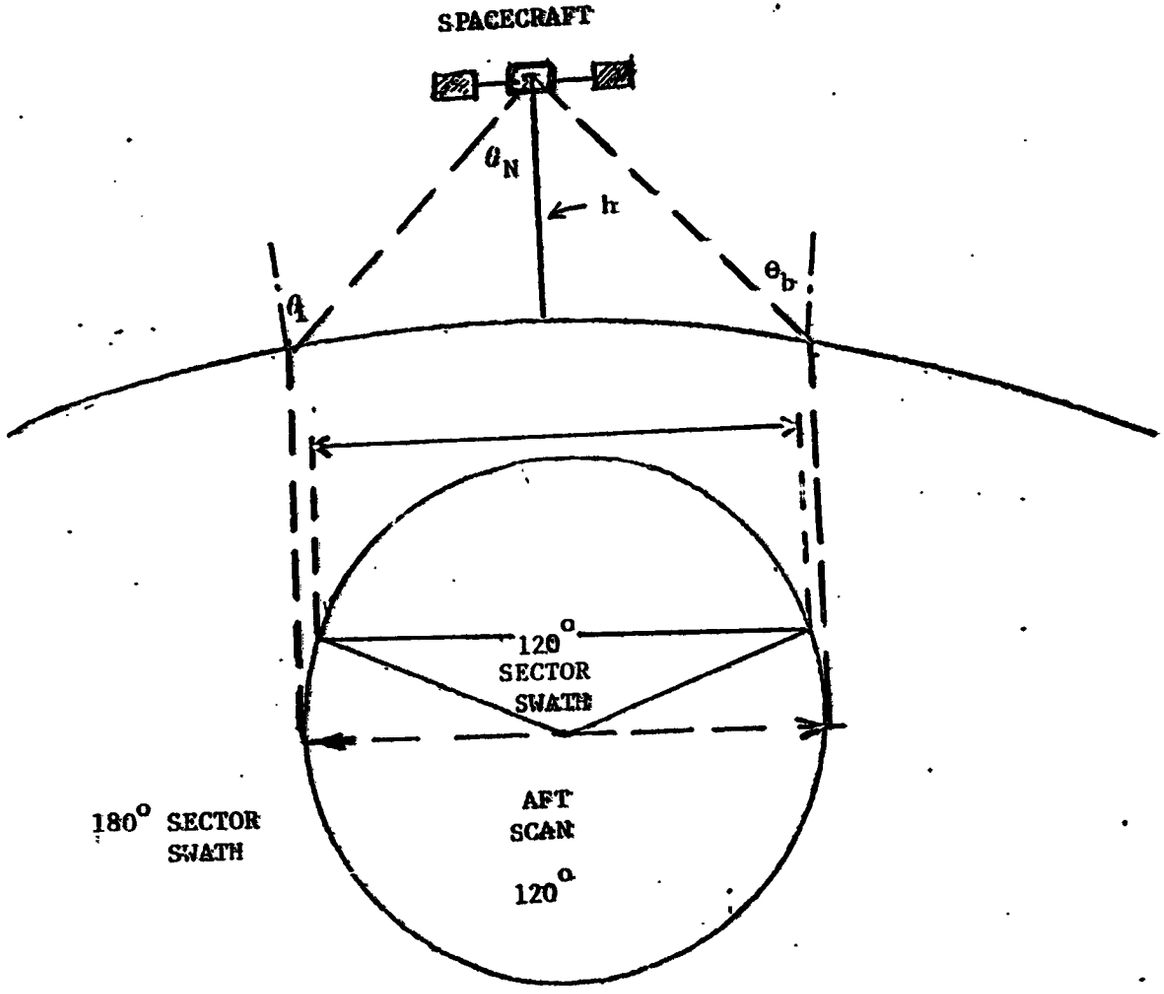

Figure 4.1-29 Microwave Radiometer Coverage

Filter C: Can the sensor meet the user performance requirements?

Yes; Under the following conditions.

- The microwave Radiometer data is used synergistically with the scatterometer data for the wind speed measurement.
- Full advantage must be taken of the antenna's 4 meter aperture (i.e.reflector is not under illuminated) to meet the 5 Km spatial resolution required for the Ice Cover-Extent.

Filter D: Are the required weight, volume and power compatible with near-term satellite systems?

Yes; Based on SEASAT & NOSS designs.

TECHNOLOGY IMPLICATIONS

The hardware technologies that need to be developed for the LAMMR are:

- Multi-Frequency Antenna Feed and Reflector Design to meet beam efficiency requirements.
- The implications of rotating a large antenna reflector at approximately 60 RPM with stringent requirements on mechanically and thermally induced distortions, must be carefully investigated.

4.1.2.4 Microwave Altimeter

Parameter Measured

The primary function of the Microwave Altimeter is to measure the pulse round-trip time and shape. These measurements are made at the satellite subtrack and are combined to provide one-second averages for the parameters measured.

The geophysical parameters measured by the Microwave Altimeter that can be used in the ocean pollution trajectory model are significant wave-height and ice thickness (inferred from altitude measurements) other parameters that can be determined by the altimeter measurements are ocean surface wind speed (at Nadir) and ocean currents.

The user requirements for the geophysical parameters measured by the altimeter are shown below:

	Ocean Current Speed	Ice Thickness	Significant Wave-Height
Precision	5 cm/sec	0.2 m	0.3 m
Accuracy	5 cm/sec	0.5 m	0.3 m
Range	0-300 cm/sec	0-50 m	0-25 m
Frequency (every N hrs)	6	24	3
Delay (hrs.)	3	6	3
Spatial Resolution	10 km	5 km	10 km

Sensor Description - Theory of Operation

A microwave altimeter is a non imaging radar capable of measuring range with extreme precision. With its antenna beam pointed towards nadir, the sensor borne in a satellite measures the distance between satellite and ocean surface. The high precision radar effectively emits a pulse of very short duration, and if the ocean surface is rough in its physical features the return pulse will have a more

gradual rise time and longer return pulse due to the "depth" of its surface. In this manner the microwave altimeter is capable of measuring the sea state, or significant wave height, designated as H 1/3. The deterministic orbit or ephemerides of the satellite can be calculated with high precision. Because of this precision, it is possible to detect fairly abrupt changes in the ocean surface elevation caused by ocean currents such as the Gulf Stream.

A diagram illustrating the effect of sea state on the return-pulse risetime characteristic is shown in Figure 4.1-30. If the sea state is low, the risetime shape will be fairly abrupt as shown by the curve labelled "0 rms waveheight". As the sea state increases in roughness, the risetime shape will become more gradual like the curve labelled 4 rms waveheight. Knowledge of the sea state can be utilized to indicate the degree of mixing of any oil spill and possibly predict the oil fate. Sea state information also can provide confirming data on oceanic wind speed at nadir.

Fairly extensive studies to investigate Gulf Stream activity using a satellite borne altimeter have been conducted by NASA Wallops. The presence of ocean currents is manifested by a change in oceanic surface slope along the cross-stream direction. The current velocity V_c is given by:

$$V_c = \frac{G}{F} \frac{H}{x}$$

where G = gravitational constant
F = Conolis parameter
H = surface height
x = cross-stream direction

By mapping the Gulf Stream area from many satellite passes differing in ground track, the ocean current characteristics have been recorded. Single satellite passes extending for a period of about one month have been necessary for this characterization.

FIGURE 4.1-30

FORMATION OF PROCESSING GATES FROM ALTIMETER WAVEFORM SAMPLES

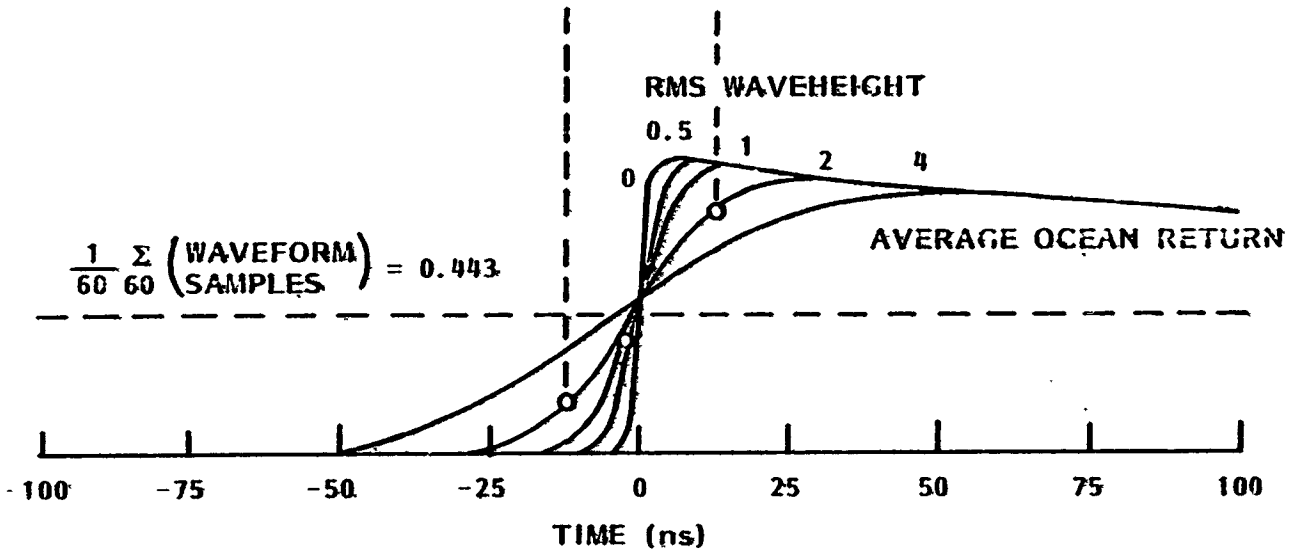

Sensor Description - Ocean Pollution Mission

The Microwave Altimeter for this application operates at 13.5 GHz ± 160 MHz and is essentially a short pulse, chirpped radar operating in a pulse-width-limited mode. It transmits 2 kilowatt pulses, chipped over a 320 MHz bandwidth at a 1020 Hz pulse repetition frequency. The signal processor uses digital filter techniques to provide 60 samples, separated by 3.125 nanoseconds of each return pulse in order to determine the return pulse shape.

Figure 4.1-31 illustrates the pulse limited illuminated area and a typical return pulse shape.

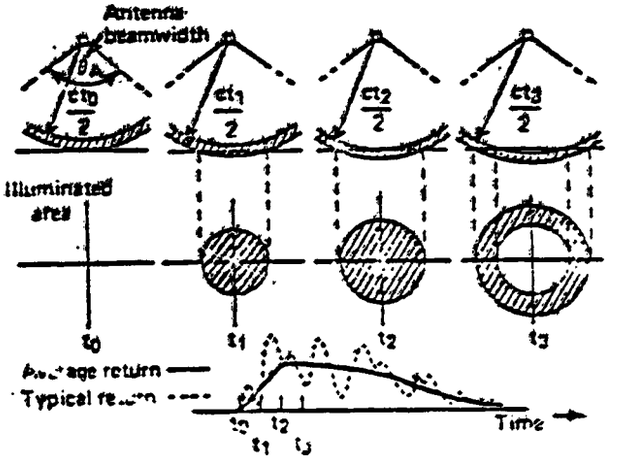

Figure 4.1-31 Pulsewidth Limited Geometry

Figure 4.1-32 is a functional block diagram of the Microwave Altimeter. One of the key features of this instrument is the utilization of the "full-deramp" technique where no compression filter is required in the receiver but, instead, a properly timed local oscillator pulse is generated that duplicates the linear - FM ("chirp") modulation of the transmit pulse.

Figure 4.1-33 shows the configuration of the Altimeter flown on Seasat-A as well as its heritage. It is highly probable that a similar Altimeter will fly on the NOSS spacecraft.

GENERAL ELECTRIC

space division

FIGURE 4.1-32
ALTIMETER BLOCK DIAGRAM

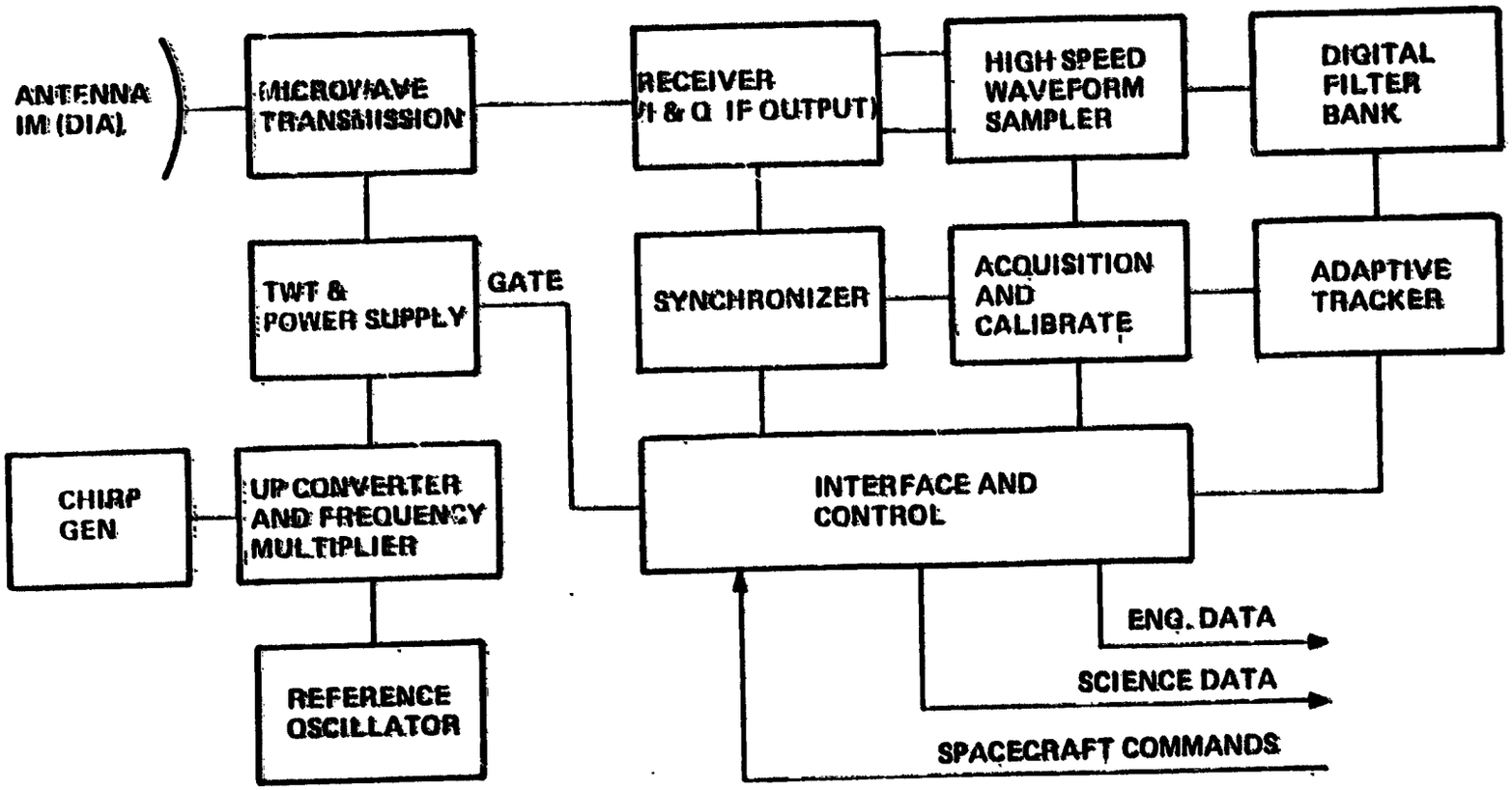

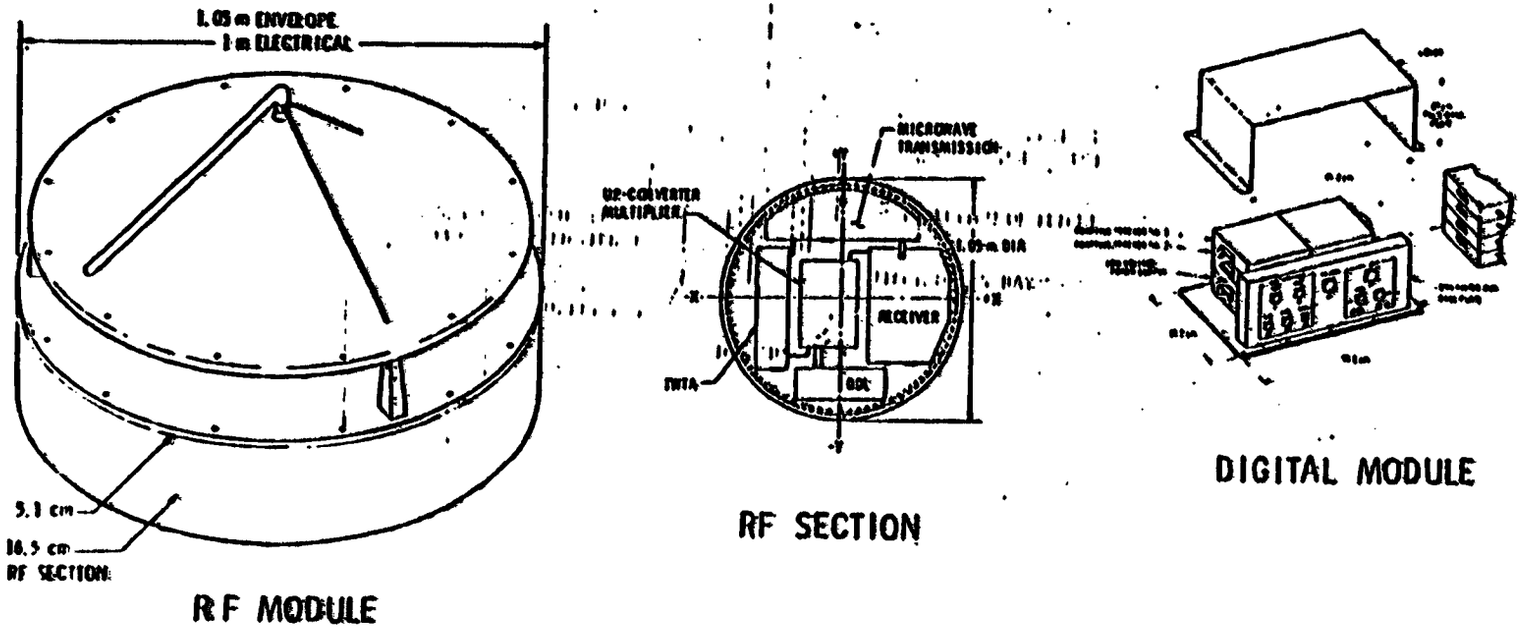

HERITAGE:SKYLAB,GEOS C, AAFE

Figure 4.1-33 Seasat Radar Altimeter Package Configuration

Performance Parameters

The Microwave Altimeter performance is determined by the σ_h factor which is defined as height noise. The equation for height noise performance as a function of signal to noise ratio is included below and a plot of this equation is shown in Figure 4.1-34

$$\sigma_h = \frac{\sigma_p}{0.8\, N_g H} \left[1 + \frac{1}{SNR}\right]$$

where:

σ_h = height noise (in meters),

$\sigma_p = \sqrt{(N_g \sigma_T)^2 + \sigma_s^2}$

N_g = number of gates combined to form tracking gate,

σ_T = system ...nt target resolution 0.426 cT,

T = 3.125 ns,

c = speed of light = 3×10^8 m/s,

σ_s = rms waveheight (in meters)

H = number of independent measurements equals PRF x avg time, and

SNR = power signal-to-noise ratio.

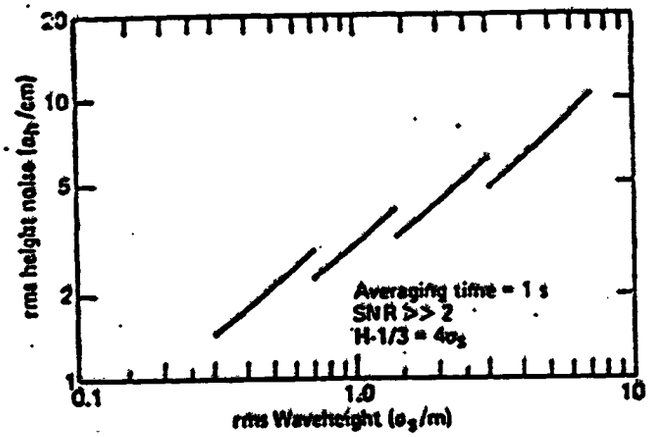

Figure 4.1-34 Inherent Precision Capability versus Waveheight

Assessment of Sensor Suitability

Filter A: Is the relationship between observable and measurement well developed?

Yes; Algorithms have been developed for use on Seasat-A data which will provide significant waveheight (H 1/3) and ice thickness and ocean currents as inferred by small variations in apparent spacecraft altitude.

Filter B: Is there sufficient sensitivity from orbit?

Yes; but with the limitations described in Filter C.

Filter C: Can the sensor meet the user performance requirements?

Partially; The sensitivity is adequate for measuring significant waveheight (H 1/3) and somewhat marginal for ocean current and ice thickness. Spatial resolution is the biggest limitation, since the instrument is a "spot" detector with nadir pointing.

Filter D: Are the required Wt. Vol. and power compatible with near-term satellite systems? Yes.

4.1.3 ASSESSMENT OF OPTICAL SENSORS AND SENSING TECHNIQUES

Oceanic pollution originating from oil spills and domestic/industrial waste disposal, were analyzed relative to remote sensing in the UV/Visible/IR spectrum. The principal applications examined dealt with the detection, mapping of the areal extent (and boundaries), and species identification relative to oil spills and waste dumps. With respect to pollutant quantification, measurement of the thickness of oil spills, as well as the concentration of waste pollutants were examined.

As a preface to the discussion of specific sensors and sensing techniques, we are presenting a brief summary of the general capabilities and limitations inherent in optical of sensing of ocean pollution parameters.

Atmospheric Attenuation Effects

The spectral atmospheric transmission over a path length corresponding to the total effective atmosphere is compared to that along slant ranges occurred with existing platforms.

The monochromatic transmittance along a path ΔL in the atmosphere is given by:

$$T = \exp\ (-\alpha \cdot \Delta L) \qquad (1)$$

where α is an attenuation coefficient and $\alpha = \sigma + K$ (2)

where σ is the scattering coefficient and K is the absorption coefficient.

The transmittance along j layers of atmosphere is:

$$T_j = \exp\ (-\Sigma_j \alpha_j \cdot \Delta L) \qquad (3)$$

where $\Delta L = \Delta Z_j \sec\theta$ for $\theta \leq 70^\circ$, (4)

and ΔZ_j = vertical distance increment

θ = zenith angle

Values of σ and K for Z_j = 1 Km as a function of altitude between 0 and 100 Km for several monochromatic wavelengths in the ultraviolet, visible and near IR spectral regions are used to solve equation (3). The cases that were examined included a vertical path, a standard mid-latitude summer atmosphere, and sensor platforms located above-atmosphere and at 1.0 Km altitude. The above-atmosphere case represents a spacecraft platform, the 1.0 Km altitude represents the operating region of aircraft systems. The results are shown by the "ultraviolet/visible/near-IR" bars plotted on Figure 4.1.3-1.

Based in transmissivity charts, average transmission in relatively broad infrared bands was computed. Their use results in the "thermal IR" data shown on Figure 4.1.3-1.

From this figure it is noted that overall atmospheric transmission is not severely degraded in the near-IR and thermal IR bands when moving from a low altitude aircraft to a platform above the atmosphere. The degradation becomes significant in the visible spectral region and severe in the ultraviolet.

It is to be noted that the data of Figure 4.1.3-1 corresponds to ideal conditions. Operation in the ultraviolet, visible and IR will be prevented in the case of significant haze and/or cloud cover, i.e., these spectral regions do not allow "all weather" operation.

Day/Night Capability

Passive sensing in the near UV, visible and near IR generally depend upon reflected solar light and therefore are performed in daylight. The exception is the use of starlight, diffuse illumination, and lunar albedo, in certain low-light-level sensing in the visible spectrum. Thermal IR measurements will depend on emission from the ocean surface, and are performed during the day or night.

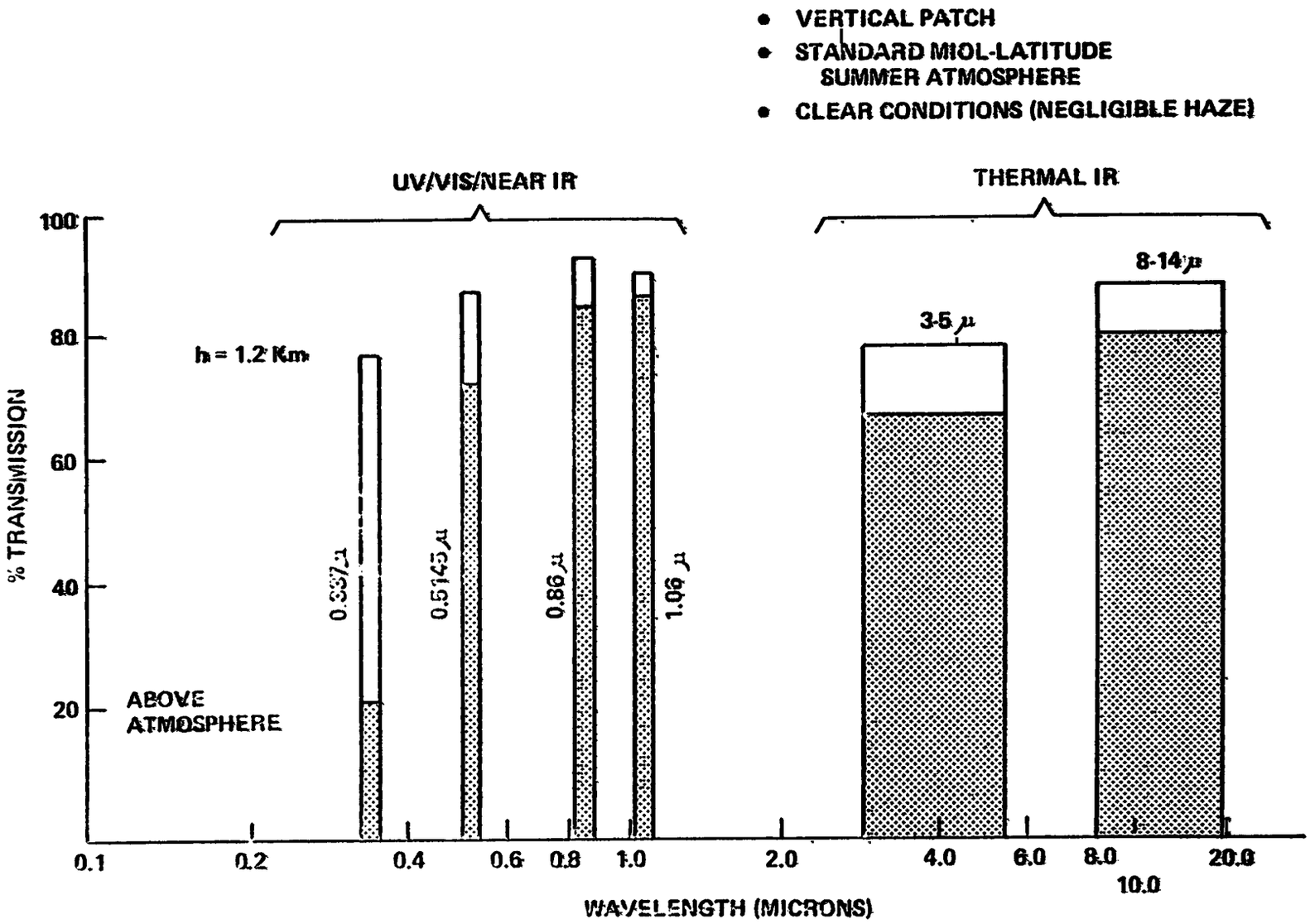

Figure 1.1.3-1. Spectral Atmospheric Transmission

Active techniques using laser illumination can be performed anytime, but with less contrast during daytime. The use of laser illumination in the Fraunhoffer absorption bands has been suggested as a possible means of increasing the contrast even under maximum solar flux conditions.

Cloud Cover

A basic limitation of optical sensing of pollutants on an operational basis is the intermittent obscuration due to cloud cover. For instance, the following approximate set of statistics apply to the north and south sectors of the U.S. east and west coastal region. (The data is extrapolated from world-wide statistics in the NASA-Marshall Study: "World-Wide Cloud Cover Distributions for Use in Computer Simulations", NASA-CR-61226, as discussed in Ref. 129.)

In the winter, typically in January, the probability of cloud-free conditions is less than 10% in all sectors except the south-western coast which has an average probability of 37%. In the summer, typically July, the probability of cloud free condition is slightly less in the southwest: 31%. However, the requirement for 100% cloud-free condition may be too stringent, since it is possible to obtain significant data in partial cloud cover. Examining the probabilities of less than 30% cloud cover, a 12-15% improvement is seen in all sectors, with the maximum probability still in the south-western coastal area, namely 50% in the winter and 43% in the summer.

Reflected Light from Oil Slicks

Reflectance contrast between oil and the surrounding ocean water is the primary means of optical detection in the near UV, Visible and Near Infrared spectrum. Both oil and ocean water absorb and reflect incident light, but the net reflection of light on oil is higher than that on water. Fluorescence of oil is caused by the re-emission of a portion of the absorbed UV energy, at a different wavelength than the incident light. This phenomenon is exploited

in the important technique of Laser Fluorosensing, which will be discussed in Section 4.1.3.1.4. (References 39, 41).

In the visible spectrum, the index of refraction of most fossil hydrocarbons is higher than that of ocean water. Experiments have shown that reflection of oil is the visible region between 0.4 microns and 0.6 microns offers less contrast than that below 0.4 microns and above 0.6 microns. Another method of detection uses reflectance contrast from ocean surface glitter. Wind stresses on the ocean surface produce capillary wave activity which is easily detected from space in terms of reflected solar light. Since an oil film suppresses capillary activity, the presence of oil is evidenced as an area of reduced reflection. It was found by Deutsch, Strong and Estes (Ref. 87) that the observations are possible when the elevation angle is equal to or greater than 40°; in Landsat, for instance, the optimum elevation angle is 55°.

Radiance contrasts is the near-infrared region of 0.75 to 1.1 micron can also be useful in daytime monitoring of oil slicks.

IR Emission from Oil Slicks

The IR emittance of oil varies with type of oil, oil thickness and aging stage. Factors affecting oil/water contrast in the thermal infrared region (e.g. 8-13 micron) are differential thermal conductivity, absorption of solar energy, evaporation rates, and oil thickness. Temperature differentials in the water, due to surface currents, thermal convection, and local upwelling can produce ambiguities in the sensing of oil slicks.

Waste Disposal Pollutant Surface Characteristics

Among the major categories of waste disposal pollutants, which include acid waste, sewage sludge, pharmaceutical waste, and dredge material, only portions of the acid wastes have positive buoyancy. The remainder of the materials

sink within 4 to 8 hours after being dumped into the ocean, therefore making detection improbable using sampling frequencies (e.g. from space) of once or twice per day. Detection of sewage plumes from sources such as ocean outfalls is possible due to the persistent flow sewage water into colder ocean, a condition that sets up connection as evidenced by a higher surface water temperature in those regions where sewage diffusion is taking place. A thin film of oil often forms in areas where sewage is discharged into the sea, due to the presence of some oil in the waste material.

Spectral Reflectance of Ocean Dumped Wastes

Significant contrast between the radiance of waste plumes and the surrounding water makes it possible to detect and map the extent of these plumes through aerial and space observations. The contrast varies with pollutant material, concentration (or dilution), observation sun-angle, and atmospheric effects. Johnson (ref. 70) has been successful in normalizing the environmental variables of a scene by in-scene background elimination. The technique uses radiance ratio vs. wavelength characteristic curves as signatures for materials such as acid industrial waste, sewage sludge, and biodigested waste. Figure 4.1.3-2 shows examples of such ratio curves. Step-wise regression analysis has been performed to extract pollution concentration information from aerial data (ref. 70).

Ambiguities exist in the interpretation of spectral radiance data to differentiate - for instance - between waste pollution and clouds (in spacecraft data) and between waste pollution and sediment. Classification techniques to circumvent these ambiguities have been developed by Moeller, Simmonds and Morrison, and have been employed by Klemas (ref. 140). The techniques employ "eigenvector" analysis utilizing various spectral bands as variables. The angular separation between vectors in a plot of radiance at the various wavelengths becomes the

discriminating factor.

Sensor/Sensing Technique Categories

The following subsections related to optical sensing are sub-divided into three categories:

1. Sensors currently operated aboard aircraft platforms
2. Existing or planned spacecraft sensors
3. A dedicated space based ocean pollution optical sensor.

Sensors in each category were assessed relative to their suitability to satisfy the requirements of the oceanic pollution missions. The methodology for the assessment was described in Section 4.1.1, and the requirements in Section 3.3.

4.1.3.1 Electro-Optical Sensors Employed in Airborne Detection

The approach taken relative to this first category of sensors was to assess specific airborne sensors which have either operationally or experimentally proven capabilities for pollution monitoring. The assessment consists of an extrapolation of the airborne electro-optical sensor capabilities to space-based capabilities in advanced versions of the sensor for adaptation to the space environment and different viewing parameters (e.g. altitude, atmospheric windows). Table 4.1.3.1-1 shows the sensors considered in this category, and the general use of the data relative to the oil pollution mission.

4.1.3.1.1 Low Light Level Television (L^3 TV)

Parameters Measured

Airborne L^3 TV sensors have been primarily used for the detection and areal mapping of oil slicks. The signature mechanism is the relative reflected sunlight return as set by the difference in reflectivity between the oil and sea water.

TABLE 4.1.3.1-1.

ELECTRO-OPTICAL SENSORS EMPLOYED IN AIRBORNE OIL DETECTION SYSTEMS

- LOW LIGHT LEVEL TELEVISION (L^3TV) CAMERA
  - DETECTION
  - AREAL INFORMATION
- ULTRA VIOLET/INFRARED (UV/IR) SCANNER
  - DETECTION
  - OIL CHARACTERIZATION
  - AREAL INFORMATION
  - SURFACE TEMPERATURE
- MULTI SPECTRAL SCANNER (MSS)
  - DETECTION
  - OIL CHARACTERIZATION
  - AREAL INFORMATION
  - SURFACE TEMPERATURE
- FLUORESCENCE SENSORS
  - DETECTION
  - OIL TYPE
  - OIL THICKNESS
- POLARIMETER
  - DETECTION
  - SEA STATE
- PHOTOGRAPHIC FILM CAMERAS
  - DETECTION
  - AREAL INFORMATION

The reflectivity difference is strongest in the ultraviolet. The L^3 TV sensors thus commonly operate in the near UV (0.3μm-0.4μm); this near UV region was not considered out of the question from the point-of-view of atmospheric transmissivity, based on the previous analysis as evidenced in Figure 4.1.3-1.

In some cases, a rotating polarizing filter is employed to detect polarization differences between the reflected sunlight from sea water and the oil slick. Rotation of the filter produces a flashing image when observing an oil slick, providing a discrimination and detection aid.

Detection and mapping of oil in water is possible due to the higher reflectivity of oil than water, up to 50% higher in the spectral region in question.

Since the reflectance of oil is dependent on oil type and slick thickness, the potentiality for classification and quantification thus exists, however, data interpretation in this application requires additional signature analysis and data base accrual. Synergistic use of other sensor data, e.g. microwave; may be necessary to separate the variables of oil type and thickness.

Description of the Sensor

The components of the L^3 TV sensor are shown in Figure 4.1.3.1.1-1.

FIGURE 4.1.3.1.1-1

LOW LIGHT LEVEL TV (L^3TV) SENSOR

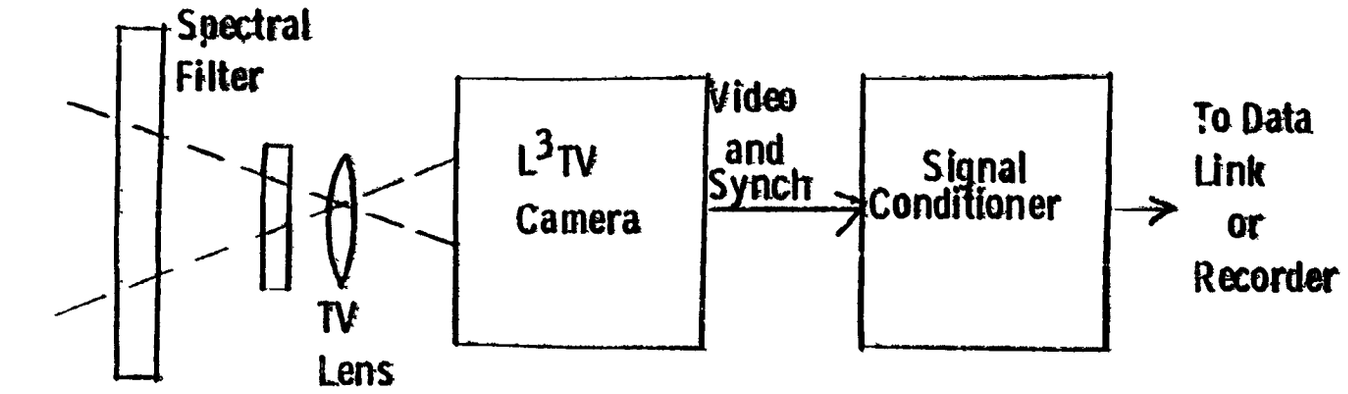

- LOW LIGHT LEVEL TV CAMERA
  - SILICON VIDICON
- ROTATING POLARIZER AND UV-NEAR IR SPECTRAL FILTER
  - ENHANCE OIL-WATER CONTRAST
- FAST (F/2) OPTIC
  - OPTIMIZE SIGNAL-TO-NOISE RATIO
- PROVEN OIL SLICK DETECTION CAPABILITY WHEN OPERATED ON AIRCRAFT PLATFORMS

The detailed characteristics of a typical airborne L^3 TV system successfully employed in oil slick detection are presented in Table 4.1.3.1-1.

TABLE 4.1.3.1-1 L^3 TV CHARACTERISTICS

(1) Television pickup tube: NEWVICON

- Spectral response from somewhat less than 0.4 micron to 0.8 micron
- Slightly greater sensitivity than standard silicon diode vidicon

(2) Lens: Fuji 8:1 Zoom

- Speed = F/2
- Focal length adjustable from 12.5 mm to 100 mm

(3) Spectral Filter: Kodak 18A

- Primary spectral response in 0.3 - 0.4 micron region
- Some spectral response in 0.65 - 0.85 micron region

(4) Provision of a rotating polarizing filter for a detection and discrimination aid.

Performance Parameters

Detectivity

The television system observes an extended scene, i.e., the oil slick is assumed to completely fill at least one resolution element. For this condition, the signal-to-noise ratio will scale as $\frac{1}{F^2}$, where F is the lens speed; if all other conditions are equal.

In moving from an aircraft platform to a spacecraft platform, the condition which significantly changes is atmosphere transmission. Considering the

response of the Kodak 18A filter and the data of Figure 1, the primary effect of this change will be in the near ultraviolet, i.e., in the region of 0.35 to 0.4 micron. Considering secant scaling with zenith angle, a reduction in atmospheric transmission by a nominal factor of up to 4 at this wavelength is for zenith angles between 0° and 45° is inferred from Figure 4.1.3-1. The resultant scaling of optics speed is:

$$\frac{(F_{airborne})^2}{(F_{spacecraft})^2} = \frac{(2)^2}{(F_{spacecraft})^2} = 4$$

$$F_{spacecraft} = 1.0$$

The requirement is thus for a relatively "fast" lens, but not excessive in terms of mechanization constraints. The L^3TV sensor thus passes the "detectivity" filter.

Resolution/Field-of-View

Modulation transfer function (MTF) representative of the baseline television pickup tube is shown by Figure 4.1.3.1.1-2. The computations on the figure convert the MTF to an effective resolution element size. These are performed using methodology described in Reference 152. An effective resolution element diameter of 7.14×10^{-2} mm is indicated at the retina center. The average size over the entire retina is taken as 1×10^{-1} mm, a nominal factor of 1.5 larger than the center value. The effective raster is 0.5 inch (12.7 mm) horizontal and 0.375 inch (9.53 mm) vertical. 127 horizontal resolution element and 95 vertical resolution elements are thus available.

The horizontal dimension is assigned to the cross-line-of-sight direction. The corresponding at-ocean foot print thus corresponds to the 12.7 mm retina dimension.

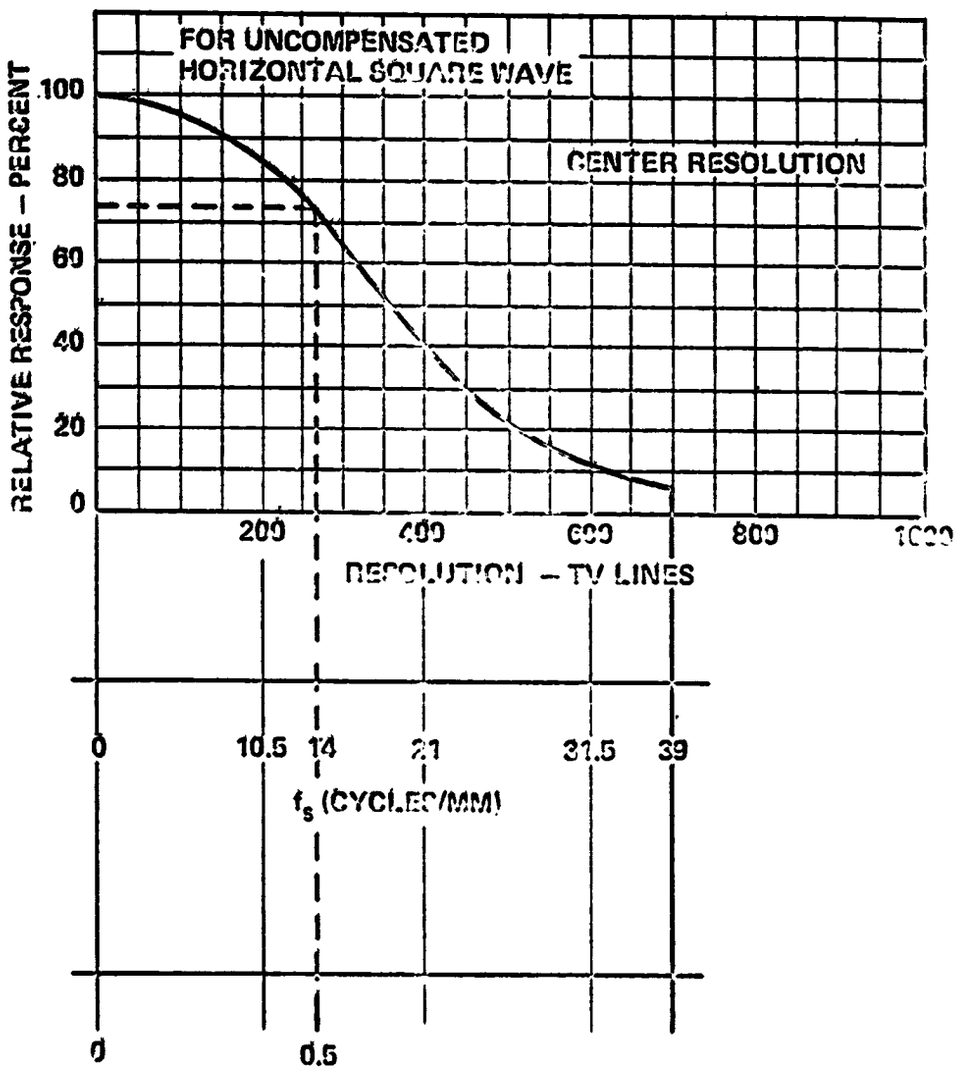

Figure 4.1.3.1.1-2 TV Sensor Resolution

The foot print of the vertical dimension (in the projected line-of-sight direction) corresponds to the 9.5 mm dimension divided by the cosine of the zenith angle. For a representative zenith angle in the region of 45 degrees, the field-of-view foot print is then nominally square.

A representative spacecraft altitude of 570 Km was used in the analysis, although higher altitudes would also be applicable. At a zenith angle of 45 degrees, the slant range is then 5.70×10^2 Km/cos 45° = 8×10^2 Km. The field-of-view of the television camera is given by:

$$FOV = \frac{D}{f.l.} \quad \text{radian} \qquad (1)$$

where D is the horizontal retina dimension = 12.7 mm and f.l. is the lens focal length in mm. The size of the ocean foot print is given by:

$$S = (R)\ (FOV) = \frac{(R)\ (D)}{f.l.} \quad \text{Km} \qquad (2)$$

where R is the slant range = 8×10^2 Km.

The required lens focal length as a function of S is computed from Equation (2). The corresponding lens diameter is given by:

$$D_o = \frac{f.l.}{F} \qquad (3)$$

where F is the optics F-number, earlier established as 1.0.

The system angular resolution is given by:

$$\Delta\Theta = \frac{\Delta X}{f.l.} \quad \text{rad} \qquad (4)$$

where ΔX is the retina resolution element size of 1×10^{-1} mm as determined by the method shown on Figure 4.1.3.1.1-2. The foot print size of $\Delta\Theta$ (ΔS_C) in the cross line-of-sight direction is given by:

$$\Delta S_C = R \cdot \Delta\Theta = (9.9 \times 10^{2})(\Delta\Theta) \text{ Km} \qquad (5)$$

The foot print size of $\Delta\Theta$ in the projected dimension along the line-of-sight is given by:

$$S_L = \frac{R \cdot \Delta\Theta}{\cos\Theta} = \frac{(9.9 \times 10^2)\ (\Delta\Theta)}{\cos\Theta}\ \text{Km} \qquad (6)$$

where Θ is the zenith angle, taken to be in the region of 45 degrees.

Note that the size of an optics diffraction limited 1σ Gaussian point spread function (PSF) diameter is approximately $\frac{\lambda}{D_o}$, where T_1 is the wavelength and D_o is the optics diameter. The ratio of this quantity to the instantaneous resolution element size $\Delta\Theta$ as given by Equation (4) is:

$$\frac{\frac{\lambda}{D_o}}{\frac{\Delta X}{f.l.}} = \frac{\frac{\lambda}{D_o}}{\frac{\Delta X}{1 \cdot D_o}} = \frac{\frac{0.4 \times 10^{-4}\ \text{cm}}{D_o}}{\frac{1 \times 10^{-2}\ \text{cm}}{1}} = 4.0 \times 10^{-3}$$

The optics blur circle will thus contribute a negligible effect to overall resolution element size.

Figure 4.1.3.1.1-3 shows plots of lens diameter at at-scene field-of-view versus cross line-of-sight at-scene resolution. These curves provide parametric trade-offs of these quantities. For example, a resolution of 1.0 Km corresponds to a field-of-view of 115 Km and a lens diameter of 8 cm. If 0.03 Km resolution is required, the field-of-view is decreased to 3.3 Km and the lens diameter is increased to 260 cm.

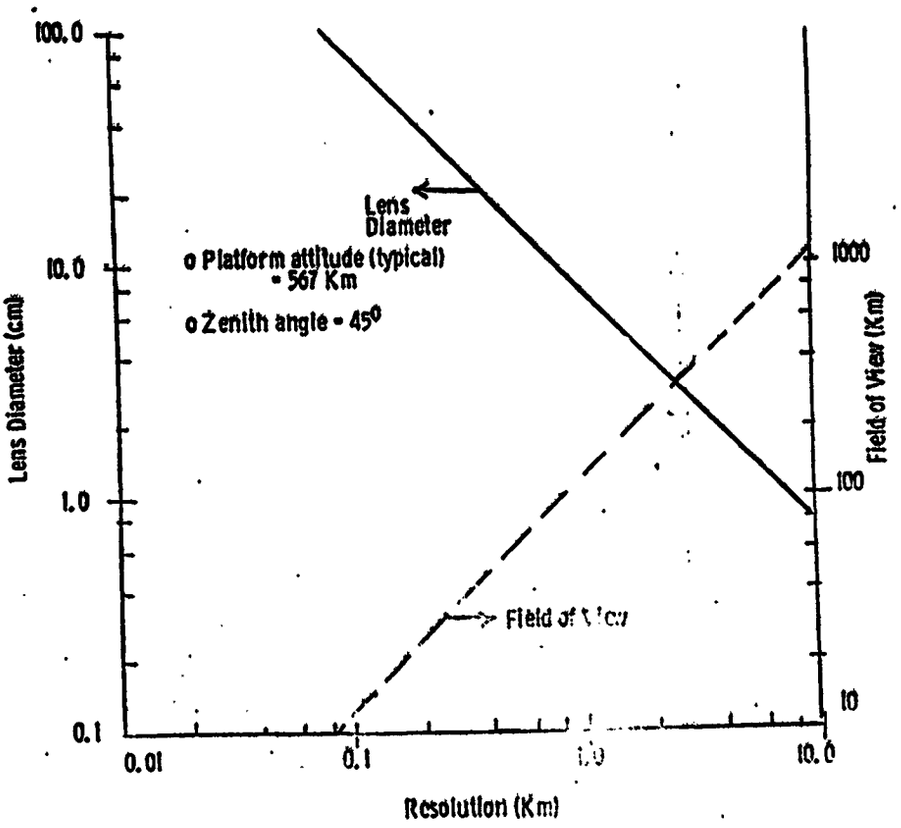

Figure 4.1.3.1.1-3. Lens Diameter and Field of View vs. Resolution For Space-Based L^3 TV Sensor

Size/Weight/Power

Television systems have previously been operated aboard remote-sensing space vehicles, for example; the return beam vidicon (RBV) camera on LANDSAT. This indicates general compatability of the L^3TV system with spacecraft size, weight, and power constraints.

Assessment of Sensor Suitability

The assessment of L^3TV capabilities for the space based application is summarized in Table 4.1.3.1.1-2. As noted, the unsatisfactory swath width/resolution tradeoffs make the sensor unsuitable for the space based system. Specifically, with 30 m to 100 m resolution and a swath width of 390 km, the optics size required for this application would not be practical.

TABLE 4.1.3.1.1-2 L^3 TV ASSESSMENT SUMMARY

- o Passes Filter "A" (Development and Operational Status)
  - Proven Capability in Current Airborne Systems (LAOSS)
- o Passes Filter "B" (Detectivity)
  - Factor of 4 Detectivity Increase Required to Overcome Increased Atmospheric Attenuation
  - Can be Achieved by going to Faster Lens and/or More Sensitive Television Pick-up Tube.
    - -- F/1.0 Optic
    - -- Silicon Intensified Target (SIT) Vidicon
- o Filter "C" (Degree to which User Requirements are met)
  - Resolution, Swath Width and Optics Size are a Parametric Trade-off, for example:

RESOLUTION (KM)	SWATH WIDTH (KM)	OPTICS SIZE (CM)
0.03	3.3	260
1.0	110.0	8
0.5	55.0	16

- o Does Not Pass Filter "C"
  - Small Swath Width at 30 M Resolution
  - All User Requirements Not Met

4.1.3.1.2 UV/IR Scanner

Parameters Measured

The UV/IR line scanner has been primarily employed in oil slick detection. It provides scanned detectors in the ultraviolet and thermal infrared spectral regions. Typical detector types are a silicon photodiode for the UV and mercury cadmium telluride (Hg Cd Te) in the infrared.

In the ultraviolet, reflected solar radiation is observed. UV detection is based upon the reflectivity difference of an oil slick and adjacent clean water areas. The parameters measured by the UV channel are equivalent to those of the L^3 TV, as discussed in Section 4.3.1.1.

The thermal infrared channel detects and images the oil slick by means of the temperature difference between the oil and water. The infrared emittance from oil is a function of oil type. The oil emittance varies with bulk thickness when the bulk emittance of the oil is significantly different from that of water.

If an oil film exists on water, the thermal exchange with the atmosphere is altered. The apparent observed temperature differences which result, however, are significantly modified by cloud radiance reflected by the oil. This effect is strong enough to cause contrast reversal for the condition of a clear versus an overcast sky. The apparent radiometric temperature difference is also effected by other factors such as thermal conductivity, evaporation rate of water, and evaporation rate of volatiles from the oil pollutants. The specific relationships are not clearly understood, therefore, the use of the thermal infrared data for classification and quantification of oil slicks is subject to significant uncertainty.

Description of the Sensor

The UV/IR sensor concept is shown in Figure 4.1.3.1.2-1. Instruments of this type are presently operated by the United States Coast Guard and the Canada Centre for Remote Sensing (References 149, 150, and 153). These define the baseline characteristics of a representative operational airborne sensor as:

1. Spectral Channels

   UV: one channel in the 0.3 to 0.4 micron region

   IR: one or two channels in the 8-14 micron region (8-9 micron and/or broadband)

2. Instantaneous Field of View

   Linear: $\Delta\theta = 2.5 \times 10^{-3}$ rad.

   Solid: $\Omega = 6.25 \times 10^{-6}$ ster.

FIGURE 4.1.3.1.2-1

ULTRA VIOLET/INFRARED (UV/IR) SCANNER

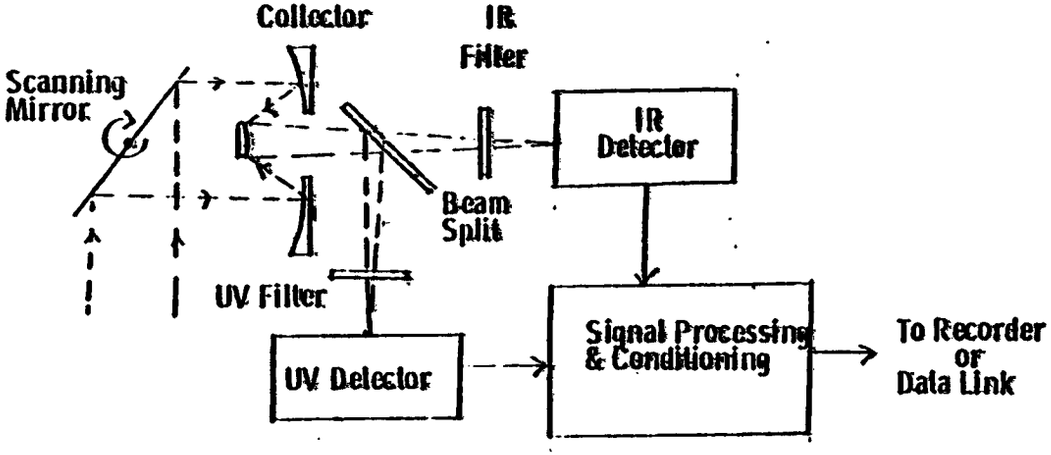

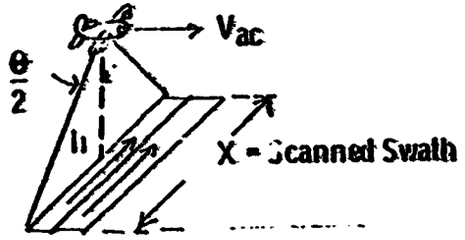

- LINE SCANNER
- UV AND IR CHANNELS

  0.35 - 0.4 MICRON

  8 - 14 MICRONS
- $A_0\Omega$ = OPTICS THROUGH PUT = 2.5×10^{-4} cm^2 - ster

  $A = 40\ cm^2$

  $\Omega = 6.25 \times 10^{-6}$ ster
- θ = SCANNED FIELD OF VIEW = 100^0
- SCAN RATE = 80 - 100 SCANS/SEC FOR AIRCRAFT SYSTEM
- PROVEN OIL SLICK DETECTION CAPABILITY WHEN OPERATED ABOARD AIRCRAFT PLATFORMS

3. Scanned Field of View: 100 degrees

4. Scan Methodology

   Mirror scan perpendicular to aircraft longitudinal axis

   Forward scan by platform motion

5. Optics $A \cdot \Omega$ product:

   $A \cdot \Omega = 40\ cm^2 \times 6.25 \times 10^{-6}$ ster.

   $= 2.5 \times 10^{-4}\ cm^2$ - ster.

6. Optics Efficiency = 0.4
   (Effective $A \cdot \Omega = 2.5 \times 10^{-4} \times 0.4 = 1 \times 10^{-4}\ cm^2$ - ster.

7. Scan Rate: 80 to 100 scans/sec.

Performance Parameters

Detectivity

Operation against a resolved scene is assumed, i.e., the oil slick fills at least a resolution element. Under this condition, a prime factor determining the detectivity is the increase in atmospheric attenuation occurring when raising the sensor from a location near the earth's surface to one above the atmosphere. From Figure 4.1.3.1-1, the increase in atmospheric attenuation for this condition is noted as a factor of 4 for the UV. The corresponding factor in the 8-14 micron IR region is 1.2. The UV channel thus suffers the most severe detectivity degradation due to atmospheric attenuation.

A common reflecting optical collector with following splitting of the collected energy to the UV and IR channels is assumed. The required $A \cdot \Omega$ product to offset the increased atmospheric attenuation is set by the maximum requirement set by the UV channel. The required value is noted as:

$$A \cdot \Omega = 2.5 \times 10^{-4} \times 4 = 1 \times 10^{-3}\ cm^2 \text{ - ster.}$$

Scanning Geometry

The detector for each channel is scanned in the direction perpendicular to the aircraft longitudinal axis (flight direction) by a rotating mirror. For a spacecraft platform altitude of 570 km the at-ocean width vs. active scan angle is given by Figure 4.1.3.1.2-2. The computations are based upon a flat-earth approximation, taken as a valid assumption at 570 km platform altitude.

Figure 4.1.3.1.2-2. Swath Width vs. Scan Angle For Platform at 567 Km Altitude (UV/IR Scanner)

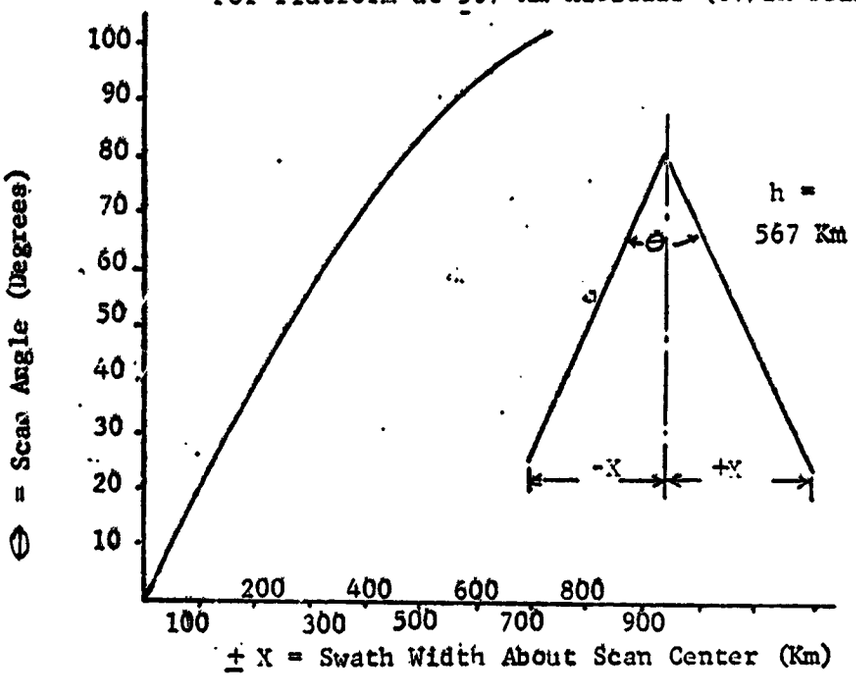

Effect of Scanning Conditions on Detectivity

It is assumed that design of the scanning subsystem will take into account the angular velocity V/R of image motion, where V is the ground velocity of the suborbital point with respect to the platform, and R is the range. The scan time T_s is set such that the detector instantaneous field of view is displaced along the flight direction by $R \cdot \Delta\theta$ at the beginning of successive active scan intervals, where $\Delta\theta$ is the detector instantaneous field of view in radians.

For the airborne platform, representative values of V and R are 150 mph (67m/sec) and 1000 ft (305 m), respectively. The corresponding $\frac{V}{R}$ ratio is 0.22 rad/sec. This closely compares with the design value of 0.20 given in Reference 14. The corresponding scan time is thus:

$$R \cdot \Delta\Theta = V \cdot T_s \qquad (14)$$

and, for the aircraft platform:

$$T_s = \frac{R \cdot \Delta\Theta}{V} = \frac{\Delta\Theta}{0.2} = 5 \cdot \Delta\Theta$$

For the satellite platform at 568 km altitude, V is 7.0 km/sec. Thus:

$$\frac{V}{R} = \frac{7.0 \frac{km}{sec}}{567\ km} = 0.0123$$

Then, for the satellite platform:

$$T_s = \frac{\Delta\Theta}{0.0123} = 81.1 \cdot \Delta\Theta$$

The scan time for the satellite platform is then 81.1/5 = 16 times that of the aircraft platform for equivalent angular resolution.

The signal-to-noise ratio (S/N) scales with $\frac{1}{\sqrt{\Delta f}}$, where Δf is the noise bandwidth of the signal processing electronics. Δf is proportional to $\frac{1}{t_d}$, where t_d is the dwell time, given by:

$$t_d = \frac{\Delta\Theta}{\Theta} \cdot T_s \cdot \epsilon \qquad (15)$$

where ϵ is the scanning efficiency. Signal-to-noise ratio thus scales as:

$$\frac{1}{\sqrt{\Delta f}} \sim T_s \qquad (16)$$

and an advantage will be gained if T_s is increased. As shown earlier, T_s is 16 times greater for the satellite system than for the baseline system due to V/R considerations for equivalent $\Delta\Theta/\Theta$ and ϵ. This provides increased S/N

by a factor of $\sqrt{16} = 4$ and by happenstance nullifies the earlier-estimated factor of 4 degradation due to atmospheric attenuation.

Parametric Satellite System Performance Calculations

Performance of the satellite-borne system are parameterized to other combinations of scan extent and instantaneous field of view by the following computations.

The required $A \cdot \Omega$ product is given by:

$$A \cdot \Omega = \frac{(4)}{K} (2.5 \times 10^{-4}) \text{ cm}^2 - \text{ster}. \qquad (17)$$

where A is the true physical aperture area, 4 is the atmospheric attenuation degradation and K is the factor by which the increased value of T_s improves the S/N at the satellite platform. Substituting in equations (14) and (15), S/N scales as:

$$S/N \sim \frac{1}{\sqrt{\Delta f}} = \frac{\Delta\theta}{\sqrt{\theta}} \sqrt{\frac{R \cdot \epsilon}{V}} \qquad (17)$$

$\Delta\theta$ and θ for the baseline are 2.5×10^{-3} radian and $100^\circ = 1.75$ radian, respectively. For these conditions, K = 4. Then, for other values of $\Delta\theta$ and θ and constant $R \cdot \epsilon / V$:

$$\frac{4}{K} = \frac{\left(\frac{2.5 \times 10^{-3}}{\sqrt{1.75}}\right)}{\left(\frac{\Delta\theta_{rad}}{\sqrt{\theta_{rad}}}\right)}$$

and,

$$K = 4. \frac{\Delta\theta_{rad} \cdot \sqrt{1.75}}{2.5 \times 10^{-3} \cdot \sqrt{\theta_{rad}}} \qquad (18)$$

Values of K as thus computed for $\theta = 50^{\circ}$ (0.873 rad) and 25° (0.436 rad) alone with values of $\Delta\theta$ between 1×10^{-4} rad and 5×10^{-3} rad are substituted into equation (17) to calculate corresponding values of $A\Omega$. The quantity Ω is set as $(\Delta\theta)^2$ to estimate the required value of aperture area A and thus aperture diameter d_o.

Resulting curves of optics diameter d_o vs. resolution at the ocean surface are shown on Figure 4.1.3.1.2-3. The indicated swath widths are total size, i.e., twice the $\pm X$ values previously shown on Figure 4.1.3.1.2-2.

The curves as shown apply to duplicating S/N achieved with the airborne sensor in the UV channel at the satellite platform conditions. Better performance should be achieved in the IR channel(s) since the IR atmospheric attenuation increase is $\frac{1.2}{4} = 0.3$ that of the UV case. Thus, the sensor passes the detectivity filter.

Assessment of Sensor Suitability

The assessment for the UV/IR Scanner is summarized in Table 4.1.3.1.2-1. As shown, the requirements for the spacebased application are not met since acceptable resolution cannot be achieved at reasonable optics size and swath

FIGURE 4.1.3.1.2-3

OPTICS DIAMETER VS. RESOLUTION AND SWATH WIDTH FOR UV/IR SCANNER

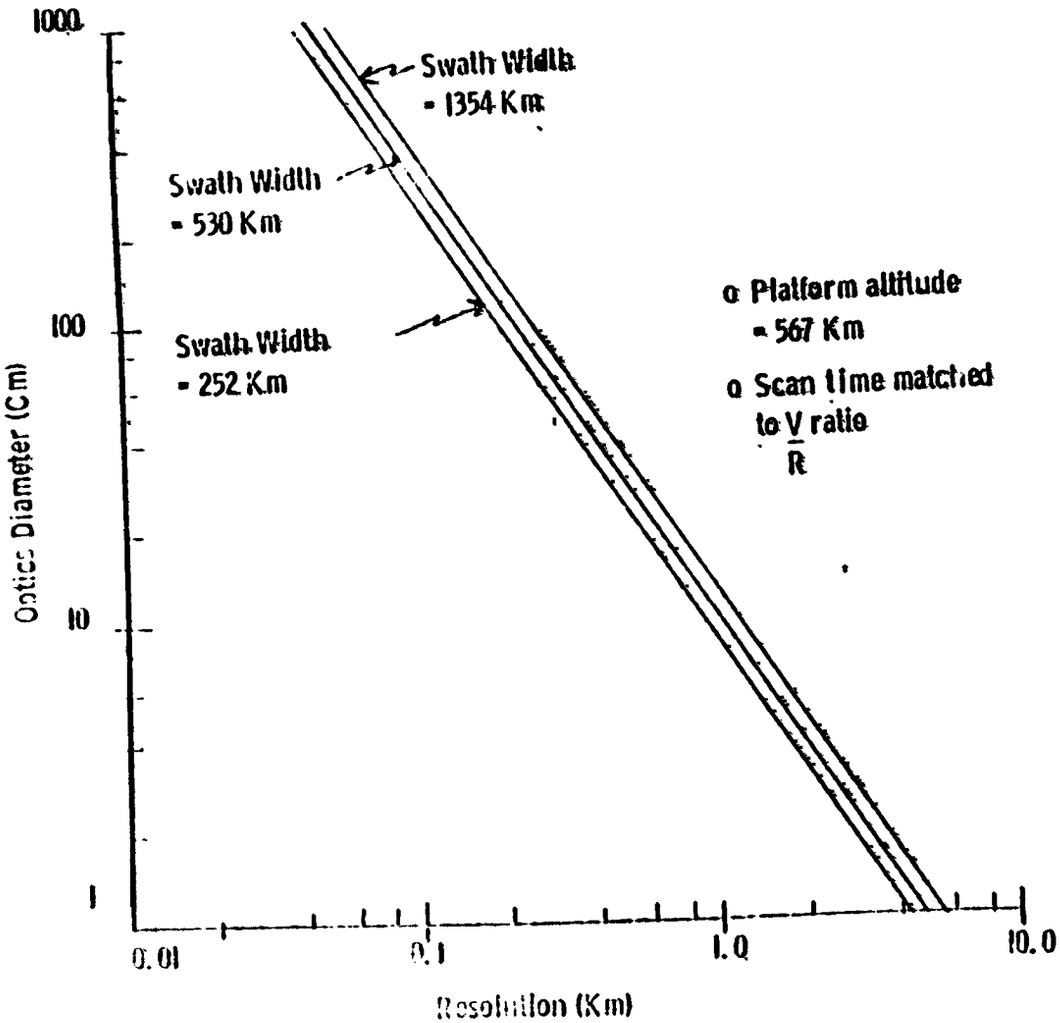

TABLE 4.1.3.1.2-1

UV/IR SCANNER ASSESSMENT SUMMARY

- PASSES FILTER #A (DEVELOPMENT AND OPERATIONAL STATUS)
  - PROVEN CAPABILITY IN CURRENT AIRBORNE SYSTEMS (E.G., CANADIAN CENTRE FOR REMOTE SENSING)
- PASSES FILTER #B (DETECTIVITY)
  - MOST SEVERE DEGRADATION CAUSED BY DECREASE IN ATMOSPHERE TRANSMISSION IN UV CHANNEL
    - FACTOR OF 4
  - CAN BE OVERCOME BY INCREASING OPTICS THROUGHPUT AND/OR DECREASING SCAN SPEED
    - LOWER $\frac{V}{R}$ RATIO FOR SPACECRAFT PLATFORM
- DOES NOT PASS FILTER #C (DEGREE TO WHICH USER REQUIREMENTS ARE MET)
  - RESOLUTION, SWATH WIDTH, AND OPTICS SIZE ARE A PARAMETRIC TRADEOFF; FOR EXAMPLE,

RESOLUTION (KM)	SWATH WIDTH (KM)	OPTIC SIZE (CM)
0.03	252	> 1000
0.1	1350	400
1.0	1350	12
2.0	530	3.6

  - CANNOT ACHIEVE 0.03 KM RESOLUTION AT REASONABLE OPTIC SIZE AND SWATH WIDTH

ALL USER REQUIREMENTS NOT MET

4.1.3.1.3 Airborne Multispectral Scanner

Parameters Measured

Airborne Multi-spectral scanners enhance the detection and identification of objects by making use of the contrast ratios that exist in narrow spectral bands. The spectral region generally covered includes the near-ultraviolet, visible, and near infrared. This type of instrument has been successfully operated against several pollutant types including oil slicks, acid plumes, sewage sludge, and bio-digested industrial wastes. The data provided yields synoptic classification and quantification of the polluted area.

Classification is accomplished by measurement of the spectral signature as established by the relative pollutant - water radiance in several narrow spectral channels. Quantification, i.e., oil slick thickness or pollutant concentration, is established by the magnitude of the radiance in selected spectral channels.

Description of the Sensor

The Airborne Multispectral Scanner Sensor (AMSS) concept is sketched in Figure 4.1.3.1.3-1. A representative system has been successfully operated by Entera Environmental Consultants, Ltd. Ottawa, Ontario for the Canada Centre for Remote Sensing (CCRS). The sensor characteristics (References 150, 153 and 156) are summarized below.

The airborne multispectral scanner is similar to the UV/IR scanner discussed in Section 4.1.3.1.2. The key difference is that, in the MSS, the UV channel of the UV/IR scanner is replaced with a dispersing spectrometer. Detectors are provided to give several narrow spectral channels from the UV to the near-IR. Representative spectral channels are those of the CCRS instrument.

FIGURE 4.1.3.1.3-1

MULTI-SPECTRAL SCANNER (E.G., CCRS-MSS)

- SIMILAR TO UV/IR SCANNER WITH UV CHANNEL REPLACED BY SPECTROMETER

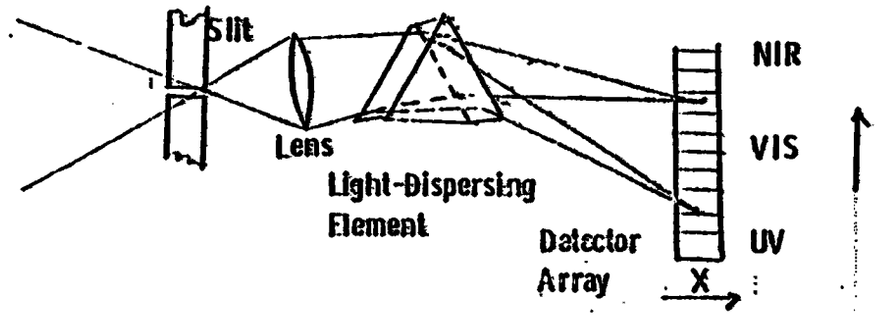

- DISPERSED SPECTRUM SAMPLED BY DETECTOR ARRAY TO PROVIDE SEVERAL NARROW CHANNELS IN UV, VIS, AND NIR (MICRON).

0.38 - 0.42	0.60 - 0.65
0.42 - 0.45	0.65 - 0.69
0.45 - 0.5	0.70 - 0.79
0.50 - 0.55	0.80 - 0.89
0.55 - 0.6	0.92 - 1.1

- ALSO PROVIDES THERMAL IR CHANNEL(S)
- PROVEN METHOD OF OIL SLICK SENSING FROM AN AIRCRAFT PLATFORM

These are:

0.38 - 0.42 micron	0.6 - 0.65 micron
0.42 - 0.45 micron	0.65 - 0.69 micron
0.45 - 0.5 micron	0.70 - 0.79 micron
0.5 - 0.55 micron	0.80 - 0.89 micron
0.55 - 0.6 micron	0.92 - 1.1 micron

Performance Parameters

Operational experience with the CCRS instruments indicates that adequate detectivity in the oil spill application is achieved in all spectral channels, except the first two, centered at 0.4μ and 0.43μ, which tend to give noisy data, apparently due to the narrow spectral bandwidth. This indicates need for an increased A.Ω product for the MSS as compared to the UV/IR scanner. An increase by a factor of 3 or 4 appears appropriate. This corresponds to an increase in optics diameter by a factor of $\sqrt{4} = 2$ for the parametric performance curves shown previously on Figure 4.1.3.1.2-3.

Assessment of Sensor Suitability

The assessment summary for the AMSS is equivalent to that as discussed above for the UV/IR scanner. The requirements for the spacebased application are not met since acceptable resolution cannot be obtained at reasonable optics size and adequate swath-width.

4.1.3.1.4 Fluorescence Sensor

Parameters Measured

Oil and other pollutants absorb light, especially in the ultraviolet, and re-emit the energy at longer wavelengths. A basic source of UV excitation is solar energy. The Fraunhofer line discriminator technique employs solar excitation. The observable is the depth of the Fraunhofer dark lines of the reflected solar spectrum compared to the depth of the lines in the incident

solar radiation. This technique suffers three major drawbacks (Reference 143):

1. It is not operable in the presence of cloud cover;
2. It cannot be used at night;
3. The main source of background noise is also the excitation source.

These drawbacks can be overcome by use of a laser as the excitation source. A representative system employing an N_2 laser at 0.337 microns is described in Reference 144. Tests verify ability to discriminate oil from sea water. Also, the ratio of fluorescent emission at 0.433 microns and 0.533 microns allowed identification of several oil types. The amplitude of the fluorescent signal is a function of oil thickness, providing a corresponding additional measurement capability. These effects are illustrated in Figure 4.1.3.1.4-1

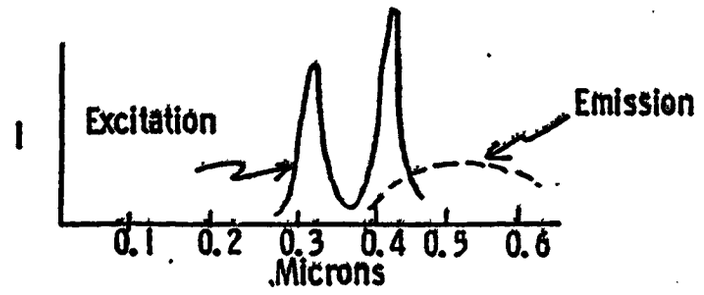

Excitation and Emission Spectra of a Oil Sample

Laser fluorosensing systems have been employed similarly for classification and quantification of other pollutants such as pulp mill effluents, chlorophylls, and phytoplanktons.

Description of the Sensor

The characteristics of a representative laser fluorescence sensor are summarized in Table 4.1.3.1.4-1

Performance Parameters

Detectivity

The assumption is made that the flourescent coefficient:

$$\epsilon_f \sim \frac{\text{watts emitted}}{\text{watts incident}} = \frac{\dot{N}_e}{\dot{N}_i} \qquad (19)$$

TABLE 4.1.3.1.4-1

REPRESENTATIVE AIRBORNE LASER-STIMULATED SYSTEM PARAMETERS *

- o N_2 LASER
  - o PEAK PULSE POWER = 100 Kw
  - o PULSE LENGTH = 10 NANOSECONDS
  - o DIVERGENCE SOLID ANGLE = 4×10^{-6} ster
  - o λ = 0.337 MICRON
- o S-20 PHOTOMULTIPHER RECEIVER
  - o EMI 9558 PHOTOMULTIPHER
  - o OPTICS DIAMETER = 30 cm
- o PER-PULSE SIGNAL TO NOISE RATIO = 25
  - o 1.0 Km AIRCRAFT ALTITUDE
  - o 25 Km VISIBILITY

* SOURCE: AN INVESTIGATION OF OIL FLUORESCENCE AS A TECHNIQUE FOR THE REMOTE SENSING OF OIL SPILLS (BY JOHN F. FANTASIA)

is equivalent to that of the measurements described in Reference 144. W_i is given by:

$$W_i = P_L \cdot T_{a,L} \cdot T_{o,L} \quad \text{watt} \tag{20}$$

where P_L = Laser power (watt)

$T_{a,L}$ = atmospheric transmission in laser path

$T_{o,L}$ = Laser optics transmission.

W_e is then given by:

$$W_e = W_i \in_f = P_L \cdot T_{a,L} \cdot T_{o,L} \cdot \in_f \quad \text{watt} \tag{21}$$

The radiant intensity is then:

$$J_e = \frac{P_L \cdot T_{a,L} \cdot T_{o,L} \cdot \in_f}{\pi} \quad \frac{\text{watt}}{\text{ster.}} \tag{22}$$

and the radiance is:

$$N_e = \frac{P_L \cdot T_{a,L} \cdot T_{o,L} \cdot \in_f}{\pi R^2 \Omega_L} \quad \frac{\text{watt}}{\text{cm}^2 \cdot \text{ster.}} \tag{23}$$

where R is the range in cm and Ω_L is the laser beam solid angle in steradians.

An optimum condition is assumed, wherein the fluorescent spot fills the receiver field of view. This requires that the boresight error between the laser and receiver be negligible. The power on the receiver detector is:

$$P_d = A_r \cdot \Omega_r \cdot N_e \cdot T_{a,r} \cdot T_{o,r} \tag{24}$$

where: A_r = reciever aperture area (cm^2)

Ω_r = receiver solid angle field of view, identical to $\Omega_L = \Omega$ for conditions assumed.

$T_{a,r}$ = atmospheric transmission along the receiver path

$T_{o,r}$ = receiver optics transmission.

Thus, substituting from equation (23)

$$P_d = \frac{A_r \cdot T_{a,r} \cdot T_{o,r} \cdot P_L \cdot T_{a,L} \cdot T_{o,L} \cdot \epsilon f}{\pi R^2}$$

$$= \frac{d_r^2 \cdot T_{a,r} \cdot T_{o,r} \cdot P_L \cdot T_{a,L} \cdot T_{o,L} \cdot \epsilon f}{R^2} \text{ watt} \quad (25)$$

To scale to other conditions of range and reciever optics size, let P_d remain constant with changing A_r and d_r.

$$\frac{\left[\frac{d_{r,1}^2 \cdot T_{a,r,1} \cdot T_{o,r,1} \cdot P_{L,1} \cdot T_{a,L,1} \cdot T_{o,L,1} \cdot \epsilon f}{R_1^2}\right]}{\left[\frac{d_{r,2}^2 \cdot T_{a,r,2} \cdot T_{o,r,2} \cdot P_{L,2} \cdot T_{a,L,2} \cdot T_{o,L,2} \cdot f}{R_2^2}\right]} = 1$$

$$P_{L,1} = P_{L,2} \frac{R_1^2}{R_2^2} \frac{T_{a,r,2} \cdot T_{a,L,2}}{T_{a,r,i} \cdot T_{a,L,1}} \frac{d_{r,2}^2}{d_{r,1}^2} \text{ watt} \quad (26)$$

where the subscript 1 refers to the spacebased system, the subscript 2 refers to the baseline airborne system, and $T_{o,L,1} = T_{o,L,2}$.

Thus, for:

$R_1 = 567$ Km $\quad T_{a,r,1} = 0.6$

$R_2 = 1.0$ Km $\quad T_{a,r,2} = 0.9$

$T_{a,L,1} = 0.2$ $\quad d_{r,2} = 30$ cm

$T_{a,L,2} = 0.8$

$$P_{L,1} = \frac{1.74 \times 10^{14}}{d_{r,1}^2} \text{ watt} \quad (27)$$

Figure 4.1.3.1.4-2 shows a plot of $d_{r,1}$ vs. $P_{L,1}$ for the spacebased scenario. The curve indicates need for a laser peak power in the region of 10^9 watts for a receiver

FIGURE 4.1.3.1.4-2
RECEIVER OPTICS DIAMETER VS LASER POWER FOR SPACE-BASED LASER-STIMULATED FLUORESCENCE SENSOR

$$P_{L,1} = P_{L,2} \cdot \frac{T_{a,r,2}\, T_{a,L,2}}{T_{a,r,1}\, T_{a,L,1}} \cdot \frac{\left(d_{r,2}^{\,2}\right)}{\left(d_{r,1}^{\,2}\right)} \cdot \frac{R_1^{\,2}}{R_2^{\,2}} = \frac{1.74 \times 10^{14}}{d_{r,1}^{2}}$$

P_L = LASER POWER

$T_{a,r}$ = ATMOSPHERIC TRANSMISSION FOR RECEIVER

$T_{a,L}$ = ATMOSPHERIC TRANSMISSION FOR LASER

d_r = RECEIVER OPTICS DIAMETER

R = RANGE

SUBSCRIPT 1 ≡ SPACE-BASED SYSTEM

SUBSCRIPT 2 ≡ BASELINE AIRBORNE SYSTEM

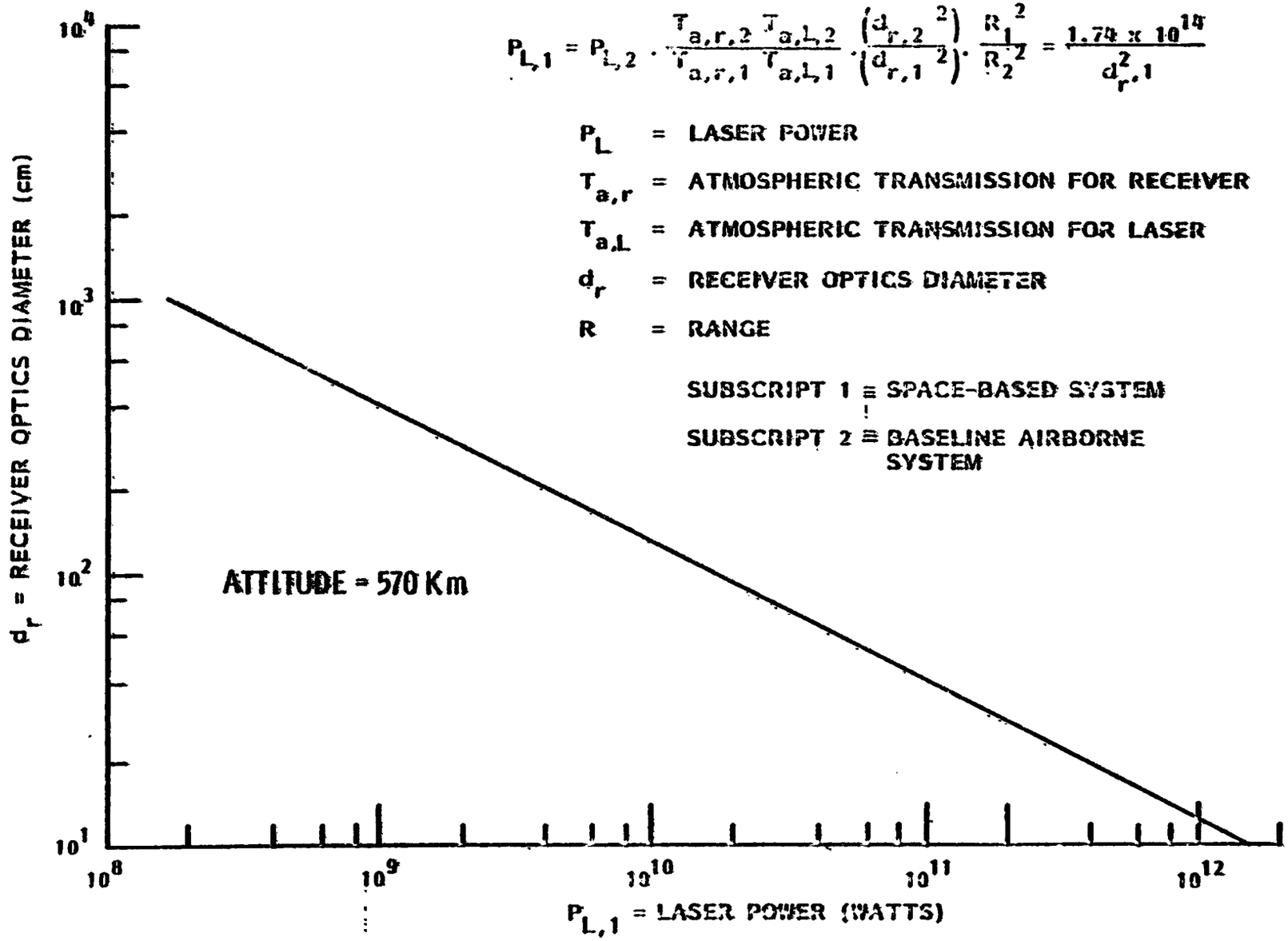

aperture diameter of 4.0 m, the maximum allowable dimension. For more desirable smaller sizes, in the region of 10 to 50 cm, the required laser power is in the order of 10^{11} to 10^{12} watts. Discussion with a manufacturer of N_2 and other UV lasers (Reference 12) indicates that these laser requirements exceed current capability by orders of magnitude. This is corroborated by available literature on the state of the art. This indicates that the laser-stimulated fluorescence sensor does not pass the detectivity filter, at least for the immediate interim.

Sensor Performance Assessment

The performance assessment summary for the laser-stimulated fluorescence sensor is given in Table 4.1.3.1.4-2. The technique is not considered appropriate to immediate spacebased application due to technology constraints.

TABLE 4.1.3.1.4-2 FLUORESCENCE SENSOR ASSESSMENT SUMMARY

- PASSES FILTER #A (DEVELOPMENT AND OPERATIONAL STATUS)
  - PROVEN CAPABILITY IN CURRENT AIRBORNE SYSTEMS
- DOES NOT PASS FILTER #B (DETECTIVITY)
  - MAXIMUM AVAILABLE LASER PEAK PULSE POWER IN REGION 10^7 - 10^8 WATTS REQUIRES RECEIVER OPTICS DIAMETER 10 METERS
- NOT CONSIDERED FURTHER FOR IMMEDIATE APPLICATION DUE TO LOW DETECTIVITY WITH CURRENT INSTRUMENTATION APPROACH
- PROVIDES A POTENTIALLY POWERFUL OIL SPILL DETECTION AND CHARACTERIZATION METHOD AND SHOULD BE CONSIDERED FOR FAR-TERM (POST 1991) SPACE SYSTEMS
  - LARGE DEPLOYABLE OPTICS
  - COHERENT DETECTION

Some indication (Reference 158) exists that laser technology advances and use of large deployable optics, of size comparable to proposed radar antennas, will make the laser fluorescencing method feasible for later generation systems. Since the technique is a potentially powerful detection, classification, and

quantization method; it should be considered for the far term (post 1991) [illegible].

4.1.3.1.5 Polarimeter

Parameters Measured

Measurements and modeling predict that the emitted radiation from the sea is polarized, with the percent polarization dependent on the sea state. Experimental measurements (Reference 151 indicate percent increase in polarity from 15% to 50%, comparing the return from a smooth sea with that from a sea-state corresponding to a wind velocity of 3 meters/sec. The measurements were made at various spectral channels in the 1 to 12 micron region. The polarimeter thus provides potential means of measuring sea state, and thus the existence of oil-dampening of wave action.

Description of the Sensor

A representative polarimeter configuration (Reference 151 is shown by Figure 4.1.3.1 5-1. The instrument employs a Si: As detector and a 39 mm diameter F/1.6 optic.

Sensor Performance Assessment

Available information indicates that polarimetry has received but limited experimental use in measuring sea-state. No evidence of significant operational history exists. The technique is thus considered as not passing Filter A. (Development and Operational Status.) Thus, it is not considered further for the spacebased system.

4.1.3.1.6 Summary of Current Airborne Sensor Capabilities in the Spacebased Application. The conclusions drawn are summarized in Table 4.1.3.1.6-1. As shown, none of the current airborne electro-optical sensors are considered appropriate to extrapolation for an immediate or mid-term spacebased system.

FIGURE 4.1.3.1.5-1
POLARIMETER

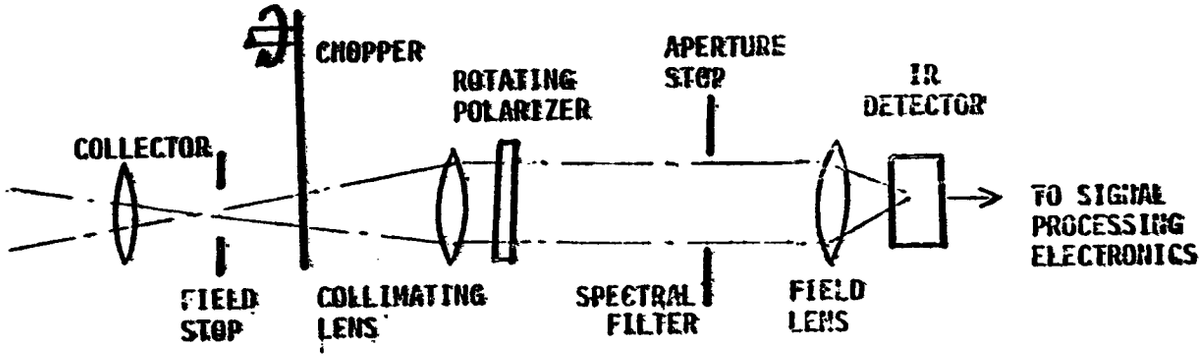

- % POLARIZATION OF SELF-EMISSION FROM SEA WATER IS DEPENDENT ON SURFACE ROUGHNESS
- EXPERIMENTAL MEASUREMENTS IN 1-12 MICRON REGION
  - REFERENCE (SMOOTH) SEA -15% POLARIZATION
  - WIND VELOCITY 3 m/sec -50% POLARIZATION
- SENSOR CHARACTERISTICS
  - FIELD OF VIEW = 1 DEGREE (1.75×10^{-2} rad)
  - COLLECTOR - 39 mm DIA, 63 mm F.L.
  - SI: AS DETECTOR

ASSESSMENT: SENSOR DOES NOT PASS FILTER NO. A (DEVELOPMENT & OPERATIONAL STATUS) DUE TO LIMITED EXPERIMENTAL EXPERIENCE.

TABLE 4.1.3.1.6-1

AIRBORNE OPTICAL SENSOR SUMMARY

- CURRENTLY EMPLOYED AIRBORNE OPTICAL SENSORS ARE NOT DIRECTLY ADAPTABLE TO A SPACE-BASED SYSTEM
  - INADEQUATE RESOLUTION AT ACCEPTABLE SWATH WIDTH FOR LOW LIGHT LEVEL TELEVISION CAMERA
  - EXCESSIVE OPTICS SIZE FOR MECHANICALLY SCANNED AND LASER-STIMULATED FLUORESCENCE SENSORS
  - REQUIREMENT FOR FILM PROCESSING FOR PHOTOGRAPHIC CAMERAS

- LASER-STIMULATED FLUORESCENCE IS A POWERFUL MEANS OF OIL SLICK MONITORING AND SHOULD BE CONSIDERED FOR LATER GENERATION SYSTEMS
  - PRESENT TECHNIQUES EMPLOY NON-COHERENT DETECTION
  - ADDITIONAL DETECTIVITY REQUIRED FOR SATELLITE USE POTENTIALLY AVAILABLE WITH LARGE DEPLOYABLE OPTICS AND ADVANCED COHERENT DETECTION TECHNOLOGY

4.1.3.2 Existing Spacebased Optical Sensors

Introduction and Summary

A comprehensive set of operational and developmental spacecraft sensors were assessed for applicability to ocean pollution monitoring missions. Since these were instruments of known space capability in the spacebased application, their suitability assessment performance analysis was less detailed than that performed for the existing airborne sensors as discussed in Section 4.1.2.1. The assessment indicated that several existing sensors were capable of supplying low resolution data of use in this mission. None were capable of supplying the high resolution data ($\approx$ 30 m) required for the primary functions of detection, areal mapping, classification, and quantification.

Parameters Measured

The existing spacecraft optical sensors are capable of measuring user requirements for ancillary data such as air temperature (17 Km resolution), sea surface temperature (1.0 Km resolution) weather front detection (8.0 Km resolution).

Representative Sensors

Representative existing spacecraft sensors of use in this mission are listed in Table 4.1.3.2-1.

4.1.3.3 Thematic Mapper

The Thematic Mapper (TM), a scanning sensor under development for use with Landsat-D, was analyzed for suitability to this mission since it will constitute the primary sensor for that near-term observational system. It is a "whisk broom" scan instrument with five spectral channels in the visible-near infrared and one spectral channel in the thermal infrared.

TABLE 4.1.3.2-1

REPRESENTATIVE EXISTING SPACECRAFT
OPTICAL SENSORS

- TIROS-N OPERATIONAL VERTICAL SOUNDER (TOVS)
  - . ATMOSPHERIC SOUNDER
    - . TROPOSPHERIC SUBSYSTEM (HIRS-2)
      - 20 SPECTRAL CHANNELS
        0.7 UM (VISIBLE)
        3.7 UM - 11 UM INFRARED REGION
        15 UM CO_2
      - GROUND RESOLUTION AT SUBPOINT = 17 KM
      - GLOBAL COVERAGE
      - ORBIT ALTITUDE = 870 KM
  - . MOPS MEASUREMENT
    - AIR TEMPERATURE AT OCEAN SURFACE
    - ACCURACY = 1^0C

TOVS MEETS MOPS REQUIREMENTS FOR AIR TEMPERATURE MEASUREMENTS

- VISIBLE INFRARED SPIN SCAN RADIOMETER (VISSR)
  - . SYNCHRONOUS METSAT (SMS)
    - GEOSTATIONARY OPERATIONAL ENVIRONMENTAL SATELLITE (GOES 1, B&C)
  - . IMAGING RADIOMETER
    - 0.55 - 0.70 MICRON
    - 10.0 - 12.6 MICRON
  - . MOPS MEASUREMENTS: MONITORING OF WEATHER FRONTS INFERRED FROM RADIANCE MEASUREMENT
    - ACCURACY 0.4^0K
    - RANGE 180^0 - 315^0K
    - POLE-TO-POLE COVERAGE
    - RESOLUTION 8.0 KM
      36,900 KM ORBIT

VISSR MEETS THE MOPS REQUIREMENTS FOR WEATHER FRONT DETECTION

- TIROS-N ADVANCED VERY HIGH RESOLUTION RADIOMETER (AVHRR)
  - . IMAGING RADIOMETER
    - 0.55 UM - 0.90 UM
    - 0.725 UM - 1.10 UM
    - 3.55 UM - 3.93 UM
    - 10.5 UM - 11.5 UM
    - 11.5 UM - 12.5 UM
  - . GROUND RESOLUTION AT SUBPOINT = 1.1 KM
  - . GLOBAL COVERAGE
  - . 870 KM ORBIT
  - . MOPS MEASUREMENT
    - SEA SURFACE TEMPERATURE
      - . NE ΔT = 0.12^0C
      - . RANGE (IR) = 240^0K - 320^0K

AVHRR MEETS MOPS REQUIREMENTS FOR SURFACE TEMPERATURE MEASUREMENTS

- COASTAL ZONE COLOR SCANNER (CZCS)
  - . APPLICATION: NOSS
  - . MULTI-CHANNEL SCANNING RADIOMETER
    - FIVE SPECTRAL CHANNELS IN REGION 0.43 - 0.80 MICRON
    - ONE INFRARED CHANNEL (10.5 - 12.5 MICRON)
  - . MOPS MEASUREMENTS: SURFACE TEMP.
    - NE ΔT 0.35^0K
    - SWATH WIDTH 1566 KM
    - RESOLUTION 0.825 KM

CZCS MEETS MOPS REQUIREMENTS FOR SURFACE TEMPERATURE MEASUREMENTS

The following detailed discussion shows that the TM sensor is of potential utility to this mission, however, its effectiveness is somewhat limited in the areas of detectivity and swath width.

Parameters Measured

The TM, designed for Landsat missions, may also perform pollutant detection classification, and areal mapping. Its applicability to observation of pollutants such as oil spills, acid dumps, sewage sludge, and other wastes is considered here. The observables in the visible are the relative water and pollutant reflectivities and the pollutant spectral signature. The observables in the thermal infrared are water-pollutant temperature difference and pollutant temperature. The TM sensor also serves to reduce the false alarm rate associated with oil spill detection by the microwave radars, for example; as caused by ship wakes and wind spills.

Description of the Sensor (Reference 114)

The Thematic Mapper (TM) is carried on Landsat D. It is a "whiskbroom" scan device providing a 185 Km swath. It contains 5 spectral channels in the visible-near IR spectral region and one channel in the thermal infrared (10.4 μm - 12.5 μm). A seventh channel covering 2.08 μm - 2.35 μm) is also planned. Angular resolution is 43 μrad in the visible-near IR and 174 μrad in the thermal infrared, corresponding to ground resolutions of 30 meters and 120 meters, respectively, at Landsat-D orbital altitude. Two of the visible spectral channels, one in the blue-green (0.45 μ m - 0.52 μ m) and one in the yellow-orange (0.52 μ m - 0.60 μm) are of particular interest to this mission; as is the thermal infrared channel.

Performance Parameters

For the visible channels, the signal to noise ratios at the indicated values of ground in-band radiance are as listed below.

Channel No.	$\Delta\lambda$ (μm)	SNR	Radiance (watt/cm^2 - ster)
1	0.45 - 0.52	32	2.8×10^{-4}
2	0.52 - 0.60	35	2.4×10^{-4}

The noise equivalent temperature difference (NETD) is 0.5°K for the thermal infrared channel (Reference 114).

The noise equivalent radiance (NER) for the visible channels is obtained by dividing the above noted radiances by the SNR.

Channel #1:

$$NER = \frac{2.8 \times 10^{-4}}{32} = 8.75 \times 10^{-6} \text{ watt/cm}^2 - \text{ster}$$

Channel #2:

$$NER = \frac{2.4 \times 10^{-4}}{35} = 6.86 \times 10^{-6} \text{ watt/cm}^2 - \text{ster}$$

Considering the uncertainties associated with atmospheric transmission, these are taken to correspond to a nominal value of 7.8×10^{-6} watt/cm^2 - ster for each channel. The corresponding value of noise equivalent incremental reflectance ($NE \cdot \Delta\rho$) is computed by the following method.

The incremental radiance between clear and polluted water areas is

$$\Delta N = \frac{H_o}{\pi} \rho_w - \frac{H_o}{\pi} \rho_o$$

$$= \frac{H_o}{\pi} (\rho_w - \rho_o) \qquad (1)$$

where:

H_o = solar irradiance at ocean surface = 8.26×10^{-3} watt/cm^2 for channel 1 and 9.44×10^{-3} watt/cm^2 for Channel 2. (In-band values at sun zenith angle = 60°).

ρ_w = clear water reflectivity

ρ_o = polluted water reflectivity

Due to the aforementioned atmospheric transmission uncertainties, a nominal value of 8.85×10^{-3} watt/cm^2 is assumed for H_o in both Channels 1 and 2.

The NE $\cdot \Delta \rho$ is the value of $(P_w - P_o)$ obtained when ΔN equals the NER:

$$NER = \left(\frac{H_o}{\pi}\right)(NE \cdot \Delta P) \qquad (2)$$

$$2.8 \times 10^{-6} = \frac{(8.85 \times 10^{-3})}{\pi} (NE \cdot \Delta \rho)$$

$$NE \cdot \Delta \rho = 2.76 \times 10^{-3} \text{ (ratio)}$$
$$= 0.28 \text{ (\%)}$$

The performance in the visible may also be expressed in terms of minimum detectable contrast (MDC), defined as:

$$MDC = \frac{N_w - N_o}{N_w} \qquad (3)$$

where N_w = clear water radiance and N_o = polluted water radiance.

Figure 4.1.3.3-1 shows MDC vs. background radiance for the Thematic Mapper as elsewhere computed. At the value sea water radiance (2.8×10^{-4} watt/cm^2 - ster) noted, the MDC is 3.17%. For H_o = 8.[illegible] watt/cm^2 as used in solution of equation (2):

$$MDC = \frac{2.8 \times 10^{-4} - N_o}{2.8 \times 10^{-4}} = 0.0317$$

$$N_o = 2.8 \times 10^{-4} - (0.0317)(2.8 \times 10^{-4}) = 2.71 \times 10^{-4} \text{ watt/cm}^2 \text{ - ster}$$

$$NER = N_w - N_o = 2.8 \times 10^{-4} - 2.71 \times 10^{-4}$$
$$= 8.8 \times 10^{-6} \text{ watt/cm}^2 \text{ - ster}$$

From: Equation (2)

$$NER = \frac{H_o}{\pi} (NE \cdot \Delta \rho)$$

$$8.8 \times 10^{-6} = \frac{8.85 \times 10^{-3}}{\pi} NE \cdot \Delta \rho$$

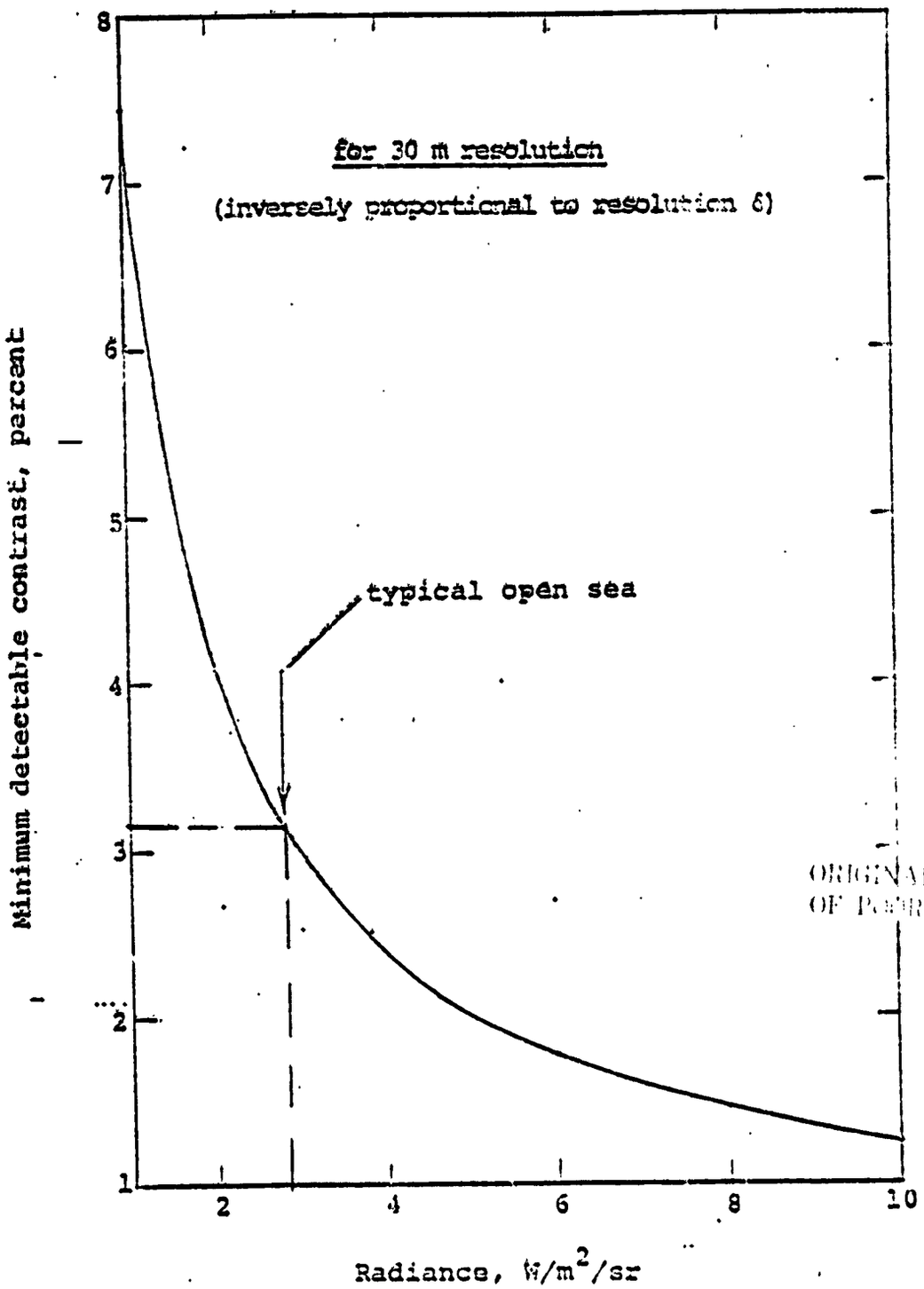

Figure 4.1.3.3-1 Minimum detectable contrast in thematic mapper, Landsat D

$$NE \cdot \Delta\rho = 0.00315 \text{ (ratio)}$$

$$= 0.315\%$$

This value correlates reasonably with the directly computer valve of 0.28% obtained from equation (2), the assumed solar angle, and the TM performance quoted in Reference .

For the infrared channel, the noise - equivalent temperature difference (NETD) is 0.5°K against a 300°K background (Reference 1).

Assessment of TM Sensor Suitability

The TM sensor analyzed using the standard sensor evaluation matrix (filters) as described in the introduction to Section 4.1.2. The assessment for each of the four filter criteria is summarized below.

Filter A - Development and Operational Status

The TM is presently a developmental instrument, based on an earlier whisk-broom scanner, the Landsat Multispectral Scanner (MSS). Based on the promising experimental results measuring waste pollution plumes and oil slicks using Landsat imagery, the TM should also be considered a candidate instrument for use in the ocean pollution missions. Environmental effects need to be better understood, both in the TM visible and thermal IR channels. The basic measurement techniques are developed, however, based or knowledge of the relationship between visible reflectance and thermal IR radiance and the presence of surface pollutants.

The TM is considered as passing this first filter, on the basis of previous experimental results using the MSS and airborne multispectral scanners.

Filter B - Detectivity/Sensitivity

In the visible, incremental reflectance between clear water and water polluted by representative substances typically ranges between about 3% to somewhat less than 1%. Signal to noise ratio will thus be in the region of 10 down to somewhat less than 3, considering the predicted NE $\cdot \Delta \rho$ of 0.03%. At least for the upper end of this range, the signal to noise ratio should be adequate. Some degree of image enhancement may be necessary at the lower end of the range.

NETD requirements in the infrared for pollutant detection are not completely defined. For surface temperature measurements, the general user requirement is for a precision (as limited by the NETD) of 0.5°C. The corresponding accuracy requirement is typically 1°C. The ability to achieve this degree of accuracy in terms of inexact knowledge of emissivity and atmospheric effect is not clearly established.

The TM thus Passes Filter B for the Visible Channels with the proviso that some degree of image enhancement may be required at the lower range of water-pollutant $\Delta \rho$ values.

Filter C - Performance Suitability

The desired resolution for detection and areal mapping is 10 meters. This is not met by the 30 meter visible and 120 meter infrared TM capability. The 30 meter capability, however, should yield useful data in the visible in many if not most cases. The resolution requirements for ancillary measurements such as surface temperature are less severe, in the region of 1 Km or greater. These are met by the TM.

For coastal zone coverage, a swath width of about 375 Km is desireable. This is greater than the 185 Km swath width of the TM.

The TM thus Does Not Rigorously Pass Filter C. If data from the instrument is available, however, the degree of attenuation introduced by Filter C is not considered large enough to preclude its use.

Filter D - Compatibility with Spacecraft

The TM is designed for operation on Landsat-D, therefore the TM passes this filter.

Performance Summary

The TM sensor is of potential utility to the Ocean Pollution Mission. Its effectiveness is decreased somewhat when the assessment is based on the most severe requirements, namely:

a. Resolution of 30 meters (visible) and 120 meters (IR) as compared to ideal requirement of 10 meters.

b. Swath width of 185 Km as compared requirement for 375 Km.

In addition, the assessment shows that the sensor has marginal detectivity in the visible channels, possibly requiring image enhancement under low-level signature conditions.

4.1.3.4 Dedicated Optical Sensor

Introduction

The conceptual design of an optical sensor meeting the overall requirements for water pollutant detection, areal mapping, classification, and quantification from orbit has been defined. The instrument employs linear detector arrays which provide coverage of several spectral channels in the 0.4 μm - 0.7 μm and thermal infrared spectral regions, in a pushbroom scan, mode. The arrays are pointable in the cross-track direction to allow the selection of specific cross-track swath regions. This capability minimizes the required array size for continuous coastal zone coverage. The Pointable Optical Linear Array configuration results in the acronym of POLA.

Late in the study, the concept of a dedicated sensor employing a pointable optical mosaic array (POMA) emerged. This concept allows selection of spectral channel center wavelengths and spectral bandwidths on command as appropriate to given mission (type of pollutant observation) requirements.

A detailed discussion of the POLA sensor is contained in this section. For the POMA, only the system concept is presented; this sensor could be considered as an alternative or an advanced version of POLA.

Parameters Measured

The dedicated optical sensor performs the functions of pollutant detection, areal mapping, classification, and quantification. It is configured to be applicable to the general requirements of ocean pollution measurements. In addition to oil spill monitoring, it is applicable to observation of other pollutants such as acid dumps, sewage sludge, and bio-degradable industrial wastes. The observables in the visible spectrum are the relative water and pollutant reflectivities and the pollutant spectral signature. The observables in the thermal infrared are water-pollutant temperature differences and pollutant temperature. The dedicated optical sensor also serves to reduce the false alarm rate associated with oil slick detection by the microwave radars, for example; as caused by ship wakes and wind slicks.

Description of the Sensor

The POLA sensor concept, the detailed sensor parameters for the visible spectral channels and the detailed characteristics of the 8.0 - 12.5 μm thermal infrared channels is, for given resolution, optics size and number of detectors are tradeoffs with detectivity (signal-to-noise performance, and swath width. Representative optics diameter is 21 cm. For 375 Km swath width, each visible spectral channel employs 1.25×10^4 detectors and the array length is 22.5 cm. For the infrared, 3.75×10^3 detectors are employed at an array length of 19.1 cm.

Performance Parameters

Visible Spectral Channels

Definition of NE $\Delta\rho$

The basic figure-of-merit for detectivity is the noise equivalent incremental reflectivity (NE Δ P). This quantity is the difference in pollutant - water percent reflectivity giving a signal-to-rms-noise ratio of 1.0.

The concept of NE $\Delta\rho$ is shown in Figure 4.1.3.4-1. The total signal level at the sensor output consist of components from atmospheric background and that of the ocean surface. Also depicted in that figure is, how the output voltage might vary as a Linear array of detectors is sampled along its length.

In the following discussion of sensor performance, the sensor-generated rms noise level is e_n. The dc level of the atmospheric background radiance deflection $L_s N_b$. The dc level of the radiance of the unpolluted water is N_w and the dc level of the radiance of the pollutant is N_p. The rms noise level $e_n^1 > e_n$ contains both sensor and background noise.

The requirement for detection is that the signal change corresponding to $N_w - N_p$ can be recognized in the presence of the noise e_n^1. The dc level is a pedestal which can be removed by slicing. It thus represents a dynamic range requirement rather than a detectivity problem. The contrast is then expressed as:

$$\text{Contrast} = C = \frac{\frac{H_s}{\pi}\rho_w - \frac{H_s}{\pi}\rho_p}{\frac{H_s}{\pi}\rho_w}$$

$$= \frac{\rho_w - \rho_p}{\rho_w} = \frac{\Delta\rho}{\rho_w} \qquad (28)$$

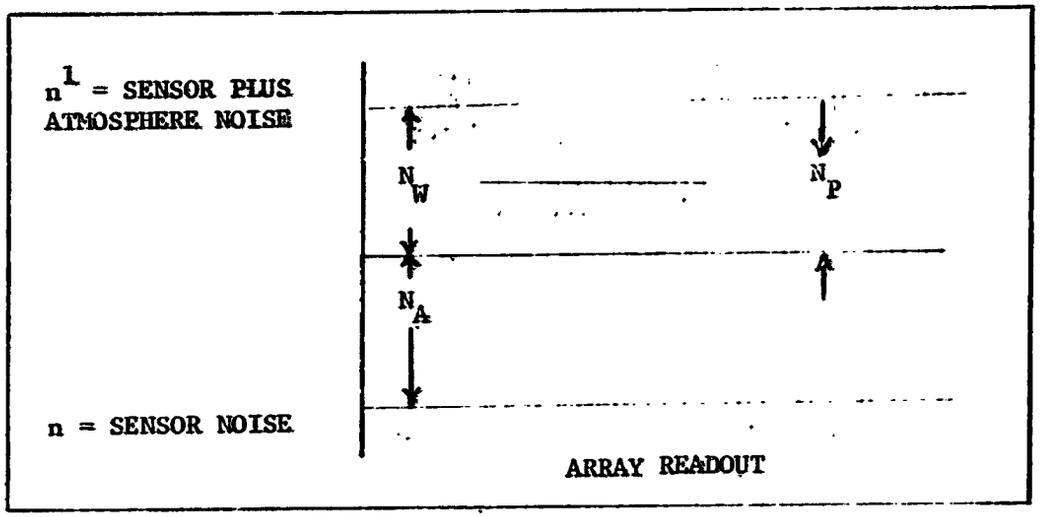

- N_A = ATMOSPHERE RADIANCE
- N_W = WATER RADIANCE = $\frac{Hs}{\pi} \rho_W$
  Hs = SOLAR IRRADIANCE
  ρ_W = WATER REFLECTIVITY
- N_P = POLLUTANT RADIANCE = $\frac{Hs}{\pi} \rho_P$
  ρ_P = POLLUTANT REFLECTIVITY

- N_A REMOVED BY THRESHOLDING
- CONTRAST = $C = \dfrac{\frac{Hs}{\pi}\rho_W - \frac{Hs}{\pi}\rho_P}{\frac{Hs}{\pi}\rho_W} = \dfrac{\rho_W - \rho_P}{\rho_W} = \dfrac{\Delta\rho}{\rho_W}$
- S/N $\dfrac{Hs, Ta\Delta\rho}{\pi . n^1}$ = 1.0 AT NE, $\Delta\rho$
- $NE\ \Delta\rho = \dfrac{\pi n^1}{HsTa}$

$\Delta\rho = C\ \rho_W$

FIGURE 4.1.3.4-1. DEFINITION OF CONTRAST AND NE $\Delta\rho$

where the quantities are as identified on Figure 12.

The signal to noise ratio is proportional to the quantity $\frac{H_s \cdot T_a \cdot \rho}{\pi \cdot n^1}$

where n^1 is the noise equivalent radiance corresponding to e_n^1 and T_a is the atmospheric transmission. Thus:

$$S/N = \frac{H_s \cdot T_a \cdot \Delta\rho}{\pi \cdot n^1} \tag{29}$$

NE$\Delta\rho$ is the value of $\Delta\rho$ at signal-to-noise = 1.0. Thus:

$$NE\Delta\rho = \frac{\pi \cdot n^1}{H_s T_a} \tag{30}$$

Sensor Signal-to-Noise Ratio Predictions

The following analysis is based upon the characteristics of General Electric's intrinsic silicon CID arrays. Operation under electronic noise limited conditions is assumed. Noise equivalent power for this case is defined in terms of noise equivalent carriers by the method shown in Table 4.1.3.4-1.

For the equations given on Table 4.1.3.4-1 the integration time t_i is:

$$t_i = \frac{\Delta X}{V_s} \tag{31}$$

where ΔX = ground resolution (meters)

V_s = spacecraft velocity (meters/sec),

and Δf is given by:

$$\Delta f = \frac{n}{t_i} \tag{32}$$

where n is the number of detectors in the array, proportional to swath width.

The quantity M is the detector quantum efficiency, ... is 0.5.

The signal to noise ratio is given by:

$$S/N = \frac{\pi \cdot \Delta N \cdot A_d \cdot T_o \cdot T_a}{4.f^2 \cdot NEP} \tag{34}$$

TABLE 4.1.3.4-1 POLA SENSOR

DEFINITION OF NOISE EQUIVALENT POWER (NEP)

- LIMITING NOISE IS JOHNSON NOISE IN READOUT AND PREAMPLIFIER

  $\bullet\ V_n \sqrt{h2} = 6.4 \times 10^{-9}$ VOLT AT PREAMPLIFIER INPUT

- EQUIVALENT NOISE CARRIERS PER INTEGRATION TIME GIVEN BY

$$N_e = \frac{Vn \sqrt{h2} \bullet \sqrt{\Delta f} \bullet C_i}{q} = \frac{(6.4 \times 10^{-9} v)\ (\sqrt{\Delta f})\ (15 \times 10^{-12} f)}{1.6 \times 10^{-19}\ \text{coulomb}} = 0.6 \sqrt{\Delta f}\ \text{CARRIERS/}_i$$

- $\Delta f = \dfrac{\text{NUMBER OF DETECTORS}}{\text{INTEGRATION TIME}} = \dfrac{n}{t_i}$

- $N_e = \dfrac{0.6 \sqrt{n}}{t_i}$

- $\text{NEP} = \dfrac{N_e\ hc}{\eta m t_i} = \dfrac{(0.6)\ (\sqrt{n})\ (6.63 \times 10^{-34}\ \text{watt-sec}^2)\ (3 \times 10^{-10}\ \frac{\text{cm}}{\text{sec}})}{(0.44 \times 10^{-4}\ \text{cm})\ (0.5)\ t_i \bullet t_i^{-11})} = \dfrac{(5.42 \times 10^{-19}) \sqrt{n}}{(t_i)\ \frac{3}{2}}$

$= (1.92 \times 10^{-15}) \sqrt{n}$ watt for $\Delta x = 30$ m, $h = 700$ Km, $\lambda = 0.44$ μm, and quantum efficiency (η) = 0.5

C-3

189

where: ΔN corresponds to $\frac{H_s \cdot T_a \cdot \Delta\rho}{\pi}$ as shown on Figure 4.1.3.3-1.

A_d = detector element area = 1×10^{-6} cm^2

T_a = atmospheric transmission = 0.667

T_o = optics/filter effective transmission, assumed = 0.45

F = optics F - number.

S/N is a function of swath width, for other given conditions, per the effect of equation (32). The NE $\Delta\rho$ corresponds to the value of $\Delta\rho$ at which the signal to noise ratio is unity. According parametric computation of NE $\Delta\rho$ vs. swath width is shown on Figure 4.1.3.3-2. The optics sizes (D_o) shown are the diameters corresponding to the indicated F-numbers at the focal length required for 30 meters ground detector subtense.

From Figure 4.1.3.4-2, values of NE $\Delta\rho$ of 0.16% at 375 Km swath width and 0.11% at 185 Km swath width are noted for an optics diameter of 21 cm. Annual values of $\Delta\rho$ for various pollutant - water combinations are shown on Table 4.1.3.4-2. These are significantly higher than the noise equivalent values shown on that figure, indicating the effectiveness of the POLA approach.

The performance as calculated above can be increased by providing m rows of detectors, each of n elements. Use of time delay integration (TDI) or longer exposure time with image motion compensation will then decrease NE $\cdot \Delta\rho$ by $\sqrt{m}$. This approach is not further considered for a multispectral sensors due to the large number of detectors required for significant improvement.

Array Length and Clock Rate vs. Swath Width

The clock rate, i.e., readout rate; is obtained by dividing the integration time by the number of detectors:

$$t_d = \frac{t_i}{n} \qquad (35)$$

FIGURE 4.1.3.4-2

NE $\cdot \Delta \rho$ VS. SWATH WIDTH FOR POLA SENSOR
(VISIBLE SPECTRAL CHANNELS)

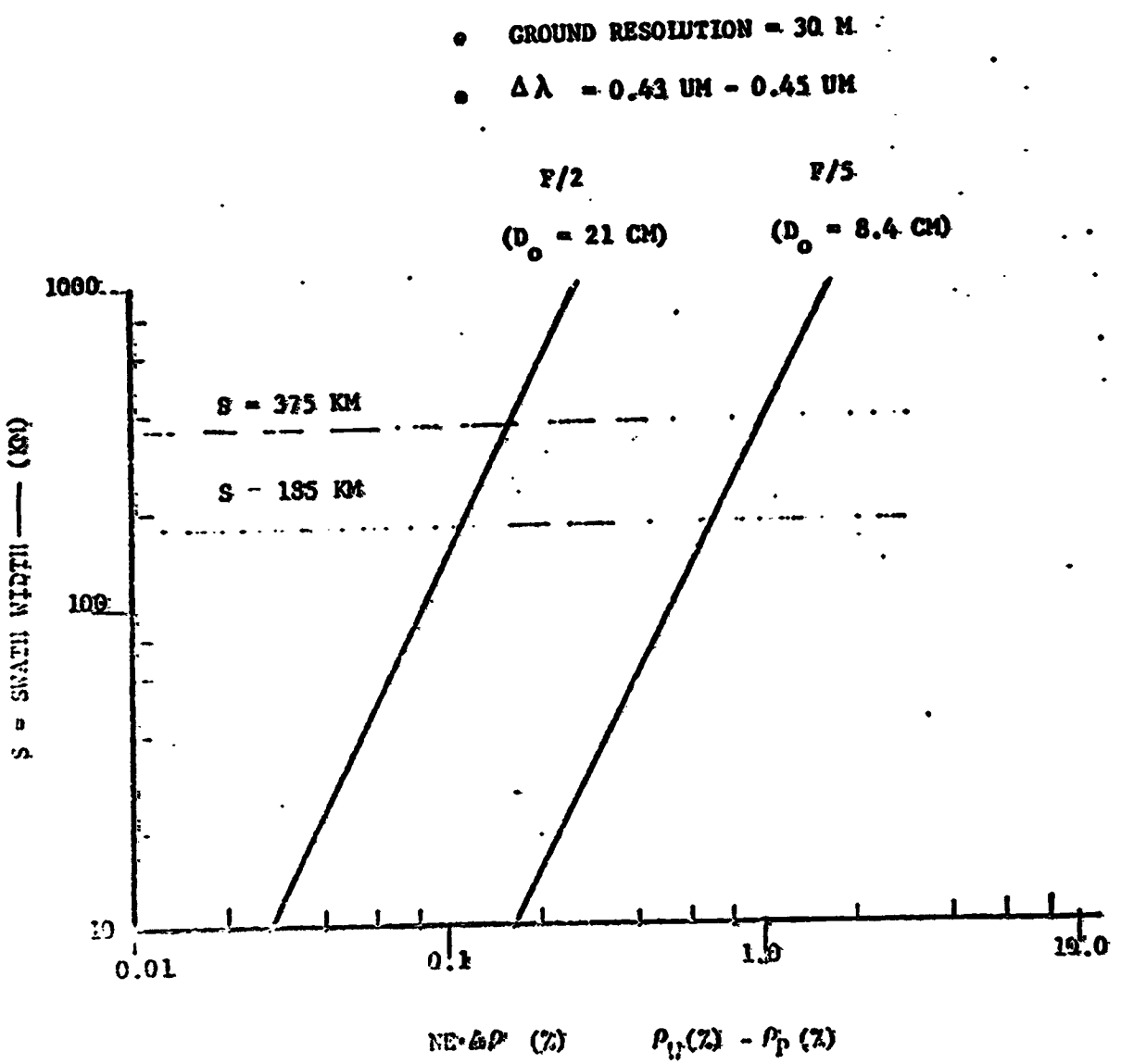

GENERAL ELECTRIC

space division

TABLE 4.1.3.4-2

INCREMENTAL REFLECTANCE ($\Delta\rho$) FOR REPRESENTATIVE SEA WATER POLLUTANTS

POLLUTANT	PLATFORM/SENSOR	WAVELENGTH	$\Delta\rho = \rho_{\omega} - \rho_{p}$ %	INVESTIGATORS
OIL SLICK	LANDSAT/ERTS-1	0.5μM = 0.6μM	2.67% (CENTER) 0.81% (EDGE)	G. GOLDMAN AND R. HORVATH (ERIM)
		0.6μM - 0.7μM	2.41% (CENTER) 0.4% EDGE)	
ACID PLUME (30 MINUTES AFTER DUMP)	AIRCRAFT AT 3.0 KM/ MODULAR MULTISPECTRAL SCANNER (MSS)	0.44μM - 0.49μM	0.82%	R. JOHNSON (NASA/LANGLEY)
		0.66μM - 0.70μM	1.46%	
SEWAGE SLUDGE (60 MINUTES AFTER DUMP)	↓	0.44μM - 0.49μM	1.11%	↓
		0.36μM - 0.79μM	1.3%	
LIQ DIGESTED INDUSTRIAL WASTE (30 MINUTES AFTER DUMP)	↓	0.66μM - 0.70μM	0.42%	↓

* ρ_W = WATER REFLECTIVITY = $\frac{N_W \pi}{\text{SOLAR IRRADIANCE}}$

ρ_P = POLLUTANT REFLECTIVITY = $\frac{N_p \pi}{\text{SOLAR IRRADIANCE}}$

$$\text{Clock Rate} = \frac{1}{t_d} = \frac{n}{t_1} = \frac{n}{4.3 \times 10^{-3} \text{ sec}} \text{ hz} \qquad (36)$$

Physical limitations on array fabrication will probably restrict maximum available clock rate to the order of 1 mhz for the 1980 - 1981 period.

Array length is obtained by multiplying the detector element size by the number of detectors.

$$L_a = n\sqrt{A_d} = (n)\ (1 \times 10^{-3})\ \text{cm.} \qquad (37)$$

Clock rate and array length for the visible spectral channels vs. swath width are shown by the plots of Figure 4.1.3.4-3.

Number of Detectors vs. Swath Width

Total number of detectors for the visible spectral channels vs. swath width is shown by Figure 4.1.3-4-3a.

8.0 - 12.5 μm Infrared Spectral Channel

Noise Equivalent Incremental Temperature (NE$\cdot\Delta$T)

For the infrared spectral channel, the figure of merit for detectivity is the noise equivalent incremental temperature (NE$\cdot\Delta$T). This is defined in a manner equivalent to NE$\cdot\Delta\rho$ excepting that the signal corresponds to the temperature rather than the reflectivity difference for the water and pollutant. The observable is the self-emitted energy from the water and pollutant areas.

For 100 meter ground resolution, 700 Km spacecraft altitude, and 0.0051 cm detector size, the lens focal length is 35.7 cm. For the 21 cm and 8.4 cm optics diameters evaluated for the visible channels, the corresponding F-numbers are 4.25 and 17.

Background limited infrared photoconductor (BLIP) operation is assumed. The total background is taken as that from a 300°K unity-emissivity scene plus

Figure 4.1.3.4-3

DETECTOR ARRAY LENGTH AND CLOCK RATE VS. SWATH WIDTH
FOR ROIA SENSOR
(VISIBLE SPECTRAL CHANNELS)

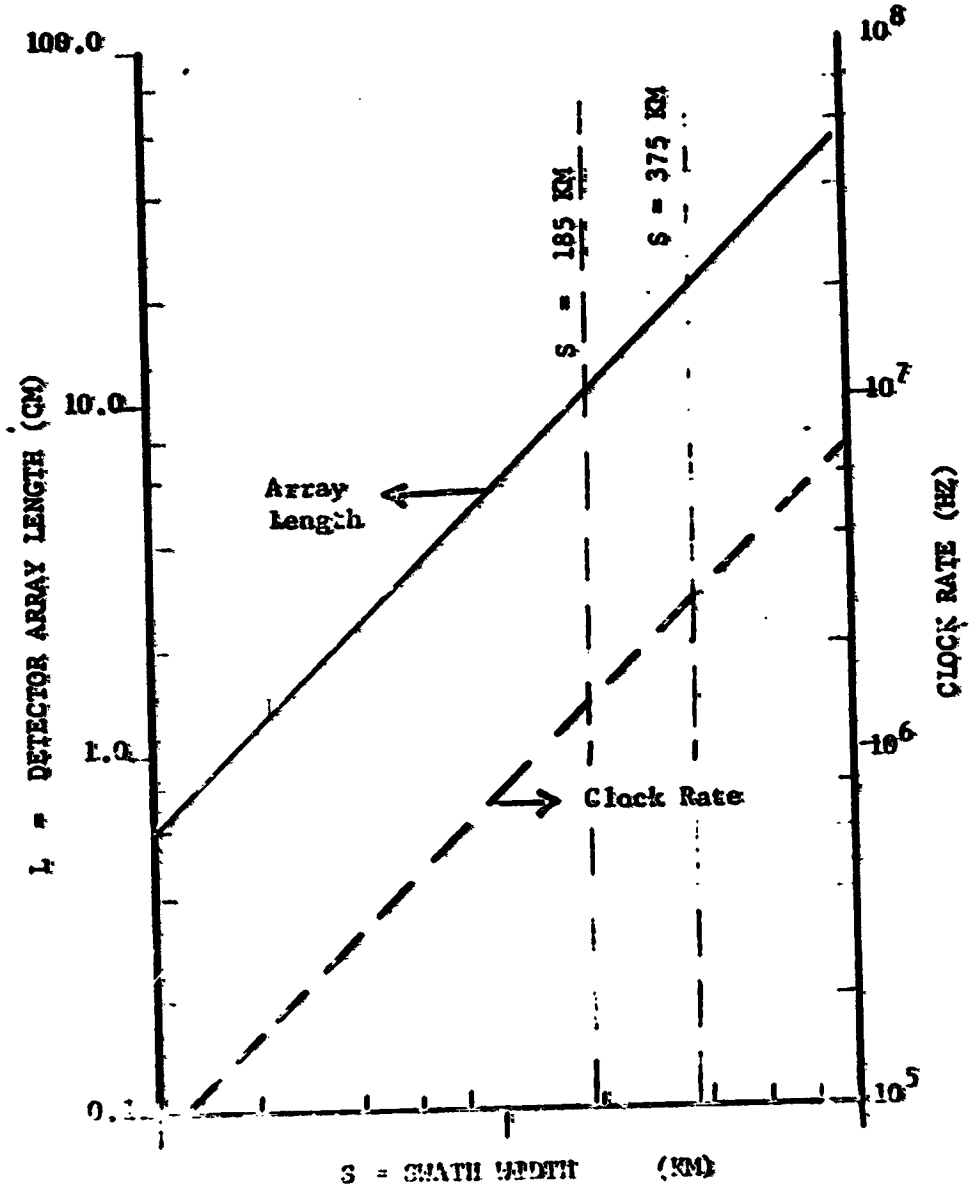

GENERAL ELECTRIC

space division

igure 4.1.3.4-3a

NUMBER OF DETECTORS PER SPECTRAL CHANNEL VS. SWATH
FOR POLA SENSOR
(VISIBLE SPECTRAL CHANNELS)

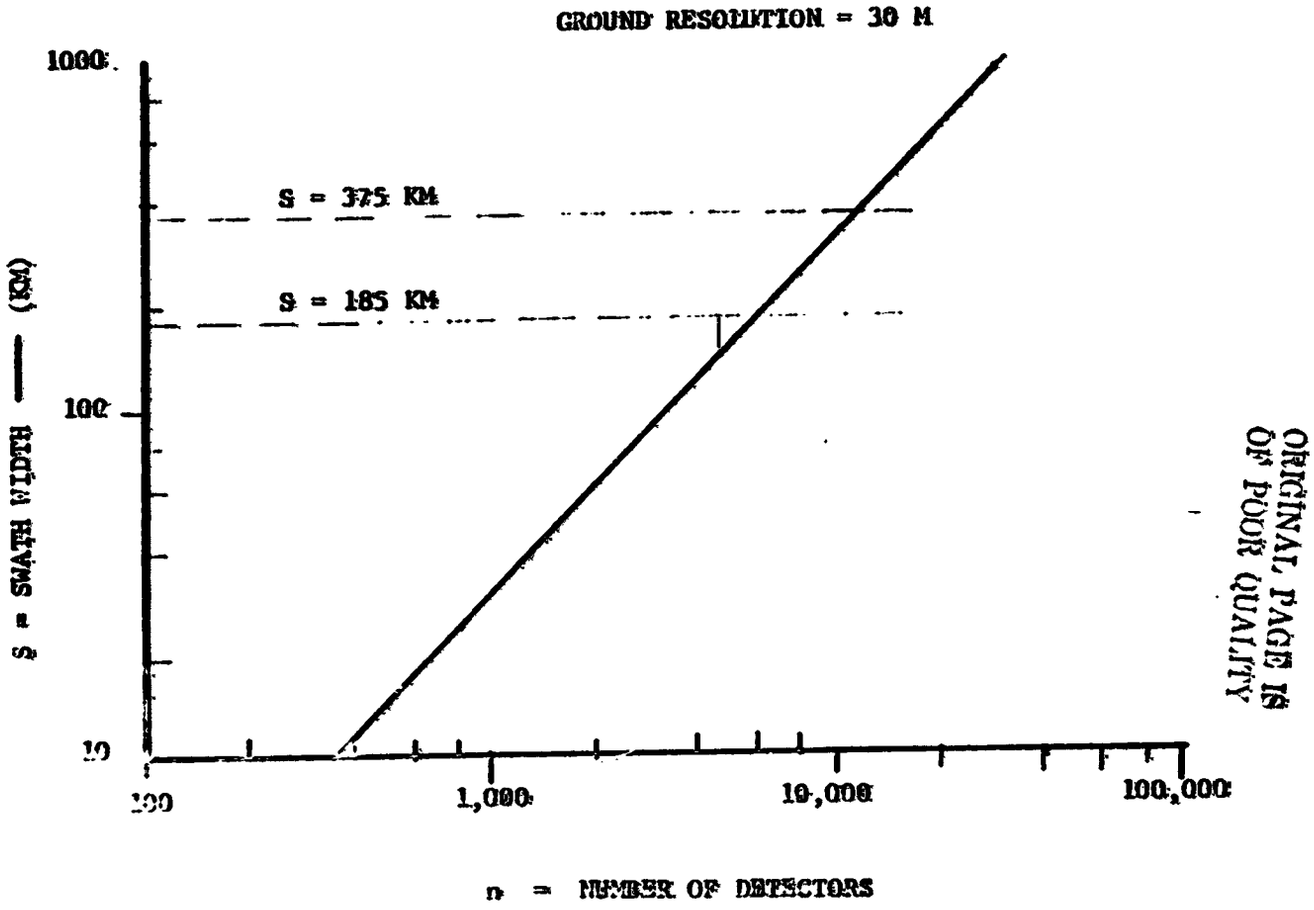

the contribution from an uncooled (300°K) lens. The lens contribution to background is estimated from that of an uncooled (300°K) optic equivalent to the F/1.7 POLA case. This lens, earlier employed with a sensor operating in the 8-14 m region, is a cassegrain system operating behind an IRTRAN-2 window. For the F/4.25 case, the lens background irradiance at the focal plane at F/1.7 is scaled as F^{-2}, i.e., multiplical by $1.7^2/4.25^2$. For the BLIP case,

$$D^*_{BLIP} = \frac{\lambda}{2hc}\sqrt{\frac{M}{\phi_B}} \qquad (38)$$

where λ = wavelength (micron)

h = Planck's constant = 6.63×10^{-34} watt sec.^{2}

c = velocity of light = 3×10^{10} cm/sec

M = detector quantum efficiency = 0.2

ϕ_B = Background irradiance at focal plane (photon/sec-cm^2).

For F/1.7, ϕ_B is computed as 1.21×10^{17} photon/sec-cm^2.
At F/4.25, ϕ_B is computed as 1.93×10^{16} photon/sec-cm^2.
The corresponding values of D^*_{BLIP} are 3.31×10^{10} at F/1.7 and 8.29×10^{10} at F/4.25.

Photoconductive detector elements with individual preamplifiers are also assumed. In this case, the noise bandwidth is equivalent to the integration time = frame time = t_i. The frame time is given by:

$$t_i = \frac{\Delta X}{V_s} = \frac{100 \text{ m}}{7 \times 10^3 \text{ m/sec}} = 1.43 \times 10^{-2} \text{ sec}$$

which is equivalent to equation (31) excepting that ΔX is 100 meters rather than 30 meters. ΔF is taken as the reciprocal of t_i, = 70 hz. The BLIP noise equivalent power is then given by:

$$NEP_{BLIP} = \sqrt{\frac{A_d \quad F}{D^*_{BLIP}}}$$

$$= \frac{(0.0051) \quad 70}{3.31 \times 10^{10}} = 1.29 \times 10^{-12} \text{ watt at F/1.7}$$

$$= \frac{(0.0051) \quad 70}{8.29 \times 10^{10}} = 5.14 \times 10^{-13} \text{ watt at F/4.25}$$

The signal-to-noise ratio is given by:

$$S/N = \frac{\pi \cdot A_d \cdot \Delta N \cdot T_o \cdot T_a}{4 \cdot F^2 \cdot NEP_{BLIP}} \qquad (39)$$

where

A_d = detector area = $(0.0051)^2$ cm

ΔN = incremental radiance between scene and 300°K background in sensor spectral passband (watt/cm^2-ster)

T_o = optics transmission = 0.35

T_a = atmospheric transmission = 0.7

The temperature difference ΔT is related to ΔN, for small values of ΔT, by the expression:

$$\Delta N (T, \Delta T, \lambda, \Delta\lambda, \epsilon) = K (T, \lambda, \Delta\lambda, \epsilon) \Delta T \qquad (40)$$

where for the given conditions $K \cong 7 \times 10^{-5}$.

Corresponding values of signal-to-noise ratio are plotted vs. ΔT in Figure 4.1.3.4-4. From the curves NEΔT is noted in the region of 0.01°K for 21 cm optics and about twice this value for 8.4 cm optics.

POLA Assessment Summary

The instrument characteristics are summarized in Table 4.1.3.4-3.

Figure 4.1.3.4-4

IDEAL BORA INFRARED PERFORMANCE

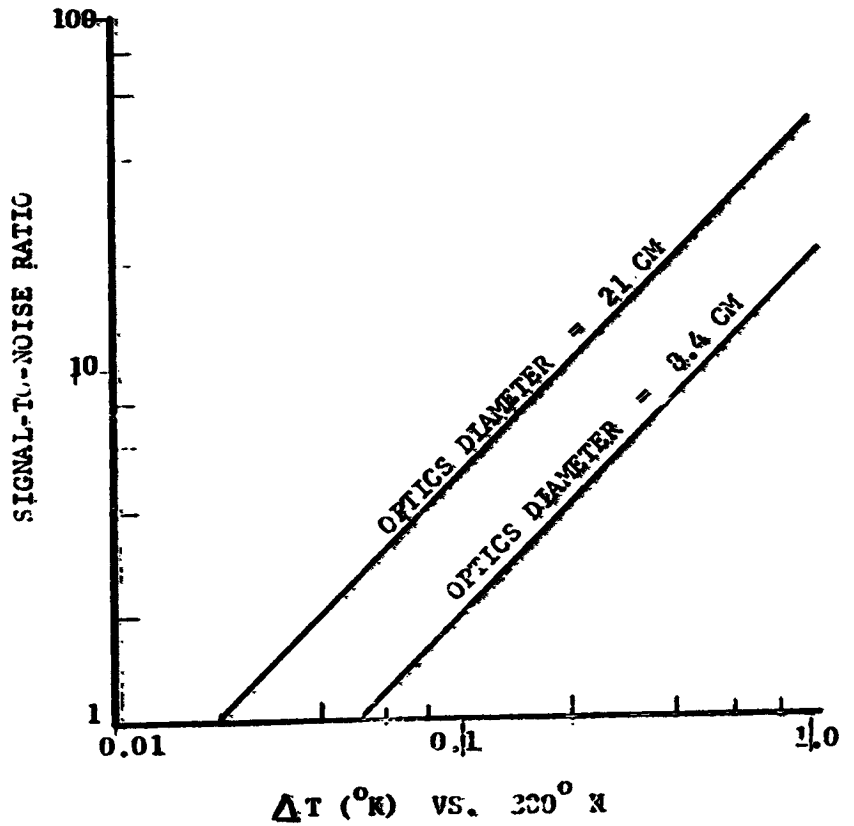

- $\Delta\lambda$ = 8.0 μM - 12.5 μM
- D^*_{BLIP} FOR CONDITIONS OF:
  - η = 0.2
  - SCENE BACKGROUND 300° K ΔT = 1.0
  - 300° K LENS FOR REPRESENTATIVE OPTICS MECHANIZATION AND COMPONENT EMISSIVITIES
- GROUND RESOLUTION = 100 METERS
- SENSOR ALTITUDE = 700 KM
- ATMOSPHERE TRANSMISSION = 0.7

Table 4.1.3.4-3

WAVELENGTH REGION	SWATH WIDTH (KM)	RESOLUTION (M)	NE·ΔP	NE δ AT (°K)	NUMBER OF DETECTORS PER SPECTRAL CHANNEL	ARRAY LENGTH (CM)	OPTICS DIAMETER (CM)
VISIBLE	375	30	0.16%		1.25×10^4	22.9	21
	185	30	0.11%		6.17×10^3	11.1	21
8.0-12.5UM	375	100		0.01	3.75×10^3	19.1	21
	185	100		0.02	1.85×10^3	9.44	8.4

A high sensor sensitivity is made possible primarily through the increase in integration time in POLA, as compared with conventional sweep-scan instruments. This sensitivity margin will be particularly useful is mapping waste plume characteristics, where swath tonal differences are significant is identifying pollutant type and concentration.

The features of pointability and wide swath are important is providing the necessary areal/temporal coverage, as will be discussed in Section 5.2.2.

Due to the development cycle for this new instrument, it is anticipated that it would be available in the mid-term time frame (post 1987).

POMA Sensor

An alternate design approach for the POLA Sensor employing a mosaic CID array focal plane and operating in the visible spectral region has been identified. The instrument is identified by the acronym POMA. (Pointable Optical Mosaic Array).

The POMA is basically a spectrometer which provides cross-track spatial resolution in the array column direction and spectral resolution in the array row direction. The design concept is sketched in Figure 4.1.3.4-5.

The CID mosaic arrays have random access capability. For the POMA application, this allows selected rows to be interrogated by command. The result is the ability to select given center wavelengths and bandwidths for the spectral channels as dictated by specific mission requirements. Operational flexibility

Figure 4.1.3.4-5

POINTABLE OPTICAL MOSAIC ARRAY (POMA) SENSOR CONCEPT
(ALTERNATIVE MECHANIZATION APPROACH TO POIA)

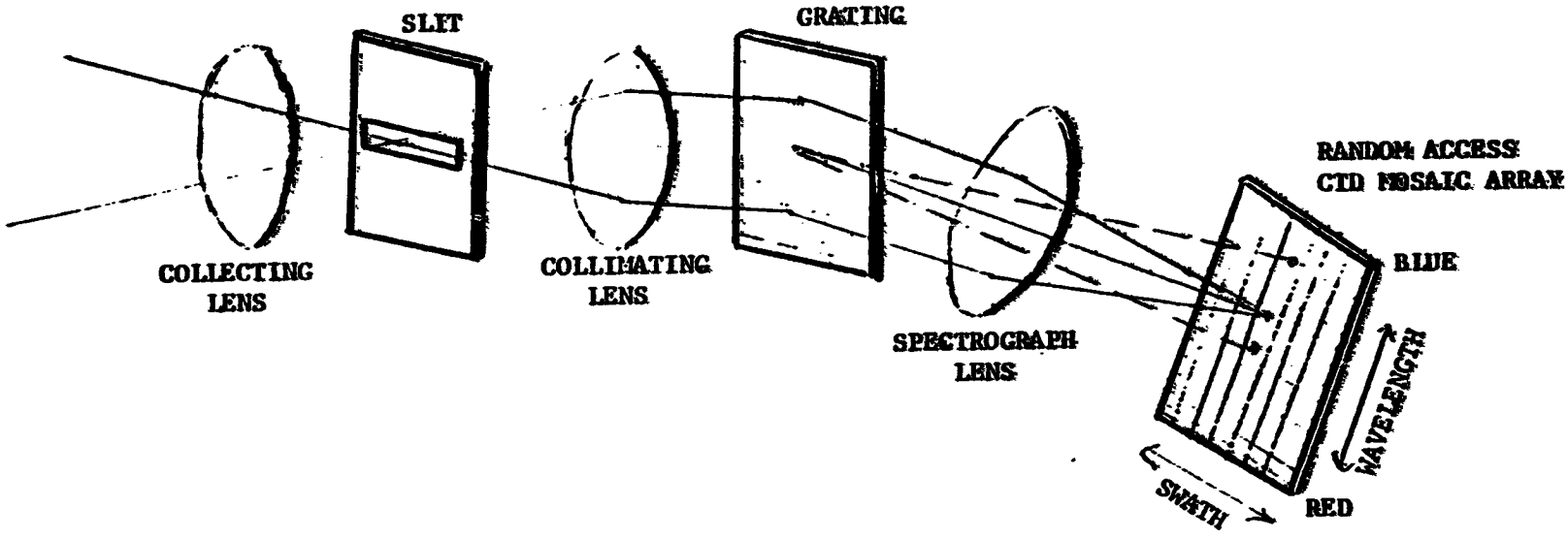

- MOSAIC CHARGE INJECTION DEVICE (CID) FOCAL PLANE
  - SPATIAL RESOLUTION IN COLUMN DIRECTION
  - SPECTRAL RESOLUTION IN ROW DIRECTION
  - SELECTABLE WAVELENGTH SPECTRAL BANDWIDTHS TAILORED TO SPECIFIC MISSION NEEDS

is thus provided as compared to the fixed spectral channels of the baseline POLA sensor. The POMA array switching command and control logic is shown by Figure 4.1.3.4-6.

The POMA sensor concept emerged late in the study. Sensor performance thus has not been examined to the extent of the POLA instrument. The POMA concept, however, is considered a versatile approach of promise.

SUMMARY OF SELECTED OPTICAL SENSORS

- Adaptation and modification of existing airborne sensors for use in space platforms is not a suitable approach.
- Existing spacecraft sensors can meet some MOPS requirements involving low resolution requirements.
- The overall MOPS requirement in the optical range can be met by a dedicated spacebased optical sensor.

Figure 4.1.4.3-6
POMA ARRAY LOGIC

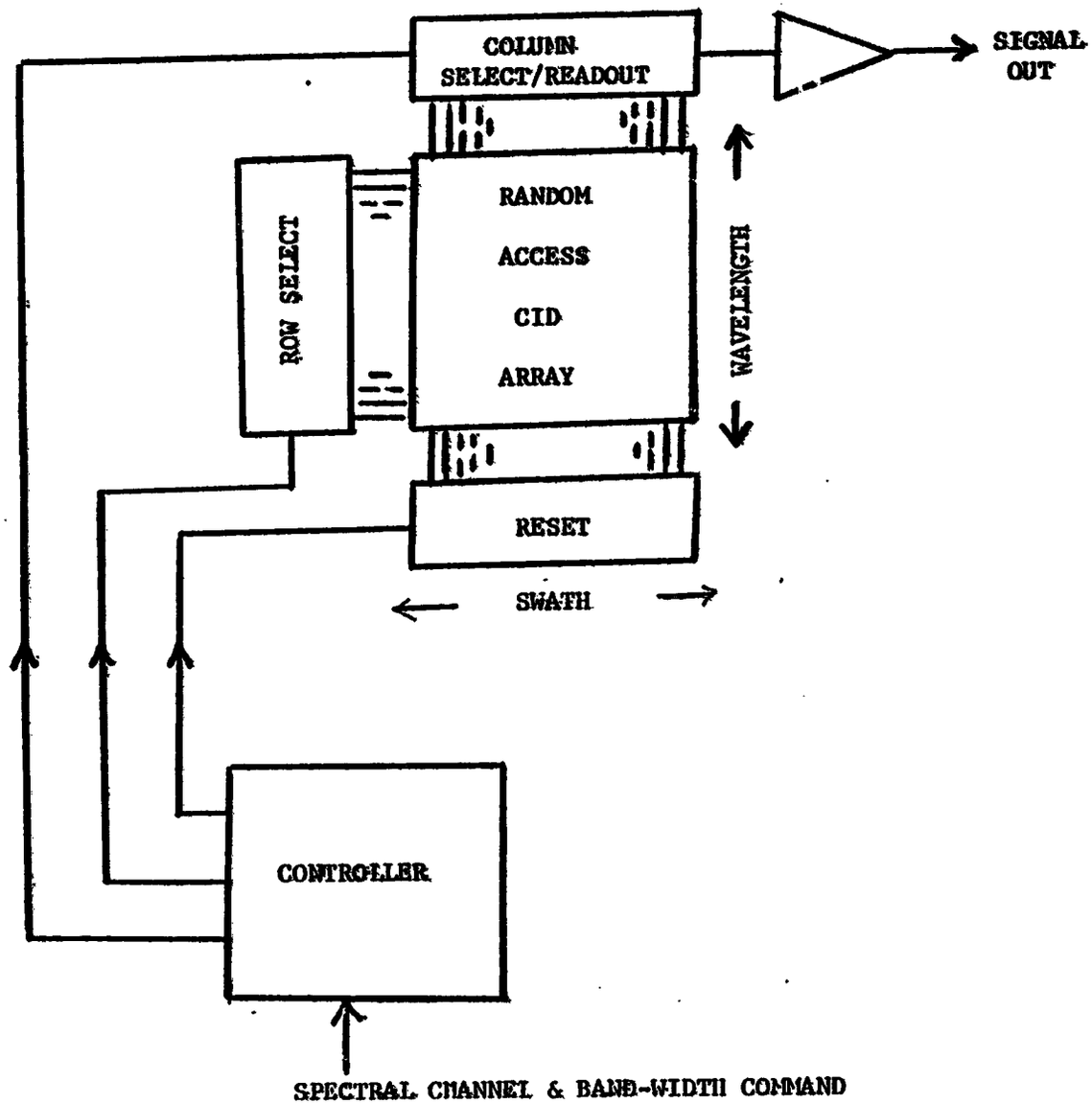

4.2 PLATFORMS

This section identifies the principal spacecraft, aircraft and surface platforms considered as candidates for the ocean pollution mission. Consideration of specific platforms, rather than hypothetical, dedicated platforms, is intended in order to make the results more realistic, since it is assumed that the ocean pollution monitoring system will be shared with other multi-mission systems. This added degree of realism holds true even though some of the platforms such as NOSS and ICEX have not been fully defined as yet. By dealing with real constraints and necessary compromises, the sensitivity of the system to this sharing of elements is evaluated and a baseline is established. This baseline, in turn, may be refined or corrected in the future, on the basis of more current information on the satellites, surveillance aircraft and surface platforms.

4.2.1 OCEANOGRAPHIC SATELLITE

The Natural Oceanic Satellite System (NOSS) is planned for launch in 1984. The Flight Segment consists of the spacecraft, Airborne Support Equipment, Ground Support Equipment and Software. The system's goals are to satisfy the need for synoptic data on ocean environmental parameters by NOAA and DOD. Table 4.2-1 shows a summary of the NOSS measurement goals as extracted from the NOSS Technical Requirements Document.

The sensor complement for NOSS includes a microwave altimeter, multichannel passive microwave radiometer, scanning spectro-radiometer (Coastal Zone Color Scanner), and scatterometer. The system includes a Surface Data Acquisition System and Receiver/ Processing Assembly interfacing with the Global Positioning System.

The nominal orbit for NOSS is a seven-synchronous orbit near 700 km altitude. The final orbit selection will be prepared as a result of parametric analyses in the Phase B NOSS Study.

Table 4.2-1. NOSS Goals

Parameter	Precision	Absolute Accuracy	Range	Frequency	Delay	Grid Size	Horizontal Resolution
Wind							
Speed	0.5 m/s	2 m/s	0 to 50 m/s	12 hrs	3 hrs	200 km	25 km
Direction	5°	10°	0° to 360°	12 hrs	3 hrs	200 km	25 km
Sea Surf. Temp.							
Global	0.25°C	1.0°C	-2°C to 35°C	3 days	12 hrs	200 km	25 km
Local	0.10°C	0.5°C	-2°C to 35°C	1 day	12 hrs	10 km	10 km
Waves (Sea State)							
Sign. Wave Ht.	0.3 m	0.3 m	0 to 25 m	12 hrs	3 hrs	100 km	25 km
Amplitude Components	0.7 m	0.7 m	1 to 8 m	12 hrs	3 hrs	100 km	25 km
Wave Length Components	10%	10%	6 to 1000 m	12 hrs	3 hrs	100 km	25 km
Direction	10°						
Ice							
Cover	15%	15%	0 to 100%	3 days	12 hrs	20 km	20 km
Thickness	2 m	2 m	0.25 to 50 m	3 days	12 hrs	50 km	50 km
Age	New, 1st yr multi-yr	New, 1st yr multi-yr	0 to 3 yrs	3 days	12 hrs	20 km	20 km
Sheet Height	0.1 m change	0.5 m change	-5 to +5 m/yr	1 yr	30 days	TBD	10 km
Bergs	N/A	+2 km of true location	N/A	2 days	12 hrs	N/A	0.1 km
Water Mass Definition							
Chlorophyll	10% (mg/m^3)	Within factor of 2	0.1 to 100 mg/m^3	2 days	8 hrs	TBD	0.4 km
Turbidity	0.1 PPM	Lo, Med, Hi	0 to TBD	1 day	10 hrs	TBD	0.4 km
Horizontal Surface Currents							
Speed	5 cm/s	5 cm/s	0 to 250 cm/s	1 day	1 day	100 km	20 km
Direction	10°	10°	0° to 360°	1 day	1 day	100 km	20 km

The types of measurements to be performed by this system correlate very well with those needed by the ocean pollution mission in the area of inputs to pollutant motion and impact models. These are, however, mission-specific requirements which are different than the NOSS goals as stated in Table 4.2-1. The most significant difference: the ocean pollution mission requires finer spatial resolution, typically 10 Km footprint as compared with the NOSS goals ranging from 20 to 50 Km.

4.2.2 SATELLITE FOR ICE PROCESSES AND CLIMATE EXPERIMENT MISSION (ICEX)

An important assumption in the study was the availability in the near time frame, a satellite that would have microwave imaging capability. The ICEX mission, formerly identified with the ICESAT concept, was selected as the baseline since it requires a synthetic aperture radar (SAR) with characteristics similar to those of the ocean pollution mission. Sharing of this SAR imaging capability is particularly appropriate since ICEX requires coverage of the Arctic and Antarctic regions whereas the U.S. ocean pollution mission requires coverage of the lower latitudes, nominally for 50°N. to the Tropic of Cancer. Thus, a pointable SAR may optimize coverage over the 200-mile coastal zone without interferring with the primary satellite mission which is related to ice surveys in the near-polar regions. Other sensors, in addition to the SAR, that were assumed to be part of the ICEX were a scatterometer, altimeter and passive microwave radiometer. The implementation of the ICEX mission is still considering several options, all of which include the use of SAR.

The orbit for ICEX has not been definitely established, however, the baseline orbit assumed for this study was a two-day repeater 725 Km altitude, 93° inclination. An alternate orbit considered is a three day repeater, 891 Km altitude, 92° inclination.

4.2.3 EARTH RESOURCES SATELLITES

The Landsat-D and Operational Earth Resource Satellite (OERS) systems constitutes the primary platforms considered in this category. These satellites will perform surveys related to the disciplines of Agriculture, Geology, Hydrology, and Land Usage.

Landsat-D will carry a Multispectral Scanner and Thematic Mapper, both mechanically scanned imaging spectro-radiometers. Its orbit will be a 20-day repeater, sun-synchronous kilometer altitude.

The primary sensors on OERS will be a Thematic Mapper and a Multispectral Resources Sampler (MRS). The latter is a concept of a pointable multi-spectral linear array with high resolution and narrow swath width.

The data derived from these satellites will be useful in coordinating and complementing microwave (all-weather) data. In addition to the limitation due to cloud cover conditions, the earth resources platforms will have orbits and swath widths that are not compatible with those ocean pollution sub-missions related to surveillance and detection of pollutants.

4.2.4 METEOROLOGICAL SATELLITES

The civilian operational environmental satellite program uses two satellite systems, the Tiros-N and Geostationary Operational Environment al Satellite.

Tiros-N is third-generation operational polar orbiting system for the following mission objectives: (a) atmospheric cloud cover monitoring on a regular, global basis; (b) sounding the atmosphere on a regular, global basis; (c) continuous monitoring of environmental features in the western hemisphere; (d) collection and relay of environmental data from remote platforms; (e) applying satellite data to improve environmental services. The sensors on-board Tiros are: The Tiros Operational Vertical Sounder (TOVS), Advanced Very High Resolution Radiometer (AVHRR), a Space Environment Monitor and a Data Collection System (referred to as ARGOS). Tiros derived

information that is useful in the ocean pollution mission includes ocean surface temperature, weather points and air temperature near the surface. The Tiros orbit has a 98.9° inclination, is sun-synchronous, and has an altitude of 854 kilometers.

The GOES system performs meteorological observations for the following purposes: (a) continuous storm tracking, (b) cloud analysis, (c) surface temperature mapping, (d) space environment sun/earth interaction, (e) remote sensor data relay. The mission sensors onboard GOES are the Visible and Infrared Spin Scan Radiometer (VISSR) and the Space Environmental Monitor. The potential contributions of GOES to the ocean pollution mission is in synoptic, low spatial resolution measurements of ocean surface currents, ocean current boundaries, and weather fronts.

4.2.5 AIRCRAFT

Airborne Oil Surveillance System (AOSS II)

The U.S. Coast Guard operates an oil surveillance system on board a C-130 aircraft. AOSS surveillance patrols are routinely scheduled; also, a large portion of the AOSS flight time is in support of monitoring missions for reported spills. Flight time capability of the aircraft is in excess of 12 hours. The payload complement of the AOSS II includes the following:

- Oil Surveillance Detection Radar (ODSR-94)
- Line Scanner covering the frequencies 8-13 microns (channels 1 & 2) and 0.32-0.3 micron
- Passive Microwave Imager (37 GHz) equipped with TV monitor & video recorder
- Aerial Reconnaissance Camera in the visible and near IR.

ARI (Aireye) Remote Sensing System

The U.S. Coast Guard is developing an airborne, real-time, all-weather, day/night remote sensing system that will detect oil pollutants and identify violating vessels. The system, designated "Aireye", will be installed on six of the 41 new Falcon 20G jet aircraft (military designation HU-25A) purchased by the Coast Guard to replace the aging HU-16E Grumman Albatross as its medium range surveillance aircraft. The

sensor system will include a side looking airborne radar, two-channel infrared/ ultraviolet line scanner, aerial reconnaissance camera, airborne data annotation system, and a control, display and record console. To identify polluting vessels at night, an active gated television (AGTV) also is being developed for inclusion in the Aireye system. The AGTV will use a one-watt, pulsed, lead vapor laser illuminator and will be capable of recording vessel names at night from a slant range of 700 meters. In addition to an active and passive mode, the AGTV will be capable of both computer and manual target acquisition and tracking. Each of the sensors will produce annotated, hard copy imagery suitable for prosecution of polluting vessels.

4.2.6 OCEAN-SURFACE PLATFORMS

Moored Buoys*

The National Data Buoy Office has deployed meteorological and surface oceanographic environmental reporting data buoys in various gulf and ocean regions to provide synoptic data to the National Weather Service (NWS) and to provide a data base for scientific studies. At least 21 moored buoys use reporting environmental data on an operational basis. These deep ocean moored buoys measure wind speed and direction, air temperature, barometric pressure, sea surface temperature, wave spectra and, at a limited number of sites, subsurface temperatures. Data is telemetered on an operational 3-hour synoptic basis via the SMS/GOES satellite to the National Environmental Satellite Service (NESS) and then via landline to the National Meteorological Center (NMC). Environmental data from many other sources is assimilated, and meteorological and oceanographic forecast data products produced for dissemination to the user community. In this application, the moored buoy is used as an in situ primary data source, and SMS/GOES is used as an efficient data telemetry relay.

* Descriptions are obtained from "Geostationary and Orbiting Satellites Applied to Remote Ocean Buoy Data Acquisition", by Dr. E. G. Kerut and Dr. G. Haas, presented at the 13th International Symposium on Remote Sensing of Environment, April 1979.

Oceanographic satellite data is presently available largely on an experimental basis. Oceanic environment parameters being measured either directly or indirectly include temperature, radiation budget, surface vector wind field, and wave height and spectra. In order to achieve the precision desired in the future, ancillary data will usually be required. There is every reason to mix surface and satellite data, so that space-derived information can be calibrated and validated by in situ surface measurements.

Drifting Buoys

These are low-cost, expendable, non-fixed buoys capable of performing in-situ measurements and being tracked by satellites on a global basis. With the launching of polar-orbiting satellites capable of data collection and relay, as well as position determination from suitably instrumented surface sensor platforms, impetus has been given to the development of low-cost, expendable drifting buoy systems capable of unattended operation on a global basis.

Communications and position fixing depend upon the operation of a low-cost UHF transmitter on the buoy, which sends data to a specialized electronics package on board a polar-orbiting satellite. The satellite in turn relays the data to a ground station. Relative motion between the satellite and buoy produces a Doppler effect on the frequency of the rf link. This frequency shift is processed along with the satellite orbital track to derive buoy position. Experience with position-fixing has found the accuracy to be well within 5 km rms for the NIMBUS-6 satellite. The operational Tiros-N satellite is providing position-fix accuracies of about 1 km. Tiros data telemetered from a surface platform (drifting buoy) is transmitted to ground stations in the U.S., then collected during each satellite pass by NESS for transmittal to France, where Service ARGOS processes the environmental parameters and determines the platform position. Data dissemination is via the Global Telecommunications Service, for timely worldwide distribution and use.

Drifting buoys have been used primarily as in situ environmental measurement systems. However, scientists are now investigating the future use of drifting buoys in conjunction with remote satellite measurements as a calibration or model validation tool, or to enhance the present satellite measurement capability. During early process-oriented experiments, drogued drifting buoys were used as Langrangian trackers to describe near-surface currents. Position data from subsequent satellite passes was used to plot buoy trajectories or the Lagrangian measurement of surface current. Much scientific and engineering work remains to relate Lagrangian and Eulerian measurements, and to verify analytically and/or experimentally Lagrangian measurement accuracies, i.e., the slippage of the drogue buoy system in the parcel of water mass to be described. However, a potentially powerful tool is available to the oceanographer to describe ocean currents over the large spatial and temporal scales at a cost unattainable heretofore.

4.3 SUPPORT SYSTEMS

The system elements identified below provide services in support of data transmission reduction, and navigation.

Tracking and Data Relay Satellite (TDRS)

This system, to be launched on the eighth Shuttle flight, will provide position information of the sensor-carrying satellites in low earth orbit, and early data to the ground station. Wide and narrow-band data can be transmitted, making use of the following capabilities.

High Data Rate Users

Single Access	Data Rate Forward	Return	Satellite Antenna
S-Band (2.0-2.3 gHz)	to 300 kbps	12 mbps	two 4.9 m gimballed antennas 2.5° beam
K-Band (13.8-15.1 gHz)	to 25 mbps	to 50 mbps Shuttle-geared service: a) 3 digital channels 50 mbps	
		or b) 2 digital channels to 2 mbps and 4.2-mc analog or TV channel	

Low Data Rate Users

Multiple Access			
S-Band	10 kbps	50 kbps	20-element phased array antenna 12.9° FOV

This system is particularly suited for the transmission of real-time data from wide-band sensors such as the SAR and POLA. Use of the single access K-band channel, however, would require scheduling integration with other high-data rate users such as Landsat & OERS.

Fleet Numerical System

This is a Navy facility for computation of meteorological and oceanographic data and transmission to the various Ocean testers. The completed parameters include wind speed, wind direction, sea surface temperature, ice-related parameters, moisture content and significant wave-height.

Applications Data Service (ADS)

A proposed NASA system, it will allow multiple external users to access NASA data bases.

4.4 DATA SYSTEM FOR OCEAN POLLUTION MISSIONS

An analysis was performed to determine viable means for routing and processing the ocean pollution data from the sensors to the user facilities. Several unique aspects of this application needed to be considered: (1) the temporal requirements specified by the users suggests real-time or very near real-time processing; (2) the multi-platform, multi-user nature of the system necessitates a flexible and versatile system; (3) since many of the system elements are shared with other systems, maximum use should be made of the available data processing capabilities.

Following is a statement of the requirements, followed by a description of the concept of the data processing system and its evolution.

4.4.1 DATA SYSTEM REQUIREMENTS

The requirements were based on the measurements specified by the users and also on assumptions relative to the type of monitoring system that would be feasible during the various time-frames. Particularly significant in the user requirements are the frequency and data delays as shown previously in Table 3.2-2. For instance, measurements related to pollutant detection and monitoring need sampling frequencies of twice daily, and a delay ranging from three (3) to six (6) hours. Similarly, a particularly significant assumption is the use of a Synthetic Aperture Radar (SAR) and Pointable Optical Linear Array (POLA) as primary sensors for oil spills and waste pollution detection. The general functions of the Data Processing System (DPS) will be as follows:

1. Process image data on oil spills and ocean-wastes and transmit outline of affected area, location, and pollutant identification to users in the field (e.g., USCG On-Site-Coordinators).
2. Process weather and oceanographic data (e.g., relative to winds, currents, waves, air-sea interface) for near-real-time input to pollutant fate and impact models and updating of environmental data bases.

Sources for these data will include multiple spacecraft (e.g., NOSS, platform for ICEX, OERS, operational metsats); aircraft (e.g., AOSS, ARI); and surface platforms (e.g. ships

TABLE 4.4-1. DPS PRINCIPAL SENSOR PROCESSING REQUIREMENTS

SENSOR	MEASUREMENT FUNCTION IN PRIMARY MISSION*	PROCESS FUNCTION IN PRIMARY MISSION*	DPS MEASUREMENT FUNCTION	MDPS PROCESSES
SAR	ICE MEASUREMENTS	RADAR CROSS SECTION → ICE COVER	OCEAN POLLUTION DETECTION	FINAL STAGE: INFORMATION EXTRACTION
POLA	**	*	OCEAN POLLUTION DETECTION	FULL PROCESSING
SCATTEROMETER	WINDS	BACKSCATTER → WIND SPEED & DIRECTION	WINDS	TWO-DIMENSIONAL CORRELATION (OVERLAYING) WITH POLLUTION IMAGE DATA AND OTHER GEOPHYSICAL PARAMETERS
PASSIVE M-WAVE RADIOMETER	TEMPERATURES	BRIGHTNESS TEMPERATURE → SURF. TEMPERATURE	TEMPERATURES	
ALTIMETER	SURFACE TOPOGRAPHY	RETURN PULSE SHAPE →	WAVE HEIGHT	

* "PRIMARY" MISSION REFERS TO NOSS OR ICEX MISSIONS FOR WHICH THE SYSTEMS WILL BE DESIGNED.

** MISSION-UNIQUE SENSOR.

and buoys). Although the primary missions of the space and surface platforms are not related to ocean pollution, it is assumed that the acquisition and processing of the data for the Ocean Pollution Missions can be effected cooperatively. This entails making optimum use of the data processing facilities of those systems whenever it is cost effective, as well as using the dedicated DPS for mission - unique processing functions. Table 4.4-1 illustrates the principal measurement and processing functions of both the primary missions and Ocean Pollution Mission.

A preliminary analysis was performed to estimate the processing rate and complexity associated with this application. A summary of the bits per second and instructions per second associated with the principal sensors is shown in Table 4.4-2. The method for performing these estimates is exemplified in Table 4.4-3A and B, which shows the bases for the estimates relative to the optical sensor ("POLA"). These are shown in terms of the various parameters, such as number of arithmetic operations and memory cycles; instructions per pixel, processing "overhead" allowance, and special allowances/adjustments. Several assumptions pertinent to this example were:

a. Estimates assumed no on-board data processing.

b. Sizing of operations was based on studies on Landsat and linear array sensors.

c. The various stages of processing of the bit-stream included:

   Data Extraction - bit synchronization, line synchronization, and formatting.

   Radiometric Correction - adjustment for radiance biases in the data.

   Information Extraction - discrimination of pixels that correspond to a specific "signature".

   Geometric Correction - compensating for image distortions; assumed to be applicable solely to "signature" discriminated pixels, to reduce the amount of processing.

d. "Overhead allowance" was handled as a fixed multiplier on each processing stage.

e. Operating Instructions:

Addition was assumed to require 3 instructions per operation.

Multiplication was assumed to require 15 instructions per operation.

Memory Cycle was assumed to require 2 instructions per operation.

TABLE 4.4-2. DPS PROCESSING REQUIREMENTS

INSTRUMENT PROCESSING	RAW DATA RATE (BITS PER SEC.)	MAX. EQUIVALENT IPS*	
		REALTIME	1/10 REAL TIME
- SCATTEROMETER	4.9 K	3.4 M	340 K
- PASSIVE MICROWAVE RADIOMETER	16.9 K	2.8 M	280 K
- ALTIMETER	8.5 K	46 M	4.6 K
- POLA	68 M	1500 M**	150 M **
- SAR	77.5 M	105 M	10.5 M

* IPS = Instructions per second in the associated software.

** Basis for these estimates is shown in the example on Table 4.4-3.

In addition to the processing requirements discussed above, the analysis included an estimation of the storage requirements associated with the types of data bases associated with this application. Table 4.4-4 shows the estimated data quantity for meteorological, oceanographic and ocean pollution data bases. In this table, a distinction is made between "latest" data related to current or near-current conditions, and "historical" data which is used to determine statistics of oceanic conditions over a long period.

TABLE 4.4-3A. PROCESSING REQUIREMENTS OPTICAL SENSOR

- ESTIMATED PROCESSING:

1 - BASIC PROCESSING ESTIMATE BY STAGE

	ADD	MULT.	MEM. CYCLE
D/E	1		2
R/C			2
I/E	8	8	8
G/C	4		8

2 - UNLOADED/LOADED INSTRUCTIONS PER PIXEL

	ADD	MULT.	MEM. CYCLE	UNLOADED TOTAL	O/H	LOADED TOTAL
D/E	3		4	7	1.5	12
R/C			4	4	1.5	6
I/E	24	120	16	160	2.5	400
G/C	12		16	28	2.5	70

3 - ALLOWANCES* FOR CLOUD COVER AND LIMITED NUMBER OF PIXELS WITH THE DESIRED SIGNATURE

STAGE	% OF VIS/ NEAR IR PIXELS	% OF THERMAL IR PIXELS TO EACH STAGE
D/E	100	100
R/C	35	100
I/E	35	100
G/C	4	10

* ASSUMES IN-LINE CLOUD COVER SCREENING, 65% OF VISIBLE/NEAR INFRARED PIXELS OBSCURED BY "CLOUDS", AND 10% OF CLASSIFIED PIXELS HAVING THE DESIRED "SIGNATURE".

D/E = DATA EXTRACTION; R/C = RADIOMETRIC CORRECTION; I/E = INFORMATION EXTRACTION; G/C = GEOMETRIC CORRECTION

TABLE 4.4-3B. PROCESSING REQUIREMENTS
OPTICAL SENSOR

4 - ADJUSTED PER PIXEL PROCESSING ESTIMATES:

- VISIBLE/NEAR IR: 156.0 INSTRUCTIONS/PIXEL
- THERMAL IR: 425 INSTRUCTIONS/PIXEL

5 - FINAL OPTICAL PROCESSING ESTIMATE

	PIXELS/SECOND		PROCESSING RATE (INSTRUCTIONS/SECOND)
VISIBLE/NEAR IR (3 CHANNELS)	$8.33(10^6)$ x 156.9 INSTR/PIXEL	=	$1.306(10^9)$
THERMAL IR (2 CHANNELS)	$0.5(10^6)$ x 425 INSTR/PIXEL	=	$0.212(10^9)$
	REAL TIME PROCESSING: TOTAL	=	$1.52(10^9)$ INSTR/SECOND
	1/10 REAL TIME PROCESSING: TOTAL	=	$152(10^6)$ INSTR/SECOND

TABLE 4.4-4. DATA BASES REQUIREMENTS

DATA	QUANTITY (BITS)	UPDATE RATE
METEOROLOGICAL (LATEST)	12×10^6	3-6 HRS
METEOROLOGICAL (HISTORICAL)	1.2×10^9	3 HRS
OCEANOGRAPHIC (LATEST)	26×10^6	3-6 HRS
OCEANOGRAPHIC (HISTORICAL)	2.5×10^9	3 HRS
OCEAN POLLUTION (HISTORY)	4.2×10^6/ YEAR	N/A

4.4.2 DATA MANAGEMENT SYSTEM CONCEPT

An initial concept of the data processing system was formulated, first, by determining the type of equipment that would permit implementation of the sensor data processing and data base storage requirements, and second, by determining the data path and interfaces between the various multi-function processors.

The following list shows generic types of processing equipment that were found suitable for processing the sensor data (ref. Table 4.4-2).

1. SAR, real-time data: hardware processor
2. SAR, one-tenth real time: very large computer or a hardware processor.
3. POLA, real-time or one-tenth real-time data: hardware processor.
4. Scatterometer, real-time data: large computer or a hardware processor.
5. Scatterometer, one-tenth real-time: mini-computer.
6. Passive Microwave Radiometer, real-time: large computer or a hardware processor.

The evolution of the DPS is envisioned to culminate in the full-capability, centralized system by the mid-term period (1988 - 1991). The interfaces between that midterm DPS and other system elements are depicted in Figure 4.4-1. Each spacecraft ground data system will provide data at various stages of processing to the DPS, where specialized processing for the ocean pollution mission is performed prior to routing the data to the local command post. The extent of processing in the individual spacecraft system facilities will depend on the compatibility between the requirements of the primary mission and those of the Ocean Pollution Mission, as well as the inherent capabilities of the S/C data system. For instance, the data grid size requirements for wind speed and velocity are more stringent for the subject mission than that for the NOSS missions, therefore a feasible approach is to augment only the data acquisition capabilities of the spacecraft to meet the higher resolution requirements of this mission over the 200 mile-zone, but perform the wind speed and direction related processes in the DPS. However, a refinement of this approach would be to perform some of the "Phase I" processing functions, related to data sequencing and formatting, within the NOSS data system if the system could handle the extra load without any interference with the primary S/C mission.

The airborne and surface data is routed directly to the local command post, but some of the data needed for correlation with S/C data is relayed to the DPS. An example of this type of correlation data is the altimeter data from the Advanced ARI and some data from the buoy data collection systems; these are merged with S/C altimeter data to produce the required coverage of significant wave height measurements within the pollution-affected area.

One of the main features of the Mid-Term DPS will be the centralization of the processing functions for the pollution fate and impact models. Many multi-purpose and specialized models serving various user needs will be utilized in this facility; however, development and initial demonstration of models would be performed in separate user facilities.

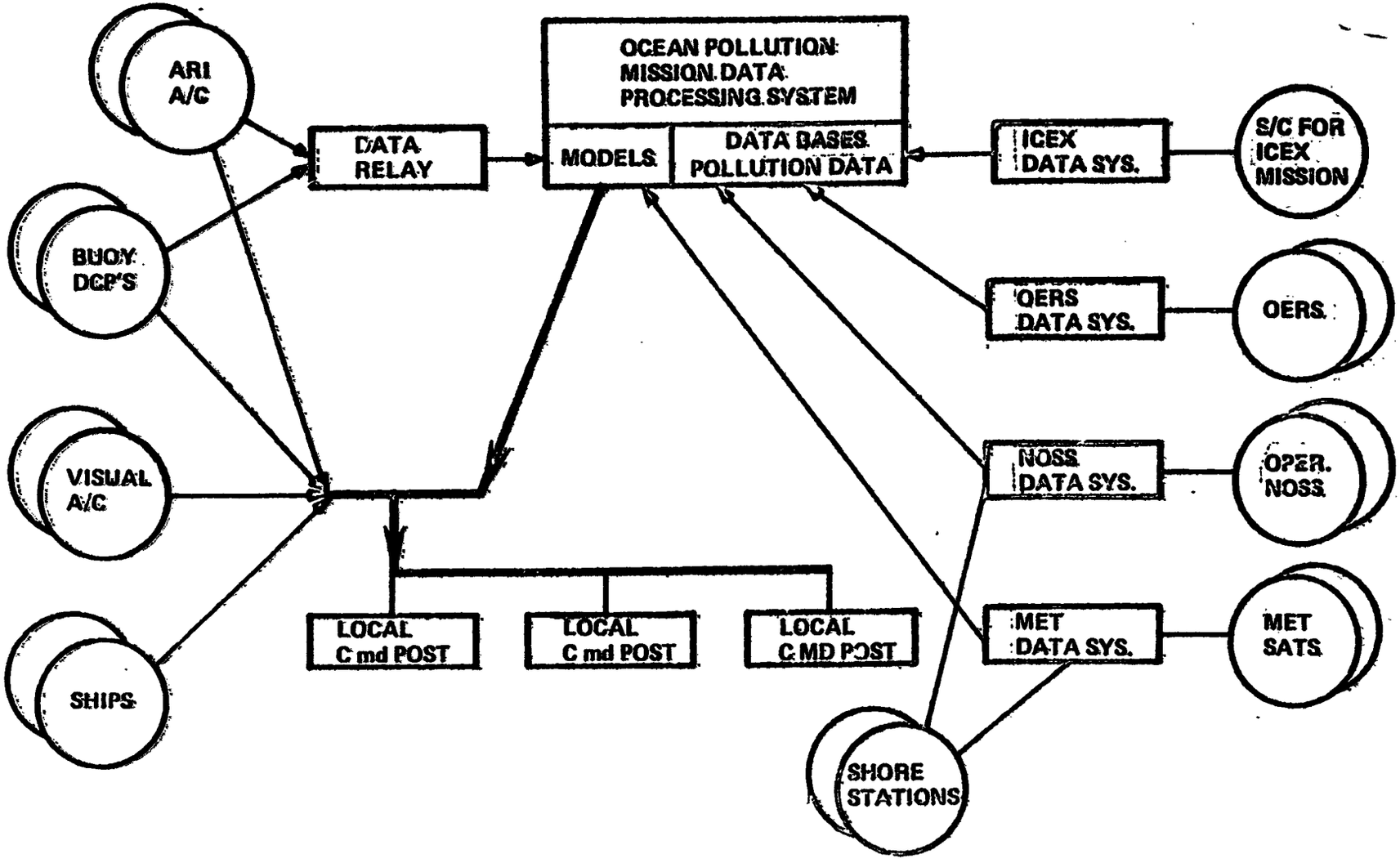

Figure 4.4-1. Mid-Term DPS Concept

By contrast, the Near Term System (1984-87) is not envisioned as having centralized models; instead, it will perform the mission-unique processing functions and route the data to the various facilities where models are being used. Another difference between the systems for the two time frames is that the Near-Term DPS will not perform automated data correlation between aircraft and surface platform data and spacecraft data, whereas the Mid-Term System will perform these functions.

The DPS operation will make optimum utilization of man's interaction with the data and his assessment of the data within the content of the overall mission situation and existing environmental conditions. Figure 4.4-2 depicts a concept of the DPS facility, with expert personnel located at the various consoles. The consoles will be able to display individual-sensor data or correlated (overlayed) sensor data. It will be able to control the inputs to the models and data bases as well as to gain access to selected data in those models and data bases.

The components and interfaces of the Mid-Term DPS are depicted in Figure 4.4-3. Sensor data is routed through the Format Decoder and appropriate Phase I, II and III processors (Phase I relates to sequencing and formatting, Phase II deals with calibration functions and Phase III encompasses actual information extraction). A "Master Computer" serves as the data manager, directly controlling Phases I and II functions, and through a mini-computer, the Phase III functions for SAR and POLA. The processed sensor data is routed to the operator consoles, data bases and correlating processor. The function of the latter is to permit the two-dimensional correlation of diverse data, as exemplified by the following combinations: microwave and optical (SAR & POLA) image data of polluted areas, microwave image data and wind fields, optical image data and sea state, wind fields and ocean surface currents, present vs. predicted oil spill areal extent.

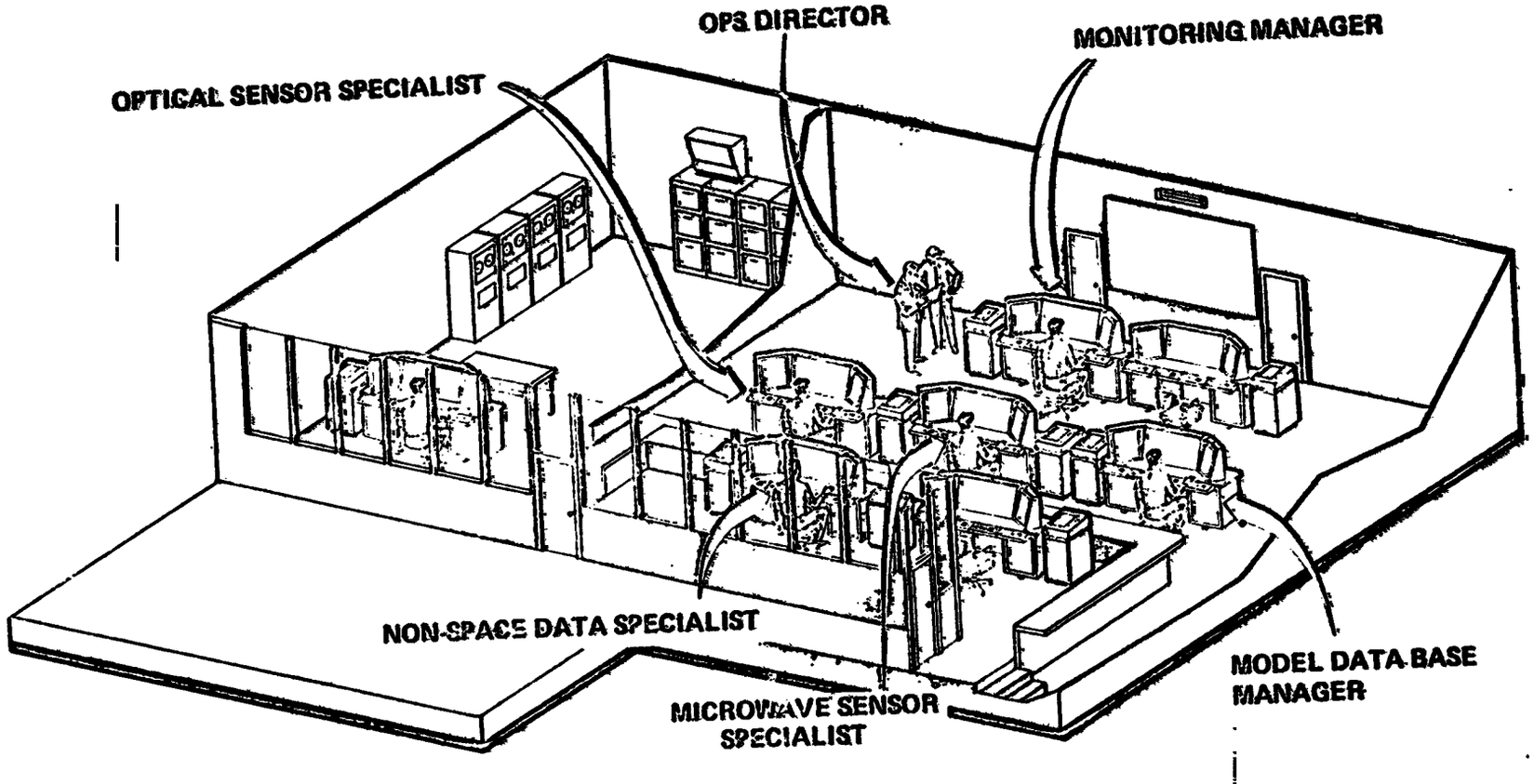

Figure 4.1-2. Data Processing Facility

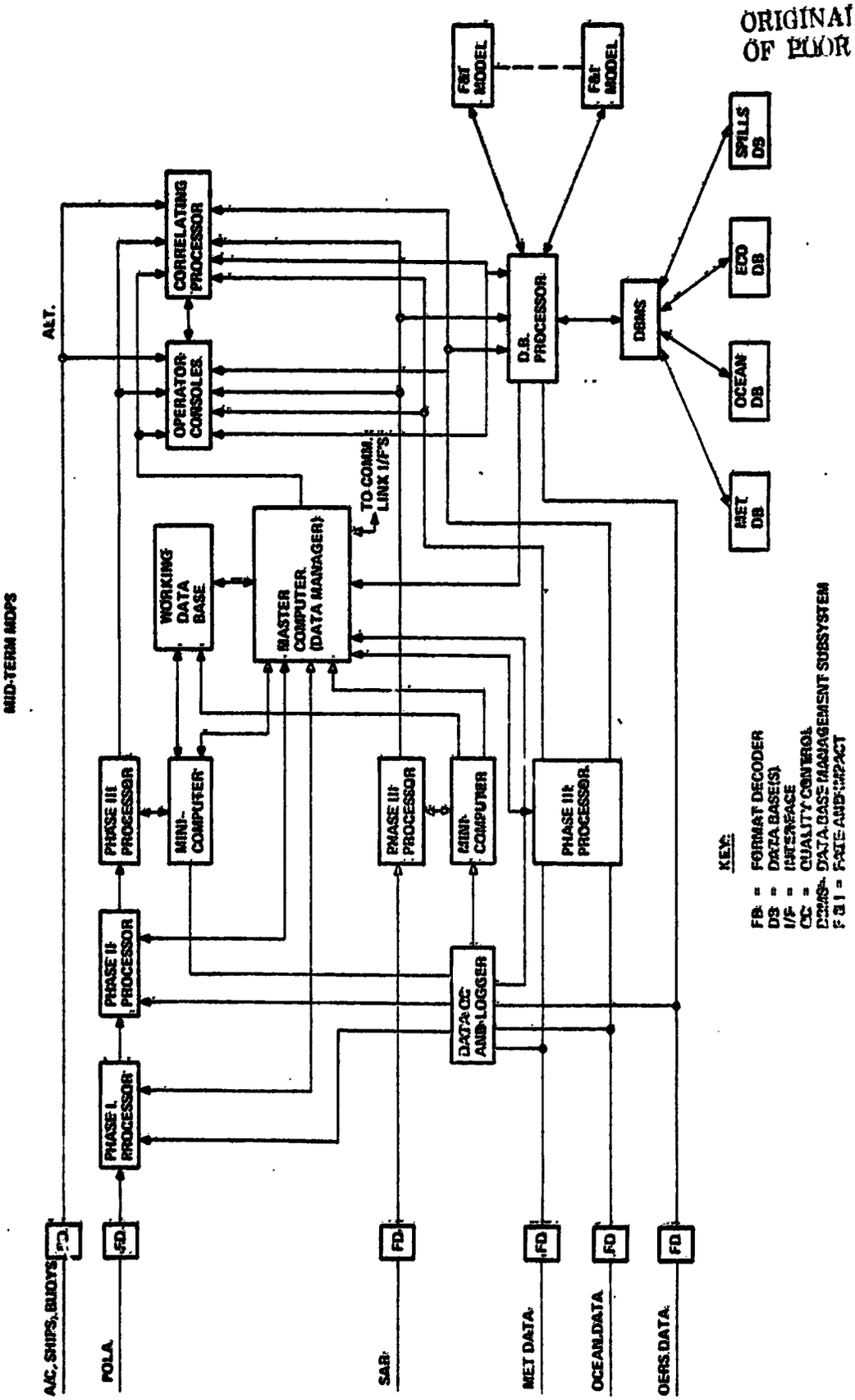

Figure 4.4-3. Mid-Term EPS

In summary, the Ocean Pollution Mission Data Processing System is a preliminary concept of a versatile, evolutionary system that will permit optimum utilization of various data from multiple platforms. It is a "nerve center" that provides the required organization and focus to these diverse data; without the DPS, each primary user would have to establish lesser capability processing centers and complex interfaces with several systems.

SECTION 5
SYSTEM CONCEPTS AND TRADEOFFS

- MISSION OPERATIONS ANALYSIS
- COASTAL COVERAGE ANALYSIS
- SYSTEM OPTIONS
- RELATIVE COST AND EFFECTIVENESS OF SYSTEM OPTIONS

SECTION 5

SYSTEM CONCEPTS AND TRADEOFFS

The previous sections have covered the ocean pollution information needs of many users and the state-of-the-art of the important elements (sensors, platforms, data processing, communication, positioning) which either currently or in the future may support these needs. This section will develop a set of system concepts (syntheses of various system element candidates) based on a logical structuring of the user community needs and the realities of operating such complex systems. Finally the several options will be compared based on relative costs and levels of support of the ocean pollution missions.

5.1 MISSION OPERATIONS ANALYSIS

The first step in synthesizing the available technologies into operational systems requires a clear statement of the missions to be supported. Up to this point, we have the knowledge and measurement requirements of key users as presented in Section 3.

5.1.1 OCEAN POLLUTION MISSIONS

A formal structure of the ocean pollution measurement missions and goals was developed through (1) personal contacts with system operators, users, designers, researchers, etc., (2) a thorough review of documentation -- technical, legislative, and programmatic, and (3) first-hand experience as a member of the remote sensing applications community. Table 5.1-1 enumerates and defines 10 major sub-missions comprising the two broadest missions: (1) Surveillance and Monitoring and (2) Modeling.

TABLE 5.1-1. FUNCTIONAL DEFINITIONS OF THE 10 OCEAN POLLUTION SUB-MISSIONS

SURVEILLANCE & MONITORING	FUNCTIONS INCLUDED
1. DETECTION	1. SURVEILLANCE & DETECTION OF UNREPORTED OIL SPILLS OR WASTE DUMPS, WHETHER ACCIDENTAL OR DELIBERATE
2. MAPPING & TRACKING	2. MEASUREMENT OF THE AREAL EXTENT & BOUNDARIES OF THE POLLUTION; DETERMINING THE LOCATION; TRACKING THE CHANGE IN AREA, SHAPE & LOCATION VS. TIME.
3. QUANTIFICATION AREAL	3. MEASURING THE OIL VOLUME THROUGH AREAL EXTENT & THICKNESS MAPPING; INFERRING WASTE POLLUTANT QUANTITY BY AREAL EXTENT & SURFACE CONCENTRATION.
4. POLLUTANT CLASSIFICATION	4. TYPE OF OIL: CRUDE CLASS, REFINED OIL CLASS, AGED VS. NEW SPILL; TYPE OF WASTE: ACID CLASS, SLUDGE, BIO-DIGESTED WASTE.
5. POLLUTER IDENTIFICATION	5. DESIGNATION & LOCATION OF SHIP, OFF-SHORE FACILITY OR COASTAL POINT SOURCE.
6. SYNOPTIC U.S. COASTAL POLLUTION MONITORING & DATA BASE BUILDING	6. ESTABLISHED AND PERIODIC UPDATING OF AMOUNT, DISTRIBUTION & TYPE OF VARIOUS POLLUTANTS WITHIN THE U.S. 200 N. MI COASTAL ZONE.
7. SYNOPTIC GLOBAL POLLUTION MONITORING & DATA BASE BUILDING (IMPLEMENTATION OF THIS MISSION IS NOT ADDRESSED IN THE STUDY)	7. SAME AS (6) ABOVE FOR ALL OCEAN AREAS, AS A MEASURE OF GLOBAL POLLUTION.
MODELING	
8. FATE MODELING	8. PREDICTION OF OIL OR WASTE POLLUTION TRAJECTORY AND SPREADING CHARACTERISTICS; APPLIES TO ACTUAL SPILLS/DUMPS THREATENING COASTAL AREAS, OR POTENTIAL POLLUTION (E.G. FROM AN EXISTING & PROPOSED OFF-SHORE OIL WELL)
9. IMPACT/RISK MODELING	9. ASSESSING THE POTENTIAL DETRIMENTAL EFFECTS TO SENSITIVE COASTAL BIOLOGICAL OR RECREATIONAL RESOURCES; PREDICTING THE PROBABILITY OF OCCURRENCE BASED ON OCEAN & METEOROLOGICAL STATISTICAL DATA.
10. SYNOPTIC OCEANOGRAPHIC/ METEOROLOGICAL/ECOLOGICAL MONITORING & DATA BASE BUILDING	10. ESTABLISHMENT AND PERIODIC UPDATING OF A DATA BASES OF OCEANOGRAPHIC, METEORLOGICAL AND ECOLOGICAL STATISTICS USEFUL IN FATE AND IMPACT MODELING.

Each sub-mission covers certain discrete performance objectives of one or more user. References 120 and 121, for example, cover the objectives of Coast Guard pollution surveillance systems and are contained within MOPS sub-missions 1 through 5.

Whereas the sub-missions were defined to be mutually exclusive to preclude overlap, they may be supportive of each other. For example, Mapping and Tracking has the two-dimensional (areal) extent of the pollutant as a principal output, whereas Quantification adds the third dimension -- thickness -- in further characterizing the pollutant in terms of quantity. Since the observable phenomena that correspond to pollutant area and thickness relate to different observables and different measurement techniques, it is appropriate to make them different system sub-missions.

In another instance, the division is geographical as in separating the U.S. Coastal Pollution Data Base sub-mission from the Global Pollution Data Base sub-mission. Comparable reasoning led to the definition of all 10 discrete sub-missions. The total set of 10 covers all clearly-identified U.S. user agency goals in ocean pollution -- whether oil or other than oil -- that are amenable to support by this study's technologies.

5.1.2 MISSION SUPPORT LOGIC

In order to understand the dynamics of systems which can or will perform these sub-missions, the logic interrelating the sub-missions was developed. Figure 5.1-1 illustrates the top level logic which is practiced in the surveillance, monitoring, and response activities (including model operation) associated with ocean pollution. At this level, all pollution is broadly divided into (1) that which is reported to the system from outside, and (2) that which the system must itself detect (Sub-mission 1). A data base of coastal pollution monitoring information (U.S. and

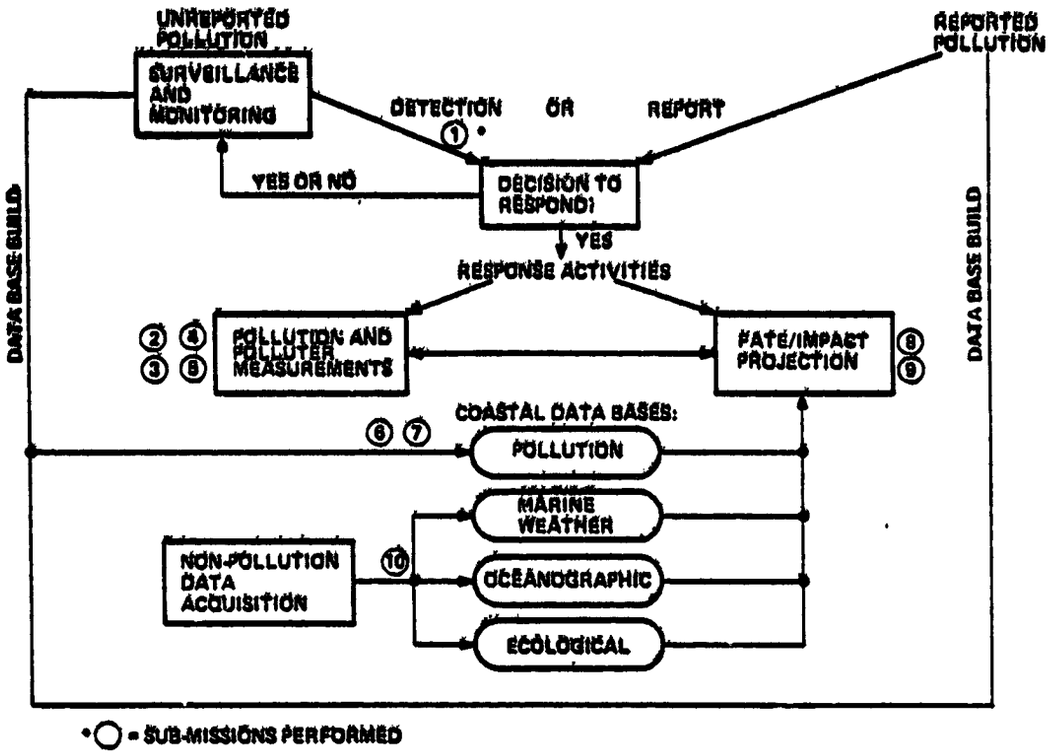

Figure 5.1-1. Top-Level Ocean Pollution Monitoring Logic

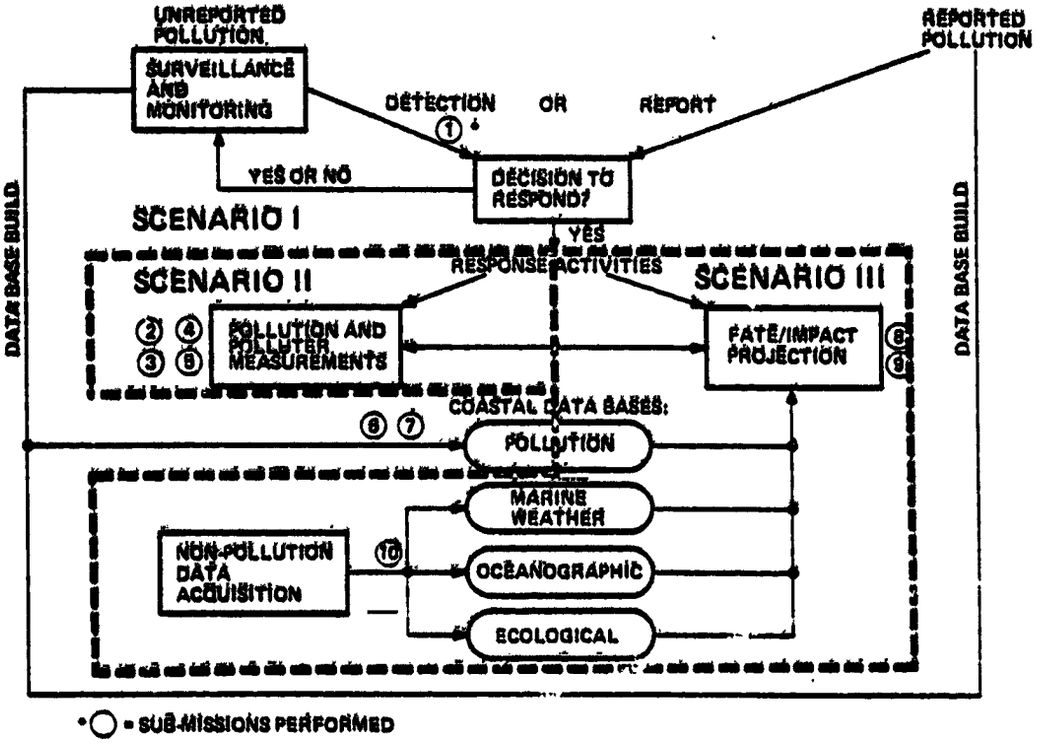

Figure 5.1-2. Top-Level Ocean Pollution Monitoring Logic with Scenarios Shown

global) is maintained from these external reports and surveillance system detection inputs (Sub-missions 6 and 7).

Initial assessment of the detected or reported pollution results in a decision to further respond or not. Response measurements to characterize the pollutant or polluter are covered by Sub-missions 2, 3, 4, and 5. Projections of the oil trajectory (fate) or impact on sensitive (biological, recreational, etc.) areas are made by computerized models (Sub-missions 8 and 9). The model inputs come from real-time response measurements and several continuously updated data bases (Sub-missions 6, 7, and 10).

5.1.3 OPERATIONAL SCENARIOS

The sub-mission definition and support logic just discussed now enables us to address potential systems in the context of employment scenarios, such as those delineated in Figure 5.1-2.

These three discrete scenarios for operationally employing candidate system elements are:

- Pollution Surveillance and Monitoring (Scenario I)
- Pollution and Polluter Measurements (Scenario II)
- Fate and Impact Projection (Scenario II)

Figure 5.1-2 specifies (1) the boundaries of each scenario within the support logic and (2) the sub-missions performed.

These scenarios were developed to identify where major system elements would fit and how they would relate to each other in their sub-mission support roles. Figure 5.1-3 shows the place of the scenarios in screening and further specifying candidate elements for the system concepts to be synthesized. Emphasis was placed on staying generic in the element specification and emplacing all candidates (space, air, and surface) in their potential operational roles.

In addition to the system elements covered in Section 4 -- sensors, platforms, and communication, positioning, and data processing support -- other types of elements must be included to envision self-contained operations.

These additional elements are: facilities, key organizations, and key personnel. Table 5.1-2 gives a generic breakdown of these categories and the primary candidates to play these (or similar) operational roles. Following the details on some of these additional system elements, each of the 3 operational scenarios is discussed at length.

5.1.3.1 Organizational and Personnel Support

An understanding of the roles of organizations and people in the various scenarios was obtained by document review and personal interviews at agencies with pertinent responsibilities. Thus, insight was gained into current and evolving practices in similar scenarios. The single most useful document is known as the "National Contingency Plan" (Reference 159) and it covers the "coordinated and integrated response by Federal agencies to protect the environment from the damaging effects of pollution discharges." Published by the CEQ (Council on Environmental Quality)

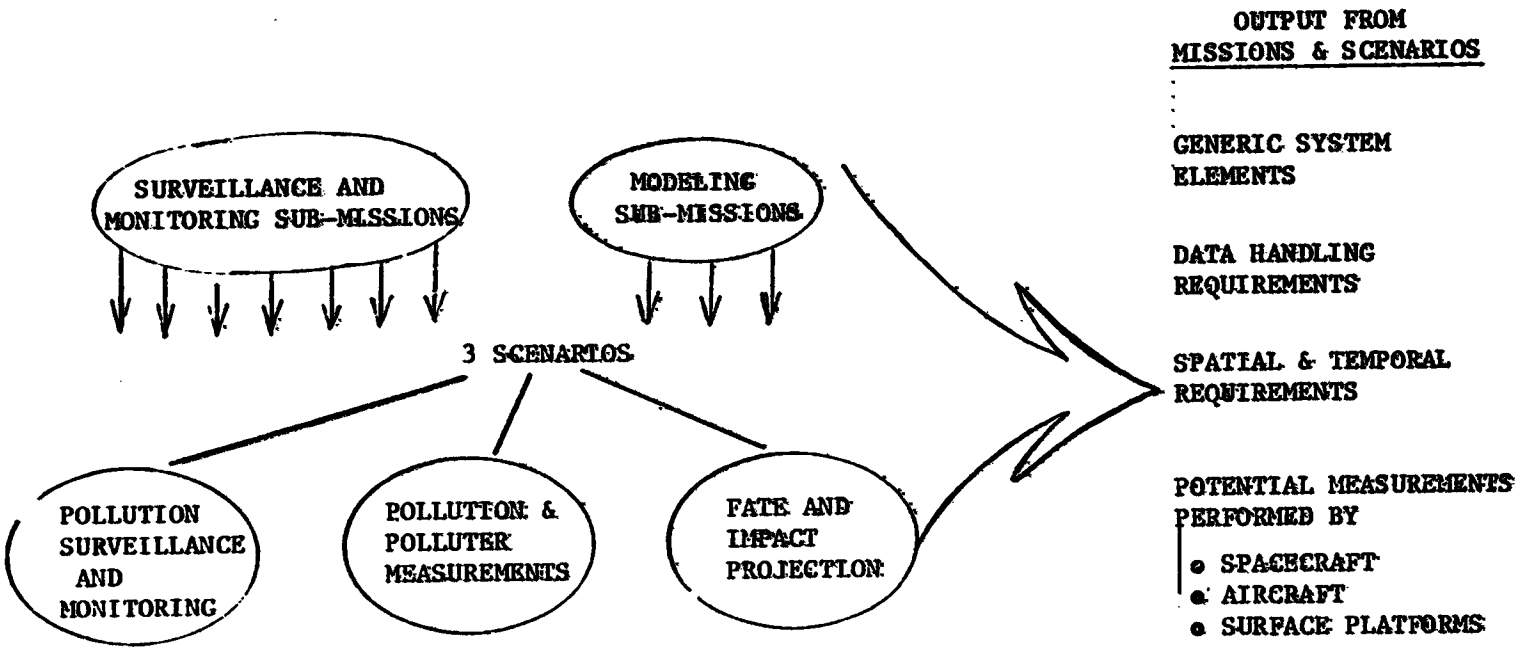

FIGURE 5.1-3. USE OF THE OPERATIONAL SCENARIOS IN SCREENING AND DEFINING SYSTEM ELEMENTS

TABLE 5.1-2 OTHER SUPPORT ELEMENTS

GENERIC BREAKDOWN	SPECIFIC CANDIDATES
1. FACILITIES	
A. OPS CONTROL	LCP (LOCAL COMMAND POST) RRC (REGIONAL RESPONSE CENTER) NRC (NATIONAL RESPONSE CENTER)
B. DATA PROCESSING	ON-BOARD AIRCRAFT (AOSS/ARI) DATA SYSTEMS CENTER* (DSC/ARI) MODEL OPERATI[illegible] (FATE/IMPACT) LOCAL CONTRACTOR LABS EPA PHOTO LAB (LAS VEGAS) MOPS DATA PROCESSING SYSTEM *
2. PERFORMING ORGANIZATIONS	
A. PLANNING AND ADVISORY	MOPS STAFF* NRT (NATIONAL RESPONSE TEAM) RRT (REGIONAL RESPONSE TEAM) CHEMTREC (PRIVATE HAZARDOUS SPILL INFORMATION CLEARINGHOUSE)
B. OPERATIONAL RESPONSE	MOPS STAFF* NATIONAL STRIKE FORCE - STRIKE TEAMS - ENVIRONMENTAL RESPONSE TEAM EMERGENCY TASK FORCES SPILLED OIL RESEARCH (SOR) TEAM
3. KEY CONTROLLING PERSONNEL	ON-SCENE COORDINATOR (OSC) — SCIENTIFIC SUPPORT COORDINATOR (SSC) NUMEROUS OTHER INDIVIDUALS ON THE NATIONAL AND REGIONAL RESPONSE TEAMS, SOR TEAM, STRIKE TEAM, MOPS STAFF*, ETC.

* CANDIDATES WHICH ARE NOT CURRENTLY IN EXISTENCE

based on multi-agency inputs provided by the NRT (National Response Team), it is the Federal "umbrella" document for various agencies' continuous responsibilities and specific response roles.

Figure 5.1-4 illustrates the level of involvement of different agencies and the interrelationships of key agencies and personnel in policy and operations. The paragraphs below describe those key groups (e.g., the NRT) and personnel (e.g., the OSC).

In a nutshell, the overall Federal response is directed by either (1) the Coast Guard for coastal and certain inland waters (such as the Great Lakes) or (2) the EPA for the remainder of the inland navigable waters. The response is broken into five phases:

Phase I - Discovery and Notification
Phase II - Evaluation and Initiation of Action
Phase III - Containment and Countermeasures
Phase IV - Removal, Mitigation, and Disposal
Phase V - Documentation and Cost Recovery

These phases are implemented and directed by the OSC only as required and generally depend on (1) the size of the discharge (minor, medium, or major) and (2) the response actions of the "discharger" and his parent agency, country, etc. The authority behind the National Contingency Plan is primarily the Federal Water Pollution Act (as amended in 1977).

Scientific expertise during a pollution response action is focussed through the SSC (Scientific Support Coordinator), generally a NOAA individual. He is both the scientific pollution effects advisor to the OSC and coordinator of real-time spill fate and impact projection activities.

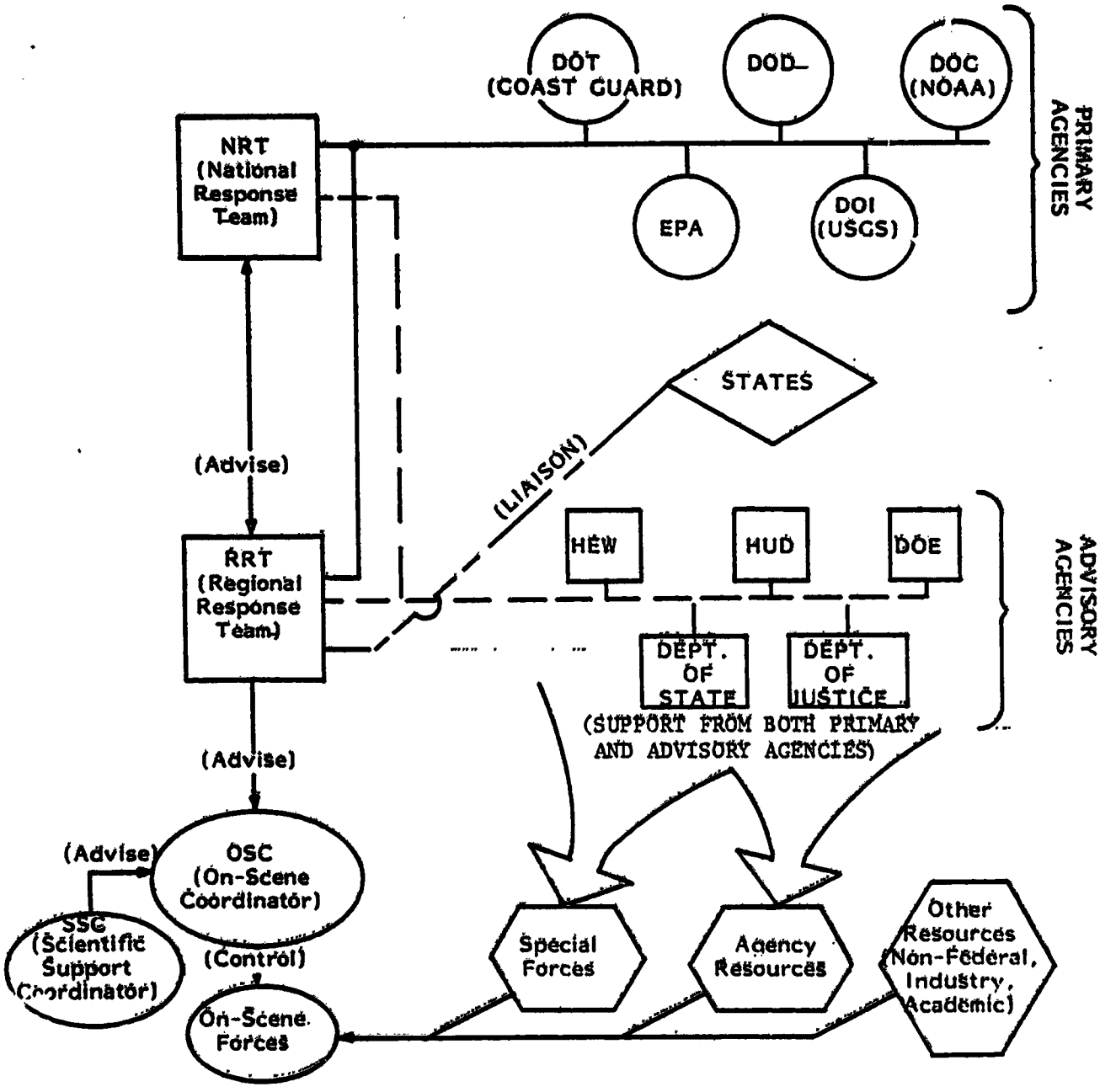

FIGURE 5.1-4 NATIONAL CONTINGENCY PLAN
ORGANIZATIONAL RELATIONSHIPS

Key facilities, organizations, and personnel covered by the National Contingency Plan are described below.

a. NRT (National Response Team), see Figure 5.1-5

(1) Consists of representatives from the Primary and Advisory Agencies. It serves as the National body for planning and preparedness actions prior to a pollution discharge and for coordination and advice during a pollution discharge.

(2) Except for periods of activation because of a pollution incident, the representative of EPA is the Chairman and the representative of DOT is Vice-Chairman of NRT. The vice-chairman maintains records of the NRT activities along with National and regional plans for pollution response. When NRT is activated for a pollution incident, the Chairman is the representative of EPA or DOT, depending upon the area in which the response is taking place.

(3) When not activated for a pollution discharge, serves as a standing committee to recommend needed policy changes in the response organization, to revise the National Contingency Plan as needed and to evaluate the preparedness of the Agencies and effectiveness of plans for coping with pollution discharges.

(4) Acts as an emergency response team in the event of a discharge involving oil or hazardous substances which (a) exceeds the response capability of the region in which it occurs; (b) transects regional boundaries; (c) involves significant numbers of persons or nationally significant amounts of property; or (d) when requested by any Primary Agency representative. Each representative, or an appropriate alternate, shall be notified immediately by telephone of activation of NRT.

b. NRC (National Response Center), See Figure 5.1-5

(1) Physical facilities established at Headquarters, U.S. Coast Guard, Washington, D.C., for coordination and control of a pollution emergency if a national level involvement is needed.

(2) Communications center continuously manned.

(3) U.S. Coast Guard provides

- Communications
- Latest marine charts from various agencies
- Tech. library
- Plotting and display capability

FIGURE 5.1-5 HIGHLIGHTS OF NRT AND NRC

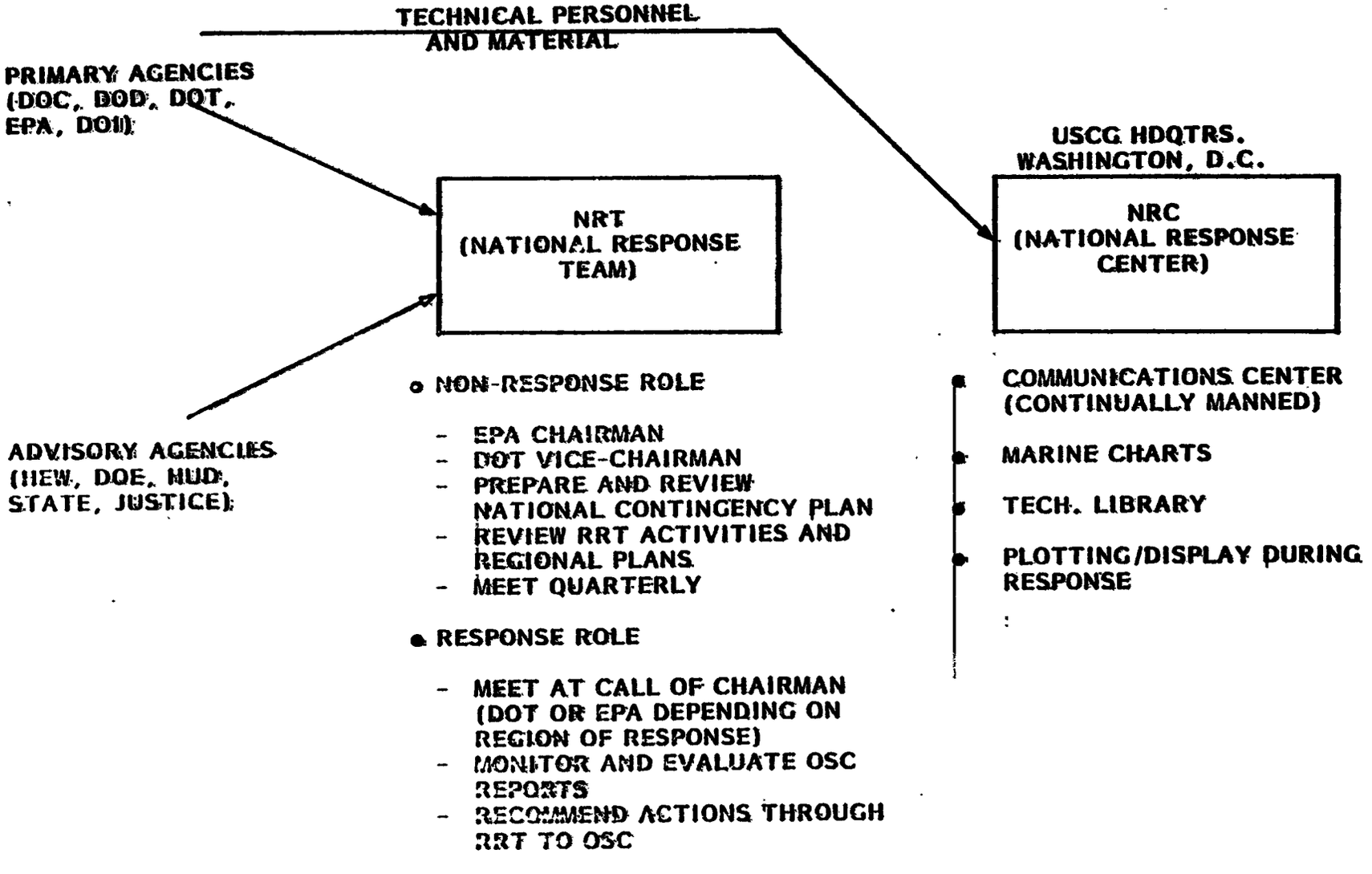

(4) Primary Agencies furnish competent technical personnel to man the NRC as requested, furnish appropriate technical manuals and materials, and such additional administrative support as required to operate the NRC effectively and efficiently.

c. RRT (Regional Response Team), see Figure 5.1-6:

(1) Consists of regional representatives of the Primary and selected Advisory Agencies, as appropriate. Acts within its region as an emergency response team performing response functions similar to those described for NRT. RRT also performs review and advisory functions relative to the regional plan similar to those prescribed for NRT at the National level. Additionally, the RRT determines the duration and extent of the Federal response, and when a shift of on-scene coordination from the predesignated OSC to another OSC is indicated by the circumstances or progress of a pollution discharge.

(2) Each Primary Agency designates one member and a minimum of one alternate member to the RRT. Each Advisory Agency may designate a member.

(3) Each of the States lying within a region is invited to furnish liaison to the RRT for planning and preparedness activities. When the Team is activated for a pollution emergency, the affected State or States are invited to participate in RRT deliberations.

(4) The RRT is activated automatically in the event of a major or potential major discharge. The RRT is activated during any other pollution emergency by an oral request from any Primary Agency representative to the Chairman of the team.

(5) The Chairman may require assembly of all or selected members of the team at the emergency center during a pollution response operation to provide technical support and assistance to the OSC.

(6) Regional Contingency Plans are developed for each region (Standard Federal Regions, see Figure 5.1-7.)

d. RRC (Regional Response Center), see Figure 5.1-6:

The RRC is the regional site for pollution emergency response activities. It is accommodated in quarters described in each regional plan and provides communications, information storage and other necessary personnel and facilities to promote the proper functioning and administration of regional pollution emergency response operations.

FIGURE 5.1-6 HIGHLIGHTS OF RRT AND RRC

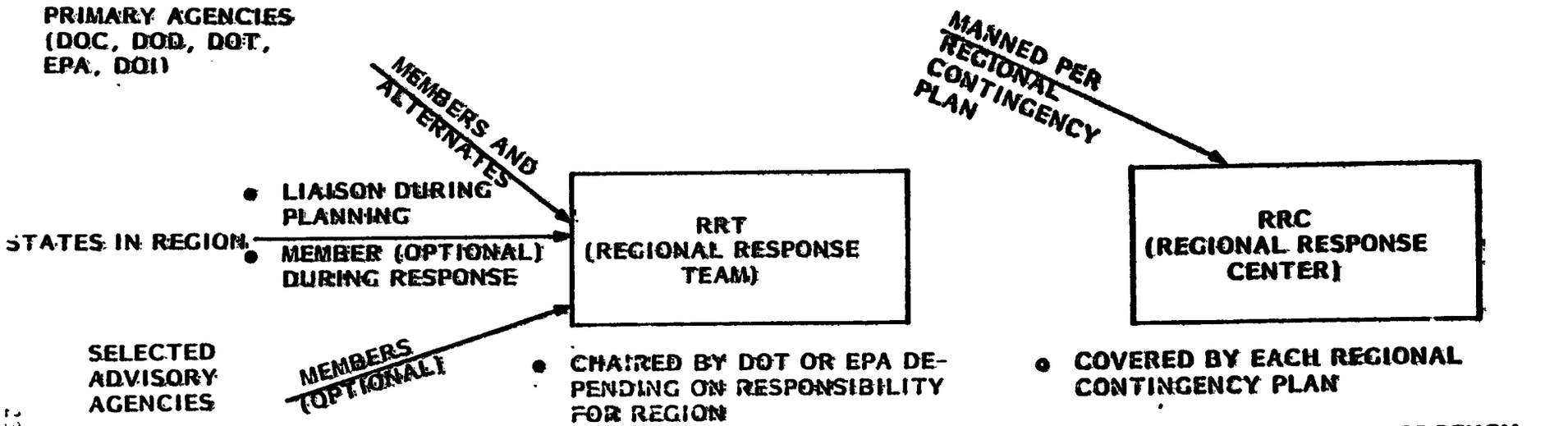

- CHAIRED BY DOT OR EPA DEPENDING ON RESPONSIBILITY FOR REGION
- NON-RESPONSE ROLE
  - PREPARE AND REVIEW REGIONAL CONTINGENCY PLAN
- RESPONSE ROLE
  - ACTIVATED AUTOMATICALLY FOR MAJOR OR POTENTIAL MAJOR SPILL IN REGION
  - MAY BE ACTIVATED FOR ANY RESPONSE AT REQUEST OF ANY PRIMARY AGENCY
  - SUPPORT AND ASSISTANCE TO OSC
  - PASS ON RECOMMENDATIONS OF NRT

- COVERED BY EACH REGIONAL CONTINGENCY PLAN
- ONE PER REGION FOR EMERGENCY RESPONSE ACTIVITIES
- COMMUNICATIONS, INFORMATION STORAGE, AND NECESSARY SUPPORT FACILITIES AND PERSONNEL

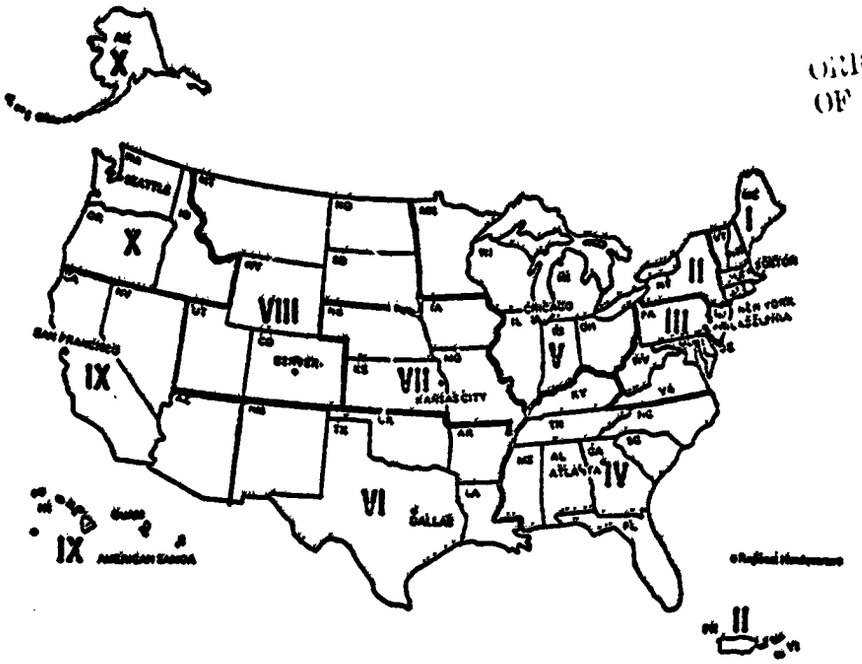

FIGURE 5.1-7 STANDARD FEDERAL REGIONS USED FOR REGIONAL RESPONSE ACTIVITIES

e. OSC (On-Scene Coordinator):

Coordination and direction of Federal pollution control efforts at the scene of a discharge or potential discharge are accomplished through the OSC, predesignated by regional plan to coordinate and direct such pollution control activities in each area of the region. This is either a Coast Guard or EPA individual, depending on responsibility for the waters impacted. In the event of a discharge of oil or hazardous substance, the first official on the site from the agency having regional responsibility assumes coordination of activities until the arrival of the predesignated OSC.

Specifically, the OSC:

(1) Determines pertinent facts about a particular discharge, such as its potential impact on human health and welfare; the nature, amount, and location of material discharged; the probable direction and time of travel of the material; the resources and installations which may be affected and the priorities for protecting them.

(2) Initiates and directs as required Phase II, Phase III and Phase IV operations. Advice provided by the EPA representative on the RRT on use of chemicals in Phase III and Phase IV operations in response to discharges of oil or hazardous substances is generally binding on the OSC.

(3) Calls upon and directs the deployment of needed resources in accordance with the regional plan to evaluate the magnitude of the discharge and to initiate and continue removal operations.

(4) Provides necessary support activities and documentation for Phase V activities.

(5) Informs and coordinates closely with RRT to ensure the maximum effectiveness of the Federal effort in protecting the natural resources and the environment from pollution damage.

f. Special Forces (National Strike Force (NSF) and Emergency Task Forces)

The NSF provides assistance to the OSC at his request during Phase III, IV, and V operations. The NSF is formed around the U.S. Coast Guard Strike Teams (one each for the East, West, and Gulf Coasts) augmented as required by the EPA Environmental Response Team. When possible, the NSF will

provide training to the Emergency Task Forces and participate with the Regional Response Team in Regional Contingency Plan development.

(1) The Strike Teams established by the U.S. Coast Guard are able to provide communications support, advice and assistance for oil and hazardous substances removal. These teams include expertise in ship salvage, diving, and removal techniques and methodology.

(2) The Environmental Response Team established by EPA to carry out the Agency's disaster and emergency responsibilities can provide the OSC and NSF with advice on the environmental effects of oil and hazardous substances discharges, and removal and mitigation of the effects of such discharges. This team includes expertise in biology, chemistry, engineering and, when necessary, meteorology and oceanography.

(3) The Emergency Task Forces consist of trained personnel with adequate supplies of oil and hazardous pollution control equipment and materials and detailed discharge removal plans for their areas of responsibility. The Emergency Task Forces are established by the Agency in each region responsible for providing the OSC.

5.1.3.2 Scenario I: Pollution Surveillance and Monitoring

Figure 5.1-8 illustrates the envisioned elements with the potential to perform key roles in support of these MOPS sub-missions (1, 6, and 7). Note that there are numerous current and planned sensor platforms (air and space) which have some capability for detection of different types of marine pollution. They span a range of techniques -- including visual, optical, and microwave -- and coverage characteristics, such as area and frequency. Geosynchronous space developments.

Space sensors with their wide fields of view and frequent revisit times combined with aircraft sensors for close-in verification and relatively limited area coverage appear to have complementary roles. In situ detection devices are also included, especially as an adjunct to remote sensing in congested (harbor/port) areas.

FIGURE 5.1-8 POLLUTION SURVEILLANCE AND MONITORING:
SCENARIO I

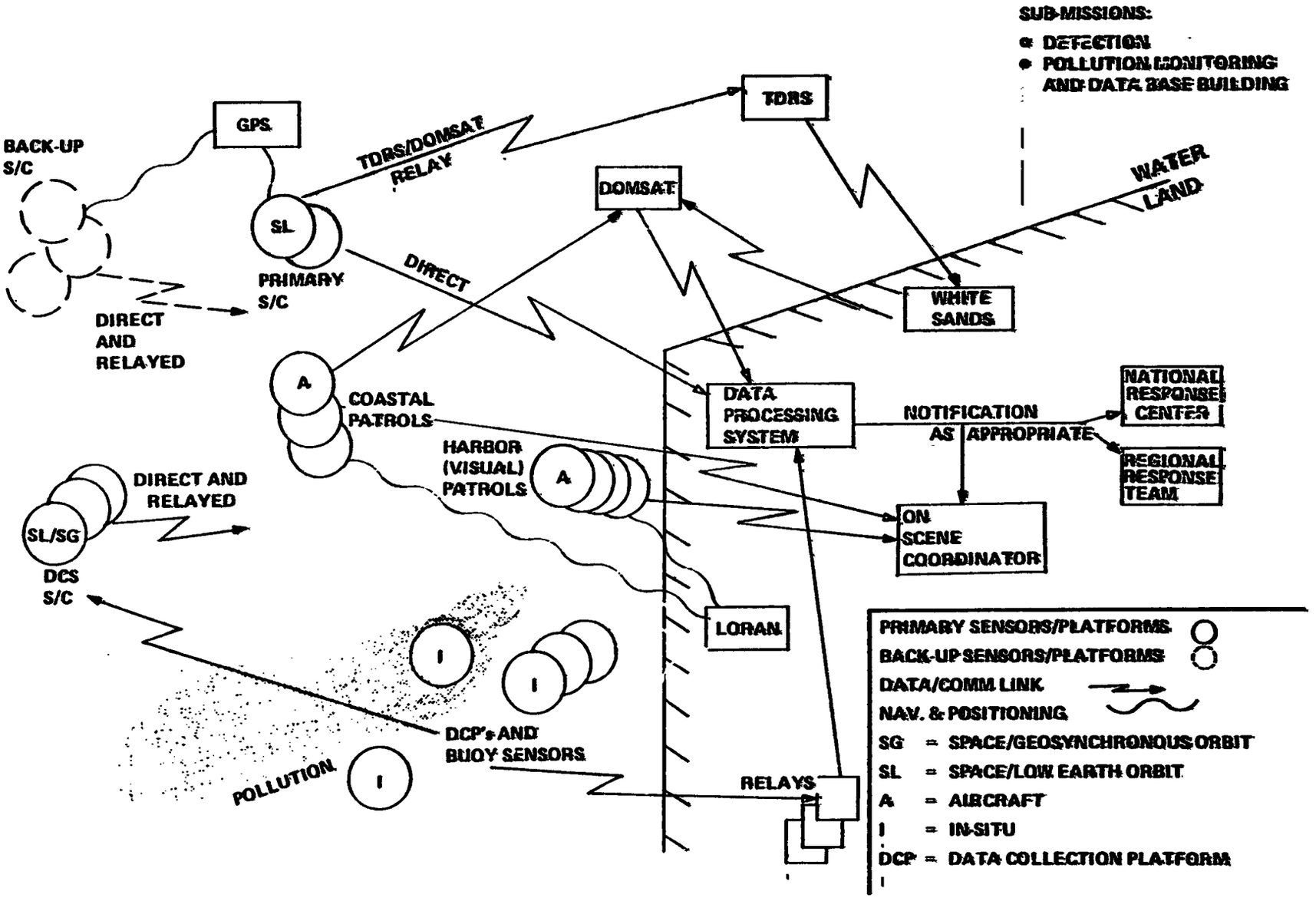

The high data rates associated with such extensive daily surveillance dictate wideband comm links (perhaps TDRSS and/or DOMSAT). The near real-time detection requirement and high data rates imply a significant, dedicated data processing system. The scenario illustrates personnel and organizations requiring rapid information on detected potential pollution.

5.1.3.3 Scenario II: Pollution and Polluter Measurements

The pollution detection (or report) from Scenario I initiates the response activities shown in Figure 5.1-9 as Scenario II. A timeline of possible response activities, such as Figure 5.1-10, is useful to understand the interplay and operational coordination of the many and varied elements in this scenario. Frequently, the first response steps will be to deploy aircraft or close-by ships to verify the suspected pollution. Following verification, these same platforms identify and document suspected polluters in the area (sub-mission 5) and begin their pollutant measurements (sub-missions 2, 3, and 4).

Mapping the areal extent and tracking the movement can generally be best handled by aircraft but for very large area targets -- such as the 1979 Bay of Campeche oil spill -- the synoptic view from space is a highly useful adjunct.

Near-surface (aircraft) and surface (ships, buoys) platforms are the only reliable means of pollutant classification and quantification within the mid-term time frame.

Almost all of the platforms and most of the sensors in this scenario are the same as Scenario I; so similar data comm link and platform navigation and positioning support are needed. In this response mode, a more complex set of organizational and personnel interactions is underway, including law enforcement and clean-up direction and monitoring at the local, regional, and national levels.

FIGURE 5.1-9 POLLUTION AND POLLUTER MEASUREMENTS: SCENARIO II

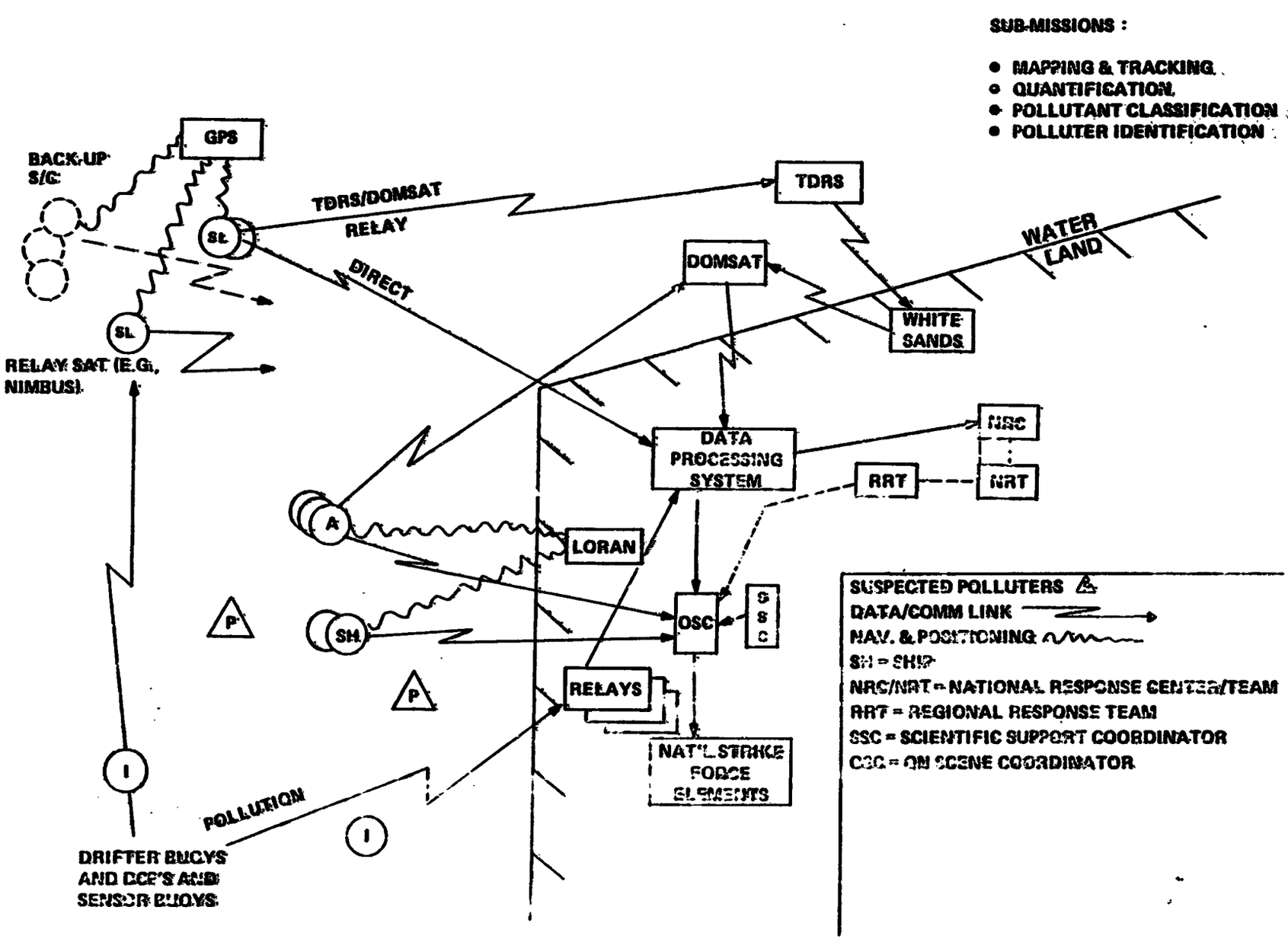

FIGURE 5.1-10 RESPONSE TIMELINE (SCENARIO II)

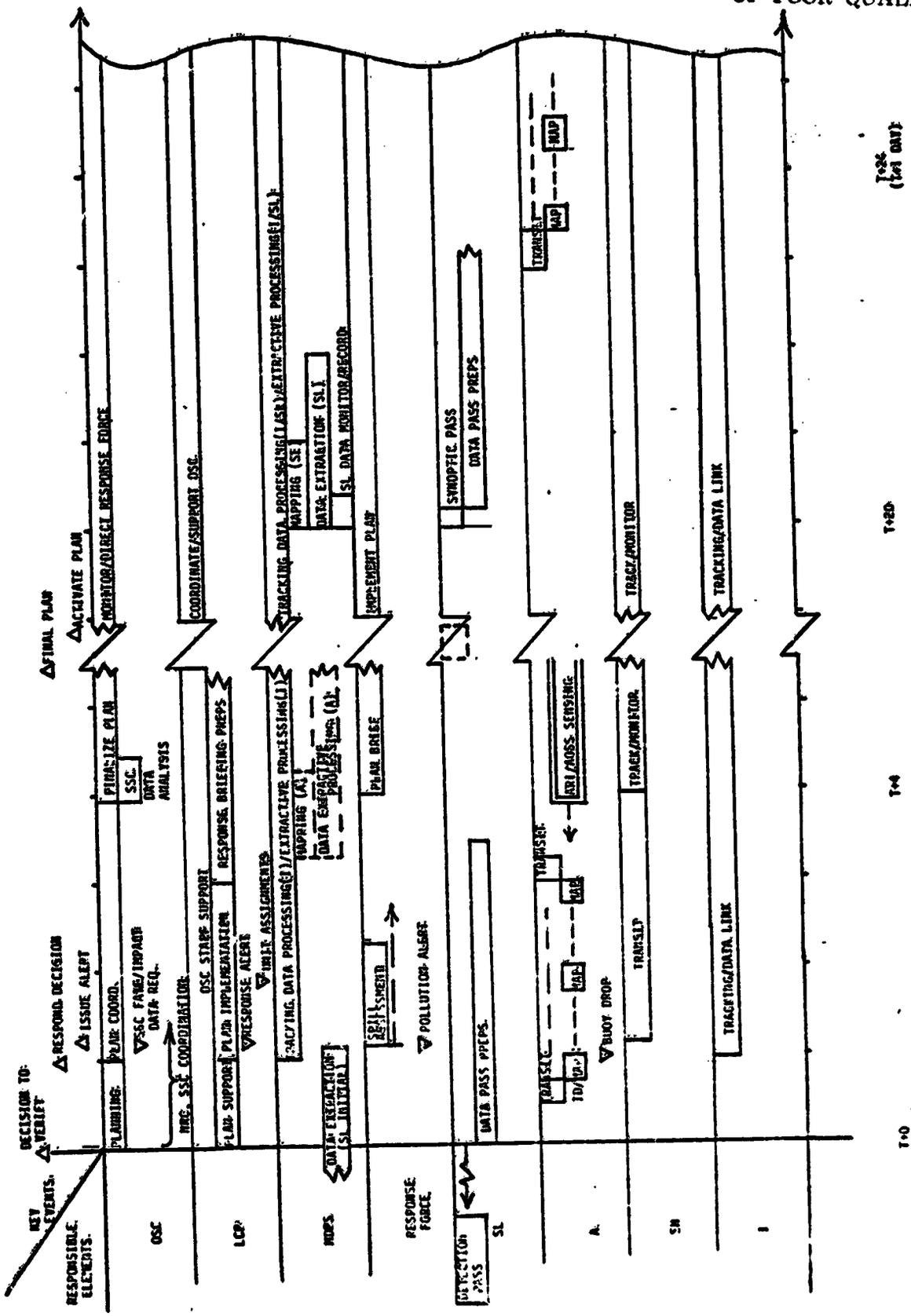

5.1.3.4 Scenario III: Fate and Impact Projection

As Figure 5.1-11 portrays, sensors on platforms at all levels are needed in support of various predictive models used to project the pollution trajectory and potential impact on sensitive areas. Numerous spacecraft (weather satellites; land, sea, and ice observers) currently do and will in the future play an important role in maintaining the meteorological, oceanographic, and ecological data bases necessary for model operation. A range of surface platforms (moored buoys, drifting buoys, ships, coastal/headland stations) provide critical, in situ measurements which enhance the accuracy of the remote sensing data. Mobile close-in platforms (aircraft and ships) are particularly helpful in real-time response activities in providing the models with fine scale, accurate local measurements from which to project. Thus, a wide set of space, air, and surface platforms — most of which already exist — together with their data processing systems, support this scenario of (1) routine data base building and model development and (2) model projections in pollution response activities.

FIGURE 5.1-11 FATE AND IMPACT PROJECTION: SCENARIO III

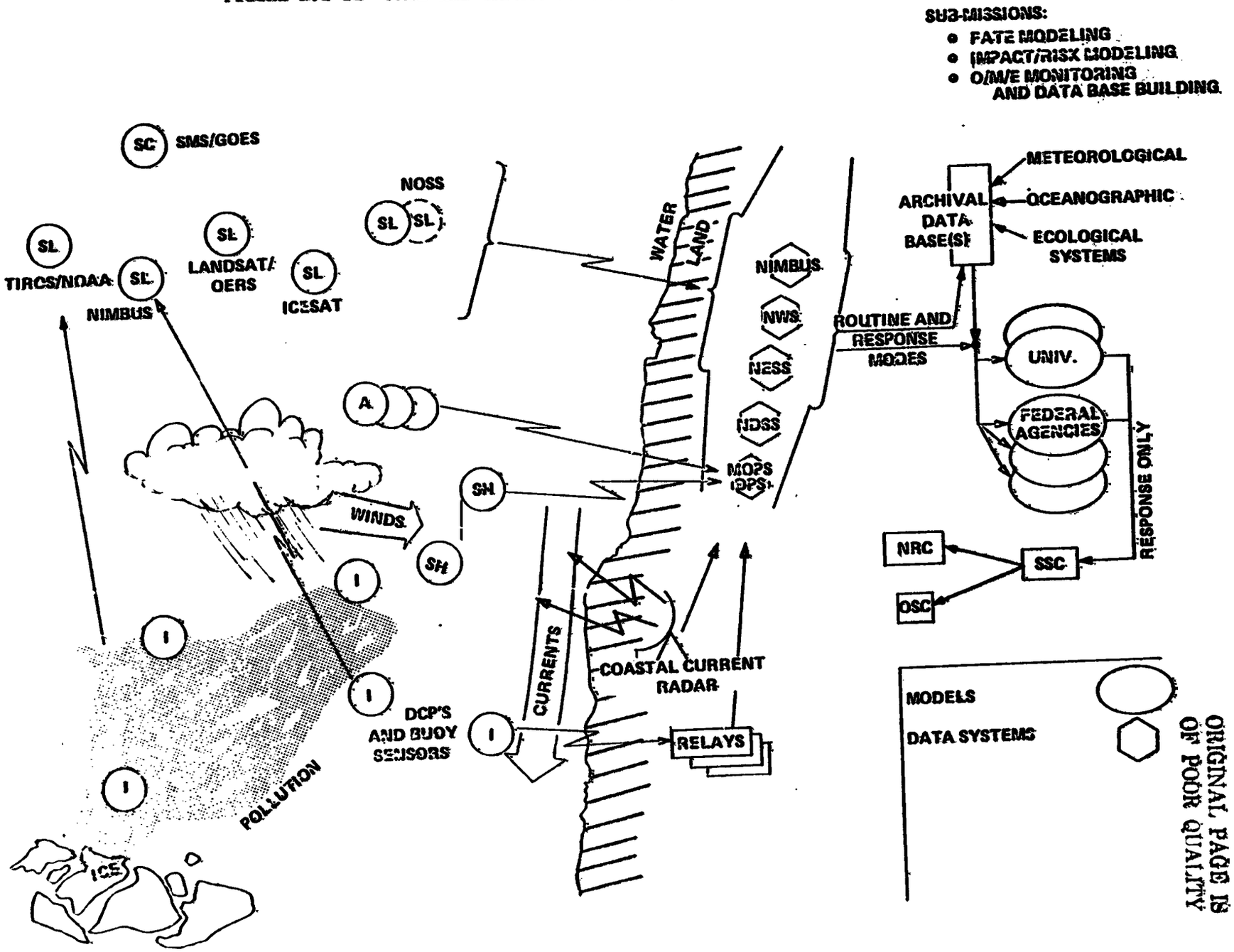

5.2 COASTAL COVERAGE ANALYSIS

5.2.1 SUMMARY

5.2.1.1 Analysis Objectives and Methodology

The various remote sensing options for coastal area coverage called for an in-depth trade analysis. Specifically, different platform/sensor options could not be compared to each other without quantitative estimates of their performance in support of MOPS mission needs. The following shows the general approach to these trade studies.

PLATFORM/SENSOR COVERAGE ANALYSES

- Identify Sensors Critical to MOPS Mission Success
- Define Coverage Objectives (Areal, Temporal) for those Sensors
- Perform Orbital Simulation and Parametric Trade Studies to Quantify the Performance of Various Options in Meeting Objectives.

Two critical remote sensing needs were selected from Table 3.4-1 for coverage assessment. The front end of pollution response activities -- detection of possible coastal zone pollution -- requires frequent broad area surveillance, such as that provided by high resolution imaging sensors. The details of possible airborne and spaceborne candidates were presented in Sections 4.1.2 and 4.1.3; in-depth analysis of their capability to meet daily broad area pollution detection needs is discussed below in section 5.2.3. The most demanding temporal frequency need is for fate modeling input data in the area of wind measurements: every six hours for direction and every three hours for speed. Section 4.1.2 above details the capability of the space-borne scatterometer to provide these data; section 5.2.4 below assess the temporal resolution possible with assumed platform/sensor configurations.

Two techniques were developed for performing these coverage analyses. The first employed graphical plots -- computer and hand-drawn overlays of various orbits and ground swaths of interest on the U.S. coastal zones. This technique was useful in characterizing broad differences among orbit/sensor options and assessing the relative impact of critical sensor parameters (such as field of view, day/night and active/passive sensing, and pointability) and critical orbit parameters (such as repeat cycle options, inclination, and altitude). Furthermore, manual plotting of computer-generated target acquisitions was used in the latter part of the areal and fractional coverage analysis to estimate portions of (1) redundant coverage and (2) inaccessibility of the various orbit/sensor/target zone combinations.

The second technique utilized a computer simulation (entitled COASTCOVER) to assess the absolute and relative performance of a number of orbit/sensor options. The motivation for obtaining accurate quantitative results, the options addressed, and the results themselves are presented in the following sections.

5.2.1.2 Results and Conclusions

Numerous analysis results are listed in their respective sections below: graphical coverage analysis (5.2.3.1), COASTCOVER areal coverage (5.2.3.2.1.1), COASTCOVER fractional coverage (5.2.3.2.1.2), and parametric sensitivity (5.2.3.2.2). The key results, with their associated conclusions, follow. All relate to the missions, orbit options, sensor characteristics, and target zones presented in section 5.2.2 below.

GENERAL

1. While the graphical plotting technique was useful for some qualitative conclusions, particularly on the impact of key parameters (inclination,

longitude of ascending node, access swath width) -- it was not adequate for accurate coverage trade-offs. COASTCOVER -- a flexible, computer simulation -- was developed and provided the needed outputs for orbit/sensor trade-offs.

COASTAL ZONE SURVEILLANCE MISSION

2. In terms of total coastal area covered (some redundantly) by several orbit/sensor options:

a. A SAR can image about 2700 (10^3) Km^2 of U.S. coastal zone in an average day. Aircraft, imaging a 20 n. mi. swath at 200 knots, would require about 200 mission-hours per day to cover the same area.

b. An optical imager can cover only about 25-30% of the SAR capability due to high coastal cloud cover, no night imaging, and sun lighting constraints.

3. In terms of a "bottom line" objective of total U.S. coastal coverage once a day, two potential spacecraft/aircraft mixes are recommended for further consideration. Both are based on a wide-swath (350-400 Km) pointable SAR with a $\pm$750 Km access swath:

a. Two spacecraft in a 3-day (Case II) repeat cycle, supplemented by aircraft only in the Gulf zone.

b. One spacecraft in a 1-day (Case IV) repeat cycle, with significant aircraft supplementation in all zones except the Atlantic.

4. To meet the same objective as 3 above with optical space sensing is much more difficult. Three to four times the number of platform/sensor combinations as in 3a. and b. above would be required. Even with that multiplicity of spacecraft heavy coastal cloud cover and sun lighting constraints preclude high confidence in meeting the daily objective. Geosynchronous spacecraft would be a more logical approach to the temporal resolution requirement, but are not forecast as a viable alternative within the mid-term time frame.

5. The Gulf coastal zone is significantly more difficult to cover than the other areas due to its east-west orientation and width and its low latitude.

6. Sensor duty cycles of about 2% (23-27 minutes per day) are needed for this mission and these target zones, regardless of orbit/sensor configuration. This reinforces the concpet of shared roles for this sensor (or sensors) with other missions and/or nations.

FATE MODEL INPUT MISSION

7. To meet the critical wind temporal resolution requirements of 3 hours (speed) and 6 hours (direction) with microwave scatterometers in typical NOSS and ICEX orbits would require at least 8 total platforms for wind speed and at least 4 total platforms for wind direction.

5.2.2 TRADE-OFF OPTIONS AND ASSUMPTIONS

5.2.2.1 Missions

These coverage analyses addressed the driving missions for the key ocean pollution remote sensors based on the section 3.3 user requirements. The high resolution imaging sensors -- both radar and passive optical -- are most heavily challenged by the detection and areal mapping need. The less stringent of the temporal resolution requirements was taken as the mission for the

imaging sensor: once daily coverage of the U.S. coastal zone out to 200 n. mi. rather than once every 12 hours out to 50 n. mi. Section 5.2.3 covers those analyses in detail.

To investigate critical high frequency fate model inputs (not currently provided by other sensing systems), the use of synoptic-coverage spacecraft microwave scatterometers for once every 3-6 hours wind measurements was taken as the mission. Section 5.2.4 summarizes that temporal coverage analysis.

5.2.2.2 Target Zones

Figure 5.2-1 illustrates the four U.S. coastal zones used as targets for coverage by the various sensor/platform options. Following are the area estimates by zone out to 200 n. mi. off the coast (generated by the COASTCOVER simulation):

ATLANTIC:	1320 (10^3) Km^2
GULF:	800 (10^3) Km^2
PACIFIC:	950 (10^3) Km^2
ALASKA:	650 (10^3) Km^2
(only as far west as Kodiak Island)	
TOTAL OF ALL FOUR:	3720 (10^3) Km^2

5.2.2.3 Sensors/Platforms

As discussed in detail earlier, the study position has been to seek other similar missions in order to share their sensor and platform costs and capabilities.

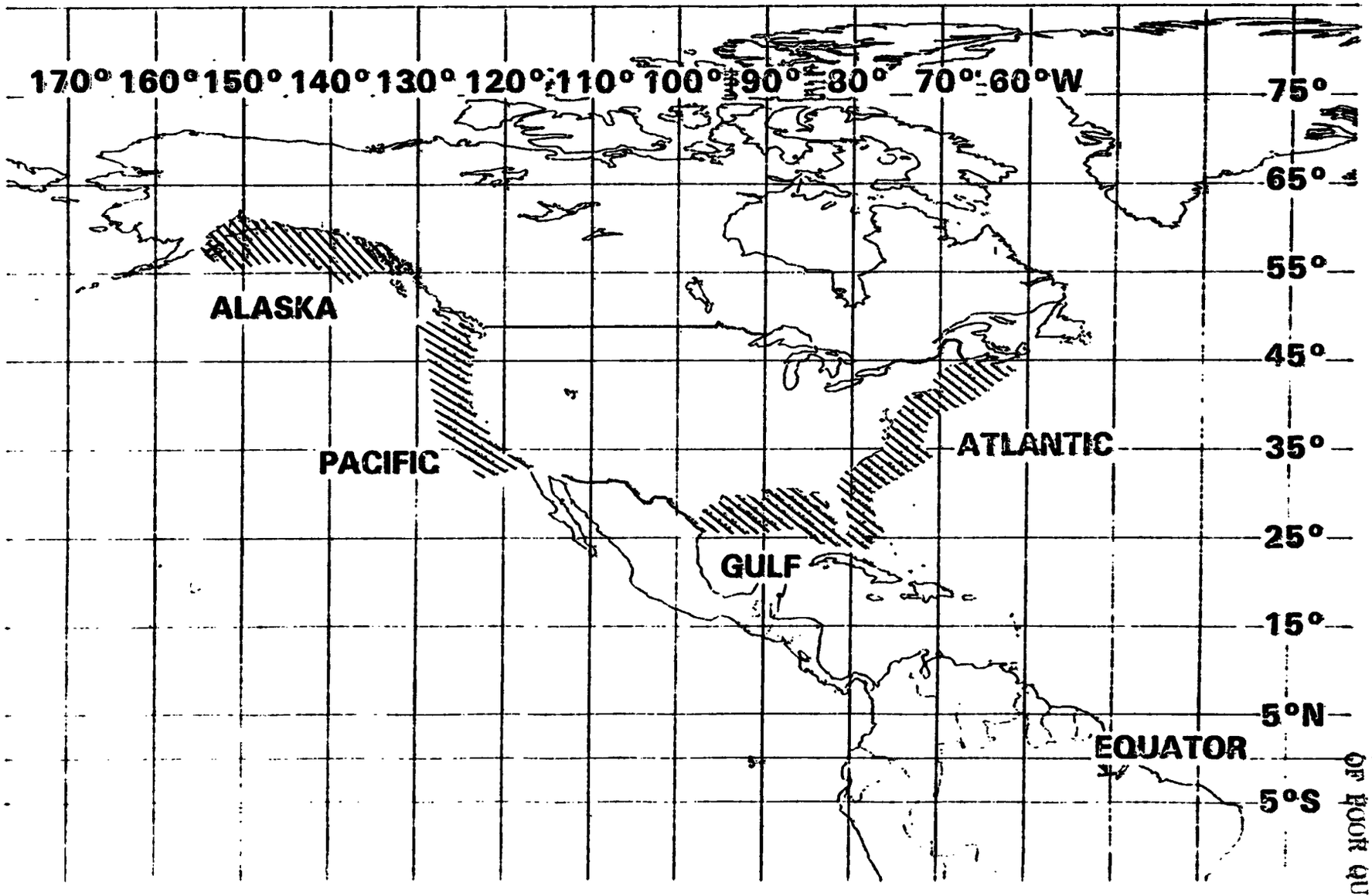

Figure 5.2-1. The Four U.S. Coastal Zones Used as System Targets

This has led to only one potential SAR shared-mission possibility: ICEX. The most attractive high resolution optical imagers within our time frame are the MSS and TM (Landsat D) and the pointable sensor proposed for the Operational Earth Resources System (OERS). However, none of these instruments fits our wide area daily coverage need due to narrowness of swath, lack of pointability, and/or too long a repeat cycle. Thus, the proposed wide-swath pointable optical linear array (POLA) is assumed to piggyback on the SAR platform (ICEX).

Figure 5.2-2 shows the currently-proposed swathing patterns for the pointable imagers and non-pointable scatterometer. Figure 5.2-3 illustrates the employment of the imager against the Atlantic coastal zone.

Aircraft sensors and platforms directly of use to our mission include the ARI and advanced ARI, discussed above. The large number of these relatively narrow swath systems required to meet the wide area daily surveillance mission by themselves points toward their suggested role in a mixed-platform system: covering part of the Gulf zone and filling in gaps or increasing coverage frequency as needed elsewhere.

5.2.2.4 Orbits

The three different low earth orbits addressed in great detail by the COASTCOVER simulation are:

1. 2-day non-sun synchronous: the current ICEX program preference (Case I in Table 5.2-1)
2. 3-day non-sun synchronous: a SAR study - proposed ICEX orbit (Reference 133); Case II in Table 5.2-1)
3. 1-day sun-synchronous: assumed alternative to simplify the use of the optical sensors (Cases III and IV in Table 5.2-1)

Figure 5.2-2. SENSOR SWATHING PATTERNS

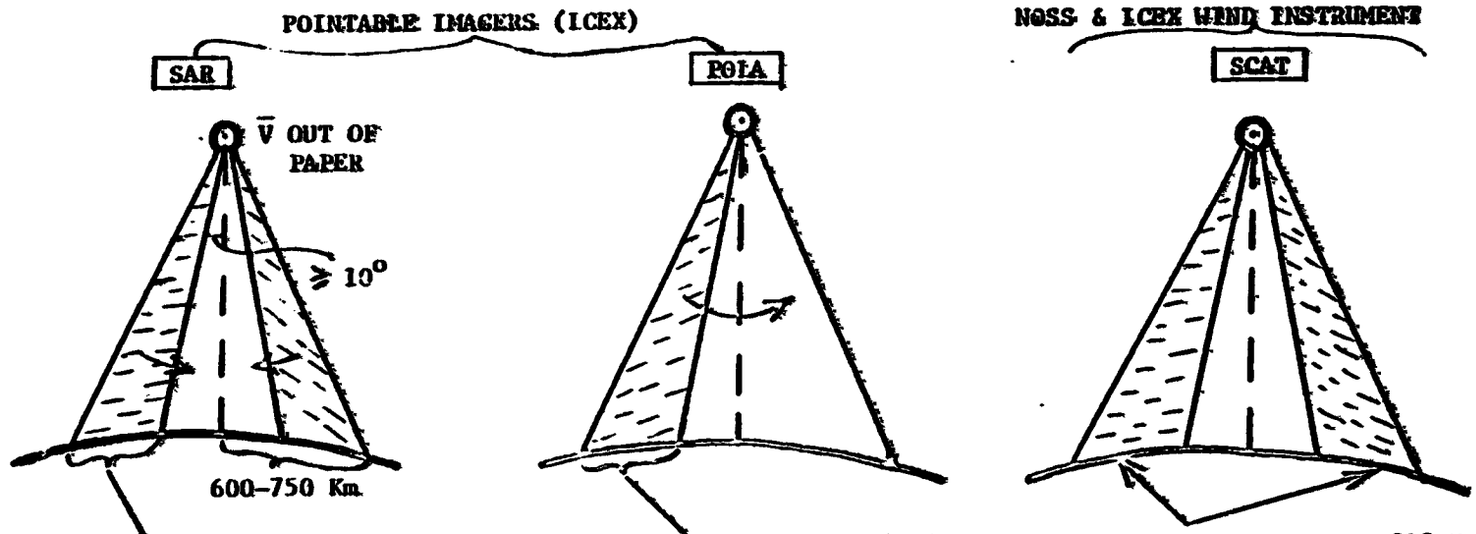

- ACTUAL SWATH: 345–392 Km ON EITHER SIDE
- POINTABLE OUT TO 600–750 Km AND AS CLOSE IN TO NADIR AS 10°
- TOTAL ACCESS SWATH: 1200–1500 Km WIDE

- ACTUAL SWATH: 345–392 Km
- POINTABLE WITHIN 600–750 Km ON EITHER SIDE OF NADIR
- TOTAL ACCESS SWATH: 1200–1500 Km

- ACTUAL SWATHS: 518 Km (NOSS) OR 551 Km (ICEX) ON BOTH SIDES OF NADIR
- NON-POINTABLE
- 560 Km (NOSS) OR 600 Km (ICEX) WIDE "BLIND" SPOT AT NADIR

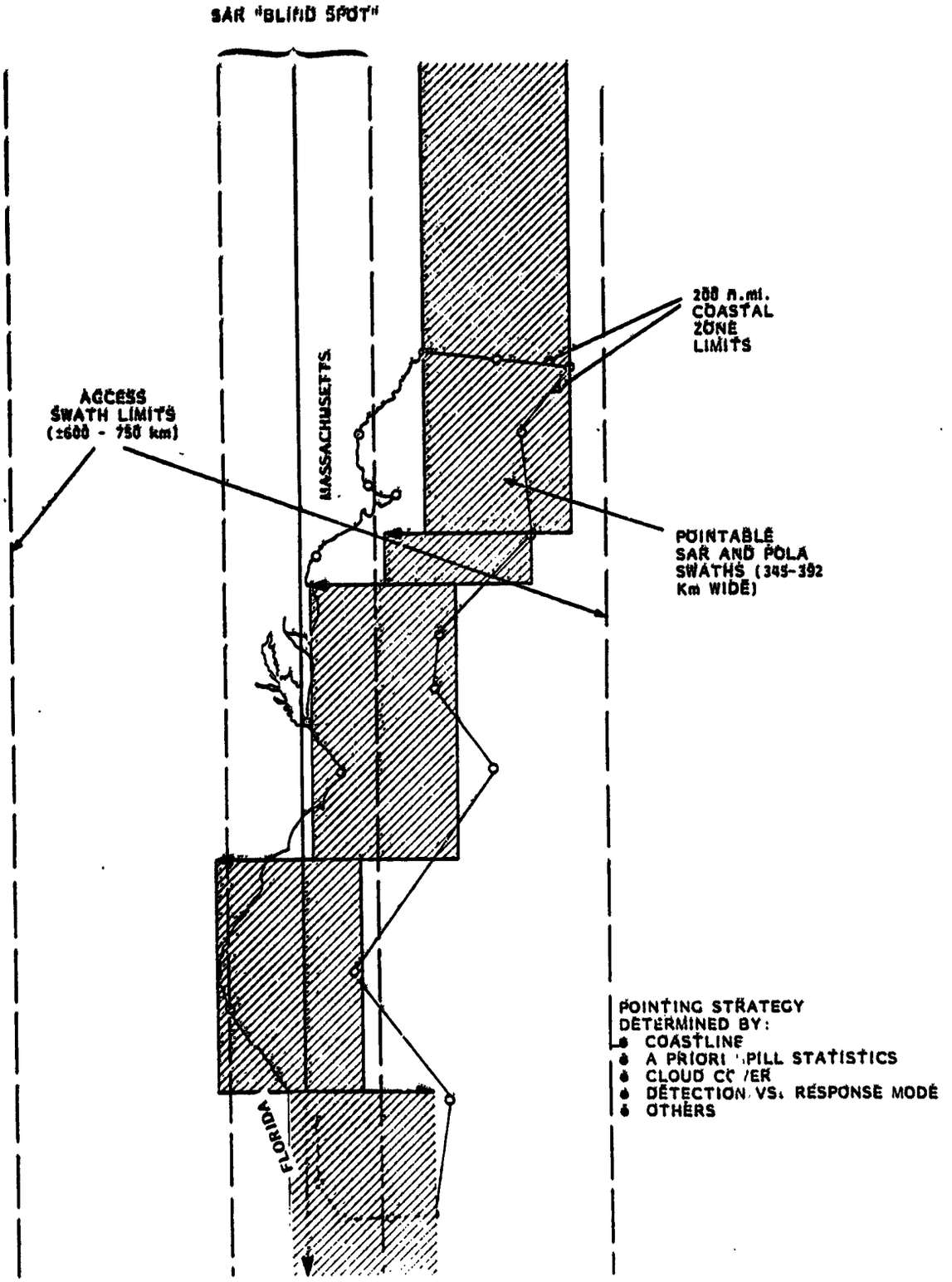

Figure 5.2-3. Primary Detection Sensors, Pointable for Optimum Coverage

TABLE 5.2-1: SUMMARY OF ORBIT/SENSOR CONFIGURATIONS EXAMINED

CASE #	ORBITAL PARAMETERS A**	I	SS/NSS	RC	SENSOR CHARACTERISTICS TYPE	SWATH	P/NP	COMMENTS
I. A.	725.6 Km	93°	NSS	2 DAYS	SAR/POLA	345 Km	P	POINTABLE AND NON-POINTABLE VERSIONS OF 2 POSSIBLE ICEX ORBITS
B.	725.6 Km	93°	NSS	2 DAYS	SAR/POLA	345 Km	NP	
II. A.	780.5 Km	92°	NSS	3 DAYS	SAR/POLA	356 Km	P	
B.	780.5 Km	92°	NSS	3 DAYS	SAR/POLA	356 Km	NP	
III. A.	891.1 Km	99°	SS	1 DAY	SAR/POLA	392 Km	P	• EFFECT OF NODAL CROSSING LONGITUDE ON 1-DAY REPEATERS INVESTIGATED (CASE III vs. CASE IV)
B.	891.1 Km	99°	SS	1 DAY	SAR/POLA	392 Km	NP	
C.	891.1 Km	99°	SS	1 DAY	SAR/POLA	392 Km	P***	• EFFECT OF WIDER ACCESS SWATH INVESTIGATED (CASES III.C. AND IV.C.)
IV.**** A.	891.1 Km	99°	SS	1 DAY	SAR/POLA	392 Km	P	
B.	891.1 Km	99°	SS	1 DAY	SAR/POLA	392 Km	NP	
C.	891.1 Km	99°	SS	1 DAY	SAR/POLA	392 Km	P***	
V.	725.6 Km	93°	NSS	2 DAYS	SCAT	551.2 Km	NP	TEMPORAL RESOLUTION INVESTIGATED FOR FIXED SWATH SCATTEROMETERS IN POSSIBLE ICEX (CASE V) AND NOSS (CASE VI)
VI.	671.7 Km	98.072°	SS	3 DAYS	SCAT	518.1 Km	NP	

* ALL ORBITS ARE CIRCULAR WITH LONGITUDE OF ASCENDING NODE = -83° UNLESS OTHERWISE SPECIFIED

** KEY TO COLUMN HEADINGS:

A: ALTITUDE
I: INCLINATION
SS/NSS: SUN SYNCHRONOUS OR NON-SUN SYNCHRONOUS
RC: REPEAT CYCLE
TYPE: SENSOR WHOSE COVERAGE WAS ASSESSED
SWATH: CROSS-TRACK GROUND SWATH VIEWED BY SENSOR
P/NP: POINTABLE OR NON-POINTABLE SENSOR FIELD OF VIEW (WITHIN ACCESS SWATH ±600 Km ON EITHER SIDE UNLESS OTHERWISE SPECIFIED)

*** WIDER ACCESS SWATH (±750 Km ON EITHER SIDE)

**** SAME AS CASE III EXCEPT LONGITUDE OF ASCENDING NODE = -76° (SELECTED TO GIVE EXCELLENT ATLANTIC ZONE COVERAGE)

5.2.3 AREAL COVERAGE ANALYSIS

5.2.3.1 Graphical Plotting Technique

A previously-developed orbital simulation computer program and automated ground track/earth map plotting program were used to generated graphical overlays of various orbits for screening and qualitative coverage estimates. Figure 5.2-4 is an example of a sensor access pattern for a 1200-km ground swath along the U.S. coastline. The following orbits were examined by this technique to assess their relative merits and sensitivity to varying sensor and orbit parameters for the daily coastal zone detection mission:

- Two sun-synchronous 1-day repeaters
- Two other sun-synchronous repeaters (3-day and 6-day)
- Two non-sun-synchronous 1-day repeaters.

The results of these investigations are shown in Figures 5.2-5 through 5.2-8 for altitudes in the Landsat/NOSS/marsat/ICEX regime (700-900 Km) and Figure 5.2-9 for the lower altitude Shuttle sortie regime.

The advantages of this technique are visibility and flexibility. Once the ground track and swath visuals were prepared, the analyst could quickly assess the impact of varying swath width, inclination, nodal crossing longitude, and other key parameters. Some of the results of these graphical plot trade-offs are shown in Figure 5.2-10..

The disadvantage of this technique is that it cannot easily provide accurate numerical answers. Given the assumption of a space sensor field of view pointable on either side of nadir with an actual ground swath narrower than the ground access swath, there are too many variables to approximate the target area covered (not simply

FIGURE 5.2-4 DAILY SENSOR ACCESS FOR A NON-SUN-SYNCHRONOUS ONE-DAY REPEATER (893 KM, 110° INCLINATION)

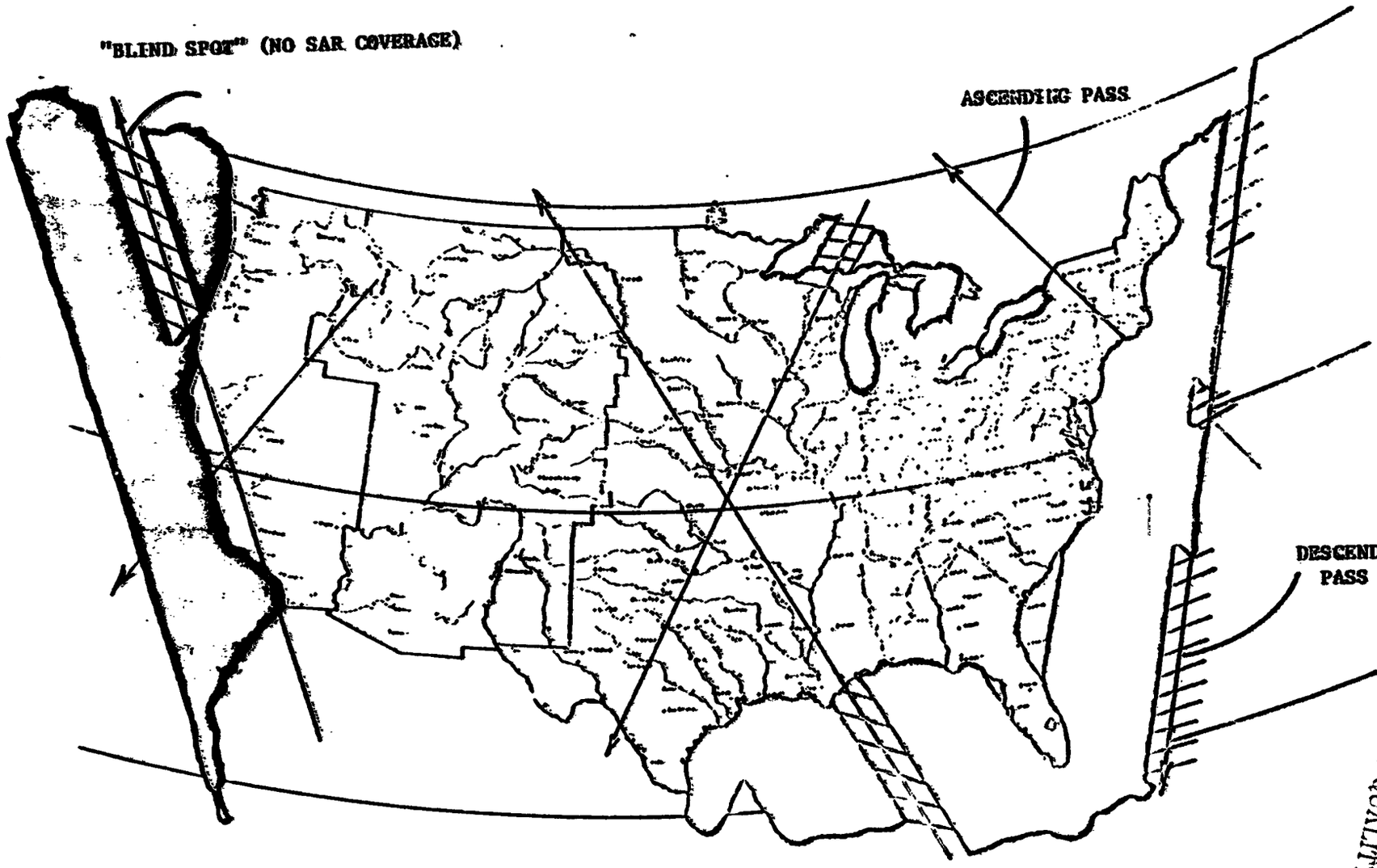

FIGURE 5-2-5. COVERAGE BY SUN-SYNCHRONOUS 1-DAY REPEATER

GENERAL

- GROUND TRACKS REPEAT DAILY (14 ORBITS) -- SOME COASTAL AREAS NEVER ACCESSIBLE
- POINTABLE SENSORS LEAD TO DIFFERENT AREAS MAPPED ON DIFFERENT DAYS
- OPTIMUM COVERAGE EXAMINED GRAPHICALLY BY VARYING THE ORBITAL PLANE ORIENTATION (LONGITUDE OF ASCENDING NODE):

OPTION 1: WESTERN FOCUS

- GOOD-TO-EXCELLENT COVERAGE: WEST COAST AND GULF OF ALASKA
- POOR-TO-NO COVERAGE: EASTERN GULF COAST AND SOUTHERN EAST COAST

OPTION 2: EASTERN FOCUS

- GOOD COVERAGE: EAST COAST, WEST COAST, AND GULF OF ALASKA
- POOR COVERAGE: GULF OF MEXICO

OPTION 3: GULF FOCUS

- GOOD-TO-EXCELLENT COVERAGE: GULF OF MEXICO AND GULF OF ALASKA
- FAIR-TO-GOOD COVERAGE: WEST COAST
- POOR-TO-NO COVERAGE: EAST COAST

A ONE-DAY REPEATER AT SUN-SYNCHRONOUS INCLINATIONS CANNOT MAP BOTH THE EAST COAST AND GULF OF MEXICO

FIGURE 5.2-6 COVERAGE BY SUN-SYNCHRONOUS 3-DAY REPEATER

GENERAL

- GROUND TRACKS REPEAT EVERY 3 DAYS (43 ORBITS)
- ALL COASTAL AREAS ARE ACCESSIBLE AT LEAST 3 (AND AS MANY AS 6) TIMES IN EVERY 3-DAY CYCLE
- MANY TARGET POINTS ARE ACCESSIBLE EVERY DAY; FEW ARE INACCESSIBLE FOR MORE THAN ONE DAY OUT OF THREE

BY SPECIFIC AREA

- FOR TYPICAL TARGET POINTS

LATITUDE	LOCATION	ACCESSIBILITY DAY #			
		SENSORS	1	2	3
25°	FLORIDA KEYS	OPTICAL MICROWAVE	X	X	
		MICROWAVE ONLY	X		X
35°	SANTA BARBARA	O/M	X	X	
		M		X	X
40°	PHILADELPHIA (NY, BOSTON, GREAT LAKES)	O/M	X	X	
		M		X	X
60°	GULF OF ALASKA	O/M	X	X	X
		M	X	X	X

ONE (OF SEVERAL) ORBIT/FOV "SOLUTIONS" THAT PERMIT ACCESS TO A HIGH PERCENTAGE OF TARGET AREAS DAILY

FIGURE 5.2-7. COVERAGE BY SUN-SYNCHRONOUS 6-DAY REPEATER

GENERAL

- GROUND TRACKS REPEAT EVERY 6 DAYS (85 ORBITS)
- ALL COASTAL AREAS ARE ACCESSIBLE AT LEAST 6 (AND AS MANY AS 12) TIMES IN EVERY 6-DAY CYCLE
- MOST TARGET POINTS ARE ACCESSIBLE FOR AT LEAST 3 DAYS IN A ROW AND INACCESSIBLE FOR NOT MORE THAN 3 DAYS IN A ROW
- OVER A 6-DAY PERIOD, ALL COASTAL AREAS CAN BE TOTALLY MAPPED AT LEAST TWICE (EXCLUDING MICROWAVE "BLIND SPOT" AREAS)

BY SPECIFIC AREA

- TABLE SHOWS WORST CASE

LATITUDE	LOCATION	ACCESSIBILITY DAY #						
		SENSORS	1	2	3	4	5	6
25°	FLORIDA KEYS	OPTICAL MICROWAVE		X	X	X		
		MICROWAVE ONLY		X	X	X		
35°	SANTA BARBARA	O/M		X	X	X	X	
		M			X	X	X	
40°	PHILADELPHIA (NY, BOSTON, GREAT LAKES)	O/M	X	X	X			
		M			X	X	X	X
60°	GULF OF ALASKA	O/M	X	X	X	X	X	X
		M	X	X	X		X	X

- EXCELLENT COVERAGE FROM MID-ATLANTIC NORTH
- PROMISING OPTION FOR HIGH FREQUENCY COVERAGE BY COMBINED AIRCRAFT/SPACECRAFT PLATFORMS

FIGURE 5.2-8 COVERAGE BY NON-SUN-SYNCHRONOUS 1-DAY REPEATER
(ILLUSTRATED IN FIGURE 5.2-4)

GENERAL

- GROUND TRACKS REPEAT DAILY (14 ORBITS)
- MOST OF COASTAL AREA ACCESSIBLE
- POINTABLE SENSORS LEAD TO DIFFERENT AREAS MAPPED ON DIFFERENT DAYS

ADVANTAGES

- GROUND TRACK FOR 110° INCLINATION "FITS" COASTAL SLOPE BETTER THAN NEAR-POLAR
- ALMOST COMPLETE DAILY ACCESS FOR HIGHEST TRAFFIC AREAS
- TWICE DAILY COVERAGE FOR SIGNIFICANT PARTS OF SOUTHERN CALIFORNIA, NORTHERN EAST COAST, AND HOUSTON REGION

DISADVANTAGES

- LIGHTING CONDITIONS FOR OPTICAL SENSOR CHANGE FROM DAY TO DAY
- 110° INCLINATION MAY MEAN TOO LITTLE POLAR COVERAGE FOR ICEX MISSION

FIGURE 5.2-9 TWO LOWER ALTITUDE OPTIONS

- 57° INCLINATION, 263.4 km, 1000 km SWATH
- NON-SUN SYNCH., ONE-DAY REPEATER (16 ORBITS)
- POTENTIAL SHUTTLE SORTIE FROM KSC

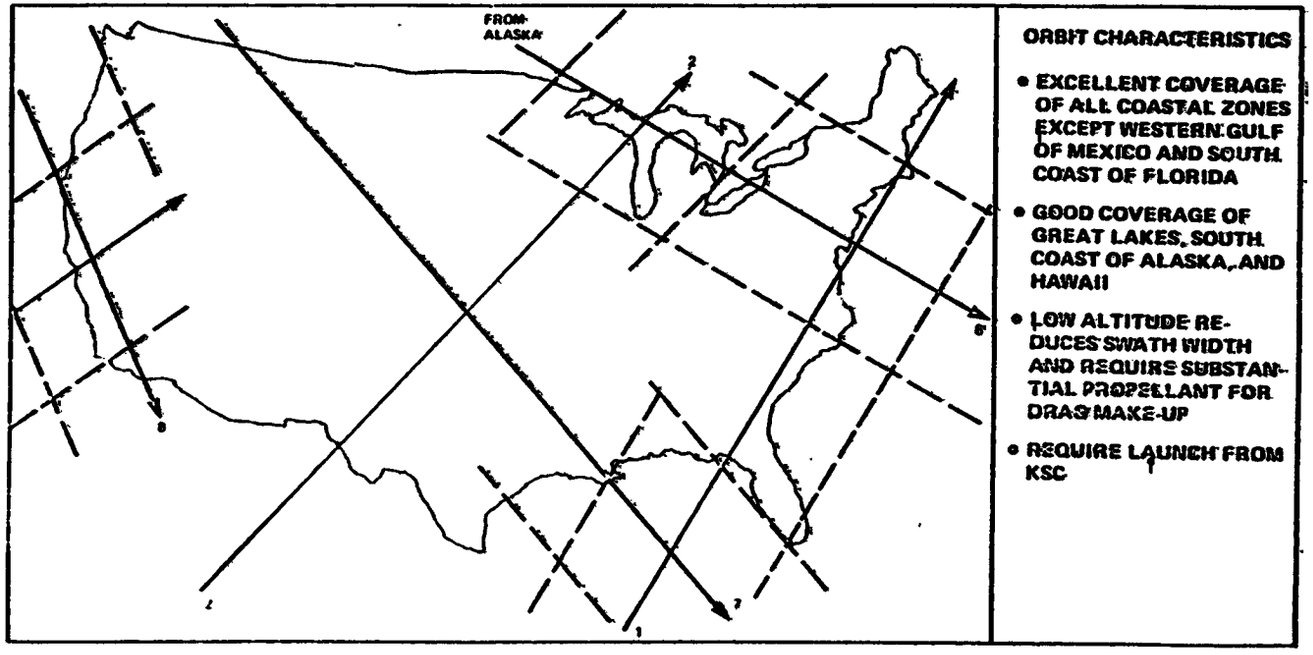

FIGURE 5.2-9 TWO LOWER ALTITUDE OPTIONS (Cont)

- NEAR-POLAR, 566.8 km, 1000 km SWATH
- SUN SYNCH., ONE-DAY REPEATER (15 ORBITS)
- POTENTIAL SHUTTLE SORTIE FROM VAFB

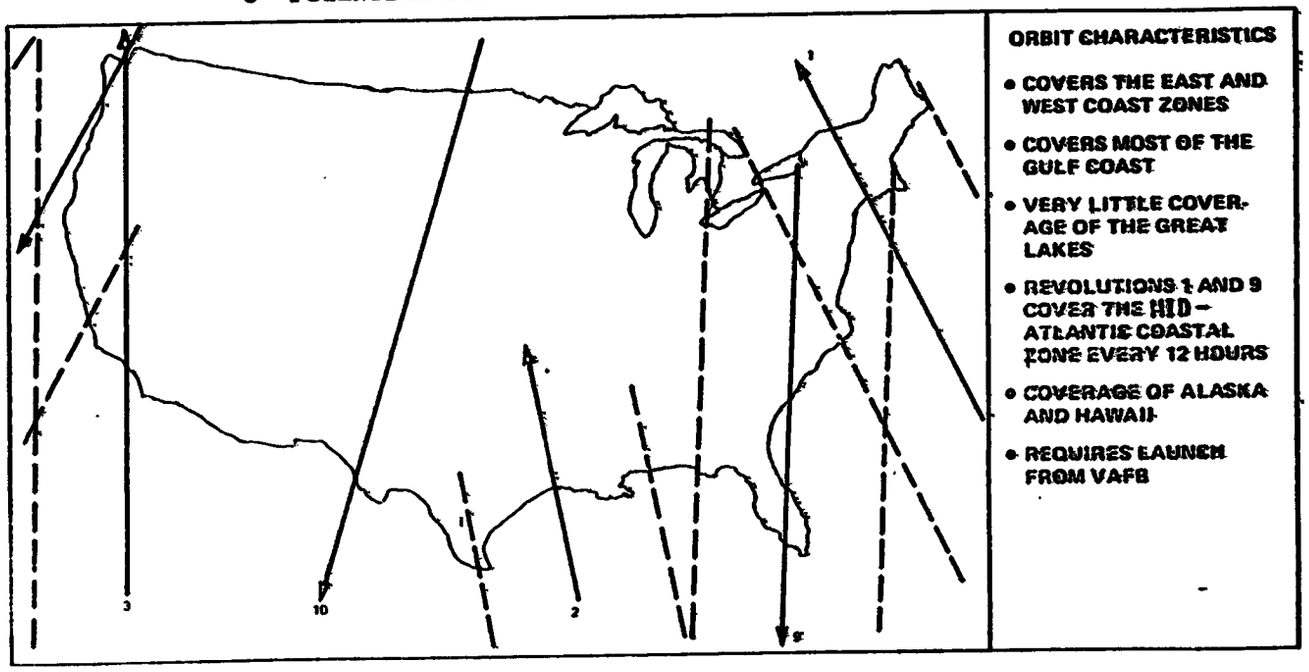

FIGURE 5.2-10 RESULTS OF GRAPHICAL COVERAGE ANALYSIS

- ONE-DAY REPEATERS
  - NOT ENOUGH ORBITS TO ACCESS ALL COASTAL AREAS
  - NON-SUN-SYNCHRONOUS GIVE BETTER COVERAGE BUT OPTICAL SENSOR LESS USEFUL
- MULTIPLE-DAY REPEATERS
  - THREE-DAY CASE OFFERS ONE POTENTIAL "SOLUTION" TO DAILY COASTAL AREA COVERAGE; OTHERS ARE BEING IDENTIFIED
  - GENERALLY MORE ORBITS/REPEAT CYCLE AND HIGHER LATITUDES PROVIDE BETTER COVERAGE BUT NOT NECESSARILY
  - COMPUTER SIMULATION WILL PROVIDE QUANTITATIVE COVERAGE ESTIMATES FOR A NUMBER OF ORBITAL OPTIONS
- MULTIPLE SPACECRAFT REQUIRED FOR TOTAL DAILY COASTAL DETECTION MAPPING REGARDLESS OF ORBIT SELECTED
- OTHER ALTERNATIVES
  - MOPS PALLET ON PERIODIC SHUTTLE SORTIES TO SUPPLEMENT FREE FLYER
  - GEOSYNCHRONOUS SPACECRAFT: SENSORS NOT LIKELY IN THE NEAR-TO-MID-TERM

accessible) during a repeat cycle. This became especially true as the parameters of each orbit were varied and the number of orbits examined was increased. A flexible, rapid response tool to give accurate coverage estimates for a wide range of orbit and sensor parameter options was needed. Consequently, a computer program was developed and is discussed in the next section.

5.2.3.2 COASTCOVER: Computer Simulation for Coverage Analysis

In order to determine accurate coverage figures for a range of orbits and sensor swath parameters and pointing options, a computer simulation was developed. Known as COASTCOVER, the software is listed in Appendix A, which also contains some simulation results.

Basically, as highlighted in Figure 5.2-11, it comprises several subroutines built upon the already-existing standard orbital simulation (DK9) which transform orbit, target, and remote sensor characteristics into accessible and actual ground swath widths and accumulated ground area covered during discrete passes through a target zone. Flexibility has been built into the program to allow for sensor FOV pointability, inaccessibility of viewing close in to nadir for side-looking microwave instruments (the "blind spot"), and area accumulation options to simulate one or two-sided viewing, pointable or fixed - FOV instruments, and "blind spot" or "no blind spot" instruments.

Section 5.2.2 discussed and illustrated the viewing and target options selected for assessment. The following sections detail the results of the COASTCOVER simulations in (1) comparing various discrete orbit/sensor options in performing the ocean pollution surveillance mission and (2) analyzing the sensitivity of coverage results to parameters such as access swath width, sensor pointability, and orbital plane orientation.

5.2.3.2.1 Coverage Results for a Set of Orbit/Sensor Configurations

COASTCOVER was run on many different orbit/sensor configurations to examine the surveillance capability for microwave and optical imaging sensors against the four main U.S. coastal zones illustrated in Section 5.2.2 above: Atlantic, Gulf, Pacific, and Alaska. The ten configurations of most current interest (based on the logic of 5.2.2 above) are summarized as Cases I through IV in Table 5.2-1.

Cases V and VI will be covered in Section 5.2.4 since they were run for temporal (not areal) coverage analysis.

5.2.3.2.1.1 COASTCOVER Areal Coverage Calculations. The detailed coverage figures for each of the ten cases are provided in Appendix A in Tables A-1 through A-40. Each table presents the areal coverage for each pass throughout the repeat cycle (1, 2, or 3 days) for one of the four target zones. In addition to the pass-by-pass and day-by-day detials of type of pass (ascending or descending) and side of sub-satellite track (east or west), the results were accumulated in several useful ways:

ASCENDING, DESCENDING AND COMBINED GRAND TOTALS:

The relative contribution of type of pass over the whole repeat cycle can be seen here. This is particularly useful for optical instruments where sun lighting conditions are critical. For the two sun-synchronous orbits (Cases III and IV), only the descending passes would be used for passive optical sensing in a typical scenario.

"NO BLIND SPOT" SENSOR TOTAL:

This simulation option "allowed" the sensor to see area within the radar "blind spot" (as an optical sensor could). Typically, this increased the areal coverage capability over the COMBINED GRAND TOTAL.

"ONE-SIDE ONLY" SENSOR TOTALS:

While the above totals assumed the field of view could access both sides of nadir, this option assumed one-side only (as for a Seasat-type one antenna SAR sensor). The effect of which side on the coverage totals is shown by the two totals.

DAILY AVERAGE ACCESS TIME:

The daily sum of the number of minutes coverage for each pass across a target zone was averaged over a repeat cycle. This figure is useful for sensor duty cycle esitmates.

FIGURE 5.2-11: COASTCOVER
A COMPUTER SIMULATION FOR COASTAL COVERAGE ANALYSIS

- USES STANDARD ORBITAL MISSION MODEL
- SUBROUTINES COMPUTE SENSOR SWATH AREAS WHICH COVER TARGET ZONES
- INPUTS:
  - ORBITAL ELEMENTS
  - SENSOR FIELD OF VIEW
  - TARGET ZONES
- OUTPUTS:
  - GROUND TRACK - FOR EACH COASTAL ZONE
  - SWATH EDGES - FOR EACH SENSOR SWATH
  - TARGET AREA COVERED - FOR EACH SATELLITE

Those detailed results are summarized for each case for each target zone (and the overall U.S. coastal zone) in Tables 5.2-2 through 5.2-6. Each table allows easy comparison of the ten cases in terms of average daily areal coverage, as well as showing the "all-orbit means". While these numbers will be further used in later discussions of sensitivity to variation of parameters, a few points may be made here:

1. A SAR wide-swath imaging sensor (with blind spot) can cover about 2700 (10^3) Km^2 of the U.S. Coastal Zone on an average day. (Some of this area is redundantly covered.) For 200 Knot aircraft with 20 nm swath width (disregarding their blind spot), about 200 mission-hours per day could provide the same coverage.

2. A pointable width-swath optical imager (such as the POLA) can cover about 750 (10^3) Km^2 of U.S. Coastal Zone on an average day (assuming 50% coastal cloud cover, descending passes only, and no blind spot).

3. The Gulf of Mexico is the most poorly covered target zone due to the combination of its east-to-west width ($\geq$ 1500 Km), its low latitude (minimizes swath sidelap), and the high orbital inclinations.

4. Sensor duty cycles of only about 2% (23 to 27 minutes a day) are indicated for this mission and these target zones.

5.2.3.2.1.2 Fractional Coverage Estimates. The "bottom line" coverage question is not simply -- how much area can be surveyed daily by each orbit/sensor configuration? -- but rather -- what fraction of the target zone is covered daily by each configuration? A corollary question is: how much target area is never surveyed by a given configuration? To arrive at these estimates, the quantiative areal coverage estimates of COASTCOVER were combined with graphical plot estimates of daily coverage redundancy. The COASTCOVER Latitude/longitude claculations for each coverage pass were used togathet with the graphical plotting techniques of section 5.2.3.1 to esitmate a daily average NRF (Non-Redundancy Factor) for each of the ten cases for each target zone. This factor adjusts the daily areal coverage for those areas covered multiple times. It could range from 1.0 for no daily coverage redundancy down to less than 0.5 (where 0.5 means all area covered on an average day is covered an average of twice).

TABLE 5.2-2: AREAL COVERAGE COMPARISON

TARGET ZONE: ATLANTIC

TARGET ZONE AREA: 1320 (10^3) Km^2

CASE #	# OF DAYS/ REPEAT CYCLE	AVERAGE # OF PASSES/ DAY	AVERAGE DAILY COVERAGE TIME	AVERAGE DAILY COVERAGE (1000 Km^2)			
				ASCENDING	DESCENDING	TOTAL (W/BLIND SPOT)	TOTAL (W/O BLIND SPOT)
I. A	2	3	10 MIN.	501	475	976	1066
B	2	2.5	8 MIN	440	370	810	901
II. A	3	2.3	10 MIN.	422	539	961	1141
B	3	2.3	9 MIN.	329	455	784	966
III. A	1	2	5 MIN.	331	85	416	470
B	1	2	4 MIN.	303	51	354	408
C	1	3	6 MIN.	418	248	666	717
IV. A	1	3	11 MIN.	639	775	1414	1462
B	1	3	11 MIN.	571	685	1256	1306
C	1	3	12 MIN.	732	959	1691	1739
ALL-ORBIT MEANS:	2.6		8.6 MIN.	469	464	933	1018

TABLE 5.2-3: AREAL COVERAGE COMPARISON

TARGET ZONE: GULF

TARGET ZONE AREA: 800 (10^3) Km^2

CASE #	# OF DAYS/ REPEAT CYCLE	AVERAGE # OF PASSES/ DAY	AVERAGE DAILY COVERAGE TIME	AVERAGE DAILY COVERAGE (1000 Km^2)			
				ASCENDING	DESCENDING	TOTAL (W/BLIND SPOT)	TOTAL (W/O BLIND SPOT)
I. A	2	3	4 MIN.	215	208	423	436
B	2	2	3 MIN.	177	165	342	361
II. A	3	2.3	3 MIN.	224	198	422	449
B	3	2	4 MIN.	198	174	372	401
III. A	1	2	4 MIN.	310	287	597	597
B	1	2	4 MIN.	292	287	579	582
C	1	2	4 MIN.	355	287	642	642
IV. A	1	2	4 MIN.	263	225	488	622
B	1	2	4 MIN.	262	219	481	620
C	1	2	4 MIN.	266	236	502	624
ALL-ORBIT MEANS:		2.1	3.8 MIN.	256	229	485	533

TABLE 5.2-4: ARSAL COVERAGE COMPARISON

TARGET ZONE: PACIFIC

TARGET ZONE AREA: 950 (10^3) Km^2

CASE #	# OF DAYS/ REPEAT CYCLE	AVERAGE # OF PASSES/ DAY	AVERAGE DAILY COVERAGE TIME	AVERAGE DAILY COVERAGE (1000 Km^2)			
				ASCENDING	DESCENDING	TOTAL (W/BLIND SPOT)	TOTAL (W/O BLIND SPOT)
I. A	2	1.5	7 MIN.	202	491	693	909
B	2	1.5	7 MIN.	199	384	583	799
II. A	3	1.7	7 MIN.	419	408	827	949
B	3	1.7	7 MIN.	382	374	756	880
III. A	1	2	9 MIN.	731	169	900	900
B	1	2	8 MIN.	654	151	805	805
C	1	2	9 MIN.	887	325	1212	1212
IV. A	1	1	4 MIN.	0	404	404	635
B	1	1	4 MIN.	0	374	374	611
C	1	2	6 MIN.	30	470	500	728
ALL-ORBIT MEANS:	1.5		6.8 MIN.	350	355	705	843

TABLE 5.2-5: AREAL COVERAGE COMPARISON

TARGET ZONE: ALASKA

TARGET ZONE AREA: 650 (1.0^3) Km^2

CASE #	# OF DAYS/ REPEAT CYCLE	AVERAGE # OF PASSES/ DAY	AVERAGE DAILY COVERAGE TIME	AVERAGE DAILY COVERAGE (1000 Km^2)			
				ASCENDING	DESCENDING	TOTAL (W/BLIND SPOT)	TOTAL(W/O BLIND SPOT)
I. A	2	3	6 MIN.	316	310	626	647
B	2	3	6 MIN.	260	253	513	541
II. A	3	3.3	6 MIN.	287	267	554	621
B	3	3	5 MIN.	250	212	462	534
III. A	1	4	8 MIN.	270	388	658	699
B	1	4	6 MIN.	229	357	586	623
C	1	4	8 MIN.	437	446	883	926
IV. A	1	2	4 MIN.	323	244	567	613
B	1	2	4 MIN.	306	244	550	598
C	1	2	4 MIN.	336	234	570	622
ALL-ORBIT MEANS:		3.0	5.7 MIN.	301	295	596	642

TABLE 5.2-6 : AREAL COVERAGE COMPARISON

TARGET ZONE: ALL FOUR U.S. COASTAL ZONES

TARGET ZONE AREA: 3720 (10^3) Km^2

CASE #	# OF DAYS/ REPEAT CYCLE	AVERAGE # OF PASSES/ DAY	AVERAGE DAILY COVERAGE TIME	AVERAGE DAILY COVERAGE (1000 Km^2)			
				ASCENDING	DESCENDING	TOTAL (W/BLIND SPOT)	TOTAL(W/O BLIND SPOT)
I.A.	2	11	27 MIN.	1235	1483	2781	3057
B.	2	9	24 MIN.	1075	1173	2248	2601
II.A.	3	10	26 MIN.	1351	1412	2763	3160
B.	3	9	25 MIN.	1159	1215	2374	2788
III.A.	1	10	26 MIN.	1642	929	2571	2666
B.	1	10	22 MIN.	1478	846	2324	2418
C.	1	11	27 MIN.	2097	1306	3403	3497
IV. A.	1	8	23 MIN.	1225	1648	2873	3332
B.	1	8	23 MIN.	1139	1522	2661	3135
C.	1	9	26 MIN.	1364	1899	3263	3713
ALL-ORBIT MEANS:		9.5	24.9	1377	1343	2720	3036

Tables 5.2-7 through 5.2-10 present the NRF and resulting fractional coverage estimates for each orbit/sensor case and each of the four coastal target zones. Table 5.2-11 is a case-by-case comparison for the total of the four zones. In addition to the NRF estimates just described, a pseudo-coverage fraction (PCF) was calculated, ratioing daily areal coverage to the total target zone area. Redundancy was then accounted for by multiplying the PCF by the NRF to arrive at a daily coverage fraction (DCF).

This "bottom line" estimate of the performance of each orbit/sensor configuration in meeting the total daily surveillance objective (DCF = 1) should be thoughtfully applied. A DCF of 0.5 does mean that half the target zone will be surveyed on an average day but it does not necessarily mean that two spacecraft with this orbit/sensor configuration can survey all the target zone on an average day. That is due to some fraction of the target zone never being accessible to some orbit/sensor configurations; this fraction was estimated and is presented in the same tables as PNA (Percent Never Accessible). These five tables can thus be used to fully compare the ten cases considered as to their "bottom line" performance of the daily surveillance mission. A few general results are cited here:

1. The average adjustment for redundancy for all orbits and target zone latitudes and orientations is to downgrade the area surveyed by about 25% (NRF = 0.75). For these near-polar orbits, the east-west oriented zones (Gulf and Alaska) experience significantly higher redundancy than the north-south oriented zones (Atlantic and Pacific).

2. As was the case with areal coverage, the fractional coverage of the Gulf (DCF$\approx$0.4) is significantly lower than the other three zones (DCF$\approx$ 0.55 to 0.59).

3. The fractions that are never accessible (PNA) are directly proportional to one factor (east-west zone width) and inversely proportional to two factors (latitude and number of days (and/or orbits) per repeat cycle). Case II -- the 3-day repeater -- allows access to the entire U.S. coastal zone except for a small part of the Gulf. The one-day repeaters -- Cases III and IV -- leave large areas (greater than 25%) inaccessible.

TABLE 5.2-7 : FRACTIONAL COVERAGE COMPARISON

TARGET ZONE: ATLANTIC

TARGET ZONE AREA: 1320 (10^3) Km^2

CASE #	NRF	PCF		DCF		PNA	
		W/BLIND SPOT	W/O BLIND SPOT	W/BLIND SPOT	W/O BLIND SPOT	W/BLIND SPOT	W/O BLIND SPOT
I. A.	0.85	0.74	0.81	0.63	0.69	5%	0%
B.	0.90	0.61	0.68	0.55	0.61	5%	0%
II. A.	0.70	0.73	0.86	0.51	0.61	0%	0%
B.	0.75	0.59	0.73	0.45	0.55	5%	0%
III. A.	0.9	0.32	0.36	0.28	0.32	55%	45%
B.	0.95	0.27	0.31	0.25	0.29	65%	55%
C.	0.85	0.50	0.54	0.43	0.46	35%	30%
IV A.	0.75	1.07	1.11	0.80	0.83	10%	5%
B.	0.80	0.95	0.99	0.76	0.79	15%	10%
C.	0.70	1.28	1.32	0.90	0.92	0%	0%
ALL ORBIT MEANS:	0.82	0.71	0.77	0.56	0.61	20%	15%

NRF: Non-Redundancy Factor = Adjustment factor to account for area covered multiple times on an average orbit day. (NRF = 0.5 means that the portion of area covered is covered an average of twice each day of the repeat cycle).

PCF: Pseudo-Coverage Fraction = Average Daily Coverage Total ÷ Target Zone Area (does not account for redundant coverage).

DCF: Daily Coverage Fraction = NRF x PCF (adjusts the PCF for estimated redundant coverage).

PNA: Percent Never Accessible = Percent of target zone never accessible (within the FOV) through the entire repeat cycle.

TABLE 5.2-8 : FRACTIONAL COVERAGE COMPARISON

TARGET ZONE: GULF

TARGET ZONE AREA: 800 (10^3) Km^2

CASE #	NRF	PCF		DCF		PNA	
		W/BLIND SPOT	W/O BLIND SPOT	W/BLIND SPOT	W/O BLIND SPOT	W/BLIND SPOT	W/O BLIND SPOT
I. A.	0.70	0.53	0.55	0.37	0.38	25%	5%
B.	0.75	0.43	0.45	0.32	0.34	35%	15%
II. A.	0.80	0.53	0.56	0.42	0.45	5%	0%
B.	0.85	0.47	0.50	0.40	0.43	10%	0%
III. A.	0.60	0.75	0.75	0.45	0.45	20%	10%
B.	0.60	0.72	0.73	0.43	0.44	25%	15%
C.	0.60	0.80	0.80	0.48	0.48	10%	0%
IV A.	0.60	0.61	0.78	0.37	0.47	55%	45%
B.	0.60	0.60	0.78	0.36	0.47	60%	50%
C.	0.60	0.63	0.78	0.38	0.47	45%	35%
ALL-ORBIT MEANS:	0.67	0.61	0.69	0.40	0.44	29%	18%

NRF: Non-Redundancy Factor = Adjustment factor to account for area covered multiple times on an average orbit day (NRF = 0.5 means that the portion of area covered is covered an average of twice each day of the repeat cycle).

PCF: Pseudo-Coverage Fraction = Average Daily Coverage Total ÷ Target Zone Area (does not account for redundant coverage).

DCF: Daily Coverage Fraction = NRF x PCF (adjusts the PCF for estimated redundant coverage).

PNA: Percent Never Accessible = Percent of target zone never accessible (within the FOV) through the entire repeat cycle.

TABLE 5.2-9 : FRACTIONAL COVERAGE COMPARISON

TARGET ZONE: PACIFIC

TARGET ZONE AREA: 950 (10^3) Km^2

CASE #	NRF	PCF		DCF		PNA	
		W/BLIND SPOT	W/O BLIND SPOT	W/BLIND SPOT	W/O BLIND SPOT	W/BLIND SPOT	W/O BLIND SPOT
I. A.	0.65	0.73	0.96	0.47	0.62	2%	0%
B.	0.70	0.61	0.84	0.43	0.59	5%	0%
II. A.	0.70	0.87	1.00	0.61	0.70	0%	0%
B.	0.75	0.80	0.93	0.60	0.69	0%	0%
III. A.	0.80	0.95	0.95	0.76	0.76	10%	10%
B.	0.85	0.85	0.85	0.72	0.72	20%	20%
C.	0.75	1.28	1.28	0.96	0.96	0%	0%
IV A.	1.0	0.43	0.67	0.43	0.67	40%	25%
B.	1.0	0.39	0.64	0.39	0.64	45%	30%
C.	1.0	0.53	0.77	0.53	0.77	20%	5%
ALL-ORBIT MEANS:	0.82	0.74	0.89	0.59	0.71	14%	9%

NRF: Non-Redundancy Factor = Adjustment factor to account for area covered multiple times on an average orbit day (NRF = 0.5 means that the portion of area covered is covered an average of twice each day of the repeat cycle).

PCF: Pseudo-Coverage Fraction = Average Daily Coverage Total ÷ Target Zone Area (does not account for redundant coverage).

DCF: Daily Coverage Fraction = NRF x PCF (adjusts the PCF for estimated redundant coverage).

PNA: Percent Never Accessible = Percent of target zone never accessible (within the FOV) through the entire repeat cycle.

TABLE 5.2-10 : FRACTIONAL COVERAGE COMPARISON

TARGET ZONE: ALASKA

TARGET ZONE AREA: 650 (10^3) Km^2

CASE #	NRF	PCF		DCF		PNA	
		W/BLIND SPOT	W/O BLIND SPOT	W/BLIND SPOT	W/O BLIND SPOT	W/BLIND SPOT	W/O BLIND SPOT
I. A.	0.65	0.96	1.00	0.63	0.65	15%	0%
B.	0.65	0.79	0.83	0.51	0.54	18%	0%
II. A.	0.65	0.85	0.96	0.55	0.62	0%	0%
B.	0.65	0.71	0.82	0.46	0.53	0%	0%
III. A.	0.55	1.01	1.08	0.56	0.59	8%	0%
B.	0.55	0.90	0.96	0.50	0.53	12%	5%
C.	0.55	1.36	1.42	0.75	0.78	5%	0%
IV A.	0.60	0.87	0.94	0.52	0.56	20%	10%
B.	0.60	0.85	0.92	0.51	0.55	25%	15%
C.	0.60	0.88	0.96	0.53	0.57	15%	0%
ALL-ORBIT MEANS:	0.61	0.92	0.99	0.55	0.59	12%	3%

NRF: Non-Redundancy Factor = Adjustment factor to account for area covered multiple times on an average orbit day (NRF = 0.5 means that the portion of area covered is covered an average of twice each day of the repeat cycle).

PCF: Pseudo-Coverage Fraction = Average Daily Coverage Total ÷ Target Zone Area (does not account for redundant coverage).

DCF: Daily Coverage Fraction = NRF x PCF (adjusts the PCF for estimated redundant coverage).

PNA: Percent Never Accessible = Percent of target zone never accessible (within the FOV) through the entire repeat cycle.

TABLE 5.2-11 : FRACTIONAL COVERAGE COMPARISON

TARGET ZONE: ALL FOUR U.S. COASTAL ZONES

TARGET ZONE AREA: 3720 (10^3) Km^2

CASE #	NRF	PCF		DCF		PNA	
		W/BLIND SPOT	W/O BLIND SPOT	W/BLIND SPOT	W/O BLIND SPOT	W/BLIND SPOT	W/O BLIND SPOT
I. A.	0.73	0.73	0.83	0.53	0.60	10%	1%
B.	0.77	0.60	0.70	0.46	0.53	14%	3%
II. A.	0.71	0.74	0.85	0.52	0.60	1%	0%
B.	0.75	0.64	0.75	0.48	0.56	4%	0%
III. A.	0.75	0.69	0.72	0.49	0.51	28%	21%
B.	0.78	0.62	0.65	0.45	0.47	36%	29%
C.	0.72	0.91	0.92	0.63	0.65	15%	11%
IV A.	0.76	0.77	0.90	0.56	0.67	29%	20%
B.	0.77	0.71	0.84	0.54	0.64	34%	25%
C.	0.74	0.88	1.00	0.63	0.72	17%	9%
ALL-ORBIT MEANS:	0.75	0.73	0.82	0.53	0.60	19%	12%

NRF: Non-Redundancy Factor = Adjustment factor to account for area covered multiple times on an average orbit day (NRF = 0.5 means that the portion of area covered is covered an average of twice each day of the repeat cycle).

PCF: Pseudo-Coverage Fraction = Average Daily Coverage Total ÷ Target Zone Area (does not account for redundant coverage).

DCF: Daily Coverage Fraction = NRF x PCF (adjusts the PCF for estimated redundant coverage).

PNA: Percent Never Accessible = Percent of target zone never accessible (within the FOV) through the entire repeat cycle.

4. On the basis of maximizing average daily coverage (DCF) and minimizing areas never covered (PNA), Case II is slightly superior to Case I and much superior to Cases III and IV, considering all four U.S. coastal zones together. For each target zone by itself, a different orbit might be preferred -- for example, Case IV.C. for the Atlantic

5. For all four coastal zones taken together, the DCF has a tight range across the eight ±600 Km access swath cases: from 0.45 to 0.56 with a mean value of 0.50. On the other hand, the PNA has a wide range depending on which of the 8 orbits is chosen.

5.2.3.2.2 Sensitivity to Variation of Key Parameters

The above conclusions are fairly general for the ten coverage cases simulated. The following paragraphs illustrate some of the power of a flexible computer simulation in assessing the specific effect of variability in key orbital and sensor parameters.

Figures 5.2-11 through 5.2-15 illustrate the performance of each of the 10 cases -- measured by DCF and PNA -- for the four coastal zones taken together and individually. Cases are plotted such that better coverage will result in movement up the page (higher DCF) and/or to the left (lower PNA). Thus, an orbit/sensor configuration that covers the entire zone daily (DCF = 1) and has no area never accessible (PNA = 0%) will be in the upper left-hand corner. This graphical rendering of performance allows the reader to accurately compare orbits quickly on a zone-by-zone or total U.S. basis. It greatly facilitates analysis of sensitivity to key parameters and supports the following points.

5.2.3.2.2.1 Sensor Pointability. In all cases, adding pointability to the sensor improved the coverage capability (9% average). The degree of improvement, however was wide; ranging from only 1-2% up to 24% (using DCF as the measure). When redundancy of coverage is disregarded and PCF is used as the measure, improvement is even greater (an average of 14% versus 9% average for DCF).

FIGURE 5.2-11 : ALL FOUR U.S. COASTAL ZONES COVERAGE COMPARISON

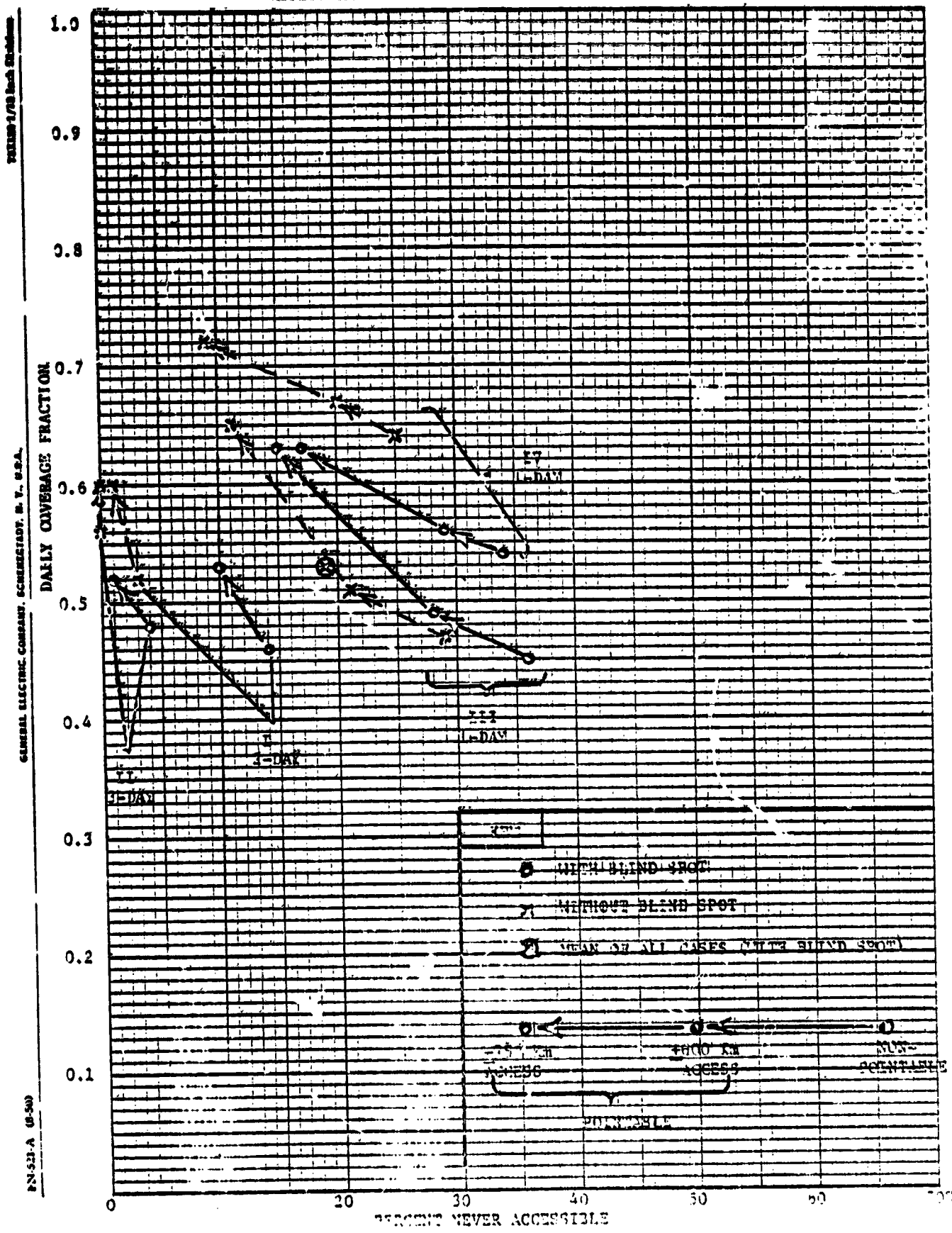

FIGURE 5.2-12 : ATLANTIC ZONE COVERAGE COMPARISON

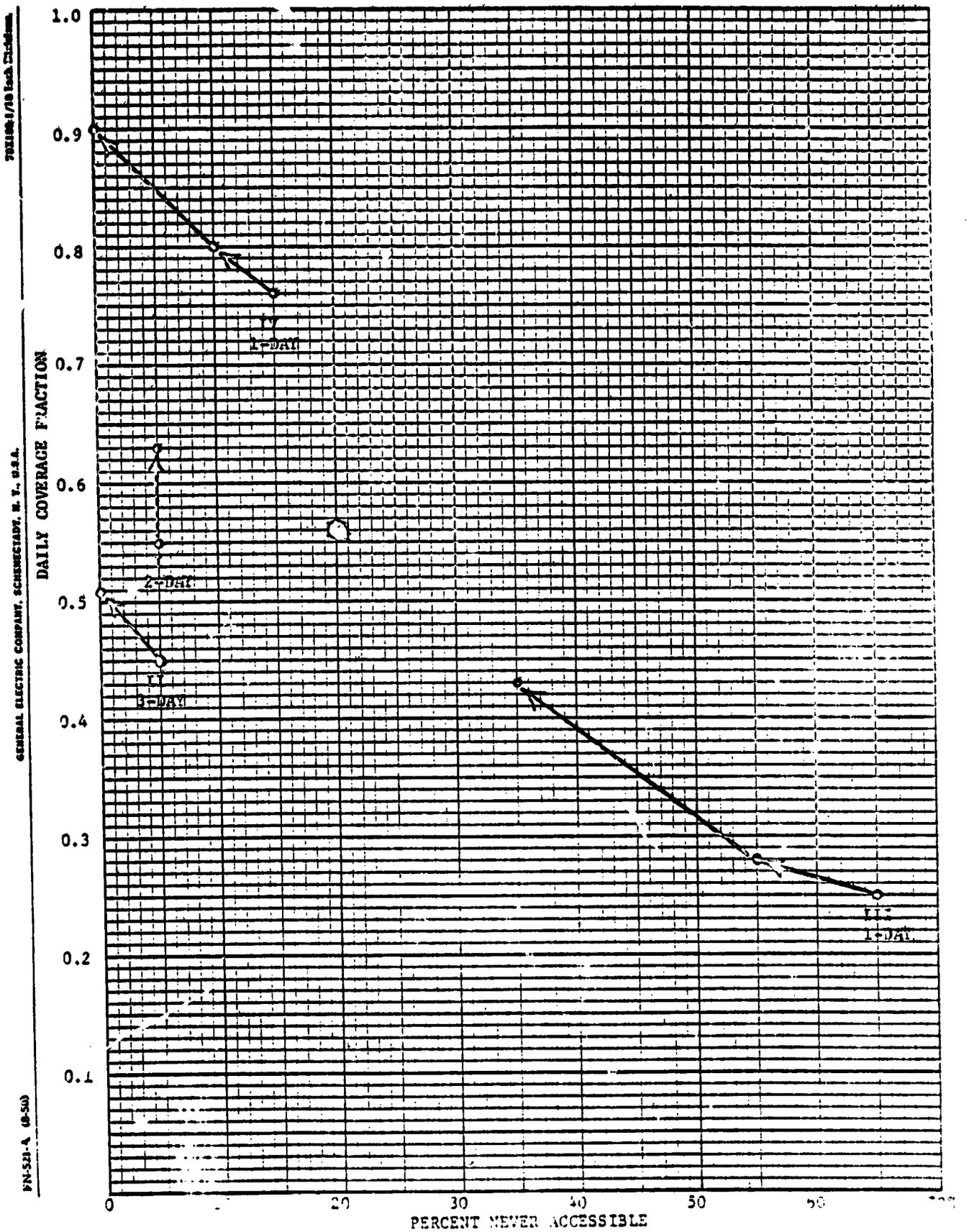

C-4

FIGURE 5.2-13: GULF ZONE COVERAGE COMPARISON

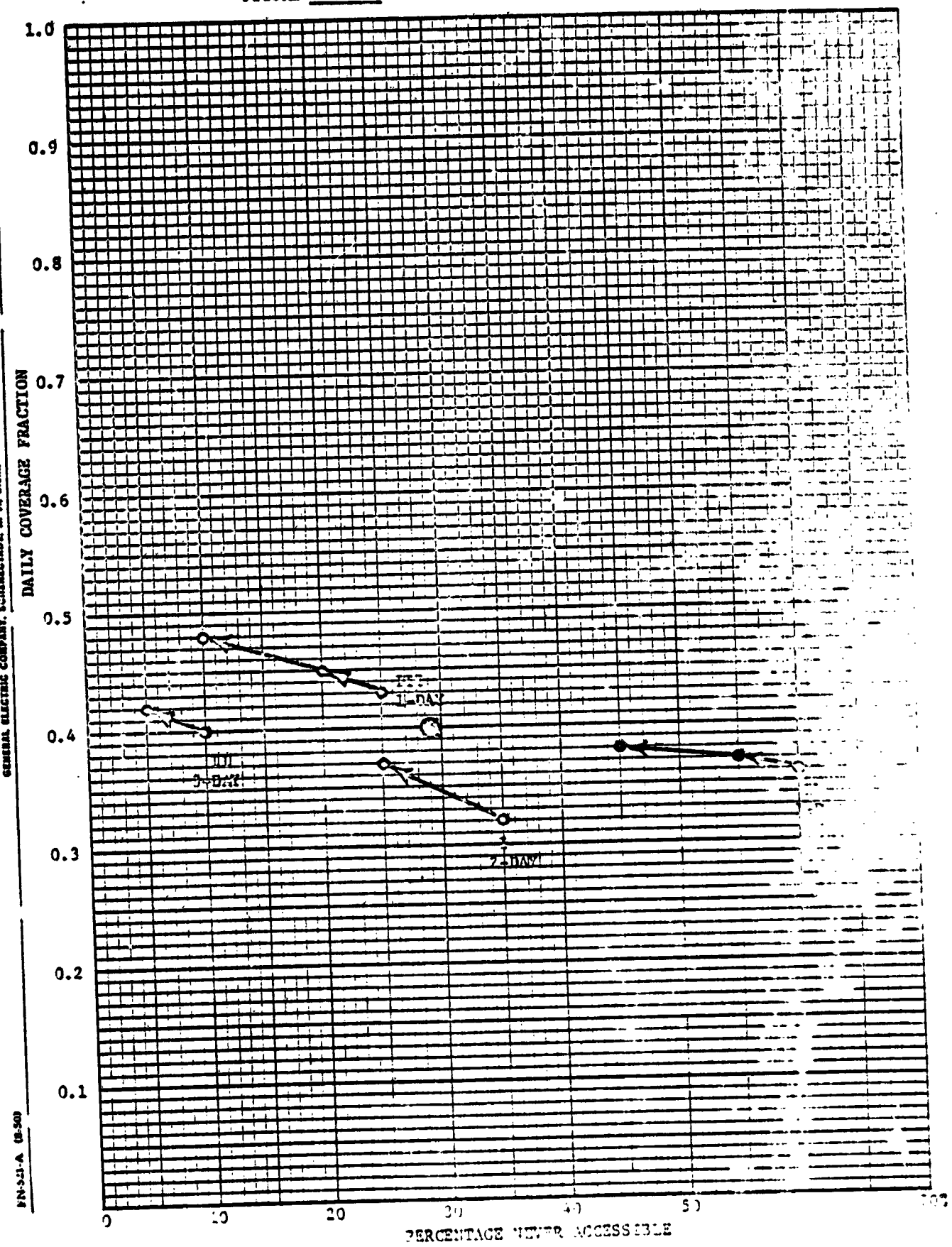

FIGURE 5.2-14: PACIFIC ZONE COVERAGE COMPARISON

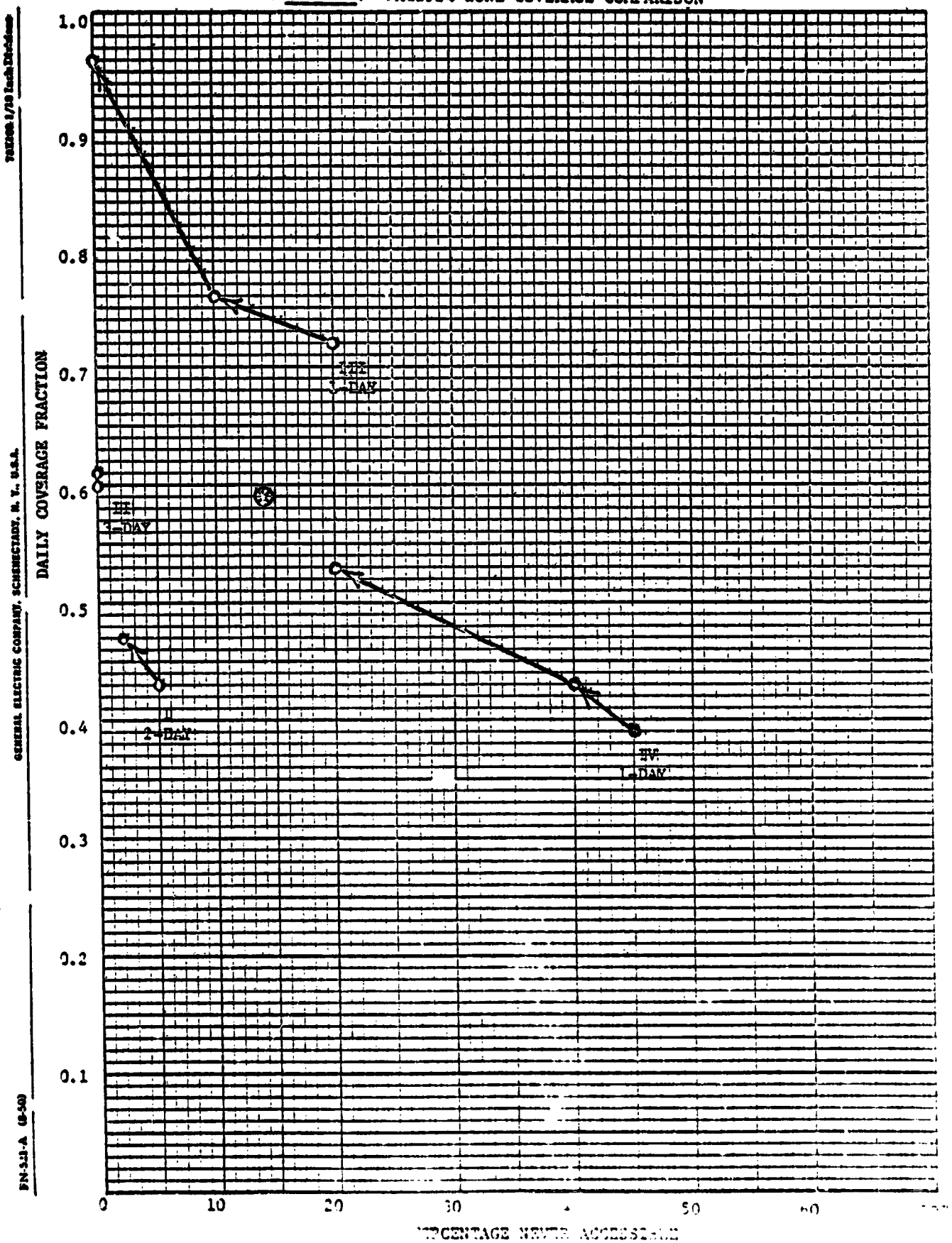

FIGURE 5.2-15: ALASKA ZONE COVERAGE COMPARISON

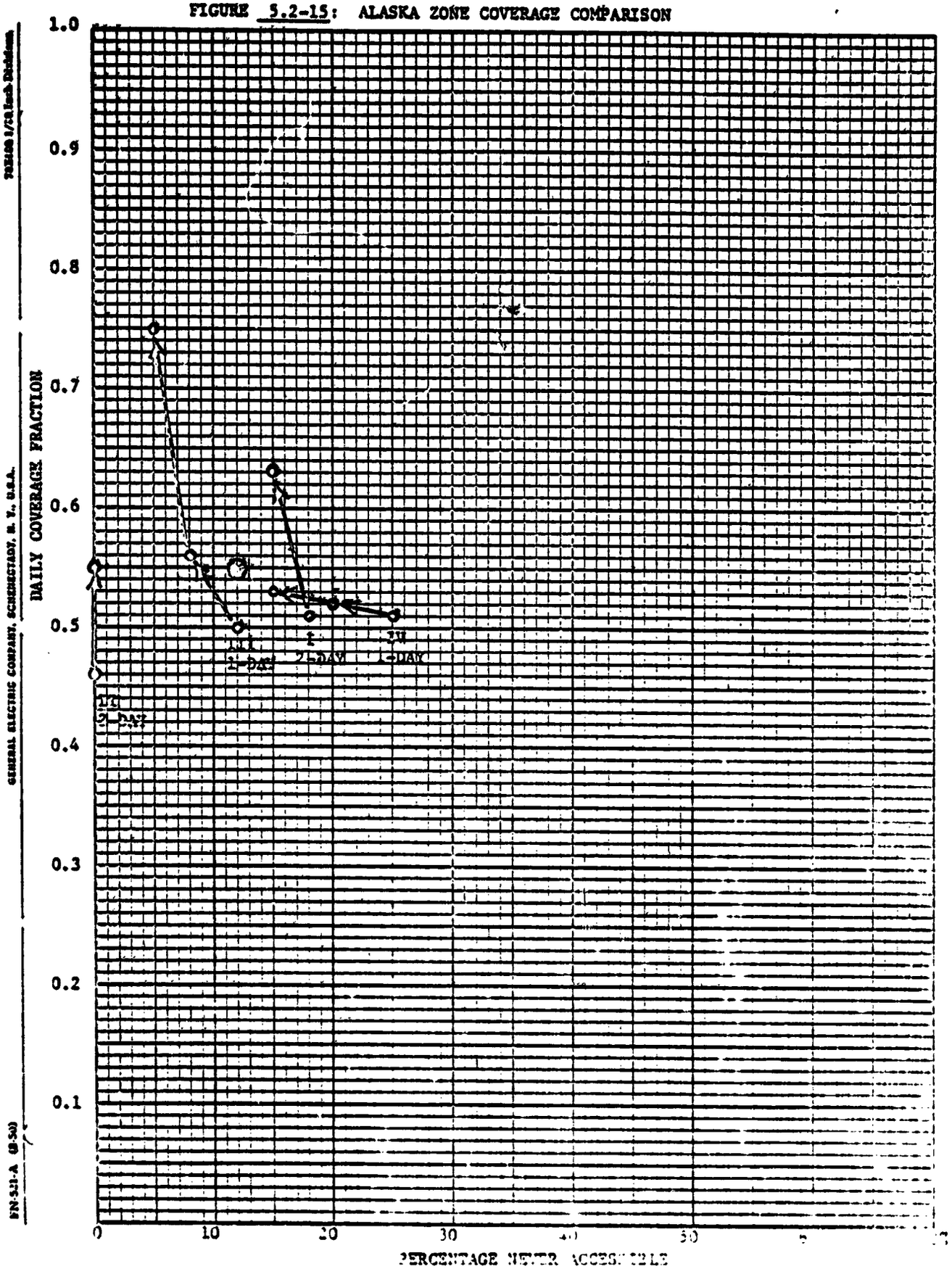

5.2.3.2.2.2 Access Swath Width. Cases III and IV each have two pointable options, one with an access swath of ±600 Km and one with ±750 Km. The coverage improvement is roughly proportional to the additional access width within which the sensor can be pointed: about 50 Km or 10% for the ±600 Km cases versus about 200 Km or 36% for the ±750 Km cases. Suffice it to note that additional access always improves coverage markedly.

5.2.3.2.2.3 Number of Days (and/or Orbits) Per Repeat Cycle.

For the total U.S. case and for almost all of the individual zones, coverage in terms of PNA improves proportionally with an increase in the repeat cycle days or orbits. On the other hand, coverage in terms of DCF is not predictably related to repeat cycle length.

5.2.3.2.2.4 Target Zone

Inspection of the individual zone mean coverage values quickly illustrates that the Gulf zone is significantly more poorly covered. This is due to a combination of low latitude, east-west extent, and near-polar orbits.

Conversely, the Alaskan zone can be seen to be significantly easier to cover, in terms of PNA. This is due to the compression of interswath ground distance as a function of increasing latitude.

5.2.3.2.2.5 Orbital Plane Orientation (Longitude of Ascending Node)

The effects of orbital plane orientation are most pronounced for short repeat cycle orbits. As an example, a 14-orbit, one-day repeater with 400 Km ground swath misses about two-thirds of the earth at 35° latitude even when both ascending and descending passes are used. Careful selection of the nodal crossing point allows excellent high-frequency coverage of some areas -- at the expense of poor coverage of others. The Case III and IV coverage for the Atlantic and Pacific zones (Figures 5.2-13 and 5.2-14) emphasize this. Case III gave excellent coverage of the Pacific with a

longitude of ascending node of -83° (83° W) at the cost of terrible coverage of the Atlantic. A nodal crossing (Case IV, -76°) selected to optimally cover the Atlantic greatly reduced the Pacific and Gulf coverage. At sun-synchronous inclinations, the Atlantic and Pacific zones are "out of phase" for good 1-day repeat cycle coverage.

5.2.3.2.2.6 Blind Spot Effect

Figure 5.2-11 shows the general impact of the radar blind spot on coverage. Removing the blind spot around nadir ($\pm 10^{\circ}$ nadir angle) increases the coverage for all cases, in terms of both DCF and PNA. To assume this improvement for optical imaging (with no blind spot) would be very misleading, however. The combination of no night sensing, cloud obscuration, haze effects, and sun angle problems (especially with non-sun synchronous orbits) in fact brings the optical imager coverage far below the SAR (with blind spot).

5.2.4 TEMPORAL RESOLUTION INVESTIGATION

COASTCOVER has been used in temporal as well as spatial coverage analysis. In its present configuration, it can generate latitude - longitude figures for the edge of variable swaths across terrestrial target zones as a function of orbital time. These figures presently must be hand-plotted and the resulting coverage areas analyzed to extract observational frequencies for coastal zones for selected repeating orbits and sensor options. Future program modifications could automate both the swath plotting and the area vs. time aspects of the analysis.

Under this contract, an investigation of a critical temporal coverage problem -- the need for frequent, broad area, wind measurements -- was performed. The following were the sensor, platform, orbit, and target zone options selected for temporal frequency assessment:

a. SENSOR: a microwave scatterometer with a wide swath (several hundred km) on both sides of the sub-satellite track providing backscatter measurements needed for frequent wind data inputs critical to fate model projections.

b. PLATFORM: such a sensor is planned for the proposed mid-1980's NOSS spacecraft and a duplicate is assumed on a mid-1980's ICEX spacecraft.

c. ORBIT: ICEX and NOSS orbits based on current program information are shown as cases V and VI of Table 5.2-1. The ground swaths were calculated to fit the orbital parameters and current NOSS scatterometer earth incidence angle constraints of 25° to [illegible]

d. TARGET ZONES: as discussed earlier, the Atlantic [illegible] zones are the highest density zones in terms of [illegible] and pollution incidence and were selected as [illegible] this temporal coverage analysis. Furthermore, [illegible] due to its southerly latitudes and east-west orientation [illegible] vides

the most difficult challenge for high frequency temporal coverage among the four U.S. coastal target zones.

The COASTCOVER program was therefore run for total repeat cycles for the configurations just discussed. The results are highlighted in Table 5.2-12. The pattern of coverage for the Gulf for each platform is illustrated in Figures 5.2-16 and 5.2-17. The longitude of ascending node used was -83°; a change in this parameter would affect the position of different coverage frequency segments within the zone but would not significantly impact the zone fractions with different coverage frequencies.

Combined spacecraft coverage frequency patterns can be produced by numerically or graphically overlaying the individual ICEX and NOSS patterns (Figure 5.2-16 plus Figure 5.2-17, for instance). The result, shown in Figure 5.2-18 for the Gulf, is a more complex coverage pattern for each zone with coverage frequencies quantized in more levels, ranging from less than 1 up to 3.3 average observations per day. No more than 10-20% of each zone would receive the high frequency (3.3) coverage and the average coverage across the zones for the combined platforms would be around two observations per day.

The results from this investigation for the assumed orbits can be compared to the user requirements discussed in section 3.3. In order to meet the wind speed and direction requirements of updates once each three and six hours, respectively, some combination of multiple NOSS and/or ICEX scatterometer platforms would clearly be necessary. Based on an average coverage rate of two observations per day for the combined coverage by one of each platform, about four total platforms would be needed to attain every six hour coverage, whereas about eight total platforms would be necessary for every three hour coverage.

TABLE 5.2-12 : SUMMARY OF TEMPORAL COVERAGE BY NOSS AND ICEX SCATTEROMETERS

TARGET ZONE	PLATFORM	REPEAT CYCLE	COVERAGE FREQUENCY		FRACTION OF ZONE
			OBSERV./REPEAT CYCLE	AVER.OBSERV./DAY	
ATLANTIC	ICEX	2 DAYS	0	0	15%
			1	0.5	14%
			2	1.0	32%
			3	1.5	15%
			4	2.0	23%
ATLANTIC	NOSS	3 DAYS	2	0.7	25%
			3	1.0	41%
			4	1.3	34%
GULF	ICEX	2 DAYS	0	0	36%
			1	0.5	7%
			2	1.0	14%
			3	1.5	6%
			4	2.0	37%
GULF	NOSS	3 DAYS	1	0.3	1%
			2	0.7	46%
			3	1.0	25%
			4	1.3	28%

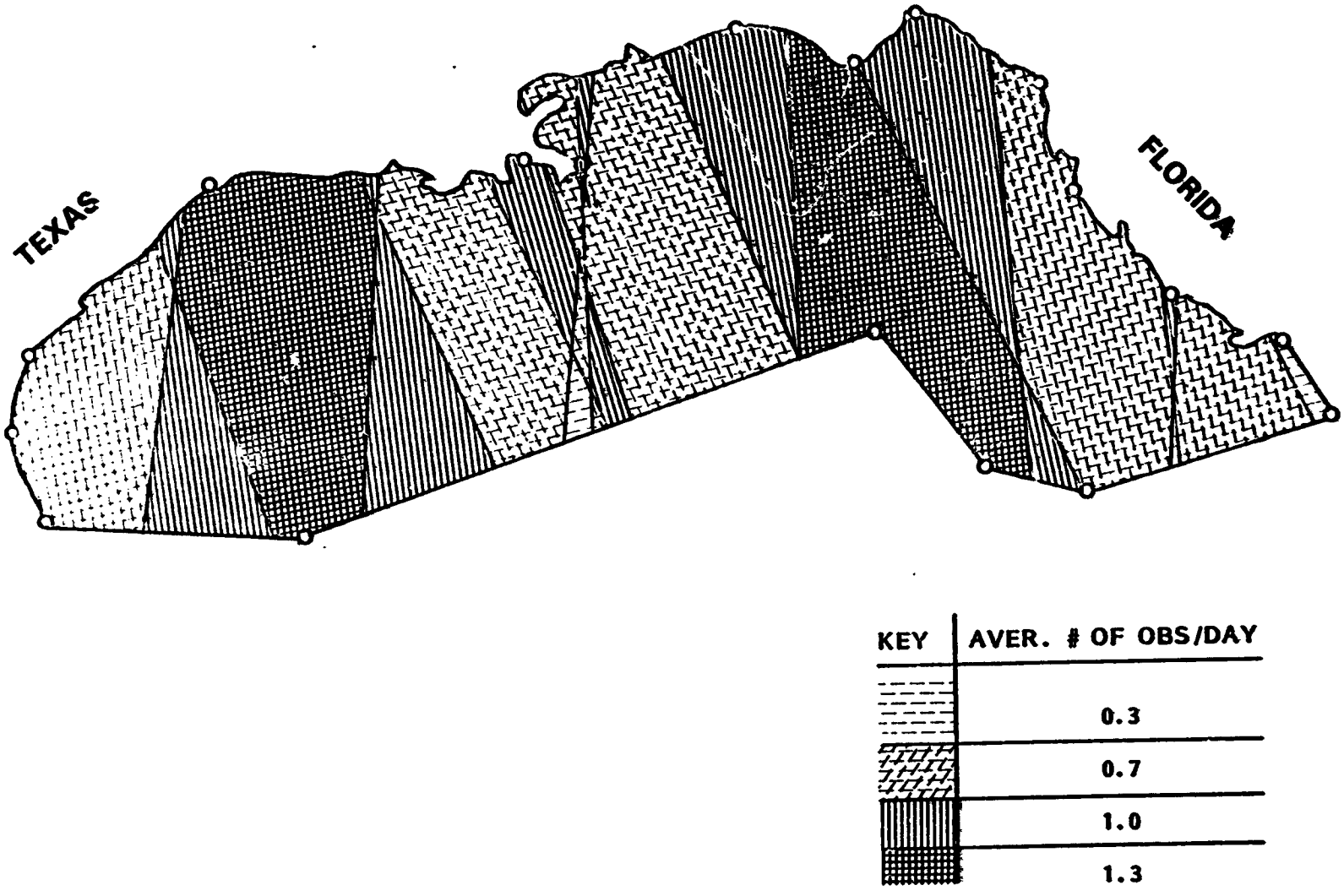

Figure 5.2-16. NOSS 3-Day Repeater Temporal Coverage of Gulf Coastal Zone

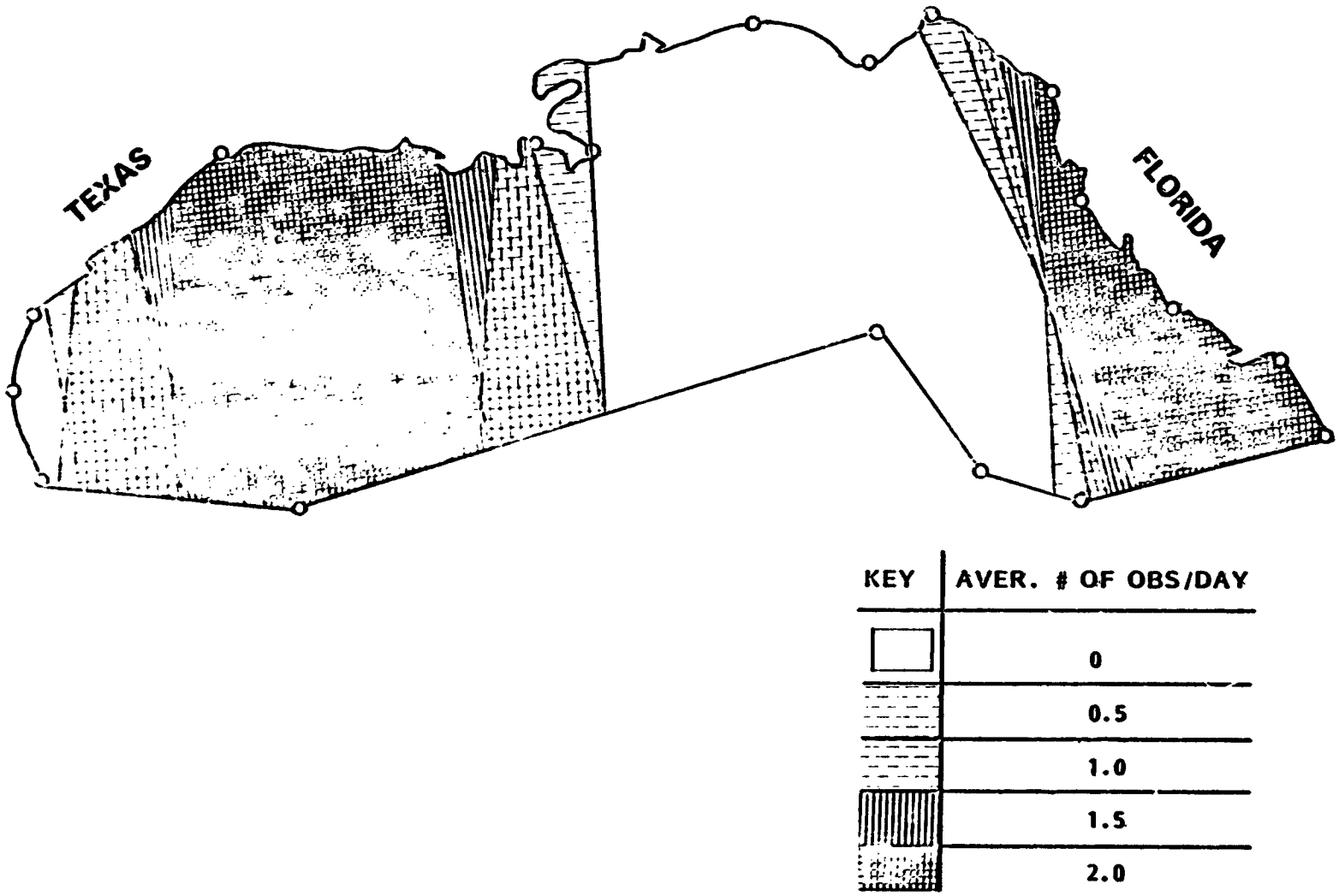

Figure 5.2-17. ICEX 2-Day Repeater Temporal Coverage of Gulf Coastal Zone

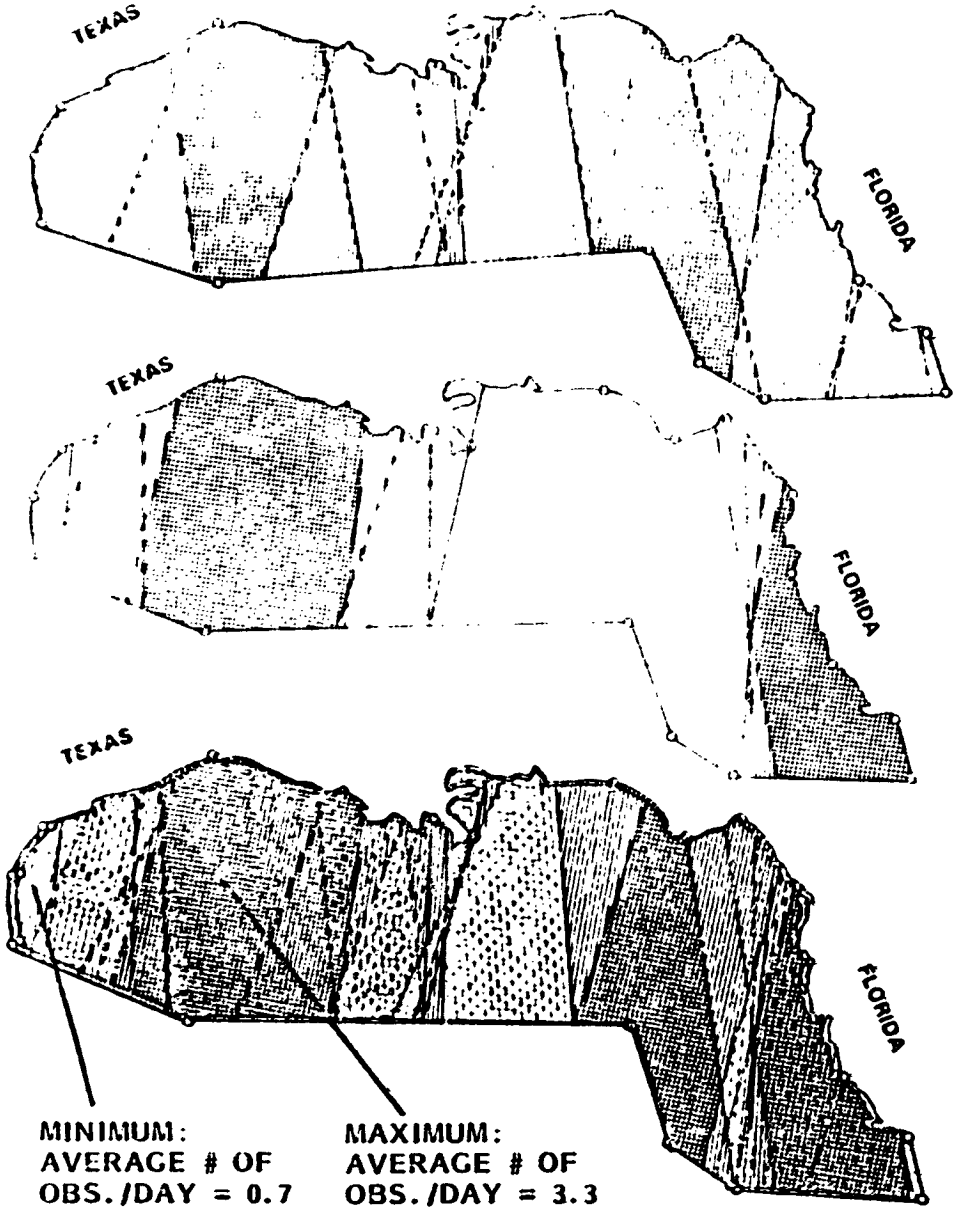

NOSS TEMPORAL COVERAGE
(REFERENCE FIGURE 5.2-16)

PLUS

ICEX TEMPORAL COVERAGE
(REFERENCE FIGURE 5.2-17)

YIELDS

COMBINED NOSS/ICEX
SCATTEROMETER
TEMPORAL COVERAGE
PATTERN

Figure 5.2-18. An Example of Combined NOSS/ICEX Temporal Coverage

5.3 SYSTEM OPTIONS

Having now structured the users' information requirements into specific submission goals and a set of operational scenarios forming the context for meeting those goals, the selection of specific system elements can be addressed.

These various generic and specific system elements, in Section 4 and 5.1, may then be combined in many possible system options, each providing a particular level of support of the user requirements and mission needs. The candidate elements selected and the several discrete system options synthesized are discussed in the following sections.

5.3.1 SYSTEM ELEMENT SCREENING AND SELECTION

The sensor screening and selection process was covered in Section 4.1. This, combined with the measurement needs of the 10 sub-missions leads to a matrix of sensor type (e.g., high resolution SAR, scatterometer, etc.) versus sub-mission supported. The added factors of utility and timing of applicable platforms (as covered in Section 4.2) for these sensors results in a platform and sensor employment concept as presented in Table 5.3-1. Note that the pertinent sensors for each sub-mission are enumerated:

- for platforms at each of three levels: space, air, and surface
- for both the near-term (1984-87) and mid-term (1988-91) time frames, and
- for either all ocean pollutants or just those other than oil.

Table 5.3-2 provides a brief descriptive review of each of the sensors and platforms which may now be considered for synthesis into a system option.

Figure 5.3-1 shows the projected phasing of the various key system elements, including reference to a possible centralized MOPS Data Processing System (MDPS).

5.3.2 SYNTHESIS OF SYSTEM OPTIONS

Beginning with the selected sensor/platform list (Table 5.3-1) and based on (1) qualitative and quantitative trade-off analyses (sections 3.4 and 5.2, for example), (2) insight into the users' applications of various system elements, (3) the relative maturity of critical technologies, and (4) other programmatic considerations; several discrete system mix options were defined and are highlighted in Figure 5.3-2. The six options selected and detailed on the following pages range from a maximum support option (I) through a no cost option (VI), which employs the capabilities of the various currently-active, planned, and proposed systems through the next decade. With each individual

			SPACECRAFT													AIRCRAFT										SURFACE					
			TOPEX					NOSS					OERS		MET SATS	ARI			AARI						USCG	BUOYS		SHIPS	COASTAL	
	SUB-MISSIONS		SCAT	ALT	SAR	PMR	POLA	SCAT	ALT	SMMR	C/A	CLR	TM	MLA	VARIOUS	SLAR	UV/IR	TV	SAR	UV/IR	TV	PMR	ALT	LSF	VISUAL	MB	DB	M/O	ODSS	CCR	MS
SURVEILLANCE & MONITORING	DETECTION	N			X								X			X	X	X							X						
		M			X		X							X					X			X	X		X						
	MAPPING & TRACKING	N			X	X				X	X		X			X	X	X							X		X				
		M			X	X	X			X		X		X					X			X	X		X	X	X				
	QUANTIFICATION	N									(X)		(X)				(X)								X						
		M					(X)					(X)		(X)							(X)	X	X		X						
	POLLUTANT CLASSIFICATION	N									(X)		(X)																		
		M					(X)					(X)		(X)										X								
	POLLUTER IDENTIFICATION	N																X							X			(X)			
		M																			X				X			(X)			
	SYNOPTIC U.S. COASTAL POLLUTION MON'G. & DATA BASE BUILD	N			X	X				X	X		X			X	X	X							X			(X)			
		M			X	X	X			X		X		X					X			X	X		X	X			(X)			
	SYNOPTIC GLOBAL POLLUTION MON'G & DATA BASE BUILD	N			X	X				X	X		X																		
		M			X	X	X			X		X		X																		
MODELING	FATE MODELING	N	X	X	X	X		X	X	X	X		X		X	X	X	X									X	X		X	
		M	X	X	X	X	X	X	X	X		X		X	X				X	X	X	X	X				X	X		X	X
	IMPACT/RISK MODELING	N	X	X	X	X		X	X	X	X		X		X	X	X	X									X	X		X	
		M	X	X	X	X	X	X	X	X		X		X	X				X	X	X	X	X				X	X		X	X
	SYNOPTIC O/M/E MONITORING AND DATA BASE BUILD	N	X	X	X	X		X	X	X	X		X		X	X	X	X									X	X		X	
		M	X	X	X	X	X	X	X	X		X	X		X				X	X	X	X	X				X	X		X	X

N = NEAR TERM (1984-87)
M = MID-TERM (1988-91)

X = FOR OIL AND OTHER OCEAN POLLUTANTS
(X) = FOR POLLUTANTS OTHER THAN OIL ONLY

ADPI	- ADVANCED AIRBORNE REMOTE INSTRUMENTATION	MB	- MOORED BUOYS	PMR	- PASSIVE MICROWAVE RADIOMETER
ALT	- ALTIMETER	METSATS	- METEOROLOGICAL SATELLITES	POLA	- POINTABLE OPTICAL LINEAR ARRAY
API	- AIRBORNE REMOTE INSTRUMENTATION	MLA	- MULTISPECTRAL LINEAR ARRAY	SAR	- SYNTHETIC APERTURE RADAR
C/A	- COASTAL ZONE COLOR SCANNER/ADV VERY HIGH RESOLUTION RADIOMETER (CZCS/AVHRR)	M/O	- METEOROLOGICAL & OCEANOGRAPHIC SENSING SYSTEMS	SCAT	- SCATTEROMETER
CCR	- COASTAL CURRENT RADAR	MS	- METEOROLOGICAL STATIONS	SLAR	- SIDE-LOOKING AIRBORNE RADAR
CLR	- OCEAN LIDAR	NOSS	- NATIONAL OCEANIC SATELLITE SYSTEM	SMMR	- SCANNING MULTICHANNEL MICROWAVE RADIOMETER
DB	- DRIFTING BUOYS	ODSS	- OCEAN DUMPING SURVEILLANCE SYSTEM	TM	- THEMATIC MAPPER
LSF	- LASER STIMULATED FLUOROSENSOR	OERS	- OPERATIONAL EARTH RESOURCES SYSTEM	USCG	- U.S. COAST GUARD
				UV/IR	- ULTRAVIOLET/INFRARED LINE SCANNER

Table 5.3-1 Platforms and Sensors (Employment Concept)

(Table is repeated from Section 2.0 for the reader's convenience)

TABLE 5.3-2

KEY TO SENSOR/PLATFORM EMPLOYMENT MATRIX

NAME	ACRONYM	DESCRIPTION
ICESAT	ICESAT	PROPOSED NASA POLAR REGION SURVEILLANCE PROGRAM; SENSOR PACKAGE BASED ON ICESAT AND MOPS REQUIREMENTS
SCATTEROMETER	SCAT	ACTIVE MICROWAVE SENSOR (GENERIC TITLE -- CONFIGURATION NOT FIRM)
ALTIMETER	ALT	ACTIVE MICROWAVE SENSOR -- MULTIBEAM VERSION (GENERIC TITLE -- CONFIGURATION NOT FIRM)
SYNTHETIC APERTURE RADAR	SAR	ACTIVE MICROWAVE IMAGING SENSOR (GENERIC TITLE -- CONFIGURATION NOT FIRM)
PASSIVE MICROWAVE RADIOMETER	PMR	PASSIVE MULTIFREQUENCY MICROWAVE SENSOR (GENERIC TITLE -- CONFIGURATION NOT FIRM)
POINTABLE OPTICAL LINEAR ARRAY	POLA	PUSHBROOM-TYPE OPTICAL LINEAR ARRAY SENSOR (HIGH RESOLUTION, WIDE SWATH, POINTABLE SENSOR SUGGESTED FOR MOPS)
NATIONAL OCEANIC SATELLITE SYSTEM	NOSS	PLANNED TRI-AGENCY (NASA/DOC/DOD) OCEAN SURVEILLANCE PROGRAM; DEVELOPMENTAL SPACECRAFT IN THE NEAR-TERM AND OPERATIONAL SPACECRAFT IN THE MID-TERM
SCATTEROMETER	SCAT	ACTIVE MICROWAVE SENSOR (GENERIC TITLE -- CONFIGURATION NOT FIRM)
ALTIMETER	ALT	SAME AS ABOVE
SCANNING MULTICHANNEL MICROWAVE RADIOMETER	SMMR	LARGE-APERTURE (3-4 METER) PASSIVE MULTIFREQUENCY MICROWAVE SENSOR (SEVERAL LOW RESOLUTION, WIDE SWATH OPTIONS BEING CONSIDERED)
COASTAL ZONE COLOR SCANNER/ADVANCED VERY HIGH RESOLUTION RADIOMETER	C/A (CZCS/AVHRR)	SCANNING MULTISPECTRAL OPTICAL SPECTRO-RADIOMETERS BASED ON CURRENTLY OPERATING INSTRUMENTS (2 OPTICAL SENSORS -- NEAR-TERM CONFIGURATION NOT FIRM)

TABLE 5.3-2 (CONTINUED)

KEY TO SENSOR/PLATFORM EMPLOYMENT MATRIX (CONT'D)

NAME	ACRONYM	DESCRIPTION
COLORIMETER	CIR	PUSHBROOM-TYPE OPTICAL LINEAR ARRAY SENSOR (SINGLE OPTICAL SENSOR SUGGESTED TO REPLACE C/A IN MID-TERM)
OPERATIONAL EARTH RESOURCES SYSTEM	OERS	PROPOSED MULTIAGENCY OPERATIONAL FOLLOW-ON TO LANDSAT
THEMATIC MAPPER	TM	SCANNING MULTISPECTRAL OPTICAL SPECTRO-RADIOMETER (HIGH RESOLUTION, MEDIUM SWATH SENSOR BEING DEVELOPED FOR LANDSAT-D)
MULTISPECTRAL LINEAR ARRAY	MLA	PUSHBROOM-TYPE OPTICAL LINEAR ARRAY SENSOR (GENERIC TITLE -- CONFIGURATION NOT FIRM)
METEOROLOGICAL SATELLITES	METSATS	ANY OF THE CURRENT OR NEXT GENERATION OPERATIONAL METEOROLOGICAL SATELLITE PROGRAMS; INCLUDES GEOSYNCHRONOUS SPACECRAFT SUCH AS GOES (U.S.) AND METEOSAT (ESA) AND POLAR ORBITERS SUCH AS NOAA/TIROS-N (U.S. NOAA) AND DMSP (U.S. DOD)
VARIOUS MET SENSORS	AVHRR, OLS, VISSR, ETC.	ANY OF THE CURRENT OR NEXT GENERATION METSAT SENSORS -- OPTICAL AND MICROWAVE, BOTH ACTIVE AND PASSIVE
AIRBORNE REMOTE INSTRUMENTATION	ARI	PLANNED U.S. COAST GUARD AIRBORNE REMOTE SENSING SYSTEM FOR MONITORING OF COASTAL ZONE WATER POLLUTION
SIDE-LOOKING AIRBORNE RADAR	SLAR	ACTIVE MICROWAVE IMAGING SENSOR (REAL APERTURE VERSION)
ULTRAVIOLET/INFRARED LINE SCANNER	UV/IR	SCANNING OPTICAL (ULTRAVIOLET AND THERMAL INFRARED) IMAGING RADIOMETER
ACTIVE GATED TELEVISION	TV	PASSIVE (LOW LIGHT LEVEL) AND ACTIVE GATED (USING A PULSED LEAD VAPOR LASER) INTENSIFIER TELEVISION SYSTEM

TABLE 5.3-2 (CONTINUED)

KEY TO SENSOR/PLATFORM EMPLOYMENT MATRIX (CONT'D)

NAME	ACRONYM	DESCRIPTION
ADVANCED AIRBORNE REMOTE INSTRUMENTATION	AARI	POSSIBLE FOLLOW-ON OPERATIONAL AIRBORNE REMOTE SENSING SYSTEM FOR COASTAL ZONE MONITORING
SYNTHETIC APERTURE RADAR	SAR	ACTIVE MICROWAVE IMAGING SENSOR (SYNTHETIC APERTURE SUGGESTED FOR AARI)
PASSIVE MICROWAVE RADIOMETER	PMR	PASSIVE MICROWAVE IMAGING SENSOR SUGGESTED FOR AARI (GENERIC TITLE -- CONFIGURATION NOT FIRM)
ALTIMETER	ALT	ACTIVE MICROWAVE SENSOR SUGGESTED FOR AARI (GENERIC TITLE -- CONFIGURATION NOT FIRM)
LASER STIMULATED FLUOROSENSOR	LSF	ACTIVE (LASER SOURCE) OPTICAL SENSOR SUGGESTED FOR AARI (GENERIC TITLE -- CONFIGURATION NOT FIRM)
ULTRAVIOLET/INFRARED LINE SCANNER ACTIVE GATED TELEVISION	UV/IR TV	(SAME AS FOR ARI)
MOORED BUOYS	MB	DATA COLLECTING MOORED (OR FIXED POSITION) BUOYS (GENERIC TITLE -- MANY CONFIGURATIONS)
DRIFTING BUOYS	DB	DATA COLLECTING OR POSITION TRANSMITTING DRIFTING (NOT FIXED POSITION) BUOYS (GENERIC TITLE -- MANY CONFIGURATIONS)
METEOROLOGICAL AND OCEANOGRAPHIC SENSING SYSTEMS	M/O	SHIP-BORNE MET AND OCEANOGRAPHIC DATA MEASUREMENT SYSTEMS
OCEAN DUMPING SURVEILLANCE SYSTEM	ODSS	OPERATIONAL U.S. COAST GUARD OCEAN DUMPING MONITORING SYSTEM ("BLACK BOX" AND SENSORS ON DUMPING VESSELS)
COASTAL CURRENT RADAR	CCR	HF RADAR FOR OFF-SHORE COASTAL CURRENT MEASUREMENTS BEING DEVELOPED BY NOAA
METEOROLOGICAL STATIONS	MS	ANY OF THE AUTOMATED OR NON-AUTOMATED COASTAL MET STATIONS PROVIDING ROUTINE WEATHER INFORMATION

FIGURE 5.3-1 KEY SYSTEM ELEMENT PHASING

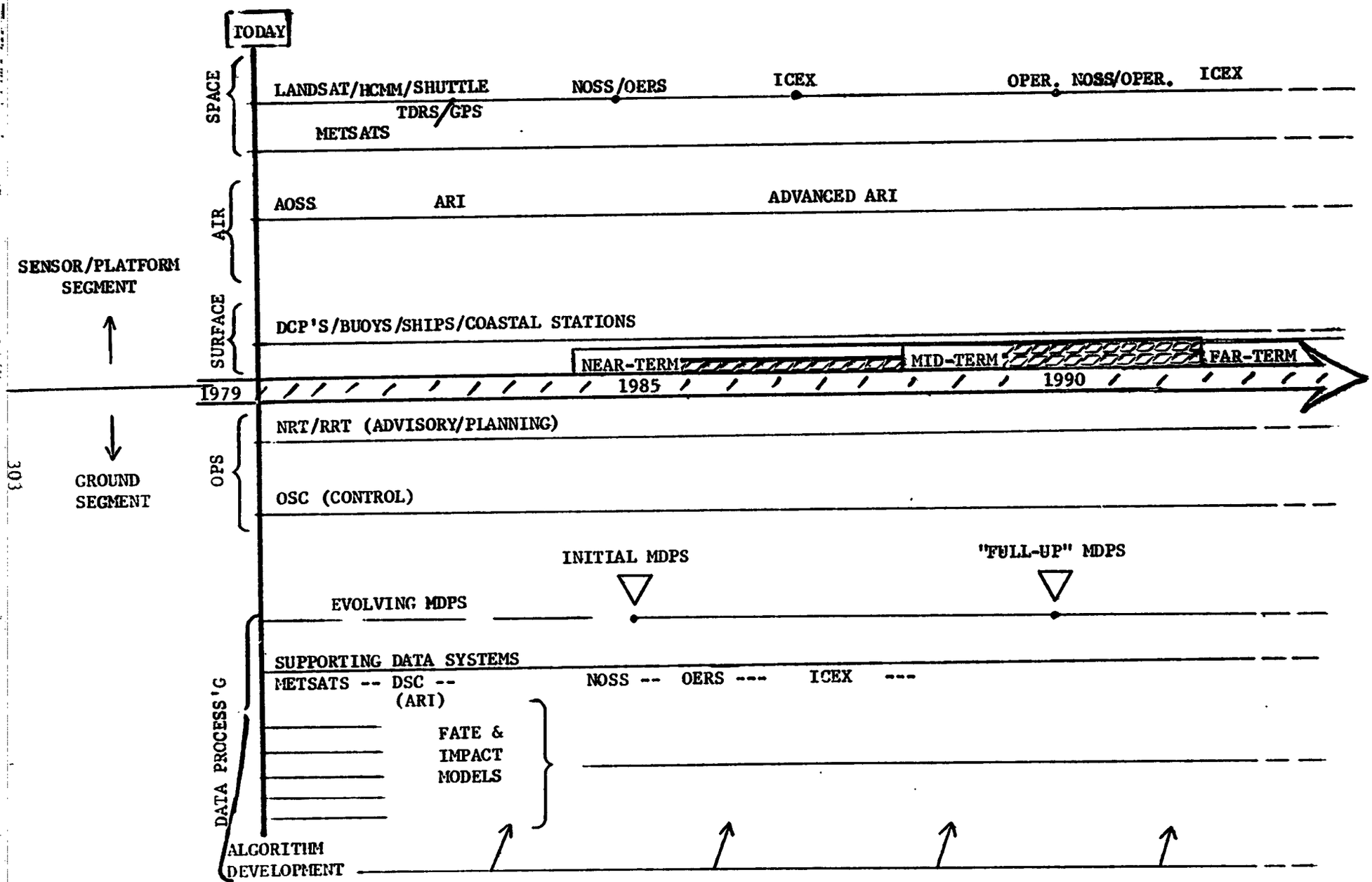

Major Element	Hi.-Res. Mult. Space Imaging Option I	Med.-Res. Mult. Space Imaging Option II	Med.-Res. Single Space Imaging Option III	Predominantly Aircraft Imaging Option IV	Minimum Cost Improved Data Usage Option V	No Modifications Option VI
Platform/Sensors						
• Space	NOSS • Scatterometer • P.M-wave rad. • Altimeter ICEX, • SAR, • POLA } 30 meters resolution	Same as I except SAR/POLA resolution reduced to 100 meters	Same as I except SAR resolution reduced to 100 meters, and elimination of POLA	Same as VI except increased usage of existing earth observing spacecraft	Same as VI except increased usage of existing earth observing spacecraft	No significant use of space sensing, except METSAT data base support
• Air	USCG-ARI Advanced ARI • SAR • Laser Fluor. • PMR • Radar Altimeter			Increased ARI-Fleet (80-100 Aircraft)	Same as VI	USCG-ARI Advanced ARI
• Surface	Buoys Ships Coastal Stations			Same as VI	Same as VI	Buoys Ships Coastal Stations
Data System	Centralized Data Processing System (CDPS)	Adjusted for 100 meters resolution	Adjusted for 100 meter res. and no POLA	Limited capability centralized facility	Add to VI: • OSC User Terminal • Info. extraction relationships	No major oceanic pollution data processing
COMM Link	TDRS/DOMSATS (Very wide band)	Wideband but reduced bandwidth from I	Wideband but reduced bandwidth from II	Improved user terminals, leased lines	Phone lines from ground stations	

Figure 5.3-2 Highlights Of System Mix Options

option write-up is a figure, showing the time-phasing of the selected system elements. Options I through III employ various levels of enhanced spacecraft remote sensing techniques, whereas option IV utilizes primarily aircraft for pollution detection. Option V was included to provide a minimum cost appr ach to make the most of planned and proposed remote sensing systems by augmenting the communications and data presentation elements. Option VI is a no cost (no MOPS system) future used as a performance baseline. The approximate relative cost and effectiveness of each option is estimated and compared in Section 5.4.

5.3.2.1 Option I: High Resolution, Multiple Space Imaging (Reference Fig. 5.3-3)

Option I features advanced technology sensors at all three levels - in space, in the air, and on the surface. The pointable high resolution synthetic aperture radar and optical multispectral linear array will provide primary and corroborative imaging data on ocean pollutants over a large percentage of the 200 nautical mile coastal zone on a daily basis. How large a percentage will depend on the ICEX, SAR, and POLA parameters in the near-term plus the advanced ARI SAR parameters in the mid-term. Oil spilled into the marine environment - whether by accident or intentionally - will be resolvable by these sensors under certain weather and/or viewing conditions.

The synoptic spacecraft detection and monitoring capabilities will assist the aircraft and surface platforms by defining the high probability spill areas (for frequent close-in surveillance) and by providing the initial detection of suspected pollution in progress to which the aircraft and/or nearby ships may respond and make their short-range measurements of the pollutant and potential polluter. State-of-the-art sensors - such as synthetic aperture radar, laser fluorosensing, and passive microwave imaging - will enhance the aircraft's abilit-

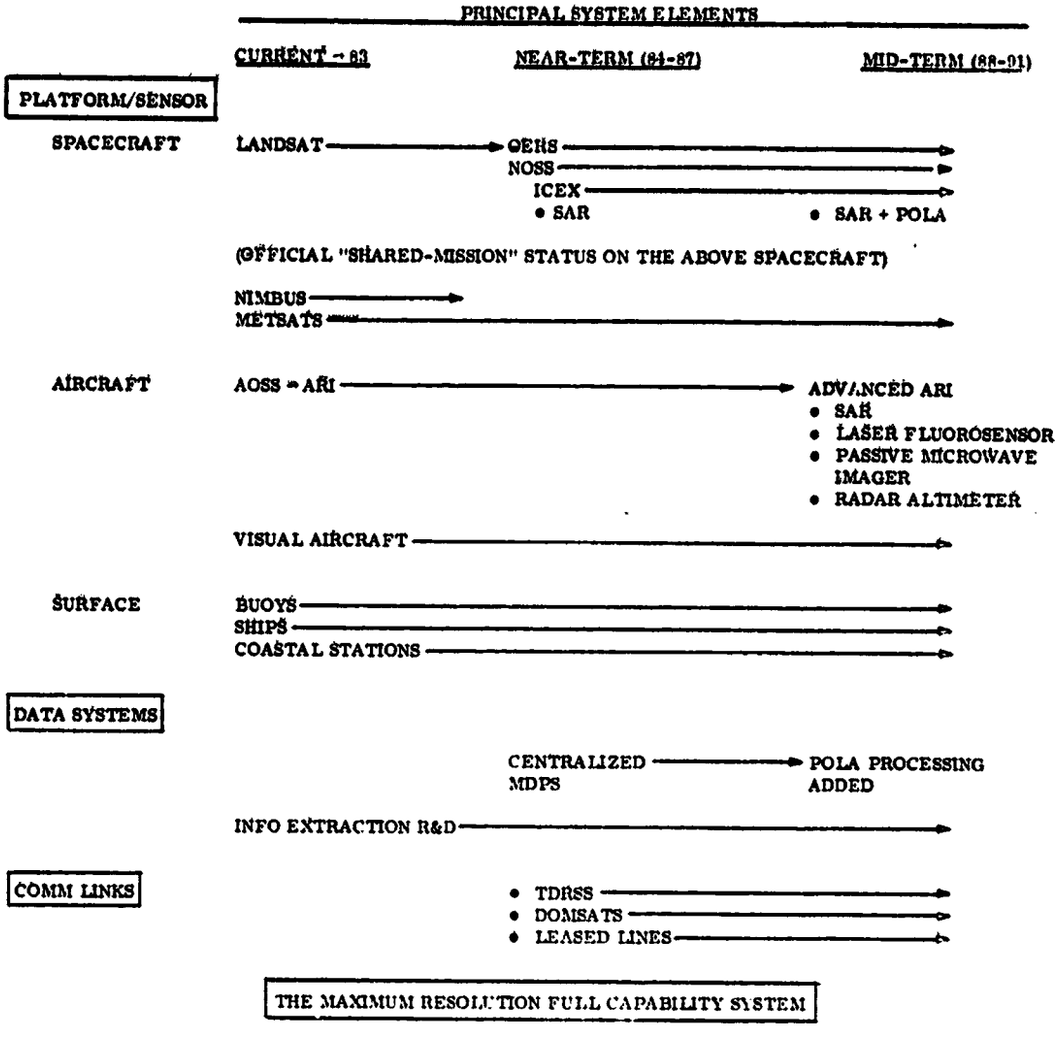

- TWO STATE-OF-THE ART POLLUTION DETECTION SENSORS ON SPACECRAFT: SYNTHETIC APERTURE RADAR (SAR) AND POINTABLE OPTICAL LINEAR ARRAY (POLA)
  - HIGH RESOLUTION: 30 METER GROUND RESOLUTION ELEMENT
  - WIDE SWATH: 375 km POINTABLE WITHIN A 1200 km (± 600 km) ACCESS SWATH
  - X-BAND RADAR
  - MULTISPECTRAL OPTICAL (VISIBLE AND THERMAL INFRARED)
- SEVERAL IMPROVED SENSORS SUGGESTED FOR "ADVANCED ARI" AIRCRAFT:
  - SAR TO IMPROVE RADAR SWATH CAPABILITY AND RESOLUTION
  - LASER FLUOROSENSOR: POLLUTANT CLASSIFICATION
  - PMI: POLLUTANT THICKNESS
  - RADAR ALTIMETER: LOCALIZED SEA STATE DATA
- CENTRALIZED MDPS AND WIDE-BAND COMM LINKS NEEDED TO ENABLE NEAR REAL-TIME PROCESSING OF SEVERAL HIGH DATA RATE SOURCES
- MAJOR R&D PROGRAM FOR INFORMATION EXTRACTION ALGORITHMS NEEDED:
  - MULTIPLE SOURCE REGISTRATION
  - CLOUD COVER SCREENING
  - FEATURE/PATTERN RECOGNITION
  - TREATMENT OF "SIGNATURE" AMBIGUITIES

Figure 5.3-3. High Resolution, Multiple Space Imaging -- SYSTEM OPTION 1

to identify and quantify the pollutant.

The fate and impact modelling effort will be supported by a suite of meteorological and oceanographic sensing devices at all levels. However, as shown in Section 5.2.4, full support of the model input temporal resolution requirements (for example, every 6 hour wind data) would require multiple NOSS and/or multiple ICEX platforms.

The high sensor data rates (both space and air) will require wide band communication links such as those of TDRSS and domestic COMSATS.

In addition to making maximum use of existing data systems - including NOSS, NESS, and NWS - a major MOPS data processing system will be developed and implemented. It will be the full capability version described in Section 4.3 incorporating special processing for the space SAR and POLA, and high speed "smart" correlation processing from the various platforms and sensors in order to minimize the false alarm rate. An immediate and ambitious information extraction research program is envisioned to develop the necessary software for the system implementation shown.

5.3.2.2 Option II: Medium Resolution, Multiple Space Imaging (Ref. Fig. 5.3-4)

Option II differs from Option I primarily in the resolution level of the spacecraft pollution detection sensors - now 100 m as opposed to 30 m. This resolution change will degrade the space detection capabilities against the intentional operational discharges of small ships and newer and/or fast non-tankers, based on the analysis discussed in Section 3.4. This class of oil pollution may be frequent in occurrence, but is comparatively low in overall volume. The pollution response and model input capabilities of this option are virtually unchanged from Option I.

Another significant modification due to the change in resolution is in the data communication and processing systems. Reduced space sensor data rates in turn reduce the wide band communication link requirements and permit down-sizing of certain components in the data processing system.

As in Option I, the development of information extraction algorithms for processing these data will be a major challenge throughout the program timeline.

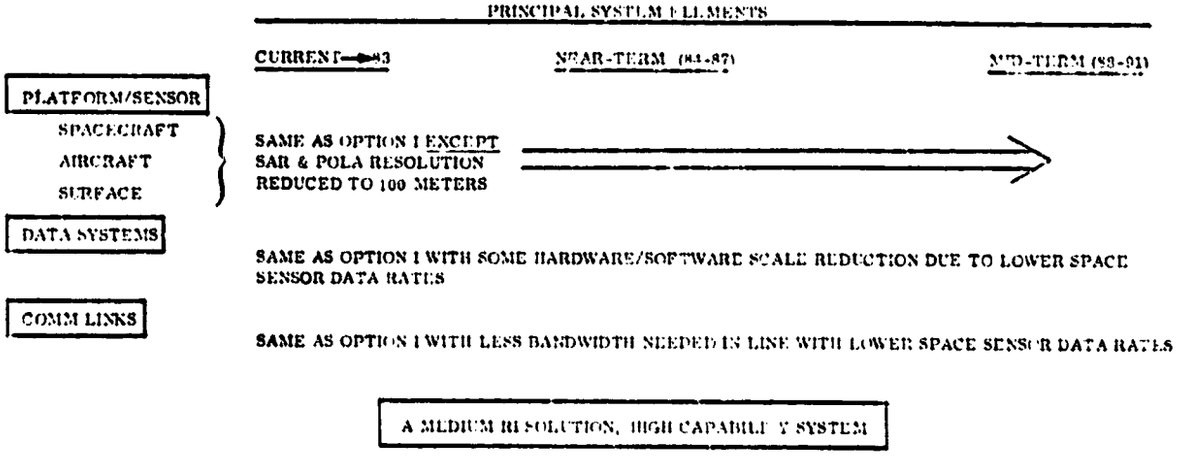

Figure 5.3-4. Medium Resolution, Multiple Space Imaging -- SYSTEM OPTION II

5.3.2.3 Option III: Medium Resolution, Single Space Imaging (Ref. Fig. 5.3-5)

Option III will retain the Option II capabilities of the primary space detection sensor (SAR) but not include the corroborating optical sensor (POLA). Synoptic space detection and monitoring of marine oil pollution, both day and night under a wide range of weather conditions, will still be a feature of this option.

Further communications data link savings will be effected by the deletion of the high rate POLA sensor and major cost savings within the data processing system will be possible because of the removal of the POLA processor.

Full aircraft and surface detection and response capabilities will remain in this option, as well as multi-level data acquisition providing inputs for the fate and impact models.

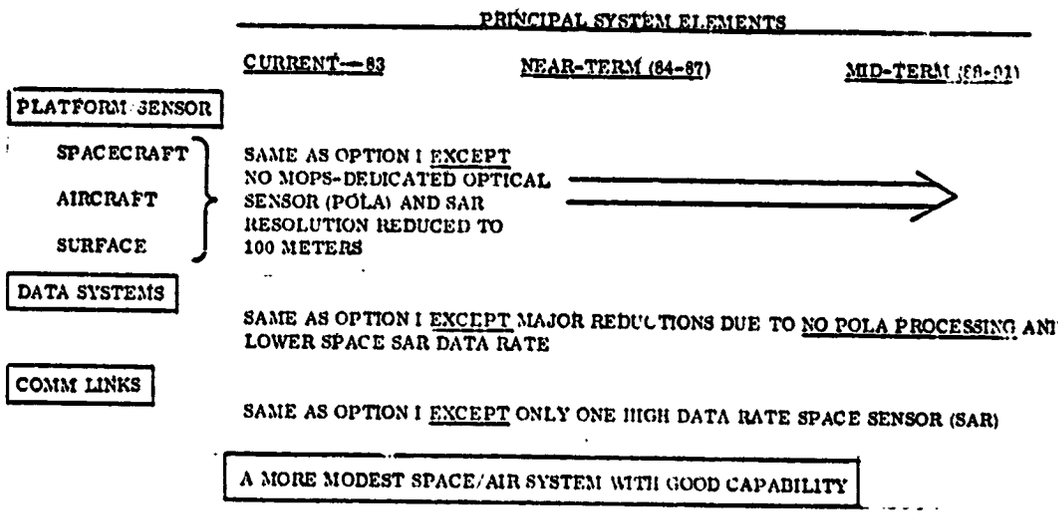

- ONLY ONE MOPS-DEDICATED POLLUTION IMAGING SPACE SENSOR
- GOOD DAILY SYNOPTIC IMAGING CAPABILITY OF LARGE PART OF COASTAL ZONE IN MOST WEATHER BUT:
  - LITTLE CHANCE OF NEAR REAL-TIME CORROBORATION OF MANY SUSPECTED SPILLS
  - MORE RELIANCE ON AIRCRAFT AND NON-DEDICATED SPACE SENSORS FOR DETECTION BACK-UP
- DATA PROCESSING SYSTEM COMPARED TO OPTIONS I AND II:
  - SIGNIFICANTLY SMALLER (NO POLA)
  - INFO EXTRACTION R&D STILL MAJOR FRONT-END NEED
  - NEED FOR CORRELATION PROCESSING USING MORE DIVERSE, INTERMITTENTLY AVAILABLE DATA SOURCES

Figure 5.3-5. Medium Resolution, Single Space Imaging -- SYSTEM OPTION III

5.3.2.4 Option IV: Predominantly Aircraft Imaging (Reference Figure 5.3-6) Option IV represents a major change in approach to the wide area pollution surveillance and monitoring mission - the employment of a much larger fleet of aircraft in lieu of dedicated space imaging sensors. The estimated fleet size for full, all weather coverage of the U.S. coastal zone with aircraft is a strong function of the resolution and type of imaging radar employed. Approximate numbers of aircraft required to provide daily flights over the U.S. coastal zone range from on the order of 100 for real aperture radar systems down to approximately 30 for synthetic aperture systems. Balanced against the improved response capabilities for rapid close-in pollution and polluter measurements attendant to such a large aircraft fleet are 1) the greatly increased operating and maintenance costs of a large aircraft fleet and 2) the loss of the synoptic coastal zone view provided by dedicated spacecraft sensors.

Data communications and processing systems will be different from the previous options and must support a greatly increased number of data acquisition platforms, each with much lower data rates than the comparable space sensors. It is envisioned that a centralized MOPS data processing system would be required in both the near and mid terms but would have a limited capability in the near term compared to Options I through III. While providing model users with the same archival and processing capabilities as in the earlier Options, the use of onboard processing for SLAR imagery will eliminate that portion of the MDPS. In the mid term, it is possible that the processing of SAR imagery from the aircraft will be handled in the MDPS in a centralized fashion (utilizing data relay via wideband leased phone lines) rather than having onboard SAR processing for each aircraft.

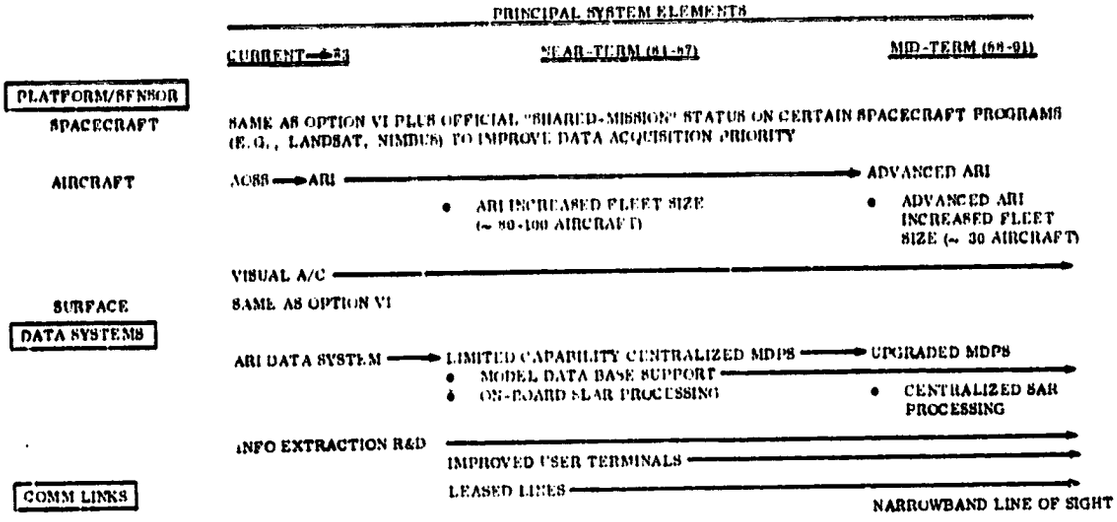

Figure 5.3-6. Predominantly Aircraft Imaging - Option IV

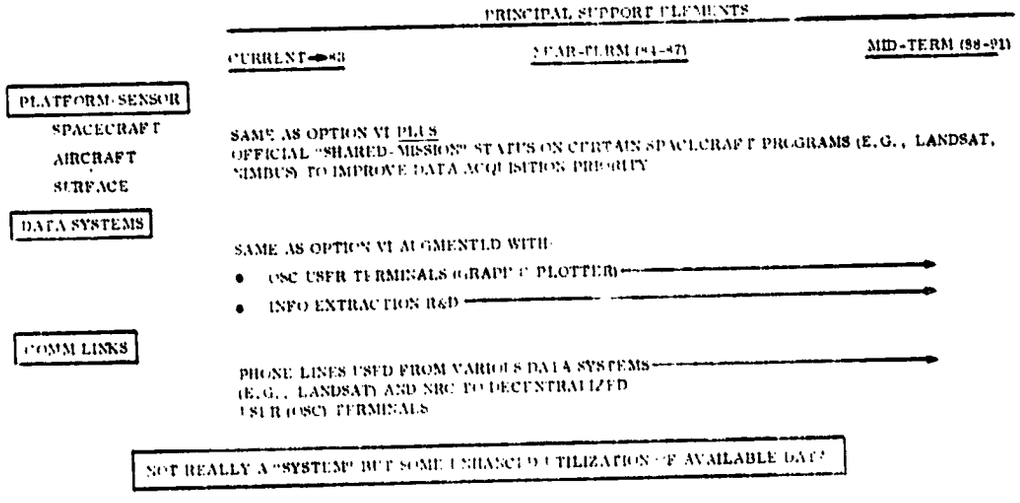

Figure 5.3-7. Minimum Cost/Improved Data Usage - Option V

5.3.2.5 Option V: Minimum Cost/Improved Data Usage (Reference Figure 5.3-7) Option V is a minimum cost approach to make the best use of existing ocean pollution data sources as soon as possible. Data sources would include the current and planned Coast Guard aircraft sensing systems and all space sensors with demonstrated or potential applicability. Notable in the latter category are the high optical and microwave sensors proposed for the Operational Earth Resources System and the ICEX system, both planned for the mid 1980's. Furthermore, the meteorological and oceanographic space sensing capabilities of the various METSATS and proposed NOSS spacecraft would be included. The MOPS approach is to make program arrangements to share usage of the appropriate space sensors without impacting performance of the primary missions.

The outstanding feature of this option is the acquisition, distribution, and presentation of data from already existing sources. To meet the low cost goal, phone lines (in some cases leased lines) would augment the already-built communications links of the parent systems, providing low rate data to multiple user terminals within the MOPS network. These terminals could be graphic plotters, for example, located in the numerous Coast Guard OSC (On Scene Coordinator) offices and in Washington (National Response Center). Thus, at minimum expense, available data for pollution response activities would be rapidly provided to the primary user in the field, with some flexibility in presentation of the data and mobility in placement of the data terminals.

5.3.2.6 Option VI: No MOPS-Specific Modifications (Reference figure 5.3-8) Option VI is the no cost future baseline. Surveillance and monitoring capabilities will be provided as presently planned by Coast Guard remote sensing aircraft and certain planned and proposed spacecraft. The frequency and breadth of coverage will be significantly less than with any of Options I through IV.

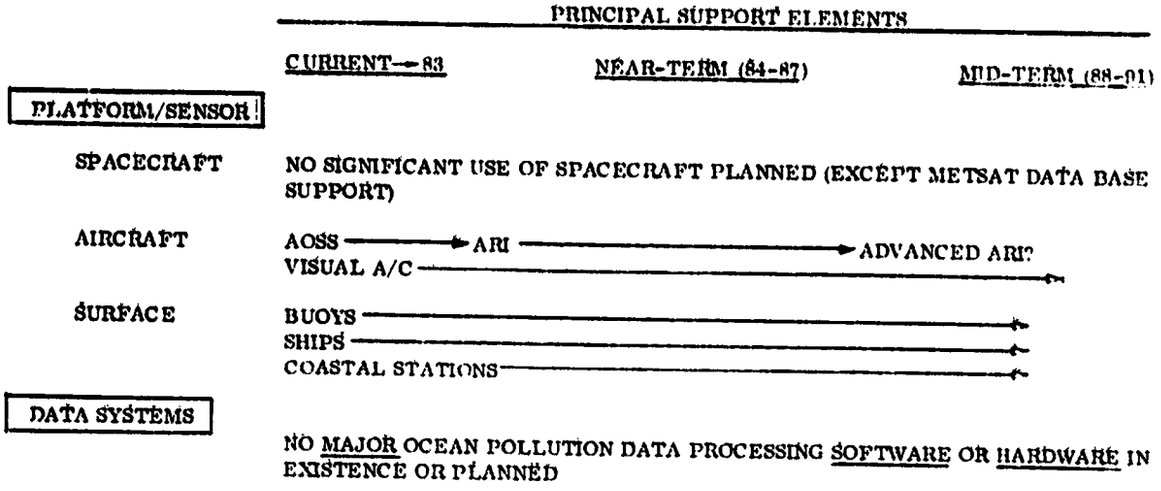

Figure 5.3-8. No Cost/No MOPS Modifications - Option VI

The lack of frequent, synoptic imaging capability that has precluded more than occasional surveillance of the current Gulf of Mexico oil well blow-out (IXTOC I, beginning June 1979) would continue under this option.

Furthermore, the disaggregated data sources (meteorological, oceanographic, and ecological) available for use in fate and impact models would not have the benefit of the common archiving and distribution provided under the several proposed MOPS data processing system options.

5.4 RELATIVE COST AND EFFECTIVENESS OF SYSTEM OPTIONS

Having defined several discrete system mix and capability options and developed a set of structured scenarios within which different elements of each option play their parts, "semi-quantitative" scoring of the options was performed.

5.4.1 EFFECTIVENESS SCORING METHODOLOGY

In addressing the effectiveness of each option, a number of performance criteria were considered. Two slightly different ways of approaching performance were settled upon:

- o Parametric support, using relative satisfaction of performance parameters such as spatial resolution and frequency of data acquisition.
- o Mission support, estimating each option's performance in the context of the scenarios previously defined.

Using a scale of 1 to 10 -- ranging from almost no satisfaction (1) to full satisfaction (10) of the criterion or scenario sub-missions -- a subjective score for each option vis-a-vis each of the criteria or scenarios was established. Table 5.4-1 presents these scores, together with the two effectiveness totals (Parametric and Mission Support). Each option's total scores have been normalized

TABLE 5.4-1. RELATIVE SCORE OF SYSTEM OPTIONS

		OPTION # I	II	III	IV	V	VI
PARAMETRIC CRITERIA	SPATIAL RESOLUTION	9	7	7	7	7	7
	TEMPORAL RESOLUTION	8	8	6	9	2	1
	AREAL COVERAGE	8	8	6	9	3	1
	TIMELINESS (INFO TO USER)	8	8	8	9	4	1
	EFFECTIVENESS SCORES *	23	21	17	24	6	0
	**	24	20	15	25	5	0
5 SCENARIOS (10 SUB-MISSIONS)	SCENARIO I: OIL	9	8	7	9	4	3
	SCENARIO I: OTO***	6	5	3	5	2	1
	SCENARIO II: OIL	8	7	6	9	5	4
	SCENARIO II: OTO***	7	6	5	8	4	3
	SCENARIO III	8	8	8	8	4	3
RELATIVE COST • INCREMENTAL TO OPTION VI • NORMALIZED TO OPTION I		1.0	.5	.3	8.0	.01	

* SUM OF CRITERIA SCORES MINUS OPTION VI SUM
** SUM OF SCENARIO SCORES MINUS OPTION VI SUM
***OTO: POLLUTANTS OTHER THAN OIL

by subtracting out the no system/no cost (Option VI) scores.

5.4.2 RELATIVE COST SCORING METHODOLOGY

Similarly, a relative cost score for each option was estimated. The cost estimating process addressed only major costs incremental to the Option VI (no cost) baseline. Moreover, emphasis was placed on the relative rather than absolute level of these costs across options. The elements costed were an option-specific set selected from the following list:

a. Added platforms
b. Platform modifications
c. Added sensors
d. Sensor modifications
e. Major operations and maintenance increases
f. Data processing hardware and software
g. Communications links
h. Information extraction R&D
i. Hardware R&D

Option IV costs, for example, are driven by items a, c, d, and e. Option I, on the other hand, has items c, d, and f as the major cost drivers.

The resulting relative cost scores are displayed at the bottom of Table 5.4-1 as the estimated costs over and above the baseline (Option VI) normalized by the "full-up" space/air system (Option I) cost.

5.4.3 DISCUSSION OF RESULTS

Concerning the precision of scores shown in Table 5.4-1, it is acknowledged that (1) there are numerous non-trivial assumptions which underlie each effectiveness score and each relative cost, and (2) we are quantifying system concepts extending a dozen years into the future on which even preliminary designs have not been established for some of the system elements. In light of this, the numbers are used in a relative rather than absolute sense. Furthermore, the study's conclusions and recommendations (covered throughout this Final

Report) were arrived at by the study process rather than application of cost and effectiveness scores. On the other hand, it is noted that these scores support the other sections' comclusions. More than that, they add the strength of relative numbers to certain system option comparisons:

- Whether viewed in terms of parametric performance or capability to support the several scenarios, the effectiveness scores for each option are virtually the same.
- The medium resolution multiple sensor option (II) is attractive, since it is only slightly less effective than the high resolution option (I) while it is significantly less costly than Option I.
- Option IV, which calls on a relatively narrow coverage capability platform (aircraft) to play the wide area coverage role (through a large fleet size), is both the most effective (slightly) and most costly (exorbitantly) option.
- At the other end of the capability scale, Option V yields relatively low effectiveness for much lower costs than the high capability systems (Options I through IV). By design, it yields slightly improved support from existing and planned systems at a modest cost.

SECTION 6
REFERENCES

SECTION 6

REFERENCES

1. Polcyn, F. C. and Sattinger, I. J.: A Summary of Remote Sensing in the New York Bight, Environmental Research Institute of Michigan, Report No. 131200-I-F, March 1979.

2. White, J. R., Freezer, D. R., and Vollmers, R. R.: U.S. Coast Guard Utilization of Remote Sensing Techniques for Ocean Surveillance, U.S. Department of Transportation, USCG.

3. Takuzo Sato, et al: Laser Radar for Remote Detection of Oil Spills, Applied Optics, Vol. 17, No. 23, Dec. 1978.

4. Hollinger, J. P. and Menella, R. A.: Oil Spills: Measurements of Their Distributions and Volumes by Multifrequency Microwave Radiometery, American Association for Advancement of Science publication, Volume 181, pp. 54-56.

5. Troy, Jr., E. and Hollinger, J. P.: The Measurement of Oil Spill Volume by a Passive Microwave Imager, NRL Memo Report 3515.

6. Hollinger, J. P. and Kenney, J. E.: Evaluation of a Passive Microwave Technique for the Measurement of Oil Film Thickness in a Test Tank Environment, NRL Memo Report 3308.

7. Hollinger, J. P.: The Determination of Oil Slick Thickness by Means of Multifrequency Passive Microwave Techniques, NRL Memorandum Report 2953.

8. Sorensen, B. M.: Recommendations from the International Workshop on Remote Sensing Sea Truth Data, Commission of the European Communities Joint Research Centre, Ispra, Italy.

9. Center for Ocean Management Studies at Univ. of Rhode Island: In the Wake of the Argo Merchant, Proceedings of a Symposium, Aug., 1978.

10. Backlund, L.: Airborne Oil Spill Surveillance System in Sweden, Proceedings of the 1979 Oil Spill Conference, March 1979.

11. Meeks, D., Bommarito, J., Schwantje, R., and Edgerton, A.: Transfer, Installation, and Flight Testing of the Modified Airborne Oil Surveillance System (AOSS II) in a HC-130B Aircraft, Final Report to U.S. Coast Guard, CG-D-60-77, August 1977.

12. Sherman, J. W.: Aerospace Remote Sensing in Oceanography, paper presented at 7th Session of the Working Group in International Oceanographic Data Exchange of the (U.N.) Intergovernmental Oceanographic Commission.

13. Hovis, W. A. and Leung, K. C.: Remote Sensing of Ocean Color, Optical Engineering, pp. 150-166, March/April 1977.

14. Private communications with Lt. Cmdr. J. Spreter, U.S. Coast Guard Base, Gloucester City, N. J., 1979.

15. Nagler, R. G. and Candless, S. W.: Operational Oceanographic Satellites, Jet Propulsion Laboratory.

16. Stringer, J. G.: Dumping and the Marine Environment, NOAA Magazine, pp. 41-45, October 1977.

17. Klemas, V.: Monitoring Coastal Water Properties and Current Circulation with Spacecraft, Instrument Society of America reprint.

18. National Academy of Sciences, Petroleum in the Marine Environment, Proceedings of Workshop on Inputs, Fates, and the Effects of Petroleum in the Marine Environment, May 21-25, 1973, Airlie, Va., 1975.

19. Edgerton A. T. and Trender, D.T.: Oceanographic Applications of Remote Sensing with Passive Microwave Techniques, Abstract from 6th Symposium of Remote Sensing of the Environment.

20. Rather, J. D., Gerry, E. T. and Neiders, G. W.: Assessment of the Benefits and Feasibility of Laser Remote Sneasing from Spacecraft and Earth Orbit, final report by W. J. Shafer Associates, Inc., May 1977.

21. Morley, L. W. et al: Ocean Information and Management Systems, paper presented at the 4th Canadian Symposium on Remote Sensing.

22. Kritikos, H. N.: Investigation of Hydrodynamic Transport Processes of the Saronikos Gulf, Moore School of Engineering, U. of Pennsylvania proposal.

23. Thomas, R. K. and Kritikos, H. N.: Measurement of Sea-State by R. F. Interferometry, IEEE Transactions on Geoscience Electronics, Vol. GE 13, No. 2.

24. Washburn, J. F. and Sandness, G. A.: Detection, Identification and Quantification Techniques for Spills of Hazardous Chemicals, summary report of study by Batelle Pacific Northwest Laboratories.

25. Nelson-Smith, A.: Oil Pollution and Marine Ecology, Plenum Press, 1973.

26. Lehr, W. E.: Remote Sensing of Southern California Oil Pollution Experiment, U.S. Coast Guard Report No. P3-203-194.

27. Salkowski, M. J.: Detection of Oil Contamination in Sea Water, I.I.T. Research Institute Report No. IITRI-C6055-22.

28. Howard, D.D.: Microwave Monitoring of Sea Water Contamination of Navy Fuel Oils, Naval Research Laboratory Report No. 6552.

29. Goldman, G. C. and Horvath, R.: The Feasibility of Oil Pollution Detection and Monitoring from Space, U.S. Coast Guard Report No. CG-D-117-75.

30. Rudder, C. L.: Aerial Detection of Spill Sources, E.P.A. Report No. EPA-R2-73-289.

31. Mostert, N.: Supership, Alfred A. Knopf, 1974.

32. Horstein, B.: The Appearance and Visibility of Thin Oil Films on Water, Environmental Protection Agency Report, EPA-R2-72-039, August 1972.

33. Horstein, B.: The Appearance and Visibility of Thin Oil Films on Water, EPA Report No. EPA-R2-72-039.

34. Grizzle, P. L. and Coleman, H J.: IR Analysis Techniques for Oil Identification, Energy Research and Development Administration.

35. Aukland, J. C.: Oil Pollution Detection and Discrimination by Remote Sensing Techniques, Spectran Incorporated, Report AD-716-349.

36. Heigl, J. J.: Oil/Water Interface Detector Laboratory Evaluation, Esso Research & Engineering Co., Report COM-74-1012.

37. Federal Regulation: Part 610 - Discharge of Oil, issued under Section 11(b) (3) of the Federal Water Pollution Control Act, as amended (84 Stat. 92 33 U.S.C. 1161), and printed in the Federal Register, Vol. 55, No. 177, September 11, 1970.

38. Croswell, W. F., et al: Summary Report of the Ad Hoc Committee on Space Monitoring of Oil Spills, Langley Research Center, 1978.

39. Fantasia, J. F. et al: An Investigation of Oil Fluorescence as a Technique for the Remote Sensing of Oil Spills, U.S. Coast Guard, Report No. FB-203-585.

40. Estes, J. E.: Remote Sensing Techniques and Methodologies Related to Conservation Division OCS Activities, Summary paper from Potential Applications of Remote Sensing for Conservation Divisions Outer Continental Shelf Data Acquisition Program, Feb. 1977.

41. Measures, R. M.: The Development of an Airborne Remote Laser Fluorosensor for Use in Oil Pollution Detection and Hydrologic Studies, Canada Centre for Remote Sensing, UTIAS Report No. 175.

42. Johnson, G. L.: Detection of Oil Contamination in Sea Water - Vol. III, IIT Research Institute, Report IITRI-C6065-66.

43. Salkowski, M. J.: Detection of Oil Contamination in Sea Water - Vol. II, IIT Research Institute, Report IITRI C6065-22.

44. Welch, R. I.: A Feasibility Demonstration of an Aerial Surveillance Spill Prevention System, Environmental Protection Agency Report #15080H0L01/72.

45. Horvath, R., Morgan, W. L. and Spellicy, R.: Measurements Program for Oil-Slick Characteristics, Willow Run Laboratories, Report No. 2766-7-F.

46. Burns, W. and Herz, M. J.: Development and Field Testing of a Light Aircraft Oil Surveillance System (LAOSS), The Oceanic Society, Report No. NASA-CR-2739.

47. Edgerton, A. T. and Trexler, D. T.: Radiometric Detection of Oil Slicks, Aerojet General Corporation, Report SD-1335-1.

48. Mohr, D., McCormack, K. et al: Oil Spill Surveillance System Study, Office of Air & Water Programs, EPA, Report EPA-R2-73-215.

49. Status Report: U.S. Coast Guard Airborne Oil Surveillance System (AOSS), Aerojet Electrosystems Company, DOT Report.

50. Hayes, R. M.: "Smart" Remote Sensor Needs for U.S. Coast Guard Ocean Environment Missions, AIAA/NASA Conference on Smart Sensors, paper no. 78-1721, Nov. 14-16, 1978.

51. Nagler, R. G.: Satellite Measurement Capabilities for Environmental and Research Observations, Jet Propulsion Laboratory.

52. Chism, S. B, et al: Advanced Sensors and Applications Study, Lockheed Electronics Company, Report N77-26590.

53. Nagler, R. G. and Sherry, E. J.: Global Services Satellite Circa 1995, Volume II, Jet Propulsion Laboratory, Report on the Joint Technology Enablement Study, 1978.

54. Perryman, D. C.: General Climatology and Wind/Wave Statistics for Offshore Newfoundland, Ocean Routes, Inc.

55. Kuo, C. F. and Talay, T. A.: Remote Monitoring of a Thermal Plume, National Aeronautics and Space Administration, NASA Technical Memorandum 80125.

56. Cassis, R. H. and Siegelin, D.: A Water Quality Monitoring System for NOAA Data Buoys, paper presented at the International Seminar & Exposition on Water Resources Instrumentation, June 1974.

57. Pollack, A. M. and Stolzenbach, K. D.: Crisis Science: Investigations in Response to the Argo Merchant Oil Spill, Massachusetts Institute of Technology, Report 78-308-Cmw.

58. Remote Sensing of Hydrocarbon Pollution, Centre Nationale pour l'Exploitation des Oceans, France.

59. NOAA Data Buoy Office: NDBO Fiscal Year 1979 Technical Requirements, U.S. Dept. of Commerce, NOAA Office of R&D, Report reference: CC8-[illegible].

60. Welch, R. I.: A Feasibility Demonstration of an Aerial Surveillance Spill Prevention System, Environmental Protection Agency, Office of Research and Monitoring, Report 15080HOL01.

61. Goldberg, E. D.: Marine Pollution Monitoring: Strategies for a National Program, Scripps Institute of Oceanography Workshop held at Santa Catalina Marine Biological Laboratory, Oct. 1972.

62. Proceedings of the 1979 Oil Spill Conference, American Petroleum Institute, Environmental Protection Agency, U.S. Coast Guard, March [illegible]

63. Bressel, C. N., Wisotsky, S. R., and Vander Velde, W. E.: Use of the Fast Fourier Transform in Evaluation of Laser Raman and Fluorescence Decay Times, Optical Engineering, March-April 1978.

64. Chandler, P. B.: Aerial and Orbital Remote Sensing of Water Quality, North American Rockwell Corp.

65. Klemas, V., Davis, G. R., and Henry, R. D.: Satellite and Current Drogue Studies of Ocean-Disposed Waste Drift, Journal WPCF, May 1977.

66. Bristow, M.P.F.: Airborne Monitoring of Surface Water Pollutants by Fluorescence Spectroscopy, Canada Centre for Remote Sensing, Dept. of Energy, Mines & Resources.

67. Douglas, D. G., Blahnik, C. E., Hilbers, G. R.: SRI Wave Staff Buoy, Stanford Research Institute, Sept. 1975.

68. Graf, K. A., Tremain, D. E. and Guthart, H.: Induced-Current Interaction with Waves, Office of Naval Research Field Projects Programs, Final Technical Report, April 1975.

69. Bowker, D. E., Witte, W. G.: The Use of Landsat for Monitoring Water Parameters in the Coastal Zone, AIAA 1977 Joint Conference on Satellite Applications of Marine Operations, November 1977.

70. Johnson, R. W.: Application of Remote Sensing to Marine Pollution and Oceanography Studies, Second Working Conference on Oceanographic Data Systems, Sept. 1978.

71. Johnson, R. W., et al: Monitoring the Temporal Dispension of a Sewage Sludge Plume in the New York Bight by Remote Sensing, 44th Annual Meeting of the American Society of Photogrammetry, Feb-Mar. 1978.

72. Johnson, R. W.: Multispectral Analysis of Ocean Dumped Materials, Eleventh International Symposium on Remote Sensing of Environment, April 1977.

73. Schroeffer, G. J.: A Philosophy of Water Pollution Control - Past and Present, Journal WPCF, Sept. 1978.

74. Demolishing Myths about Ocean Disposal, Journal WPCF, Sept. 1978.

75. Costle, D. M.: Ocean Dumping in the United States, U.S. Environmental Protection Agency, Sixth Annual Report, Jan.-Dec. 1977.

76. 1977 Report to Congress on Administration of Ocean Dumping Activities, U.S Army Corps of Engineers, June 1978.

77. 1978 Report to Congress on Administration of Ocean Dumping Activities, Dept. of Transportation, U.S. Coast Guard, March 1979.

78. Whitlock, C. H., Kuo, C. Y.: A Regression for Evaluation and Quantification for Water Quality Parameters from Remote Sensing Data, Thirteenth International Symposium on Remote Sensing of the Environment, April 1979.

79. Report to the Congress on Ocean Dumping Research January through December 1977, U.S. Department of Commerce, August 1978.

80. Maul, G. A., Gordon, H. R.: On the Use of the Earth Resources Technology Satellite (Landsat-1) in Optical Oceanography, Remote Sensing of Environment, 1975.

81. Maul, G. A.: Locating and Interpreting Hand-Held Photographs Over the Ocean, A Gulf of Mexico Example from the Apollo-Soyuz Test Project, Remote Sensing of Environment, 1978.

82. Graf, K. A., et al: Induced-Current Effects on Microwave Backscatter, IEEE Transactions on Antennas and Propagation, Jan. 1977.

83. Maul, G. A.: Recent Progress in the Remote Sensing of Ocean Surface Currents, Marine Technology Society Journal, 1976.

84. Maul, G. A., et al: Geostationary Satellite Observations of Gulf Stream Meaders: Infrared Measurements and Time Series Analysis, Journal of Geophysical Research, December 1978.

85. Maul, G. A.: Recent Progress in the Remote Sensing of Ocean Surface Currents, Marine Technology Society, 1976.

86. Maul, G. A.: The Annual Cycle of the Gulf Loop Current Part I: Observations During a One Year Time Series, Sears Foundation: Journal of Research, February 1977.

87. Deutsch, M., et al: Use of Landsat Data for the Detection of Marine Oil Slicks, Offshore Technology Conference, May 1977.

88. Surveillance of Environmental Pollution and Resources by Electromagnetic Waves, NATO Advanced Studies Institute Series, ISBN 90-277-0949-1, April 1978.

89. Boxer, B.: Mediterranean Action Plan: An Interim Evaluation, Science, Vol. 202, November 1978.

90. Graf, K. A.: Guthart, H.: Velocity Effects in Synthetic Apertures, IEEE Transactions on Antennas and Propagation, Vol. AP-17, September 1969.

91. Gloarsen, P., Barath, F. T.: A Scanning Multi-Channel Microwave Radiometer for Nimbus-G and Seasat-A, IEEE Journal of Oceanic Engineering, Vo. OE-2, No. 2, April 1977.

92. Milgram, J. H., and Van Houten, R. J.: Mechanics of a Strained Layer of Floating Oil Above a Water Current, Journal of Hydronautics, Vol. 12, No. 3, July 1978.

93. Myers, E. P. and Gunnerson, C. G.: Hydrocarbons in the Ocean, MESA Special Report, U.S. Department of Commerce, April 1976.

94. Bureau of Land Managements Outer Continental Shelf Task Team: The Environmental Quality Monitoring Report, U.S. Dept. of Commerce, February 1976.

95. Hovis, W. A.: Ocean Color Imagery - Coastal Zone Color Scanner, First Comprehensive Symposium on the Practical Application of Earth Resources Survey Data, Vol. 1, I-C.

96. Shelves, T. C.: Remote Measurements of Water Pollution with a Lidar Polarimeter, Remote Sensing Center, Texas A&M University.

97. Lewis, B. W., and Collins, V. G.: Remotely Sensed and Laboratory Spectral Signatures of an Ocean-Dumped Acid Waste, NASA Technical Note, NASA-TN-D Langley Research Center, July 1977.

98. Waldichuk, M.: Global Marine Pollution, Inter-Governmental Oceanographic Commission, Technical Series, 1977.

99. A Comprehensive Plan for the Global Investigation of Pollution in the Marine Environment and Baseline Study Guidelines, Inter-Governmental Oceanographic Commission Technical Series, June 1976.

100. Junghans, R. and Zachariason, R.: The Integrated Global Ocean Station System (IGOSS), Environmental Data Service, July 1974.

101. Rudder, C. L., et al: Aerial Detection of Spill Sources, Office of Research and Development, U.S. Environmental Protection Agency, EPA-R2-73-289, Sept. 1973.

102. Welch, R. I.: Aerial Spill Prevention Surveillance during Sub-Optimum Weather, Office of Research and Development, U.S. Environmental Protection Agency, EPA-R2-73-243, September 1973.

103. Rudder, C. L., et al: Aerial Surveillance Spill Prevention System, EPA-R2-72-007, Office of Research and Monitoring, U.S. Environmental Protection Agency, August 1972.

104. Slack, J. R. et al: An Oil Spill Risk Analysis for the Southern California (Proposed Sale 48) Outer Continental Shelf Lease Area, U.S. Geological Survey, Water Resources Division, October 1978.

105. Lichte, H. W., and Breslin, M. C.: Performance Testing of Three Offshore Skimming Devices, EPA-600/7-78-082, U.S. Environmental Protection Agency, May 1978.

106. Clarke, P. F., et al: A Guide to Obtaining Information from the USGS 1978, Geological Survey Circular 777, U.S. Dept. of Interior, 1978.

107. White, P. G., et al: Development and Flight Test of the Multi-Channel Ocean Color Sensor (MOCS), NASA Contractor Report, NASA CR-2311, Langley Research Center, October 1973.

108. Ehrenspeck, H., et al: Oil Spill and Oil Pollution Reports Vol. 5, No. 1, PB-281671, Industrial Environmental Research Lab., April 1978.

109. Marine Pollution Monitoring (Petroleum), NBS Special Publication 409, National Bureau of Standards Symposium & Workshop, December 1974.

110. Cutrona, L. J.: Synthetic Aperture Radar, in Radar Handbook, M. I. Skolnik, Ed., New York: McGraw-Hill, 1970, Ch. 23, pp. 23.1-23.25.

111. Harger, R. O.: Synthetic Aperture Radar Systems, Theory and Design, New York: Academic Press, 1970.

112. Tomiyasu, K.: Tutorial Review of Synthetic Aperture Radar (SAR) with Applications to Imaging of the Ocean Surface, Proc. IEEE, Vol. 66, pp. 563-583, May 1978.

113. Matthews, R. E. (Editor): Active Microwave Sensor Technology, Ch. 5, Active Microwave Workshop Report, NASA-SP-37 .

114. Thematic Mapper, Hughes Aircraft, Document No. D4596. SCG 80198R, prepared for NASA-GSFC, June 1978.

115. Conner, W., et al: A Small Oil Spill at West Falmouth, EPA (600/9-79-007), U.S. Environmental Protection Agency, Office of Research and Development, March 1979.

116. Hovis, W. A. and Knoll, J. S.: Optical Measurements of Crude Oil Samples under Simulated Conditions, NOAA Technical Memorandum NESS 105, U. S. Department of Commerce, October 1979.

117. Anderson, A. G., et al: Microwave Remote Sensing from Space for Earth Resources Survey, NTIS, No. NRC/CORSEERS-77/1, National Academy of Sciences, 1977.

118. Jordan, R. and Held, D.: The Seasat-A Synthetic Aperture Radar, IEEE International Microwave Symposium, 1979, Orlando, Florida.

119. Claasen, J. P.: Short Study of a Scanning SAR for Hydrological Monitoring on a Global Basis, Tech Rpt. #205-1, Contract NAS-5-22384, U. Kansas Remote Sensing Lab, September 1975.

120. Cutrona, L. J.: Comparison of Sonar System Performance Achievable Using Synthetic Aperture Techniques with the Performance Achievable by More Conventional Means, J. Acoust. Soc. AM., Vol. 52, pp. 336-348, August 1975.

121. Johnson, R. W., et al: Quantitative Mapping of Suspended Solids in Wastewater Sludge Plumes in the New York Bight Apex, Journal WPCF, October 1977.

122. Huffaker, R. M., Editor, et al: Feasibility Study of Satellite-Borne Lidar Global Wind Monitoring System, NOAA Technical Memorandum ERL WPL-37, Wave Propagation Laboratory, September 1978.

123. McGoogan, J. et al: Real Time Determination of Geophysical Parameters from a Multibeam Altimeter, NASA Wallops, paper no. AIAA 78-1735.

124. Excerpts from Text in Oil Spill Prevention and Removal, published by Noys Data Corp.

125. Lissauer, I. M., Welsh, J. P., and Hufford, G. L.: Environmental Risk of Beaufort Sea Oil Spills - A Management Tool, MTS Journal, Vol. II, No. 1, 1977.

126. NOAA Program Development Plan for Seasat-A Research and Applications, NOAA S/T 77-2858, U.S. Dept. of Commerce, July 1977.

127. Woolever, G. F., et al: Utilization of Remote Sensing Techniques for U.S. Coast Guard Missions, U.S. Coast Guard Research and Development Center, Groton, Conn.

128. Tomiyasu, K. : Synthetic Aperture Radar with Elevation-Plane Scanned Antenna Beam for Swath Coverage, in Digest IEEE 1979 Int. Antenna and Propagation Symposium, pp. 208-210, 1979.

129. Smith, D. M.: Summary Report - Cloud Probabilities and Expected Values of Coverage, PIR *U-3860-DMS-342, General Electric Co., December 1969.

130. Gjessing, D. T. and Nordo, J.: Environmental Surveillance (Remote Probing, Pollution Monitoring), Ref. 70159/76/B/NDRE/DTG/RB/204.1 - NATO, Norwegian Defense Research Establishment, January 1976.

131. Ohlhorst, C. W.: Quantitative Mapping by Remote Sensing of an Ocean Acid-Waste Dump, NASA Technical Paper 1275, NASA Scientific and Technical Information Office, October 1978.

132. Tomiyasu, K.: Central Swath Mapping by a Future Satellite-Borne Fan-Beam Microwave Scatterometer for Inferring Global Ocean Wind Fields, IEEG Journal of Oceanic Engineering, Vol.OE-3, No. 3, July 1978.

133. Tomiyasu, K. et al: Feasibility Study Radar for Ice Processes and Climate Studies, Spacecraft Dept. Document No. 79SDS4219, General Electric Co., April 1979.

134. Sabins Jr., F. F.: Remote Sensing Principles and Interpretation, W. H. Freeman and Company, San Francisco, 1978.

135. Catoe, C. E., and McLean, J. T.: A Multispectral Look at Oil Pollution Detection, Monitoring, and Law Enforcement.

136. Alexander, L. M. (Editor), et al: U.S. Coastal Belt Conflict, Resolution, and Promise Center for Ocean Management Studies, Univ. of Rhode Island, June 1977.

137. Moders, C.N.K., et al: Climate and Fisheries, Center for Ocean Management Studies Workshop, Univ. of Rhode Island, March 1978.

138. Polcyn, F. C., and Sattinger, I. J.: Marine Ecosystems Analysis Program: A Summary of Remote Sensing Investigations in the New York Bight, Report No. 131200-1-F, Enfironmental Research Institute of Michigan, U.S. Dept of Commerce, March 1979.

139. Meeks, D. C. et al: Installation and Flight Testing of the Modified Airborne Oil Surveillance System (AOSS II) in a HC-130B Aircraft - Final Report, Rpt. #5546, Aerojet Electrosystems Company, August 1977.

140. Klemas, V., and Philpot, W. D.: Remote Sensing of Ocean Dumped Waste Drift and Dispersion, First International Ocean Dumping Symposium, Univ. of Rhode Island, October 1978.

141. Harrison, E. F. and Green, R. N.: Orbit Analysis for Coastal Zone Oceanography Observations, J. Spacecraft, Vol. II, No. 3, March 1974.

142. Hawkins, R. K. and Gray, A. L. et al: Observation of Two Test Oil Spills with a Microwave Scatterometer and a Synthetic Aperture Radar (SAR), Workshop of the NATO-CCMS Pilot Study on the Use of Remote Sensing for the Control of Marine Pollution, April 1979.

143. Philpot, W., and Klemas, V.: Detection of Ocean Waste in the New York Bight, N79-21637 Final Report, Delaware University, March 1979.

144. Bayma, R. W. and McInnes, P. A.: Aperture Size and Ambiguity Constraints for a Synthetic Aperture Radar, in Record IEEE 1975 Int. Radar Conf., pp. 499-504, 1975.

145. Kirk, Jr. J. C.: A Discussion of Digital Processing in Synthetic Aperture Radar, IBM J. Res. Develop., Vol. 21, pp. 415-432, September 1977.

146. Van de Lindt, W. J.: Digital Technique for Generating Synthetic Aperture Radar Images, IBM J. Res. Develop., Vol. 21, pp. 415-432, September 1977.

147. Stow, W. K.: Total Earth Resources System for the Shuttle Era, General Electric Space Division report DRL no. T-880(MA-129TA), December 1975.

148. Transfer, Installation, and Flight Testing of the Modified Airborne Oil Surveillance System (AOSS II) in a HC-130B Aircraft, U.S. Coast Guard Rpt. No. CG-D-60-77, U.S. Coast Guard, Office of Research and Development.

149. Vollmers, R., et al: Airborne Spill Detection and Tracking System, Ad Hoc Committee on Space Monitoring of Oil Spills, U.S. Coast Guard, February 1978.

150. Thomson, Dr. V. and Gulatsi, R.: Informal Communication, Intera, between Environmental Consultants and General Electric Co., February 1979.

151. Egan, W. G., and Hilgeman, T.: Polarimeter Measures Sea State Characteristics Using Emitted Infrared Radiation, paper presented to Eleventh International Symposium of Remote Sensing of the Environment, Environmental Research Institute, April 1977.

152. Seyrafi, K.: Electro-Optical Systems Analysis, Electro-Optical Research Company, 1973.

153. McCall, W., and Gulatsi, R.: Informal Communication, Intera, between Environmental Consultants Ltd. and General Electric Co., February 1979.

154. Pratt, W. K.: Laser Systems Communications, Jonn Wiley & Sons, 1969.

155. Gulatsi, R. and Manchel, G.: Telecon, General Electric Co. and Lumonns Research Ltd., February 1979.

156. Thomson, V. and Gulatsi, R.: Informal Communication, Entera, Environmental Consultants, Ltd. and General Electric Co., February 1979.

157. Specification - Airborne Infrared/Ultraviolet Line Scanner Set, Dept. of Transportation, U.S. Coast Guard, Office of Research and Development, June 1978.

158. Assessment of the Benefits and Feasibility of Laser Remote Sensing from Spacecraft and Earth Orbit, Final Report for Jet Propulsion Laboratory, Calif. Institute of Technology Contract #954673, W. J. Shafer Associated, May 1977.

159. National Oil and Hazardous Substances Pollution Contingency Plan, Title 40, Chapter 5, Federal Register, Vol. 40, No. 28, February 10, 1975.

SECTION 7
APPENDICES

APPENDIX A — A COASTAL COVERAGE COMPUTER SIMULATION

APPENDIX B — A COMPARISON OF TIME STEPS FOR OIL SPILL MONITORING (BY DR. PETER CARMILLON AND KURT HANSEN, UNIVERSITY OF RHODE ISLAND)

APPENDIX C — PASSIVE REMOTE SENSING OF OFF-SHORE POLLUTANTS SUBCONTRACT REPORT BY TETRA-TECH., INC.)

APPENDIX A: COASTCOVER -- A COASTAL COVERAGE COMPUTER SIMULATION

I. PROGRAM LISTING (FORTRAN IV)

```
C          PROGRAM-COASTCOVER
C
C
C  THIS PROGRAM CALCULATES THE LATITUDE AND LONGITUDE OF POINTS ALONG
C  THE UPPER AND LOWER EDGES OF A SWATH SEEN BY A SATELLITE INAN EARTH
C  ORBIT. THE WIDTH OF THE SWATH IS SPECIFIED BY AN ELEVATION ANGLE:
C  AN OBSERVER ON EARTH WOULD BE IN THE SWATH IF HE COULD SEE THE
C SATELLITE WITHOUT LOOKING BELOW THE ELEVATION ANGLE. THIS PROGRAM
C  IS DERIVED FROM THE DK9 PROGRAM AND MOST OF THE INPUTS ARE THE SAME.
C  THIS VERSION OF COASTCOVER COMPUTES THE SURFACE AREA DEFINED WITHIN ONE
C      OF SEVERAL CLOSED COASTAL ZONES THAT IS COVERED AT EACH CROSSING OF
C      THE SPACECRAFT SENSOR GROUND SWATH.
C
C
C    THIS VERSION USES METRIC INPUT/OUTPUT, ENGLISH UNITS INTERNALLY.
C
C
C
C  INPUTS:
C    A,E,INC,WPZERO,PSIZERO,DEL-T,NDT : SAME AS FOR DK9
C    SELEV  : ELEVATION ANGLE AS DESCRIBED ABOVE (DEGREES)
C    LATOLD : A DUMMY LATITUDE THAT TELLS THE PROGRAM WHETHER THE SAT-
C             IS GOING NORTH OR SOUTH. F IT IS HEADING NORTH, LATOLD
C             SHOULD BE SOUTH OF THE STARTING LATITUDE; IF IT IS HEADING
C             SOUTH, LATOLD SHOULD BE NORTH OF THE STARTING LATITUDE.
C
C  OUTPUT:
C    LATUP,LONUP : LATITUDE AND LONGITUDE OF POINTS ON THE UPPER EDGE
C                  OF THE SWATH
C    LATLOW,LONLOW : LATITUDE AND LONGITUDE OF POINTS ON THE LOWER EDGE
C                    OF THE SWATH
C
     REAL LATCUR,LONCUR,LATOLD,LATUP,LONUP,LATLOW,LONLOW
      REAL LATUPO,LONUPO,LATLOO,LONLOO,LATUPI,LONUPI,LATLOI,LONLOI
      DIMENSION WBDO(24,13),WBDI(24,13),EBDO(24,13), EBDI(24,13)
      COMMON NUMW,NUME,SSLAT,SSLONG
      COMMON  NEX,NWX,NEY,NWY,NEZ,NWZ
     COMMON  SLOPSW,CEPTSW,SLOPSE,CEPTSE, SLOPAV,CEPTAV
    COMMON SEBW,SEBE,SWBE,SWBW
     CHARACTER  ALPH1*6, ALPH2*6, ALPH3*6,  BET1*6,
     &    BET2*6,  BET3*6,  GAM1*6,GAM2*6,GAM3*6
C
  RE=3444.
 PI=3.1415926535
  CJ=1.62405E-3
        R=180./PI
       CONVRG=.0001
       WE=.2506844773
       GMU=2.25901E8
      * * * * * * * * *
     PRINT,"A,E,INC,WPZERO,PSIZERO,DEL-T,NDT"
```

```
C    INPUT THE NUMBER OF LINES IN BOUNDARY TABLE
     DO 999  III=1,4
C     READ,NUMW,NUME,LIMSWA
      READ,NUMW,NUME,ACTSWA
C     INPUT WEST BOUNDARIES
C
C     WBD IS WEST BOUNDARY
C    J=1 IS LINE NUMBER
C     J=2  IS LATITUDE
C     J=3 IS LONGITUDE
C
      DO 28  N=1,NUMW
      READ, (WBDO(N,J), J=1,3)
      28  CONTINUE
      DO 27  N=1,NUMW
     DO 26   J=1,3
       WBDI(N,J)=WBDO(N,J)
     26  CONTINUE
     27  CONTINUE
C
C   CALCULATE SLOPES AND INTERCEPTS OF BOUNDARY SEGMENTS.
     DO 25  N=1,NUMW
C
C     WBDO(N,4) IS THE SLOPE
C
      WBDO(N,4) = (WBDO(N,2) - WBDO(N+1,2))/
     &    (WBDO(N,3) - WBDO(N+1,3))
      IF(N.EQ.NUMW) WBDO(N,4) =0.0
      WBDI(N,4)=WBDO(N,4)
C
C     WBDO(N,5) IS THE Y INTERCEPT OF THE BOUNDARY
     WBDO(N,5) = WBDO(N,2) - WBDO(N,4)*WBDO(N,3)
      IF(N.EQ.NUMW)  WBDO(N,5)=100.0
      WBDI(N,5) = WBDO(N,5)
     25  CONTINUE
C
C
C     INPUT EAST BOUNDARIES
C
C      EBDO IS EAST BOUNDARY COORDINATES
C
      DO 30 N=1,NUME
      READ, (EBDO(N,J), J=1,3)
      30 CONTINUE
      DO 35   N=1,NUME
     DO 34  J=1,3
      EBDI(N,J) = EBDO(N,J)
     34  CONTINUE
      35  CONTINUE
C
C     EBDO(K,4) IS THE BOUNDARY SLOPE
C
     DO 32  K=1,NUME
     EBDO(K,4) = (EBDO(K,2)- EBDO(K+1,2))/
     &   (EBDO(K,3) - EBDO(K+1,3))
```

```
      IF (K.EQ.NUME)  EBDO(K,4) = 0.0
       EBDI(K,4) = EBDO(K,4)
C     EBDO(K,5) IS THE Y INTERCEPT OF THE BOUNDARY.
C
       EBDO(K,5) = EBDO(K,2) - EBDO(K,4)*EBDO(K,3)
       IF(K.EQ.NUME) EBDO(K,5)=100.0

       EBDI(K,5) = EBDO(K,5)
    32  CONTINUE
C
C
C
     1  READ,AMET,E,XI,WPZ,PSI,TLIM
       READ,LATOLD
       A=AMET/1.852
C      ENTER BOUNDARIES OF REGION TO BE SWATHED
       READ,TOP,BOT,EAST,WEST
C        ENTER EVEVATION ANGLE
     2  CONTINUE
       READ,SELEVO,SELEVI
       IPRNT=3
       POINT=0.0
       SELEVO = SELEVO/R
       SELEVI = SELEVI/R
     3 T=0.
       ACCUM = 0.0
      TACCMB=0.0
      WP=WPZ
        ELNGND=PSI
          EMM=0.
          XMM=SQRT(GMU/A**3)
D=(A/RE)*(1.-E*E)
OMEGN=-2.*PI*CJ*COS(XI/R)
 OMEGP=PI*CJ*(4.-5.*SIN(XI/R)**2)
 OMGDOT=R*OMEGN/D**2
 WPDOT=R*OMEGP/D**2
 TMINS=2.*PI*SQRT(A**3/GMU)
   DT=TMINS/180.0
 DOMG=DT*OMGDOT/TMINS
 DWP=DT*WPDOT/TMINS
PRINT 103
PRINT,"  T (MIN)        OMGDOT(DEG/DAY)  WPDOT(DEG/DAY)"
 PRINT,TMINS,OMGDOT*1440./TMINS,WPDOT*1440./TMINS
PRINT 103
  4 WRITE(6,205)
   205  FORMAT(1H1,2X,4HTIME,5X,7HTR ANOM,4X,3HLAT,4X,4HLONG,8X,
&     8HVELOCITY,
&    5X,5HSELAT,5X,6H SELON,5X,6H SWLAT,4X,7H SWLON ,2X,
&     8HA-WEST  ,8HA-EAST  ,4X,8H ACCUM  ///)
    PRINT,"OUTER ELEVATION ANGLE IS          ",R*SELEVO
    PRINT,"INNER ELEVATION ANGLE IS          ",R*SELEVI
 5 CONTINUE
    DOMG=DT*OMGDOT/TMINS
    DWP=DT*OMGDOT/TMINS
       EMM=XMM*T
       ECCO=EMM
```

```
1610   901 ECC=EMM+E*SIN(ECCO)
1620       IF(ABS(ECC-ECCO)-CONVRG)903,903,902
1630   902 ECCO=ECC
1640       GO TO 901
1650   903 THT2=ATAN(SQRT((1.+E)/(1.-E))*TAN(ECC/2.))
1660       THETA=2.*THT2*R
1670       IF(THETA.LT.0.) THETA=THETA+360.
1680       P=A*(1.-E*E)
1690       CTH=COS(2.*THT2)
1700       RAD=P/(1.+E*CTH)
1710       THDOT=R*SQRT(GMU/P**3)*(1.+E*CTH)**2
1720       THTDD=R*(-2.*GMU*E*SIN(2.*THT2)/RAD**3)
1730       VSQ=GMU*(2./RAD -1./A)
1740        VSQ=VSQ+.01
1750       V=SQRT(VSQ)
1760       VHOR=RAD*THDOT/R
1770       VVERT=SQRT(VSQ-VHOR*VHOR)
1780   IF (THETA.GT.180.)VVERT=-1.*VVERT
1790       GAM=R*ARSIN(VVERT/V)
1800       V=V*6076.115/60.
1810    V=0.3048*V
1820       PHI=WP+THETA
1830       SSLAT=R*ARSIN(SIN(XI/R)*SIN(PHI/R))
1840       X=COS(PHI/R)
1850  Y=SIN(PHI/R)*COS(XI/R)
1860  Z=SIN(PHI/R)*SIN(XI/R)
1870       SSLONG= ELNGND-WE*T+ATAN2(Y,X)*R+1440.
1880       NREV=SSLONG/360.
1890       SSLONG=SSLONG-360.*NREV
1900 495 CONTINUE
1910 496 CONTINUE
1920   905  CONTINUE
1930C
1940C
1950C   TEST PRESENT POSITION AGAINST BOUNDY OF AREA OF INTEREST.
1960C
1970C
1980   IF(SSLAT.LT.BOT.OR.SSLAT.GE.TOP)  GO TO 899
1990   IF(SSLONG.LT.WEST.OR.SSLONG.GT.EAST)  GO TO 899
2000C       *          *        *          *          *
2010C       SUBROUTINE SWATH CALLED HERE
2020C       *          *        *          *          *
2030C  CALCULATE THE SWATH WIDTH
2040    SWDTHO = ARCOS((RE/RAD)*COS(SELEVO))-SELEVO
2050    SWDTHO = SWDTHO*R
2060    SWDTHI = ARCOS((RE/RAD)*COS(SELEVI))-SELEVI
2070    SWDTHI = SWDTHI*R
2080    WIDEO=(SWDTHO/360.0)*40075.0
2090    WIDEI=(SWDTHI/360.0)*40075.0
```

```
2100   DT=TMINS/360.0
2110    DOMG=DT*OMGDOT/TMINS
2120    DWP=DT*WPDOT/TMINS
2130C   **   **   **   **   **   **
2140   CALL SWATH(SSLAT,SSLONG,LATOLD,SWDTHO,
2150  &    LATUPO,LONUPO,LATLOO,LONLOO,XI)
2160   CALL SWATH(SSLAT,SSLONG,LATOLD,SWDTHI,LATUPI,
2170  &   LONUPI,LATLOI,LONLOI,XI)
2180C
2190C  DEFINE THE LAT AND LONG. OF SWATH ENDS.
2200C
2210C
2220C   SE MEANS EAST END OF THE SWATH, SO SELON IS THE
2230C    THE LONGITUDE OF THEEAST EDGE OF THE CURRENT SWATH POINT.
2240C    SW IS THE WEST EDGE OF THE SWATH, ETC.
2250C
2260C
2270C
2280   SELONO = AMAX1(LONUPO,LONLOO)
2290   SELONI = AMAX1(LONUPI,LONLOI)
2300   SWLONO = AMIN1(LONUPO,LONLOO)
2310   SWLONI = AMIN1(LONUPI,LONLOI)
2320C
2330   ISEO = 100*SELONO
2340   ISEI = 100*SELONI
2350   ISWO = 100*SWLONO
2360   ISWI = 100*SWLONI
2370   NUPO = 100*LONUPO
2380   NUPI = 100*LONUPI
2390   LOWO = 100*LONLOO
2400   LOWI = 100*LONLOI
2410   IF(ISEO.EQ.NUPO)   SELATO=LATUPO
2420   IF(ISEI.EO.NUPI)  SELATI=LATUPI
2430   IF(ISEO.EQ.LOWO)  SELATO=LATLOO
2440   IF(ISEI.EQ.LOWI)  SELATI=LATLOI
2450   IF(ISWO.EQ.NUPO)  SWLATO=LATUPO
2460   IF(ISWI.EQ.NUPI)  SWLATI=LATUPI
2470   IF(ISWO.EQ.LOWO)  SWLATO=LATLOO
2480   IF(ISWI.EQ.LOWI)  SWLATI=LATLOI
2490C
2500C   NE AND NW ARE LINE NUMBERS, EAST OR WEST, THAT DEFINE
2510C    LATITUDE AND  LONGITUDE IN THE BOUNDARY TABLE.
2520C    X  IS WEST EDGE OF SWATH
2530C    Y  IS CENTER OF SWATH
2540C    Z  IS EAST EDGE OF SWATH
2550C
2560C
2570     DO 40 N=1,NUMW
2580    IF(SWLATO.LT.WBDO(1,2)) NWX=0
2590   IF(SWLATO.GT.WBDO(N,2).AND.SWLATO.LT.WBDO(N+1,2)) NWX=N
2600   IF(SWLATO.GE.WBDO(NUMW,2))  NWX=NUMW
2610    40  CONTINUE
```

```
2620C
2630C
2640      DO 41  JK=1,NUME
2650      IF(SWLATO.LT.EBDO(1,2))  NEX=0
2660     IF(SWLATO.GT.EBDO(JK,2).AND.SWLATO.LT.EBDO(JK+1,2))
2670&     NEX=JK
2680     IF(SWLATO.GT.EBDO(NUME,2))  NEX=NUME
2690  41   CONTINUE
2700C
2710    CALL EDGE(WBDO,EBDO,NEX,NWX,SWLATO,SWBE,SWBW)
2720C
2730C
2740     DO 42 K=1,NUME
2750    IF(SELATO.LT.EBDO(1,2))  NEZ=0
2760   IF(SELATO.GT.EBDO(K,2).AND.SELATO.LT.EBDO(K+1,2)) NEZ=K
2770   IF(SELATO.GE.EBDO(NUME,2))  NEZ=NUME
2780    42  CONTINUE
2790C
2800 DO 43 JIL=1,NUMW
2810     IF(SELATO.LT.WBDO(1,2))  NWZ=0
2820     IF(SELATO.GT.WBDO(JIL,2).AND.SELATO.LT.WBDO(JIL+1,2))
2830&    NWZ=JIL
2840     IF(SELATO.GT.WBDO(NUMW,2))  NWZ=NUMW
2850    43   CONTINUE
2860C
2870C
2880    CALL EDGE(WBDO,EBDO,NEZ,NWZ,SELATO,SEBE,SEBW)
2890     DO 45 JIM=1,NUME
2900    IF(SSLAT.LT.EBDO(1,2))  NEY=0
2910    IF(SSLAT.GT.EBDO(JIM,2).AND.SSLAT.LT.EBDO(JIM+1,2))
2920&    NEY=JIM
2930    IF(SSLAT.GE.EBDO(NUME,2))   NEY=NUME
2940     45 CONTINUE
2950    DO 49   JA=1,NUMW
2960     IF(SSLAT.LT.WBDO(1,2))   NWY=0
2970    IF(SSLAT.GT.WBDO(JA,2).AND.SSLAT.LE.WBDO(JA+1,2))
2980&    NWY=JA
2990     IF(SSLAT.GT.WBDO(NUMW,2))  NWY=NUMW
3000    49   CONTINUE
3010C
3020C
3030    CALL EDGE(WBDO,EBDO,NEY,NWY,SSLAT,SSBE,SSBW)
3040C
3050C
3060C
3070C
3080   GO TO  333
3090    331  CONTINUE
3100C     WRITE(6,201)
3110    WRITE(6,103)
3120C    WRITE(6,202)  SEBW,SEBE,SELONO,SELATO,N3,N4,SLOPSE,CEPTSE,FRACE
3130C    WRITE(6,202)  SSBW,SSBE,SSLONG,SSLAT,NWY,NEY,SLOPAV,CEPTAV,SSLONG
3140C     WRITE(6,202)  SWBW,SWBE,SWLONO,  SWLATO,N1,N2,SLOPSW,CEPTSW,FRACW
3150C
3160   GO TO 63
3170   333  CONTINUE
```

```
3180C
3190      IF(SELONO.GE.SEBE.AND.SELONO.LT.SEBW)  GO TO 61
3200      IF(SSLONG.GE.SSBE.AND.SSLONG.LT.SSBW)  GO TO 61
3210      IF(SWLONO.GE.SWBE.AND.SWLONO.LT.SWBW)  GO TO 61
3220      IF(SELONO.GE.SEBW.AND.SELONO.LE.SEBE)  GO TO 61
3230      IF(SSLONG.GE.SSBW.AND.SSLONG.LE.SSBE)  GO TO 61
3240      IF(SWLONO.GE.SWBW.AND.SWLONO.LE.SWBE)  GO TO 61
3250      IF(SWLONO.GE.SWBW.AND.SELONO.LE.SEBE)  GO TO 61
3260     IF(SSLAT.GT.BOT.OR.SSLAT.LE.TOP)  GO TO 61
3270     IF(SSLONG.GT.WEST.OR.SSLONG.LE.EAST) GO TO 61
3280C
3290    AEASTO = 0.0
3300    AEASTI=0.0
3310    AWESTO=0.0
3320    AWESTI=0.0
3330    PWESTO=0.0
3340    PWESTI=0.0
3350    PEASTO=0.0
3360    PEASTI=0.0
3370C
3380    GO TO 63
3390     61  CONTINUE
3400     DT=TMINS/720.0
3410     DOMG=DT*OMGDOT/TMINS
3420     DWP=DT*WPDOT/TMINS
3430     **    **    **    **    **    **
3440     IF(IPRNT.EQ.2)  WRITE(6,205)
3450     IF(IPRNT.EQ.2)  WRITE(6,200)  T,THETA,SSLAT,SSLONG,
3460&    V,SELATO,SELONO,SWLATO,SWLONO,SLOPSW,SLOPSE,DT*1000.
3470     CALL AREA(WBDO,EBDO,SELONO,SELATO,SWLONO,SWLATO,FRACEO,
3480   &  FRACWO,N1O,N2O,N3O,N4O)
3490     CALL AREA(WBDI,EBDI,SELONI,SELATI,SWLONI,SWLATI,FRACEI,
3500   & FRACWI,N1I,N2I,N3I,N4I)
3510    ACTEO=FRACEO*WIDEO
3511    TOTEST=AMIN1(ACTEO,ACTSWA)
3520    ACTEI=FRACEI*WIDEI
3530    ACTENT=ACTEO-ACTEI
3540    ACTWO=FRACWO*WIDEO
3541    TOTWST=AMIN1(ACTWO,ACTSWA)
3542    COMTOT=TOTWST+TOTEST
3543    CMBTOT=AMIN1(COMTOT,ACTSWA)
3550    ACTWI=FRACWI*WIDEI
3560    ACTWNT=ACTWO-ACTWI
3570    IF(ACTENT.LT.0.0)  ACTENT=0.0
3580    IF(ACTWNT.LT.0.0)  ACTWNT=0.0
3581    IF(CMBTOT.LT.0.0)  CMBTOT=0.0
3590     WRITE (6,222) FRACEO,WIDEO,ACTEO,FRACEI,WIDEI,ACTEI,ACTENT
3600     WRITE (6,223) FRACWO,WIDEO,ACTWO,FRACWI,WIDEI,ACTWI,ACTWNT
3610    222 FORMAT(34HEAST FRACTIONS AND COVERAGE ARE    ,7(F7.3,3X),/)
3620    223 FORMAT(34HWEST FRACTIONS AND COVERAGE ARE    ,7(F7.3,3X),/)
```

```
3630C  IF(LIMSWA.EQ.2) FLIM=580./600.
3640C   LIM   IS INPUT DATA TO DEFINE IF SWATH WIDTH IS LIMITED
3650C
3660C    IF(LIMSWA.NE.2) FLIM=1.0
3670C   IF(FRACE.GE.FLIM) FRACE=FLIM
3680C   IF(FRACW.GE.FLIM) FRACW=FLIM
3690C   CONST = (SWIDTH/360.0)*40.0751*(DT*60.0)*V/1000.)
3700C    AEAST = FRACE*CONST
3710    IF (ACTENT.GE.ACTSWA)  ACTENT = ACTSWA
3720    IF (ACTWNT.GE.ACTSWA)  ACTWNT = ACTSWA
3730    AEAST = (ACTENT/1000.)*(DT*60.0)*(V/1000.)
3740    AWEST = (ACTWNT/1000.)*(DT*60.0)*(V/1000.)
3741    ACMTOT=(CMBTOT/1000.)*(DT*60.)*(V/1000.)
3750C    AWEST = FRACW*CONST
3760    PEAST=0.0
3770    PWEST=0.0
3780    IF(AEAST.GE.AWEST)  PEAST=AEAST
3790    IF(AEAST.LE.0.0)  PEAST=0.0
3800    IF(AWEST.GT.AEAST)  PWEST=AWEST
3810    IF(AWEST.LE.0.0) PWEST=0.0
3820C    WIDE=(SWIDTH/360.0)*40075.0
3830C
3840  GO TO 331
3850C
3860     63   CONTINUE
3870C
3880     ACCUM=ACCUM + AWEST +AEAST
3881    TACCMB=TACCMB+ACMTOT
3890    TOTW=TOTW+AWEST
3900    TOTE=TOTE+AEAST
3910    PCCUM=PCCUM + AMAX1(PWEST,PEAST)
3920    POINT=POINT + AMAX1(PWEST,PEAST)
3930    IF(SSLAT.GT.LATOLD)  BET2="ASCEND"
3940    IF(SSLAT.LT.LATOLD)   BET2="DESCEN"
3950    ALPH1="TIME"
3960    ALPH2="OMEGA"
3970    ALPH3="WIDTH"
3980    BET1="WEST"
3990    BET3="EAST"
4000    GAM1="WEST"
4010    GAM2="SSAT"
4020    GAM3="EAST"
4030    IF(N10.GT.0) CUT1=WBDO(N10,12)
4040    IF(N10.EO.0) CUT1=SWBW
4050    IF(N20.GT.0)  CUT2=WBDO(N20,13)
4060    IF(N20.EQ.0)  CUT2=SWBE
4070    IF(N30.GT.0)  CUT3=EBDO(N30,12)
4080    IF(N30.EQ.0)  CUT3=SEBW
4090    IF(N40.GT.0)  CUT4=EBDO(N40,13)
4100    IF(N40.EQ.0)  CUT4=SEBE
4110C
4120C
4130    IF(IPRNT.LE.2)
```

```
4140&  WRITE(6,200) T,THETA,SSLAT,SSLONG,V,SELATO,SELONO,SWLATO,SWLONO,
4150&    AWEST,AEAST,ACCUM
4160C
4170    WRITE(6,220) ALPH1,T,BET1,SWLONO,SWLATO,N1O,CUT1,N3O,CUT3,
4180&     FRACWO,AWEST, GAM1,TOTW,PWEST
4190    WRITE(6,220) ALPH2,THETA,BET2,SSLONG,SSLAT,NWY,SSBW,
4200&      NEY,SSBE,SSLONG,ACCUM,GAM2,ACCUM,PCCUM
4210    WRITE(6,220)  ALPH3,WIDEO,BET3,SELONO,SELATO,N2O,CUT2,
4220&     N4O,CUT4,FRACEO,AEAST,GAM3,TOTE,PEAST
4231   WRITE(6,203)  TACCMB
4250C
4260    220 FORMAT(1H ,A6,3X,F8.3,2X,A6,3X,2(F8.3,2X),2(I4,2X,F8.3,2X),
4270&    F8.6,3X,F7.2,3X,A6,3X,F7.2,3X,F7.2)
4280C
4290   200  FORMAT(1HO,F8.2,3X,F6.2,3X,F6.2,3X,F6.2,3X,F6.2,3X,F10.1,3X,4(4X,F6.2),
4300&   2X,2(2X,F6.2),2X,F10.2//)
4310   201  FORMAT(1H ,4X,9HBOUND-W  ,4X,9HBOUND-E  ,3X,9H  LONG   ,
4320&    3X,9H   LAT   ,6HNWEST ,6H NEAST ,3X,5HSLOPE,5X,4HCEPT)
4330    202  FORMAT(1H ,4X,4(F11.4),2(I6),2(2X,F11.5)2X,F7.5)
4331   203  FORMAT(35HNO BLIND SPOT SENSOR COVERAGE IS   ,F9.3,////)
4340C
4350C
4360   GO TO 904
4370C
4380C  END OF MODIFICATION
4390C       *     *          :         *         *
4400  899  CONTINUE
4410    ACCUM = 0.0
4420    PCCUM=0.0
4430    TOTW=0.0
4440    TOTE=0.0
4450    DT=TMINS/180.0
4460    DOMG=DT*OMGDOT/TMINS
4470    DWP=DT*WPDOT/TMINS
4480C
4490   904  CONTINUE
4500   LATOLD = SSLAT
4510    ELNGND = ELNGND + DOMG
4520  WP=WP+DWP
4530    IPT=0
4540  910 T=T+DT
4550    IF(T.LE.TLIM) GO TO 5
4560    PRINT 103
4570    PRINT,"AREA ACCUMULATION FOR POINTING SENSOR IS  ",POINT
4580  PRINT 103
4590C   PRINT,"FINISHED? 1-YES; 2-NO"
4600C  ICONTI=1,END.  ICONTI=2,NEW ORBIT,ETC.  ICONTI=3, NEW SWATH
4610   READ, ICONTI,LIMSWA
4620   GOTO(999,1,2),ICONTI
4630  100 FORMAT(F8.2,F9.2,2(F8.2),F10.3,F12.3,F9.3,F8.2)
4640 101 FORMAT(F8.2,F9.2,F8.2,F7.2,F9.2,F10.2,F9.2,F8.2,I4)
4650 102 FORMAT(32X,5(F8.2))
4660 103 FORMAT(//)
4670 999  CONTINUE
4680   STOP
4690       END
```

```
4700C
4710C
4720 SUBROUTINE SWATH(LATCUR,LONCUR,LATOLD,SWIDTH,LATUP,LONUP,LATLOW,
4730&       LONLOW,BINCL)
4740C
4750C   THIS SUBROUTINE TAKES THE LATITUDE AND LONGITUDE OF A NADIR POINT
4760C   AND RETURNS THE LATTITUDES AND LOGITUDES OF POINTS ON THE UPPER
4770C   AND LOWER EDGES OF A SWATH SEEN BY THE SATELLITE.
4780C
4790C   INPUT VARIABLES (NOTE: ALL ANGLES ARE IN DEGREES):
4800C
4810C      LATCUR = CURRENT LATTITUDE OF NADIR
4820C      LONCUR = CURRENT LONGITUDE  "   "
4830C      LATOLD = LATITUDE OF PREVIOUS NADIR POINT
4840C      BINCL  = ANGLE OF INCLINATION OF THE ORBIT
4850C      SWIDTH = DISTANCE FROM THE NADIR POINT TO THE EDGE OF THE
4860C               SWATH ( IN DEGREES OF ARC ALONG A GREAT CIRCLE)
4870C
4880C   OUTPUT VARIABLES:
4890C
4900C      LATUP  = LATITUDE OF POINT ON THE UPPER EDGE OF THE SWATH
4910C      LONUP  = LONGITUDE "   "    "  "    "     "   "  "    "
4920C      LATLOW = LATITUDE  "   "    "  "  LOWER   "   "  "    "
4930C      LONLOW = LONGITUDE "   "    "  "    "     "   "  "    "
4940C
4950    REAL LATCUR,LONCUR,LATOLD,LATUP,LONUP,LATLOW,LONLOW,NINETY
4960C
4970    PI = 3.14159265358979323846
4980    NINETY = PI/2.0
4990C
5000C   FIRST CONVERT ALL THE INPUT VARIABLES TO RADIANS
5010C
5020    LATCUR = LATCUR*PI/180.
5030    LONCUR = LONCUR*PI/180.
5040    LATOLD = LATOLD*PI/180.
5050    WIDTH  = SWIDTH*PI/180.
5060    B      = BINCL*PI/180.
5070C
5080C   CALCULATE THE ARCS FOR THE UPPER TRACE
5090C
5100  ANGA = ARSIN(COS(B)/COS(LATCUR))
5110  ANGALP = NINETY - ANGA
5120  POLCUR = NINETY - LATCUR
5130  POLUP  = ARCOS(COS(WIDTH)*COS(POLCUR)+SIN(WIDTH)*SIN(POLCUR)*
5140&          COS(ANGALP))
5150  ANG GAM = ARCOS((COS(WIDTH)-COS(POLUP)*COS(POLCUR))/
5160&           (SIN(POLUP)*SIN(POLCUR)))
5170C
5180C   CLACULATE THE ARCS FOR THE LOWER TRACE
5190C
```

```
5200  ANG DEL = ANG A + NINETY
5210  POLLOW = ARCOS(COS(WIDTH)*COS(POLCUR)+SIN(WIDTH)*SIN(POLCUR)*
5220&           COS(ANGDEL))
5230  ANG PHI =ARCOS((COS(WIDTH)-COS(POLCUR)*COS(POLLOW))/
5240&             (SIN(POLCUR)*SIN(POLLOW)))
5250C
5260C   CALCULATE LATITUDE & LONGITUDE OF UPPER & LOWER TRACES
5270C
5280   IF(LATCUR.LT.LATOLD) GOTO 10
5290C    YOU'RE HERE IF THE SATELLITE IS HEADING NORTH
5300      LATUP = NINETY - POLUP
5310      LONUP = LONCUR - ANGGAM
5320      LATLOW= NINETY - POLLOW
5330      LONLOW= LONCUR + ANGPHI
5340      GOTO 20
5350C
5360C    YOU'RE HERE IF THE SATELLITE IS HEADING SOUTH
5370#10    LATUP = NINETY - POLUP
5380       LONUP = LONCUR + ANGGAM
5390       LATLOW= NINETY - POLLOW
5400       LONLOW= LONCUR - ANGPHI
5410C
5420C  CONVERT EVERYTHING BACK TO DEGREES
5430C
5440#20  LATUP = LATUP * 180./PI
5450     LATLOW= LATLOW*  180./PI
5460     LONUP = LONUP*180./PI
5470     LONLOW= LONLOW*180./PI
5480     LATOLD= LATCUR*180./PI
5490    LATCUR = LATCUR*180./PI
5500    LONCUR= LONCUR* 180./PI
5510   RETURN
5520   END
5530C
5540C
5550C   THIS ROUTINE TAKES THE LATITUDE OF A POINT, AND FROM THE
5560C    INPUT TABL;LE OF BOUNDARIES RETURNS THE EAST AND WEST
5570C    BOUNDARIES FOR THE INPUT LATITUDE.
5580C
5590C
5600    SUBROUTINE EDGE(WB,EB,NE,NW,XLAT,ELONG,WLONG)
5610    DIMENSION WB(24,13),EB(24,13)
5620    COMMON  NUMW,NUME
5630C
5640    ELONG=EB(NE,3) + (EB(NE,3)-EB(NE+1,3))/
5650&   (EB(NE,2)-EB(NE+1,2))*(XLAT-EB(NE,2))
5660  IF(NE.EQ.0)  ELONG=EB(1,3)
5670    IF(NE.EQ.NUME)    ELONG=EB(NUME,3)
5680    WLONG = WB(NW,3) + (WB(NW,3)-WB(NW+1,3))/
5690&   (WB(NW,2) - WB(NW+1,2))*(XLAT - WB(NW,2))
5700    IF(NW.EQ.0)  WLONG=WB(1,3)
5710    IF(NW.EQ.NUMW)  WLONG=WB(NUMW,3)
5720      RETURN
5730    END
```

```
5740C
5750C
5760    SUBROUTINE AREA(WB,EB,SELON,SELAT,SWLON,SWLAT,FRACE,FRACW,N1,N2,
5770   &    N3,N4)
5780C
5790C
5800C     THIS ROUTINE TAKES THE COORDINATES OF A CLOSED ZONE
5810C        AND THE POINTS FROM A GROUND TRACE (SWATH) AND
5820C        CALCULATES THE AREA COMMON TO ZONE AND SWATH.
5830     DIMENSION WB(24,13),EB(24,13)
5840    COMMON NUMW,NUME,SSLAT,SSLONG
5850       COMMON    NEX,NWX,NEY,NWY,NEZ,NWZ
5860    COMMON  SLOPSW,CEPTSW,SLOPSE,CEPTSE,SLOPAV,CEPTAV
5870    COMMON SEBW,SEBE,SWBE,SWBW
5880C
5890C    REJECT ANY SWATHS COMPLETELY NORTH OR SOUTH OF THE ZONE.
5900C    PRINT,"AREA SUBROUTINE CALLED. SSLAT IS     ",SSLAT
5910    N1=0
5920    NR1=0
5930    NRR1=0
5940    N2=0
5950    NR2=0
5960    NRR2=0
5970    N3=0
5980    NR3=0
5990    NRR3=0
6000    N4=0
6010    NR4=0
6020    NRR4=0
6030    JIM=0
6040    JEAN=0
6050     EDGE1=0.0
6060     EDGE2=0.0
6070     EDGE3=0.0
6080     EDGE4=0.0
6090     IREW=0
6100     IREE=0
6110     FRACE=0.0
6120     FRACW=0.0
6130C
6140    IF(NUME.LE.0) NUME = 1
6150    IF(NUMW.LE.0)  NUMW = 1
6160C
6170    SNOR=AMIN1(SELAT, SWLAT)
6180     SSOUTH=AMAX1(SELAT,SWLAT)
6190    DUMWH = 0.0
6200    DUMWL=90.0
6210    DUMEH=0.0
6220    DUMEL=90.0
6230   DO 101  MW=1,NUMW
6240    DUMWL=AMIN1(WB(MW,2),DUMWL)
6250    DUMWH=AMAX1(WB(MW,2),DUMWH)
6260   101  CONTINUE
```

```
      DO 102  NW=1,NUME
       DUMEL=AMIN1(EB(NW,2),DUMEL)
       DUMEH=AMAX1(EB(NW,2),DUMEH)
  102  CONTINUE
       BNOR=AMAX1(DUMWH,DUMEH)
       BSOUTH=AMIN1(DUMWL,DUMEL)
        IF(SNOR.GE.BNOR)  GO TO 198
         IF(SSOUTH.LE.BSOUTH)   GO TO 198
C
C
C     EQUATIONS OF LINES ARE IN THE FORM
C        Y = MX +B;  WHERE M IS THE SLOPE (SLOP) OF
C     OF THE LINE, AND B IS THE Y INTERCEPT (CEPT).
C    HENCE, SLOPSW IS THE SLOPE OF THE SWATH, FROM
C    THE CENTER TO THE WEST SIDE.  O, SLOPSE IS THE
C    SLOPE OF THE SWATH, FROM THE CENTER TO THE EAST
C    EDGE.
C
C    THE INTERSECTIONS OF THE SWATH WITH THE BOUNDARY
C    LINES ARE COMPUTED AND STORED IN THE BOUNDARY
C     TABLES IN COLUMNS 7,8,9 FOR WEST INTERSECTIONS,
C     AND COLUMNS 9,10,11 FOR EAST INTERSECTIONS.
C    EACH SET IS LATITUDE, LONGITUDE, AND "FLAG"
C    FOR EACH LINE OF THE INPUT BOUNDARY TABLE.
C
       SLOPSW = (SWLAT-SSLAT)/(SWLON-SSLONG)
       CEPTSW = SWLAT - SLOPSW*SWLON
      SLOPSE = (SSLAT - SELAT)/(SSLONG-SELON)
       CEPTSE = (SELAT - SLOPSE*SELON)
      SLOPAV = (SWLAT-SELAT)/(SWLON-SELON)
      CEPTAV = SELAT - SLOPAV*SELON
C
      DO 100  JO=1,NUMW
C
C     CHECKING FOR PARALLEL LINES!
C
      K=0
      WB(JO,12)=0.0
      WB(JO,13)=0.0
C
      IF(ABS(SLOPSW-WB(JO,4)).LT.0.01)      K=1
      IF(K.EQ.1)  WB(JO,7)=350.
      IF(K.EQ.1)  GO TO 50
      WB(JO,7) = (WB(JO,5)-CEPTSW)/
     &  (SLOPSW-WB(JO,4))
   50 CONTINUE
      IF(ABS(SLOPSE-WB(JO,4)).LT.0.01)  K=2
      IF(K.EQ.2)  WB(JO,10)=350.
      IF(K.EQ.2) GO TO 51
      WB(JO,10) = (WB(JO,5)-CEPTSE)/
     &  (SLOPSE-WB(JO,4))
   51 CONTINUE
      WB(JO,6) = WB(JO,4)*WB(JO,7) + WB(JO,5)
       WB(JO,9)= WB(JO,4)*WB(JO,10) + WB(JO,5)
```

```
6810C
6820    CALL FLAG(WB(JO,2),WB(JO,3),WB(JO+1,2),WB(JO+1,3),
6830&    WB(JO,6),WB(JO,7),WB(JO,8))
6840     IF (WB(JO,8).GT.0.0)  EDGE1=WB(JO,8)
6850C
6860    IF(WB(JO,8) GE.SWLON.AND.WB(JO,8).LE.SSLONG)
6870&    WB(JO,12)=WB(JO,8)
6880    IF(WB(JO,12).GT.0.0.AND.N1.EQ
6890    IF(WB(JO,12).GT.0.0.AND.N1.GT.0.AND.N1.LT.JO)  NR1=JO
6900    IF(WB(JO,12).GT.0.0.AND.NR1.GT.0.AND.NR1.LT.JO) NRR1=JO
6910    IF(NRR1.GT.0)  WRITE(6,500) NRR1,WB(JO,6),WB(JO,7)
6920C
6930   CALL FLAG(WB(JO,2),WB(JO,3),WB(JO+1,2),WB(JO+1,3),
6940&    WB(JO,9),WB(JO,10),WB(JO,11))
6950     IF(WB(JO,11).GT.0.0)  EDGE2=WB(JO,11)
6960C
6970    IF(WB(JO,11).GE.SSLONG.AND.WB(JO,11).LE.SELON)
6980&    WB(JO,13)=WB(JO,11)
6990    IF(WB(JO,13).GT.0.0.AND.N2.EO.0)  N2=JO
7000    IF(WB(JO,13).GT.0.0.AND.N2.GT.0.AND.N2.LT.JO)  NR2=JO
7010    IF(WB(JO,13).GT.0.0.AND.NR2.GT.0.AND.NR2.LT.JO)  NRR2=JO
7020    IF(NRR2.GT.0) WRITE(6, 500) NRR2,WB(JO,9),WB(JO,10)
7030   100  CONTINUE
7040C
7050   DO 120  JIL=1,NUME
7060    K=0
7070    EB(JIL,12)=0.0
7080    EB(JIL,13)=0.0
7090C
7100    IF(ABS(SLOPSE-EB(JIL,4)).LT.0.01)    K=3
7110    IF(K.EQ.3) EB(JIL,10)=350.
7120    IF(K.EQ.3) GO TO 53
7130    EB(JIL,10) = (EB(JIL,5)-CEPTSE)/
7140&    (SLOP3E-EB(JIL,4))
7150    53 CONTINUE
7160    IF(ABS(SLOPSW-EB(JIL,4)).LT.0.01)  K=4
7170    IF(K.EO.4)  EB(JIL,7)=350.
7180    IF(K.EQ.4) GO TO 54
7190    EB(JIL,7) = (EB(JIL,5)-CEPTSW)/
7200&    (SLOPSW-EB(JIL,4))
7210    54 CONTINUE
7220    EB(JIL,9) = EB(JIL,4)*EB(JIL,10) + EB(JIL,5)
7230    EB(JIL,6) = EB(JIL,4)*EB(JIL,7) + EB(JIL,5)
7240C
7250    CALL FLAG (EB(JIL,2),EB(JIL,3),EB(JIL+1,2),EB(JIL+1,3),
7260&    EB(JIL,6),EB(JIL,7),EB(JIL,8))
7270C
7280    IF(EB(JIL,8).GE.SWLON.AND.EB(JIL,8).LE.SSLONG)
7290&    EB(JIL,12)=EB(JIL,8)
7300    IF(EB(JIL,8).GT.0.0)    EDGE3=EB(JIL,8)
7310    IF(EB(JIL,12).GT.0.0.AND.N3.EO.0)  N3=JIL
7320    IF(EB(JIL,12).GT.0.0.AND.N3.GT.0.AND.N3.LT.JIL)  NR3=JIL
7330    IF(EB(JIL,12).GT.0.0.AND.NR3.GT.0.AND.NR3.LT.JIL)  NRR3=JIL
7340    IF(NRR3.GT.0)  WRITE(6,500) NRR3,EB(JIL,6),EB(JIL,7)
7350C
```

```
7360   CALL FLAG(EB(JIL,2),EB(JIL,3),EB(JIL+1,2),EB(JIL+1,3),
7370&   EB(JIL,9),EB(JIL,10),EB(JIL,11))
7380   IF(EB(JIL,11).GT.0.0)  EDGE4=EB(JIL,11)
7390C
7400   IF(EB(JIL,11).GE.SSLONG.AND.EB(JIL,11).LE.SELON)
7410&   EB(JIL,13)=EB(JIL,11)
7420   IF(EB(JIL,13).GT.0.0.AND.N4.EQ.0)  N4=JIL
7430   IF(EB(JIL,13).GT.0.0.AND.N4.GT.0.AND.N4.LT.JIL) NR4=JIL
7440   IF(EB(JIL,13).GT.0.0.AND.NR4.GT.0.AND.NR4.LT.JIL) NRR4=JIL
7450    IF(NRR4.GT.0)   WRITE(6,500)  NRR4,EB(JIL,9),EB(JIL,10)
7460   120   CONTINUE
7470    IF(WB(N1,1).LT.0.0.OR.WB(N3,1).LT.0.0)  IREW=2
7480   IF(EB(N2,1).LT.0.0.OR.EB(N4,1).LT.0.0)   IREE=2
7490C
7500   WHALF=SWLON-SSLONG
7510   IF(NR1.GT.0.OR.NR3.GT.0)  GO TO 250
7520    IF(N3.GT.0.AND.N1.EQ.0)  JIM=1
7530   IF(JIM.EQ.1.AND.EB(N3,6).LT.EB(N3+1,2))   FRACW=ABS((EB(N3,12)-
7531&   SWLON)/WHALF)
7532   IF(JIM.EQ.1.AND.EB(N3,6).GE.EB(N3+1,2))   FRACW=1.-ABS((EB(N3,12)-
7533&   SWLON)/WHALF)
7540    IF(N3.GT.0.AND.N1.GT.0)   JIM=2
7550    IF(JIM.EQ.2) FRACW=(WB(N1,12)-EB(N3,12))/WHALF
7560    IF(N3.EQ.0.AND.N1.GT.0)   JIM=3
7570   IF(JIM.EQ.3.AND.WB(N1,6).LT.WB(N1+1,2))   FRACW=ABS((WB(N1,12)-
7571&   SSLONG)/WHALF)
7572   IF(JIM.EQ.3.AND.WB(N1,6).GE.WB(N1+1,2))   FRACW=1.-ABS((WB(N1,12)-
7573&   SSLONG)/WHALF)
7590    IF(JIM.EQ.3.AND.IREW.EQ.2)  FRACW=  ((SWLON-WB(N1,12))
7600&   /WHALF)
7610    IF(N3.EQ.0.AND.N1.EQ.0)  JIM=4
7620   IF(JIM.EQ.4.AND.(SSLONG.LE.EDGE3).AND.(SWLON.GT.EDGE1)) FRACW=1.0
7630C
7640   250   IF(NR1.GT.0.AND.WB(N1,4).GE.0.0)   FRACW=ABS((WB(NR1,12)-
7641&   WB(N1,12))/WHALF)
7642   IF(NR1.GT.0.AND.WB(N1,4).LT.0.0)  FRACW=1.-ABS((WB(NR1,12)-
7643&   WB(N1,12))/WHALF)
7644   IF(NR3.GT.0.AND.EB(N3,4).LT.0.0)  FRACW=ABS((EB(NR3,12)-
7645&   EB(N3,12))/WHALF)
7646   IF(NR3.GT.0.AND.EB(N3,4).GE.0.0)  FRACW=1.-ABS((EB(NR3,12)-
7647&   EB(N3,12))/WHALF)
7660C
7670C
7680C
7690    EHALF=SELON-SSLONG
7700   IF(NR2.GT.0.OR.NR4.GT.0)  GO TO 300
7710    IF(N2.EQ.0.AND.N4.EQ.0)  JEAN=1
7720   IF(JEAN.EQ.1.AND.(SSLONG.GT.EDGE2).AND.(SELON.LE.EDGE4)) FRACE=1.0
7730    IF(N2.EQ.0.AND.N4.GT.0)  JEAN=2
7740   IF(JEAN.EQ.2.AND.EB(N4,9).LT.EB(N4+1,2))   FRACE=ABS((EB(N4,12)-
7741&   SSLONG)/EHALF)
7742   IF(JEAN.EQ.2.AND.EB(N4,9).GE.EB(N4+1,2))   FRACE=1.-ABS((EB(N4,
7743&   13)-SSLONG)/EHALF)
```

```
      IF(JEAN.EQ.2.AND.IREE.EQ.2) FRACE=  ((SELON-EB(N4,13))
     &  /EHALF)
      IF(N2.GT.0.AND.N4.EQ.0)   JEAN=3
     IF(JEAN.EQ.3.AND.WB(N2,9).GE.WB(N2+1,2))   FRACE=ABS((WB(N2,13)-
     &  SSLONG)/EHALF)
     IF(JEAN.EQ.3.AND.WB(N2,9).LT.WB(N2+1,2))   FRACE=1.-ABS((WB(N2,
     &  13)-SSLONG)/EHALF)
      IF(N2.GT.0.AND.N4.GT.0)   JEAN=4
      IF(JEAN.EQ.4) FRACE=(EB(N4,13)-WB(N2,13))/EHALF
C
  300   IF(NR2.GT.0.AND.WB(N2,4).GE.0.0)  FRACE=ABS((WB(NR2,13)-
     &  WB(N2,13))/EHALF)
     IF(NR2.GT.0.AND.WB(N2,4).LT.0.0)   FRACE=1.-ABS((WB(NR2,13)-
     &  WB(N2,13))/EHALF)
     IF(NR4.GT.0.AND.EB(N4,4).LT.0.0)   FRACE=ABS((EB(NR4,13)-
     &  EB(N4,13))/EHALF)
     IF(NR4.GT.0.AND.EB(N4,4).GE.0.0)   FRACE=1.-ABS((EB(NR4,13)-
     &  EB(N4,13))/EHALF)
C
C
  488  FORMAT(1H0,2(I5,2X,F9.4),4(3X,I5)//)
C
  500  FORMAT(1H0,35HRE-ENTRANT BOUNDARIES; THIS POINT IS,
     &   19H THIRD INTERSECTION,2X,I5,2(2X,F9.4)//)
C
     NO=2
      IF(NO.EQ.2) GO TO 199
     WRITE(6,188)
     DO 130  KIL=1,NUMW
     WRITE(6,200) (WB(KIL,J),J=1,13)
     130   CONTINUE
C
      WRITE(6,488) N1,EDGE1,N2,EDGE2,NR1,NRR1,NR2,NRR2
C
C
     WRITE(6,188)
     DO 140  LIL=1,NUME
     WRITE(6,200)  (EB(LIL,J), J=1,13)
     140   CONTINUE
C
      WRITE(6,488) N3,EDGE3,N4,EDGE4,NR3,NRR3,NR4,NRR4
C
C
C
```

```
8110C     WRITE (6,404) SLOPBWX,CEPTBWX,SLOPSW,CEPTSW,SLOPBEZ,CEPTBEZ,
8120C&     SECTWX,SECTEZ,SECTWZ,SECTEX
8130    404  FORMAT(1H0,10(2X,F9.3)//)
8140C
8150    188  FORMAT(1H0,4X,4HLINE,4X,3HLAT,4X,4HLONG,10X,
8160&    5HSLOPE,4X,9HINTERCEPT,4X,6HWBOUND,4X,4HWLON,
8170& 6X,5HWFLAG,3X,6HEBOUND,4X,4HELON,7X,5HEFLAG,2X,6H(X,13),1X,6H(X,13)//)
8180C
8190    200  FORMAT(1H ,3(2X,F7.3),2(2X,F10.4)
8200&    ,2(2X,F8.4),3X,F5.1,2(1X,F8.4),3X,3(2X,F5.1))
8210C
8220     GO TO 199
8230    198   CONTINUE
8240C
8250c
8260C     PRINT,"       JUMP BACK FROM SUBROUTINE   *****  "
8270 199   CONTINUE
8280      RETURN
8290      END
8300C
8310C
8320    SUBROUTINE FLAG(BLAT1,BLON1,BLAT2,BLON2,SLAT,SLON,FLAGGE)
8330C
8340C  RESET TIC AND FLAGGE TO ZERO BEFORE NEXT CASE
8350C
8360    TIC=0.00
8370    FLAGGE=0.00
8380C
8390C  TEST TO SEE IF INTERCEPT MEETS LATITUDE TEST
8400C
8410    IF((SLAT.GE.BLAT1.AND.SLAT.LE.BLAT2).OR.
8420&   (SLAT.LE.BLAT1.AND.SLAT.GE.BLAT2))  TIC=2.00
8430C
8440C   TEST INTERCEPT AGAINST LONGITUDE BOUNDARIES
8450C
8460    IF(TIC.GT.1.00.AND.((SLON.GE.BLON1.AND.SLON.LE.BLON2).OR.
8470&    SLON.LE.BLON1.AND.SLON.GE.BLON2))  FLAGGE=SLON
8480C
8490    RETURN
8500END
```

II. PROGRAM OUTPUT

a. Sample Simulation Output

Numerous print options have been used to develop and utilize the flexibility of COASTCOVER to compare orbit/sensor configurations and perform sensitivity analyses. Figure A-1 is a primary print option for final coverage computations. The key numbers in the sample output (A, B, C, etc.) are explained; the few that are not explained are either redundant or related to intermediate calculations needed for final answers.

b. Tabular Summaries of Zone-by-Zone Simulation Results for Ten Cases

Tables A-1 through A-40 list the pass-by-pass coverage results of simulations for each target zone for the 10 orbit/sensor configurations (Cases I through IV, Table 5.2-1).

ORIGINAL PAGE IS
OF POOR QUALITY

FIGURE A-1: SAMPLE OF COASTCOVER OUTPUT

Results of one time step along orbit (one of several print options)

```
                                     A        B        C          D        E         F        G

EAST FRACTIONS AND COVERAGE ARE    0.660   472.937  312.285     1.000   128.026   128.026   184.259
WEST FRACTIONS AND COVERAGE ARE    1.000   472.937  472.937     1.000   128.026   128.026   344.911
            H                          J                                                       K                L        M
TIME     214.621  WEST          210.833   56.722  0   206.017  0   204.416  1.000000    21.38  WEST    26.73    21.38
OMEGA     58.000  000000        218.555   57.374  8   204.741  4   223.867  ********   157.87  SSAT   197.87   141.10
WIDTH    472.937  EAST          226.452   57.541  3   224.524  4   223.769  0.660310    11.42  EAST   131.14     0.
NO BLIND SPOT SENSOR COVERAGE IS   164.025
                                     N

EAST FRACTIONS AND COVERAGE ARE    0.606   472.937  286.820     1.000   128.026   128.026   158.795
WEST FRACTIONS AND COVERAGE ARE    1.000   472.937  472.937     1.000   128.026   128.026   344.911

TIME     214.759  WEST          210.608   57.209  0   205.064  0   205.325  1.000000    21.38  WEST    48.11    21.38
OMEGA     58.500  000000        218.430   57.872  9   204.934  4   223.425  ********   189.10  SSAT   189.10   182.48
WIDTH    472.937  EAST          226.435   58.039  0   224.014  5   223.285  0.606467     9.84  EAST   140.98     0.
NO BLIND SPOT SENSOR COVERAGE IS   185.413
```

A: Fraction of outer swath in target zone
B: Outer access swath width (km)
C: Width of target zone covered by outer access swath (km)
D: Fraction of inner swath in target zone
E: Inner access swath width (km)
F: Width of target zone covered by inner access swath (km)
G: Net target zone width accessible (km)
H: Orbit time (minutes), central angle (degrees), and outer access swath width (km)
J: Longitude and latitude of sub-satellite point and west and east outer access swath limits
K: West side (top number) and east side (bottom number) area (in 10^3 Km^2) viewable during this time step
L: West side, total, and east side viewable areas (in 10^3 Km^2) accumulated during this pass over the target zone
M: West side or east side (maximum of top or bottom number from K above) area viewed by pointable sensor during this time step and accumulation (middle number) of this pointable option during this pass over the target zone (all in 10^3 Km^2)
N: Area (in 10^3 Km^2) accumulated during this repeat cycle by a pointable sensor option not limited by the blind spot (i.e., no inner swath limit)

TABLE A-1

ORBITAL COVERAGE SIMULATION

CASE IA : 2 - DAY [illegible], 2450 SWATH POINTACLE SENSOR

TARGET ZONE: ATLANTIC

DAY#	PASS#	ACCESS TIME	ASCENDING WEST	ASCENDING EAST	DESCENDING WEST	DESCENDING EAST	DAILY SUB-TOTALS ASCENDING	DAILY SUB-TOTALS DESCENDING
1	1	2 MIN.		26				
	2	2 MIN.			85		71	174 } 1
	3	2 MIN.				11		
	1	1 MIN	31	240				
2		1 MIN			111	280	241	774 } 2
	2	2 MIN	211					

DAILY AVERAGE ACCESS TIME = 1 MIN

GRAND TOTAL: 1002 ASCENDING + 952 DESCENDING = 1954

"NO BLIND SPOT" SENSOR TOTAL: 2131

"ONE-SIDE ONLY" SENSOR TOTALS:

ASCENDING WEST/DESCENDING EAST: 1021

ASCENDING EAST/DESCENDING WEST: 951

NOTE: All Coverage Figures are in 1000 Km^2

TABLE A-2
ORBITAL COVERAGE SIMULATION

CASE TA : 2 - DAY [illegible] SWATH [illegible] SENSOR

TARGET ZONE: [illegible]

DAY#	PASS#	ACCESS TIME	ASCENDING WEST	ASCENDING EAST	DESCENDING WEST	DESCENDING EAST	DAILY SUB-TOTALS ASCENDING	DAILY SUB-TOTALS DESCENDING
1	1	MIN.	1 1	105				
	2	2 MIN.			178	67	392	245
	3		(NEGLIGIBLE)					
	4	1 MIN.		139				
	5	1 MIN.			13		139	17
	6	1 MIN				151		

ORIGINAL PAGE IS OF POOR QUALITY

GRAND TOTAL: 431 ASCENDING + 415 DESCENDING = 846

DAILY AVERAGE ACCESS TIME = 1 MIN.

"NO BLIND SPOT" SENSOR TOTAL: 12

"ONE-SIDE ONLY" SENSOR TOTALS:

ASCENDING WEST/DESCENDING EAST: 411

ASCENDING EAST/DESCENDING WEST: 42

NOTE: All Coverage Figures are in 1000 Km^2

TABLE A-3

ORBITAL COVERAGE SIMULATION

CASE IA : 1 - DAY Min in Nov. 34° SWATH RAINBOW SENSOR

TARGET ZONE: PACIFIC

DAY#	PASS#	ACCESS TIME	ASCENDING WEST	ASCENDING EAST	DESCENDING WEST	DESCENDING EAST	DAILY SUB-TOTALS ASCENDING	DAILY SUB-TOTALS DESCENDING
1	1	3 MIN.				308	0	308
2	2	5 MIN.	404				404	674
	3	5 MIN.			548	126		

DAILY AVERAGE ACCESS TIME = 7 MIN.

GRAND TOTAL:

404 ASCENDING

\+ 970 DESCENDING

= 1374

"NO BLIND SPOT" SENSOR TOTAL: 1317

"ONE-SIDE ONLY" SENSOR TOTALS:

ASCENDING WEST/DESCENDING EAST: 1274

ASCENDING EAST/DESCENDING WEST: 952

NOTE: All Coverage Figures are in 1000 Km^2

TABLE A-4

ORBITAL COVERAGE SIMULATION

CASE IA : 2 - DAY [illegible], 3[illegible] SWATH POINTAPLE SENSOR

TARGET ZONE: ALASKA

DAY#	PASS#	ACCESS TIME	ASCENDING WEST	ASCENDING EAST	DESCENDING WEST	DESCENDING EAST	DAILY SUB-TOTALS ASCENDING	DAILY SUB-TOTALS DESCENDING	
1	1	2 MIN.	156	118			274	[illegible]	1
	2	2 MIN.			195	196			
	"	- MIN.							
2	1	2 MIN.	176				358	22[illegible]	2
	"	2 MIN.		182					
	"	2 MIN.			73	156			

DAILY AVERAGE ACCESS TIME = 6 MIN.

GRAND TOTAL: 632 ASCENDING + [illegible] DESCENDING = 1252

"NO BLIND SPOT" SENSOR TOTAL: 1293

"ONE-SIDE ONLY" SENSOR TOTALS:

ASCENDING WEST/DESCENDING EAST: 684

ASCENDING EAST/DESCENDING WEST: [illegible]

NOTE: All Coverage Figures are in 1000 Km^2

TABLE A-5

ORBITAL COVERAGE SIMULATION

CASE IP : 2 - DAY [illegible], [illegible] SWATH N-N-[illegible] SENSOR

TARGET ZONE: [illegible]

DAY#	PASS#	ACCESS TIME	ASCENDING WEST	ASCENDING EAST	DESCENDING WEST	DESCENDING EAST	DAILY SUB-TOTALS ASCENDING	DAILY SUB-TOTALS DESCEND
	1	1 Min			25			
	2	1 Min,				[illegible]	[illegible]	1
	3	[illegible]	358	271				
	4	6 Min.			436	465	[illegible]	[illegible]
	5	[illegible]	224					

DAILY AVERAGE ACCESS TIME = [illegible]

GRAND TOTAL: 879 ASCEND

\+ 741 DESCEN

= 1620

"NO BLIND SPOT" SENSOR TOTAL: 1802

"ONE-SIDE ONLY" SENSOR TOTALS:

ASCENDING WEST/DESCENDING EAST: 861

ASCENDING EAST/DESCENDING WEST: 741

NOTE: All Coverage Figures are in 1000 Km^2

TABLE A-6

ORBITAL COVERAGE SIMULATION

CASE IV : 2 - DAY … , 345 km SWATH NON-R… SENSOR

TARGET ZONE: GULF

DAY#	PASS#	ACCESS TIME	ASCENDING WEST	ASCENDING EAST	DESCENDING WEST	DESCENDING EAST	DAILY SUB-TOTALS ASCENDING	DAILY SUB-TOTALS DESCENDING
1	1	2 MIN.	198	78			276	236
	2	2 MIN.			171	65		
2	3	1 MIN.		78			78	94
	4	1 MIN.				94		

… AVERAGE ACCESS TIME = 3 MIN.

GRAND TOTAL: 354 ASCENDING
+ 330 DESCENDING
= 684

"NO BLIND SPOT" SENSOR TOTAL: 722

"ONE-SIDE ONLY" SENSOR TOTALS:

ASCENDING WEST/DESCENDING EAST: 351

ASCENDING EAST/DESCENDING WEST: 321

Note: All Coverage Figures are in 1000 Km^2

TABLE A-7

ORBITAL COVERAGE SIMULATION

CASE IC : 2 - DAY NON SYNC. 345 n.m. SWATH NON ROTATABLE SENSOR

TARGET ZONE: PACIFIC

DAY#	PASS#	ACCESS TIME	ASCENDING WEST	ASCENDING EAST	DESCENDING WEST	DESCENDING EAST	DAILY SUB-TOTALS ASCENDING	DAILY SUB-TOTALS DESCENDING
1	1	3 MIN.				162	0	162 } 1
	2	5 MIN.	318				318	600 } 2
	3	7 MIN.			480	126		

GRAND TOTAL: 318 ASCENDING + 768 DESCENDING = 1166

DAILY AVERAGE ACCESS TIME = 7 MIN.

"NO BLIND SPOT" SENSOR TOTAL: 1578

"ONE-SIDE ONLY" SENSOR TOTALS:

ASCENDING WEST/DESCENDING EAST: 288

ASCENDING EAST/DESCENDING WEST: 576

NOTE: All Coverage Figures are in 1000 Km^2

TABLE A-8

ORBITAL COVERAGE SIMULATION

CASE T2 : 2 - DAY NON-SYNCH. 345 KM SWATH NON-RANGE SENSOR

TARGET ZONE: ALASKA

DAY#	PASS#	ACCESS TIME	ASCENDING WEST	ASCENDING EAST	DESCENDING WEST	DESCENDING EAST	DAILY SUB-TOTALS ASCENDING	DAILY SUB-TOTALS DESCENDING
1	1	2 MIN.	154	120				
	2	2 MIN.			136		274	305 } 1
	3	2 MIN.				169		
2	1	2 MIN.	82					
	2	2 MIN.		163			245	202 } 2
	3	2 MIN.			91	111		

DAILY AVERAGE ACCESS TIME = 2 MIN

GRAND TOTAL: 519 ASCENDING + 507 DESCENDING = 1026

"NO BLIND SPOT" SENSOR TOTAL: 1051

"ONE-SIDE ONLY" SENSOR TOTALS:

ASCENDING WEST/DESCENDING EAST: 516

ASCENDING EAST/DESCENDING WEST: 510

NOTE: All Coverage Figures are in 1000 Km^2

TABLE A-9

ORBITAL COVERAGE SIMULATION

CASE 2 A : 3 - DAY [illegible], [illegible] SWATH [illegible] SENSOR

TARGET ZONE: ATLANTIC

DAY#	PASS#	ACCESS TIME	ASCENDING WEST	ASCENDING EAST	DESCENDING WEST	DESCENDING EAST	DAILY SUB-TOTALS ASCENDING	DAILY SUB-TOTALS DESCENDING
1	1	5 MIN.		70				
	2	2 MIN.			232		459	232
	3	5 MIN.	33	34				
2	4	5 MIN.				599	[illegible]	[illegible]
	5	6 MIN	29	2[illegible]3				
[illegible]	6	[illegible] MIN			507	380	249	[illegible]
	7	[illegible] MIN	249					

DAILY AVERAGE ACCESS TIME = [illegible] MIN.

GRAND TOTAL: [illegible] ASCENDING

\+ [illegible] DESCENDING

= 2882

"NO BLIND SPOT" SENSOR TOTAL: [illegible]

"ONE-SIDE ONLY" SENSOR TOTALS:

ASCENDING WEST/DESCENDING EAST: 1451

ASCENDING EAST/DESCENDING WEST: 423

NOTE: All Coverage Figures are in 1000 Km^2

TABLE A-10

ORBITAL COVERAGE SIMULATION

CASE II A : 3 - DAY Nov. 3rd, 350 km SWATH POINTABLE SENSOR

TARGET ZONE: GULF

DAY#	PASS#	ACCESS TIME	ASCENDING WEST	ASCENDING EAST	DESCENDING WEST	DESCENDING EAST	DAILY SUB-TOTALS ASCENDING	DAILY SUB-TOTALS DESCENDING	
1	1	2 MIN.	191	103					
	2	2 MIN.			39	171	490	216	1
	3	2 MIN.	196						
	4	2 MIN.			215		181	215	2
	5	1 MIN.		181					
	6				(NEGLIGIBLE)				
	7	1 MIN.			162		0	162	3

GRAND TOTAL: 671 ASCENDING + 593 DESCENDING = 1264

[illegible] ACCESS TIME = 3 MIN.

"NO BLIND SPOT" SENSOR TOTAL: 1346

"ONE-SIDE ONLY" SENSOR TOTALS:

ASCENDING WEST/DESCENDING EAST: 726

ASCENDING EAST/DESCENDING WEST: 538

NOTE: All Coverage Figures are in 1000 Km²

TABLE A-11
ORBITAL COVERAGE SIMULATION

CASE IIA: B - DAY [illegible], 356km SWATH [illegible] SENSOR
TARGET ZONE: [illegible]

DAY#	PASS#	ACCESS TIME	ASCENDING WEST	ASCENDING EAST	DESCENDING WEST	DESCENDING EAST	DAILY SUB-TOTALS ASCENDING	DAILY SUB-TOTALS DESCENDING	
1	1	1 MIN.				19	0	19	1
2	2	5 MIN.		665			665	521	2
	3	4 MIN.				521			
3	4	5 MIN.	511	81			592	685	3
	5	5 MIN.			547	138			

DAILY AVERAGE ACCESS TIME = 7 MIN.

GRAND TOTAL: 1257 ASCENDING
+ 1225 DESCENDING
= 2482

"NO BLIND SPOT" SENSOR TOTAL: 2845

"ONE-SIDE ONLY" SENSOR TOTALS:

ASCENDING WEST/DESCENDING EAST: 1159

ASCENDING EAST/DESCENDING WEST: 1273

NOTE: All Coverage Figures are in 1000 Km^2

TABLE A-12

ORBITAL COVERAGE SIMULATION

CASE IIA : 3 - DAY [illegible], [illegible] SWATH POINTABLE SENSOR

TARGET ZONE: ALASKA

DAY#	PASS#	ACCESS TIME	ASCENDING WEST	ASCENDING EAST	DESCENDING WEST	DESCENDING EAST	DAILY SUB-TOTALS ASCENDING	DAILY SUB-TOTALS DESCENDING
1	1	2 MIN.	174	83				
	2	2 MIN.			216		257	322
	3	2 MIN.				106		
2	4	2 MIN.	260					
	[illegible]	[illegible]		[illegible]				
	[illegible]	[illegible]			94		[illegible]	282
	7	[illegible]				188		
	[illegible]	[illegible]	[illegible]					
	1	[illegible]		178			191	172
	[illegible]	[illegible]			241	172		

DAILY AVERAGE ACCESS TIME = [illegible]

GRAND TOTAL: [illegible] ASCENDING

\+ [illegible] DESCENDING

= 1062

"NO BLIND SPOT" SENSOR TOTAL: [illegible]

"ONE-SIDE ONLY" SENSOR TOTALS:

ASCENDING WEST/DESCENDING EAST: 113

ASCENDING EAST/DESCENDING WEST: 141

NOTE: All Coverage Figures are in 1000 Km^2

TABLE-A-13

ORBITAL COVERAGE SIMULATION

CASE II B : 3 - DAY Non Sun-Sync. 350 km SWATH NON-POINTABLE SENSOR

TARGET ZONE: ATLANTIC

DAY#	PASS#	ACCESS TIME	ASCENDING WEST	ASCENDING EAST	DESCENDING WEST	DESCENDING EAST	DAILY SUB-TOTALS ASCENDING	DAILY SUB-TOTALS DESCENDING	
1	1		(NEGLIGIBLE)						
	2	2 MIN.			174		299	174	1
	3	5 MIN.	33	266					
2	4	5 MIN.				489	463	489	2
	5	5 MIN.	226	237					
3	6	6 MIN.			430	271	226	701	3
	7	3 MIN.	226						

DAILY AVERAGE ACCESS TIME = 9 MIN.

GRAND TOTAL: 988 ASCENDING + 1364 DESCENDING = 2352

"NO BLIND SPOT" SENSOR TOTAL: 2897

"ONE-SIDE ONLY" SENSOR TOTALS:

ASCENDING WEST/DESCENDING EAST: 1245

ASCENDING EAST/DESCENDING WEST: 1107

NOTE: All Coverage Figures are in 1000 Km^2

TABLE A-14

ORBITAL COVERAGE SIMULATION

CASE IIP : 3 - DAY NON-SUN-SYNC. 350 km SWATH NON-PAINTABLE SENSOR

TARGET ZONE: GULF

DAY#	PASS#	ACCESS TIME	ASCENDING WEST	ASCENDING EAST	DESCENDING WEST	DESCENDING EAST	DAILY SUB-TOTALS ASCENDING	DAILY SUB-TOTALS DESCENDING	
1	1	2 MIN.	207	83					
	2	2 MIN			33	164	413	197	1
	3	2 MIN.	123						
2	4	2 MIN.			213		180	213	2
	5	2 MIN.		180					
-	6	2 MIN				113	0	113	3

GRAND TOTAL: 593 ASCENDING + 523 DESCENDING = 1116

DAILY AVERAGE ACCESS TIME = 4 MIN.

"NO BLIND SPOT" SENSOR TOTAL: 1202

"ONE-SIDE ONLY" SENSOR TOTALS:

ASCENDING WEST/DESCENDING EAST: [illegible]

ASCENDING EAST/DESCENDING WEST: [illegible]

NOTE: All Coverage Figures are in 1000 km^2

TABLE A-15

ORBITAL COVERAGE SIMULATION

CASE IIB: 3 - DAY NON SUN SYNC 556KM SWATH NON-POINTABLE SENSOR

TARGET ZONE: PACIFIC

DAY#	PASS#	ACCESS TIME	ASCENDING WEST	ASCENDING EAST	DESCENDING WEST	DESCENDING EAST	DAILY SUB-TOTALS ASCENDING	DAILY SUB-TOTALS DESCENDING	
1	1				(NEGLIGIBLE)		0	0	1
2	2	6 MIN.		556			556	459	2
	3	4 MIN.			459				
3	4	5 MIN.	510	81			591	663	3
	5	5 MIN.			525	138			

DAILY AVERAGE ACCESS TIME = 7 MIN.

GRAND TOTAL: 1147 ASCENDING + 1122 DESCENDING = 2269

"NO BLIND SPOT" SENSOR TOTAL: 2639

"ONE-SIDE ONLY" SENSOR TOTALS:

ASCENDING WEST/DESCENDING EAST: 1147

ASCENDING EAST/DESCENDING WEST: 1122

NOTE All [illegible] Swaths are in 1000 KM²

TABLE A-15

ORBITAL COVERAGE SIMULATION

CASE T.C : 3 - DAY 1 PM, 3.6 SWATH Non-Pointable SENSOR

TARGET ZONE: ALASKA

DAY#	PASS#	ACCESS TIME	ASCENDING WEST	ASCENDING EAST	DESCENDING WEST	DESCENDING EAST	DAILY SUB-TOTALS ASCENDING	DAILY SUB-TOTALS DESCENDING	
1	1	2 MIN.	168	83			251	250	1
	2	2 MIN.			197				
	3	1 MIN.				53			
2	4	2 MIN.	222				329	219	2
	5	1 MIN		107					
	6	1 MIN.			38				
	7	2 MIN.				181			
	8	2 MIN.		161			169	166	3
	9	2 MIN.			55	111			

DAILY AVERAGE ACCESS TIME = 5 MIN.

GRAND TOTAL: 749 ASCENDING + 635 DESCENDING = 1384

"NO BLIND SPOT" SENSOR TOTAL: 1601

"ONE-SIDE ONLY" SENSOR TOTALS:

ASCENDING WEST/DESCENDING EAST: 735

ASCENDING EAST/DESCENDING WEST. 649

NOTE: All Coverage Figures are in 1000 Km^2

TABLE A-17

ORBITAL COVERAGE SIMULATION

CASE III A : 1 - DAY [illegible], [illegible] km SWATH POINTABLE SENSOR

TARGET ZONE: ATLANTIC

DAY#	PASS#	ACCESS TIME	ASCENDING WEST	ASCENDING EAST	DESCENDING WEST	DESCENDING EAST	DAILY SUB-TOTALS ASCENDING	DAILY SUB-TOTALS DESCENDING
1		2 MIN.			85			
	2	3 MIN.	246	52			331	85

DAILY AVERAGE ACCESS TIME = 5 MIN

GRAND TOTAL: 331 ASCENDING

\+ 85 DESCENDING

= 416

"NO BLIND SPOT" SENSOR TOTAL: 470

"ONE-SIDE ONLY" SENSOR TOTALS:

ASCENDING WEST/DESCENDING EAST: 298

ASCENDING EAST/DESCENDING WEST: 172

NOTE: All Coverage Figures are in 1000 Km^2

TABLE A-18

ORBITAL COVERAGE SIMULATION

CASE [illegible] : 1 - DAY [illegible] SWATH [illegible] SENSOR

TARGET ZONE: [illegible]

DAY #	PASS #	ACCESS TIME	ASCENDING WEST	ASCENDING EAST	DESCENDING WEST	DESCENDING EAST	DAILY SUB-TOTALS ASCENDING	DAILY SUB-TOTALS DESCENDING
	1	2 MIN.	25	25			310	287
	2	2 MIN.			11	213		

DAILY AVERAGE ACCESS TIME = 1 HR.

GRAND TOTAL: 310 ASCENDING + 287 DESCENDING = 597

"NO BLIND SPOT" SENSOR TOTAL: 597

"ONE-SIDE ONLY" SENSOR TOTALS:

ASCENDING WEST/DESCENDING EAST: 238

ASCENDING EAST/DESCENDING WEST: 359

All Coverage Figures are in 1000 km^2

TABLE A-19

ORBITAL COVERAGE SIMULATION

CASE IIIA : 1 - DAY SUN-SYNCH, 3200 NM SWATH POINTABLE SENSOR

TARGET ZONE: PACIFIC

DAY#	PASS#	ACCESS TIME	ASCENDING WEST	ASCENDING EAST	DESCENDING WEST	DESCENDING EAST	DAILY SUB-TOTALS ASCENDING	DAILY SUB-TOTALS DESCENDING
1	1	6 MIN.	731				731	169
	2	3 MIN.				169		

DAILY AVERAGE ACCESS TIME = 9 MIN.

GRAND TOTAL:

731 ASCENDING

\+ 169 DESCENDING

= 900

"NO BLIND SPOT" SENSOR TOTAL: 900

"ONE-SIDE ONLY" SENSOR TOTALS:

ASCENDING WEST/DESCENDING EAST: 900

ASCENDING EAST/DESCENDING WEST: 0

NOTE: All Coverage Figures are in 1000 Km^2

TABLE A-20

ORBITAL COVERAGE SIMULATION

CASE NIA: 1 - DAY SUN-SYNC., 392 km SWATH POINTABLE SENSOR

TARGET ZONE: ALASKA

DAY #	PASS #	ACCESS TIME	ASCENDING WEST	ASCENDING EAST	DESCENDING WEST	DESCENDING EAST	DAILY SUB-TOTALS ASCENDING	DAILY SUB-TOTALS DESCENDING
	1	2 MIN.	78					
	2	2 MIN.		192			270	388
	3	2 MIN.			162			
	4	2 MIN.				226		

DAILY AVERAGE ACCESS TIME = 8 MIN.

GRAND TOTAL: 270 ASCENDING + 388 DESCENDING = 658

"NO BLIND SPOT" SENSOR TOTAL: 619

"ONE-SIDE ONLY" SENSOR TOTALS:

ASCENDING WEST/DESCENDING EAST: 39-1

ASCENDING EAST/DESCENDING WEST: 39-1

NOTE: All Coverage Figures are in 1000 Km^2

TABLE A-21

ORBITAL COVERAGE SIMULATION

CASE: [illegible] : 1 - DAY [illegible] 212 K.M. SWATH NON-FOVEATED SENSOR

TARGET ZONE: ATLANTIC

PASS#	ACCESS TIME	ASCENDING WEST	ASCENDING EAST	DESCENDING WEST	DESCENDING EAST	DAILY SUB-TOTALS ASCENDING	DAILY SUB-TOTALS DESCENDING
1	1 MIN.			51		303	51
2	3 MIN.	220	83				

DAILY AVERAGE ACCESS TIME = 4 MIN.

GRAND TOTAL:

303 ASCENDING

\+ 51 DESCENDING

= 354

"NO BLIND SPOT" SENSOR TOTAL: 408

"ONE-SIDE ONLY" SENSOR TOTALS:

ASCENDING WEST/DESCENDING EAST: 220

ASCENDING EAST/DESCENDING WEST: 134

NOTE: All Coverage Figures are in 1000 Km^2

TABLE A-22

ORBITAL COVERAGE SIMULATION

CASE III-B: 1 - DAY [illegible], 392 Km SWATH NON-[illegible] SENSOR

TARGET ZONE: GULF

ORBIT#	PASS#	ACCESS TIME	ASCENDING WEST	ASCENDING EAST	DESCENDING WEST	DESCENDING EAST	DAILY SUB-TOTALS ASCENDING	DAILY SUB-TOTALS DESCENDING
1	1	2 MIN.	25	267			292	281
	2	2 MIN.			75	212		

GRAND TOTAL: 292 ASCENDING + 281 DESCENDING = 579

DAILY AVERAGE ACCESS TIME = 4 MIN.

"NO BLIND SPOT" SENSOR TOTAL: 582

"ONE-SIDE ONLY" SENSOR TOTALS:

ASCENDING WEST/DESCENDING EAST: 237

ASCENDING EAST/DESCENDING WEST: 342

NOTE: All Coverage Figures are in 1000 Km^2

TABEL A-23

ORBITAL COVERAGE SIMULATION

CASE TTP: 1 - DAY Sept. 1966, 392 km SWATH NON-POINTING SENSOR

TARGET ZONE: PACIFIC

DAY#	PASS#	ACCESS TIME	ASCENDING WEST	ASCENDING EAST	DESCENDING WEST	DESCENDING EAST	DAILY SUB-TOTALS ASCENDING	DAILY SUB-TOTALS DESCENDING
1	1	6 MIN.	654				654	151 } 1
	2	2 MIN.				151		

DAILY AVERAGE ACCESS TIME = 8 MIN.

GRAND TOTAL: 654 ASCENDING + 151 DESCENDING = 805

"NO BLIND SPOT" SENSOR TOTAL: 805

"ONE-SIDE ONLY" SENSOR TOTALS:

ASCENDING WEST/DESCENDING EAST: 805

ASCENDING EAST/DESCENDING WEST: 0

NOTE: All Coverage Figures are in 1000 km^2

TABLE A-24

ORBITAL COVERAGE SIMULATION

CASE TI2 : 1 - DAY SUN SYNC., 312 Km SWATH NOMINAL SENSOR

TARGET ZONE: ACTUAL

DAY#	PASS#	ACCESS TIME	ASCENDING WEST	ASCENDING EAST	DESCENDING WEST	DESCENDING EAST	DAILY SUB-TOTALS ASCENDING	DAILY SUB-TOTALS DESCENDING
1	1	2 MIN.	42					
	2	1 MIN.		187			229	357
	3	1 MIN.			137			
	4	2 MIN.				220		

DAILY AVERAGE ACCESS TIME = 6 MIN.

GRAND TOTAL:

229 ASCENDING

\+ 357 DESCENDING

= 586

"NO BLIND SPOT" SENSOR TOTAL: 673

"ONE-SIDE ONLY" SENSOR TOTALS:

ASCENDING WEST/DESCENDING EAST:

ASCENDING EAST/DESCENDING WEST:

NOTE: All Coverage Figures are in 1000 Km²

TABLE A-25

ORBITAL COVERAGE SIMULATION

CASE IIIC : 1 - DAY [illegible], 372 km SWATH POINTABLE SENSOR

TARGET ZONE: ATLANTIC

DAY#	PASS#	ACCESS TIME	ASCENDING WEST	ASCENDING EAST	DESCENDING WEST	DESCENDING EAST	DAILY SUB-TOTALS ASCENDING	DAILY SUB-TOTALS DESCENDING
1	1	2 MIN.			200			
	2	1 MIN.				48	418	248 } 1
	3	3 MIN.	353	65				

DAILY AVERAGE ACCESS TIME = 6 MIN.

GRAND TOTAL:

418 ASCENDING

\+ 248 DESCENDING

= 666

"NO BLIND SPOT" SENSOR TOTAL: 717

"ONE-SIDE ONLY" SENSOR TOTALS:

ASCENDING WEST/DESCENDING EAST: 401

ASCENDING EAST/DESCENDING WEST: 265

NOTE: All Coverage Figures are in 1000 Km^2

TABLE A-26

ORBITAL COVERAGE SIMULATION

CASE IIIC : 1 - DAY SUN-SYNCH. 392 km SWATH POINTABLE SENSOR

TARGET ZONE: GULF

DAY#	PASS#	ACCESS TIME	ASCENDING WEST	ASCENDING EAST	DESCENDING WEST	DESCENDING EAST	DAILY SUB-TOTALS ASCENDING	DAILY SUB-TOTALS DESCENDING
1	1	2 MIN.	50	305			355	287
	2	2 MIN.			75	212		

DAILY AVERAGE ACCESS TIME = 1 MIN

GRAND TOTAL:

355 ASCENDING

\+ 287 DESCENDING

= 642

"NO BLIND SPOT" SENSOR TOTAL: 642

"ONE-SIDE ONLY" SENSOR TOTALS:

ASCENDING WEST/DESCENDING EAST: 262

ASCENDING EAST/DESCENDING WEST: 380

NOTE: All Coverage Figures are in 1000 Km^2

TABLE A-27
ORBITAL COVERAGE SIMULATION

CASE IIIC : 1 - DAY Sun-Sync., 342.6 KM SWATH POINTABLE SENSOR
TARGET ZONE: PACIFIC

DAY#	PASS#	ACCESS TIME	ASCENDING WEST	ASCENDING EAST	DESCENDING WEST	DESCENDING EAST	DAILY SUB-TOTALS ASCENDING	DAILY SUB-TOTALS DESCENDING
1	1	6 MIN.	887				887	325 } 1
	2	3 MIN.				325		

DAILY AVERAGE ACCESS TIME = 9 MIN.

GRAND TOTAL:
887 ASCENDING
+ 325 DESCENDING
= 1212

"NO BLIND SPOT" SENSOR TOTAL: 1212

"ONE-SIDE ONLY" SENSOR TOTALS:

ASCENDING WEST/DESCENDING EAST: 1212

ASCENDING EAST/DESCENDING WEST: 0

NOTE: All Coverage Figures are in 1000 Km^2

TABLE A-28

ORBITAL COVERAGE SIMULATION

CASE IIIC: 1 - DAY SUN-SYNCH. 3.92 km SWATH POINTABLE SENSOR

TARGET ZONE: ALASKA

DAY#	PASS#	ACCESS TIME	ASCENDING WEST	ASCENDING EAST	DESCENDING WEST	DESCENDING EAST	DAILY SUB-TOTALS ASCENDING	DAILY SUB-TOTALS DESCENDING
1	1	2 MIN.	209					
	2	2 MIN.		228			437	446
	3	2 MIN.			219			
	4	2 MIN.				227		

DAILY AVERAGE ACCESS TIME = 8 MIN.

GRAND TOTAL: 437 ASCENDING + 446 DESCENDING = 883

"NO BLIND SPOT" SENSOR TOTAL: 926

"ONE-SIDE ONLY" SENSOR TOTALS:

ASCENDING WEST/DESCENDING EAST: 436

ASCENDING EAST/DESCENDING WEST: 447

NOTE: All Coverage Figures are in 1000 Km^2

TABLE A-29

ORBITAL COVERAGE SIMULATION

CASE IVA : 1 - DAY SUN-SYNCH, 392km SWATH POINTABLE SENSOR

TARGET ZONE: ATLANTIC

DAY#	PASS#	ACCESS TIME	ASCENDING WEST	ASCENDING EAST	DESCENDING WEST	DESCENDING EAST	DAILY SUB-TOTALS ASCENDING	DAILY SUB-TOTALS DESCENDING
	1	5 MIN.		430				
	2	6 MIN.				775	639	775
	3	2 MIN	209					

DAILY AVERAGE ACCESS TIME = 11 MIN.

GRAND TOTAL: 639 ASCENDING + 775 DESCENDING = 1414

"NO BLIND SPOT" SENSOR TOTAL: 1162

"ONE-SIDE ONLY" SENSOR TOTALS:

ASCENDING WEST/DESCENDING EAST: 1.-1

ASCENDING EAST/DESCENDING WEST: -1-

NOTE: All Coverage Figures are in 1000 Km^2

TABLE A-30

ORBITAL COVERAGE SIMULATION

CASE IV A : 1 - DAY ION SAMA, 3124 m SWATH PANORAMIC SENSOR

TARGET ZONE: GULF

DAY#	PASS#	ACCESS TIME	ASCENDING WEST	ASCENDING EAST	DESCENDING WEST	DESCENDING EAST	DAILY SUB-TOTALS ASCENDING	DAILY SUB-TOTALS DESCENDING
1	1	2 MIN.	263				263	229 61
	2	2 MIN.			209	16		

377

DAILY AVERAGE ACCESS TIME = 4 MIN.

GRAND TOTAL: 263 ASCENDING + 229 DESCENDING = 492

"NO BLIND SPOT" SENSOR TOTAL: 422

"ONE-SIDE ONLY" SENSOR TOTALS:

ASCENDING WEST/DESCENDING EAST: 37

ASCENDING EAST/DESCENDING WEST: 33

NOTE: All Coverage Figures are in 1000 Km^2

TABLE A-31

ORBITAL COVERAGE SIMULATION

CASE: VA : 1 - DAY ON EACH, 392 Km SWATH PONTIAC SENSOR

TARGET ZONE: PACIFIC

DAY#	PASS#	ACCESS TIME	ASCENDING WEST	ASCENDING EAST	DESCENDING WEST	DESCENDING EAST	DAILY SUB-TOTALS ASCENDING	DAILY SUB-TOTALS DESCENDING
1	1	1 MIN.			33	371	0	404

DAILY AVERAGE ACCESS TIME = 1 MIN.

GRAND TOTAL: 0 ASCENDING + 404 DESCENDING = 404

"NO BLIND SPOT" SENSOR TOTAL: 635

"ONE-SIDE ONLY" SENSOR TOTALS:

ASCENDING WEST/DESCENDING EAST: 371

ASCENDING EAST/DESCENDING WEST: 33

NOTE: All Coverage Figures are in 1000 Km^2

TABLE A-32

ORBITAL COVERAGE SIMULATION

CASE 12 : 1 - DAY SUN-SYNCH, 392 KM SWATH POINTABLE SENSOR

TARGET ZONE: ALASKA

DAY#	PASS#	ACCESS TIME	ASCENDING WEST	ASCENDING EAST	DESCENDING WEST	DESCENDING EAST	DAILY SUB-TOTALS ASCENDING	DAILY SUB-TOTALS DESCENDING
1	1	2 MIN.	82	241			323	244
	2	2 MIN.			45	199		

SEE NEXT PAGE FOR DAILY SUB-TOTALS

329

GRAND TOTAL: 323 ASCENDING + 244 DESCENDING = 567

DAILY AVERAGE ACCESS TIME = 4 MIN.

"NO BLIND SPOT" SENSOR TOTAL: 613

"ONE-SIDE ONLY" SENSOR TOTALS:

ASCENDING WEST/DESCENDING EAST: 244

ASCENDING EAST/DESCENDING WEST: 241

NOTE: All Coverage Figures are in 1000 Km^2

TABLE A-33

ORBITAL COVERAGE SIMULATION

CASE IVB : 1 - DAY SUN-SYNCH. 392 Km SWATH NON-POINTABLE SENSOR

TARGET ZONE: ATLANTIC

ACCESS TIME	ASCENDING WEST	ASCENDING EAST	DESCENDING WEST	DESCENDING EAST	DAILY SUB-TOTALS ASCENDING	DAILY SUB-TOTALS DESCENDING
3 MIN.		384				
6 MIN.			685		571	1
2 MIN.	187					

SS TIME = 11 MIN.

GRAND TOTAL: 571 ASCENDING + 685 DESCENDING = 1256

"NO BLIND SPOT" SENSOR TOTAL: 1256

"ONE-SIDE ONLY" SENSOR TOTALS:

ASCENDING WEST/DESCENDING EAST: 571

ASCENDING EAST/DESCENDING WEST: 685

NOTE: All Coverage Figures are in 1000 Km^2

TABLE A-34

ORBITAL COVERAGE SIMULATION

CASE TVB : 1 - DAY SUN SYNC H. 392 KM SWATH: NON-POINTABLE SENSOR

TARGET ONE: GULF

DAY #	PASS #	ACCESS TIME	ASCENDING WEST	ASCENDING EAST	DESCENDING WEST	DESCENDING EAST	DAILY TOTAL ASCENDING	DAILY TOTAL DESCENDING
1	1	2 MIN.	262				262	219
	2	2 MIN.			204	15		

381

GRAND TOTAL: 262 ASCENDING + 219 DESCENDING = 481

DAILY AVERAGE ACCESS TIME = 1 MIN.

"NO BLIND SPOT" SENSOR TOTAL: 262

"ONE-SIDE ONLY" SENSOR TOTALS:

ASCENDING WEST/DESCENDING EAST: 277

ASCENDING EAST/DESCENDING WEST: 204

NOTE: All Coverage Figures are in 1000 Km^2

TABLE A-35
ORBITAL COVERAGE SIMULATION

CASE IIB : 1 - DAY SUN SYNCH. 322 km SWATH NON-POINTABLE SENSOR
TARGET ZONE: PACIFIC

DAY#	PASS#	ACCESS TIME	ASCENDING WEST	ASCENDING EAST	DESCENDING WEST	DESCENDING EAST	DAILY SUB-TOTALS ASCENDING	DAILY SUB-TOTALS DESCENDING
1	1	4 MIN.			30	344	0	374

382

DAILY AVERAGE ACCESS TIME = 4 MIN.

GRAND TOTAL: 0 ASCENDING
+ 374 DESCENDING
= 374

"NO BLIND SPOT" SENSOR TOTAL: 611

"ONE-SIDE ONLY" SENSOR TOTALS:

ASCENDING WEST/DESCENDING EAST: 344

ASCENDING EAST/DESCENDING WEST: 30

NOTE: All Coverage Figures are in 1000 Km^2

TABLE A-36
ORBITAL COVERAGE SIMULATION

CASE IVB : 1 - DAY SUN-SYNCH, 3124 n.m. SWATH NON-RIMTRACK SENSOR
TARGET ZONE: ALASKA

DAY#	PASS#	ACCESS TIME	ASCENDING WEST	ASCENDING EAST	DESCENDING WEST	DESCENDING EAST	DAILY SUB-TOTALS ASCENDING	DAILY SUB-TOTALS DESCENDING
1	1	2 MIN.	81	225			306	244
	2	2 MIN.			45	199		

DAILY AVERAGE ACCESS TIME = 4 MIN.

GRAND TOTAL: 306 ASCENDING
+ 244 DESCENDING
= 550

"NO BLIND SPOT" SENSOR TOTAL: 573

"ONE-SIDE ONLY" SENSOR TOTALS:

ASCENDING WEST/DESCENDING EAST: 280

ASCENDING EAST/DESCENDING WEST: 111

NOTE: All Coverage Figures are in 1000 Km^2

TABLE A-37

ORBITAL COVERAGE SIMULATION

CASE TVC : 1 - DAY IN [illegible], 392 km SWATH POINTABLE SENSOR

TARGET ZONE: ATLANTIC

DAY#	PASS#	ACCESS TIME	ASCENDING WEST	ASCENDING EAST	DESCENDING WEST	DESCENDING EAST	DAILY SUB-TOTALS ASCENDING	DAILY SUB-TOTALS DESCENDING
1	1	3 MIN.		475				
	2	7 MIN.				959	732	1434
	3	2 MIN.	257					

384

GRAND TOTAL: [illegible] ASCENDING + 1591 DESCENDING = 1691

DAILY AVERAGE ACCESS TIME = 12 MIN.

"NO BLIND SPOT" SENSOR TOTAL: 1739

"ONE-SIDE ONLY" SENSOR TOTALS:

ASCENDING WEST/DESCENDING EAST: [illegible]

ASCENDING EAST/DESCENDING WEST: [illegible]

NOTE: All Coverage Figures are in 1000 Km^2

TABLE A-38

ORBITAL COVERAGE SIMULATION

CASE: IC : 1 - DAY SUN-SYNCH, 312 KM SWATH: POINTABLE SENSOR

TARGET ZONE: GULF

DAY#	PASS#	ACCESS TIME	ASCENDING WEST	ASCENDING EAST	DESCENDING WEST	DESCENDING EAST	DAILY SUB-TOTALS ASCENDING	DAILY SUB-TOTALS DESCENDING
1	1	2 MIN.	266				266	236 1
	2	2 MIN.			227	9		

385

GRAND TOTAL: 266 ASCENDING
+ 236 DESCENDING
= 502

DAILY AVERAGE ACCESS TIME = 1 MIN

"NO BLIND SPOT" SENSOR TOTAL: 274

"ONE-SIDE ONLY" SENSOR TOTALS:

ASCENDING WEST/DESCENDING EAST: 275

ASCENDING EAST/DESCENDING WEST: 1

NOTE: All Coverage Figures are in 1000 Km^2

TABLE A-39

ORBITAL COVERAGE SIMULATION

CASE IVC : 1 - DAY SUN-SYNCH, 392 km SWATH POINTABLE SENSOR

TARGET ZONE: PACIFIC

DAY#	PASS#	ACCESS TIME	ASCENDING WEST	ASCENDING EAST	DESCENDING WEST	DESCENDING EAST	DAILY SUB-TOTALS ASCENDING	DAILY SUB-TOTALS DESCENDING
1	1	1 MIN.	30				30	
	2	5 MIN.			34	436		470

DAILY AVERAGE ACCESS TIME = 6 MIN.

GRAND TOTAL: 30 ASCENDING + 470 DESCENDING = 500

"NO BLIND SPOT" SENSOR TOTAL: 728

"ONE-SIDE ONLY" SENSOR TOTALS:

ASCENDING WEST/DESCENDING EAST: 100

ASCENDING EAST/DESCENDING WEST: 31

NOTE: All Coverage Figures are in 1000 Km^2

TABLE A-40

ORBITAL COVERAGE SIMULATION

CASE IV-C : 1 - DAY SUN-SYNCH, 512 KM SWATH POINTABLE SENSOR

TARGET ZONE: ALASKA

DAY#	PASS#	ACCESS TIME	ASCENDING WEST	ASCENDING EAST	DESCENDING WEST	DESCENDING EAST	DAILY SUB-TOTALS ASCENDING	DAILY SUB-TOTALS DESCENDING
	1	3 MIN.	82	254			336	
	2	2 MIN.			60	174		234

GRAND TOTAL: 336 ASCENDING + 234 DESCENDING = 570

DAILY AVERAGE ACCESS TIME = 4 MIN.

"NO BLIND SPOT" SENSOR TOTAL: 022

"ONE-SIDE ONLY" SENSOR TOTALS:

ASCENDING WEST/DESCENDING EAST:

ASCENDING EAST/DESCENDING WEST:

NOTE: All Coverage Figures are in 1000 Km^2

APPENDIX B

A Comparison of Time Steps for Oilspill Monitoring

Dr. Peter Cornillon
Kurt Hansen
University of Rhode Island

In this project, a total of 5 runs were done, each releasing 300,000 metric tons of medium crude oil over a 30 day period. The surface portion of the spill is represented by round circular puddles of oil called 'spillets'. There is one spillet released every day over the 30 days. The plots which refer to spillet one refers to the spillet released at time equals zero. The subsurface part of the spill is tracked by outlining the area where the concentration exceeds 50 parts per billion.

The base run consisted of a time step of three hours where the environmental data (winds and currents) were entered every time step. The other runs used a time step of three hours but entered the environmental data every 12 and 24 hours, respectively. In two of these runs, the magnitudes were averaged over the environmental time step and in the remaining two runs, the value at the beginning of the time step was used throughout the environmental time step.

It can be seen that the averaging had little affect on the positions of the first spillet but taking a discrete value at the beginning of the time step increased the distances between the spillet for each case. Figures 1 and 2 show all three cases at 10, 20, 30 and 40 days. By 40 days the spillet reaches the edge of the study area and thus does not move again.

Figures 3 and 4 show the difference between the twelve and twenty-four time step cases for the averaged and discrete case. The remaining figures show the surface and subsurface portion of the spill at 10, 20, 30 and 40 days. Here, as before, the spillets are piling up at the edge of the study area by day forty. The previous plots which were done for the 12 and 24 hour time step are for the averaged case.

Table 1. Positions of Spillet One

Days	Time Step for Environmental Data		
	3 Hours	12 Hours (average)	24 Hours (average)
10	66.46W 41.15N	66.50W 41.10n	66.45W 41.14N
20	65.39W 40.35N	65.45W 40.35N	65.42W 40.31N
30	65.82W 39.79N	65.97W 39.85N	65.85W 39.78N
40	65.14W 39.45N	65.25W 39.43N	65.00W 39.44N

Table 2. Positions of Spillet One
(Not averaged)

	Time Step for Environmental Data	
Days	12 Hours	24 Hours
10	66.50W 40.94N	65.92W 40.93N
20	65.50W 40.45N	65.02W 40.31N
30	65.80W 39.83N	65.40N 39.58N
40	65.24W 39.44N	65.09W 39.45N

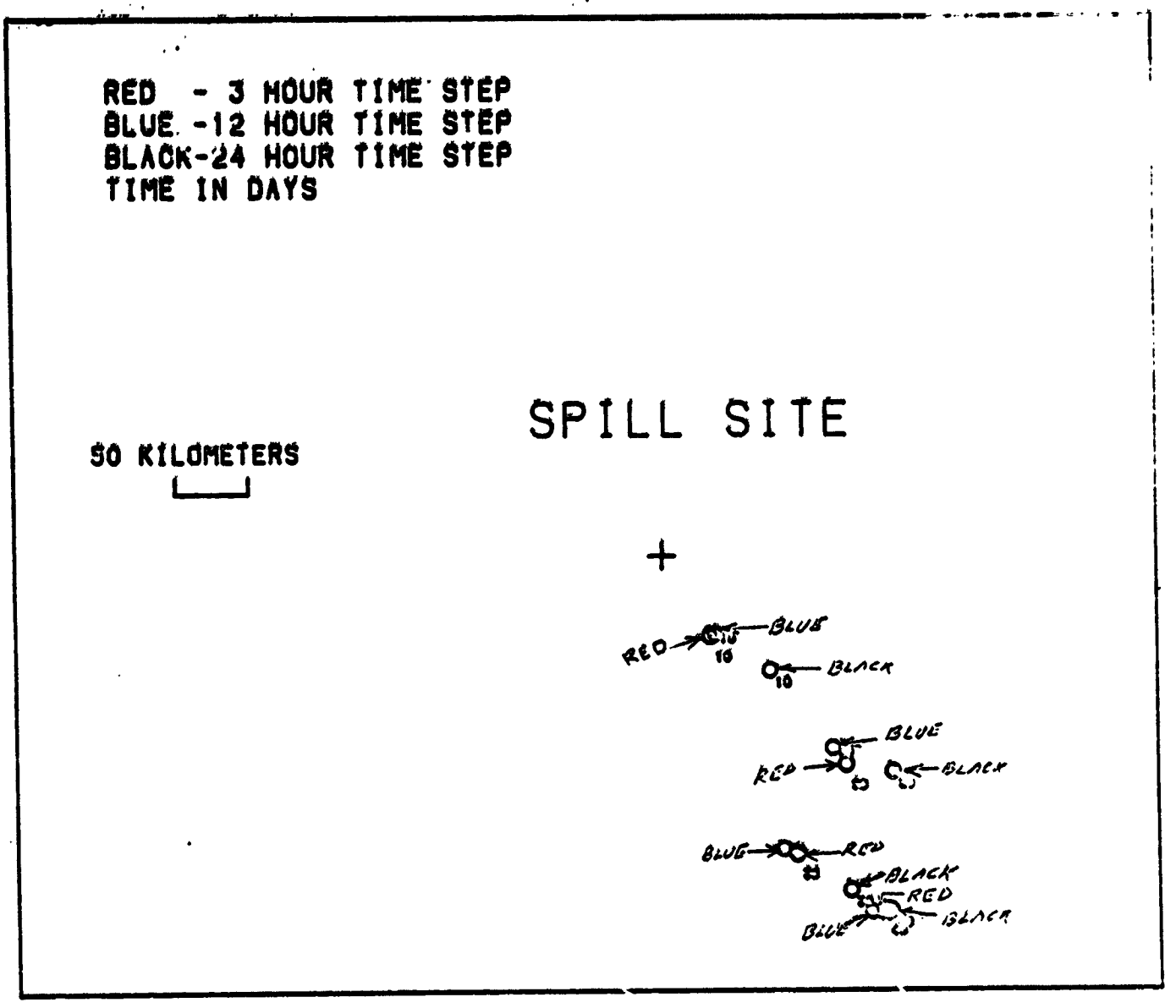

Figure 1. Position of Spillet One Using Discrete Data

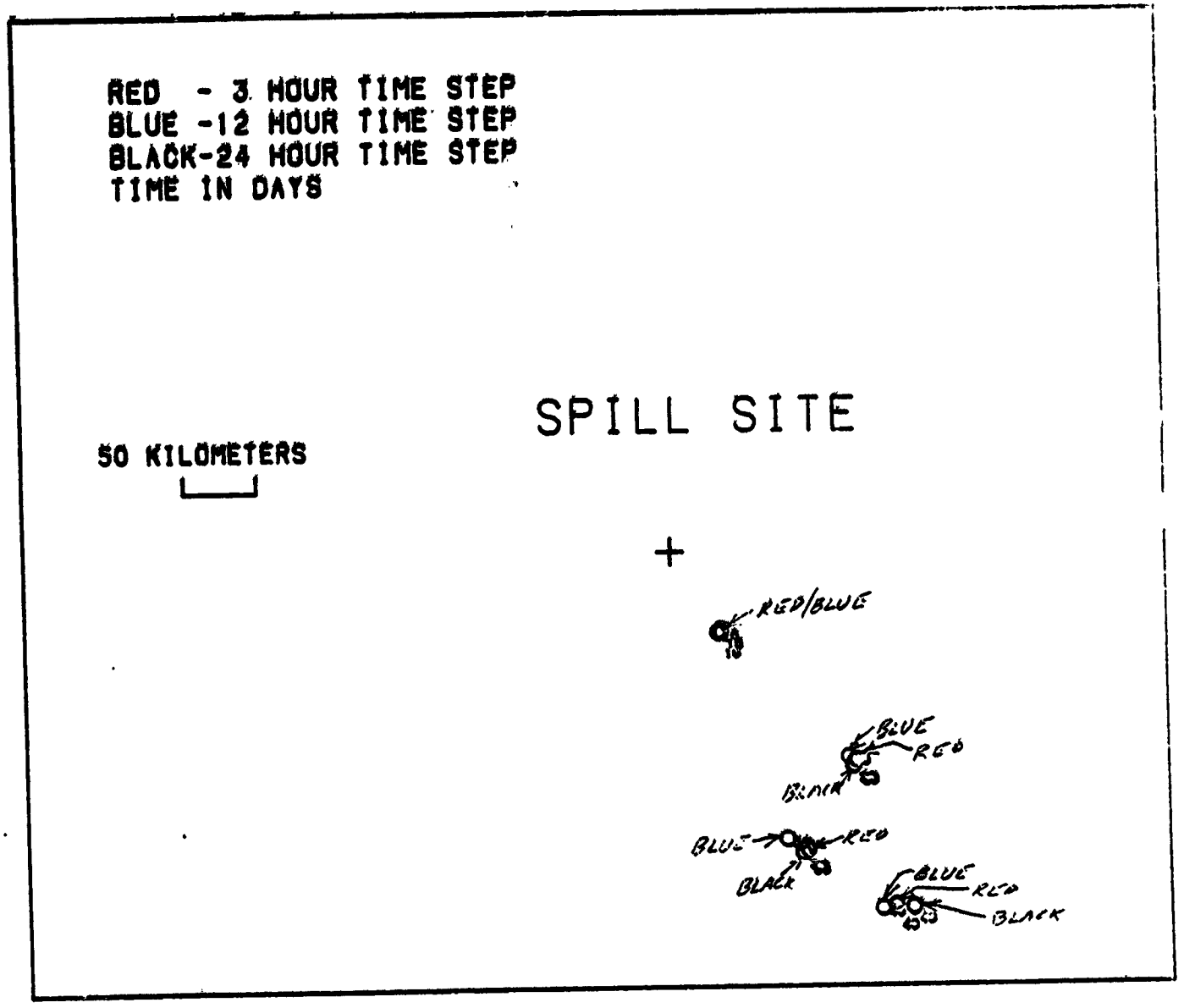

Figure 2. Position of Spillet Using Averaged Data

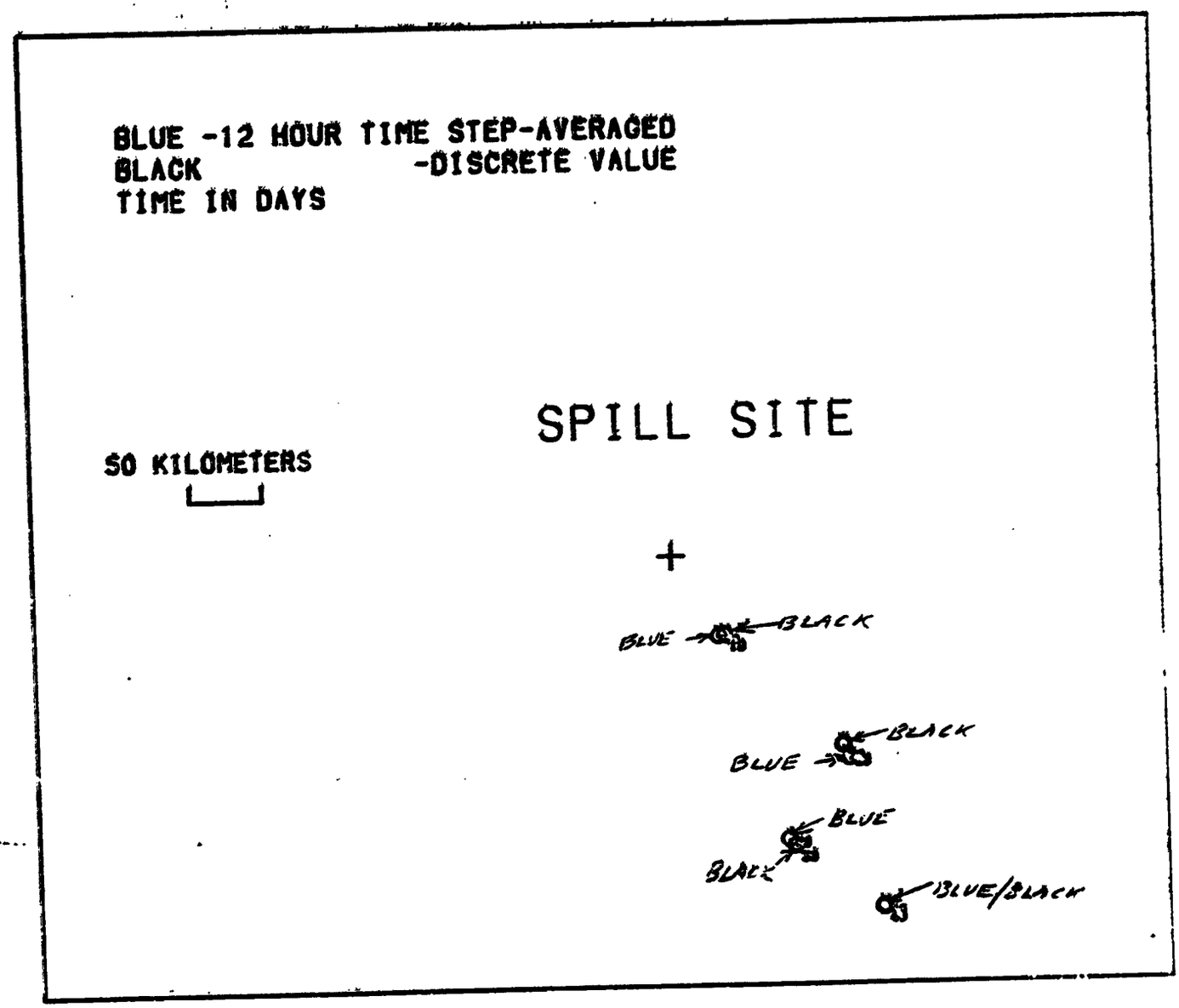

Figure 3. Comparison of the Positions of Spillet One for Time Step of 12 Hours.

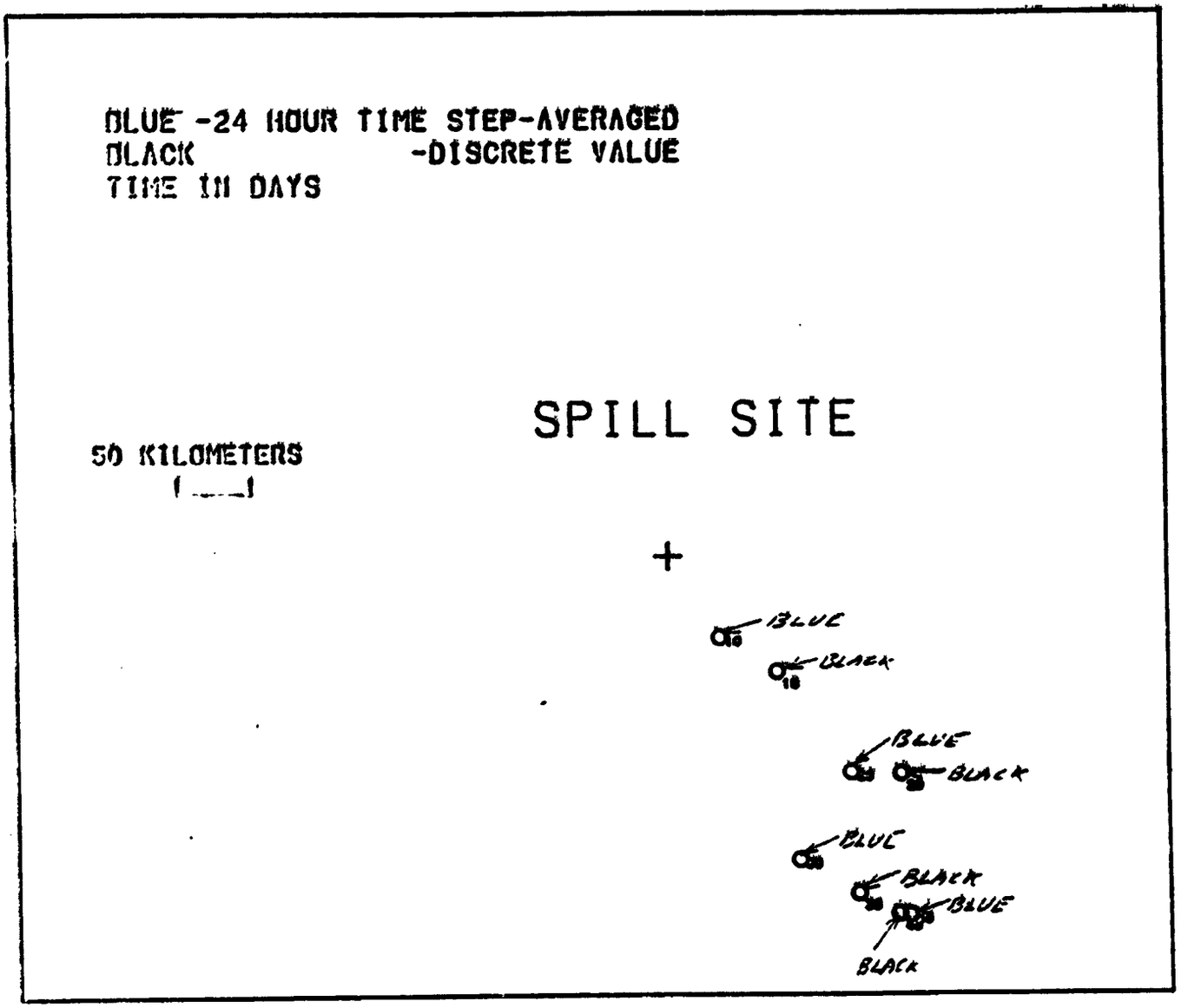

Figure 4. Comparison of the Positions of Spillet One for Time Step of 24 Hours.

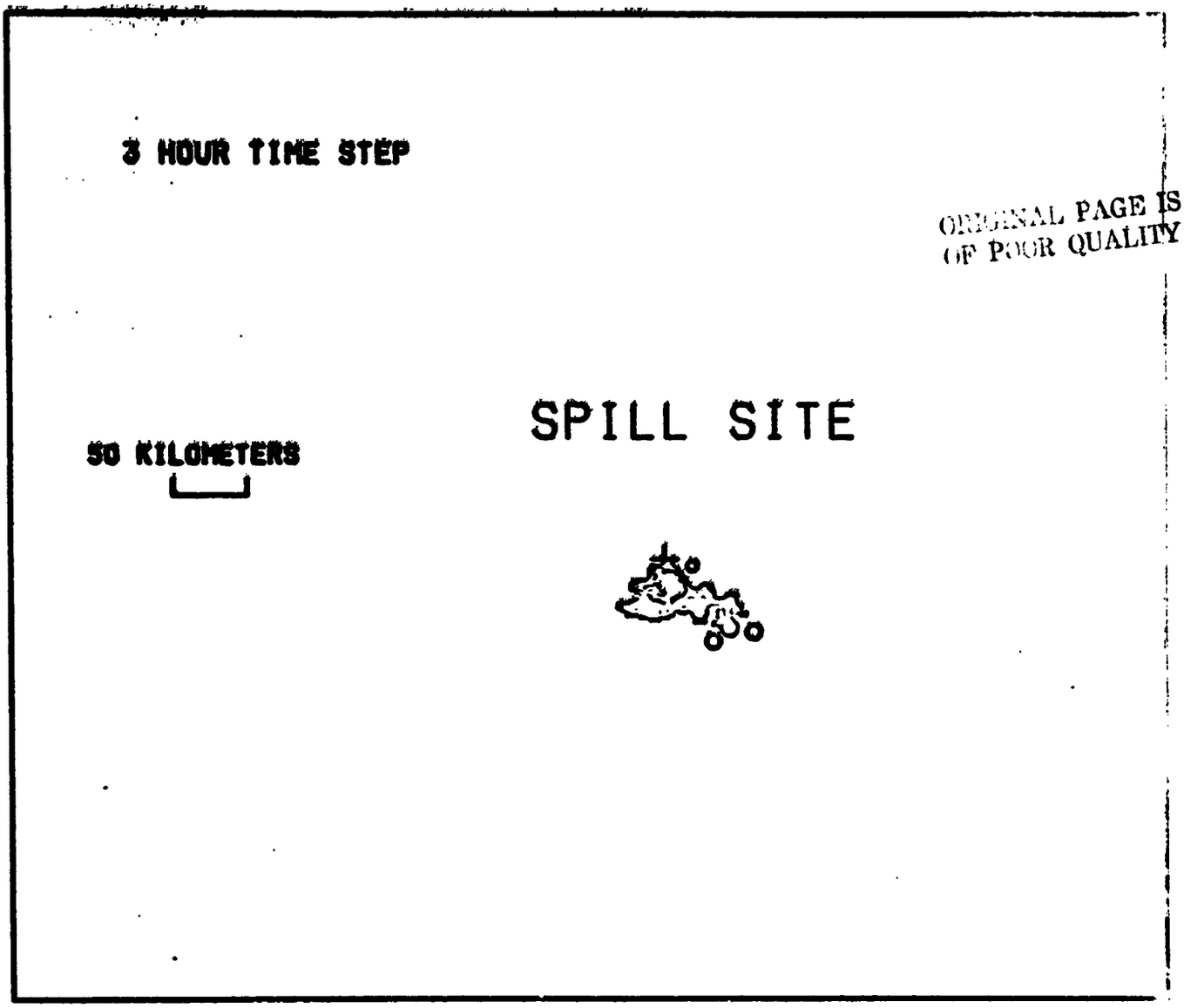

Figure 5. Surface and Subsurface Portions of Oilspill at Time Equals 10 Days.

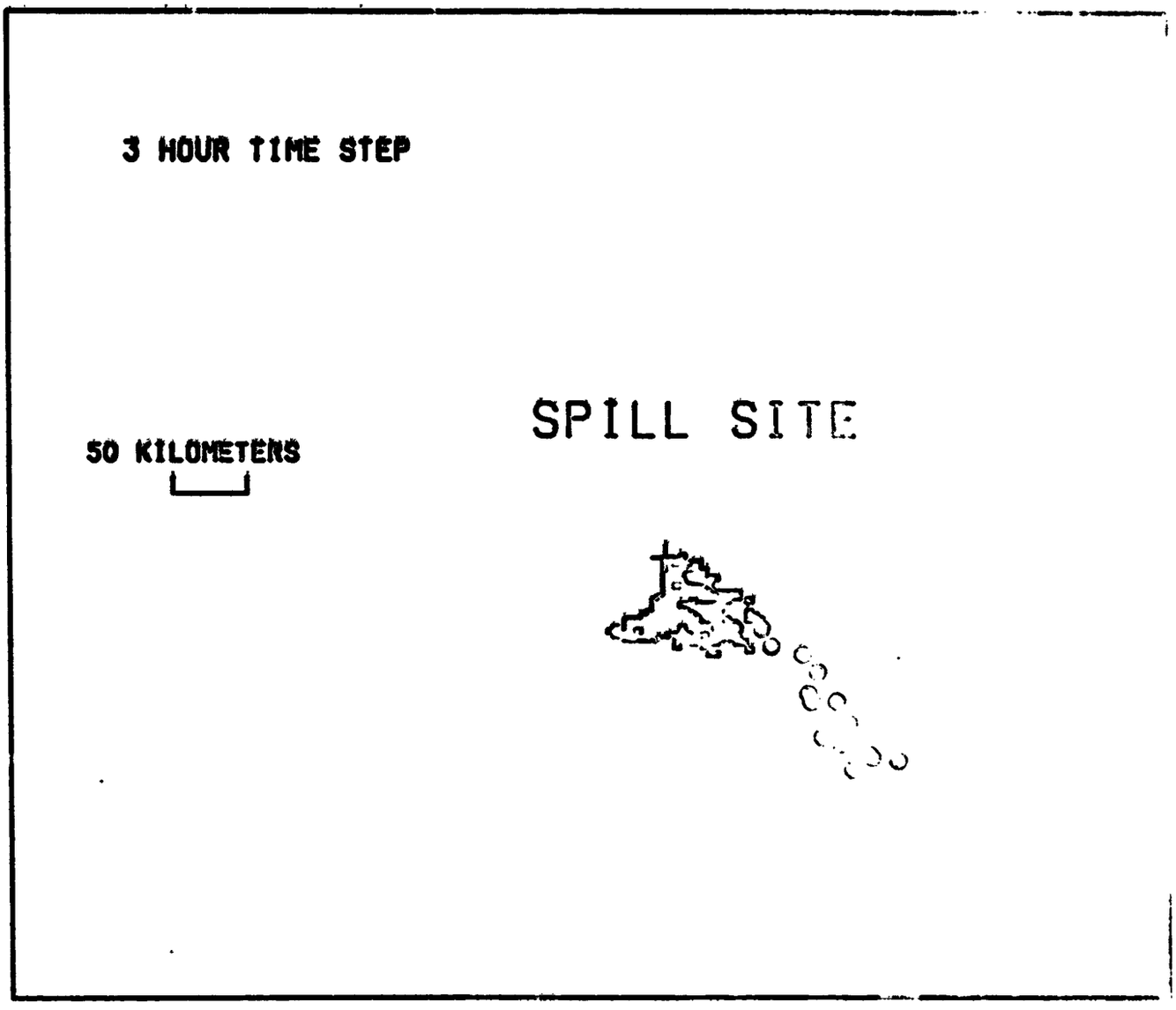

Figure 6. Surface and Subsurface Portions of Oilspill at Time Equals 20 Days.

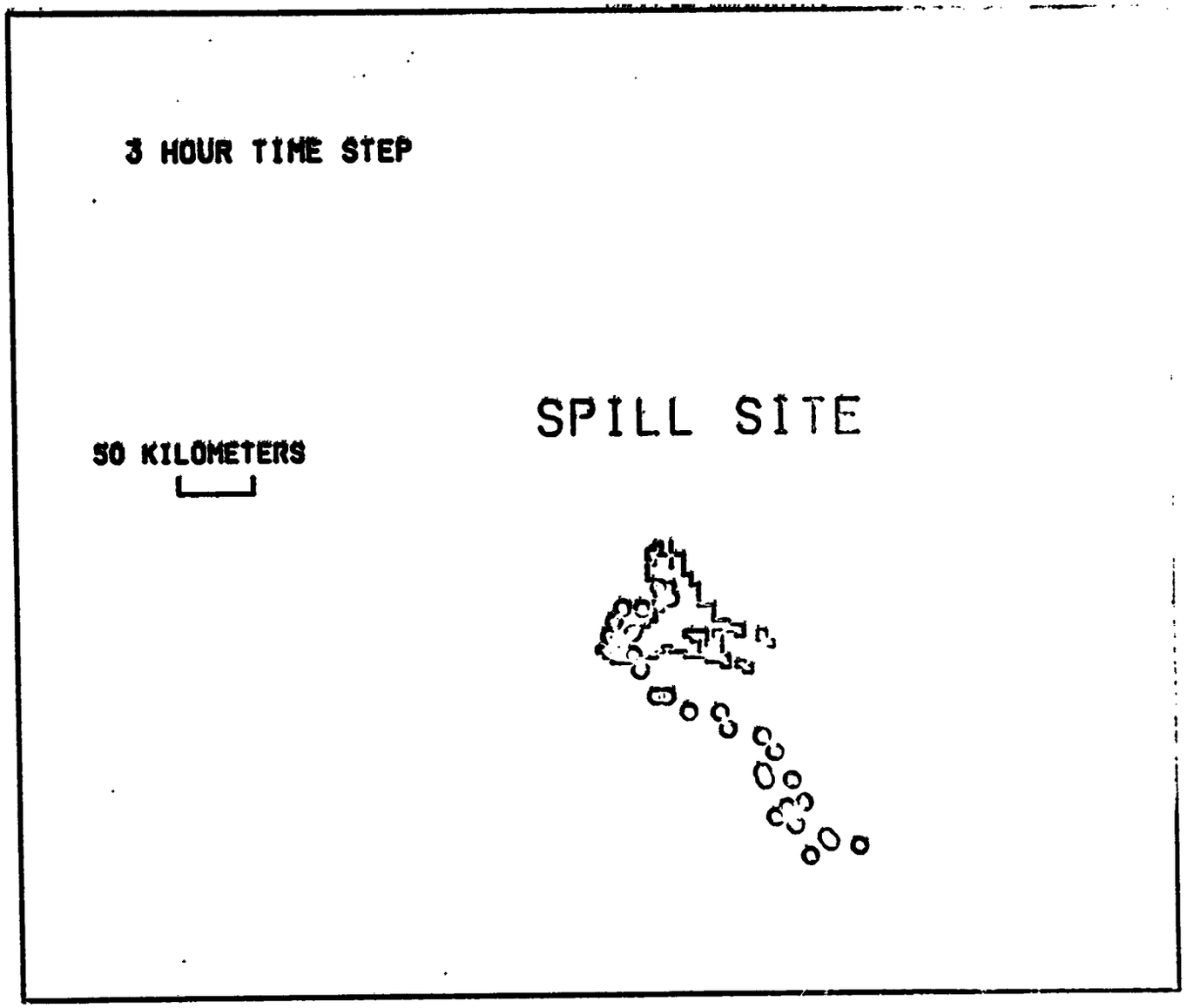

Figure 7. Surface and Subsurface Portions of Oilspill at Time Equals 30 Days.

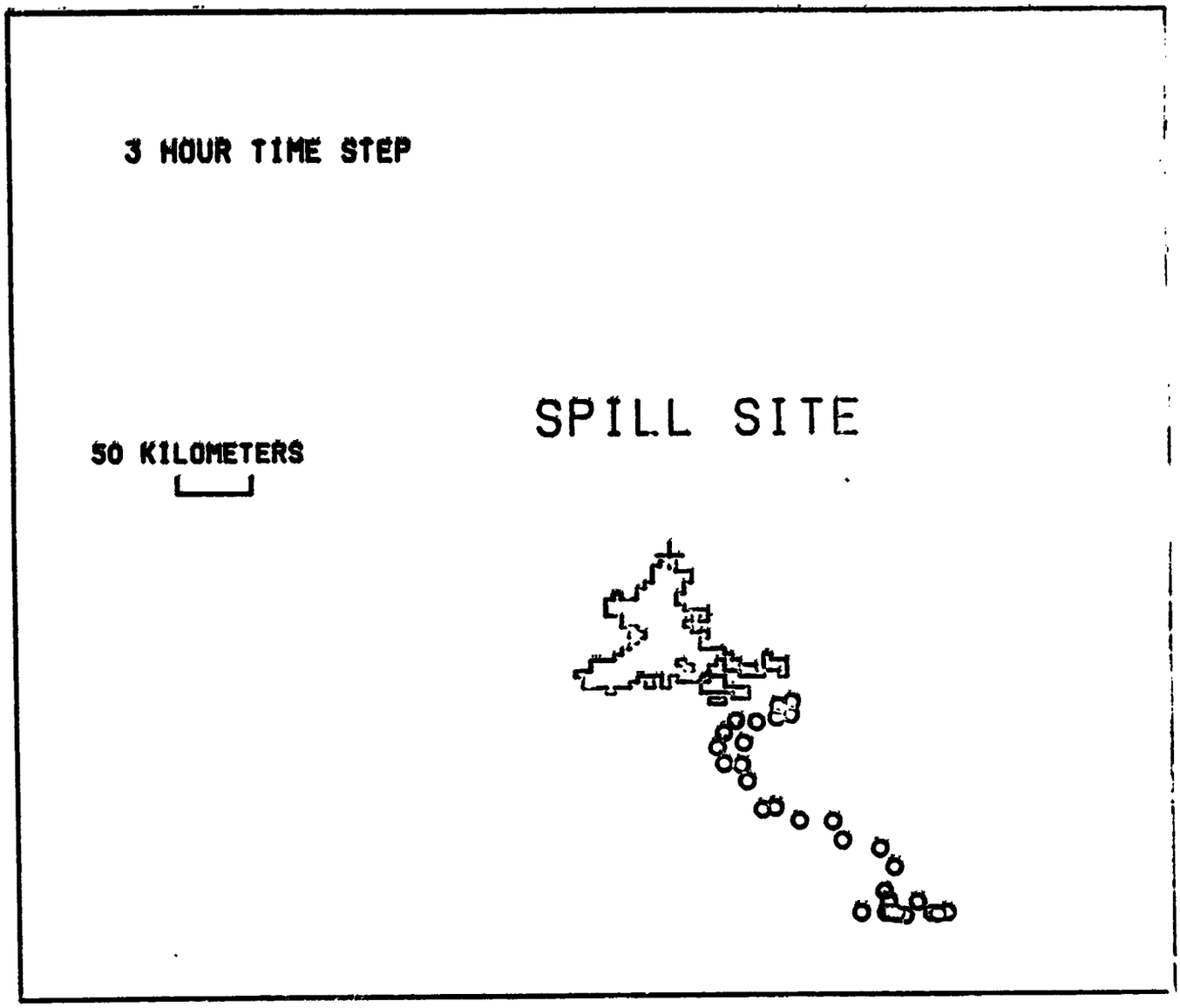

Figure 8. Surface and Subsurface Portions of the Oilspill at Time Equals 40 Days.

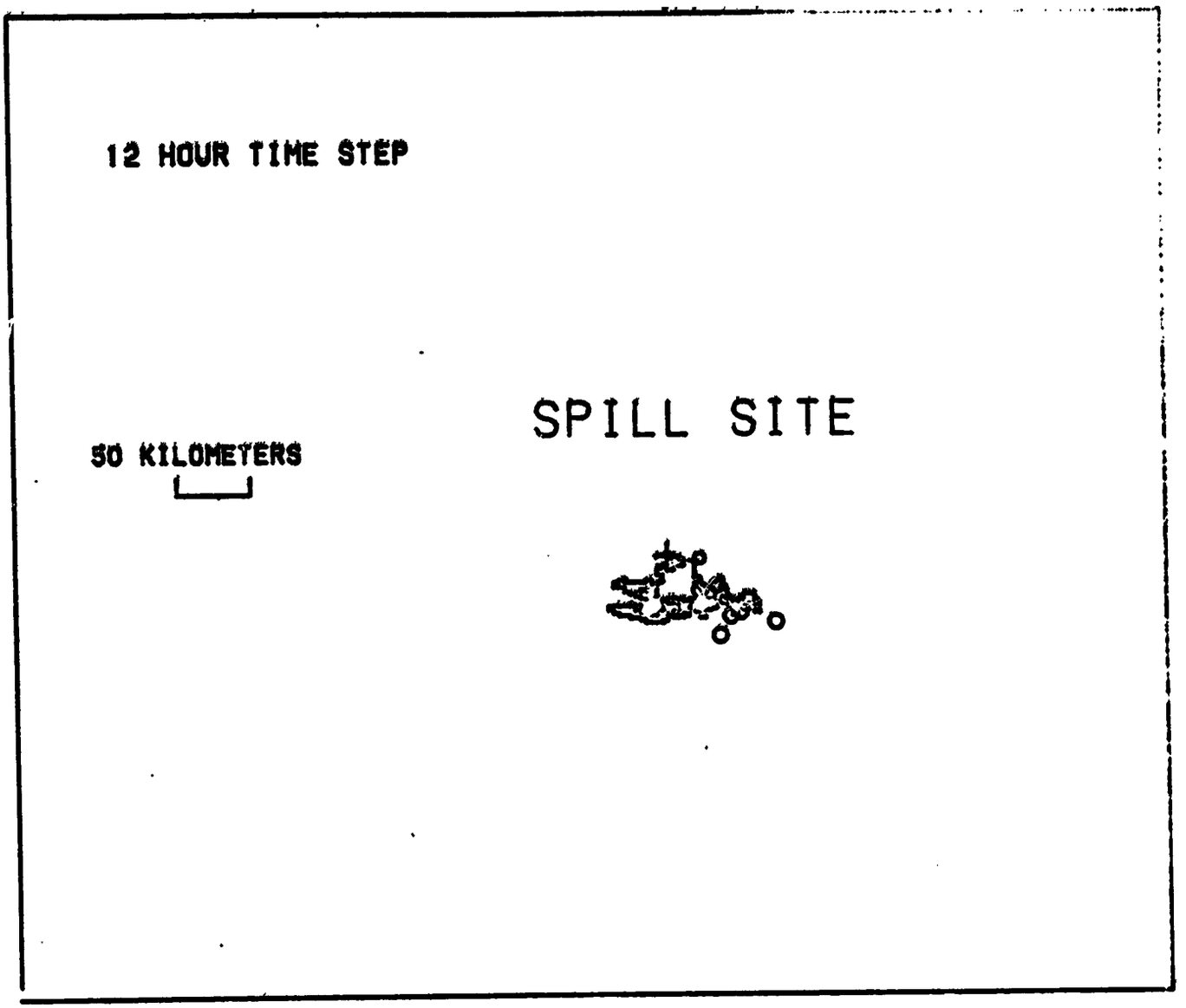

Figure 9. Surface and Subsurface Portions of the Oilspill at Time Equals 10 Days.

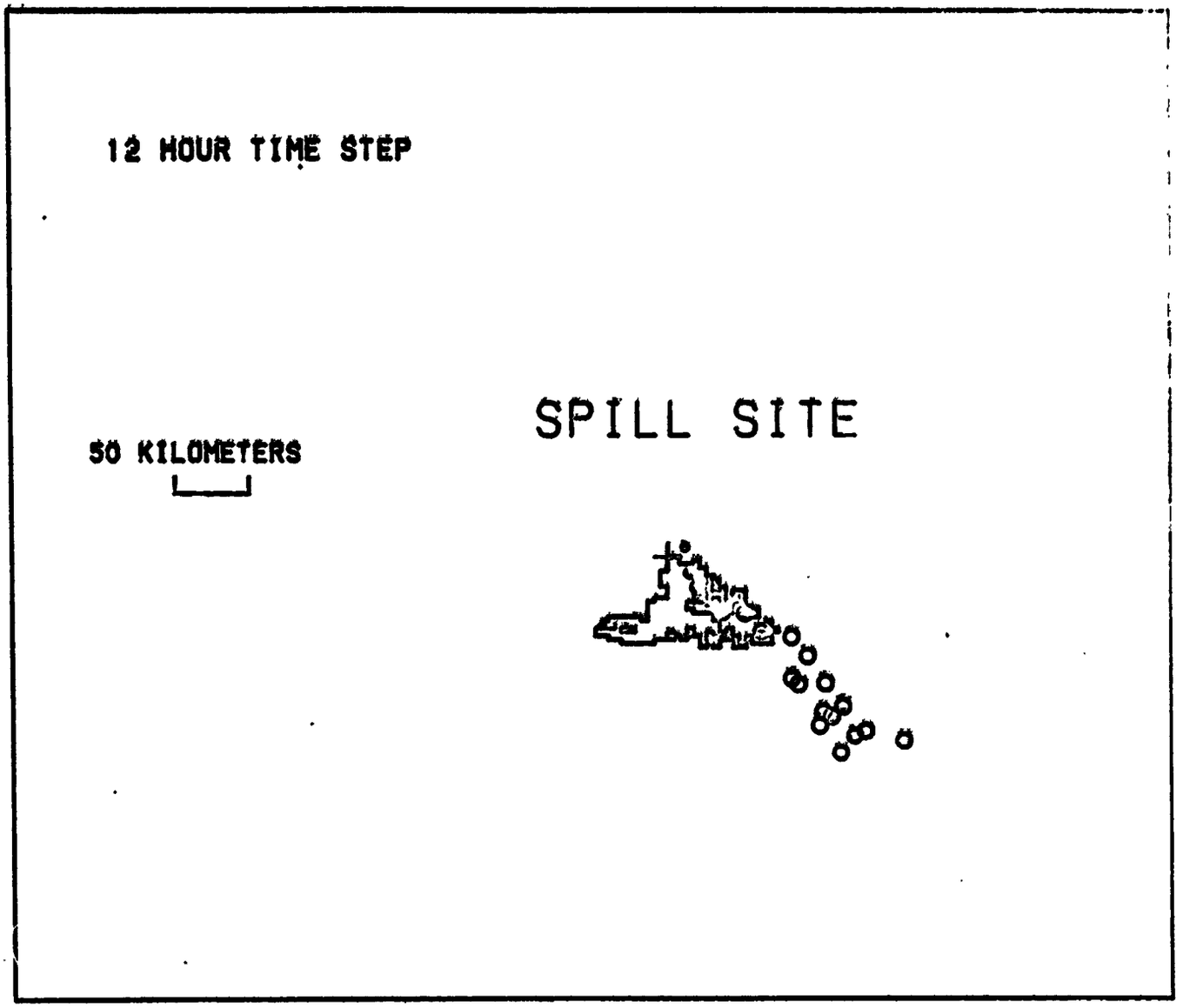

Figure 10. Surface and Subsurface Portions of the Oilspillat Time Equals 20 Days.

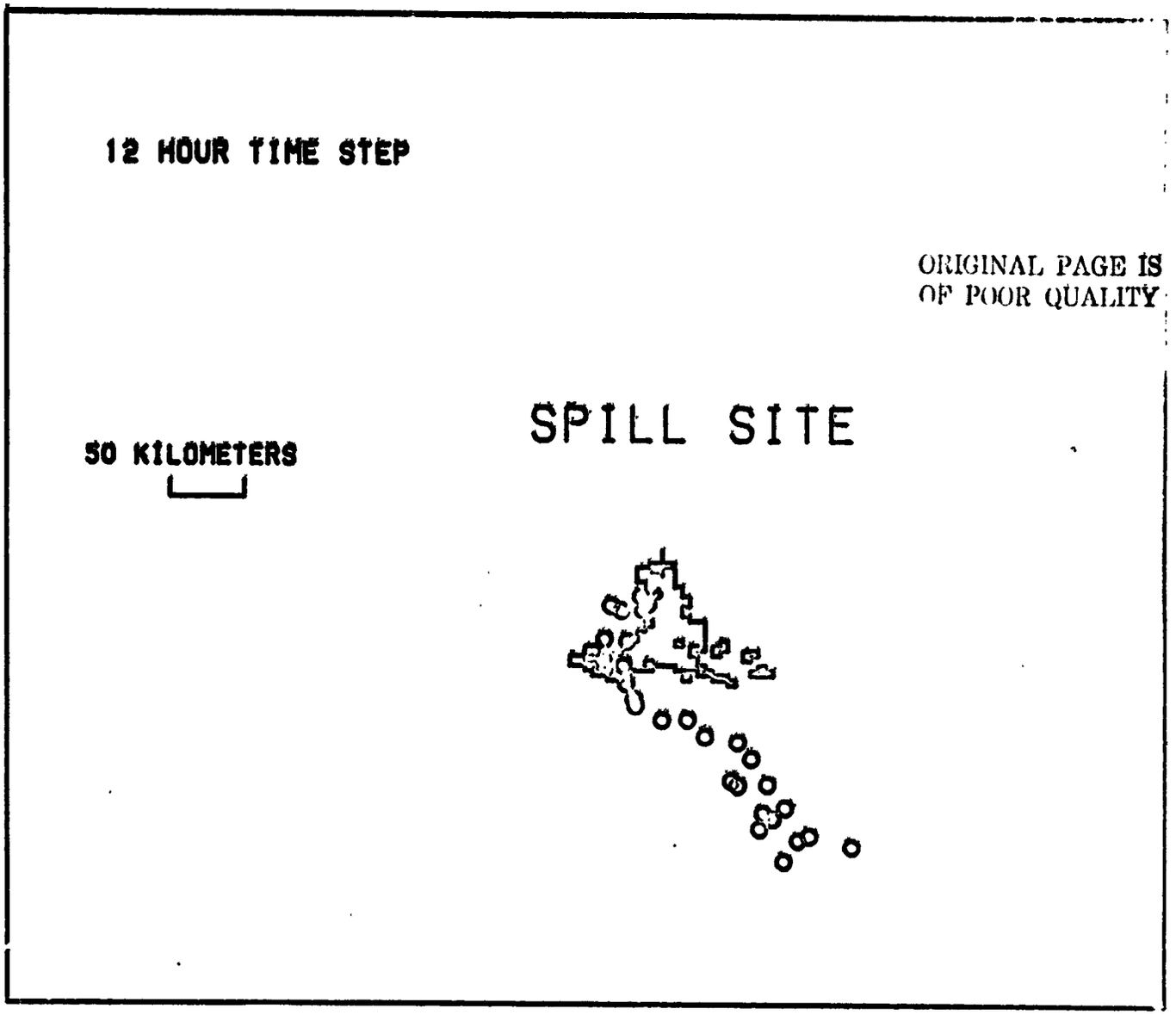

Figure 11. Surface and Subsurface Portions of the Oilspill at Time Equals 30 Days.

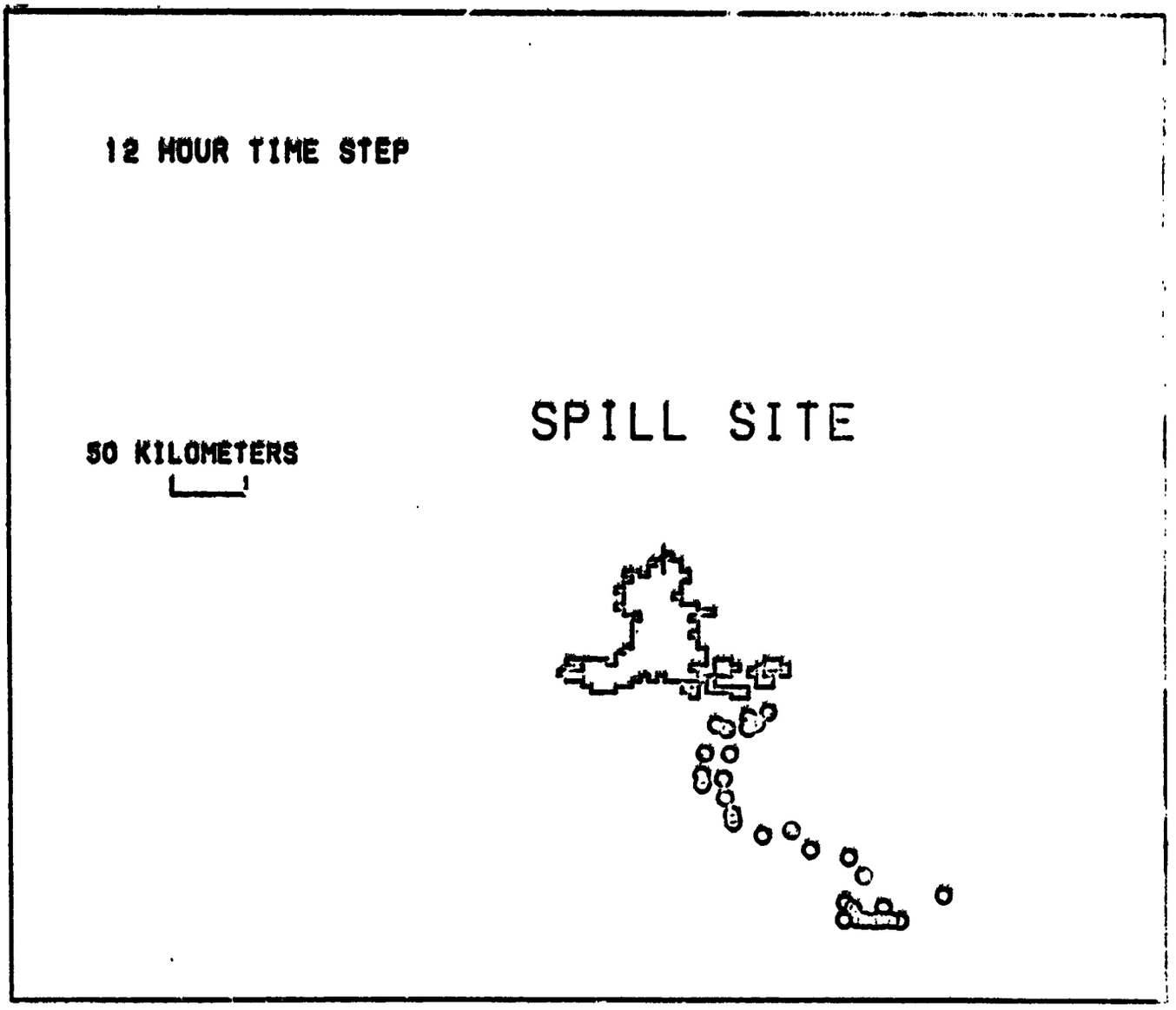

Figure 12. Surface and Subsurface Portions of the Oilspill at Time Equals 40 Days.

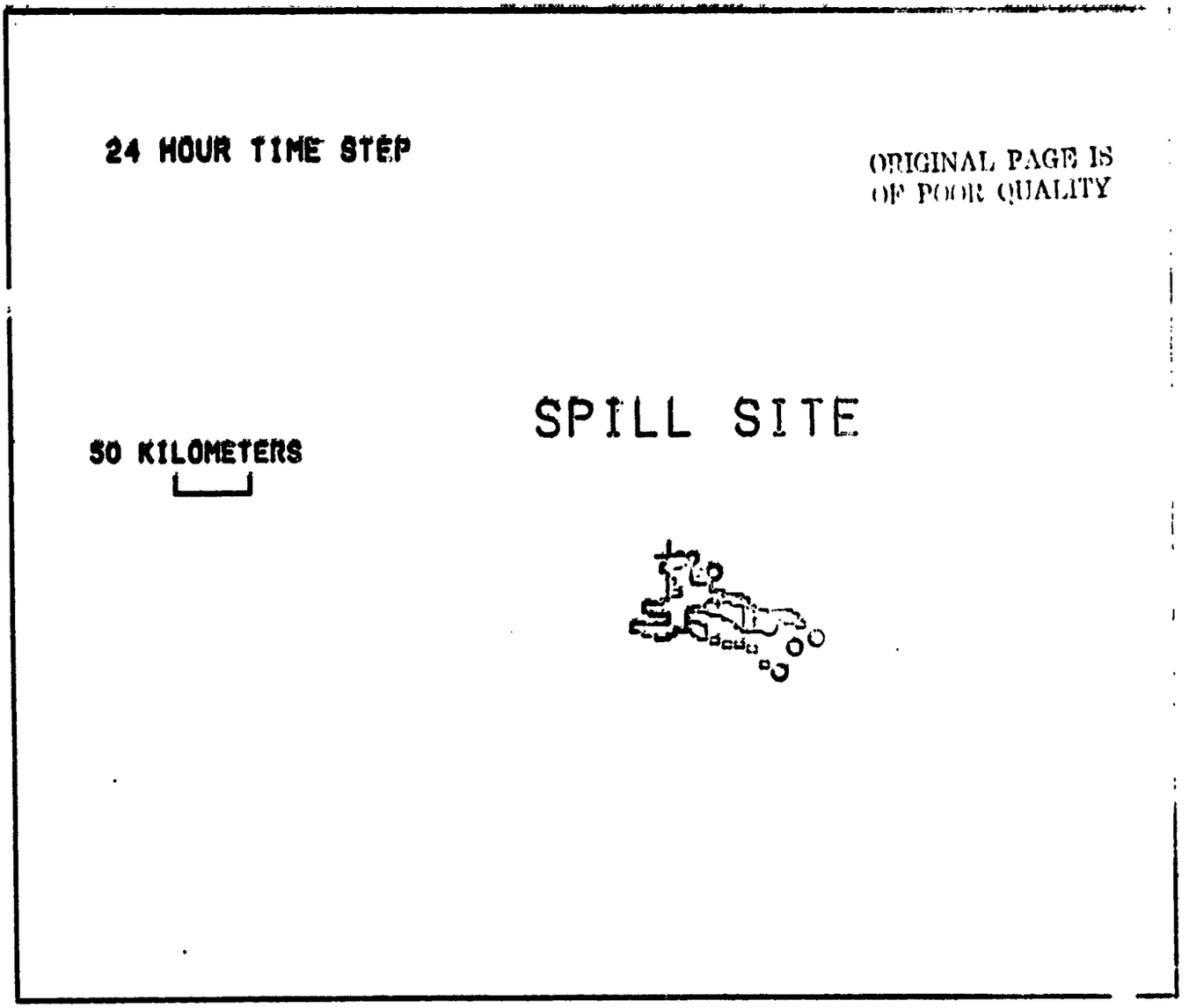

Figure 13. Surface and Subsurface Portions of the Oilspill at Time Equals 10 Days.

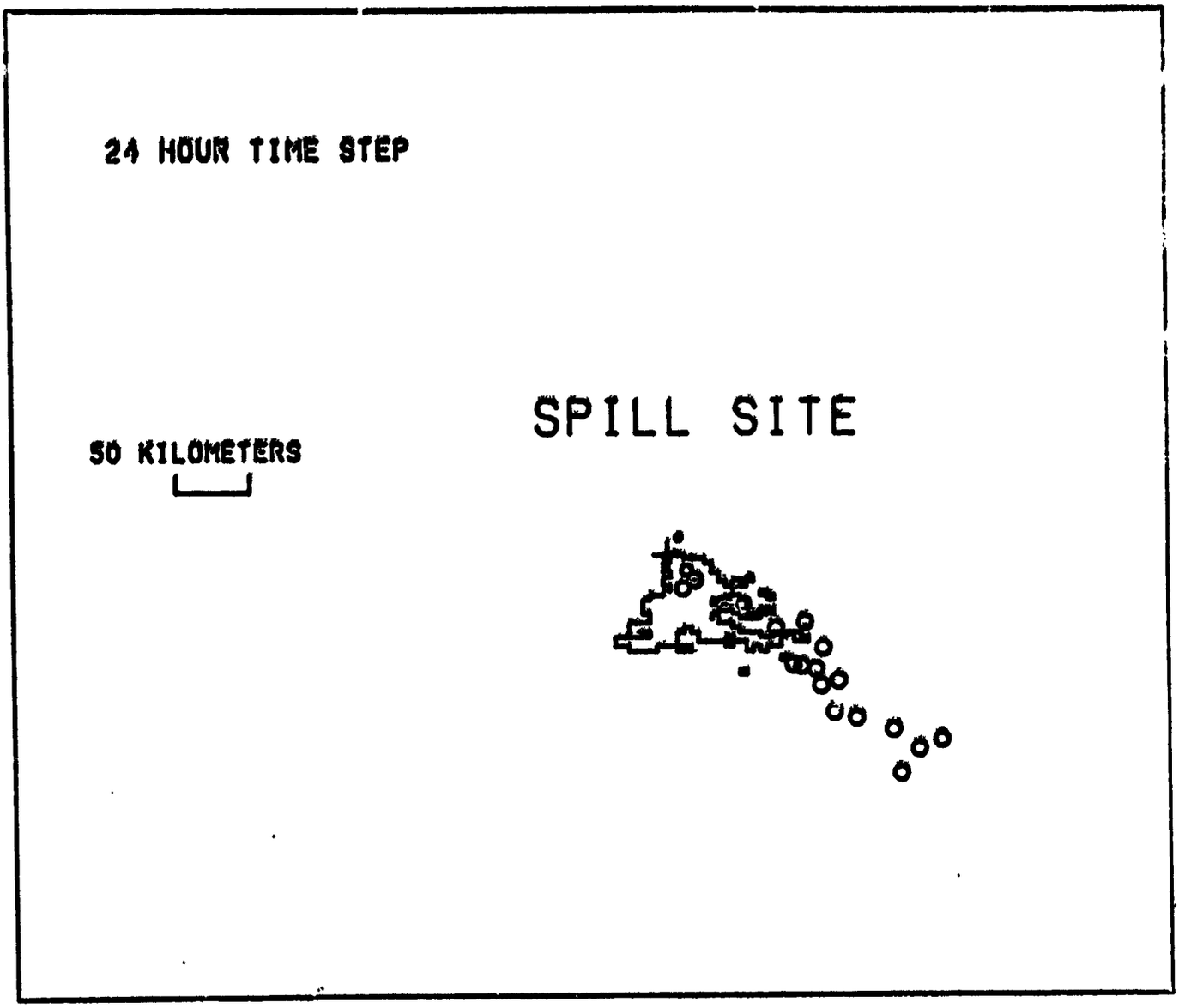

Figure 14. Surface and Subsurface Portions of the Oilspill at Time equals 20 Days.

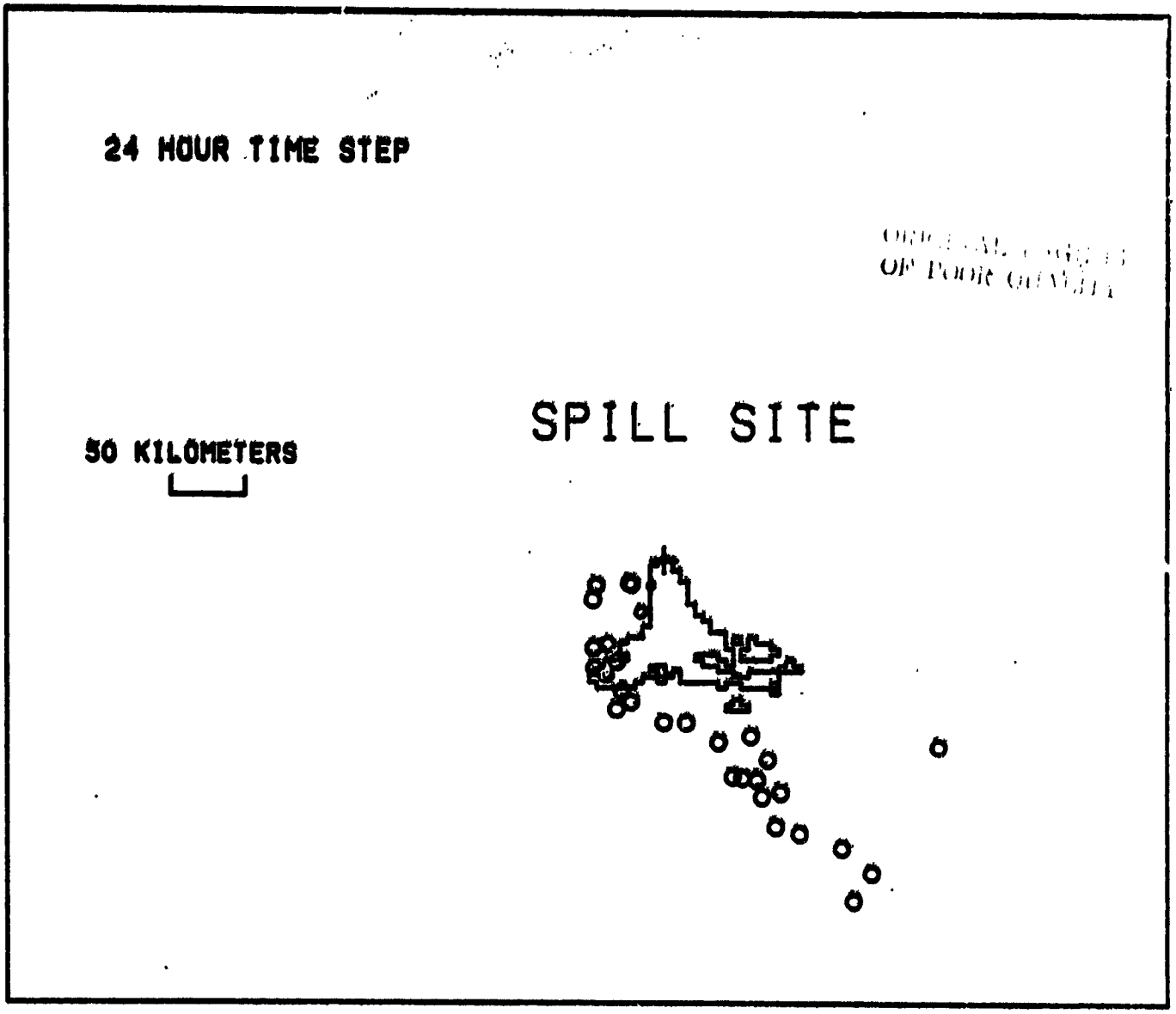

Figure 15. Surface and Subsurface Portions of the Oilspill at Time Equals 30 Days.

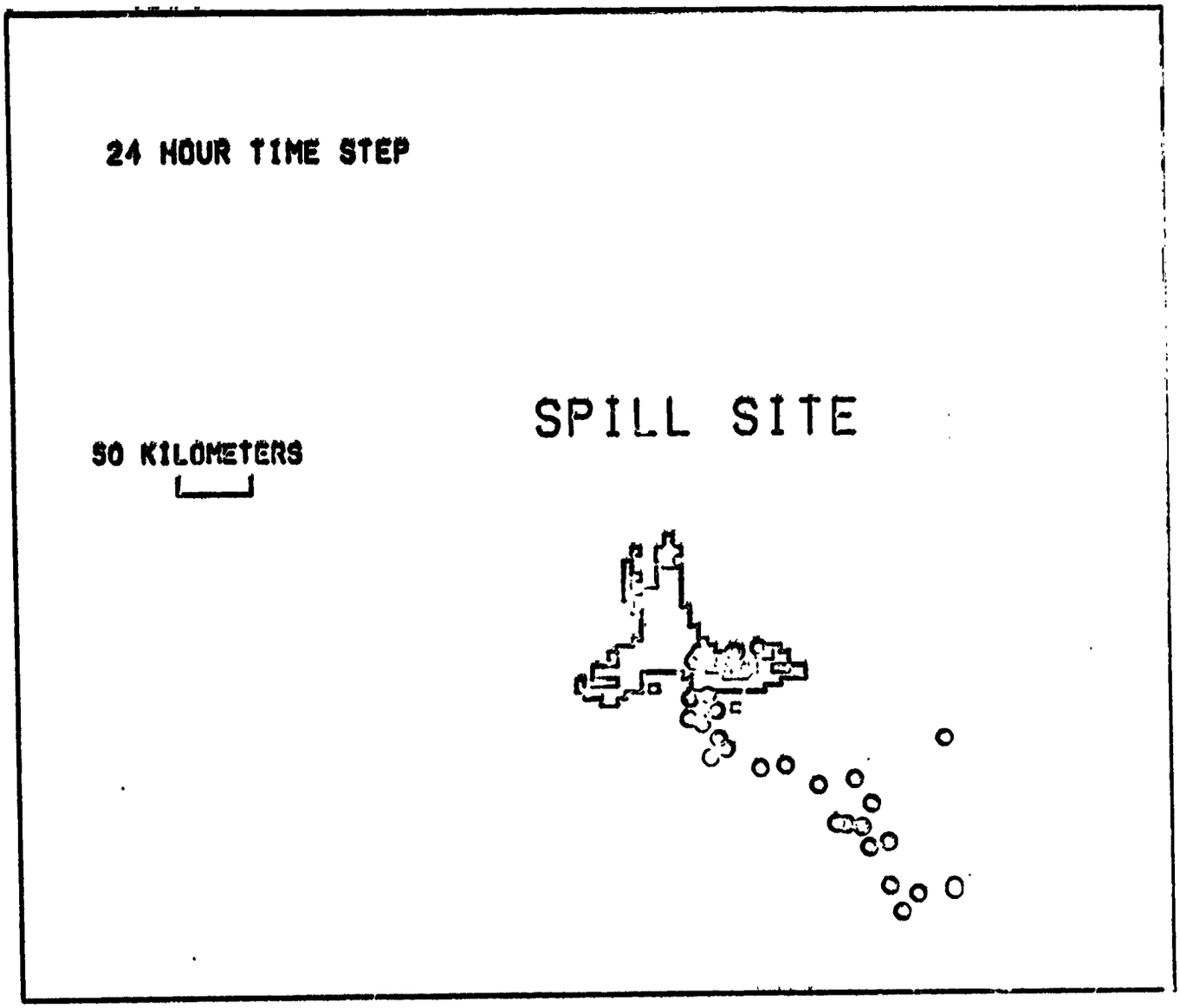

Figure 16. Surface and Subsurface Portions of the Oilspill at Time Equals 40 Days.

APPENDIX C

PASSIVE REMOTE SENSING OF OFF-SHORE POLLUTANTS

TC 5009

May 1979

TABLE OF CONTENTS
(APPENDIX C)

PASSIVE REMOTE SENSING OF OFF-SHORE POLLUTANTS

INTRODUCTION

In this report we discuss satellite detection and monitoring of off-shore dumped pollutants, other than oil. Following EPA guidelines, we divide the pollutants into four categories:

- acid waste
- industrial waste
- sewage sludge
- dredge material

Off-shore dumps consist of material that sink, or at the very least do not remain on the water surface. Of the three portions of the spectrum, visible, infrared and microwave, only the first that penetrates the water can sense waste concentration. The major problem in the visible band is to get around weather and atmospheric haze.

The results of the analyses in this report confirm the intuitive notion that all three satellite based sensors have the required sensitivity to do the job, but only the visible has sufficient spatial resolution. However, none of the sensing techniques allow a clean cut extraction of the pollutant signature from the background. We assert that the problem of pollution monitoring is not a sensor problem but a problem of mathematical modeling and data processing.

Part 1 of this report presents tables that summarize EPA pollution monitoring requirements, the significant parameters that should be measured and how well sensors in the three spectral bands, visible, infrared, and microwave fulfill these requirements. Part 2, the bulk of the report gives all the calculations, trade-offs and limitations of the three sensor systems.

PART 1: SUMMARY TABLES

1. PERMISSIBLE OFFSHORE DUMPS: USER (EPA) REQUIREMENT MATRIX

	PRECISION (relative accuracy)	ACCURACY (absolute accuracy)	RANGE	FREQUENCY	TIME DELAY (hrs) Time between event sighting and user getting data	SPATIAL RESOLUTION
OCEAN POLLUTION DUMP SIZE/SHAPE	million metric tons Acid 1.3 Industrial 1.4 Sewage 4.7	NA	Area(km^2) Depth (m) 40 to 1550 20 to 200	Discharge rate (tons/km) 20 to 200 Freq. of Trip daily, weekly, biweekly, bimonthly, and bi/yearly	.25	NA
OCEAN POLLUTION DUMP COORDINATES	200m	200 m	Acid Wastes (NY Bight) $40^{o}16'N-40^{o}20'N$ $73^{o}36'W-73^{o}40'W$ Industrial (NY Bight) $38^{o}40'N-39^{o}00'N$ $72^{o}00'W-72^{o}30'W$ Industrial (Puerto Rico) $19^{o}10'N-19^{o}20'N$ $66^{o}35'W-66^{o}50'W$	NA	NA	NA
POLLUTANT IDENTIFICATION	acid waste industrial waste sewage sludge	NA	NA	NA	NA	20m
POLLUTANT CONCENTRATION	concentration must be obtained from Permittee		1:10 to $1:10^{5}$	NA	NA	NA

II. SATELLITE PASSIVE SENSORS

	Visible	Infrared	Microwave
Wavelength	480 nm 680 nm	10.6μm 3.8μm	1 cm (30 GHz)
Spectral Band	30 nm	2μm .8μm	3 GHz
Sensor Number or Area	100 cm^2	100 sensors	N sensors
Dwell Time	38s	150μs	150 N μsec
Collecting Aperture	10 cm diameter	30 cm diameter	10 m diameter
Sensitivity	Min. Det. Cont. = .04%	10 mk 50 mk	.5K
Efficiency	1%	50%	-----
Spatial Resolution	30 m x 30 m	100m x 100m 240m x 240m	1 km x 1 km
Altitude	1 Mm	1 Mm	1 Mm
Swath Width crosstrack	1 Mm	1 Mm	1 Mm
Swath Width downtrack	10 km	NA	NA

III. RECOMMENDED MEASUREMENTS

	VISIBLE	INFRARED	MICROWAVE
POLLUTANT			
Identification	Spectral Radiance	Radiometric Temperature	Radiometric Temperature?
Concentration	Spectral Transmissivity Spectral Reflectivity	NA	NA
Constituents	Spectral Transmissivity Spectral Reflectivity	Spectral Emissivity	Spectral Emissivity ?
BACKGROUND			
Atmosphere			
Absorption	Transmittance	Transmittance	Transmittance
Scattering	Path Radiance	NA	NA
OCEAN			
Sea State	Reflectivity vs wind	Angular radiometric temperature	Angular radiometric temperature
Surface Temperature	NA	Radiometric Temperature	NA
Absorption	Diffuse Reflectance	Spectral Emissivity	NA
Scattering	Diffuse Reflectance	NA	NA

IV.1 - SENSOR FILTER SUMMARY

SENSOR NAME:	2-Band Passive Visible Radiometer (480 nm ± 15 nm 680 nm ± 15 nm)
HERITAGE:	LANDSAT D
APPLICABLE MEASUREMENT(S):	Radiance Contrast
FILTER A: IS THE RELATIONSHIP BETWEEN OBSERVABLE & MEASUREMENT WELL DEVELOPED?	Limited by weather and haze
FILTER B: IS THERE SUFFICIENT SENSITIVITY FROM ORBIT?	Yes
FILTER C: CAN THE SENSOR MEET THE USER PERFORMANCE REQUIREMENTS?	Yes
FILTER D: ARE THE REQUIRED WT, VOL, & POWER COMPATIBLE WITH NEAR-TERM SATELLITE SYSTEMS?	Yes

IV.2 SENSOR FILTER SUMMARY

SENSOR NAME:	2-Band Passive IR Scanning Radiometer (new sensor) (3.8μm ± 10%, 10.6μm ± 10%)
HERITAGE:	Tetra Tech 2-wavelength radiometer
APPLICABLE MEASUREMENT(S):	Thermodynamic Temperature of Sea Surface
FILTER A: IS THE RELATIONSHIP BETWEEN OBSERVABLE & MEASUREMENT WELL DEVELOPED?	Yes
FILTER B: IS THERE SUFFICIENT SENSITIVITY FROM ORBIT?	Yes, with large focal plane cooled arrays
FILTER C: CAN THE SENSOR MEET THE USER PERFORMANCE REQUIREMENTS?	Not the required 30 m plume width. Spatial resolution is 100 m @ 10.6μm & 240 m @ 3.8μm
FILTER D: ARE THE REQUIRED WT, VOL, & POWER COMPATIBLE WITH NEAR-TERM SATELLITE SYSTEMS?	Yes

IV.3 SENSOR FILTER SUMMARY

SENSOR NAME:	Passive Microwave Scanning Radiometer (λ - 1 cm)
HERITAGE:	NASA LRC
APPLICABLE MEASUREMENT(S):	Sea Surface Slope Statistics
FILTER A: IS THE RELATIONSHIP BETWEEN OBSERVABLE & MEASUREMENT WELL DEVELOPED?	Moderately well
FILTER B: IS THERE SUFFICIENT SENSITIVITY FROM ORBIT?	No
FILTER C: CAN THE SENSOR MEET THE USER PERFORMANCE REQUIREMENTS?	No
FILTER D: ARE THE REQUIRED WT, VOL, & POWER COMPATIBLE WITH NEAR-TERM SATELLITE SYSTEMS?	Yes

PART 2: SENSORS

In the following we present the results of our trade-off between sensitivity and resolution for three satellite based sensors

- visible imaging radiometer
- infrared scanning radiometer
- microwave scanning radiometer

1.0 OPTICAL RADIOMETRY

We have studied satellite sensors to investigate the feasibility of seeing low-contrast patterns in color on the sea surface. The feasibility divides into two questions. First, what existing or planned satellites provide a capability suitable for a demonstration. The short answer is that NASA LandSat D scheduled for launch in 1983 should provide 3% contrast in a 30 x 30 meter pixel, slightly smeared in the crosstrack direction by limited electronic response time.

The second question is, What capability can be achieved in a satellite package optimized for pollution detection? In this case NASA's present radiometric methods are inappropriate because they have traded off contrast and resolution in order to achieve absolute radiometric calibration. If we forego absolute measurements, it is possible to optimize for recognition of low-contrast patterns that represent spilled pollutant. This leads to a sensor that performs more like a low-light-level television system.

The following sections address the two questions. The first describes the radiometer aboard LandSat D, and the second describes possibilities for a system dedicated to the pollution detection problem.

1.1 LandSat D: Thematic Mapper

This satellite carries a radiometer that scans a swath 100 nautical miles wide on the earth's surface. In the visible range of interest are two color bands, a blue-green one from 450 to 520 nm and yellow-orange from 520 to 600 nm. Each band uses an array of 16 silicon photodiodes as detectors. A mechanical scanner sweeps the crosstrack direction while orbital motion scans along track.

The relevant properties of the LandSat D radiometer appear in Table 1 along with the symbols used to denote these quantities in the equations

TABLE 1: PROPERTIES OF LandSat D

Swath width: S = 185 km

Altitude: H = 1 Mm

Velocity, equivalent surface: V = 6.6 km/sec

Detectors in array: N = 16

Footprint (square pixel) size: δ = 30 meters

Dwell time: τ = 10μsec

Spectral radiance of the sea: L_λ = 0.035 W/sr/m^2/nm

Filter pass, Band 1: b = 80 nm

Telescope efficiency: η = 0.2

Aperture diameter: d = 40 cm

Detector responsivity: R = 0.6/volt

Thermal noise, spectral density: kT = 4 x 10^{-21} watt/Hz

(T = 290 kelvin)

Electron's charge: e = 1.6 x 10^{-19} coulomb

Detector/amplifier bandwidth: B = 50 kHz

Noise resistance: R = 1.0 x 10^9 ohms

(feedback resistor for transimpedance amplifier)

that follow. The area coverage rate is the product of velocity V by swath width S:

$$\dot{A} = VS = 1220 \text{ km}^2/\text{sec},$$

From this we derive the dwell time τ that one of the 16 sensors inspects each pixel (δ by δ) on the sea surface:

$$\tau = N\delta^2/\dot{A} = 10\mu\text{sec}$$

Note that $N\delta^2$ is the footprint of the N sensors on the earth surface.

The scene (sea and air above it) has a certain radiance L (watt/m^2/steradian) that is focused on the detector where power p produces current I:

$$p = L \text{ (efficiency) (area) (solid angle)}$$
$$\text{(solid angle)} = \text{(aperture area/altitude}^2) = \pi d^2/4H^2$$
$$p = L\eta\delta^2 (\pi d^2/4H^2)$$
$$\frac{p}{L} = \frac{\pi}{4}\eta \left(\frac{\delta d}{h}\right)^2 = 22.6 \times 10^{-12} \text{ m}^2 \qquad (1)$$

The light detector is a silicon photodiode that converts electric current with typical responsivity R = 0.6 amps/watt. To facilitate calculations that follow, we use one factor K to convert sea radiance to detector current I:

$$K \equiv \frac{I}{L} = \frac{I}{p}\,\frac{p}{L} = R\,\frac{p}{L} = 13.6 \times 10^{-12} \text{ m}^2\text{sr/volt} \qquad (2)$$

We shall estimate the noise current i_n in the detector and use K to convert it to a minimum detectable radiance (MDL) on the sea surface:

$$MDL = i_n/K \qquad (3)$$

Two types of noise limit performance of the system, shot and thermal (Johnson), given by the following:

$$i_s^2 = 2eIB \tag{4a}$$

$$i_t^2 = 4kTB/R \tag{4b}$$

$$i_n^2 = i_s^2 + i_t^2 \tag{5}$$

Here R is the load resistance across the photodiode, or the feedback resistance in the case of a circuit with a transimpedance amplifier. Normally thermal noise would limit the performance of a photodiode, but in this case NASA has used a newly developed sensor with a transimpedance amplifier. The equivalent noise resistance is remarkably high, $R = 10^9$ ohms.

Substituting Eqs. 4a and 4b in 5, and using Eqs. 2 and 3 gives

$$MDL = \sqrt{(C_1 + C_2 L)\, B} \tag{6}$$

where

$$C_1 = 4kT/K^2R \qquad C_2 = 2e/K \tag{7}$$

and

$$C_1 B = 4.35 \times 10^{-3}\ (W/m^2/sr)^2$$

$$C_2 B = 1.18 \times 10^{-3}\ W/m^2/sr \tag{8}$$

We have plotted Eq. 6 in Figure 1 in the form MDL/L, which is the minimum detectable contrast. One point on this curve is particularly significant at a radiance of $L_s = 2.8\ W/m^2/sr$. This value is typical of scene radiance looking at open ocean (no clouds). The minimum detectable

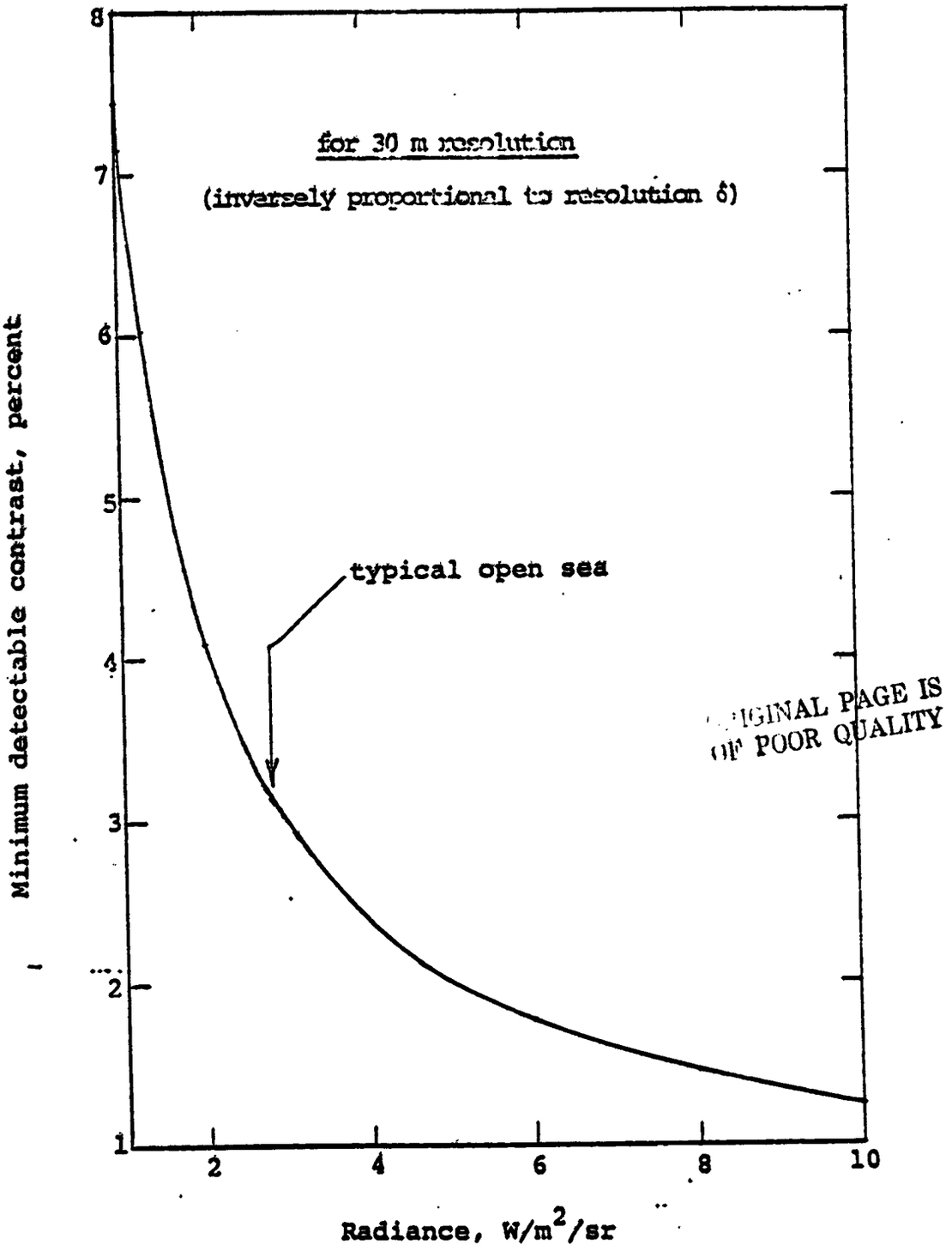

Fig. 1. Minimum detectable contrast in thematic mapper, Landsat D

contrast is 3.1%, and its reciprocal is the signal-to-noise ratio in terms of photocurrent (I/i_n), namely 32. It happens that NASA has specified this same signal-to-noise ratio at the same radiance in its contract with Hughes Santa Barbara Research Center. The saturation radiance is 10 $W/m^2/sr$ at which the specified signal-to-noise is 85, a bit higher than our estimate of 79 (reciprocal of 1.3% in Figure 1).

We estimated the radiance of the sea by first averaging its spectral radiance (see in Figures 12, 13 and 14 of Roswell Austin's paper in Optical Aspects of Oceanography, edited by Jerlov and Nielsen and reproduced in the Appendix). The average spectral radiance L_λ = 0.035 $W/m^2/sr/nm$, multiplied by the filter pass band, b = 80 nm, then gives the result we used:

$$L_s = L_\lambda b = 2.8\ W/m^2/sr. \quad \text{(in the blue-green)}$$

The same graphs indicate that only 14% (a seventh) of the light comes from the sea surface; the rest is backscattered by air. Of the part from the sea, about a third is surface reflection. Thus 10% of the radiance at the radiometer is light that has penetrated the sea. Presumably this percentage is improved by avoiding sun glint.

Finally, the frequency response of the thematic mapper rolls off at B = 50kHz = $1/2\tau$, and so the radiance in one pixel spills over a bit into the next one or two pixels in the crosstrack scan direction.

1.2 Dedicated Imaging Sensor

This section discusses a satellite package dedicated to those applications in which the main problem is to see low-contrast patterns. The best approach is to use a large array of sensors to increase the dwell time on each pixel (compared to LandSat D). An ordinary television camera has in effect an array of about 250,000 sensors occupying a total area of about one square inch. It would be reasonable to assume a total photosensitive area as large as 100 cm^2, which can be divided into vari-

ous numbers of pixels (TV lines) depending on the trade-off between contrast and resolution. If common television camera tubes were used, 17 of them would be required to achieve this area in each color band, i.e. 51 for a tri-color system. However, oversized tubes or some other advanced solid-state image sensor would reduce the total number of devices. We shall leave the question of size open and denote the photosensitive area by a.

A wide swath is very desirable to catch as many breaks in the clouds as possible. We assume that the width equals the altitude, i.e.

$$X = H = 1 \text{ Mm} \tag{9}$$

as shown in Figure 2. In the direction along track, the field of view is smaller to avoid excessive photosensitive area,

$$a = xy \tag{10}$$

(see Figure 2). If Y denotes the dimension of the field of view along track, then the dwell time is

$$T = Y/V \tag{11}$$

It will be advantageous to make this time as long as possible, even 10 seconds or more, to average out clutter from the sea surface. This feature requires some form of motion compensation, but the result is rewarding because it will very thoroughly remove statistical fluctuations in sun glint, and to some extent those due to patches of foam. Depending on sea state and wind, this can be a great advantage over previous NASA radiometers that essentially "freeze" the instantaneous clutter in each pixel.

Let us assume a fairly advanced system with fast optics, say a focal ratio of two:

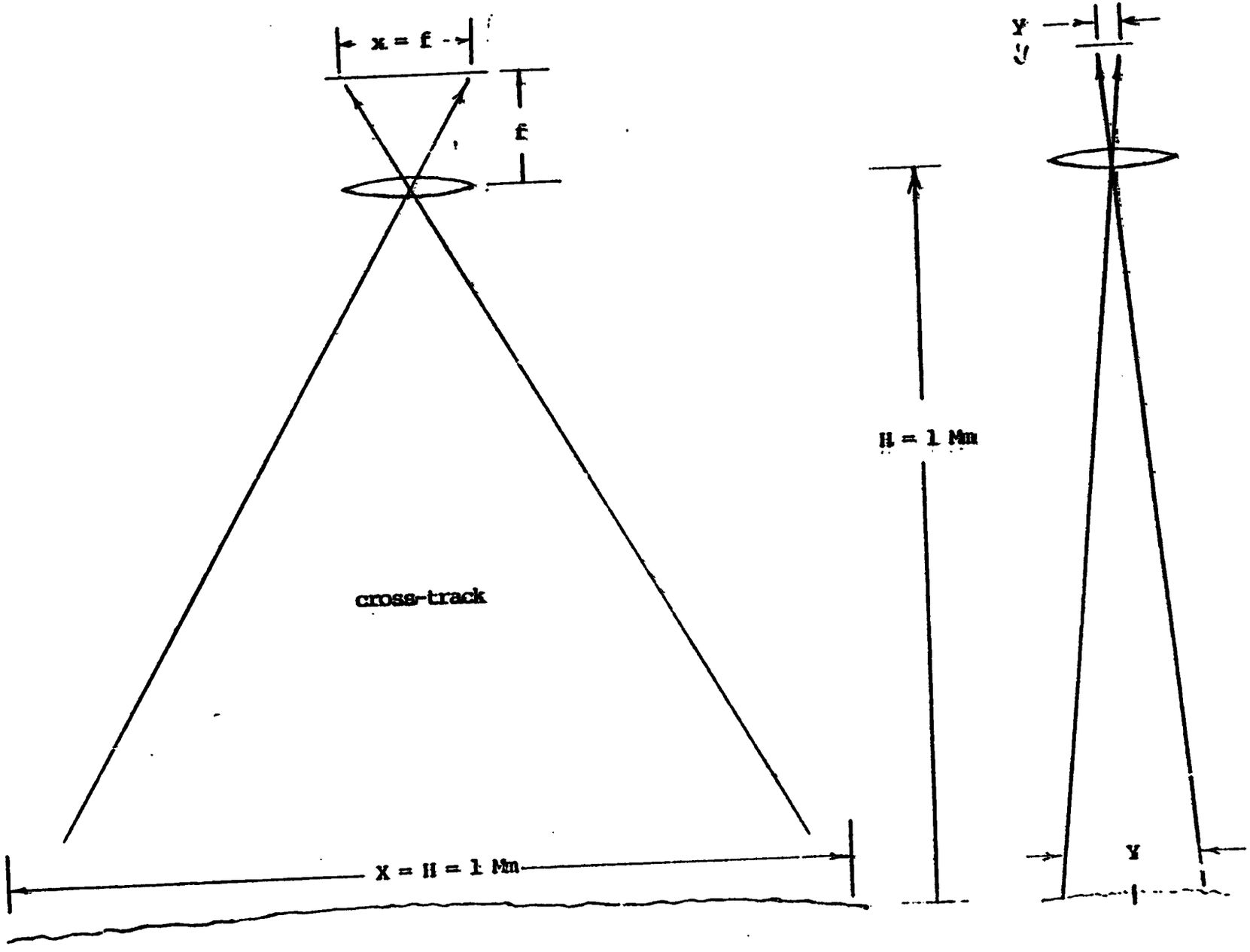

Fig. 2. Optical geometry

$$f/d = 2. \tag{12}$$

Any faster optics would not work well with an interference filter to limit the band to $\Delta\lambda = b$. Equation 12 determines the solid angle of rays into one point on the focal plane:

$$\Omega = (\pi/4)\ (d/f)^2 = \pi/16 \tag{13}$$

Apart from an optical efficiency factor η_o, the image has the same radiance as the object, namely

$$L_s = L_\lambda b \tag{14}$$

where L_λ is the spectral radiance and b the filter bandwidth. Thus the number of photons collected in the entire field of view is

$$N_\phi = (L_s/h\nu)\eta_o a\Omega\ T \tag{15}$$

and the number in each pixel is

$$n_\phi = \frac{N_\phi \delta^2}{XY} = \frac{\pi}{16}\ \frac{\eta_o L_s}{h\nu}\ \frac{a\delta^2}{VH} \tag{16}$$

where Equations 9, 11, 13 and 15 have been used.

The mean number of detection events in each pixel of the photosensitive surface is

$$n_d = \eta_q n_\phi \ , \tag{17}$$

where η_q is quantum efficiency, and the standard deviation in this number is

$$\Delta n_d = \sqrt{n_d} \tag{18}$$

These equations combine to give the minimum detectable contrast

$$MDC = \frac{\Delta n_d}{n_d} = \frac{1}{\sqrt{n_q n_\phi}} \qquad (19)$$

Substituting Eq. 14 in 16 in 19 gives

$$MDC = \sqrt{\frac{16}{\pi} \frac{h\nu}{n_o n_q} \frac{VH}{bL_\lambda}} \frac{1}{\delta\sqrt{a}} \qquad (20)$$

Curiously, the collecting aperture d has dropped out of this expression because it is tied to f through the focal ratio, Eq. 12, and to other factors through the geometry of Figure 2.

For plotting this expression, it is convenient to put

$$L_\lambda = \ell \Lambda \qquad (21)$$

where Λ is the peak spectral radiance when the sky is clear and the sun is high,

$$\Lambda = .035 \text{ W/m}^2\text{/sr/nm},$$

and ℓ represents all environmental losses of illumination due to sun angle, hydrometeors, or whatever. Finally we lump all losses of light together, whether in the environment or the equipment and put

$$n = \ell n_o n_d \qquad (22)$$

For example, we might have

optical transparency - .5 (mostly in the filter)
20% aperture observation - .8
detector quantum efficiency - .15

sun angle - .5
haze and Rayleigh scattering - .33

product: $\eta = .01$

In this form, Eq. (2) becomes

$$MDC = \sqrt{\frac{16}{\pi} \frac{(h\nu)\ VH}{\eta \Lambda b}} \frac{1}{\delta\sqrt{a}} \tag{23}$$

Figure 3 shows MDC versus $\delta\sqrt{a}$ (δ in meters and $\sqrt{a}$ in cm) with η as a parameter.

For example, when

$a = 100\ cm^2$ (10 by 10 detector surface),

$\delta = 30\ m, \quad \eta = 1\%$

then $MDC = 3.8 \times 10^{-4}$.

Quite clearly this is less than the natural contrast noise on the sea due to patches of foam, seaweed, windrows, and the like. Therefore, we desire a long dwell time on each resolution cell to average out these factors as much as possible. Equation 11 gives

$$T = Y/V = (y/f)\ (H/V) \tag{24}$$

where we have used

$$Y/H = y/f \tag{25}$$

which results from similar triangles in Figure 2. The factor y/f in Eq. 24 cannot in practice be made arbitrarily large to attain a long dwell time because the motion compensation becomes nonlinear and complicated as the angles involved grow large. It is beyond the scope of this study to solve such details, but for the sake of illustration, suppose

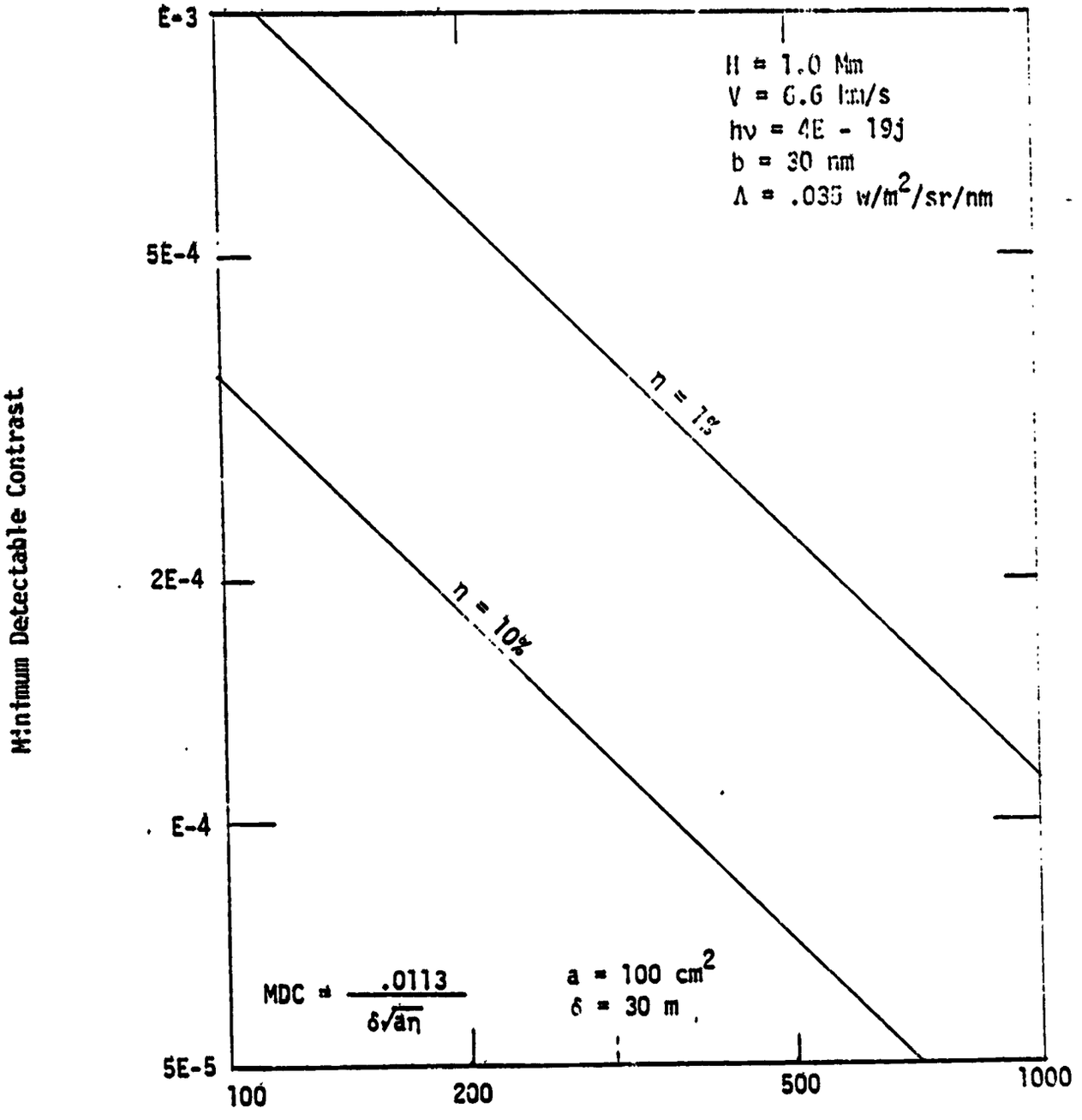

Figure 3. Minimum Detectable Contrast of Visible Radiometer

$$y/f = 1/4, \tag{26}$$

which keeps the angles quite small ($< 7^0 = \arctan y/2f$). Then Eq. 24 gives $T = 38$ sec, a nice long period that averages out nearly all foam statistics as well as sun glint. Moreover, using $x = f$ (Figure 2) and $xy = a$ (Eq. 10), we find that

$$f = 2\sqrt{a}$$

if $a = 100\ cm^2$ (previous example) then

$$f = x = 20\ cm$$
$$y = a/x = 5\ cm$$
$$d = f/2 = 10\ cm,$$

all very small and reasonable.

For the case of an aircraft platform, we have not plotted the MDC as in Figure 3 because it is so small that it is meaningless, i.e. the product VH in Eqs. 20 and 23 is even smaller. However, the dwell time for averaging out clutter is not as long. Assuming

$$H = 3\ km\ (9840\ ft)$$
$$V = 160\ m/s$$

Equations 26 and 24 give $T = 5$ sec, long enough to average out sun glint, but not much else.

2.0 INFRARED SCANNING RADIOMETRY

For our purposes, "infrared" means wavelengths from 3 to 20μm. Radiation from sea and clouds in this band consists almost entirely of thermal emission, reflected and scattered sunlight being negligible. The so-called "photographic" infrared, wavelengths near 1μm, should be classed with visible light for our purposes, because this band is a component of sunlight, and so radiometry works only during the day. Within the band of interest, there are two particularly clear "windows", one at 10.6μm and the other at 3.8μm, as shown in Figure 4. The 10.6μm band (9.6 to 11.6) is the better for three reasons. First, it provides 200 times as many photons, which overpower noise in the sensor and provide more sensitivity. Second, the long wavelength has minimum sensitivity to small particles, haze and such, because Rayleigh scattering decreases as λ^4. Finally, this window has the least atmospheric absorption (from gasses and vapors) of any optical band (including visible and ultraviolet).

When the radiometer looks vertically down at the sea, it provides an almost pure measure of the temperature of the sea surface uncorrupted by other factors. Reflected sky radiance comprises only 1 or 2% of the signal at incidence angle of 0 to 30°, but this increases to 100% at grazing incidence; see Figure 5. The observed radiance originates very close to the surface, the mean distances being

$$\begin{aligned} \zeta(3.8) &= 60\mu m = 16\lambda \\ \zeta(10.6) &= 11\mu m = 1\lambda \end{aligned} \qquad (27)$$

This means that the radiometer is very sensitive to any floating pollutant, such as an oil spill that inhibits evaporation at the surface. At the very least, a coating changes the temperature by 0.5K, which is the temperature change through the so-called conduction layer, approximately the top 1.5 mm of the sea. This is a relatively large signal, but of course it is diluted with the signal from normal water wherever the film is thin and breaking up.

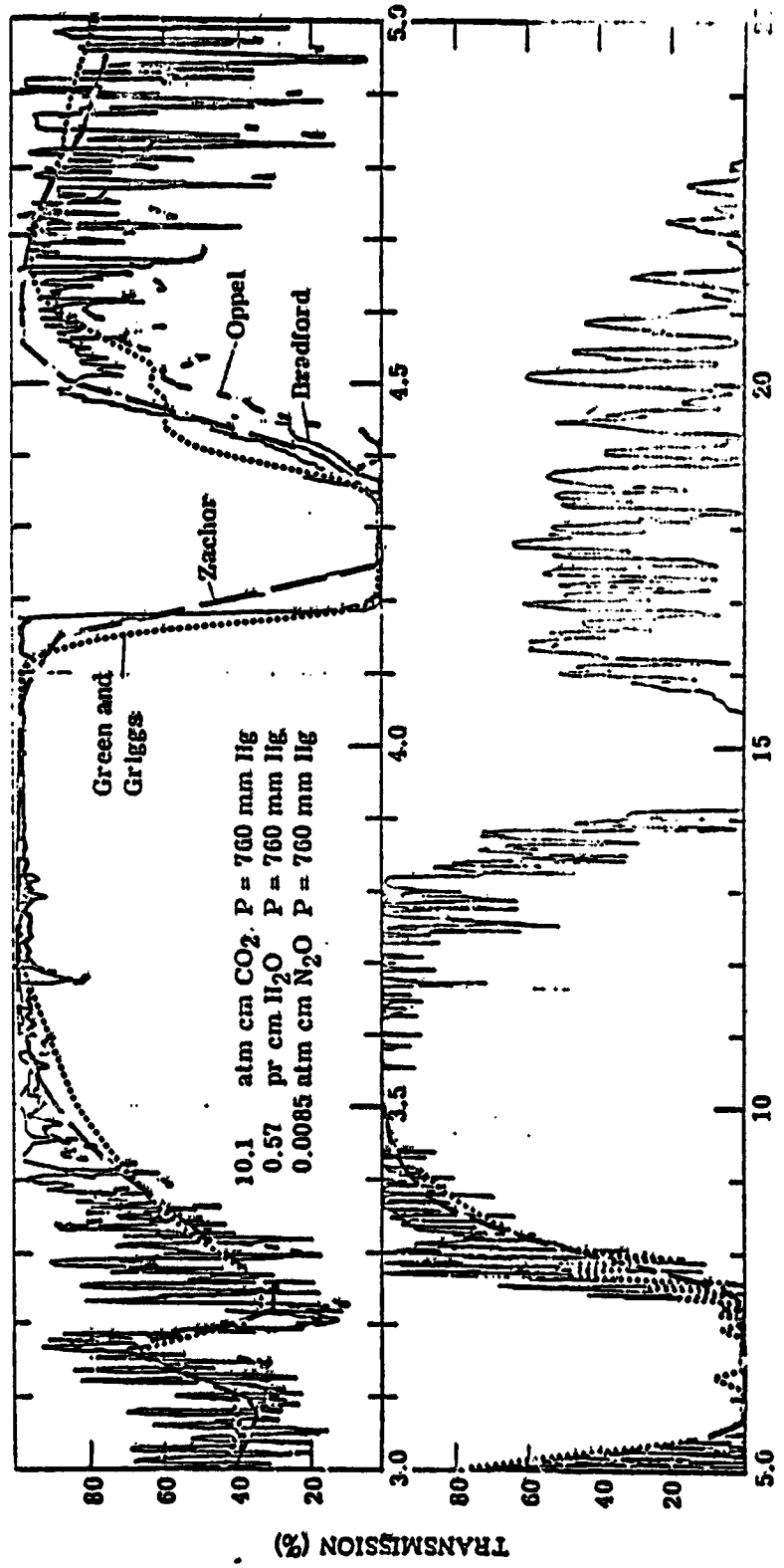

Fig. 4. Transmission over 1,000 ft Path at Sea Level

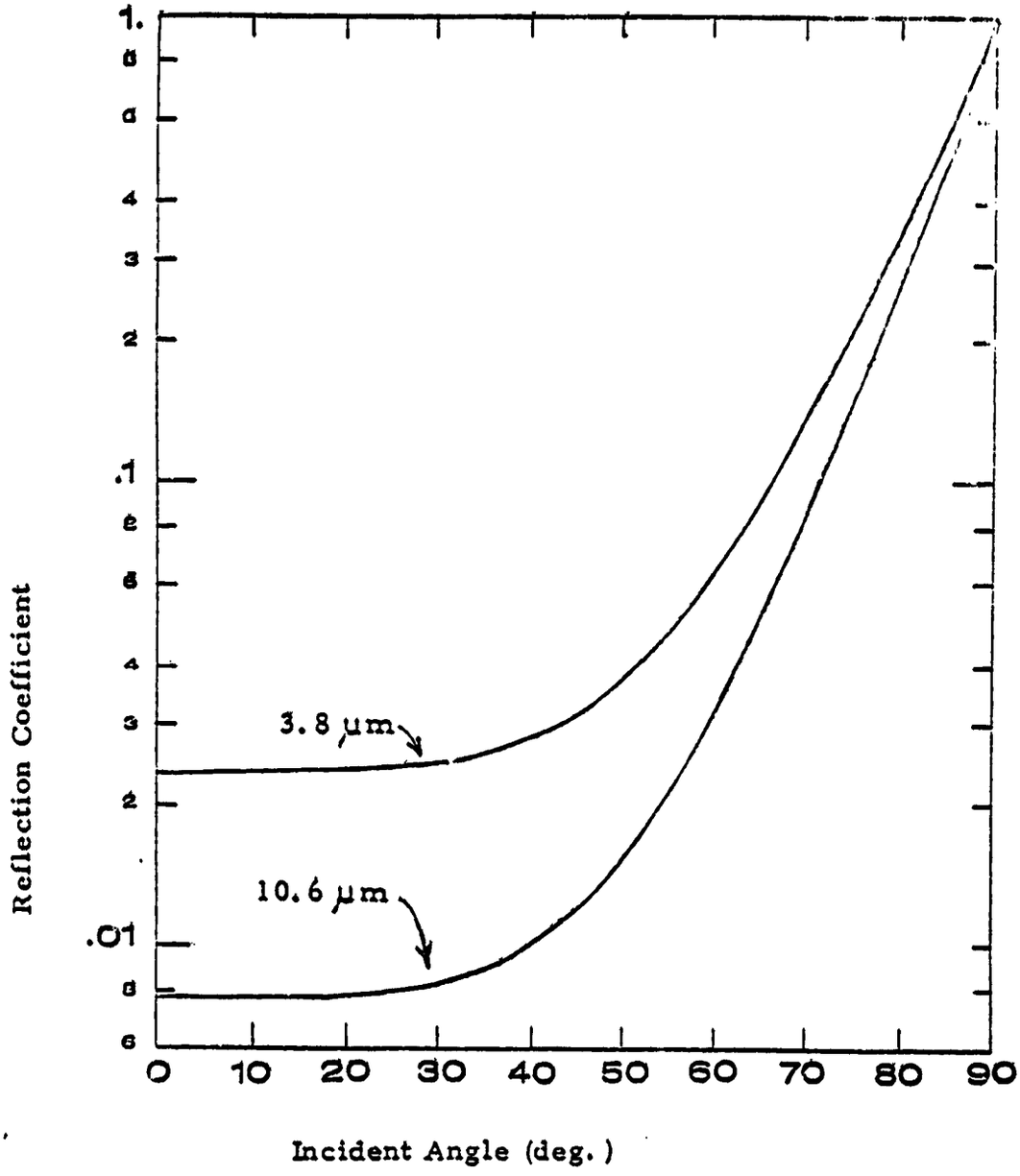

Fig. 5. Reflection Coefficient of Water

A sensitivity goal of one fiftieth this amount, i.e. 10 mK is probably appropriate. We show that an advanced satellite radiometer at 10.6um can see a $(100\ m)^2$ resolution cell with this temperature sensitivity providing it has 100 detectors in array. A radiometer at 3.8um would only resolve about $(240\ m)^2$. An airborne radiometer of the same design would be overkill, i.e. orders of magnitude excessive performance capability.

We doubt if the infrared radiometer has much sensitivity to pollutants that mix into bulk water, for then the surface effect is very small. There may be exceptions when the sun is shining on the water and the pollutant discolors it enough to raise the temperature by absorbing sunlight. Also, most chemicals release or absorb heat upon dilution, but this heat is a transient occurrence observable only when the dump is quite fresh.

2.1 Blackbody Formulas

The sea is very nearly a blackbody in the infrared with emissivity

$$\varepsilon_o = 1 - R_o = .98 \text{ to } .99$$

at normal incidence as discussed in connection with Figure 5. Thus it is appropriate to express radiance in terms of the blackbody function B:

$$L(\lambda) = \varepsilon B(\lambda,T) \text{ power/area/steradian}$$

However, for reasons discussed in Section 2.3, it is more appropriate to express blackbody radiation in terms of photons instead of the traditional formulas for power. We denote this change by using the symbol Q instead of B:

$$\varepsilon B \rightarrow \varepsilon Q, \text{ photons/sec/area/steradian}$$

We also denote spectral radiance with a subscript λ:

$$Q_\lambda = Q/b, \text{ ph/sec/area/sr/um} \qquad (28)$$

where b is the spectral bandwidth in micrometers.

In these terms, the Planck radiation formula is

$$Q_\lambda = \frac{C_q}{\lambda 4} \exp\left(-\frac{C_e}{\lambda T}\right) \tag{29}$$

where

$$C_q \equiv 2c - 6.0E26 \text{ photons} \cdot \mu m^3/sec/m^2/sr$$
$$C_e \equiv hc/k = 14388\mu m \cdot \text{kelvin} \tag{30}$$

Quantities useful for evaluating Equations 28, 29, and 30 in the two bands of interest appear in Table 2 above the dashed line. Those quantities involving temperature are evaluated at 295 kelvin. The choice of bandwidth b (fifth in the list) is governed by the need to avoid absorption lines in the air spectrum, Figure 4.

In all infrared radiometers, it is traditional to express the observed radiance in temperature units, i.e. the temperature of a blackbody that would give the same radiance as the observed value. This is quite natural because radiometers are calibrated by looking at a blackbody at a known temperature. Thus we need a formula to express a radiance increment ΔQ in terms of the equivalent temperature increment:

$$\Delta T = \Delta Q/Q' \tag{31}$$

where $Q' \equiv \partial Q/\partial T$. Differentiating Equation 29 gives the required expression:

$$\frac{Q'}{Q} = \frac{\partial}{\partial T} \ln Q_\lambda = \frac{C_e}{\lambda T^2} \tag{32}$$

or with the aid of Equation 31.

TABLE 2 USEFUL RADIOMETRIC QUANTITIES

evaluated at two wavelengths and T = 295 Kelvin

Quantity	Units	3.8μm	10.6μm
$C_e/\lambda = h\nu/k$	kelvin	3786	1357
$C_e/\lambda T = h\nu/kT$	(dimensionless)	12.83	4.601
$C_q/\lambda^4 = 2c/\lambda^4$	photons/s/m^2/sr/μm	2.88E24	4.75E22
Q_λ (Eq. 29)	ph/sec/m^2/sr/μm	7.67E18	4.77E20
b (suitable in air)	μm	0.6	2.0
$Q(295,\lambda) = Q_\lambda b$	ph/sec/m^2/sr	4.6E18	9.5E20
$Q/Q' = kT^2/h\nu$	kelvin	23.0	64.1
R_o (nomal incidence)	%	2.40	0.83
$R_o Q/Q'$	millikelvin	552	532

note only 4% difference

$$\Delta T = \frac{\Delta Q}{Q}\left(\frac{Q}{Q'}\right) = \frac{\Delta Q}{Q}\left(\frac{\lambda T^2}{C_e}\right) \tag{33}$$

or

$$\frac{\Delta T}{T} = \frac{\Delta Q}{Q}\left(\frac{\lambda T}{C_e}\right) = \frac{\Delta Q}{Q}\left(\frac{kT}{h\nu}\right) \tag{34}$$

The ratio Q/Q' for Equation 33 is listed below the dashed line in Table 2.

2.2 Natural Background Fluctuations

The last item in Table 2 gives a particularly interesting special case, the maximum effect that sky can have on the apparent temperature of the sea. Suppose the sky is completely overcast, and a radiometer beneath the overcast looks directly down at the sea. (or else a satellite radiometer looks through a small hole in the overcast) Also suppose that the temperature of the overcast is not too different from that of the sea. (A small difference, say 5K, does not matter much since the sky contributes only 1 or 2% of the radiance.) Then the sea and sky in effect form an isothermal enclosure, and the radiometer necessarily sees the thermodynamic temperature of both:

$$Q_{cloudy} = Q(T)$$

But when the sky is clear

$$Q_{clear} = \varepsilon Q(T) = (1 - R_o)\, Q(T)$$

$$\Delta Q = Q_{cloudy} - Q_{clear} = R_o Q(T)$$

and finally, using Equation 31,

$$\Delta T = \frac{\Delta Q}{Q'} = R_o \frac{Q}{Q'} \approx 540 \text{ mK} \tag{35}$$

as listed in Table 2. If the sky is partly cloudy, then the temperature increment is

$$\Delta T(f) = f(R_0 Q/Q') \tag{36}$$

where f is the fraction of cloud cover. It is not easy to determine f accurately. Since the radiometer sees a blurred image of the sky in the wind-roughened sea, one cannot say exactly how much of the sky it is seeing nor to what degree. If an estimate of f is in error 10%, then the corresponding error in temperature is

$$\Delta T = 0.1\ R_0 Q/Q' = 50\ mK, \tag{37}$$

which is about the maximum natural noise level for broken clouds, unless an auxillary sky radiometer is used to make a correction.

If radiometric temperature is measured at both 3.8 and 10.6μm, then there are two Equations 36 which in principle be solved for two unknowns, water temperature and fractional cloud cover. But a curious coincidence occurs as shown in Figure 6. The x and y axes represent the two unknowns, and the locus of possible values is plotted for each radiometric measurement. The intersection that fixes f and T_{sea} has such an extremely small angle that the solution is worthless in the presence of expected noise.

If the two radiometric temperatures, T(3.8) and T(10.6), are substracted, then both of the principal effects, i.e. T_{sea} and T_{sky}, are eliminated and some other residual effect remains. We do not know what the principal contribution is, but it is not roughness, as our computer simulations have shown. It may turn out that the residual is very sensitive to pollution. Perhaps it is the temperature difference resulting from different skin depths in the two bands, Equation 27. The thermal gradient from evaporation and heat conduction at the sea surface is $T = \partial T/\partial z = .33$ K/m, which gives

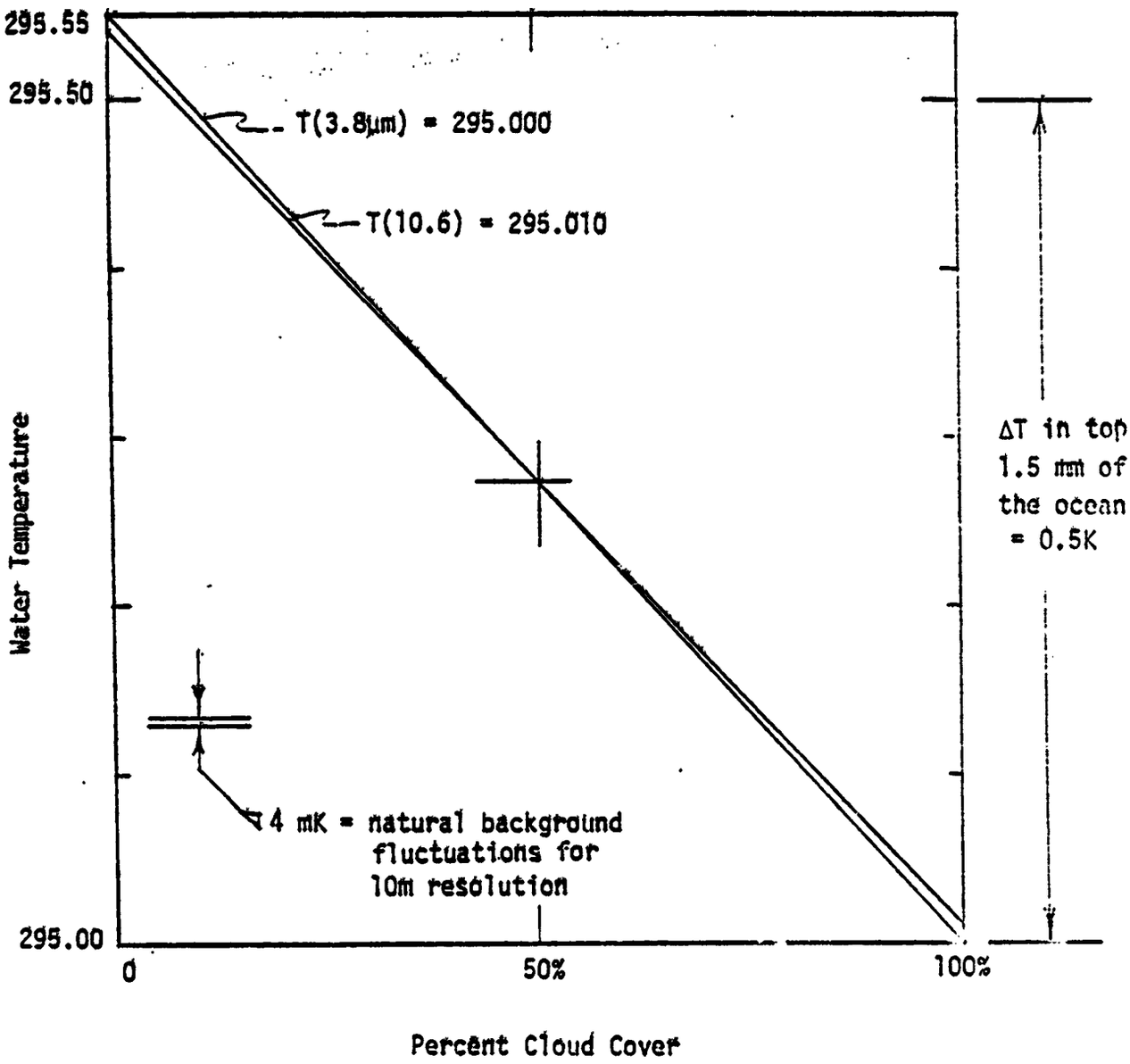

Fig. 6. Attempt to Find Both Cloud Cover and Water Temperature using Radiometric Temperature at Two Wavelengths

$$\left.\begin{aligned} \Delta_g T(3.8) &= 20 \text{ mK} \\ \Delta_g T(10.6) &= 4 \text{ mK} \end{aligned}\right\} \tag{38}$$

If the sea is not too calm, say sea state 2 or greater, then the fluctuations due to clouds, $\Delta T = 50$ mK, Equation 37 occur over large distances, comparable to the altitude of the cloud because the cloud image in the sea is blurred over about a radian. This may not interfere with the observation of pollution plumes on a smaller scale, say a few hundred meters. Over these distances the natural background noise has a variance spectrum given very roughly by

$$\left.\begin{aligned} \phi(3E\text{-}3 \text{ cycles/m}) &= 8E\text{-}3 \ K^2m^2 \\ \phi(0.3 \text{ cycles/meter}) &= 2.3E\text{-}3 \ K^2m^2 \end{aligned}\right\} \tag{39}$$

(linear interpolation (extrapolation) may be used for other frequencies). These values are very rough because they were derived from a 1-dimensional cut through space time (a ship moving at a fixed speed) in a constant field of view, and so we could only assume that the fluctuations were frozen in the sea surface as the ship moved through. In a spacial bandwidth, $\Delta\nu_x$ by $\Delta\nu_y$, the temperature variance is

$$\Delta T^2 = \phi \Delta\nu_x \, \Delta\nu_y \tag{40}$$

If we want the temperature variance in a $(10 \text{ meter})^2$ resolution cell, it is reasonable to take

$$\Delta\nu_x = \Delta\nu_y = \frac{1/2 \text{ cycle}}{10 \text{ meters}} = .05 \text{ cycles/meter} \tag{41}$$

Then Equation 40 gives

$$\Delta T = \sqrt{6E\text{-}3 \ K^2m^2} \times .05 \ m^{-1} = 4 \text{ mK} \tag{42}$$

a much reduced natural background.

2.3 Radiometer Sensitivity

A satellite radiometer must be quite sophisticated compared to an aircraft radiometer. The satellite sensor collects relatively few photons from each resolution cell on the sea surface because of its high altitude and short dwell time. We assume that the satellite radiometer employs low-noise amplifiers of the type used in LandSat D and discussed in Section 1.1. In this case, the sensitivity is limited by shot noise (photon statistics) which overpowers other sources of noise, mainly thermal noise in the amplifier. (Considerably more photons are received in the infrared than a similar radiometer for visible light.) We assume that the infrared radiometer employs cold stops and a cold filter so that radiation from warm parts within the radiometer cannot reach the detector. Thus the only shot noise is that from the field of view.

The performance of infrared detectors and radiometers has traditionally been expressed in power units using figures of merit such as NEP, D and D^*. However, since the shot noise limit is both feasible and required, it is appropriate to bypass these quantities completely and discuss sensitivity in terms of photon statistics alone. It is for this reason that the preceding formulas were expressed in terms of photon flux instead of power commencing with Equation 28.

A straightforward range equation gives the number of photons collected from each resolution cell on the sea surface:

$$n_\phi = Q(\lambda) \left(\frac{\text{dwell}}{\text{time}}\right) \left(\frac{\text{cell}}{\text{area}}\right) \left(\frac{\text{solid angle subtended}}{\text{by radiometer aperture}}\right)$$

$$n = Q(\tau) \, (\delta^2) \left(\frac{\pi d^2/4}{H^2}\right) \tag{43}$$

where d is aperture diameter and H the radiometer's altitude. The number of detection events per all is given by

$$\bar{n}_e = \eta \bar{n}_\phi \tag{44}$$

where η is an overall efficiency that includes optical transparency, aperture obscuration, and detector efficiency, the last being the efficiency in converting photons to charge carriers.

Dwell time τ depends on N_d, the number of detectors in array; the more there are, the more time each detector can spend on one cell. Assuming an efficient scan pattern, i.e. each detector is always looking at a cell within the swath of interest, the dwell time is

$$\tau = \frac{\text{area examined at any instant}}{\text{area scan rate}}$$

$$\tau = \frac{N_d \delta^2}{SV} \tag{45}$$

where S denotes swath width and V the platform velocity. Substituting Equation 45 into 43 into 44 gives

$$\bar{n}_e = \frac{\pi}{4} \frac{\eta N_d Q}{SV} \left(\frac{d\delta^2}{H}\right)^2 \tag{46}$$

Note the extreme sensitivity to resolution δ. This is because δ^2 enters into both the emission area and the dwell time.

Receiver sensitivity derives from the well known formula for the variance of photon (Poisson) statistics:

$$(\Delta n_e)^2 = \bar{n}_e \tag{47}$$

Converting to radiometric temperature uncertainty ΔT gives

$$\frac{\Delta n_e}{\bar{n}_e} = \frac{1}{\sqrt{\bar{n}_e}} = \frac{\Delta Q}{Q} = \frac{\Delta T}{T} \cdot \left(\frac{C_e}{\lambda T}\right) \tag{48}$$

where Equation 47 was used in the first step, 46 in the second, and Equation 33 in the last step. Solving for ΔT gives

$$\frac{\Delta T}{T} = \frac{\lambda T}{C_e} \frac{1}{\sqrt{n_e}} \quad , \tag{49}$$

$$\frac{\Delta T}{T} = \frac{\lambda T}{C_e} \frac{4}{\pi} \frac{SV}{\eta N_d Q} \frac{H}{d\delta^2} \tag{50}$$

We have plotted this equation in Figure 31 in the form ΔT versus δ with N_d as a parameter. Even though ΔT is not very sensitive to N_d, we chose it as a variable because the number of detectors varies so greatly in different arrays, all the way from 1 to 200 in a recent NASA development. Reasonable values assumed for other quantities are the following:

T = 295 kelvin

$C_e/\lambda T$, Q - See Table 2

S = H = 1 Mm

V = 6.6 km/sec

η = 0.5

d = 30 cm

Figure 7 shows that a 100-element array at 10.6um (solid line) provides 100-meter resolution and 10 mK sensitivity. At 3.8um (dashed lines) the performance is marginal, and either sensitivity, resolution, or both have to be compromised. On the left side of the graph the dashed lines are discontinued where the assumption of shot-noise-limited performance begins to fail.

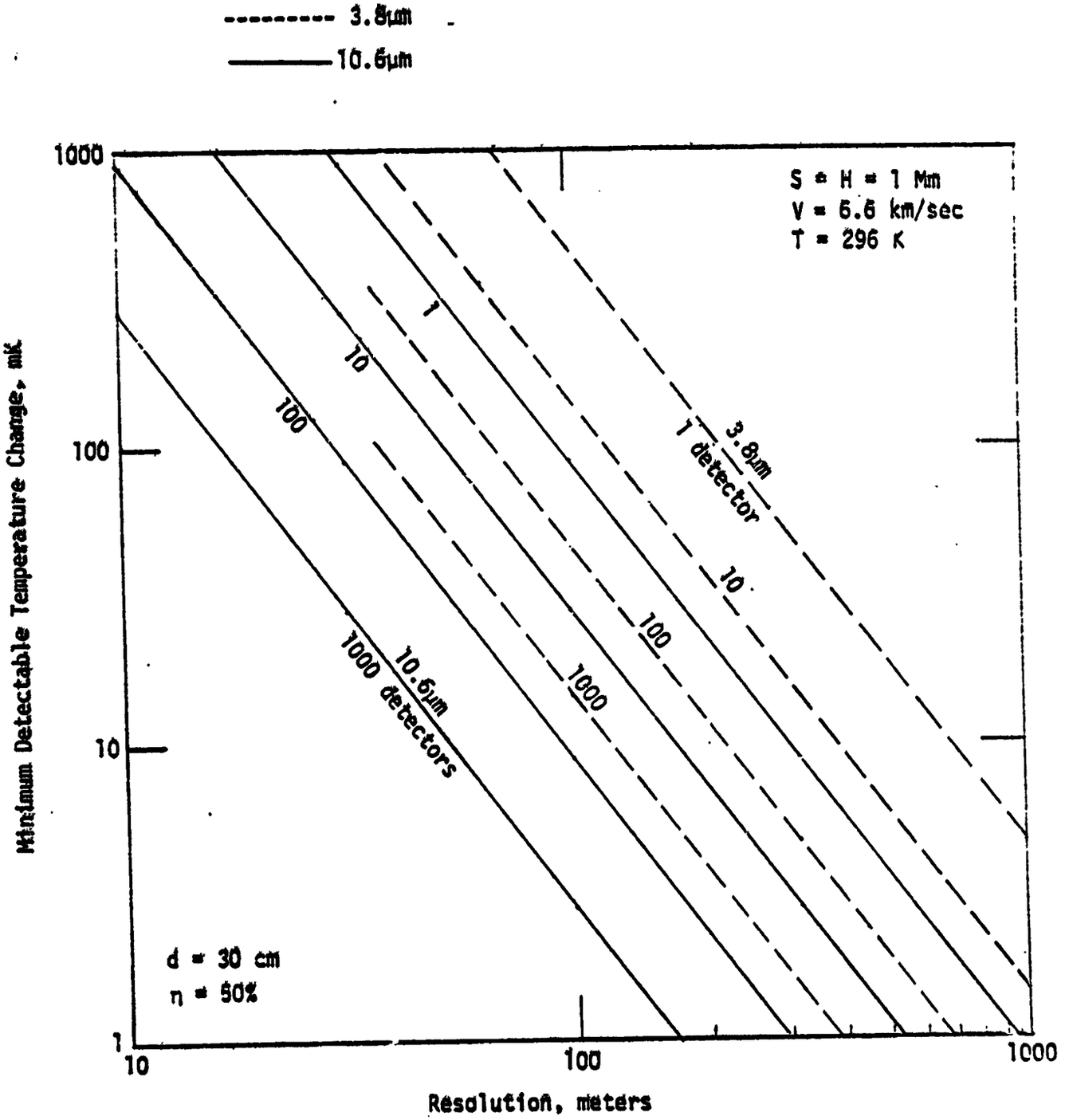

Fig. 7. Performance of Advanced Infrared Imaging Radiometer (shot noise limited) in a Satellite

3.0 MICROWAVE RADIOMETRY

We foresee a limited application of microwave radiometry for pollution sensing from satellites, although there may be some application from aircraft providing they fly beneath the clouds. The reasoning behind this conclusion follows. First, the requirement for angular resolution forces the choice of a short wavelength on the order of $\lambda = 1$ cm ($F = 30$ GHz). But the radiometer is sensitive to clouds at this wavelength, and so its use on a satellite is limited to areas with clear skys. Moreover, at these high frequencies, the radiometer is quite insensitive to sea temperature and conductivity (salinity), as discussed later. The main sensitivity that remains is surface roughness which is of great interest for detection and monitoring of oil slicks.

However, the measurement of roughness puts radiometry into direct competition with radar scatterometry, which measures the same thing. Radar has most of the advantages:

1. penetrates clouds
2. high resolution available by range gating and synthetic aperture
3. no problem with reflected cloud radiance
4. lower frequencies (e.g. L-band) usable if synthetic aperture used for angular resolution
5. cross polarization data

The only advantages for radiometry are:

6. no transmitter power
7. no clutter statistics (random interference effects)

In case of a satellite, Items 1 and 2 appear to be the driving factors. The cloud penetration (1) is very important because 70 to 80% of the ocean is covered by clouds. Also resolution (Item 2) is critical in the satellite

case as we show in Section 3.3. Item 3, problems with reflected cloud radiance is severe because reflectivity is on the order of 50%, depending on frequency and look angle. This may tip the balance in favor of radar even in the aircraft case. The fact that radar requires transmitter power and has problems with clutter statistics (implied by Items 6 and 7) is just something we shall have to work around. These matters are described in the following sections and summarized briefly in Table 3, a sort of 4-dimensional microwave matrix that considers:

- platform: satellite, aircraft
- mode: active (radar), passive (radiometer)
- sky: clear, cloudy
- sensitivity to water condition: roughness, salinity, temperature

3.1 Radiometric Temperature of Seawater

The intensity of radiation recovered in a microwave radiometer is customarily expressed as radiometric temperature T. This would be the same as thermodynamic temperature if the radiometer were pointed at a perfect absorber, but seawater is not, and so a radiometer looking at the sea sees a complicated mix of water and sky radiance reflected from various directions. The results in the case of a clear sky is that the radiometric temperature depends very little on the water temperature except at low frequencies; Stogryn [IEEE Transactions AP-15, p. 278 (Mar 67)] confirms it in a classic paper, for F = 19.4 GHz (λ = 1.5 cm), windspeeds 0 and 7 m/sec and nadir angles 0 and 50^0, as shown in Figure 8. Other investigators have found similar results, e.g. a group at Texas A&M, Figures 9 10, and 11. Figure 9 shows considerable dependence on sea temperature at 9.3 GHz (λ = 3.2 cm), but as discussed later, this frequency provides too little angular resolutions. Figures 9, 10, and 11 also show that the radiometer does not respond effectively to salinity, which might be important in some pollution studies.

TABLE 3 MICROWAVE SUMMARY

Mode	Sensitivity	Platform: Satellite — Sky: clear	Platform: Satellite — Sky: cloudy	Platform: Aircraft — Sky: clear	Platform: Aircraft — Sky: cloudy (fly under?)
Passive (radiometer)	surface roughness	POOR compared to radar which offers fa. better resolution and the following options: • range gate • synthetic aperture • cross polarization	NO Clouds require $\lambda \geq 10$cm but angular resolution requires $\lambda \leq 1$ cm	YES but not superior to radar.	POOR compared to radar since radiometer data complicated by reflected cloud radiance
	conductivity (salinity)	NO Sensitive only if $\lambda > 3$cm, but angular resolution requires $\lambda \leq 1$cm.		POOR since measure of conductivity must be disentangled from large effects of surface roughness and clouds	
	water temperature	NO Sensitive only if $\lambda \geq 10$cm, but angular resolution requires $\lambda \leq 1$cm.		Probably NO since infrared radiometer does the job with far better resolution and less interference from reflected sky and surface roughness.	

Mode	Sensitivity	Sky: clear	Sky: cloudy
Active (radar)	roughness	YES	
	conductivity	YES if long λ	
	temperature	NO	

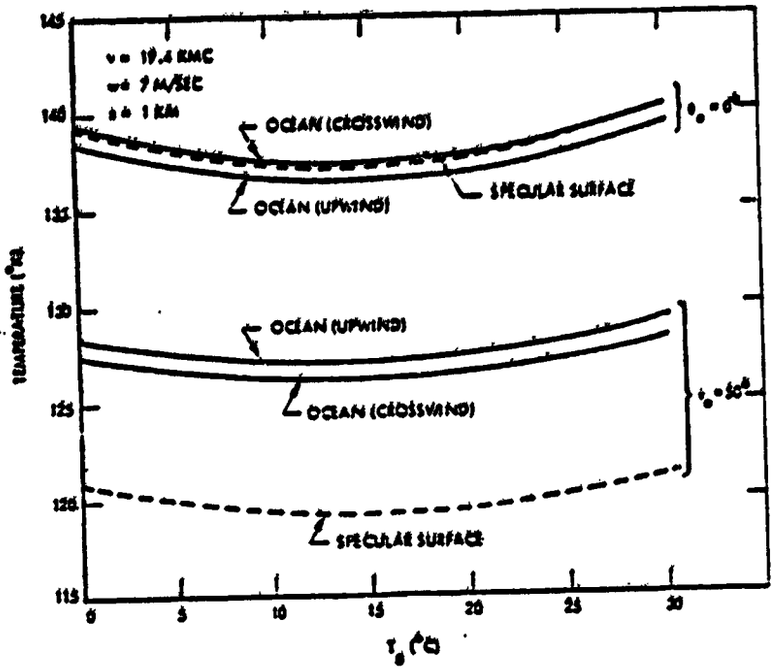

Fig. 8. Temperature of horizontally polarized radiation as a function of water temperature.

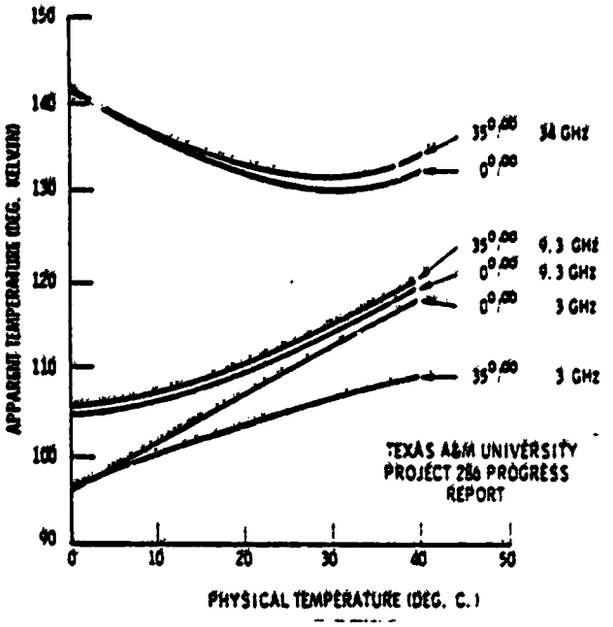

Fig. 9. Theoretically predicted curves. Brightness temperature vs. salinity and temperature.

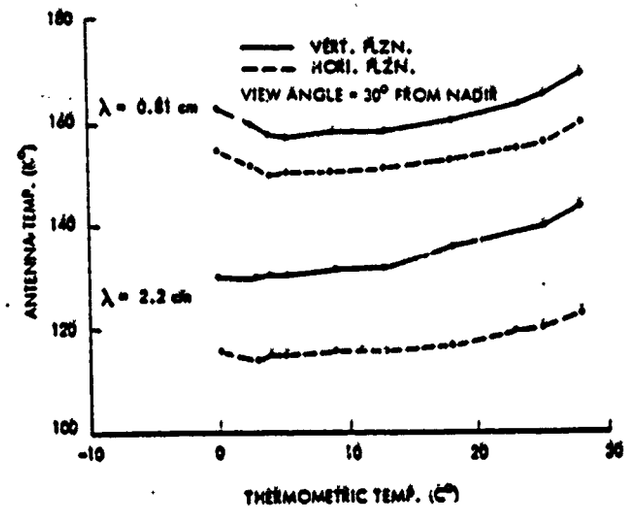

Fig. 10. Antenna brightness temperature of fresh water as a function of thermometric temperature.

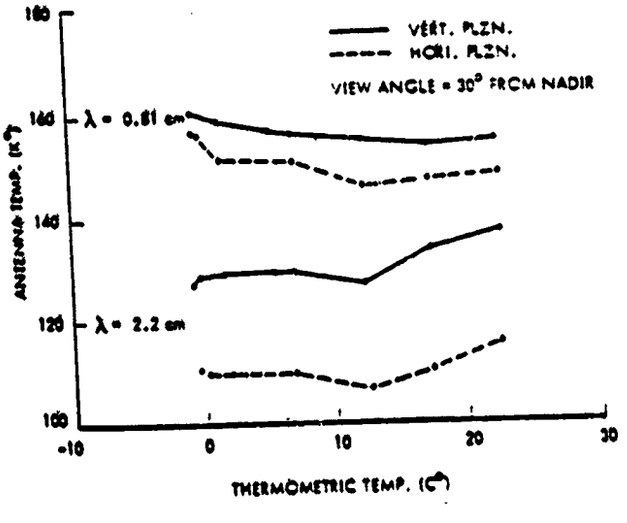

Fig. 11. Antenna brightness temperature of sea water as a function of thermometric temperature.

A microwave radiometer looking at the sea is sensitive to the angle of the water surface, and hence to wind that roughens the surface. This effect appears in curves by Stogryn reproduced here as Figures 12, 13, and 14.

3.2 Clouds

Figures 12 and 14 show that temperature sensitivity on the order of

$$\Delta T = 1 \text{ Kelvin}$$

is needed to sense small changes in surface roughness. This in turn limits the amount of interference that can be tolerated from clouds, ΔT_c. This interference is proportional to the fractional absorption A:

$$\Delta T_{cloud} \approx A T_c$$

Assuming T_c = 300 Kelvin gives A = .003. Comparing to Figure 15 shows that even a light cloud causes appreciable interference at frequencies 10 GHz or higher. But frequencies this high (see Section 3.3) are required to attain reasonable angular resolution, and so the microwave radiometer, unlike radar, simply will not be very useful in seeing through clouds.

3.3 Instrumental Limitations

The sensitivity of a microwave radiometer to temperature changes is given by

$$\Delta T = \frac{2\, T_n}{\sqrt{B\tau}} \qquad (51)$$

where T_n is the receiver noise temperature, B its bandwidth, and τ the dwell time. The factor of 2 applies strictly to a Dicke radiometer, and varies slightly with other schemes used to stabilize the gain. The dwell time needed for Equation 1 depends on platform velocity V and geometrical factors:

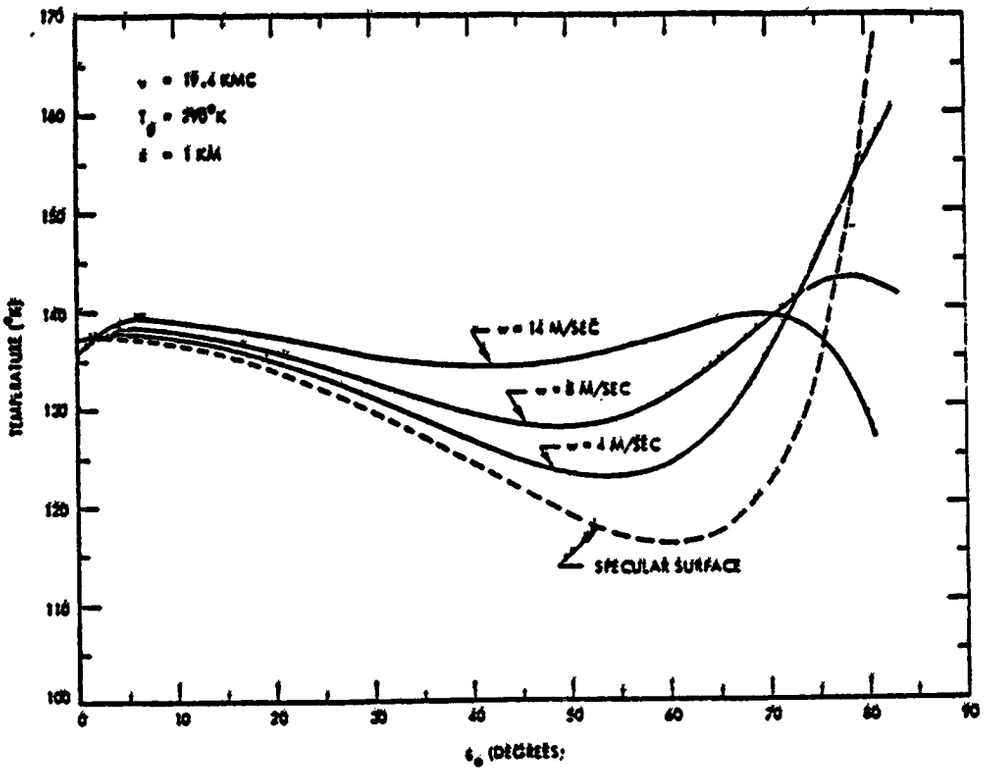

Fig. 12. Temperature of horizontally polarized radiation as a function of angle (upwind case).

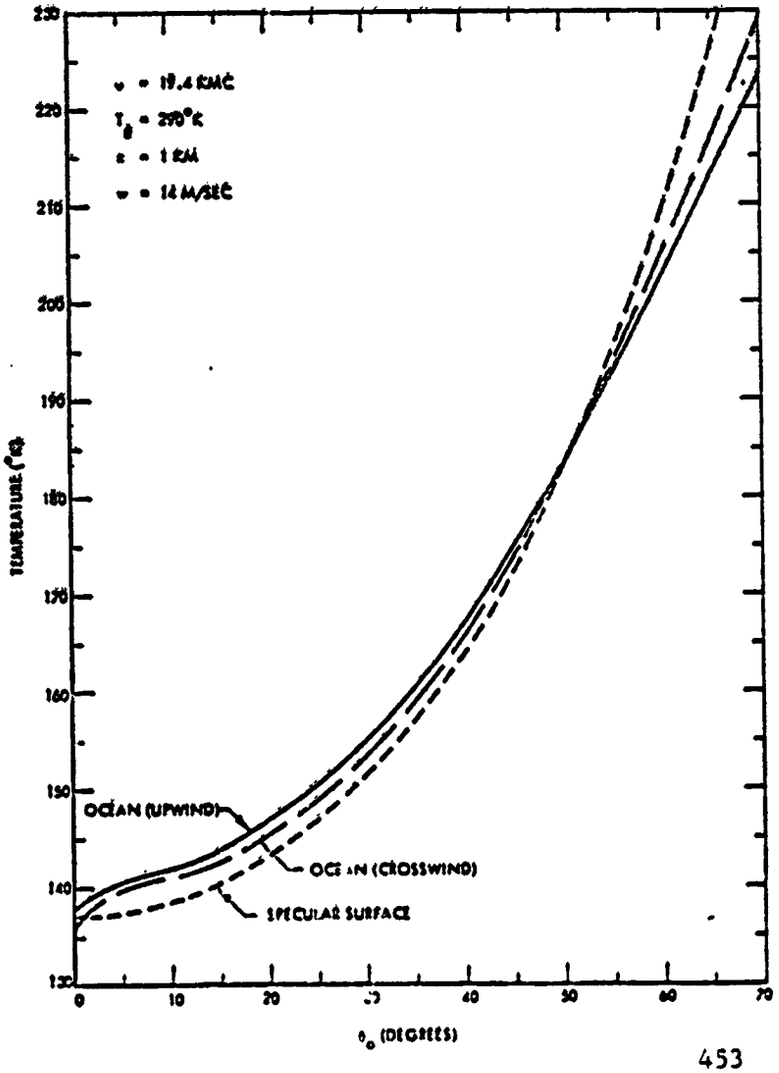

Fig. 13. Temperature of vertically polarized radiation as a function of angle.

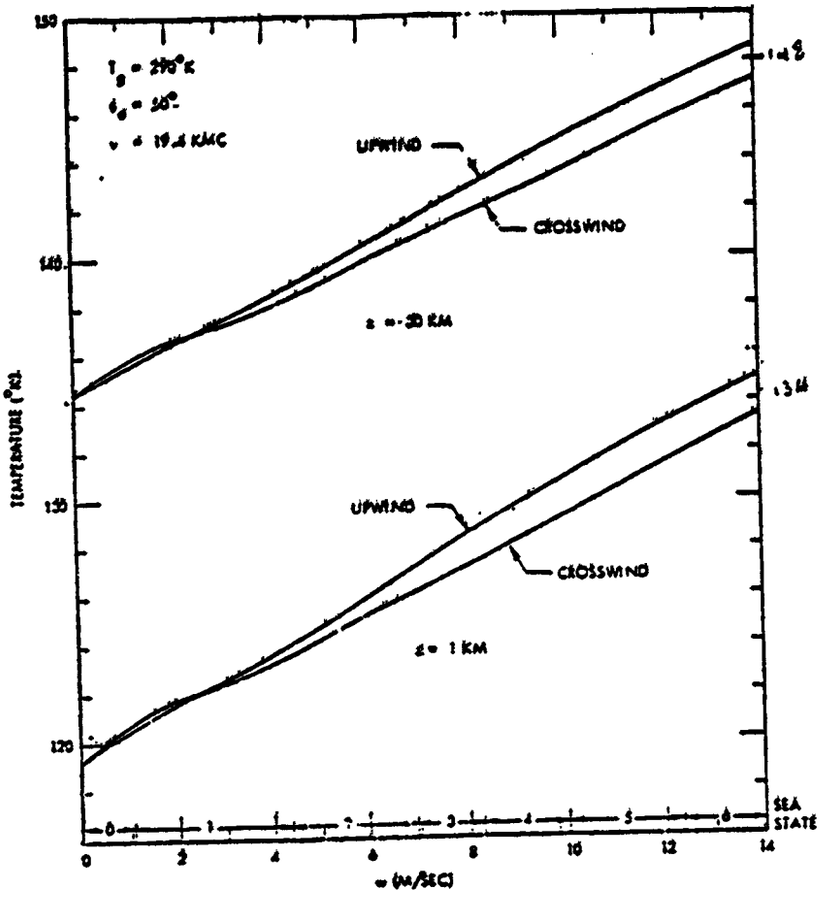

Fig. 14. Temperature of norizontally polarized radiation as a function or wind speed.

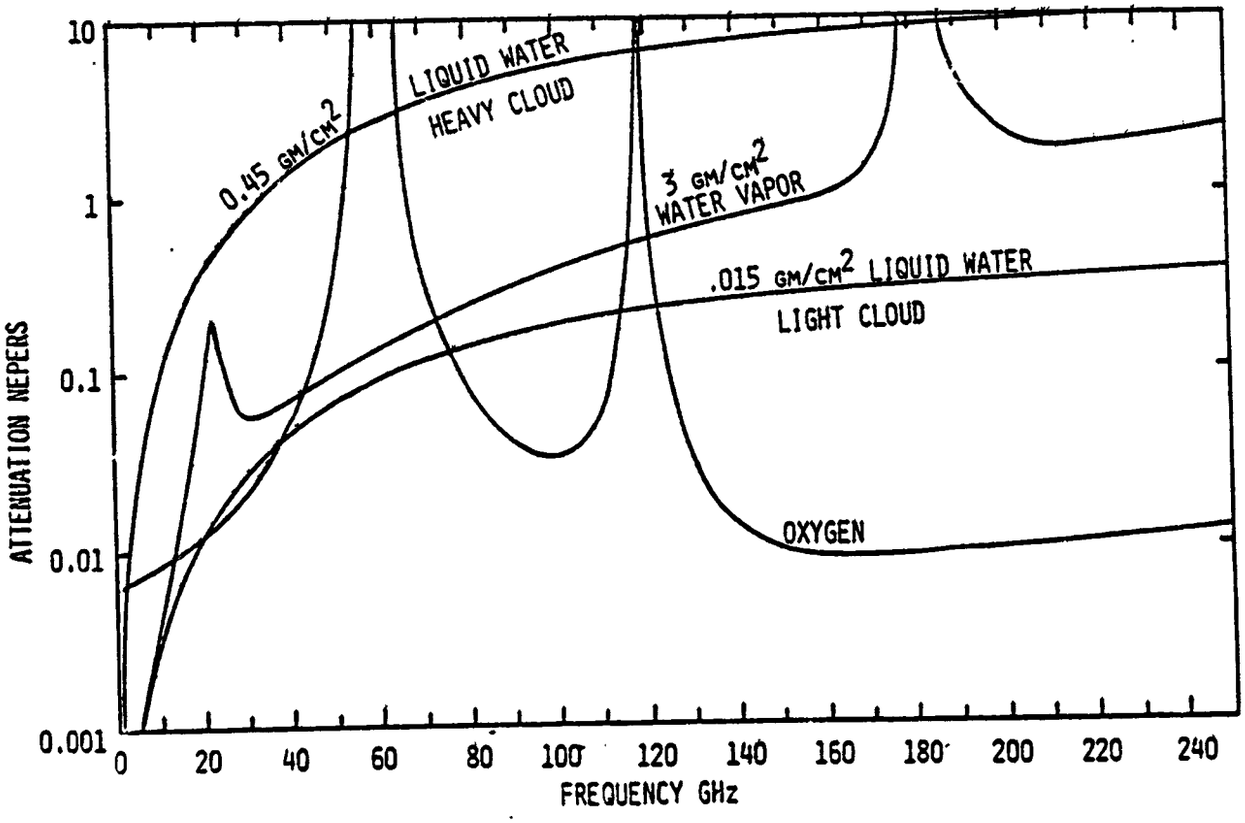

Fig. 15. Zenith microwave opacity components for a standard atmosphere, 3 gm/cm^2 columnar water vapor density and two clouds.

$$\tau = \frac{\text{resolution area}}{\text{area search rate}}$$

$$\tau = \delta^2/SV \qquad (52)$$

where S is the swath width and δ the dimension of a resolution cell (presumed square). At nadir, the resolution is approximately:

$$\delta = \lambda h/d \quad , \qquad (53)$$

where h is altitude and d aperture diameter. This equation expresses a severe bind: λ should be short for good resolution, but long to avoid excessive sensitivity to thin clouds or fog. The best one can do is use large apertures as listed in Table 4 along with assumed λ, h and resulting δ. The value δ = 1 km in the satellite column is adequate for mapping a large oil spill, but too large for many smaller dumps. Other reasonable assumptions are listed in this table along with the results from Equations 51, 52, and 53. These results show that the sensitivity is quite adequate. The real crunch is in resolution and sensitivity to clouds.

TABLE 4 RADIOMETER ASSUMPTIONS AND RESULTS

Assumptions	Satellite	Aircraft
Altitude H	1 Mm	3 km
Swath S = H	1 Mm	3 km
Velocity V	7 km/sec	160 m/s
Wavelength λ	1 cm	3 cm
Frequency F	30 GHz	10 GHz
B = F/10	3 GHz	1 GHz
Aperture diameter d	10m = 1000λ	1 meter = 33λ
Noise temperature T_n	150K	150K
Results		
Resolution δ	1 km	100 m
Dwelling time τ	140μs	20 msec
Sensitivity ΔT	0.46K	.067K

APPENDIX

Curves of Spectral Radiance

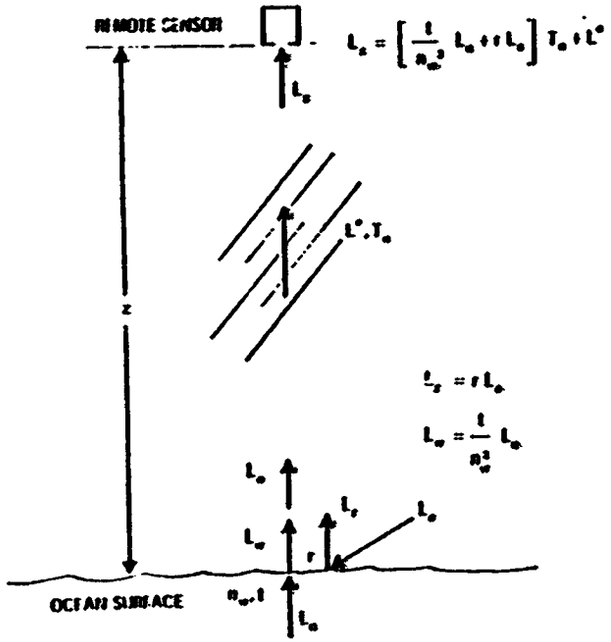

Fig. 11. Component parts of the upwelling radiance signal, L_z.

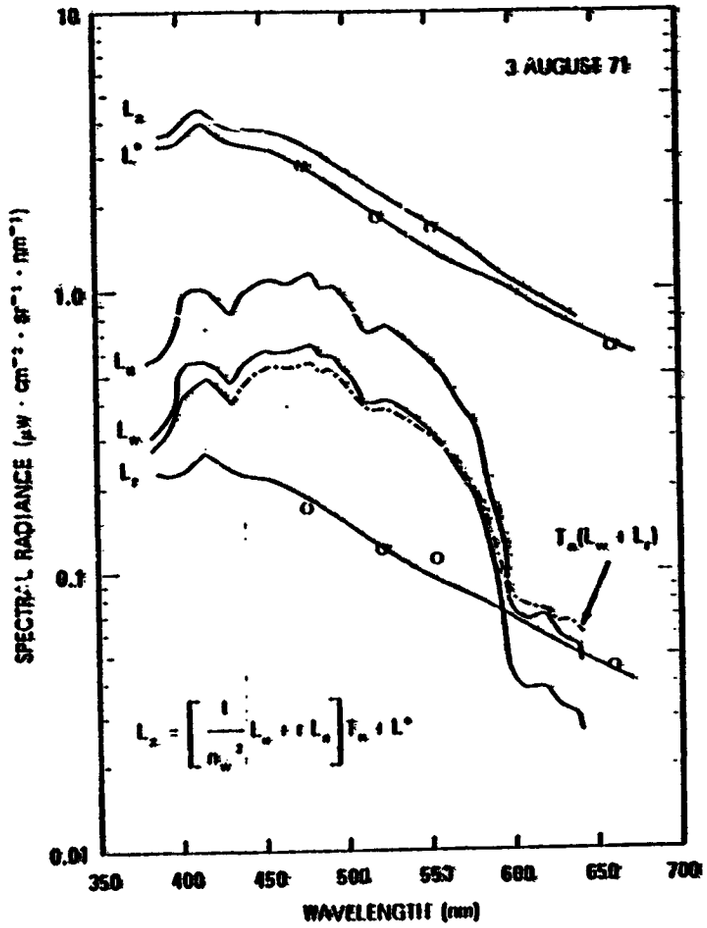

Fig. 12. Computed apparent spectral radiance of the ocean (and its components) as observed above the atmosphere. Blue-green water.

Figures by RW Austin, "Remote Sensing of Spectral Radiance," Chapter 14 in Optical Aspects of Oceanography, edited by NG Jerlov and ES Nielsen, Academic Press, NY 1974 (continued next page)

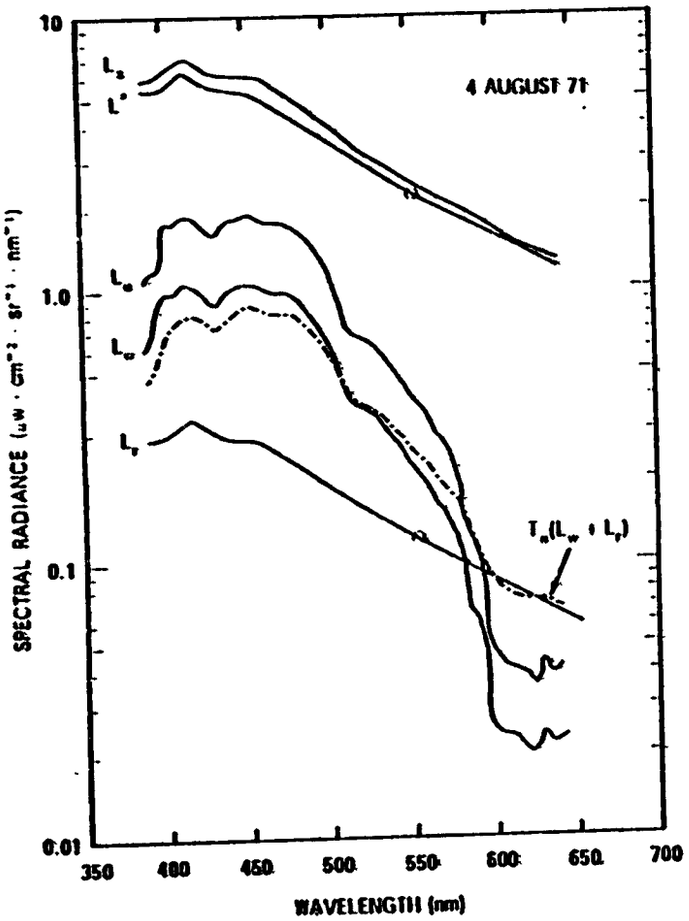

Fig. 13. Computed apparent spectral radiance of the ocean (and its components) as observed above the atmosphere. Blue water.

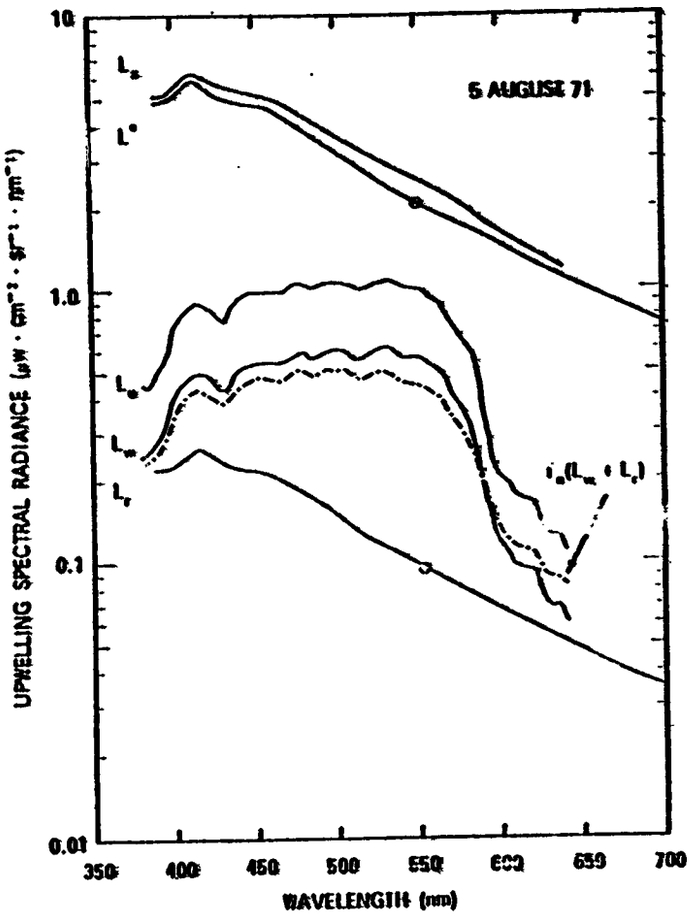

Fig. 14. Computed apparent spectral radiance of the ocean (and its components) as observed above the atmosphere. Green water.

Figures by RW Austin, concluded

1. Report No.	2. Government Accession No.	3. Recipient's Catalog No.
NASA CR-159242		

4. Title and Subtitle	5. Report Date
ASSESSMENT OF THE USE OF SPACE TECHNOLOGY IN THE MONITORING OF OIL SPILLS AND OCEAN POLLUTION-TECHNICAL VOLUME	April 1980
	6. Performing Organization Code
7. Author(s)	8. Performing Organization Report No.
U. R. Alvarado (Editor)	
	10. Work Unit No.
9. Performing Organization Name and Address	
General Electric Company Space Division Valley Forge Space Center P. O. Box 8555, Philadelphia, PA 19101	11. Contract or Grant No. NAS1-15657
	13. Type of Report and Period Covered
12. Sponsoring Agency Name and Address	Contractor Report
National Aeronautics and Space Administration Washington, DC 20546	14. Sponsoring Agency Code

15. Supplementary Notes

Contract Monitor: William F. Croswell, NASA Langley Research Center, Hampton, VA 23665

16. Abstract

The United States Congress in the NASA Authorization Act of 1978, directed NASA to investigate the potential of satellite systems and space technology to detect and monitor oil spills and ocean waste disposal in the U.S. waters. As a result, a program of spacecraft studies, was initiated along with field measurements and laboratory investigations to provide the scientific information to perform the assessment. The space system study, which is documented in this report is directed toward all weather remote sensing and surveillance where the space system would provide information to regulatory agencies for closer investigation with aircraft and ships. This volume is the Executive Summary.

17. Key Words (Suggested by Author(s))	18. Distribution Statement
OIL SPILL ASSESSMENT RADAR REMOTE SENSING RADIO REMOTE SENSING	Unclassified - Unlimited Subject Category 43

19. Security Classif. (of this report)	20. Security Classif. (of this page)	21. No. of Pages	22. Price*
Unclassified	Unclassified	462	

For sale by the National Technical Information Service, Springfield, Virginia 22161